



Hashemite Kingdom of Jordan



Jordan Journal of



Biological Sciences

An International Peer-Reviewed Scientific Journal

Financed by the Scientific Research and Innovation Support Fund



<http://jjbs.hu.edu.jo/>

المجلة الأردنية للعلوم الحياتية
Jordan Journal of Biological Sciences (JJBS)

<http://jjbs.hu.edu.jo>

Jordan Journal of Biological Sciences (JJBS) (ISSN: 1995–6673 (Print); 2307-7166 (Online)): An International Peer- Reviewed Open Access Research Journal financed by the Scientific Research and Innovation Support Fund, Ministry of Higher Education and Scientific Research, Jordan and published quarterly by the Deanship of Scientific Research , The Hashemite University, Jordan.

Editor-in-Chief

Professor Atoum, Manar F.

Molecular Biology and Genetics,
The Hashemite University

Assistant Editor

Dr. Muhannad, Massadeh I.

Microbial Biotechnology,
The Hashemite University

Editorial Board (Arranged alphabetically)

Professor Amr, Zuhair S.

Animal Ecology and Biodiversity
Jordan University of Science and Technology

Professor Hunaiti, Abdulrahim A.

Biochemistry
The University of Jordan

Professor Khleifat, Khaled M.

Microbiology and Biotechnology
Mutah University

Professor Lahham, Jamil N.

Plant Taxonomy
Yarmouk University

Professor Malkawi, Hanan I.

Microbiology and Molecular Biology
Yarmouk University

Associate Editorial Board

Professor Al-Hindi, Adnan I.

Parasitology
The Islamic University of Gaza, Faculty of Health
Sciences, Palestine

Dr Gammoh, Noor

Tumor Virology
Cancer Research UK Edinburgh Centre, University of
Edinburgh, U.K.

Professor Kasperek, Max

Natural Sciences
Editor-in-Chief, Journal Zoology in the Middle East,
Germany

Professor Krystufek, Boris

Conservation Biology
Slovenian Museum of Natural History,
Slovenia

Dr Rabei, Sami H.

Plant Ecology and Taxonomy
Botany and Microbiology Department,
Faculty of Science, Damietta University, Egypt

Professor Simerly, Calvin R.

Reproductive Biology
Department of Obstetrics/Gynecology and
Reproductive Sciences, University of
Pittsburgh, USA

Editorial Board Support Team

Language Editor

Dr. Shadi Neimneh

Publishing Layout

Eng.Mohannad Oqdeh

Submission Address

Professor Atoum, Manar F

The Hashemite University
P.O. Box 330127, Zarqa, 13115, Jordan
Phone: +962-5-3903333 ext.4147
E-Mail: jjbs@hu.edu.jo

International Advisory Board (Arranged alphabetically)

Professor Ahmad M. Khalil

Department of Biological Sciences, Faculty of Science,
Yarmouk University, Jordan

Professor Anilava Kaviraj

Department of Zoology, University of Kalyani, India

Professor Bipul Kumar Das

Faculty of Fishery Sciences W. B. University of Animal &
Fishery Sciences, India

Professor Elias Baydoun

Department of Biology, American University of Beirut
Lebanon

Professor Hala Gali-Muhtasib

Department of Biology, American University of Beirut
Lebanon

Professor Ibrahim M. AlRawashdeh

Department of Biological Sciences, Faculty of Science, Al-
Hussein Bin Talal University, Jordan

Professor João Ramalho-Santos

Department of Life Sciences, University of Coimbra, Portugal

Professor Khaled M. Al-Qaoud

Department of Biological sciences, Faculty of Science,
Yarmouk University, Jordan

Professor Mahmoud A. Ghannoum

Center for Medical Mycology and Mycology Reference
Laboratory, Department of Dermatology, Case Western
Reserve University and University Hospitals Case Medical
Center, USA

Professor Mawieh Hamad

Department of Medical Lab Sciences, College of Health
Sciences , University of Sharjah, UAE

Professor Michael D Garrick

Department of Biochemistry, State University of New York at
Buffalo, USA

Professor Nabil. A. Bashir

Department of Physiology and Biochemistry, Faculty of
Medicine, Jordan University of Science and Technology,
Jordan

Professor Nizar M. Abuharfeil

Department of Biotechnology and Genetic Engineering, Jordan
University of Science and Technology, Jordan

Professor Samih M. Tamimi

Department of Biological Sciences, Faculty of Science, The
University of Jordan, Jordan

Professor Ulrich Joger

State Museum of Natural History Braunschweig, Germany

Professor Aida I. El Makawy

Division of Genetic Engineering and Biotechnology, National
Research Center. Giza, Egypt

Professor Bechan Sharma

Department of Biochemistry, Faculty of Science University of
Allahabad, India

Professor Boguslaw Buszewski

Chair of Environmental Chemistry and Bioanalytics, Faculty of
Chemistry, Nicolaus Copernicus University Poland

Professor Gerald Schatten

Pittsburgh Development Center, Division of Developmental
and Regenerative Medicine, University of Pittsburgh, School
of Medicine, USA

Professor Hala Khyami-Horani

Department of Biological Sciences, Faculty of Science, The
University of Jordan, Jordan

Professor James R. Bamburg

Department of Biochemistry and Molecular Biology, Colorado
State University, USA

Professor Jumah M. Shakhaneh

Department of Biological Sciences, Faculty of Science, Mutah
University, Jordan

Dr. Lukmanul Hakkim Faruck

Department of Mathematics and Sciences College of Arts and
Applied Sciences, Dhofar, Oman

Professor Md. Yeamin Hossain

Department of Fisheries, Faculty of Fisheries , University of
Rajshahi, Bangladesh

Professor Mazin B. Qumsiyeh

Palestine Museum of Natural History and Palestine Institute for
Biodiversity and Sustainability, Bethlehem University,
Palestine

Professor Mohamad S. Hamada

Genetics Department, Faculty of Agriculture, Damietta
University, Egypt

Professor Nawroz Abdul-razzak Tahir

Plant Molecular Biology and Phytochemistry, University of
Sulaimani, College of Agricultural Sciences, Iraq

Professor Ratib M. AL- Ouran

Department of Biological Sciences, Faculty of Science, Mutah
University, Jordan

Professor Shtaywy S. Abdalla Abbadi

Department of Biological Sciences, Faculty of Science, The
University of Jordan, Jordan

Professor Zihad Bouslama

Department of Biology, Faculty of Science Badji Mokhtar
University, Algeria

Instructions to Authors

Scopes

Study areas include cell biology, genomics, microbiology, immunology, molecular biology, biochemistry, embryology, immunogenetics, cell and tissue culture, molecular ecology, genetic engineering and biological engineering, bioremediation and biodegradation, bioinformatics, biotechnology regulations, gene therapy, organismal biology, microbial and environmental biotechnology, marine sciences. The JJBS welcomes the submission of manuscript that meets the general criteria of significance and academic excellence. All articles published in JJBS are peer-reviewed. Papers will be published approximately one to two months after acceptance.

Type of Papers

The journal publishes high-quality original scientific papers, short communications, correspondence and case studies. Review articles are usually by invitation only. However, Review articles of current interest and high standard will be considered.

Submission of Manuscript

Manuscript, or the essence of their content, must be previously unpublished and should not be under simultaneous consideration by another journal. The authors should also declare if any similar work has been submitted to or published by another journal. They should also declare that it has not been submitted/ published elsewhere in the same form, in English or in any other language, without the written consent of the Publisher. The authors should also declare that the paper is the original work of the author(s) and not copied (in whole or in part) from any other work. All papers will be automatically checked for duplicate publication and plagiarism. If detected, appropriate action will be taken in accordance with International Ethical Guideline. By virtue of the submitted manuscript, the corresponding author acknowledges that all the co-authors have seen and approved the final version of the manuscript. The corresponding author should provide all co-authors with information regarding the manuscript, and obtain their approval before submitting any revisions. Electronic submission of manuscripts is strongly recommended, provided that the text, tables and figures are included in a single Microsoft Word file. Submit manuscript as e-mail attachment to the Editorial Office at: JJBS@hu.edu.jo. After submission, a manuscript number will be communicated to the corresponding author within 48 hours.

Peer-review Process

It is requested to submit, with the manuscript, the names, addresses and e-mail addresses of at least 4 potential reviewers. It is the sole right of the editor to decide whether or not the suggested reviewers to be used. The reviewers' comments will be sent to authors within 6-8 weeks after submission. Manuscripts and figures for review will not be returned to authors whether the editorial decision is to accept, revise, or reject. All Case Reports and Short Communication must include at least one table and/ or one figure.

Preparation of Manuscript

The manuscript should be written in English with simple lay out. The text should be prepared in single column format. Bold face, italics, subscripts, superscripts etc. can be used. Pages should be numbered consecutively, beginning with the title page and continuing through the last page of typewritten material.

The text can be divided into numbered sections with brief headings. Starting from introduction with section 1. Subsections should be numbered (for example 2.1 (then 2.1.1, 2.1.2, 2.2, etc.), up to three levels. Manuscripts in general should be organized in the following manner:

Title Page

The title page should contain a brief title, correct first name, middle initial and family name of each author and name and address of the department(s) and institution(s) from where the research was carried out for each author. The title should be without any abbreviations and it should enlighten the contents of the paper. All affiliations should be provided with a lower-case superscript number just after the author's name and in front of the appropriate address.

The name of the corresponding author should be indicated along with telephone and fax numbers (with country and area code) along with full postal address and e-mail address.

Abstract

The abstract should be concise and informative. It should not exceed **350 words** in length for full manuscript and Review article and **150 words** in case of Case Report and/ or Short Communication. It should briefly describe the purpose of the work, techniques and methods used, major findings with important data and conclusions. No references should be cited in this part. Generally non-standard abbreviations should not be used, if necessary they should be clearly defined in the abstract, at first use.

Keywords

Immediately after the abstract, **about 4-8 keywords** should be given. Use of abbreviations should be avoided, only standard abbreviations, well known in the established area may be used, if appropriate. These keywords will be used for indexing.

Abbreviations

Non-standard abbreviations should be listed and full form of each abbreviation should be given in parentheses at first use in the text.

Introduction

Provide a factual background, clearly defined problem, proposed solution, a brief literature survey and the scope and justification of the work done.

Materials and Methods

Give adequate information to allow the experiment to be reproduced. Already published methods should be mentioned with references. Significant modifications of published methods and new methods should be described in detail. Capitalize trade names and include the manufacturer's name and address. Subheading should be used.

Results

Results should be clearly described in a concise manner. Results for different parameters should be described under subheadings or in separate paragraph. Results should be explained, but largely without referring to the literature. Table or figure numbers should be mentioned in parentheses for better understanding.

Discussion

The discussion should not repeat the results, but provide detailed interpretation of data. This should interpret the significance of the findings of the work. Citations should be given in support of the findings. The results and discussion part can also be described as separate, if appropriate. The Results and Discussion sections can include subheadings, and when appropriate, both sections can be combined

Conclusions

This should briefly state the major findings of the study.

Acknowledgment

A brief acknowledgment section may be given after the conclusion section just before the references. The acknowledgment of people who provided assistance in manuscript preparation, funding for research, etc. should be listed in this section.

Tables and Figures

Tables and figures should be presented as per their appearance in the text. It is suggested that the discussion about the tables and figures should appear in the text before the appearance of the respective tables and figures. No tables or figures should be given without discussion or reference inside the text.

Tables should be explanatory enough to be understandable without any text reference. Double spacing should be maintained throughout the table, including table headings and footnotes. Table headings should be placed above the table. Footnotes should be placed below the table with superscript lowercase letters. Each table should be on a separate page, numbered consecutively in Arabic numerals.

Each figure should have a caption. The caption should be concise and typed separately, not on the figure area. Figures should be self-explanatory. Information presented in the figure should not be repeated in the table. All symbols and abbreviations used in the illustrations should be defined clearly. Figure legends should be given below the figures.

References

References should be listed alphabetically at the end of the manuscript. Every reference referred in the text must be also present in the reference list and vice versa. In the text, a reference identified by means of an author's name should be followed by the year of publication in parentheses (e.g.(Brown,2009)). For two authors, both authors' names followed by the year of publication (e.g.(Nelson and Brown, 2007)). When there are more than two authors, only the first author's name followed by "*et al.*" and the year of publication (e.g. (Abu-Elteen *et al.*, 2010)). When two or more works of an author has been published during the same year, the reference should be identified by the letters "a", "b", "c", etc., placed after the year of publication. This should be followed both in the text and reference list. e.g., Hilly, (2002a, 2002b); Hilly, and Nelson, (2004). Articles in preparation or submitted for publication, unpublished observations, personal communications, etc. should not be included in the reference list but should only be mentioned in the article text (e.g., Shtyawy,A., University of Jordan, personal communication). Journal titles should be abbreviated according to the system adopted in Biological Abstract and Index Medicus, if not included in Biological Abstract or Index Medicus journal title should be given in full. The author is responsible for the scuracy and completeness of the references and for their correct textual citation. Failure to do so may result in the paper being withdraw from the evaluation process. Example of correct reference form is given as follows:-

Reference to a journal publication:

Bloch BK. 2002. Econazole nitrate in the treatment of *Candida vaginitis*. *S Afr Med J.* , **58**:314-323.

Ogunseitan OA and Ndoye IL. 2006. Protein method for investigating mercuric reductase gene expression in aquatic environments. *Appl Environ Microbiol.*, **64**: 695-702.

Hilly MO, Adams MN and Nelson SC. 2009. Potential fly-ash utilization in agriculture. *Progress in Natural Sci.*, **19**: 1173-1186.

Reference to a book:

Brown WY and White SR.1985. **The Elements of Style**, third ed. MacMillan, New York.

Reference to a chapter in an edited book:

Mettam GR and Adams LB. 2010. How to prepare an electronic version of your article. In: Jones BS and Smith RZ (Eds.), **Introduction to the Electronic Age**. Kluwer Academic Publishers, Netherlands, pp. 281–304.

Conferences and Meetings:

Embabi NS. 1990. Environmental aspects of distribution of mangrove in the United Arab Emirates. Proceedings of the First ASWAS Conference. University of the United Arab Emirates. Al-Ain, United Arab Emirates.

Theses and Dissertations:

El-Labadi SN. 2002. Intestinal digenetic trematodes of some marine fishes from the Gulf of Aqaba. MSc dissertation, The Hashemite University, Zarqa, Jordan.

Nomenclature and Units

Internationally accepted rules and the international system of units (SI) should be used. If other units are mentioned, please give their equivalent in SI.

For biological nomenclature, the conventions of the *International Code of Botanical Nomenclature*, the *International Code of Nomenclature of Bacteria*, and the *International Code of Zoological Nomenclature* should be followed.

Scientific names of all biological creatures (crops, plants, insects, birds, mammals, etc.) should be mentioned in parentheses at first use of their English term.

Chemical nomenclature, as laid down in the *International Union of Pure and Applied Chemistry* and the official recommendations of the *IUPAC-IUB Combined Commission on Biochemical Nomenclature* should be followed. All biocides and other organic compounds must be identified by their Geneva names when first used in the text. Active ingredients of all formulations should be likewise identified.

Math formulae

All equations referred to in the text should be numbered serially at the right-hand side in parentheses. Meaning of all symbols should be given immediately after the equation at first use. Instead of root signs fractional powers should be used. Subscripts and superscripts should be presented clearly. Variables should be presented in italics. Greek letters and non-Roman symbols should be described in the margin at their first use.

To avoid any misunderstanding zero (0) and the letter O, and one (1) and the letter l should be clearly differentiated. For simple fractions use of the solidus (/) instead of a horizontal line is recommended. Levels of statistical significance such as: * $P < 0.05$, ** $P < 0.01$ and *** $P < 0.001$ do not require any further explanation.

Copyright

Submission of a manuscript clearly indicates that: the study has not been published before or is not under consideration for publication elsewhere (except as an abstract or as part of a published lecture or academic thesis); its publication is permitted by all authors and after accepted for publication it will not be submitted for publication anywhere else, in English or in any other language, without the written approval of the copyright-holder. The journal may consider manuscripts that are translations of articles originally published in another language. In this case, the consent of the journal in which the article was originally published must be obtained and the fact that the article has already been published must be made clear on submission and stated in the abstract. It is compulsory for the authors to ensure that no material submitted as part of a manuscript infringes existing copyrights, or the rights of a third party.

Ethical Consent

All manuscripts reporting the results of experimental investigation involving human subjects should include a statement confirming that each subject or subject's guardian obtains an informed consent, after the approval of the experimental protocol by a local human ethics committee or IRB. When reporting experiments on animals, authors should indicate whether the institutional and national guide for the care and use of laboratory animals was followed.

Plagiarism

The JJBS hold no responsibility for plagiarism. If a published paper is found later to be extensively plagiarized and is found to be a duplicate or redundant publication, a note of retraction will be published, and copies of the correspondence will be sent to the authors' head of institute.

Galley Proofs

The Editorial Office will send proofs of the manuscript to the corresponding author as an e-mail attachment for final proof reading and it will be the responsibility of the corresponding author to return the galley proof materials appropriately corrected within the stipulated time. Authors will be asked to check any typographical or minor clerical errors in the manuscript at this stage. No other major alteration in the manuscript is allowed. After publication authors can freely access the full text of the article as well as can download and print the PDF file.

Publication Charges

There are no page charges for publication in Jordan Journal of Biological Sciences, except for color illustrations,

Reprints

Ten (10) reprints are provided to corresponding author free of charge within two weeks after the printed journal date. For orders of more reprints, a reprint order form and prices will be sent with article proofs, which should be returned directly to the Editor for processing.

Disclaimer

Articles, communication, or editorials published by JJBS represent the sole opinions of the authors. The publisher shoulders no responsibility or liability what so ever for the use or misuse of the information published by JJBS.

Indexing

JJBS is indexed and abstracted by:

DOAJ (Directory of Open Access Journals)

Google Scholar

Journal Seek

HINARI

Index Copernicus

NDL Japanese Periodicals Index

SCIRUS

OAJSE

ISC (Islamic World Science Citation Center)

Directory of Research Journal Indexing
(DRJI)

Ulrich's

CABI

EBSCO

CAS (Chemical Abstract Service)

ETH- Citations

Open J-Gat

SCImago

Clarivate Analytics (Zoological Abstract)

Scopus

AGORA (United Nation's FAO database)

SHERPA/RoMEO (UK)

المجلة الأردنية للعلوم الحياتية
Jordan Journal of Biological Sciences (JJBS)
ISSN 1995- 6673 (Print), 2307- 7166 (Online)

<http://jjbs.hu.edu.jo>

The Hashemite University
Deanship of Scientific Research
TRANSFER OF COPYRIGHT AGREEMENT

Journal publishers and authors share a common interest in the protection of copyright: authors principally because they want their creative works to be protected from plagiarism and other unlawful uses, publishers because they need to protect their work and investment in the production, marketing and distribution of the published version of the article. In order to do so effectively, publishers request a formal written transfer of copyright from the author(s) for each article published. Publishers and authors are also concerned that the integrity of the official record of publication of an article (once refereed and published) be maintained, and in order to protect that reference value and validation process, we ask that authors recognize that distribution (including through the Internet/WWW or other on-line means) of the authoritative version of the article as published is best administered by the Publisher.

To avoid any delay in the publication of your article, please read the terms of this agreement, sign in the space provided and return the complete form to us at the address below as quickly as possible.

Article entitled:-----

Corresponding author: -----

To be published in the journal: Jordan Journal of Biological Sciences (JJBS)

I hereby assign to the Hashemite University the copyright in the manuscript identified above and any supplemental tables, illustrations or other information submitted therewith (the "article") in all forms and media (whether now known or hereafter developed), throughout the world, in all languages, for the full term of copyright and all extensions and renewals thereof, effective when and if the article is accepted for publication. This transfer includes the right to adapt the presentation of the article for use in conjunction with computer systems and programs, including reproduction or publication in machine-readable form and incorporation in electronic retrieval systems.

Authors retain or are hereby granted (without the need to obtain further permission) rights to use the article for traditional scholarship communications, for teaching, and for distribution within their institution.

- I am the sole author of the manuscript
- I am signing on behalf of all co-authors of the manuscript
- The article is a 'work made for hire' and I am signing as an authorized representative of the employing company/institution

Please mark one or more of the above boxes (as appropriate) and then sign and date the document in black ink.

Signed: _____ Name printed: _____

Title and Company (if employer representative) : _____

Date: _____

Data Protection: By submitting this form you are consenting that the personal information provided herein may be used by the Hashemite University and its affiliated institutions worldwide to contact you concerning the publishing of your article.

Please return the completed and signed original of this form by mail or fax, or a scanned copy of the signed original by e-mail, retaining a copy for your files, to:

Hashemite University
Jordan Journal of Biological Sciences
Zarqa 13115 Jordan
Fax: +962 5 3903338
Email: jjbs@hu.edu.jo

EDITORIAL PREFACE

Jordan Journal of Biological Sciences (JJBS) is a refereed, quarterly international journal financed by the Scientific Research and Innovation Support Fund, Ministry of Higher Education and Scientific Research in cooperation with the Hashemite University, Jordan. JJBS celebrated its 12th commencement this past January, 2020. JJBS was founded in 2008 to create a peer-reviewed journal that publishes high-quality research articles, reviews and short communications on novel and innovative aspects of a wide variety of biological sciences such as cell biology, developmental biology, structural biology, microbiology, entomology, molecular biology, biochemistry, medical biotechnology, biodiversity, ecology, marine biology, plant and animal biology, plant and animal physiology, genomics and bioinformatics.

We have watched the growth and success of JJBS over the years. JJBS has published 11 volumes, 45 issues and 479 articles. JJBS has been indexed by SCOPUS, CABI's Full-Text Repository, EBSCO, Clarivate Analytics- Zoological Record and recently has been included in the UGC India approved journals. JJBS Cite Score has improved from 0.18 in 2015 to 0.7 in 2019 (Last updated on 1 March, 2021) and with Scimago Institution Ranking (SJR) 0.18 (Q3) in 2019.

A group of highly valuable scholars have agreed to serve on the editorial board and this places JJBS in a position of most authoritative on biological sciences. I am honored to have six eminent associate editors from various countries. I am also delighted with our group of international advisory board members coming from 15 countries worldwide for their continuous support of JJBS. With our editorial board's cumulative experience in various fields of biological sciences, this journal brings a substantial representation of biological sciences in different disciplines. Without the service and dedication of our editorial; associate editorial and international advisory board members, JJBS would have never existed.

In the coming year, we hope that JJBS will be indexed in Clarivate Analytics and MEDLINE (the U.S. National Library of Medicine database) and others. As you read throughout this volume of JJBS, I would like to remind you that the success of our journal depends on the number of quality articles submitted for review. Accordingly, I would like to request your participation and colleagues by submitting quality manuscripts for review. One of the great benefits we can provide to our prospective authors, regardless of acceptance of their manuscripts or not, is the feedback of our review process. JJBS provides authors with high quality, helpful reviews to improve their manuscripts.

Finally, JJBS would not have succeeded without the collaboration of authors and referees. Their work is greatly appreciated. Furthermore, my thanks are also extended to The Hashemite University and the Scientific Research and Innovation Support Fund, Ministry of Higher Education and Scientific Research for their continuous financial and administrative support to JJBS.

Professor Atoum, Manar F.
March, 2021

CONTENTS

Original Articles

- 199 - 203 Phytochemical profiling and in vitro α -amylase inhibitory activity of *Glycosmis pentaphylla* (Retz.) DC.
Vinitha Saseendra Babu and Puthuparambil Madhavan Radhamany
- 205 - 211 Biochemical Effects of Low Crude Protein Diets Supplemented with Varying Methionine Concentrations
Simiat. M. Ogunbode, Eustace. A. Iyayi
- 213 - 217 *In vitro* genotoxicity study of the lambda-cyhalothrin insecticide on Sf9 insect cells line using Comet assay
Manal Saleh , Daas Ezz -din and Aroub Al-Masri
- 219 - 228 Protective effect of amino acid, Glycine in broilers fed on Imidacloprid treated rations
Enas, A. Abbas, Amany, M. Salama, Fayza, A., Sdeek, Eman, I. M. Ismail, Abdalla, S. H., Elshorbagy, I. M., Abd EL Rahman, T. A.
- 229 - 238 Enhancing Electricity Generation with the use of KMnO₄ as an electron acceptor in Microbial Fuel Cell
Adegunloye Deke Victoria, Faloni Taiwo Mercy
- 239 - 243 Neuroprotective Efficacy of *Dunaliella salina* Against Paraquat-Induced Neurotoxicity in *Drosophila melanogaster*
Mohamad Agus Salim, Muhammad Subandi and Yeni Yuniarti
- 245 - 251 Cytokine genes expression in uteri of *Bubalus bubalis* associated with endometritis infection
Dalia A. Taha, Eman R. Mahfouz, Mona A. Bibars, Nagwa A. Hassan and Othman E. Othman
- 253 – 260 Influence of drought stress on physiological traits of crossed okra varieties
Zainab G. Ahmed, Magdi A. El-Sayed
- 261 – 266 Orange Peels Valorization For Citric Acid Production Through Single And Co-Culture Fermentation
Muddassar Zafar, Hania Shah Bano and Zahid Anwar
- 267 – 270 Bioactive ingredients of different extracts of *Vitex agnus-castus L.* Fruits from Morocco and their antioxidant potential
Fatima El Kamari, Driss Ousaaid, Amal Taroq, Yassine El Atki, Iman Aouam, Badiia Lyoussi, and Abdelfattah Abdellaoui.
- 271 – 278 Thrombin protease-activated receptor inhibitors from the peel of *Ananas comosus* (L.) Merr.: an *in silico* approach
Babatunde J. Oso, Ige F. Olaoye , Anne Adeyanju and Adepeju Aberuagba
- 279 – 283 Analysis of APXs and HSPs genes responsible to respond to heat stress in tomato plants cultivated in Central Sulawesi
Astija , Musdalifah Nurdin, Syech Zainal
- 285 – 290 Effect of Garlic, Vitamin C, Vitamin E–Selenium against Bioaccumulated Organolead-Induced Cellular Injury in Liver and Spleen of Albino Rats: Pilot Study
Ziad Shraideh, Darwish Badran, Ahmed Alzbeede, Duaa Alqattan, Areej Alzbeede, Kholoud Frieihat
- 291 - 295 The Antioxidant Activity of Kelor (*Moringa oleifera* Lam.) Leaves Based on Drying Method
Devi Dwi Siskawardani, Sri Winarsih and Khwunta Khawwee
- 297 – 302 Impacts of Immunostimulant Yeast (*Saccharomyces cerevisiae*) Supplemented Feed on Growth and Blood Profile of Java Barb (*Barbonymus gonionotus*)
Diana Rachmawati , Roy Hendroko Setyobudi, Juris Burlakovs, Tita Elfitasari and Agus Heri Purnomo
- 303 – 307 The Moderating Effect of *Hypericum thymbrifolium* against Memory Loss and Alzheimer's Disease (Experimental Study in Mice)
Khayra Zerrouki ,Noureddine Djebli, Leila Gadouche , Esra Eroglu Ozkan And Afife Mat

- 309 – 316 RAPD analysis and field screening of bread wheat and barley accessions for resistance to cereal leafminer *Syringopais temperatella*
Ihab H. Ghabeish , Firas A. Al-Zyoud and Dhia S. Hassawi
- 317 – 325 Cadmium and Lead Concentrations in Water, Sediment, Fish and Prawn as Indicators of Ecological and Human Health Risk in Santubong Estuary, Malaysia
Adriana Christopher Lee, Farah Akmal Idrus , Fazimah Aziz
- 327 – 336 Durum wheat (*Triticum turgidum ssp durum*) improvement during the past 67-year in Algeria: Performance assessment of a set of local varieties under rainfed conditions of the eastern high plateaus
Leïla Haddad, Adel Bachir, Nassima Ykhelef, Amar Benmahammed, Hammena Bouzerzour
- 337 - 342 Influence of Fasting and Feed Constituents Size Variation on Broiler Performance and Intestinal Demonstrations
Asad Ali Khaskheli and Li Chou
- 343 - 352 Diversity of *Phaseolus lunatus* L. in East Java, Indonesia based on PCR-RAPD technique
Elly Purwanti, Mohamad Amin, Siti Zubaidah, Maftuchah Maftuchah, Siti Nur Hidayati, and Ahmad Fauzi
- 353 - 358 Increasing Liquidity of SSDM-Based Red Chili Farmers through Agricultural Insurance
Sri Ayu Andayani , Yayan Sumekar, Reny Sukmawani, Agus Yadi Ismail, Dadan Ramdani Nugraha and Sri Umyati
- 359 - 365 1-Pentacosanol Isolated from Stem Ethanolic Extract of *Cayratia trifolia* (L.) is A Potential Target for Prostate Cancer-In *SILICO* Approach
Sundaram Sowmya , Palanisamy Chella Perumal , Subban Ravi, Palanirajan Anusooriya, Piramanayagam Shanmughavel , Eswaran Muruges , Karri Krishna Chaithanya and Velliur Kannian Gopalakrishnan
- 367 - 372 Cloning, expression and purification of *Leishmania major* PSA-sfGFP fusion protein
Aisha Al-jaghasi, Abdul-Qader Abbady, Sahar Al-Khatib and Chadi Soukkarieh
- 373 - 197 Relevance of Nanoparticles on Micropropagation, Antioxidant Activity and Molecular Characterization of *Sequoia sempervirens* L. Plant.
Iman M. El-Sayed, Walaa H. Salama, Rasha G. Salim, Lobna S. Taha

Phytochemical profiling and in vitro α -amylase inhibitory activity of *Glycosmis pentaphylla* (Retz.) DC.

Vinitha Saseendra Babu^{1,*} and Puthuparambil Madhavan Radhamany²

¹Junior Research Fellow, Plant Reproductive Biology Laboratory, Department of Botany, University of Kerala, Kariavattom, Thiruvananthapuram, Kerala, India-695581; ²Professor, Department of Botany, University of Kerala, Kariavattom, Thiruvananthapuram, Kerala, India-695581

Received May 18, 2020; Revised July 30, 2020; Accepted July 30, 2020

Abstract

The present work has been done with an objective to analyze the phytochemical composition responsible for plausible antidiabetic effect of leaf, stem and root of *Glycosmis pentaphylla* (Retz.) DC. Fresh leaf, stem and root of *Glycosmis pentaphylla* were extracted with ethanol (EEGPle, EEGPst, EEGPro) and evaluated by phytochemical analysis for their infinite primary and secondary metabolites viz. carbohydrates, proteins, alkaloids, flavonoids, terpenoids, glycosides, saponin and phenols. The antiabetic effect was done with the help of alpha amylase inhibitory assay. Estimation of total flavonoid content (TFC) and total phenolic content (TPC) was also done to confirm the presence of these phytochemicals. The phytochemical analysis of EEGPle revealed that carbohydrates, proteins, alkaloids, flavonoids, glycosides, tannins, phenols and saponins were present, whereas, EEGPst showed the presence of proteins, alkaloids, flavonoids, phenols and terpenoids. Presence of carbohydrates, alkaloids, phenol and terpenoids were found in EEGPro. A significant hypoglycemic activity was revealed by the EEGPle [EC₅₀: (23.14±0.006) µg/mL], compared to EEGPst and EEGPro. Quantity of TFC and TPC was highest in EEGPle (112.96±3.89 mg QRE/g and 96.6±1.08 mg GAE/g extract) rather than EEGPst and EEGPro extracts. The present work suggests that EEGPle has a significantly higher anti-diabetic property than EEGPst and EEGPro. These extracts can help in preventing or slowing down the occurrence of diabetes, but a detailed analysis of these extracts is required to determine the presence of promising compound(s) responsible for their anti-diabetic potential.

Keywords: *Glycosmis pentaphylla*, Phytochemicals, Anti-diabetic activity, Hyperglycemic

1. Introduction

The demand and acceptance for medicinal plants is progressively increasing. In fact, the existence of human race depends more or else on herbal drugs. Today, most of the under-developed nations are still known to practice traditional systems of herbal medicine (Singh, 2002). This is so, as overconsumption of allopathic drugs can cause severe side effects like cardiovascular disorders, memory loss, stress, anxiety and so on (Firenzuoli and Gori, 2007). Even though the role of medicinal plants is highly appreciated, thorough knowledge has to be made before being accepted for medication. Hence, there is a need to determine the actual content and composition of crude drug extracts. Also, standardization of the active components present in plants can help in the emergence of a new millennium of preventive medicine to treat human diseases in future.

Diabetes is a serious health issue that affects millions of people and is known as the fifth leading to death (Mukesh and Namita, 2013). This disease is caused due to the metabolic disorders of proteins, fats and carbohydrates (Osadebi *et al.* 2014). It results from either insulin deficiency or malfunction as it causes an increase in blood glucose after any type of meal (Modak *et al.* 2007). Treatments like the use of insulin, pharmaceutical drugs

and controlled diet have enabled specialists to control diabetes to some extent. Modern systems of medicine have also identified several types of glucose-lowering drugs that can decelerate diabetes. These drugs have some disadvantages, including drug resistance (reduction of efficiency), side effects, and even toxicity (Hui *et al.* 2005). Medicinal plants are being used in the treatment of diabetics as they have the ability to improve the performance of pancreatic tissue by the production of insulin or reducing the glucose absorption in intestine.

The plant *Glycosmis pentaphylla* (Retz.) DC. (*G. pentaphylla*) of the citrus family, Rutaceae, is an evergreen shrub or small tree that grows up to 5 metres tall. The plant is native to China, India, Sri Lanka, Thailand, Cambodia, Vietnam, Malaysia, Indonesia and Philippines. The detailed description of plant is available elsewhere (Yoganarasimhan and Jadhav, 1996). The fruit of the plant is edible and the juice of leaves is used to treat diarrhoea, coughs, rheumatism, anaemia and jaundice (Chopra, 1969). Several authors investigated the plant for anti-inflammatory efficacy (Ahamad and Aqil, 2007), hepatoprotective activity (Nayak *et al.* 2013) antimicrobial effect (Amran *et al.* 2011) and antipyretic potential (Sarkar and Mandal, 2011).

Previous research has revealed that *G. pentaphylla* possesses anti-diabetic activity in its leaves (Gupta *et al.* 2011). But there are no reports showing comparison of the

* Corresponding author e-mail: vinithasbabu55@gmail.com.

hypoglycemic activity of the plant in its leaf, stem and root. Therefore, an attempt to explore the phytochemical composition and in vitro α -amylase inhibitory activity of ethanolic extract of *G. pentaphylla* leaf (EEGPle), stem (EEGPst) and root (EEGPro) is made.

2. Materials and Methods

2.1. Chemicals

Acarbose, Folin-Ciocalteu's reagent, quercetin (QT), gallic acid (GA), 3,5 dinitro salicylic acid (DNSA), Dimethylsulfoxide (DMSO) and α -amylase from *Aspergillus oryzae* were purchased from Sigma-Aldrich and other remaining chemicals were used of analytical grade unless otherwise specified.

2.2. Collection and authentication of plant materials

Fresh leaf, stem and root (about 5 kg) of *G. pentaphylla* were collected from Thodupuzha (Latitude: 9.8959°N; Longitude: 76.7184°E) of Kerala, India during April, 2018 to October, 2018. The leaves, stem and roots were thoroughly washed to remove foreign matters, and then shade dried for 2 weeks. Later, the identification was done as *G. pentaphylla* (Accession number KUBH 6073) by an expert taxonomist from Department of Botany, University of Kerala, India. The leaf, stem and root of *G. pentaphylla* (about 2 kg each) were separated manually, followed by shade dried. Dried leaf, stem and root were grounded with the help of a mechanical grinder into coarse powder. The generated powders (about 300 g each) were preserved in airtight containers and placed in a cool, dry and dark place until extraction.

2.3. Preparation of plant extracts

Based on literature review, it was found that ethanol possesses higher extraction efficiency due to its polarity (Snyder and Kirkland, 1979). About 200 g individual powdered sample was taken in clean, flat-bottomed amber colored glass container and soaked in 700 mL of 95% ethanol. The container was sealed and kept for several days with occasional shaking. The whole mixtures then underwent coarse filtration by pieces of cotton. Thereafter, the mixture was filtered through filter (Whatman No.1) paper and the solvent was made to evaporate under reduced pressure with the help of a rotary evaporator at 50°C to yield crude extracts. (i.e. 10.75 g for EEGPle, 6.18 g for EEGPst and 8.25 g for EEGPro). The crude ethanolic extracts thus obtained were kept at 4°C for further studies.

2.4. Qualitative phytochemical screening

Crude extracts were screened to identify the presence of primary and secondary metabolites, viz. carbohydrates, proteins, alkaloids, flavonoids, terpenoids, glycosides, tannins and saponins, using standard screening tests and phytochemical procedures (Sofowora, 1982; Harborne, 1973; Suriyamoorthy *et al.* 2014; Al-Daihan *et al.* 2013; Kapoor *et al.* 1969; Smolenski *et al.* 1974; Krishnamoorthi, 2015; Blois, 1958; Tiwari *et al.* 2011).

2.5. In vitro α -amylase inhibitory studies

The α -amylase inhibition assay was performed using 3,5 dinitro salicylic acid (DNSA) method (Miller, 1959) with slight modifications. The crude extract EEGPle, EEGPst and EEGPro was dissolved in a minimum amount of 10% DMSO and was further dissolved in buffer

((Na₂HPO₄/NaH₂PO₄ (0.02 M), NaCl (0.006 M) at pH 6.9) to give concentrations ranging from 25 to 200 µg/mL. A volume of 200 µL of α -amylase solution (2 units/mL) was mixed with 200 µL of each of the extracts and was incubated for 10 min at 30 °C. Thereafter, 200 µL of the starch solution (1% in water (w/v)) was added to each tube and incubated for 3 min. The reaction was terminated by the addition of 200 µL DNSA reagent (12 g of sodium potassium tartrate tetrahydrate in 8.0 mL of 2 M NaOH and 20 mL of 96 mM of 3,5-dinitrosalicylic acid solution) and was boiled for 10 min in a water bath at 85–90 °C. The mixture was cooled to ambient temperature and was diluted with 5 mL of distilled water, and the absorbance was measured at 540 nm using a UV-Visible spectrophotometer. The blank with 100% enzyme activity was prepared by replacing the plant extract with 200 µL of buffer. A blank reaction was similarly prepared using plant extracts at each concentration in the absence of the enzyme solution. A positive control sample was prepared using acarbose (100 µg/mL µg/ml), and the reaction was performed similarly to the reaction with plant extract as mentioned above. The % α -amylase inhibition was plotted against the extract concentration and the IC₅₀ values were obtained from the graph. The α -amylase inhibitory activity was calculated using the equation given below:

$$\% \alpha \text{ amylase inhibition} = 100 \times \frac{\text{Abs 100\% control} - \text{Abs sample}}{\text{Abs 100\% control}}$$

2.6. Total Phenolic Content (TPC)

The TPC was estimated according to Cheung *et al.* 2003. The crude extracts of *G. pentaphylla* were mixed with methanol (95%) for preparation of the stock solution (1 mg/mL). A standard, GA was also mixed with 95% methanol to prepare the 1 mg/mL concentration standard solution. For this test, 1 mL of crude extract with 1000 µg/mL concentration was mixed along with 1 mL Folin-Ciocalteu's reagent, 5 min later 10 mL volume of sodium carbonate (7%) solution was added to the mixture, and then deionized distilled water (13 mL) was added and thoroughly mixed. This mixture was kept for 90 min in the dark at 23°C and then the absorbance was recorded at 750 nm by UV spectrophotometer (Thermo Fisher Scientific G10S). Standard curve for estimation of TPC was prepared using GA standard solution (i.e. 6.25 µg/mL to 200 µg/mL) using the similar procedure as described earlier. The TPCs were expressed as mg of gallic acid equivalents (GAE) per g of the dried sample.

2.7. Total Flavonoid Content (TFC)

The TFC was estimated by method described by Park *et al.* 2008. The stock solution was prepared as mentioned in TPC. Similarly, the standard solution of QT was prepared through mixing it with 95% methanol (i.e. 1 mg/L). To estimate the TFC, 0.3 mL of the crude extract (1000 µg/mL), 3.4 mL of methanol (30%), 0.15 mL of 0.5 mol/L sodium nitrate and 0.15 mL of 0.3 mol/L aluminum chloride were mixed. Then after 5 min, 1 mL of 1 mol/L sodium hydroxide was supplemented. The obtained solution was thoroughly mixed, and absorbance was recorded at 506 nm against the reagent blank. TFCs were expressed as mg of quercetin equivalents (QRE) per g of the dried sample.

2.8. Statistical Analysis

All experimental results are expressed as mean \pm standard error (SE), and data were analysed by one-way analysis of variance ($P < 0.001$) using SPSS software (ver. 22.0; SPSS Inc., Chicago, IL, USA).

3. Results

3.1. Estimation of phytoconstituents

The phytochemical analysis in leaf, stem and root of *G. pentaphylla* revealed the existence of many important bioactive molecules in different extracts, such as carbohydrates, proteins, alkaloids, flavonoids, terpenoids, glycosides, tannins and saponins that were confirmed by colour reaction tests as shown in Table 1. Based on the intensity of the colour reaction, the EEGPle contained the highest amount of alkaloids, phenols, flavonoids and saponin, compared to EEGPst and EEGPro.

Table 1. Phytochemical composition of *G. pentaphylla* leaf, stem and root extracts

Phytochemical constituents	EEGPle	EEGPst	EEGPro
Alkaloids	-	-	-
Wagner's Test	++	+	+
Mayer's Test	++	+	-
Test for carbohydrates			
Benedict's Test	++	-	++
Fehling's Test	+++	-	+
Test for glycosides	++	-	-
Phenols	-	-	-
Ferric Chloride Test	+++	++	++
Flavonoids	-	-	-
Lead Acetate Test	+++	++	-
Alkaline reagent Test	+++	+	-
Saponins	-	-	-
Froth Test	+++	-	-
Foam Test	++	-	-
Terpenoids	-	-	-
Libermann Test	+++	++	++
Horizon Test	+++	++	++
Proteins	-	-	-
Xanthoproteic Test	+	-	-
Ninhydrin Test	+	-	+

Where, +: present (in mild amount), ++: present (in moderate amount), +++: present (in large amount), - absent, based on the power of colour generated in the reaction.

3.2. In vitro α -amylase inhibitory studies

Evaluating the plot of % α -amylase inhibition as a function of extract concentrations (Fig. 1), the EC_{50} values were calculated (Table 2). The crude EEGPle exhibited the lowest EC_{50} of $23.14 \pm 0.006 \mu\text{g/mL}$ and that of EEGPst and EEGPro were $47.15 \pm 0.003 \mu\text{g/mL}$ and $96.15 \pm 0.006 \mu\text{g/mL}$, respectively. The EC_{50} value of α -amylase inhibitory assay was acarbose < EEGPle, EEGPst and EEGPro. In comparison with the EC_{50} value acarbose, EEGPle was significantly higher ($P < 0.001$). Thus, the present result reveals that, among the three extracts,

EEGPle exerted a 72.2 % α -amylase inhibition at 200 $\mu\text{g/mL}$ concentration.

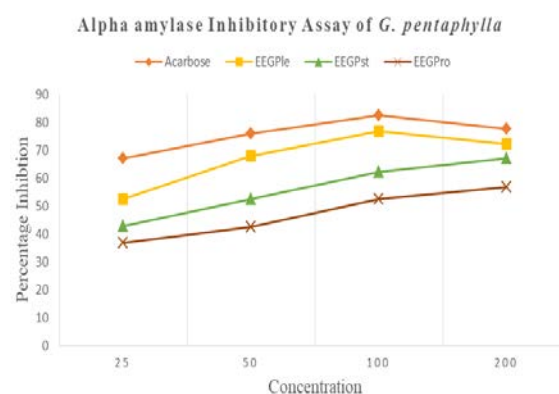


Figure 1. Percentage of α -amylase inhibition as a function of extract concentrations

Table 2. The α -amylase inhibition assay of *Glycosmis pentaphylla*

Standard/ Extract	α -amylase inhibition assay				EC_{50} value for α - amylase inhibition assay
	25 $\mu\text{g/mL}$	50 $\mu\text{g/mL}$	100 $\mu\text{g/mL}$	200 $\mu\text{g/mL}$	
Acarbose	67.0 \pm 0.70	76.0 \pm 0.70	82.4 \pm 0.50	77.6 \pm 0.50	18.12 \pm 0.005
EEGPle	52.4 \pm 0.50	67.8 \pm 0.58	76.8 \pm 0.86	72.2 \pm 0.58	23.14 \pm 0.006
EEGPst	42.8 \pm 0.58	52.4 \pm 0.50	62.2 \pm 0.58	67.0 \pm 0.70	47.15 \pm 0.003
EEGPro	36.8 \pm 0.58	42.4 \pm 0.74	52.4 \pm 0.50	56.6 \pm 0.74	96.15 \pm 0.006
Treatment	482.028***	549.293***	467.492***	192.988***	3854.772***
df (n-1)					

The representative experiment is a mean standard error followed by different superscript lowercase letters indicate significant difference between each parameter as evaluated by Duncan's Multiple Range Test. f value significant at * $P \leq 0.001$ level, NS- non-significant.

3.3. Estimation of TPC and TFC

The TPC of *G. pentaphylla* extracts was estimated from GA standard curve ($y = 0.0106x + 0.0542$), and the results were represented in milligrams of GAE. Table 5 shows that the TPC in the EEGPle, EEGPst and EEGPro varied largely and EEGPle exhibited the highest TPC. The content of flavonoid was estimated from the QCT standard curve ($y = 0.0005x + 0.029$), and the results were expressed as mg of QE (Table 3). The EEGPle showed the maximum amount of flavonoid contents followed by EEGPst and EEGPro.

Table 3. Total phenolic and flavonoid contents of *G. pentaphylla* extracts

Extracts	Total phenolic (mg GAE/g)	Total flavonoid (mg QE/g)
EEGPle	112.96 \pm 3.89	96.6 \pm 1.08
EEGPst	56.16 \pm 0.54	32.1 \pm 0.8
EEGPro	23.5 \pm 0.55	11.16 \pm 0.54

Values were expressed as mean \pm SD (n=3).

4. Discussion

In the recent past, there has been an exponential growth in the field of herbal medicine, and these drugs are gaining popularity both in developing and developed countries. This is so, as being natural entails less side effects. The traditional medicines in use are derived from medicinal plants, minerals and organic matter (Grover *et al.* 2002). Inclusion of fruits and vegetables in diet has decelerated the occurrence of chronic diseases associated with aging such as cancer, cardiovascular diseases, brain dysfunction and cataract. Also, plants serve as sources for the development of drugs in contemporary medicine. Still, there is a need to determine the safety efficacy and stability of plant derived products before being marketed. Hence, researchers are focusing on the potential of medicinal plants to be used as crude drugs. As part of this, in the present study, the phytoconstituents, and α -amylaseinhibitory activities of the ethanolic extracts of leaf, stem and root of *G. pentaphylla* were evaluated.

Secondary metabolites like flavonoids, alkaloids, tannins, terpenoids, saponins and coumarin metabolites were introduced with major impact on diabetes (Bahmani *et al.* 2014). The present study on *Glycosmis pentaphylla* has shown that several polyphenolic compounds like flavonoids, phenolic acids, and tannins are deemed as the chief constituents of plants. These metabolites have profound activity to enhance glucose utilization by regulating glucagon (Valetteet *et al.* 1984) and insulin secretion, thus implicating its role in hypoglycemic action in medicinal plants. Alkaloids have been shown to exhibit cytotoxic effect on tumour cell lines emphasizing its role in prevention of cancer, neurodegenerative diseases and chronic inflammation (Lamkadem *et al.* 2001). Bio-functionalities of these secondary metabolites present in the extracts influence the biological activities of the plants. In addition, protective ability of plant extracts against the pathological diseases is related to total phenolics and flavonoids in the plant samples as they have been recognized to exhibit various biological activities (Oyedemiet *et al.* 2011). This study suggested that among the ethanolic crude extracts of leaf, stem and root of *G. pentaphylla*, EEGPle have superior anti-diabetic potential owing to the presence of higher amount of phenols, flavonoids, and saponins. These are significantly associated to the anti-diabetic potential of these extracts.

Hyperglycemia has been a classical risk in the development of diabetes and the complications associated with diabetes. Therefore, control of blood glucose levels is critical in the early treatment of diabetes and reduction of macro- and microvascular complications. One therapeutic approach is the prevention of carbohydrate absorption after food intake, which is facilitated by inhibition of enteric enzymes including α -glucosidase and α -amylase present in the brush borders of intestine. The α -amylase inhibitory studies performed demonstrated that the extracts of *G. pentaphylla* had significant inhibitory potentials. The EC₅₀ value ($23.14 \pm 0.006 \mu\text{g/mL}$) of EEGPle is almost similar to that of acarbose ($18.12 \pm 0.005 \mu\text{g/mL}$) a widely used and marketed anti-diabetic drug. EEGPst and EEGPro also exhibited α -amylase inhibition in a dose dependent fashion. These α -amylase inhibitors terminate or decelerate the absorption of starch into the body by

blocking the hydrolysis of 1,4-glycosidic linkages of starch and other oligosaccharides into maltose, maltotriose and other simple sugars (Kumar *et al.* 2010). The highest α -amylase inhibitory activity in EEGPle is mostly due to polar compounds and is worth further investigating and isolating pure active compounds. Hence the above results suggest that EEGPle could be greatly beneficial in reducing the absorption of starch into the body; also, it can be effectively used in ayurvedic treatments.

5. Conclusion

Plant parts have been used individually or in formulations for treatment of diabetes and its complications. One of the major problems with this herbal formulation is that the active ingredients are not well-defined. Efforts are now being made to investigate mechanism of action of some of these plants using model systems. The present study suggests that ethanolic leaf extract of *G. pentaphylla* have anti-diabetic property. As a result, the leaf extracts of *G. pentaphylla* leaf may serve as a possible source of natural anti-diabetic drug. It is important to know the active components and their molecular interaction, which will help to analyse therapeutic efficacy of the product and to standardize the product.

Acknowledgement

The authors wish to thank the Head of the Department of Botany, University of Kerala, for providing necessary facilities for the completion of this work. The authors are also grateful to JOINT CSIR-UGC (Ref. No. 876/ (CSIR-UGC NET DEC. 2018)) for providing financial assistance.

References

- Ahmad I and Aqil F.2007. In vitro efficacy of bioactive extracts of 15 medicinal plants against ESBL-producing multidrug-resistant enteric bacteria. *Microbiol. Res.*, **162**: 264-275.
- Al-Daihan S, Al-Faham M, Al-Shawi N, Almayman R, Brnawi A and Zargar S. 2013. Antibacterial activity and phytochemical screening of some medicinal plants commonly used in Saudi Arabia against selected pathogenic microorganisms. *J King Saud Uni-Sci*, **25**: 115-120.
- Amran H, Farhana R, Shapna S, Rumana M and Apurba SA. 2011. Antimicrobial, antioxidant and cytotoxic effects of methanolic extracts of leaves and stems of *Glycosmis pentaphylla* (Retz.) Correa. *J. App. Pharm. Sci*, **8**: 137-140.
- Bahmani M, Golshahi H, Saki K, Rafieian-Kopaei M, Delfan B and Mohammadi T. 2014. Medicinal plants and secondary metabolites for diabetes mellitus control. *Asian Pac. J. Trop. Dis.*, **4**, S687-S692.
- Blois MS. 1958. Antioxidant determinations by the use of a stable free radical. *Nature*, **29**: 1199-1200.
- Cheung LM, Cheung PC and Ooi VEC. 2003. Antioxidant activity and total phenolics of edible mushroom extracts. *Food Chem*, **81**: 249-255.
- Chopra GS. 1969. Man and marijuana. *Int J Addict*, **4**: 215-247.
- Firenzuoli F and Gori L. 2007. Herbal medicine today: clinical and research issues. *Evid Based Complement Alternat Med*, **1**:37-40.
- Grover JK, Yadav S and Vats V. 2002. Medicinal plants of India with anti-diabetic potential. *J. Ethnopharmacol.*, **81**: 81-100.

- Gupta N, Agarwal M, Bhatia V, Jha SK and Dinesh J. 2011. In vitro antioxidant Activity of crude extracts of the plant *Glycosmis pentaphylla* Correa. *Int J Pharm Sci Rev Res*, **6**:158-62.
- Harborne JB. 1973. *Phytochemical methods: a guide to modern techniques of plant analysis*. 2nd ed. Chapman and Hall, New York.
- Hui H, Zhao X and Perfetti R. 2005. Structure and function studies of glucagon-like peptide-1 (GLP): the designing of a novel pharmacological agent for the treatment of diabetes. *Diabetes Metab Res Rev*, **21**: 313-331.
- Kapoor LD, Singh A, Kapoor SL and Shrivastava SN. 1969. Survey of Indian medicinal plants for saponins, alkaloids and flavonoids. *Lloydia*, **32**: 297-302.
- Khorasani Esmaeili A, Mat Taha R, Mohajer S and Banisalam B. 2015. Antioxidant activity and total phenolic and flavonoid content of various solvent extracts from in vivo and in vitro grown *Trifolium pratense* L. (Red Clover). *BioMed Res Int*, **1**: 643-685.
- Krishnamoorthi R. 2015. Phytochemical screening and antioxidant activity of *Justicia tranquebariensis* and *Bauhinia racemosa*. *Int J Pharmacog*, **2**: 362-367.
- Kumar BD, Mitra A and Manjunatha M. 2010. A comparative study of alpha-amylase inhibitory activities of common antidiabetic plants of Kharagpur 1 block. *Int J Green Pharm*, **4**:115-21.
- Lamkadem M, Melhaoui A, Mimouni J and Fontonge R. 2001. Cytotoxic effect and electrophysiologic activity of (R)-bgugaine, an alkylpyrrolidine alkaloid against MRC-5 fibroblasts. *Toxicol*, **39**: 485-490.
- Miller GL. 1959. Use of dinitrosalicylic acid reagent for determination of reducing sugar. *Anal Chem*, **31**: 426-8.
- Modak M, Dixit P, Londhe J, Ghaskadbi S and Devasagayam TPA. 2007. Indian herbs and herbal drugs used for the treatment of diabetes. *J Clin Biochem Nutr.*, **40**: 163.
- Mukesh R and Namita P. 2013. Medicinal Plants with Antidiabetic Potential- A review. *American-Eurasian J Agric Environ Sci.*, **13**: 81-94.
- Nayak SA, Kumar S, Satapathy K and Naik SK. 2013. In vitro plant regeneration from cotyledonary nodes of *Withania somnifera* (L.) Dunal and assessment of clonal fidelity using RAPD and ISSR markers. *Acta Physiol Plant*, **35**: 195-203.
- Osadebe PO, Odoh EU and Uzor PF. 2014. The search for new hypoglycemic agents from plants. *Afr J Pharmacol*, **8**: 292-303.
- Oyedemi SO, Yakubu MT and Afolayan AJ. 2011. Antidiabetic activities of aqueous leaves extract of *Leonotis leonurus* in streptozotocin induced diabetic rats. *J Med Plant Res*, **5**: 119-125.
- Park YS, Jung ST, Kang SG, Heo BK, Arancibia-Avila P and Toledo F. 2008. Antioxidants and proteins in ethylene-treated kiwifruits. *Food Chem*, **107**: 640-648.
- Sarkar R and Mandal N. 2011. In vitro cytotoxic effect of hydroalcoholic extracts of medicinal plants on Ehrlich's Ascites Carcinoma (EAC). *International Journal of Phytomedicine*, **3**, 370.
- Singh JS. 2002. The biodiversity crisis: A multifaceted review. *Curr Sci*, **82**: 638-47.
- Smolenski SJ, Silinis H and Farnsworth NR. 1974. Alkaloids screening. *Lloydia*, **37**: 506-536.
- Snyder HL and Kirkland JJ. 1979. *Introduction to Modern Liquid Chromatography*, first ed. John Wiley, New York.
- Sofowora A. 1982. *Medicinal plants and traditional medicinal in Africa*. third ed. John Wiley, Nigeria.
- Suriyamoorthy P, Subrhamanian H and Kanagasapabathy D. 2014. Comparative phytochemical investigation of leaf, stem, flower and seed extracts of *Macrotyloma uniflorum* L. *Indo Ame J Pharma Rese*, **4**: 5415-5419.
- Tiwari P, Kumar B, Kaur M, Kaur G and Kaur H. 2011. Phytochemical screening and extraction: A review. *Int Pharmaceutica Scientia*, **1**: 98-104.
- Valette G, Sauvaire Y, Baccou JC and Ribes G. 1984. Hypocholesterolaemic effect of fenugreek seeds in dogs. *Atherosclerosis*, **50**: 105-111.
- Yoganarasimhan SN and Jadhav, D. 1996. *Medicinal plants of India*. first ed. Interline Publishers, Bangalore.

Biochemical Effects of Low Crude Protein Diets Supplemented with Varying Methionine Concentrations

Simiat. M. Ogunbode^{1*}, Eustace. A. Iyayi²

¹Chemical Sciences Department, College of Natural and Applied Sciences, Fountain University Osogbo, Osogbo, Nigeria

²Animal Science Department, Faculty of Agriculture, University of Ibadan, Ibadan, Nigeria.

Received May 2, 2020; Revised August 2, 2020; Accepted August 5, 2020

Abstract

The research investigated the consequences of decreased crude protein (CP) and methionine supplementation in diets on certain biochemical indices in broiler chicks. A total number of 135 newly hatched chicks were allotted to nine dietary treatments, 3 replicates of five birds each. Groups A-C served as the control with 20% CP and 0.6, 1.0 and 1.4% methionine supplementation. Groups D-F and G-I were placed on 17 and 14% CP diets respectively, with similar methionine supplementation as the control groups. The experiment lasted six weeks. Vital biochemical parameters studied include alkaline phosphatase, aminotransferases, superoxide dismutase, catalase, malondialdehyde, and organ-body weight ratios. Findings from the study indicated that there was a significant ($p < 0.05$) reduction in alkaline phosphatase activities of tissues of birds placed on 17 and 14% CP as correlated with birds on the control. MDA concentration was significantly ($p < 0.05$) elevated in the liver, kidney, and heart of broiler chicks fed diets with 14 and 17% CP at all methionine levels investigated when compared to control (20% CP). The low crude protein with varying methionine concentrations in broiler chick diets had no negative impact on birds' vital organs relative to whole body weight. These findings thus concluded that the functions and not size of the organs studied in broiler chicks were adversely affected at CP levels below 20%.

Keywords: Crude protein, methionine, lysine, gizzard, superoxide dismutase.

1. Introduction

Proteins are macromolecules that are made up of chains of amino acids; they play a key role in the structural build-up of body tissue (human and animal) and have a significant impact on growth as indices of performance in broiler birds (Pinchasov *et al.*, 1990). Amino acids are structurally made up of a carbon framework, a carboxyl group, an amino group with an R-chain that distinguishes one amino acid from the other (Cheeke, 2005). Protein metabolism releases these amino acids that perform several useful functions such as the up growth of the architectural parts of muscles, enzymes, and antibodies that are specific in roles in the different parts of the body (Pond, 1995, Abbasi *et al.*, 2014 and Van Emous *et al.*, 2015).

Methionine content of plant-based poultry feeds is inadequate in meeting up with the requirement of avian (NRC, 1994). This non-sufficiency mostly hinders the biodiversity quality of protein in corn cum soybean-based diets (Meirelles *et al.*, 2003, Lemme *et al.*, 2005, Kim *et al.*, 2006 and Matsushita, *et al.*, 2007). The metamorphosis of methionine to S-adenosyl methionine enhances the DNA methylation process which eventually dictates cell growth and eventual specialization (Niculescu and Zeisel, 2002). The activities of skeletal muscle tissues and meat

quality during the methylation process are also a function of methionine content of poultry diet (Liu *et al.*, 2010).

Reducing feed cost while ascertaining the effectiveness of usage of reduced protein diet has been boosted with crystalline amino acids, in this case methionine, to meet the amino acid requirement in poultry birds as reported by (NRC, 1994) is always the major target of animal nutritionists. Excess nitrogen from high crude protein diets could pose a major health challenge to the environment. Hence, reducing the cost of production and environmental pollution is germane to the poultry industry (Keshavarz, 2003; Gunawardana *et al.*, 2008 and Alagawany and Mahrose, 2014). Thus, for a safer environment, formulation of diets with well-balanced amino acids, in this case methionine, that precisely meet the needs of the birds becomes paramount. While ascertaining the adequacy of methionine to meet broiler birds' requirement, it is equally germane to monitor the biochemical enzyme activities of such diet at the organ level. It is imperative to be able to say categorically that the activities of the enzymes are being retained in the membrane or getting leaked out into the serum while feeding a low crude protein cum varying levels of methionine supplemented diets to broiler birds. This research, hence, evaluated some vital biochemical indices like alkaline phosphatase, alanine aminotransferase, catalase, superoxide dismutase, and malondialdehyde in vital tissues of broiler birds fed low protein with varying methionine concentrated diets.

* Corresponding author e-mail: oyewolar@gmail.com.

2. Materials and Methods

2.1. Source of Chemicals and Reagents

Assay kits for various enzymes activities studied in this research were sourced from Randox Laboratories, County Antrim, UK. All other reagents were of analytical grade and were prepared according to standard procedure.

2.1.1. Experimental Diets and Management of Animals

Diets essentially rich in nutritional requirements of birds (Table 1) as well as suitable for the purpose of the

Table 1. Gross Composition (Kg/100 g) of Experimental Diets

Crude Protein (%)	20	20	20	17	17	17	14	14	14
Methionine (%)	0.6	1.0	1.4	0.6	1.0	1.4	0.6	1.0	1.4
Lysine (%)	1.2	1.2	1.2	1.2	1.2	1.2	1.2	1.2	1.2
Maize	45.50	45.50	45.50	48.00	48.00	48.00	56.00	56.00	56.00
Soybean	32.00	32.00	32.00	21.00	21.00	21.00	12.00	12.00	12.00
Wheat offal	12.00	12.00	12.00	20.00	20.00	20.00	21.00	21.00	21.00
Palm oil	5.0	5.0	5.0	5.0	5.0	5.0	5.0	5.0	5.0
Dicalcium phosphate	2.40	2.22	2.00	2.50	2.45	2.05	2.50	2.19	2.00
Limestone	2.22	2.00	1.82	2.35	2.00	2.00	2.09	2.00	1.79
Premix	0.25	0.25	0.25	0.25	0.25	0.25	0.25	0.25	0.25
Salt	0.25	0.25	0.25	0.25	0.25	0.25	0.25	0.25	0.25
Methionine	0.30	0.70	1.10	0.34	0.74	1.14	0.38	0.68	1.18
Lysine	0.08	0.08	0.08	0.31	0.31	0.31	0.53	0.53	0.53
Total	100	100	100	100	100	100	100	100	100

CP-crude protein *Premix supplied the following information kg of diet: Vitamin A (12,500,000 IU), Vit D3 (2,500,000 IU), Vit E (40,000mg) Vitamin K3 (2,000mg), Vit B, (3,000mg), Vit B2 (5,500mg), Naicin (55,000mg), calcium panthothenate (11,500mg) Vit B6 (5000mg) Vit B12 (25mg), choline chloride (500, 000mg), folic acid (1,000mg), Biotin (80mg), Mn (120,000mg), Fe (100,000mg), Zn (80,000mg), Cu (8,500mg), I (1,500mg) Co (300mg), Se (120mg).

2.1.2. Experimental Design

135 newly hatched broiler chicks were distributed to nine experimental dietary treatments, three replicates of five birds each. The experimental diets consisted of 20, 17 and 14 % crude protein (CP), each with 0.6, 1.0 and 1.4 % methionine (Table 1). A diet containing 20 % CP served as the control diet. All diets had a 1.2 % isolysine content. The study lasted six weeks.

2.2. Blood Collection and Tissue Homogenate Preparation for Analysis

Birds were starved a night preceding the day of the sacrifice (at the end of feeding trial) to empty the crop. Three birds per replicate were randomly selected and weighed, then 10 mL blood sample was aspirated via the jugular vein. Aspirated blood samples were centrifuged at 3000 revolutions per minute for 10 minutes using a Bench Centrifuge 90-1, Gallenkomp, England to get serum for the various analysis. The serum collected using Pasteur pipette was kept frozen at -20°C and used within seven days of collection. Thereafter, the selected broiler birds were then sacrificed, de-feathered, reweighed to get dressing weight and then dissected to get precise organs of interest. The organs were cleaned with tissue paper to remove the attached debris. A known weight of each organ was then homogenized in an ice-cold 0.25 M sucrose solution according to the method of Ogbu and Okechukwu (2001) in order to retain the integrity of the tissues needed for analysis.

2.3. Enzyme Activities

The concentration of protein in the serum was analysed for, by the Biuret method as reported by Gornall *et al*

research were prepared in the nutrition section of the Biochemistry and Nutrition unit of Department of Chemical Sciences, Fountain University, Osogbo. Broiler birds (arbor acre) used for the study were gotten from a reputable farm (ROS farm) in Osogbo. The birds were raised in a well brightened and well-oxygenated poultry unit where feed and water were served without restriction. The experimental protocol followed the regulations of the Animal Care and Use Committee, Fountain University, Osogbo, Nigeria. Vaccinations were carried out as at when due.

(1949). Standard procedures for analysis of enzyme activities were strictly adhered to, as described for ALP by Wright *et al.* (1972); aminotransferases by Reitman and Frankel (1957); SOD by Amicerali (1999); CAT by Beers and Sizer (1952) and MDA by Reilly and Aust (1978).

2.4. Statistical Analysis

Research values were described as means \pm standard deviation (n=3). Analyses of Variance (ANOVA) accompanied by Tukey-Kramer test for nonconcurrences amongst means were utilized to ascertain any significant differences ($p < 0.05$) between variables.

3. Results

3.1. Tissues Enzymes Assay

Observable ($p < 0.05$) differences in the serum ALP activities of birds on 20% crude protein (CP) with varying methionine concentrations and those on other levels of crude protein (Table 2) were noticed. The same applies to all organs studied except the liver. Liver ALP portrayed no statistically significant ($p > 0.05$) difference among the birds placed on 20 % and those on 17% CP, regardless of the varying methionine concentrations, but significantly different for those on 14% CP. Overall, various organ ALP enzyme activities decrease with a decrease in crude protein percentage cum increase in methionine concentrations.

Serum AST activities were noticeably ($p < 0.05$) increased with a decrease in crude protein concentration of the diets (Table 3). Liver and heart AST were significantly ($p < 0.05$) higher at 20% CP inclusion level with a corresponding decrease in the activities of the enzyme in

the serum at this level. In the same vein, liver and heart AST activities decreased noticeably ($p < 0.05$), with a decrease in CP inclusion level, mostly at 14 and 17% regardless of the methionine variations, this correspondingly lead to increase in the enzyme activities of the serum at this level, except that at 17% CP and 0.6% methionine based diet, that had reduced serum activities

competing favourably with birds on 20 % CP and 0.6-1.4% methionine inclusion level.

Though there were no observable ($p > 0.05$) differences in the liver ALT enzyme activities amongst all experimental diets (control inclusive), numerically, as the crude protein decreases, liver ALT activities decrease with a concurrent elevation in the activities of the enzyme in the serum (Table 4).

Table 2. Specific activities of alkaline phosphatase (ALP- U/mg) in some organs and serum of broiler chickens fed with varying levels of crude protein and methionine supplemented diets

DIETARY TREATMENT	SERUM	LIVER	KIDNEY	HEART	GIZZARD	DUODENUM	PROVENTRICULUS
20%CP, 0.6%Met	0.49 ± 0.01 ^d	90.34±7.54 ^a	59.26±5.10 ^a	11.72±1.64 ^a	13.48±0.60 ^a	1.32±0.49 ^a	48.51±0.55 ^a
20%CP, 1.0%Met	0.49 ± 0.01 ^d	89.66 ±7.44 ^a	53.77±5.25 ^a	12.10±0.40 ^a	12.57±0.89 ^a	1.40±0.15 ^a	45.40±2.83 ^a
20%CP, 1.4%Met	0.50±0.09 ^d	85.67 ±8.98 ^a	55.08±6.12 ^a	12.02±2.02 ^a	16.84±1.45 ^a	1.37±0.05 ^a	45.24±1.44 ^a
17%CP, 0.6%Met	0.55 ± 0.05 ^c	87.45 ±6.45 ^a	44.76±4.64 ^b	7.78±0.91 ^d	10.64±1.44 ^b	0.57±0.04 ^b	40.81±0.91 ^b
17%CP, 1.0%Met	0.56±0.03 ^c	80.54 ±6.00 ^a	41.23±3.40 ^b	8.42±0.50 ^c	9.03±1.03 ^b	0.50±0.03 ^b	31.80±1.32 ^b
17%CP, 1.4%Met	0.56 ± 0.04 ^c	82.65 ±7.78 ^a	33.72±3.83 ^c	8.60±1.45 ^c	8.28±0.50 ^b	0.62±0.03 ^b	25.70±1.03 ^b
14%CP, 0.6%Met	1.96±0.03 ^a	68.17 ±1.6 ^b	23.05±3.21 ^d	9.00±1.28 ^b	6.30±0.43 ^c	0.22±0.02 ^c	15.23±0.41 ^c
14%CP, 1.0%Met	1.88±0.09 ^a	69.20 ±2.38 ^b	18.03±1.45 ^e	9.58±0.94 ^b	6.80±1.94 ^c	0.25±0.01 ^c	12.45±0.49 ^d
14%CP, 1.4%Met	1.57±0.09 ^b	65.75 ±1.45 ^c	21.02±1.12 ^d	9.62±1.08 ^b	6.01±1.77 ^c	0.20±0.01 ^c	11.32±1.65 ^d

Values are mean±SD of 3 determinations. Enzyme activities are expressed as nmol min⁻¹mg⁻¹protein.

^{a-d} Values carrying different superscripts for each organ are significantly different $P < 0.05$

Table 3. Specific activities of Aspartate Transaminase (AST-U/mg) in the liver, heart, and serum of broiler chickens fed with varying levels of crude protein and methionine supplemented diets.

DIETARY TREATMENT	SERUM	LIVER	HEART
20%CP, 0.6%Met	5.25±0.75 ^d	65.00±4.00 ^a	58.33±8.14 ^a
20%CP, 1.0%Met	6.75±0.86 ^d	58.11±3.95 ^a	57.25±0.75 ^a
20%CP, 1.4%Met	6.00±0.43 ^d	45.00±2.82 ^b	56.03±1.49 ^a
17%CP, 0.6%Met	6.50±0.50 ^d	51.33±4.03 ^b	47.00±3.00 ^b
17%CP, 1.0%Met	7.50±0.30 ^c	46.50±3.00 ^b	39.98±2.55 ^c
17%CP, 1.4%Met	8.75±0.73 ^b	45.25±4.25 ^b	36.50±3.50 ^c
14%CP, 0.6%Met	8.50±0.70 ^b	40.00±2.00 ^c	33.13±2.71 ^c
14%CP, 1.0%Met	8.90±0.30 ^b	33.50±3.50 ^d	29.33±2.89 ^c
14%CP, 1.4%Met	9.50±0.10 ^a	30.75±3.25 ^d	19.25±0.75 ^d

The results are mean ± SD of 3 determinations. Enzyme activities are expressed as nmol min⁻¹mg⁻¹protein.

^{a-d} Values carrying superscripts different from the control for each organ are significantly different ($P < 0.05$).

Table 4. Specific activities of alanine aminotransferase (ALT-U/mg) in the serum and liver of broiler chickens fed with varying levels of crude protein and methionine supplemented diets

DIETARY REATMENT	SERUM	LIVER
20%CP, 0.6%Met	2.00±0.20 ^d	21.67±1.15 ^a
20%CP, 1.0%Met	3.11±0.51 ^c	21.06±2.64 ^a
20%CP, 1.4%Met	3.33±0.25 ^c	21.33±0.76 ^a
17%CP, 0.6%Met	4.67±0.31 ^a	19.67±2.77 ^a
17%CP, 1.0%Met	3.67±0.04 ^b	20.00±1.00 ^a
17%CP, 1.4%Met	5.67±1.21 ^a	20.33±0.57 ^a
14%CP, 0.6%Met	4.67±0.51 ^a	18.67±3.21 ^a
14%CP, 1.0%Met	5.00±1.64 ^a	18.67±2.08 ^a
14%CP, 1.4%Met	6.67±1.51 ^a	19.67±2.32 ^a

Data are mean of three determinations ± SD. Specific enzyme activities are expressed as nmol min⁻¹mgprotein⁻¹.

^{a-d} Values carrying different superscripts are significantly different ($P < 0.05$).

3.2. Antioxidant enzymes assay

Statistically significant ($p < 0.05$) difference occurred in all organs' SOD activities of birds on 20% CP with varying Met concentration when compared with other diets concentration levels in the study with the exception of the activity of the enzyme in the liver (Table 5). There was no significant difference ($p > 0.05$) in the liver SOD activities of birds placed on 20% and 17% CP with varying Met concentration, but the duo was glaringly different when correlated with the performance of the enzyme on birds placed on 14% CP diet at various Met concentration.

Noticeable ($p < 0.05$) differences in the CAT activities of birds on the various CP/Met supplemented diets (table 6) were observed. 20% CP / 0.6% Met was significantly ($p < 0.05$) different from every other CP/Met combination. Overall, the activity of the enzyme reduces with a reduction in crude protein content at any methionine combination level.

Various organs malondialdehyde (MDA) level of birds on the control diet was noticeably ($p < 0.05$) lower when compared with the values obtained for birds on other (experimental) diets signifying a more toxicity level in the studied organ at percentages lower than 20% (Table 7).

Table 5. Specific activities of Superoxide Dismutase (SOD-U/ml) in some vital organs of broiler chickens fed with varying levels of crude protein and methionine supplemented diets.

DIETARY TREATMENT	LIVER	KIDNEY	HEART	DUODENUM	GIZZARD	PROVENTRICULUS
20% CP, 0.6% Met	0.55±0.04 ^a	0.67±0.15 ^a	0.42±0.07 ^a	0.37±0.06 ^a	0.43±0.01 ^b	0.69±0.02 ^a
20% CP, 1.0% Met	0.51±0.03 ^a	0.53±0.08 ^{ab}	0.41±0.55 ^a	0.25±0.05 ^{bc}	0.48±0.02 ^a	0.69±0.03 ^a
20% CP, 1.4% Met	0.58±0.01 ^a	0.48±0.01 ^b	0.39±0.09 ^a	0.25±0.02 ^b	0.41±0.01 ^{bc}	0.66±0.03 ^a
17% CP, 0.6% Met	0.58±0.08 ^a	0.39±0.02 ^c	0.37±0.10 ^b	0.28±0.03 ^b	0.26±0.01 ^e	0.47±0.09 ^b
17% CP, 1.0% Met	0.54±0.04 ^a	0.39±0.01 ^c	0.32±0.00 ^b	0.18±0.03 ^c	0.21±0.01 ^f	0.30±0.04 ^c
17% CP, 1.4% Met	0.51±0.04 ^a	0.37±0.02 ^c	0.28±0.03 ^c	0.31±0.08 ^{ab}	0.27±0.01 ^e	0.46±0.15 ^b
14% CP, 0.6% Met	0.31±0.04 ^c	0.35±0.04 ^{cd}	0.28±0.03 ^c	0.11±0.01 ^d	0.36±0.05 ^c	0.30±0.05 ^c
14% CP, 1.0% Met	0.41±0.03 ^b	0.33±0.04 ^d	0.23±0.08 ^{cd}	0.17±0.04 ^c	0.39±0.01 ^c	0.22±0.11 ^d
14% CP, 1.4% Met	0.39±0.05 ^{bc}	0.21±0.00 ^e	0.20±0.02 ^d	0.12±0.05 ^{cd}	0.35±0.20 ^{cd}	0.24±0.25 ^d

The results are mean ± SD of 3 determinations. Enzyme activities are expressed as nmol min⁻¹mg⁻¹protein.

^{a-d} Values carrying superscripts different from the control for each organ are significantly different ($P < 0.05$).

Table 6. Specific activities of catalase (CAT- U/ml) in the kidney and heart of broiler chickens fed with varying levels of crude protein and methionine supplemented diet

DIETARY TREATMENT	LIVER	KIDNEY	HEART
20% CP, 0.6% Met	37.21±1.21 ^a	42.13±4.60 ^a	52.42±4.62 ^a
20% CP, 1.0% Met	33.67±2.23 ^b	35.89±3.19 ^{ab}	45.10±1.05 ^b
20% CP, 1.4% Met	30.18±3.18 ^b	31.07±4.76 ^b	42.72±4.83 ^b
17% CP, 0.6% Met	25.13±2.38 ^c	37.83±2.30 ^{ab}	36.48±1.01 ^c
17% CP, 1.0% Met	22.01±3.49 ^c	38.27±3.76 ^{ab}	31.99±1.24 ^d
17% CP, 1.4% Met	28.08±2.92 ^c	35.86±3.33 ^{ab}	30.26±3.53 ^d
14% CP, 0.6% Met	18.82±1.55 ^d	24.67±1.80 ^c	25.68±1.13 ^e
14% CP, 1.0% Met	11.82±1.25 ^e	17.90±3.45 ^d	23.09±1.61 ^{ef}
14% CP, 1.4% Met	13.08±1.12 ^e	15.13±1.49 ^d	21.82±1.25 ^f

The results are mean ± SD of 3 determinations. Enzyme activities are expressed as nmol min⁻¹mg⁻¹protein.

^{a-d} Values carrying superscripts different from the control for each organ are significantly different ($P < 0.05$).

Table 7. Malondialdehyde (MDA- n mol/ml) concentrations in some vital organs of broiler chickens fed with varying levels of crude protein and methionine supplemented diets

DIETARY TREATMENT	LIVER (x10-9)	KIDNEY (x10-9)	HEART (x10-9)	GIZZARD (x10-9)	DUODENUM (x10-9)	PROVENTRICULUS (x10-9)
20% CP, 0.6% Met	2.47±0.32 ^c	2.03±0.50 ^c	0.84±0.02 ^e	5.15±0.50 ^e	8.42±0.05 ^f	7.19±1.20 ^d
20% CP, 1.0% Met	2.21±0.33 ^c	2.69±0.01 ^c	0.87±0.09 ^e	8.68±0.31 ^d	10.01±0.31 ^e	5.50±3.90 ^d
20% CP, 1.4% Met	2.39±0.13 ^c	2.76±0.25 ^c	0.90±0.05 ^e	11.37±0.79 ^c	13.70±0.60 ^d	7.18±0.11 ^d
17% CP, 0.6% Met	3.05±0.14 ^b	16.90±2.09 ^{ab}	5.24±0.12 ^b	11.20±1.90 ^c	17.30±2.00 ^a	13.40±1.00 ^c
17% CP, 1.0% Met	3.17±0.32 ^b	18.70±2.90 ^a	8.07±1.24 ^a	15.10±2.40 ^b	14.48±0.09 ^c	13.20±2.80 ^c
17% CP, 1.4% Met	3.30±1.21 ^b	17.20±1.76 ^a	8.30±0.99 ^a	20.30±1.30 ^a	14.20±1.10 ^{bc}	16.20±4.10 ^c
14% CP, 0.6% Met	5.40±0.48 ^a	14.00±1.92 ^b	1.60±1.45 ^{de}	9.63±0.30 ^d	14.69±0.04 ^b	21.10±1.40 ^b
14% CP, 1.0% Met	5.40±0.97 ^a	15.8±1.57 ^b	2.06±0.21 ^d	13.40±1.10 ^b	16.80±2.30 ^{ab}	25.10±1.60 ^a
14% CP, 1.4% Met	5.10±0.46 ^a	17.60±1.90 ^a	3.61±0.06 ^c	17.20±2.70 ^a	18.60±2.50 ^a	27.30±2.10 ^a

The results are mean ± SD of 3 determinations. Malondialdehyde concentrations are expressed as nmol mg⁻¹ protein.

^{a-d} Values carrying superscripts different from the control for each organ are significantly different ($P < 0.05$).

3.3. Organ to Body Weight Ratio

The formulation of the experimental diet did not affect all organs that were studied (Table 8). No significant

differences ($p>0.05$) between the various organs to body ratio amongst all crude protein/methionine concentrations under investigation.

Table 8. Organ to body weight ratio (%) of broiler chickens fed with varying levels of crude protein and methionine supplemented diets ($\times 10^{-2}$).

DIETARY TREATMENT	LIVER	KIDNEY	HEART	GIZZARD	PROVEN-TRICULUS	DUODENUM
20% CP, 0.6% Met	2.50±0.01 ^a	0.38±0.02 ^a	0.58±0.02 ^a	1.90±0.50 ^a	0.40±0.10 ^a	0.60±0.10 ^a
20% CP, 1.0% Met	2.45±0.11 ^a	0.35±0.02 ^a	0.57±0.01 ^a	2.00±0.30 ^a	0.50±0.10 ^a	0.70±0.10 ^a
20% CP, 1.4% Met	2.50±0.01 ^a	0.37±0.01 ^a	0.58±0.00 ^a	2.30±0.30 ^a	0.40±0.10 ^a	0.50±0.10 ^a
17% CP, 0.6% Met	2.49±0.10 ^a	0.37±0.01 ^a	0.57±0.00 ^a	2.30±0.40 ^a	0.50±0.10 ^a	0.70±0.10 ^a
17% CP, 1.0% Met	2.51±0.02 ^a	0.36±0.03 ^a	0.57±0.03 ^a	2.60±0.50 ^a	0.50±0.10 ^a	0.50±0.20 ^a
17% CP, 1.4% Met	2.50±0.01 ^a	0.38±0.02 ^a	0.58±0.00 ^a	3.20±0.30 ^a	0.60±0.10 ^a	0.70±0.20 ^a
14% CP, 0.6% Met	2.53±0.01 ^a	0.38±0.06 ^a	0.56±0.09 ^a	1.80±0.60 ^a	0.50±0.10 ^a	0.80±0.10 ^a
14% CP, 1.0% Met	2.49±0.18 ^a	0.36±0.03 ^a	0.57±0.01 ^a	1.90±0.70 ^a	0.40±0.10 ^a	0.50±0.10 ^a
14% CP, 1.4% Met	2.50±0.01 ^a	0.38±0.09 ^a	0.56±0.08 ^a	2.50±0.20 ^a	0.50±0.01 ^a	0.80±0.20 ^a

The results are mean ± SD of 3 determinations.

^a Values carrying same superscripts with the control for each organ and serum are not significantly different ($P>0.05$).

4. Discussion

Alkaline phosphatase is an omnipresent membrane-bound glycoprotein that initiates the disintegration of phosphate monoesters at fundamental pH values. Tissue nonspecific alkaline phosphatase is found in various tissues in the human body. It plays a significant role in metabolism, especially in liver functionality and bone growth. It facilitates the breakdown of protein (Hada *et al.*, 1978 and Husni *et al.*, 2012). It had earlier been reported that significantly increased levels of ALP enzyme activities of birds on experimental diets as compared to the activity of the same enzyme for birds on the control diet might indicate damage to the liver (Arslan *et al.*, 2003 and Saeid *et al.*, 2014). This study reported a significant ($p<0.05$) decrease in ALP enzyme activities of liver and other organs of interest as correlated with the control, hence no detrimental aftermath on the activities of organs studied as it has to do with ALP activities. Serum ALP enzyme activities, on the other hand, demonstrated a progressive increase as crude protein percentages decrease. This is an indication that at reduced crude protein percentage (mostly below 20%), enzyme activities in the serum increase. This might signify more toxic enzyme activities of the serum at reduced crude protein percentage (below 20%). This aligned with the work of Samantha *et al.*; (2018) that proclaimed highest blood serum ALP activity levels in broiler birds given methionine over or above the requirement as suggested by NRC, (1994) recommendation.

Aspartate aminotransferase (AST) is an aminotransferase enzyme that initiates the metamorphosis of aspartate and carbonyl compound to oxaloacetate and glutamate. It is found in all tissues save bone, with zenithal levels mostly found in the liver and skeletal muscle (Evans, 2009). The aminotransferases (AST and ALT) are normally restricted within liver cells and are discharged into the blood when liver cells are impaired. Hence, elevated levels of AST or ALT mostly signify liver impairment (Hrapkiewicz and Medina, 2007 and Madu and Nadro, 2017). It had earlier been reported that the activities, most of the liver enzymes that are associated

with the breaking down of amino acids decline with a flat protein-based diet and invariably increases with an elevated protein-based diet (Muramatsu *et al.*, 1971; Roudbaneh *et al.*, 2013 and Ospina-Rojas *et al.*, 2014). This negates the work of Elham *et al.*; (2010) which reported the highest serum AST concentration for birds on the control diets as against other experimental diets, probably because the birds used were challenged alongside and fed with methionine and threonine concentration over and above NRC, (1994) recommendation. This is buttressing the fact that at reduced CP inclusion level, mostly below 20%, most enzymes got leaked into the serum in broiler birds.

Alanine aminotransferase (ALT), also an aminotransferase enzyme is obtained in serum and organ tissues, most importantly in the liver, though appreciable amounts also originated in the kidney, skeletal muscle, and myocardium. The enzyme is raised in serum under conditions of notable cellular loss and is always an indication of liver functionality. Nutritional intake, restraint, and drug prescription may affect plasma ALT in rodents (Evans, 2009). The observed results of the ALT are in line with the research findings of Elham *et al.*; (2010) which reported a non-significant effect on liver ALT activities especially on day 28 when birds were fed methionine and threonine above NRC, (1994) recommendation.

Superoxide dismutase (SOD) is a pristine detox enzyme and the utmost competent oxidant inhibitor in the cell. It is a crucial endogenous oxidant inhibitor enzyme that fights against free radicals. It activates the neutralization of superoxide ion (free radicals), thereby relinquishing the presumably pernicious superoxide anion that is not very risky (Herberg *et al.*, 2004; Halliwell *et al.*, 2005; Yuan *et al.*, 2010 and Dysken *et al.*, 2014). The observed results of the ALT supported the work of Subbaiah *et al.*; (2011) that proclaimed a reduction in the SOD activities of birds infected with Newcastle Disease Virus (NDV) and given dietary methionine content over and above the recommendation of NRC, (1994). On the other hand, it negated the research outcome of Jan *et al.*; (2018) which reported increased activities of SOD in the liver of turkeys fed increased dietary methionine contents over 40% above NRC, (1994) recommendation.

Catalase (CAT) is an accepted oxidation inhibitor enzyme found almost in all living tissues that uses a non-metallic bivalent element, that is, the most sufficient element in the earth's surface. The enzyme utilizes iron or manganese as an alloy and disproportionates the degeneration or diminution of the simplest peroxide to water and oxygen, hence finalizing the cleansing procedure mimicked by superoxide dismutase (Chelikani *et al.*, 2004). The observed result in this regard is in line with the research outcome of Jan *et al.*; (2018) that reported a surge in the activity of the enzyme in the intestinal wall and liver of turkey fed increase methionine content above NRC, (1994) recommendation.

Malondialdehyde (MDA) is an extremely dangerous secondary product formed partly by lipid oxidation derived free radicals. It is an enzymatic assay globally used for determining oxidative stress in the biomedical field where lipid peroxidation is a chain phenomenon giving rise to the formation of various active compounds which eventually result in cellular damage (Slatter *et al.*, 2000). The results of the MDA are in accord with the finding of Subbaiah *et al.*; (2011) that acclaimed a surge in the level of MDA of birds infected with Newcastle Disease Virus (NDV) and given dietary methionine content over and above the recommendation of NRC. A reduction in the MDA level in the liver, but a surge in the activity of the enzyme in the intestinal wall of turkey fed increased dietary methionine content above NRC, (1994) recommendation (>40%) was earlier reported by Jan *et al.*; (2018). Hepatic MDA concentration in this study was significantly influenced by crude protein/methionine combination at below 20% and 1.4% respectively. This does not align with the research outcome of Jan *et al.*; (2018) which claimed that higher methionine concentrations in the diet did not influence the hepatic MDA combination.

Organ to body weight ratio is usually an indication of impending toxic effect, in this case of experimental diet on vital organs monitored (Olayode *et al.*, 2019). The biochemical reason that warrants analyzing for relative organ weight is that mostly, organ weight changes are normally relative weight-wise to total body weight. Hence, they are usually examined to find out whether the size of the organ has changed, especially as a subset of the weight of the whole animal, which will eventually serve as an indicator of the adverse effect of drugs or experimental diets on the target organ (Nigatu *et al.*, 2017). Vital organs have been reported to obtain their nutritional requirement irrespective of other body performance demands (Cengiz and Küçükersan, 2010; Ospina-Rojas *et al.*, 2014 and Shirzadegan *et al.*, 2015). This research finding negates the work of Amr (2015) which reported a markedly highest weight of proventriculus, heart and liver of birds on the control diet (22.1% CP, 1.18% lysine and 0.52% methionine) as compared with other experimental diets when birds were fed with exuberance methionine and lysine in the presence or absence of L-Carnitine.

5. Conclusion

In conclusion, enzyme activities and not the size of the organs studied in broiler chicks were adversely affected at CP levels below 20%, up till 14%, even with methionine supplementation.

Acknowledgments

The author hereby acknowledges the input of laboratory staff of Fountain University Osogbo for their input during laboratory analysis.

References

- Abbasi MA, Mahdavi AH, Samie AH and Jahanian R. 2014. Effects of different levels of dietary crude protein and threonine on performance, humoral immune responses and intestinal morphology of broiler chicks. *Braz. J. Poult. Sci.*, **16**: 35-44.
- Alagawany M and Mahrose KM. 2014. Influence of different levels of certain essential amino acids on the performance, egg quality criteria and economics of lohmann brown laying hens. *Asian J. Poult. Sci.*, **8**: 82-96.
- Amiceralli F. 1999. Age dependent ultrastructural alterations and biochemical response of rat skeletal muscle after hypoxic or hyperoxic treatments. *Biochem Biophys. Acta*, **1453**: 105-114.
- Amr AW, Abeer A and Mohamed E. 2015. Impact of Dietary Excess Methionine and Lysine with or without Addition of L-Carnitine on Performance, Blood Lipid Profile and Litter Quality in Broilers. *Asian J Animal Vet Adv*, **10**:191-202.
- Arslan C, Cıtil M and Saatci M. 2003. Effects of L-carnitine administration on growth performance, carcass traits, blood serum parameters and abdominal fatty acid composition of ducks. *Arch Anim Nutr.* **57**:381-388.
- Beers RF and Sizer IW. 1952. A spectrophotometric method for measuring the breakdown of hydrogen peroxide by catalase. *J. Biol. Chem.* **195**, 133-140.
- Cengiz Ö and Küçükersan S. 2010. Effects of graded contents of arginine supplementation on growth performance, hematological parameters and immune system in broilers. *Revue De MedecineVeterinaire.* **161**: 409.
- Cheeke PR. **Applied Animal Nutrition: Feeds and Feeding**. 3rd Eds. Pearson Prentice Hall, Upper Saddle River, USA. ISBN-13: 9780131133310, 2005. Pages: 604.
- Chelikani P, Fita I and Loewen PC. 2004. Diversity of structures and properties among catalases. *Cell Mol Life Sci.* **61**:192-208.
- Dysken MW, Sano M, Asthana S, *et al.*, 2014. Effect of vitamin E and memantine on functional decline in Alzheimer disease: the TEAM-AD VA cooperative randomized trial. *JAMA.* **311**:33-44.
- Elham M, Azhar K, Seyed RH, Tech CL and Mohd HB. 2010. Change in Growth Performance and Liver Function Enzymes of Broiler Chickens Challenged with Infectious Bursal Disease Virus to Dietary Supplementation of Methionine and Threonine. *American Journal of Animal and Veterinary Sciences.* **5** : 20-26, ISSN 1557-4555.
- Evans GO. 2009. Animal Clinical Chemistry. CRC Press, Boca Raton FL.
- Gornall AC, Bardawill CJ and David MM. 1949. Determination of serum protein by means of biuret reaction. *J. Biol. Chem.* **177**:751-756.
- Gunawardana P, Roland DA and Bryant MM. 2008. Effect of energy and protein on performance, egg components, egg solids, egg quality and profits in molted hy-line W-36 hens. *J. Applied Poult. Res.* **17**: 432-439.
- Hada T, Higashino K, Okochi T and Yamamura Y. 1978. Kasahara-variant alkaline phosphatase in a renal cell Carcinoma Clin. Chim. Acta. **89**. 31 1-316
- Halliwell B, Rafter J and Jenner A. 2005. Health promotion by flavonoids, tocopherols, tocotrienols, and other phenols: direct or indirect effects? Antioxidant or not? *Am J Clin Nutr.* **81**:268S-276S.

- Hercberg S, Galan P, Preziosi P, *et al.*, 2004. The SU. VI. MAX Study: a randomized, placebo-controlled trial of the health effects of antioxidant vitamins and minerals. *Arch Int Med.* **164**:2335–2342.
- Hrapkiewicz K and Medina L. 2007. **Clinical Laboratory Animal Medicine**, second ed., Blackwell Publishing, Ames Iowa.
- Husni S, Ali AA and Gaber MS. 2012. Explanation of the Decrease in Alkaline phosphatase (ALP) Activity in Hemolysed Blood Samples from the Clinical Point of View: *In vitro* study. *Jordan J Biol Sci.* **5**: 2.
- Jan J, Bartłomiej T, Katarzyna O, Andrzej K, Magdalena K and Zenon Z. 2018. The effect of different dietary levels of DL-methionine and DL-hydroxy analogue on the antioxidant status of young turkeys infected with the haemorrhagic enteritis virus. *BMC Vet Res.* **14**: 404.
- Keshavarz, K. 2003. Effects of reducing dietary protein, methionine, choline, folic acid and vitamin B12 during the late stages of the egg production cycle on performance and eggshell quality. *Poultry. Sci.*, **82**: 1407-1414.
- Kim WK and Froelich CA. Jr., 2006. Patterson PH, Ricke SC. The potential to reduce poultry nitrogen emissions with dietary methionine or methionine analogues supplementation. *World's Poultry. Sci. J.* **62**:338–353.
- Lemme A, Kozłowski K, Jankowski J, Petri A and Zduńczyk Z. 2005. Responses of 36 to 63 day old BUT Big 6 turkey toms to graded dietary methionine + cysteine levels. *J. Anim. Feed Sci.* **14**:139–142.
- Liu G, Zong K, Zhang L and Cao S. 2010. Dietary methionine affect meat quality and myostatin gene exon 1 region methylation in skeletal muscle tissues of broilers. *Agri. Sci. China.* **9**:1338–1346.
- Madu JO, Nadro M. 2017. Evaluation of the Toxicological Effects of *Senecio aureus* Extract on the Liver and Hematological Parameters in Wistar Rats. *Jordan J Biol Sci.* **10**: 1.
- Matsushita K, Takahashi K and Akiba Y. 2007. Effects of adequate or marginal excess of dietary methionine hydroxyl analogue free acid on growth performance, edible meat yields and inflammatory response in female broiler chickens. *J. Poult. Sci.* **44**:265–272.
- Meirelles HT, Albuquerque R, Borgatti LMO, Souza LWO, Meister NC and Lima FR. 2003. Performance of broilers fed with different levels of methionine hydroxyl analogue and DL-methionine. *Braz. J. Poult. Sci.* **5**:69–74.
- Muramatsu K, Odagiri H, Morishita S and Takeuchi H. 1971 Effect of excess levels of individual amino acids on growth of rats fed casein diets. *J. Nutr.* 1971. **101**:1117- 1125.
- Niculescu MD and Zeisel SH. 2002. Diet, methyl donors and DNA methylation: interactions between dietary folate, methionine and choline. *J. Nutr.* **132**:2333–2335.
- Nigatu TA, Mekbebe A, Kelbessa U, Wondwossen E and Eyasu MA. 2017. Toxicological investigation of acute and chronic treatment with *Gnidia stenophylla* Gilg root extract on some blood parameters and histopathology of spleen, liver and kidney in mice. *BMC Res Notes.* **10**:625.
- NRC. 1994. **Nutrients Requirements of Poultry**. 9th Rev. Edn., National Academic Press, Washington, USA. ISBN-13: 9780309596329, Pages: 1-56.
- Ogbu SI and Okechukwu FI. 2001. The effect of storage temperature performance and body composition of broiler chicks. *Poultry Sci.* **81**: 1156-1167.
- Olayode OA, Michael OD and Gbola O. 2019. Biochemical, hematological and histopathological evaluation of the toxicity potential of the leaf extract of *Stachytarpheta cayennensis* in rats, *J Trad Compl Med.*
- Ospina-Rojas IC, Murakami AE, Duarte CRDA, Eyng C, Oliveira CALD and Janeiro V. 2014. Valine, isoleucine, arginine and glycine supplementation of low-protein diets for broiler chickens during the starter and grower phases. *British Poultry Sci.* **55** :766-73.
- Pinchasov Y, Mendonca C X and Jensen, LS. 1990. Broiler chick response to low protein diets supplemented with synthetic amino acids. *Poult. Sci.* **69**:1950–55.
- Pond WP, Church DC and Pond KR. 1995. **Basic Animal Nutrition and Feeding** . John Wiley and Sons, New York.
- Reilly CA and Aust SD. 1999. Measurement of lipid peroxidation. *Curr. Protoc. Toxicol.*
- Reitman S and Frankel SA. 1957. Colorimetric method for the determination of serum GOT and GPT. *American J Clin Pathol.*, **28**: 56-63.
- Roudbaneh MT, Babae MJ, Frooziyeh MA and Alizadeh B. 2013. Estimation of dietary threonine requirement for growth and immune responses of broilers. *J App Anim Res.* **41**: 474-483.
- Saeid SS, Reza YM and Javad N. 2014. The effects of different levels of L-carnitine and methionine on performance and blood metabolites in female broiler. *Res Opin Anim Vet Sci.* **4**:427–431.
- Samantha S, Ebrahim D, Alireza S, Mehrdad B and Antonio G Aldo P. 2018. Effects of dietary surpluses of methionine and lysine on growth performance, blood serum parameters, immune responses, and carcass traits of broilers. *Journal of Applied Animal Research.* **47** :146-153.
- Shirzadegan K, Nickkhal I and Jafari MA. 2015. Impacts of Dietary L-Threonine Supplementation on Performance and Intestinal Morphology of Broiler Chickens during Summer Time. *Iranian J Appl Animal Sci.* **5**:2 .
- Slatter DA, Bolton CH and Bailey AJ. 2000. The importance of lipid-derived malondialdehyde in diabetes mellitus. *Diabetologia* **43**: 550-557.
- Subbaiah KCV, Raniprameela D, Visweswari G, Rajendra W and Lokanatha V. 2011. Perturbations in the antioxidant metabolism during Newcastle disease virus (NDV) infection in chicken. Protective role of vitamin E. *Naturwissenschaften.* **98**:1019–26.
- Van Emous RA, Kwakkel RP, Van Krimpen MM and Hendriks WH. 2015. Effects of dietary protein levels during rearing and dietary energy levels during lay on body composition and reproduction in broiler breeder females. *Poult Sci.* **94**: 1030-1042.
- Wright PJ, Leathwood PD and Plummer DT. 1972. Enzymes in rat urine: alkaline phosphatase, *Enzymologia.* **42**: 317.
- Yuan G, Sun B, Yuan J and Wang Q. 2010. Effect of 1-methylcyclopropene on shelf life, visual quality, antioxidant enzymes and health-promoting compounds in broccoli florets. *Food Chem.* **118**:774–781.

In vitro genotoxicity study of the lambda-cyhalothrin insecticide on Sf9 insect cells line using Comet assay

Manal Saleh^{1,*}, Daas Ezz -din² and Aroub Al-Masri¹

¹National Commission for Biotechnology, (NCBT), Damascus, Syria Biomedical department -Cell Culture laboratory; ² Faculty of Agriculture, Damascus University, Damascus, Syria

Received: May 9, 2020; Revised: June 18, 2020; Accepted: August 5, 2020

Abstract

The Synthetic Pyrethroid Lambda-cyhalothrin is one of the most common and used pesticides worldwide for pest control. Its application has resulted in serious environmental hazards and health concerns and has led to the development of resistant pest populations. There are few studies of insecticide toxicity and genotoxicity on insects; therefore, in this study, we evaluated the potential genotoxic activity of Lambda-cyhalothrin using the single-cell microgel electrophoresis or comet assay (the alkaline comet assay) on Sf9 insect cell line. Four different concentrations of Lambda-cyhalothrin were used (0.5, 5, 25, and 100 µm) to treat Sf9 cells for 24 h. UVC (for 45 min) was used as a positive control. The results showed that Lambda-cyhalothrin induced a statistically significant increase in DNA damage in Sf9 insect cell line compared with negative control ($p < 0.05$), except at the 5 µm concentration. UVC induces oxidative stress as Lambda-cyhalothrin insecticide. Lambda-cyhalothrin was more genotoxic than UVC on the Sf9 cell line. This may suppose that Lambda-cyhalothrin insecticide has other genotoxic effects on the Sf9 insect cell line than what is known.

Keywords: Comet assay, DNA damage, Pyrethroid, lambda-cyhalothrin, Sf9 cells.

1. Introduction

The excessive use of synthetic pesticides in agriculture has resulted in serious environmental hazards (Packiam *et al.*, 2015), health concerns, and a spike in resistant pest populations (Giner *et al.*, 2012; Nagy *et al.*, 2014). Therefore, several assays were recently developed to evaluate the genotoxic effects of chemicals and other potent environmental toxicants in living organisms, for example, the structural chromosomal aberrations assay (SCA), micronucleus test (MN), and sister chromatid exchanges and comet assay (Mohanty *et al.*, 2011). Among these assays, single-cell gel electrophoresis or comet assay has been widely used in the detection and evaluation of genotoxic compounds in several test systems (Singh *et al.*, 1988; Collins, 2004) both *in vitro* and *in vivo* (Sasaki *et al.*, 2007).

Lambda-cyhalothrin is a synthetic pyrethroid type II insecticide that contains a cyano group widely used to control agricultural and domestic insect pests of cotton, cereals, hops, ornamentals, and vegetables. It is also used in public health applications to control insects, ticks, and flies which may act as disease vectors (Abdel Aziz and Abdel Rahem, 2010). Lambda-cyhalothrin is classified as a class D carcinogen by US EPA (US Environmental Protection Agency, 2012). It is moderately persistent in the soil environment (Saleem *et al.*, 2014).

Lambda-cyhalothrin penetrates the insect cuticle, disrupting nerve conduction within minutes by interacting with sodium channels on nerve membranes (Chakravarthi *et al.*, 2007; Shaurub and Abd El-Aziz, 2015). Upon

application, the insect suffers loss of muscular control, which results in paralysis and eventually death. There are several reports of lambda-cyhalothrin toxicity to mammals and its ability to induce oxidative stress *in vivo* and *in vitro* (Tukhtaev *et al.*, 2012). Lambda-cyhalothrin is highly toxic to fish, aquatic arthropods, and honeybees (Muranli, 2013; Aldehamee, 2015).

Some studies have reported lambda-cyhalothrin genotoxicity using structural chromosomal aberrations assay (SCA), micronucleus test (MN), and comet assay (Çelik *et al.*, 2005a, b; Naravaneni and Jamil, 2005). Most studies focused on lambda-cyhalothrin toxicity to vertebrates, including cytotoxicity (Çelik *et al.*, 2005 b), endocrine disruption (Al-Sarar, 2015; Kim *et al.*, 2015), genotoxicity like induction of micronucleus (MN), nuclear abnormalities formation on mosquitofish (Muranli and Güner, 2011) and chromosomal aberrations to *Mystus gulio* fish (Velmurugan *et al.*, 2006). Some assays also indicated immunotoxicity *in vitro* models, such as human lymphocytes (Naravaneni and Jamil, 2005) and rat bone marrow (Çelik *et al.*, 2005 a, b; Zhang *et al.*, 2010). Whereas the studies of insecticide toxicity and genotoxicity on insects were few, some studies were carried out using the *in vivo* model as the effect of lambda-cyhalothrin on desert locust, *Schistocerca gregaria* Forsk (Al Hariri and Suhail, 2001) that caused an increase in the total counts and abnormal haemocytes.

The genotoxicity of another pyrethroid insecticide” Deltamethrin “was investigated on cell-mediated immune of *Galleria mellonella* (Lepidoptera: Pyralidae) that induced genotoxic damage by micronucleus formation (Kurt and Kayış, 2015). The majority of studies focused on

* Corresponding author e-mail: manalcapno@gmail.com.

the genotoxic effect of radiation on DNA damage *in vivo* model on *Ephesia kuehniella* insect (Tuncbilek *et al.*, 2011), and *in vitro* model on Sf9 cell line resistance to DNA-damaged treatments, by radiation and hydrogen peroxide (Chandna *et al.*, 2004; Cheng *et al.*, 2009).

Comet assay was first described by Ostling & Johanson (1984), and numerous modifications have been reported to date to allow the detection of various types of DNA damage (Gaivão and Sierra, 2014). Different types of the comet assay for different purposes have been described by Collins (2004); the neutral comet assay to detect Double-strand breaks (DSB) and the alkaline comet assay to detect DNA single-strand breaks (SSB).

The most widely used method for the assessment of DNA damage is the alkaline comet assay (Nandhakumar *et al.*, 2011).

The comet assay is a micro electrophoretic technique for the direct visualization of DNA damage at the level of the individual cell (Hamdani *et al.*, 2014). DNA damage is evaluated by the proportion of DNA which migrates out of the nuclei toward the anode when individual cells or isolated nuclei, embedded in a thin agarose layer, are subjected to electrophoresis that results in a "comet-like" shape of nuclei. The Comet is examined after staining with an appropriate fluorochrome stain like ethidium bromide using a fluorescence microscope or with silver staining (Nadin *et al.*, 2001; Garcia *et al.*, 2007). The comets can be classified either by visual scoring or by using image analysis software packages (Collins, 2004; Collins *et al.*, 2008). According to visual scoring, the comets are classified into five different classes, from 0 (no tail) to 4 (almost all DNA in tail), based on the tail length and the amount of DNA present in the tail. If 100 comets are scored, and each comet assigned a value of 0 to 4 according to its class, the total score for the sample gel will be between 0 and 400 "arbitrary units or damage index" (Garcia *et al.*, 2004; 2011; Collins *et al.*, 2008; Collins *et al.*, 2014). Due to the lack of *in vitro* data on the effect of lambda-cyhalothrin on insect cells, results necessitate more genotoxicity studies of pesticides using different assays with different test materials (Bhoopendra and Nitesh, 2015).

This study aimed to investigate the *in vitro* genotoxic effects induced by analytical grade Lambda-cyhalothrin on Sf9 insect cells line as a model for lepidopteran insect cells by using the comet assay.

2. Materials and methods

2.1. Chemicals

Lambda-cyhalothrin (RS)- α -cyano-3-phenoxybenzyl (1R)-cis-3-(Z)-(2-chloro-3, 3, 3-trifluoroprop-1-enyl)-2, 2-dimethylcyclopropanecarboxylate, purity of (98.7%) were obtained from Syngenta.

A stock solution of 10 mM of lambda-cyhalothrin was prepared using DMSO (Dimethyl sulfoxide) freshly made before cell treatment.

2.2. Cell culture

The Sf9 cells derived from pupal ovarian tissue of *Spodoptera frugiperda* (Vaughn *et al.*, 1977) were purchased from Gentaur-Belgium. The culture was routinely maintained at 27°C using the incubator (Selecta) in 25-cm² culture flasks (TPP) by adding 4ml of EX-cell

medium (serum-free medium), (Sigma-Aldrich). Cells formed a monolayer and were sub-cultured every 3–4 days using (TPP) scraper.

2.3. Cell treatment

Cells were seeded into a 6 well tissue culture plate with a density of 1x10⁶ cells/ml and allowed to grow for 24 h. The cultures were then treated for 24 h with four concentrations (0.5, 5, 25 and 100 μ M) of lambda-cyhalothrin that induced inhibition of cells growth (6, 24, 39, 51%) respectively, based on previous studies, then the culture media were removed and the cells were washed with cold (PBS) Phosphate Buffer Saline (Ca⁺⁺ and Mg⁺⁺) free, and scraped, centrifuged and resuspended in 200 μ l PBS for the comet assay.

2.4. Comet assay

The comet assay was performed using the Comet Assay® Silver Staining Kit Catalog #4251-050-K (Trevigen). Alkaline Comet Assay® following the manufacturer's instructions with slight modification. Briefly, cells (1 x 10⁵ cells/ml) were mixed with molten LM Agarose (at 37°C) at a ratio of 1: 10 (v/v). Then, a 50 μ l of mixing was pipetted onto the Comet Slide™ area immediately. Cells exposed to UVC (257.3 nm) for 45 min were used as positive controls, and cells treated with DMSO alone were used as a negative control. To prevent additional damage, all the steps described above were conducted under dim light.

The slides were incubated at 4°C for 1 h to accelerate the gelling of the agarose disc and then transferred to prechilled lysis solution (cat# 4250-050-01) 40 ml with 10% DMSO incubate overnight at 4°C. Comet Slide™ was immersed in alkali unwinding solution (pH=13, 300 mM NaOH, 1 mM EDTA) at room temperature, in the dark for 30 minutes.

Slides placed in an electrophoresis slide tray, and then covered with 500 ml alkaline electrophoresis solution pH=13 (300 mM NaOH, 1 mM EDTA). Electrophoresis was performed for 30 minutes (1 Volt/cm / 300 mA). Then slides were immersed twice in dH₂O for 5 minutes then in 70% ethanol for 5 minutes. Samples were dried at 37°C for 10-15 minutes and stained with silver staining.

2.4.1. Silver Staining:

The sample area was covered with 100 μ l of prepared fixation solution :10X Fixation Additive (cat# 4254-200-05), dH₂O, methanol, glacial acetic acid, incubated for 20 minutes at room temperature, and then rinsed in dH₂O for 30 minutes. The samples were then covered with 100 μ l of prepared staining solution : dH₂O, 20X Staining Reagent #1 (cat# 4254-200-01), 20X Staining Reagent #2 (cat# 4254-200-02), 20X Staining Reagent #3 (cat# 4254-200-03), and incubated at room temperature for 5 - 20 minutes. The intensity of staining was visualized under the microscope using a 100X objective, and the reaction stopped when comets were easily visible by covering samples with 100 μ l of 5% acetic acid for 15 minutes and rinsing in dH₂O.

2.4.2. Comet analysis:

Comets (more than 50 per treatment) were captured, digitized, and copied to the computer.

Each comet was identified by a number from 0 to 4 with various degrees of DNA damage. Class 0 represents no damage with the head being large and intact and comet

without a tail. Class 1 represents slight damage with the head being large and little affected and a short tail whose length is less or equal to one head diameter. Class 2 represents medium damage with the head being large and little affected, and a short tail. Class 3 represents extensive damage with the head being reduced, long and large tail. Class 4 represents severe damage with the head being greatly reduced; long and large tail whose contour is difficult to determine due to the dispersion of small DNA fragments (Collins, 2004). Then DNA damage was calculated in AU as using the formula:

$$AU = \frac{(0 \times N_0 + 1 \times N_1 + 2 \times N_2 + 3 \times N_3 + 4 \times N_4)}{\text{\#comets analyzed}} \times 100$$

Where N₀, N₁, etc. are the numbers of comets in categories 0, 1, etc. (Garcia *et al.*, 2011).

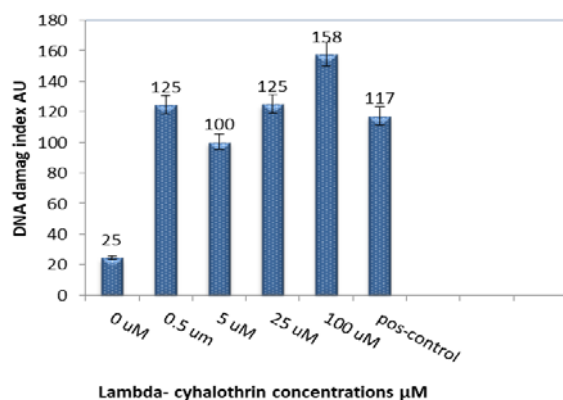
2.5. Statistical analysis

For each treatment, two slides were prepared, in two independent experiments performed. Statistical analyses were performed with the Mann-Whitney test using SPSS-17.0 Software. Error bars represent standard deviation. Results were considered statistically significant when $p < 0.05$.

3. Results

The results showed that lambda-cyhalothrin, significantly increased DNA damages in Sf9 insect cell line, compared with negative controls ($P > 0.05$), except at the 5 μM concentration, while no significant difference was observed between the all lambda -cyhalothrin concentrations and positive control, as shown in figure (1). DNA damage index was: 125,100,125,158, using concentrations (0.5, 5, 25 and 100 μM) of Lambda-cyhalothrin that induced inhibition percentage of cell growth, (6, 24, 39, 51%) respectively.

It was observed that lambda-cyhalothrin insecticide induced DNA-damage of 125 AU at the lowest concentration of 0.5 μM compared to 25 AU of untreated cells. The lowest DNA damage was measured in 100 AU at 5 μM concentration, while the higher value of damage was 158 AU at 100 μM , which is the highest concentration



of lambda -cyhalothrin insecticides tested here.

Figure 1. DNA damage induced by lambda-cyhalothrin in Sf9 insect cell line expressed in arbitrary units (AU) in the comet assay. Data are means of values of repeated experiments \pm standard deviation. A statistically significant increase ($p < 0.05$) as determined by comparing the values of DNA damage induced by various concentrations of lambda-cyhalothrin with the negative control (with 10% DMSO).

Figure 2 shows the Images of the silver-stained comet of Sf9 insect cell line, with various degrees of DNA damage. Class 0 represents undamaged cells and class 4 represents the most heavily damaged.

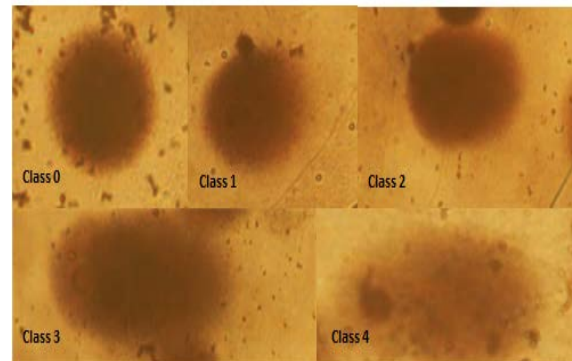


Figure 2. Visual scoring of DNA damage from 0 to 4 according to comet appearance, Study sample: Sf9 insect cells, Stain: Silver nitrate, Magnification: 200X

4. Discussion

Long-term extensive use of insecticides has been a major cause for insecticides-resistance development in insects, which creates an important problem and is a major threat to agriculture, human, and animal health.

Measuring DNA damage is a key step in a broad range of biomedical and toxicological research studies. Among several methods of detecting DNA damage, the comet assay, being very simple, cheap, and not requiring sophisticated high-cost equipment, has been most widely adopted and used.

Resistance to Pyrethroids insecticides refers to the genetic change in the insect pest genome. This genetic change can occur by two main mechanisms: 1) increased levels of detoxification enzymes resulting in metabolic resistance, and 2) target-site mutations in the voltage-gated sodium, known as knock-down resistance (kdr) (Shen *et al.*, 2016).

Lambda-cyhalothrin belongs to Pyrethroids insecticides and is used extensively in pest control. It is essential to study and analyze the cytotoxic and genotoxic effects of Lambda-cyhalothrin on both environment and human health. These studies will enable better adoptions for measures that can protect humans from the potential mutagenic, carcinogenic effects of these insecticides, and halt the development of insecticide resistance in the insect pest (Nagy *et al.*, 2014).

Most toxicity studies of the Lambda-cyhalothrin insecticide effect were performed on vertebrate's *in vivo/in vitro* model, whereas a few data are available for insects; therefore, this current research is applied on Sf9 insect cell line model using comet assay to investigate the genotoxicity of Lambda-cyhalothrin insecticide. The results indicate that Lambda-cyhalothrin insecticide is genotoxic to Sf9 insect cell line by causing DNA damage in all concentrations, which corresponds with previous studies applied on other organisms (Çelik *et al.*, 2005a,b; Naravaneni and Jamil, 2005; Zhang *et al.*, 2010; Muranli and Güner, 2011; Muranli, 2013). The DNA damage index was measured as (125,100,125,158) AU, using concentrations (0.5, 5, 25, and 100 μM) of Lambda-cyhalothrin that induced inhibition of cells growth at (6,

24, 39, 51%), respectively. It was observed that DNA damage index is related to the inhibition rate except for the 5 μM concentration, and that can be explained by that the Sf9 cell's response to DNA damage is induced by Lambda-cyhalothrin insecticide. This response includes cell cycle arrest to allow DNA repair (Remington, 2010), or cell death via apoptosis if the damage encountered is great (Chandna *et al.*, 2004).

A possible mechanism for lambda-cyhalothrin cytotoxicity could be the induction of oxidative stress by the increase in reactive oxygen species (ROS or free radicals). ROS will impair the balance between the ROS generation and antioxidant defense capability, and this will cause damage to the cell membrane lipids and proteins (Tukhtaev *et al.*, 2012), in addition to single-strand DNA breaks, (Zhang *et al.*, 2010; Fetoui *et al.*, 2015; Deeba *et al.*, 2017).

In this present study, it was found that Sf9 insect cell line is resistant to UVC effect, which explains the insignificant differences between all concentrations of Lambda-cyhalothrin and cells treated with UVC as a positive control (Cheng *et al.*, 2009). Chandna *et al.* (2004; 2010) reported that Lepidopteran insect cells are known to exhibit very high radio-resistance, which is possibly caused by a stronger antioxidant system and active DNA repair mechanisms. Previously, we reported two different populations of Sf9 cells were identified, mononucleated and polynucleated according to their nuclear number (Saleh, 2011). The endopolyploid cells (polynucleated) possibly play a role in Sf9 cells metabolism and their ability to active DNA repair, as with Ivanov and others (2003) who also reported that endopolyploid cells produced after severe genotoxic damage, which might facilitate an alternative pathway of cell survival and therefore contribute to genotoxic resistance.

Although the mode of action of UVC and lambda-cyhalothrin insecticide is one, which is inducing oxidative stress, the genotoxic effect of lambda-cyhalothrin on Sf9 insect cell line was higher than UVC, which may indicate that Lambda-cyhalothrin insecticide has an additional genotoxic effect on Sf9 insect cell line.

In conclusion, the results from this present study indicate that Lambda-cyhalothrin insecticide is genotoxic to the Sf9 insect cell line, and can cause DNA damage in all tested concentrations. DNA damage index was: 125,100,125,158, using concentrations (0.5, 5, 25 and 100 μM) of lambda-cyhalothrin that induced inhibition percentage of cells growth : (6, 24, 39, 51%), respectively. The possible mechanism by which Lambda-cyhalothrin cytotoxicity occurs is by oxidative stress induction, and additional mechanisms await further characterization.

Acknowledgments

We would like to express our appreciation to Mr. Ismael Saleh for his help in statistical analysis, and to Mrs. Banan al-sheikh and Mrs. Inas Nemer for their help in this research.

References

Abdel Aziz KB and Abdel Rahem HM. 2010. Lambda, the pyrethroid insecticide as a mutagenic agent in both somatic and germ cells. *J Am Sci*, **6**:72-81.

Aldehamee MHM. 2015. Effect of Different Concentrations of Pesticide Colti 5 (Lambda-Cyhalothrin) On Water Flea *Daphnia pulex*. *Jubpas*, **23**: 680-685.

Al-Hariri MK and Suhail ANJUM. 2001. Effect of lambda-cyhalothrin and deltamethrin on the haemocytes of Desert Locust, *Schistocerca gregaria* Forsk. *Int J Agric Biol*, **3**:81-84.

Al-Sarar AS, Abobakr Y, Bayoumi AE, and Hussein HI. 2015. Cytotoxic and genotoxic effects of abamectin, chlorfenapyr, and imidacloprid on CHO K1 cells. *Environ Sci Pollut Res*, **22**: 17041-17052.

Bhoopendra K. and Nitesh K. 2014. Immunotoxicity of Lambda-Cyhalothrin in Wistar Albino Rats. *Int J Toxicol Pharmacol Res*, **6**: 47-56.

Çelik A, Mazmanci B, Çamlica Y, Çömelekoğlu U, and Aşkin A. 2005a. Evaluation of cytogenetic effects of lambda-cyhalothrin on Wistar rat bone marrow by gavage administration. *Ecotoxicol Environ Sa*, **61**: 128-133.

Çelik A, Mazmanci B, Çamlica Y, Aşkin A, and Çömelekoğlu Ü. 2005b. Induction of micronuclei by lambda-cyhalothrin in Wistar rat bone marrow and gut epithelial cells. *Mutagenesis*, **20**: 125-129.

Chakravarthi K, Naravaneni R, and Philip GH. 2007. Study of cypermethrin cytogenesis effects on human lymphocytes using in-vitro techniques. *J Appl Sci Environ Manage*, **11**: 77 - 81.

Chandna S, Dwarakanath BS, Seth RK, Khaitan D, Adhikari JS, and Jain V. 2004. Radiation responses of Sf9, a highly radioresistant lepidopteran insect cell line. *Int J Radiat Biol*, **80**: 301-315.

Cheng IC, Lee HJ, and Wang TC. 2009. Multiple factors conferring high radioresistance in insect Sf9 cells. *Mutagenesis*, **24**: 259-269.

Collins AR. 2004. The comet assay for DNA damage and repair. *Mol. Biotechnol*, **26**: 249-261.

Collins AR, El Yamani N, Lorenzo Y, Shaposhnikov S, Brunborg G, and Azqueta A. 2014. Controlling variation in the comet assay. *Front Genet*, **5**:1-5.

Collins AR, Oscoz AA, Brunborg G, Gaivão I, Giovannelli L, Kruszewski M, Smith CC, and Štětina R. 2008. The comet assay: topical issues. *Mutagenesis*, **23**: 143-151.

Deeba F, Raza I, Muhammad N, Rahman H, ur Rehman Z, Azizullah A, Khattak B, Ullah F, and Daud MK. 2017. Chlorpyrifos and lambda cyhalothrin-induced oxidative stress in human erythrocytes: *in vitro* studies. *Toxicol Ind Health*, **33**: 297-307.

Fetoui H, Feki A, Salah GB, Kamoun H, Fakhfakh F, and Gdoura R. 2015. Exposure to lambda-cyhalothrin, a synthetic pyrethroid, increases reactive oxygen species production and induces genotoxicity in rat peripheral blood. *Toxicol Ind Health*, **31**: 433-441.

Gaivão I and Sierra LM. 2014. Drosophila comet assay: insights, uses, and future perspectives. *Front Genet*, **5**:1-8.

García O, Mandina T, Lamadrid AI, Diaz A, Remigio A, Gonzalez Y, Piloto J, Gonzalez JE and Alvarez A. 2004. Sensitivity and variability of visual scoring in the comet assay: results of an inter-laboratory scoring exercise with the use of silver staining. *Mutat Res Genet Toxicol Environ Mutagen*, **556**: 25-34.

Garcia O, Romero I, González JE and Mandina T. 2007. Measurements of DNA damage on silver-stained comets using free Internet software. *Mutat Res Genet Toxicol Environ Mutagen*, **627**: 186-190.

- García O, Romero I, González JE, Moreno DL, Cuétara E, Rivero Y, Gutiérrez A, Pérez CL, Álvarez A, Carnesolta D and Guevara I. 2011. Visual estimation of the percentage of DNA in the tail in the comet assay: Evaluation of different approaches in an intercomparison exercise. *Mutat Res Genet Toxicol Environ Mutagen*, **720**: 14-21.
- Giner M, Avilla J, Balcells M, Caccia S, and Smagghe G. 2012. Toxicity of allyl esters in insect cell lines and in *Spodoptera littoralis* larvae. *Arch Insect Biochem*, **79**: 18-30.
- Hamdani DA, Javeed A, Ashraf M, Nazir J, Ghafoor A, and Altaf I. 2014. *In vitro* cytotoxic and genotoxic evaluation to ascertain toxicological potential of ketoprofen. *Afr J Pharm Pharmacol*, **8**: 386-391.
- Ivanov A, Cragg MS, Erenpreisa J, Emzinh D, Lukman H, and Illidge TM. 2003. Endopolyploid cells produced after severe genotoxic damage have the potential to repair DNA double-strand breaks. *J Cell Sci*, **116**: 4095-4106.
- Kim CW, Go RE, and Choi KC. 2015. Treatment of BG-1 ovarian cancer cells expressing estrogen receptors with lambda-cyhalothrin and cypermethrin caused a partial estrogenicity via an estrogen receptor-dependent pathway. *Toxicol Res*, **31**:331-337.
- Kurt D and Kayaş T. 2015. Effects of the pyrethroid insecticide deltamethrin on the hemocytes of *Galleria mellonella*. *Turk J Zool*, **39**: 452-457.
- Mohanty G, Mohanty J, Dutta SK, and Jena SD. 2011. Genotoxicity testing in pesticide safety evaluation. , Pesticides in the Modern World - Pests Control and Pesticides Exposure and Toxicity Assessment. *Intech Open Access Publisher*, **614**: 403-426.
- Muranli FDG and Güner U. 2011. Induction of micronuclei and nuclear abnormalities in erythrocytes of mosquitofish (*Gambusia affinis*) following exposure to the pyrethroid insecticide lambda-cyhalothrin. *Mutat Res Genet Toxicol Environ Mutagen*, **726**: 104-108.
- Muranli FDG. 2013. Genotoxic and cytotoxic evaluation of pyrethroid insecticides λ -cyhalothrin and α -cypermethrin on human blood lymphocyte culture. *Bull Environ Contam Toxicol*, **90**: 357-363.
- Nadin SB, Vargas-Roig LM and Ciocca DR. 2001. A silver staining method for single-cell gel assay. *J Histochem Cytochem*, **49**: 1183-1186.
- Nagy K, Rác G, Matsumoto T, Ádány R, and Ádám B. 2014. Evaluation of the genotoxicity of the pyrethroid insecticide phenothrin. *Mutat Res Genet Toxicol Environ Mutagen*, **770**: 1-5.
- Nandhakumar S, Parasuraman S, Shanmugam MM, Rao KR, Chand P, and Bhat BV. 2011. Evaluation of DNA damage using single-cell gel electrophoresis (Comet Assay). *J Pharmacol Pharmacother*, **2**: 107-111.
- Naravani R and Jamil K. 2005. Evaluation of cytogenetic effects of lambda-cyhalothrin on human lymphocytes. *J Biochem Mol Toxicol*, **19**: 304-310.
- Ostling G and Johanson KJ. 1984. Micro electrophoretic study of radiation-induced DNA damages in individual mammalian cells. *Biochem Biophys Res Commun*. **123**: 291-298.
- Packiam SM, Emmanuel C, Baskar K, and Ignacimuthu S. 2015. Feeding deterrent and genotoxicity analysis of a novel phytopesticide by using comet assay against *Helicoverpa armigera* (Hübner)(Lepidoptera: Noctuidae). *Braz Arch Biol Techn*, **58**: 487-493.
- Remington SE. 2010. Cellular response to DNA damage after exposure to organophosphates *in vitro* (Doctoral dissertation, Newcastle University).
- Saleem U, Ejaz S, Ashraf M, Omer MO, Altaf I, Batool Z, Fatima R and Afzal M. 2014. Mutagenic and cytotoxic potential of Endosulfan and Lambda-cyhalothrin—*In vitro* study describing individual and combined effects of pesticides. *Int J Environ Sci*, **26**: 1471-1479.
- Saleh M.2011. The effect of insecticides on insect cell culture *in vitro*. MSc dissertation, Damascus University, Syria.
- Sasaki YF, Nakamura T, and Kawaguchi S. 2007. What is better experimental design for *in vitro* comet assay to detect chemical genotoxicity? *AATEX*, **14**: 499-504.
- Shaurub ESH and El-Aziz NMA. 2015. Biochemical effects of lambda-cyhalothrin and lufenuron on *Culex pipiens* L. (Diptera: Culicidae). *Int J Mosq Res*, **2**: 122-126.
- Shen XM, Liao CY, Lu XP, Wang Z, Wang JJ, and Dou W. 2016. Involvement of three esterase genes from *Panonychus citri* (McGregor) in fenpropathrin resistance. *Int J Mol Sci*, **17**:1-15.
- Singh NP, McCoy MT, Tice RR, and Schneider EL. 1988. A simple technique for quantitation of low levels of DNA damage in individual cells. *Exp Cell Res*, **175**: 184-191.
- Tukhtaev K, Tulemetov S, Zokirova N, and Tukhtaev N. 2012. Effect of long term exposure of low doses of lambda-cyhalothrin on the level of lipid peroxidation and antioxidant enzymes of the pregnant rats and their offspring. *J Res Health Sci*, **13**: 93-99.
- Tuncbilek AS, Kilicoglu H, Yazici N, Ozcan S, Erel Y, Canpolat U, Yay A and Bakir S. 2011. Detection of DNA Damage in *Ephesia kuehniella* by single cell gel electrophoresis after exposure to gamma radiation. *Ann Univ Craiova Agr, Montanology, Cadastre Series*, **41**: 266-269.
- U.S. EPA. **Environmental Protection Agency**. 2012. Office of Pesticide Programs: Chemicals Evaluated for Carcinogenic Potential, Annual Cancer Report.
- Vaughn J L, Goodwin R H, Tompkins G J and McCawley P. 1977.The Establishment Of Two Cell Lines From The Insect *Spodoptera Frugiperda* (Lepidoptera; Noctuidae). *In vitro*, **13**: 213- 217.
- Velmurugan B, Ambrose T, and Selvanayagam M. 2006. Genotoxic evaluation of lambda-cyhalothrin in *Mystus gulio*. *J Environ Biol*, **27**: 247-250.
- Zhang Q, Wang C, Sun L, Li L, and Zhao M. 2010. Cytotoxicity of lambda-cyhalothrin on the macrophage cell line RAW264.7. *J Environ Sci*, **22**: 428-432.

Protective effect of amino acid, Glycine in broilers fed on Imidacloprid treated rations

Enas, A. Abbas^{1,*}, Amany, M. Salama¹, Fayza, A., Sdeek², Eman, I. M. Ismail³, Abdalla, S. H.⁴, Elshorbagy, I. M.⁵, Abd EL Rahman, T. A.²

¹Department of Biochemistry, Toxicology Unit, Animal Health Research Institute (AHRI), Agriculture Research Center (ARC), Egypt

²Department of Pesticide Residue, Central Agricultural Pesticides Laboratory (CAPL), Agriculture Research Center (ARC), Egypt

³Department of Biochemistry, Zagazig Provincial Laboratory, Animal Health Research Institute (AHRI), Agriculture Research Center (ARC), Egypt;

⁴Department of Pathology, Zagazig Provincial Laboratory, Animal Health Research Institute (AHRI), Agriculture Research Center (ARC), Egypt;

⁵Department of Food Hygiene, Zagazig Provincial Laboratory, Animal Health Research Institute (AHRI), Agriculture Research Center (ARC), Egypt.

Received: May 29, 2020; Revised: July 25, 2020; Accepted: August 7, 2020

Abstract

Broiler chicks were segregated into three groups. Group 1 fed on a basal diet and served as a control, group 2 was given Imidacloprid (IM) at a dose of 50 mg/kg diet and group 3 was dietary supplemented with 0.5 % Glycine (GLY) and IM (50 mg/kg diet) for 4 weeks. Blood and tissue samples were collected on the 7th, 14th, 21st, and 28th days. The obtained findings revealed that IM residues were beyond the maximum residue limit (MRL) (0.02 ppm) and were significantly higher in muscles ranging from 0.042±0.0039 to 0.073±0.0026 ppm and in liver tissues ranging from 0.466±0.033 to 0.790±0.017 ppm throughout the experimental time interval in IM- treated chicks. IM induced a significant decline in the total erythrocytic count (TEC), packed cell volume (PCV), mean corpuscular volume (MCV), hemoglobin (Hb), mean corpuscular hemoglobin (MCH), mean corpuscular hemoglobin concentration (MCHC), total leucocytic counts (TLC) and lymphocyte percent. IM- treated chicks exhibited a significant reduction in the levels of serum acetylcholinesterase (AChE). Besides, the hepatic antioxidants activities [(superoxide dismutase (SOD), catalase (CAT) and reduced glutathione (GSH)] were significantly decreased. A significant increase in the levels of serum alanine aminotransferase (ALT), aspartate aminotransferase (AST), alkaline phosphatase (ALP), uric acid, creatinine, hepatic lipid peroxide malondialdehyde (MDA), heterophils and monocyte percent were observed in IM-treated chicks. Furthermore, IM induced a significant histopathological lesions in the liver, kidney and muscles. Conclusively, GLY supplementation inhibited IM accumulation. Therefore, IM residues were not detected in muscles, while ranging from (0.250±0.029 to 0.553±0.023) ppm in liver tissues of GLY and IM- treated chicks. Dietary GLY improved liver and kidney function and ameliorated hematological alterations, neurotoxicity, oxidative stress and histopathological lesions induced by IM.

Keywords: broiler chickens, imidacloprid, glycine, toxicity, histopathology.

1. Introduction

Neonicotinoids represent high selective toxicity to insect over vertebrate nicotinic acetylcholine receptors (nAChRs) (Matsuda Ihara, and Sattelle, 2020). Birds are potentially exposed to neonicotinoid insecticides by ingestion of coated seeds during crop planting (Bean *et al.*, 2019). Neonicotinoids have direct and indirect effects on birds through the food chain. Imidacloprid acts in the same systemic manner as other neonicotinoids. Using imidacloprid as seed treatments induces oxidative stress and poses risks to small birds (Gibbons *et al.*, 2015). Imidacloprid caused sub-lethal effects such as altered biochemical parameters in birds fed insecticide-treated wheat, at the recommended dose (Lopez-Antia *et al.*, 2013).

The histopathology of the liver of imidacloprid intoxicated mice revealed mild focal necrosis with swollen

cellular nuclei, hypertrophied blood vessels, and cytoplasmic lesions in hepatocytes, and in kidneys showed degeneration of the tubules and glomerulus (Arfat *et al.*, 2014). Imidacloprid administration at different doses in female albino mice revealed leucocytic infiltration, congestion, and dilated sinusoids, distorted central vein filled with blood in the liver (Ajay *et al.*, 2014).

The benefits of Gly supplementation during the grower period are limited as other protein related nutrients become limiting at 17.7% curd protein. Supplementation of 0.713% Gly in the grower period increased body weight gain and reduced feed conversion ratio (Hilliari *et al.*, 2020). Low protein diets are typically glycine deficient and produce poor performance. Supplementing the diet with Gly or precursors of Gly can overcome this deficiency (Hilliari *et al.*, 2019). Among the non-essential amino acids, the only amino acid glycine could potentially improve inferior performance in broilers. Glycine is important in amino acid metabolism of growing chicks and

* Corresponding author e-mail: abbasenas@gmail.com.

significantly affect serum uric acid (Awad et al., 2017). Glycine with other amino acids is involved in several crucial metabolic functions such as synthesis of creatine, haem, glutathione, and the essential synthesis of uric acid for excretion of any excess nitrogen. Glycine is a component of uric acid molecule and is directly involved in the synthesis of uric acid by providing two carbons and one nitrogen atom (Corzo, 2012).

The present study was designed to evaluate the possible effects of glycine supplementation on hematological, biochemical, and histopathological alterations associated with oxidative stress and hepato-renal disorder induced by imidacloprid toxicity in broiler chicks.

2. Materials and Methods

2.1. Imidacloprid

Imidacloprid (99.5% w/w) was manufactured by Payer Crop Science AG. R&D SIM - RT- Analytics, Frankfurt, Germany. Its molecular formula is $C_9H_{10}ClN_5O_2$, and its molecular weight is 255.7 g/M. It was diluted in distilled water to obtain the desired concentrations and mixed with diet.

2.2. Glycine

Glycine is a white, sweet-tasting crystalline solid. It is one of the simplest proteinogenic amino acids. It was obtained from El Nasr Pharmaceuticalchemicals Co. Adwic, Pure lab. Chemicals. The molecular formula of glycine is NH_2-CH_2-COOH . It has no D- or L-configuration because a single hydrogen atom is attached

to the α -C-atom where a side chain is attached for most other amino acids.

2.3. Experimental design

Broiler ration obtained from AL-Aman Foundation, Abou- Kabeer, El-Sharkya Governorate (Table 1). Diet formulation is based on nutrient requirements by Natural Resources Conversion Service (NRCS, 2003). Sixty unsexed Ross broiler chick aged one day old obtained from a local hatchery were randomly segregated into three groups (20 chicks/ pen). One day old chicks were vaccinated against Newcastle Disease (ND) and Infectious Bronchitis (IB). The chicks were reared under strict hygienic conditions in accordance with the guidelines for the care and use of experimental animals. The birds were provided with standard feed and clean water *ad libitum* and were acclimatized for 10 days prior to the experiment. The ambient temperature was 25 °C, and relative humidity was 45–55 percent, with 12 h each of dark and light cycles. The temperature of the animal house was maintained between 21-31 °C throughout the experiment.

2.4. Diets

Group1: fed on the basal diet (Table 1) and served as the control group;

Group 2: fed on the basal diet + imidacloprid at a dose of 50 mg/kg diet daily according to Ravikanth, *et al.* (2018).

Group 3: fed on the basal diet + 0.5 % glycine diet according to Hofmann *et al.* (2010) + imidacloprid at a dose of 50 mg/kg diet.

The experiment was carried out for 4 weeks. The birds were monitored for clinical signs, if any.

Table 1. Composition of the experimental basal diets

Starter- diet			Finisher grower diet		
Ingredients	Chemical composition	%	Ingredients	Chemical composition	%
Yellow corn 54.00	Protein	> 21%	Yellow corn 54.00	Protein	>19%
Soybean meal(44% Cp)	Fat	> 3.92%	Soybean meal (46% Cp)	Fat	>6.22%
Yellow corn gluten (60%)	Fibers	< 3.26%	Yellow corn gluten (60%)	Fibers	< 3.06%
Soybean oil	Energy	> 2000 K.K.	Soybean oil	Energy	> 2100 K.K.
Dicalcium Phosphate			Dicalcium Phosphate		
Limestone			Limestone		
NaCl			NaCl		
Vit+Min mix (1826)			Vit+ Min mix (1826)		
Sodium bicarbonate			Sodium bicarbonate		
DL-methionine			DL-methionine		
L-Lysine hydrochloride			L-Lysine hydrochloride		

2.5. Sampling

Serum and tissue samples were collected from birds in each group at the end of the 7th, 14th, 21st, and 28th day. Before sacrificing and drawing blood samples, birds were fasted for 2 h. Blood samples were collected from wing vein into heparinized and non-heparinized tubes. Heparinized blood was used for complete blood count. Non-heparinized blood samples were incubated at 37 °C until the blood clotted then the samples were centrifuged at 3000 r. p. m. for 15 minutes and the clear supernatant serum was separated carefully and stored at -20 °C for biochemical analysis. Birds were sacrificed by cervical

dislocation and samples of liver, kidneys, and muscle tissue samples were collected.

2.6. HPLC analysis

The ration was analyzed prior to treatments. Muscle, liver, and kidney samples were collected from birds of all groups. The cleaned and acidified extracts were transferred into auto-sampler vials and used for HPLC analysis as described in section 2.6.2. below.

2.6.1. Extraction /Partitioning

10 g of the comminuted homogenous and frozen muscles and liver samples were weighed into a 50 mL centrifuge tube, 10 mL acetonitrile and the potential

internal standard (ISTD) solution (e.g. 100 µL of an ISTD) were added and the tube was closed and shaken vigorously by hand for 1 minute. After that, a mixture of 4 g magnesium sulfate anhydrous (MgSO₄), 1g sodium chloride (NaCl), 1g Disodium hydrogencitrate sesquihydrate (Na₃ H Citrate sesquihydrate) (e.g. Aldrich 359084 or Fluka 71635) was added. The tube was closed and shaken vigorously by hand for 1 minute and centrifuged for 5 minutes at 3000 U/min.

2.6.2. Dispersive solid-phase extraction (SPE)

An aliquot of the extract is transferred into a PP-single use-centrifuge tube which contains 25 mg primary-secondary amine (PSA) and 150 mg MgSO₄ per mL extract (e.g.: for 8 mL extract 200 mg PSA and 1.2 g MgSO₄ was needed). The tube is shaken for 30 s and centrifuged (e.g. for 5 min 3000 U/min. After centrifugation, the cleaned extract is transferred into a screw cap vial, and pH is quickly adjusted to ca. 5 by adding a 5% formic acid solution in acetonitrile (v/v) (pro mL extract ca.10 µL). The cleaned and acidified extracts are transferred into auto-sampler vials and used for IM determination by the HPLC technique. HPLC analysis was performed with an Agilent 1100 HPLC system (USA), with a quaternary pump, the manual injector (Rheodyne), thermostat compartment for the column, and photodiode array detector according to (Anastassiades *et al.*, 2003). The chromatographic column was C18 Zorbax XDE (250 mm x 4.6 mm, 5 µm). The column was kept at room temperature. The flow rate of the mobile phase (acetonitrile/water = 80/20. v/v) was 0.8 mL/min., and the injection volume was 20 µL. The detection wavelength was set at 270 nm. The retention time was about 4.064 min. Residues were estimated by comparison of peak area of standards with that of the unknown or spiked samples run under identical conditions.

2.7. Evaluation of hematological parameters

Heparinized blood was used to determine total erythrocytic count (TEC). Packed cell volume (PCV), mean corpuscular volume (MCV), mean corpuscular hemoglobin (MCH), mean corpuscular hemoglobin concentration (MCHC), total leucocytic counts (TLC), differential count of leukocytes such as lymphocyte (%), heterophil (%), monocyte (%), basophil% and eosinophil (%) were estimated according to Feldman *et al.* (2000). Hemoglobin (Hb) concentration analysis was performed as described by Fairbanks and Klee (1987).

2.8. Serum Biochemical assay

Serum samples were used for biochemical analysis by UV/VIS Spectrophotometer Jasco Model 7800 using Biodignostic Kits, Cairo, Egypt. Alanine aminotransferase (ALT) aspartate aminotransferase (AST) assay is based on measuring the keto acids pyruvate or oxaloacetate formed in its derivative form, 2,4- dinitrophenylhydrazine according to Sahoo *et al.* (2014). Alkaline phosphatase (ALP) assay is based on estimating the liberated phenol colorimetrically in the presence of 4- aminophenazone and potassium ferricyanide according to Sahoo *et al.* (2014). Serum creatinine forms a colored complex with picrate in an alkaline medium and was determined according to Bogin and Keller (1987), and serum uric acid assay is based on reactions catalyzed by Uricase and Peroxidase and formation of Colored quinoneimine according to

Fosati *et al.* (1980). Serum acetylcholinesterase (AChE) activity was measured via spectrophotometer according to Ellman *et al.* (1961). This method can be accomplished by using acetylthiocholine iodide as substrate (1 mM final concentration of acetylthiocholine iodide) for measuring cholinesterase activities.

2.9. Hepatic antioxidants and lipid peroxides assay

Birds were sacrificed and the liver was rapidly removed and stored at -20 °C for estimation of antioxidants concentration separately weighed, cut into small pieces, and homogenized in an ice-cold isotonic physiological saline solution at a concentration of 0.1g/mL. The homogenates were centrifuged at 3500 rpm for 10 min at -4 °C and the supernatant was obtained and used for estimation of enzymatic and non-enzymatic antioxidant activities and lipid peroxidation by spectrophotometric methods. The assay of superoxide dismutase (purple color SOD) activity is based on the capacity of pyrogallol to autoxidize, a process highly dependent on a substrate for SOD according to (Bannister and Calabrese, 1987). The antioxidative enzyme catalase was evaluated by the reaction with a known quantity of H₂O₂. In the presence of peroxidase (HRP), remaining H₂O₂ reacts with 3,5-Dichloro -2-hydroxybenzene sulfonic acid (DHBS) and 4-aminophenazone (AAP) to form a chromophore with a color intensity inversely proportional to the amount of catalase in the original sample (Aebi,1984), reduced glutathione (GSH) was determined in tissue supernatant by a colorimetric method described by Lin Hu *et al.* (1988). Lipid peroxide formation was determined as malondialdehyde (MDA) that react with thiobarbituric acid (TBA) in acidic medium at temperature of 95°C for 30 min to form thiobarbituric acid reactive product the absorbance of the resultant pink product was measured at 534 nm according to Jentzsch, *et al.* (1996) using kits of Biodiagnostic Cairo, Egypt.

2.10. Histopathological Studies

Tissue slices of liver, kidneys, and muscles from all groups were taken on 14th and 28th days post-treatment (PT) and fixed in 10 % neutral buffered formalin (NBF) solution then dehydrated, cleared and embedded in paraffin wax. Tissue sections of 4-5 micron thickness were prepared and stained with Hematoxyline and Eosin stain (H&E) and examined microscopically (Survarna *et al.*, 2013).

2.11. Statistical analysis

Data were statistically analyzed using analyses of variance (F-test) followed by Duncan's multiple range test. A probability at a level of 0.05 or less was considered significant. Standard errors were also estimated using international business machine statistical package for social sciences (IBM SPSS) statistics program version 20.

3. Results

3.1. Pesticide residue

Starter diet and grower diet were tested before the experiment and the diets were imidacloprid free. IM residues were not detected in muscles and liver from the control group as well as in muscles from the third group treated with imidacloprid and glycine throughout all time

intervals. Imidacloprid residues were above the MRL in the liver from second and third groups and muscles of broiler chicks from second group. Imidacloprid residue was significantly higher in muscles and liver tissues of chicks from the second group treated with imidacloprid

only in comparison to the control group. However, glycine in combination with imidacloprid provoked a significant decline in IM accumulation in liver and muscle tissues (**Table 2**).

Table 2: Imidacloprid residue in tissues in mg/kg (ppm) of broilers received dietary Imidacloprid (50 mg/kg) with or without glycine (0.5%).

Samples	Groups		Control	Imidacloprid	Imidacloprid + Glycine	MRLs (Codex, 2003)
	Days					
Residues (mg/kg)	Muscles	7 th	ND a	0.042±0.0039 b	ND a*	0.02 ppm
		14 th	ND a	0.049±0.0010 b	ND a	
		21 st	ND a	0.055±0.0029 b	ND a	
		28 th	ND a	0.073±0.0026 b	ND a	
	Liver	7 th	ND a	0.466±0.033 b	0.250±0.029 c	0.02 ppm
		14 th	ND a	0.643±0.024 b	0.293±0.017 c	
		21 st	ND a	0.757±0.020 b	0.482±0.011c	
		28 th	ND a	0.790±0.017 b	0.553±0.023 c	

Data were represented as means of samples±SE. Means in the same row with different superscripts ^{a, b, c} are significantly different (Duncan multiple range test $P < 0.05$). * ND=Not Detected

3.2. Hematological study

Hematological observations revealed a significant decrease ($p < 0.05$) in mean values of TEC, Hb, PCV, MCV, MCH, MCHC, TLC, and lymphocytes %. On the other hand, IM induced a significant increase ($p < 0.05$) in heterophils % throughout all time intervals and in monocytes % on the 28th day of the experiment in the IM – treated group in comparison to the control group. These effects were significantly suppressed by glycine supplementation in the third group (**Table 3**).

3.3. Neurotoxicity and hepatorenal toxicity

Biochemical assays revealed that IM induced a significant ($p < 0.05$) inhibition in serum AChE in the second group which was relieved by glycine in the third group on the 7th, 14th, and 28th days of treatments. However, imidacloprid induced significant elevations in serum ALT, AST, uric acid, and creatinine ($p < 0.05$) in broilers received imidacloprid alone in the second group and which were significantly attenuated by glycine supplementation in the third group at all time intervals. In addition, IM evoked a significant increase in the levels of serum ALP on the 21th and 28th days of treatment which was significantly ameliorated by glycine on the 28th day of treatment (**Table 4**).

3.4. Oxidative stress

IM induced a significant reduction in the levels of hepatic CAT and GSH concentrations on the 7th, 21st, and 28th days of treatment that was significantly ameliorated on the 21st and 28th days in the third group. Nevertheless, imidacloprid induced a significant decrease in SOD activity ($P < 0.05$), while evoked a significant increase ($P < 0.05$) in lipid peroxide (MDA) at all time intervals that was significantly mitigated by glycine supplementation in the third group. and SOD (**Table 5**).

3.5. Clinical Signs

Chicks given dietary imidacloprid showed clinical signs as depression, decreased appetite, reduced feed intake, watery diarrhea, muscle tremors, ataxia and sitting on hocks.

3.6. Histopathology

Liver sections of chicks treated with IM (50 mg/kg ration) for two weeks revealed degeneration of hepatocytes with mild fatty change (Fig.A), marked dilation and congestion of blood vessels (Fig.B). Kidney showed hydropic degeneration with infiltration of inflammatory cells (Fig.C), and muscles did not reveal pathological changes after two weeks.

After four weeks of administration, the liver showed coagulative necrosis of hepatocytes accompanied by mild infiltration of inflammatory cells (Fig.D). The kidney slices revealed degeneration of tubular epithelial cells and congestion of renal blood vessels (Fig.E). Muscle tissue sections revealed inflammatory cells. (Fig.F).

Chicks were treated with imidacloprid 50 mg/kg ration and glycine 0.5% of ration after two weeks, the liver showed dilated, congested blood vessels and was surrounded by inflammatory cells infiltration (Fig.G), kidney showed hydropic degeneration in addition to inflammatory cells infiltration (Fig.H), muscles did not reveal pathological changes after two weeks, while after four weeks of administration liver showed hydropic degeneration with infiltration of few inflammatory cells (Fig.I), kidney showed mild vacuolar degeneration of tubular epithelium and few congested blood capillaries (Fig.J), and muscles showed few infiltrations of inflammatory cells around blood vessels (Fig.K).

Table 3: Effect of Imidacloprid (50 mg/kg diet) with or without glycine (0.5%) on some hematological indices of broiler chicks on 7th, 14th, 21st, and 28th days of treatments.

Parameters	Groups	Time	Control	Imidacloprid	Imidacloprid + Glycine
TEC (10 ⁶ /μL)		7 th day	2.26± 0.01a	1.66±0.06 b	2.21±0.02 a
		14 th day	2.72± 0.06 a	1.69± 0.05 b	2.56± 0.09 a
		21 st day	2.80± 0.02 a	1.76± 0.06 a	2.58± 0.09 a
		28 th day	2.85± 0.04 a	1.86± 0.02 b	2.77± 0.003 a
Hb (g/dL)		7 th day	9.67±0.09 a	7.50±0.12 b	9.73± 0.15 a
		14 th day	10.73±0.12 a	9.87±0.09b	10.23±0.18c
		21 st day	11.07±0.07a	8.27±0.22b	10.50±0.21a
		28 th day	11.40±0.12 a	9.53±0.03 b	10.73±0.17c
PCV (%)		7 th day	30.47±0.26 a	22.80±0.10 b	25.79±0.15 c
		14 th day	31.04±0.09 a	26.60±0.30 b	27.83±0.17 c
		21 st day	31.47±0.09 a	27.37±0.27 b	28.33±0.38 c
		28 th day	32.30±0.46 a	27.40±0.78 b	31.46±0.10 a
MCV (fL)		7 th day	120.90± 0.45 a	111.12 ±0.89 b	112.33± 0.33 b
		14 th day	121.53± 0.29 a	111.57±0.72b	112.93± 0.23b
		21 st day	121.03± 0.03 a	111.83±0.81 b	113.40± 0.06 b
		28 th day	122.17± 0.91 a	111.70±0.81 b	114.80± 0.56 c
MCH (pg)		7 th day	40.37±0.23 a	38.87± 0.09 b	38.89± 0.07b
		14 th day	41.29±0.29 a	39.02± 0.04 b	39.83± 0.16c
		21 st day	41.67±0.28 a	39.47± 0.12 b	39.93± 0.17 b
		28 th day	43.17±0.49 a	32.87± 0.26 b	40.30± 0.05 c
MCHC (g/dL)		7 th day	32.57± 0.30 a	31.53± 0.29 b	33.63±0.20 c
		14 th day	34.70± 0.12 a	32.63± 0.09 b	34.67± 0.17a
		21 st day	35.33± 0.15 a	32.93± 0.02 b	34.97± 0.12 a
		28 th day	37.57± 0.44 a	34.63± 0.38 b	35.83± 0.28 c
TLC (10 ³ / μL)		7 th day	23.23± 0.62 a	20.57± 0.27 b	25.10±0.61a
		14 th day	36.47± 0.83 a	21.87± 0.45 b	26.47±0.74 c
		21 st day	37.09± 0.11a	21.77± 0.54 b	27.90±0.55 c
		28 th day	37.60± 0.21a	23.47± 0.49 b	35.40±0.46c
Heterophils (%)		7 th day	34.00± 0.58 a	99.67± 0.33 b	35.47±0.86 a
		14 th day	32.83± 0.17a	99.33± 0.30 b	32.67±0.33 a
		21 st day	32.17± 0.34 a	99.33± 0.67b	33.00±0.13 a
		28 th day	24.27± 0.40a	89.77± 0.60 b	32.10±0.31c
Lymphocytes (%)		7 th day	66.00± 0.58 a	0.33± 0.02 b	64.53±0.29 a
		14 th day	67.17± 0.17a	0.66± 0.03 b	67.33±0.23 a
		21 st day	75.83± 0.28a	0.67± 0.17b	67.00±0.68c
		28 th day	75.40± 0.57a	0.93± 0.10 b	66.30±0.91 c
Monocytes (%)		7 th day	0± 0 a	0± 0 a	0± 0 a
		14 th day	0± 0 a	0± 0 a	0± 0 a
		21 st day	0± 0 a	0± 0 a	0± 0 a
		28 th day	0.1± 0.06 a	9.00± 1.69 b	0.37± 0.09a
Eosinophils (%)		7 th day	0± 0 a	0± 0 a	0± 0 a
		14 th day	0± 0 a	0.33± 0.09 a	0± 0 a
		21 st day	0± 0 a	0± 0 a	0± 0 a
		28 th day	0.20± 0.13 a	0.28± 0.14 a	0± 0 a
Basophils (%)		7 th day	0± 0 a	0± 0 a	0± 0 a
		14 th day	0± 0 a	0± 0 a	0± 0 a
		21 st day	0± 0 a	0± 0 a	0± 0 a
		28 th day	0± 0 a	0± 0 a	0± 0 a

Data were represented as means of samples±SE. Means in the same row with different superscripts ^{a,b,c} are significantly different (Duncan multiple range test P < 0.05).

Table (4): Effect of Imidacloprid (50 mg/kg diet) with or without glycine (0.5%) on some biochemical parameters in the serum of broiler chicks on 7th, 14th, 21st, and 28th days of treatments.

Parameters	Groups		Control	Imidacloprid	Imidacloprid + Glycine
	Days				
Ach E(U/L)	7 th day		1451.27±21.86 a	1311.04±6.35 b	1406.67±3.33a
	14 th day		1556.27±0.02a	1455.00±18.01b	1534.73±17.41a
	21 st day		1696.96±34.19a	1556.07±2.49 ab	1620.80±17.79ab
	28 th day		1832.50±33.80a	1588.50±17.70 b	1707.50±31.70 c
ALT(IU/L)	7 th day		10.45±0.25 a	17.92±0.13 b	13.93±0.46 c
	14 th day		13.38±0.36 a	19.90±0.49 b	14.85±0.20 c
	21 st day		15.81±0.38 a	22.35±0.20 b	16.75±0.19 a
	28 th day		17.12±0.48 a	24.16±0.32 b	18.78±0.21 c
AST (U/L)	7 th day		38.97±0.58 a	108.08±0.65 b	89.33±0.67 c
	14 th day		48.60±0.70 a	118.26±0.32 b	92.08±0.54 c
	21 st day		76.83±0.60 a	123.50±0.29 b	105.93±0.12 c
	28 th day		78.67±0.88 a	122.72±0.43 b	107.13±0.30 c
ALP (mmol/L)	7 th day		1.58±0.06 a	1.57±0.03 a	1.52±0.06 a
	14 th day		1.62±0.06 a	1.73±0.03 a	1.54±0.09 a
	21 st day		1.67±0.04 a	1.82±0.04 ab	1.72±0.02 ab
	28 th day		1.75±0.02 a	1.89±0.05 b	1.76±0.01 a
Uric acid (mg/dL)	7 th day		2.53±0.19 a	5.50±0.28 b	4.48±0.28 c
	14 th day		3.79±0.15 a	6.80±0.10 b	5.47±0.26 c
	21 st day		4.33±0.24 a	7.80±0.10 b	5.98±0.07 c
	28 th day		5.34±0.28 a	9.12±0.13 b	6.18±0.12 c
Creatinine (mg/dL)	7 th day		0.21±0.01 a	0.88±0.04 b	0.37±0.03 c
	14 th day		0.23±0.01 a	0.79±0.15 b	0.93±0.04 a
	21 st day		0.25±0.01 a	1.08±0.16 b	0.52±0.09 a
	28 th day		0.27±0.01 a	1.43±0.06 b	0.51±0.05 c

Data were represented as means of samples±SE. Means in the same row with different superscripts ^{a, b, c} are significantly different (Duncan multiple range test $P < 0.05$).

Table 5: Effect of Imidacloprid (50 mg/kg diet) with or without glycine (0.5%) on hepatic antioxidants activity and lipid peroxidation in broilers on 7th, 14th, 21st, and 28th days of treatments.

Parameter	Groups		Control	Imidacloprid	Imidacloprid + Glycine
	Time				
SOD ($\mu\text{mol/ g}$)	7 th day		34.93±0.52 a	27.90±0.46 b	41.34±0.43 c
	14 th day		36.22±0.40 a	28.23±0.62 b	42.18±0.43 c
	21 st day		37.50±0.76 a	29.23±0.39 b	50.11±0.79 c
	28 th day		38.06±0.58 a	30.83±0.33 b	60.41±0.83 c
CAT ($\mu\text{mol / g}$)	7 th day		1.67±0.12 a	1.10±0.11 b	1.16±0.12 b
	14 th day		1.87±0.09 a	1.56±0.33 a	1.73±0.12 a
	21 st day		2.03±0.08 a	1.75±0.07 ab	1.97±0.03 ab
	28 th day		2.16±0.04 a	1.83±0.06 b	2.05±0.03 a
GSH ($\mu\text{mol/ g}$)	7 th day		2.20±0.15 a	1.17±0.16 b	1.97±0.03 a
	14 th day		3.70±0.11 a	2.80±0.15 ab	3.33±0.33 ab
	21 st day		4.57±0.28 a	3.47±0.26 b	4.23±0.23 a
	28 th day		4.91±0.05 a	4.04±0.03 b	4.58±0.12 c
MDA (nmol/ g)	7 th day		6.47±0.75 a	16.66±0.44 b	12.27±0.92 c
	14 th day		7.93±0.52a	18.10±0.55 b	14.61±0.64 c
	21 st day		10.67±0.88 a	18.83±0.62 b	13.22±0.61 c
	28 th day		12.60±0.31 a	19.79±0.44 b	14.48±0.39 c

Data were represented as means of samples±SE. Means in the same row with different superscripts ^{a, b, c} are significantly different (Duncan multiple range test $P < 0.05$).

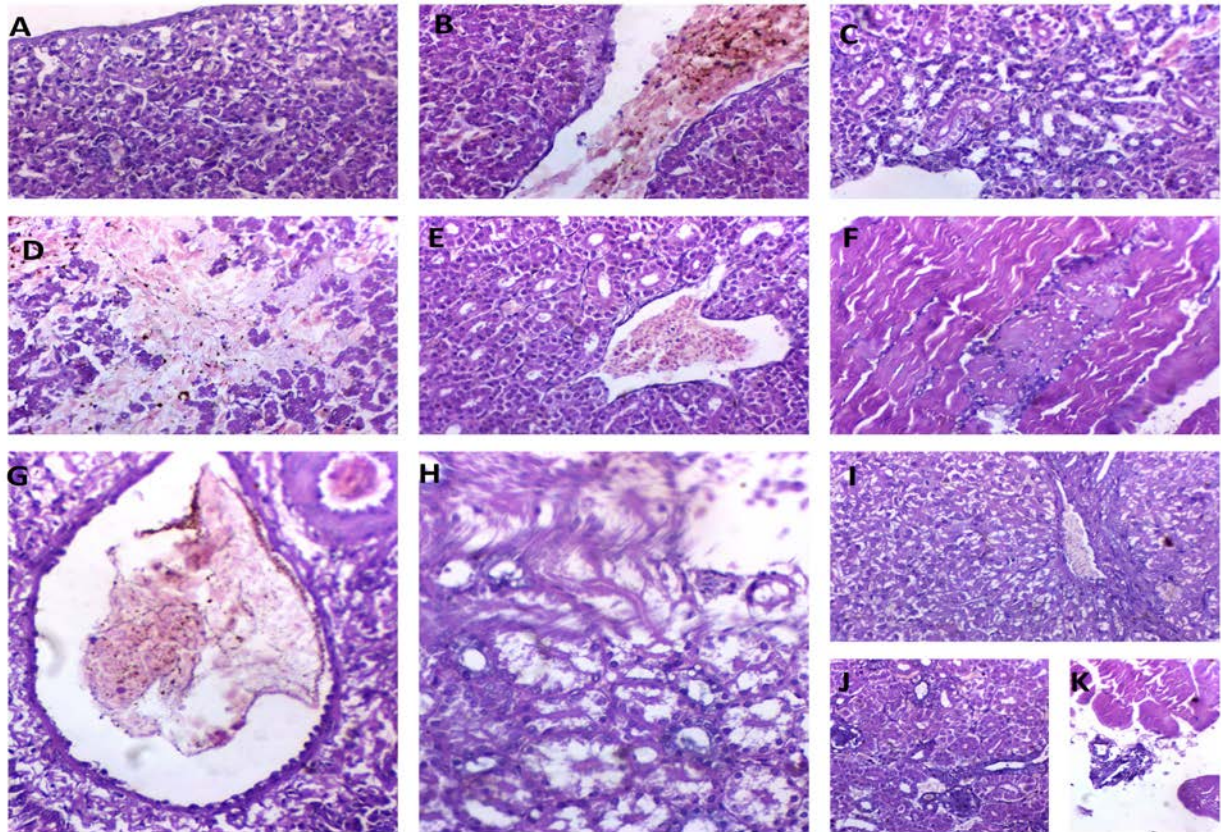


Figure A. Liver sections from second group treated with imidacloprid for two weeks showed degeneration of hepatic cells with mild fatty change (H&EX400).

Figure B. Liver sections from second group treated with imidacloprid for two weeks showed marked dilation and congestion of the central vein (H&EX400).

Figure C. Section of kidney from second group treated with imidacloprid for two weeks showed hydropic degeneration with mild infiltration of inflammatory cells (H&EX400).

Figure D. Section of liver from second group treated with imidacloprid for four weeks showed a focal area of coagulative necrosis of hepatocytes accompanied by mild infiltration of lymphocytes and heterophils. (H&EX400)

Figure E. Section of kidney from second group treated with imidacloprid for four weeks showed degeneration of tubular epithelial cells and congestion of renal blood vessels. (H&EX400)

Figure F. Section of muscle tissue from second group treated with imidacloprid for four weeks showed few infiltrations of inflammatory cells. (H&EX400).

Figure G . Liver section from third group treated with imidacloprid and glycine for two weeks showed dilated, congested blood vessels and mild infiltration of inflammatory cells (H&EX400).

Figure H. Kidney section from third group treated with imidacloprid and glycine for two weeks showed vacuolar degeneration and infiltration of inflammatory cells. (H&EX400)

Figure I. Liver section from third group treated with imidacloprid and glycine for four weeks showed vacuolar degeneration with mild infiltration of inflammatory cells. (H&EX200)

Figure J. Section of kidney from third group treated with imidacloprid and glycine for four weeks showed mild vacuolar degeneration of tubular epithelium and few congested blood capillaries. (H&EX400)

Figure K . Section of muscle from third group treated with imidacloprid and glycine for four weeks showed mild infiltration of inflammatory cells around blood vessels. (H&EX400).

4. Discussion

Imidacloprid is categorized as moderately toxic by the EPA, falling under both toxicity neonicotinoid insecticide class II and class III, (US EPA, 2012). In the present study, imidacloprid residues were above the (Codex, 2003) permissible limit (0.02 ppm) in muscles in group 2 and in liver tissue in group 2 and group 3. In accordance with the present study, Ong *et al.* (2017) observed that imidacloprid showed accumulation during the broiler breeding period and the residues at the end of the treatment period showed increment compared to the beginning of treatment period (Ong *et al.*, 2017). Imidacloprid metabolites found in the feces include glycine conjugate of methylthionicotinic acid accounted for roughly 80% of the administered doses (Tomlin, 2006). The amino acid, glycine (Gly) could be

utilized for attaching to molecules for their excretion (Forman *et al.*, 2009).

In the current study, the decline in the mean values of TEC, Hb, PCV, MCV, MCH, and MCHC could be due to the direct toxic action of IM on bone marrow, liver and kidneys which might play a vital role in hemopoiesis and erythropoietin production in respective organs (Ravikanth *et al.*, 2017). The significant reduction in total leucocytic count in the present study was in line with the findings of Sasidhar Babu *et al.* (2014) in layer chicks. The lymphocytic depletion observed in the present study might be as a result of hemorrhages in the spleen. Imidacloprid insecticide also has deleterious effects immunologically in the broiler chicks targeting the humoral immune responses (Kammon *et al.*, 2012).

Glycine is functional in the biosynthesis of the porphyrin moiety of heme groups (te Braake *et al.*, 2008).

This may explain the improvement of the hemoglobin concentration in group 2.

The neurological signs observed in chicks treated with IM could be correlated to the agonistic action of imidacloprid on nicotinic acetylcholine receptors which could induce neuromuscular paralysis (Tomizawa and Casida, 2005).

The significant reduction in the levels of antioxidant indices and the elevation of lipid peroxidation in the liver tissue in group 2 in the present study were in line with Ganguly (2013) and Ravikanth *et al.* (2018). Superoxide radicals undergo dismutation by the action of superoxide dismutase to hydrogen peroxide, while the hydrogen peroxide formed is converted to water and molecular oxygen by catalase to prevent accumulation in the cell (Halliwell, 2015).

The action of glycine is based on its cytoprotective ability from stress injury. Amino acids such as glycine can lower free radical damage by increasing glutathione production (te Braake *et al.*, 2008).

Imidacloprid exposure induced hepatotoxic and nephrotoxic damage. In addition, there is an obvious correlation between the lesions and plasma biochemical changes (Kammon *et al.*, 2010). In agreement with the current study, Ravikanth, *et al.* (2017) and Sasidhar Babu *et al.* (2014) observed an increased AST activity signifying muscular damage. Elevated ALP activities may be either primary or secondary to damage in the liver and kidneys. Bataille *et al.* (2011) recorded a decline in the active transepithelial uric acid secretion in the renal proximal tubule which may occur due to cellular stress.

In poultry, uric acid pathways are directly or indirectly dependent on glycine and its precursors (Akinde, 2014). Glycine also plays a critical role in uric acid formation for nitrogen excretion in poultry. Glycine addition decreased serum uric acid concentrations in broilers fed 1.35% Lysine (Powell *et al.*, 2009) and increased uric acid excretion (Namroud *et al.* 2010).

Moreover, the hepatic necrosis might be due to oxidative stress induced by imidacloprid that further involved in cellular protein degradation. The dilated sinusoidal spaces were due to the shrinkage and necrosis of hepatic cells. These results were in agreement with Sasidhar Babu *et al.* (2014) and Ganguly (2013). Microscopic changes in the liver revealed large areas of vacuolation, fatty degeneration, large areas of necrosis, and congested sinusoidal spaces. These results were similar to the findings of Eissa (2004) in Japanese quail and Kammon *et al.* (2010) in layer chicks. The vacuolation of hepatocytes might be due to the retention of fluid inside the cell. The cloudy swelling might be due to the reduction of energy necessary for the regulation of ion concentration of the cells (Omiamia, 2004). In addition, Kammon *et al.* (2010) in layers chicks and Ravikanth (2015) in broilers observed that imidacloprid exposure did not produce any changes in the liver cells except for mild cellular swelling in the hepatocytes and exposure of imidacloprid for 20 and 30 days produced degenerative changes in the hepatocytes and necrosis surrounded by neutrophilic infiltration and explained this lesion by oxidative stress induced by imidacloprid.

In the kidney, the vacuolar degeneration of tubular epithelial cells and hemorrhage between tubules could be due to increased glomerular filtration and capillary

permeability. The leakage of proteins causes tubular necrosis (Wankhede *et al.* 2017). These findings were in accordance with (Ravikanth *et al.*, 2017) and (Gupta and Lather, 2016).

In the present study, the imidacloprid treated chicks (Group 2) showed congestion and hemorrhage in the liver, kidney, and breast muscles. The present results were similar to that obtained by Eissa (2004), Wankhede *et al.*, (2017) and Komal (2018) who found that imidacloprid intoxication cause fatty change, congestion, necrosis of hepatocytes and nephritis.

The liver and kidney showed hydropic degeneration and mild vacuolar degeneration of tubular epithelium in group3. This improvement in the histopathological lesions may result from the sulphhydryl group of amino acid cysteine, which prevents oxidation of endogenous mitochondrial and microsomal enzymes which participate in the toxicity production. One possible mechanism by which glycine induces these responses is through an increase in the formation of cysteine (Wu, 2013). The obtained findings revealed that chicks in group 3 showed lower degree of lesion compared to group 2.

In the present study, the significant increase in glutathione production induced by glycine supplementation may explain the improvement in the histopathological lesion in group 2 and were in agreement with the findings of Eissa (2004) in Japanese quails who concluded the protective effect of glutathione against pathological changes induced by imidacloprid.

5. Conclusion

Our findings confirmed that glycine supplementation increased imidacloprid excretion and reduced the pesticide accumulation in edible organs and tissue of broiler chicks. Glycine enhanced antioxidants activity and exhibited a preventive effect against oxidative stress and neurotoxicity induced by imidacloprid. Furthermore, glycine reduced hematological alterations and improved hepato-renal function that was supported by regressive pathological lesions in the liver, kidney, and muscles.

References

- Aebi H. 1984. Catalase *in vitro*. *Methods Enzymol.*, **105**:121-6.
- Bean TG, Gross, MS, Karouna-Renier NK, Henry PFP, Schultz SL, Haldik ML, Kuivila KM and Rattner BA. 2019. Toxicokinetics of imidacloprid-coated wheat seeds in Japanese quail (*Coturnix japonica*) and an evaluation of hazard. *Environ. Sci. Technol.*, **53** (7): 3888-3897.
- Ajay K, Monika T and Sudhir, KK. 2014. Effect of sub-lethal doses of Imidacloprid on histological and biochemical parameters in female albino mice. *IOSR. Journal of Environmental Science, Toxicology and Food Technology*, **8** (1): 09-15.
- Akinde DO. 2014. Amino acid efficiency with dietary glycine supplementation: part 1 and Part 2. *World Poult Sci J.*, **70** (3): 461-474.
- Anastassiades M, Lehotay SJ, Stajnbaher D and Schenck, FJ. 2003. Fast and easy multiresidue method employing acetonitrile extraction/partitioning and dispersive solid-phase extraction for the determination of pesticide residues in produce, *J AOAC Int.*, **86**: 412- 431.

- Arfat Y, Nasir M, Muhammad UT, Maryam R, Sameer A, Fan Z, Di-Jie L, Yu-Long S., Lifang H, Chen, Z, Chong Y, Peng S and Ai-Rong Q. 2014. Effect of Imidacloprid on hepatotoxicity and nephrotoxicity in male albino mice. *Toxicology Rep.* 1: 554-561.
- Awad EA, Zulkifli I, Soleimani AF and Aljuobori A. 2017. Effects of feeding male and female broiler chickens on low-protein diets fortified with different dietary glycine levels under the hot and humid tropical climate, *Italian J Animal Sci.* 16:3, 453-461.
- Bannister, JV and Calabrese, L. 1987. Assays for superoxide dismutase, In: **Methods of Biochemical Analysis**, vol. 32, pp. 279-312, John Wiley & Sons, New York, NY, USA.
- Bataille AM, Maffeo, CL and Renfro JL. 2011. Avian renal proximal tubule urate secretion is inhibited by cellular stress-induced AMP-activated protein kinase. *Am J Physiol-Renal Physiol.*, 300: F1327-F1338.
- Bogin E and Keller P. 1987. Application of clinical biochemistry to medically relevant animal models and standardization and quality control in animal biochemistry. *J Clin Chem Clin Biochem.*, 25: 873-878.
- Codex Alimentarius Commission. 2003. **Food Standards Programme Codex Alimentarius Commission**. Joint FAO/WHO, The Netherlands .
- Corzo A. 2012. Determination of the arginine, tryptophan, and glycine ideal-protein ratios in high-yield broiler chicks. *J Appl Poult Res.* 21:79-87.
- Eissa OS. 2004. Protective effect of vitamin C and glutathione against the histopathological changes induced by imidacloprid in the liver and testis of Japanese quail. *Egyptian J Hospital Med.* 16:39-54.
- Ellman, GL, Courney KD, Andres V, Featherstone, RMA. 1961. A new and rapid colorimetric determination of acetylcholinesterase activity. *Biochem Pharmacol.* 7: 88-95.
- Fairbanks VF and Klee GG. 1987. **Biochemical Aspect of Haematology**, In: **Tietz NW, Editor. Fundamentals of Clinical Chemistry**, 3rd ed., Philadelphia: WB Saunders, pp. 803-806.
- Feldman BF, Zinkl JG and Jain NC. 2000. **Schalm's Veterinary Hematology**, 5th ed., Williams and Wilkins, Philadelphia, 21-100.
- Forman HJ, Zhang H and Rinna A. 2009. "Glutathione: overview of its protective roles, measurement, and biosynthesis. *Mol Aspects Med.* 30 (1-2): 1-12.
- Fosati P, Principe L and Berti G. 1980. Use of 3,5-dichloro-2-hydroxybenzene sulfonic acid/4-aminophenazone chromogenic system in the direct enzymatic assay of uric acid in serum and urine. *Clin Chem.* 26: 227-231.
- Ganguly S. 2013. Long term exposure to chemicals, insecticides and heavy metals causing toxicity: A Review. *Int J Pharm res biosci.* 2 (3): 333-342.
- Gibbons D, Morrissey C. and Mineau P. 2015. A review of the direct and indirect effects of neonicotinoids and fipronil on vertebrate wildlife. *Environ Sci Pollut Res.* 22:103-118.
- Gupta KRP and Lather D. 2016. Clinico-pathological studies of imidacloprid toxicity in broiler chickens. *Haryana Vet.* 55 (2): 163-165.
- Halliwell B. 2015. **Free Radicals and Other Reactive Species in Disease**, Encyclopedia of Life Sciences, pp. 1-9.
- Hilliar M, Huyen N, Girish CK, Barekatin R, Wu S, Swick RA. 2019. Supplementing glycine, serine, and threonine in low protein diets for meat type chickens. *Poult Sci.* 98(12): 6857-6865.
- Hilliar M , Hargreave G, Girish CK Barekatin R, Wu SB and Swick RA. 2020. Using crystalline amino acids to supplement broiler chicken requirements in reduced protein diets. *Poultry Sci.* 99:1551-1563.
- Hofmann AF, Hagey LR and Krasowski, MD. 2010. Bile salts of vertebrates: structural variation and possible evolutionary significance. *J Lipid Res.* 51: 226-246.
- Jentzsch AM, Bachmann H, Furst P and Biesalski HK. 1996. Improved analysis of malondialdehyde in human body fluids. *Free Rad Biol Med.* 20 (2): 251-256.
- Kammon AM, Brar RS, Banga HS, Sodhi, S. 2012. Ameliorating effects of vitamin E and selenium on immunological alterations induced by imidacloprid chronic toxicity in chickens. *J Environ Anal Toxicol.* 4:7.
- Komal (2018). A Review: Pathological studies on imidacloprid toxicity and its amelioration with vitamin C. *The Pharma Innov J.* 7(4): 999-1002.
- Lin Hu M, Dillard CJ and Tappel AL. 1988. Plasma SH and GSH measurement. *Methods Enzymol.* 233: 380-382.
- Lopez-Antia A, Ortiz-Santaliestra, ME, Francois M and Rafael M. 2013. Experimental exposure of red-legged partridges (*Alectoris rufa*) to seeds coated with imidacloprid, thiram and difenoconazole. *Ecotoxicology*, 2 (1): 125-138.
- Matsuda, Ihara M and Sattelle DB. Neonicotinoid insecticides: Molecular targets, resistance, and toxicity. *Annu Rev Pharmacol Toxicol.* 60: 241-255.
- Namroud NF, Shivazad M and Zaghari M. 2010. Impact of dietary crude protein and amino acids status on performance and some excreta characteristics of broiler chicks during 10-28 days of age. *J Anim Physio. An N.* 94: 280-286.
- NRCS. 2003. (Natural Resources Conversion Service). **Nutrient Management Technical Note No. 4 Feed and Animal Management for Poultry**. Ecological Sciences Division October 2003. (USDA) United States Department of Agriculture.
- Omiama SE. 2004. Protective effect of vitamin C and glutathione against the histopathological changes induced by imidacloprid in the liver and testis of Japanese quail. *Egypt J Hosp Med.* 16: 39-54.
- Ong S, Ab Majid AH and Ahmad H. 2017. Insecticide residues on poultry manures: Field efficacy test on selected insecticides in managing *Musca Domestica* population. *Trop Life Sci Res.* 28(2): 45-55.
- Powell S, Bidner TD and Southern, LL. 2009. The interactive effects of glycine, total sulfur amino acids, and lysine supplementation to corn-soybean meal diets on growth performance and serum uric acid and urea concentrations in broilers. *Poult Sci.*, 88: 1407-1412.
- Ravikanth V. 2015. Mixed toxicity of spinosad (SPD) and imidacloprid (IM) in broilers and its amelioration with vitamin E and silymarin M.V. Sc. Thesis (Veterinary pathology Department) SRI Venkateswara Veterinary University.
- Ravikanth VM, Lakshman, D. Madhuri and Kalakumar, B. 2017. Haematological alterations in broilers administered with imidacloprid and spinosad and its amelioration with Vitamin E and Silymarin. *Int J Curr Microbiol App Sci.* 6(4): 496-500.
- Ravikanth V, Lakshman M, Madhuri D and Kalakumar B. 2018. Effect of spinosad and imidacloprid on Serum Biochemical alterations in male broilers and Its Amelioration with vitamin E and Silymarin. *Int J Curr Microbiol App Sci.* 7(4): 2186-2192.
- Sahoo D, Rukmini M, and Ray R. 2014. Quantitative analysis of serum levels of alanine and aspartate aminotransferases, γ -Glutamyl transferase and alkaline phosphatase as predictor of liver diseases. *Am Inter J Res in Form, Appl and Nat. Scie.* 9: 51-55.
- Sasidhar Babu N, Kumar AA, Reddy AG, Amaravathi P and Hemanth I. 2014. Chronic experimental feeding of imidacloprid induced oxidative stress and amelioration with vitamin C and *Withania somnifera* in layer birds. *Int J Sci. Env ISSN Technol.* 3(5): 1679-1684.

Survarna K, Lyton C and Bancroft JD. 2013. **Bancroft's theory and practice of histological Techniques**, 7th ed. Oxford, Churchill Livingstone, Elsevier, England, pp.654.

te Braake FH, Schierbeek K, de Groof A, Vermes M, Longini G and van Goudoever J B. 2008. Glutathione synthesis rates after amino acid administration directly after birth in preterm infants. *Am J Clin Nutr.* **88**: 333-339.

Tomizawa M and Casida J E. 2005. Neonicotinoid insecticide toxicology: mechanisms of selective action. *Ann Rev Pharmacol Toxicol.* **45**: 247-268.

Tomlin CDS. 2006. **The Pesticide Manual. A world compendium**, 14th ed., British Crop Protection Council. Surrey, England: pp. 598-599.

US EPA. 2012. United States Environmental Protection Agency Ecological Risk Assessment. http://www.epa.gov/oppefed1/ecorisk_ders/toera_analysis_eco.htm. Accessed 27Oct2012.

Wankhede V, Hedau M, Ingole RS, Hajare SW and Wade MR. 2017. Histopathological alterations induced by subacute imidacloprid toxicity in Japanese quails and its amelioration by *Butea monosperma*. *J Pharmacog Phytochem.* **6 (3)**: 252-257.

Wu G. 2013. Discovery and chemistry of amino acids. In: **Amino Acids: Biochemistry and Nutrition**. CRC Press, Boca Raton, USA.

Enhancing Electricity Generation with the use of KMnO_4 as an electron acceptor in Microbial Fuel Cell

Adegunloye Deke Victoria, Faloni Taiwo Mercy*

Department of Microbiology, Federal University of Technology, Akure, Ondo State, Nigeria

Received: April 5, 2020; Revised: August 5, 2020; Accepted: August 9, 2020

Abstract

The use of potassium permanganate (KMnO_4) to enhance electricity generation in a microbial fuel cell (MFC) was evaluated. Proximate compositions of pig dung were determined. Microorganisms were isolated and identified using conventional and molecular methods. Double chamber types of MFCs were constructed. The anode chamber contained the pig dung sample, while the cathode chamber contained 0.1 M KMnO_4 . Current cum voltage were observed three times daily for a period of 40 days. Nine bacteria and five fungi were identified. *Bacillus mycoides* of the phylum Firmicutes were dominant. Before electricity generation, the highest bacterial and fungal load was from Apatapiti (2.71×10^5 cfu/g) and FUTA (2.93×10^4 sfu/g) pig dung respectively. After, the bacterial and fungal load was highest in Apatapiti (1.35×10^5 cfu/g) and South Gate (1.60×10^4 sfu/g) pig dung respectively. Generally, the highest voltage and current were from FUTA (1301 mV) and Apatapiti (4.5020 mA) pig dung, respectively. Findings revealed for the first time that pig dung yielded an output voltage as high as 3003 mV, which powered low voltage appliances conveniently. Hence, pig dung is a potential renewable electricity generation source and its use would curb environmental toxics and health hazards.

Keywords: Microbial fuel cell, pig dung, KMnO_4 , current, voltage.

1. Introduction

Energy is an integral factor for the socioeconomic growth, progress, and development of any nation. Globally, the usage of fossil fuel to generate electricity, automobile mobility and in many industrial establishments has recently recorded an alarming increasing rate, and this elicits global energy crisis simultaneously (EIA, 2013). It has been predicted from studies that fossil fuel will govern the world's energy supply and will amount to about eighty percent by 2040 (EIA, 2013).

Over the years, the demand for more animal protein to maintain an exponentially expanding population has given birth to a conspicuous and alarming increase in livestock production with sundry start-up of diverse animal farms. Simultaneously, the disposal of animal dung into the environment has been on a colossal increase, inadvertently creating a challenge in waste management unresolved (Iregbu *et al.*, 2014). Pig dung as an MFC substrate would be an advantageous alternative in electricity generation, this will thereby lead to its reduction in the environment. Also, it would abate the spurious challenges that accompany its reckless disposal and thereby generate wealth and employment for the nation.

The discovery that the metabolic activities of microorganisms could generate energy in the form of electrical current and voltage has led to a raised concentration in MFC technology (Potter, 1911). These new technologies can be adopted with promising prospects to provide energy in a sustainable mode. However, major

improvements are essential for its applications on a large scale to become feasible.

An important alternative research area in the recent approaches to electricity generation was from carbon-free renewable energy and additional power systems (Fan and Xue, 2016). Researches over the years on energy solutions revealed fossil fuels as irreplaceable completely because no solution is sufficient. With respect to this, alternatives should be sorted and sourced in mitigating this vast challenge (assuredly certain that dependence on fossil fuels cannot be sustainable due to finite supplies and pollution) (Franks and Nevin, 2010). MFC is renowned technological advancement with the capacity to meet the goals (dual) of energy production and waste management (Fan and Xue, 2016). MFC has been on the call of all, even till date with its projected relevance in recovering energy; especially electrical energy (Cao, 2019).

MFCs has been limited by quite a lot of parameters some of which include; the rate of oxidation and electron transfer to the anodes by microorganisms, nature of sample substrate, nature of proton exchange membrane (PEM), nature of the electron acceptor (catholyte) used among others (Ginkel *et al.*, 2005). The use of oxygen (aqueous or gaseous state) as an electron acceptor at the cathode chamber has been of wide acceptability owing to availability and its high redox potential (Clauwert *et al.*, 2008). Nevertheless, its poor contact with the cathode electrode in addition to the slowness in its oxygen reduction rate on the carbon electrode surface has been a major denigration that impedes its usage in MFCs (Li *et al.*, 2009). This downside of oxygen can be circumvented by enabling an increase in the amount of liquefied oxygen

* Corresponding author e-mail: fametey14@gmail.com.

in the cathode with the use of electron acceptors with high oxidizing potential. The present study explores the usage of KMnO_4 in enhancing current and voltage generation from pig dung in a microbial fuel cell.

2. Materials and Methods

2.1. Sample Collection

The used pig dung was collected from pig farms in FUTA, South Gate, and Apatapiti area of Akure, Ondo state. The samples were collected into sterile bags, labelled and conveyed straightaway into the laboratory for immediate analyses.

2.2. Proximate Analysis

Proximate composition of the moisture content, total ash, crude fat, crude fiber, protein content, and carbohydrate content of the pig dung was determined. Moisture Content was determined according to the method description of AOAC (2002). Ash content was analysed using the gravimetric method, according to AOAC (2005). The fat content was determined using the Soxhlet type of the direct solvent extraction method, according to AOAC (2010). The protein content of the sample was determined by the Micro-Kjeldahl method, according to AOAC (2005). The total carbohydrate content of each sample was estimated by "difference," according to the method description of AOAC (2010).

2.3. Isolation of Bacteria and Fungi from pig Dung

The bacteria isolates were subjected to various biochemical tests and with the use of ABIS online software, while the fungi isolates were identified by viewing under a microscope (Olympus CH) (Samson, 2007). The isolates were further identified using molecular methods to ascertain their identities.

2.4. Identification of Isolates at Molecular Level

Bacteria and fungi with the highest percentage frequency of occurrence from each sample were identified to the molecular level. This was carried out using the sequencing techniques according to the method description of Akinyemi and Oyelakin, (2014). The DNA in each isolate was extracted using the procedure of the Zymo bacterial DNA Mini-prep kit. The quality of DNA was ascertained with the use of agarose gel electrophoresis by size fractionation on 1.0 % agarose gel. The extracted genomic DNA was stored at 4°C. PCR was performed using Hi-Media Taq polymerase (500 U), Hi-media 50 mM MgCl_2 and Hi-media 10X buffer (500 U) and QIAGEN dNTPs (10 mM each). Universal 16S rRNA forward primer was used. PCR amplifications were performed with an Applied Biosystems Veriti Thermal cyclers according to the method of Akinyemi and Oyelakin, 2014. Nine μl of Hi Di Formamide with 1 μl of the amplified DNA totaling 10 μl was loaded on the machine, and the data were expressed as A, C, T, and G on the computer system. The obtained sequence was analyzed with BLAST in the National Centre for Biotechnology Information (NCBI) database. Moreover, the phylogenetic relationship of the bacteria species were compared using their existing sequences obtained from NCBI GenBank (Oyetayo, 2014).

2.5. Construction of Microbial Fuel Cell

Double chamber MFC was built according to the work of Adegunloye and Faloni (2020). The double chambers include; anode and cathode chambers with an occupying volume of one thousand and two hundred milliliters in each of the chamber. The chambers were bridged with a proton exchange membrane (PEM) contained in polyvinyl chloride pipes with dimension 14 cm by 3.7 cm, the point of connections were sealed with epoxy adhesive to avoid dripping. Two millimeters (mm) diameter of the hole was drilled into the cover lid of each chamber as wire point inputs. The chambers were filled with water up to the brim for an hour to arrest possible leakages from the joining points. Voltage and current generated from the MFC were measured with the digital multimeter (SUOER SD 9205A) and recorded at 6 hours interval each day (8 am - 8 pm) summarily making up three sessions daily (morning, afternoon, and evening) for a period of forty (40) days.

2.5.1. Proton Exchange Membrane (PEM)

The PEM consisted of NaCl (an electrolyte for proton exchange) according to the work of (Kumar *et al.*, 2012; Adegunloye and Faloni, 2020). Twenty gram (20g) of agar-agar powder was dissolved into 1000 ml of distilled water containing 75.5 g of NaCl, the mixture was boiled for about 3 minutes and cooled to room temperature (Akujobi *et al.*, 2017). The solution was afterwards dispensed into the polyvinyl chloride pipes with an enclosed end and was left to congeal at normal room temperature.

2.5.2. Filling of the Chambers

The fabricated chambers were disinfected with ethyl alcohol (85%) and radiated for fifteen minutes in an UV inoculating chamber to ensure possible contaminants are ruled out. The anodic chamber was aseptically filled with 50% of the substrate (600 g and 600 ml of pig dung and sterilized water respectively) (Kumar *et al.*, 2012). The cathodic chamber was filled with 1200 ml of 0.1 M KMnO_4 .

2.5.3. Making and Testing the Control MFC:

Six hundred (600) gram of pig dung was sterilized in the autoclave (at 121°C for 15 minutes) to exterminate the organisms embedded while its nutritional and mineral components are preserved. The anodic chamber was aseptically filled with the substrate (600 g and 600 ml of pig dung and sterilized distilled water respectively) and the chamber was air tight. The cathodic chamber was filled with 1200 ml of 0.1 M KMnO_4 as electron acceptor.

2.6. Statistical Analysis

Duncan's New Multiple Range Test and Analysis of Variance (ANOVA) using Statistical Packages for the Social Sciences (SPSS) 22.0 version was employed in the test for significance of difference between the samples from the various sites. Data are presented as mean \pm standard error (SE). The significance of each test was evaluated at the level of $P \leq 0.05$.

3. Results

3.1. Pig Dung's Proximate Composition

The proximate content of the pig dung from the three sites is presented in Table 1. The outcome specified a significant difference ($p \leq 0.05$) in the nutrient composition of the dung from the three locations. FUTA pig dung had the highest significant ($p \leq 0.05$) values for ash content,

Table 1. Pig Dung's Proximate Composition

Parameters	Ash Content (%)	Moisture Content (%)	Crude Fat Content (%)	Crude Fibre Content (%)	Protein Content (%)	Carbohydrate Content (%)	Energy Value (%)
FUTA	12.9780 ± 0.00058 ^c	18.2580 ± 3.00050 ^a	6.0520 ± 0.00058 ^c	33.2260 ± 0.00058 ^a	25.3620 ± 0.00058 ^c	1.3040 ± 0.00058 ^a	677.2460 ± 0.00058 ^b
South Gate	9.0040 ± 0.00058 ^b	16.3140 ± 0.00058 ^a	3.0250 ± 0.00058 ^a	40.4430 ± 0.00058 ^c	21.4280 ± 0.00058 ^b	9.7320 ± 0.00058 ^b	641.6820 ± 0.00058 ^a
Apatapiti	7.0700 ± 0.00577 ^a	22.3500 ± 0.00577 ^a	3.8460 ± 0.00058 ^b	33.7040 ± 0.00058 ^b	18.2630 ± 0.00058 ^a	14.7670 ± 0.00058 ^c	703.8120 ± 0.00058 ^c

3.2. The Total Aerobic Bacterial Load (TABL)

The total aerobic bacterial load is presented in Table 2. The outcome specified a significant ($p \leq 0.05$) difference in the bacterial load of the pig dung from the three locations. The TABL result from the first isolation before the MFC experiment was between 1.72×10^5 cfu/g and 2.71×10^5 cfu/g; FUTA pig dung had significantly ($p \leq 0.05$) lower TABL compared to South Gate and Apatapiti pig dung which were on the same significant difference ($p \leq 0.05$) level. The TABL result after the MFC experiment was between 5.33×10^3 cfu/g and 1.35×10^5 cfu/g; the highest significant ($p \leq 0.05$) load was from Apatapiti pig dung. The TABL was higher for the first isolation (before the experiment) across all the sites compared to the final isolation (after the experiment).

Table 2. The Total Aerobic Bacterial Load (TABL)

Pig Dung	Initial (Cfu/g)	Final (Cfu/g)
FUTA	$1.72 \times 10^5 \pm 25.44^a$	$8.90 \times 10^4 \pm 5.51^b$
South Gate	$2.71 \times 10^5 \pm 25.10^b$	$5.33 \times 10^3 \pm 0.88^a$
Apatapiti	$2.67 \times 10^5 \pm 7.06^b$	$1.35 \times 10^5 \pm 3.18^c$

3.3. The Total Aerobic Fungal Load (TAFL)

The total aerobic fungal load is presented in Table 3. The outcome specified a significant ($p \leq 0.05$) difference in the fungal load of the pig dung from the three locations. The TAFL result from the first isolation before the MFC experiment was between 3.99×10^3 cfu/g and 2.94×10^4 cfu/g; all the dungs from the different locations were on the same significant ($p \leq 0.05$) difference level. The TAFL result after the MFC experiment was between 8.01×10^3 cfu/g and 1.60×10^4 cfu/g; South Gate pig dung had significantly ($p \leq 0.05$) lower TAFL compared to Apatapiti and FUTA pig dung which were on the same significant difference ($p \leq 0.05$) level. South Gate pig dung had the highest TAFL from the first isolation (before the experiment) while Apatapiti and FUTA pig dung had the highest fungal load from the final isolation (after the experiment).

Table 3. The Total Aerobic Fungal Load (TAFL)

Pig Dung	Initial (Sfu/g)	Final (Sfu/g)
FUTA	$1.47 \times 10^4 \pm 0.88^a$	$1.60 \times 10^4 \pm 3.06^b$
South Gate	$2.94 \times 10^4 \pm 13.78^a$	$8.01 \times 10^3 \pm 0.00^a$
Apatapiti	$3.99 \times 10^3 \pm 2.00^a$	$1.53 \times 10^4 \pm 0.67^b$

crude fat content and protein content with values (12.98 ± 0.00) %, (6.05 ± 0.00) % and (25.36 ± 0.00) % respectively. Apatapiti pig dung had the highest significant ($p \leq 0.05$) values for crude fibre content, carbohydrate content and energy value with values (40.44 ± 0.00) %, (14.77 ± 0.00) % and (703.81 ± 0.00) KJ/g. There was no significant difference ($p \leq 0.05$) in the moisture content of the dung from the three locations.

3.4. Total Bacterial and Fungal Count (TBC/TFC) under Anaerobic Condition

The TBC and TFC of the pig dung under anaerobic condition after the MFC experiment is presented in Table 4. The outcome specified a significant ($p \leq 0.05$) difference in the fungal load of the pig dung from the three locations. The TBC was in a range of 4.00×10^3 cfu/g to 2.20×10^4 cfu/g; the highest significant ($p \leq 0.05$) TBC was from FUTA pig dung while the lowest was from South Gate pig dung. The TFC was between 6.33×10^3 sfu/g and 1.50×10^4 sfu/g; Apatapiti pig dung had significantly ($p \leq 0.05$) the highest TFC while there was no TFC from FUTA pig dung.

Table 4. Total Bacterial and Fungal Count (TBC/TFC) under Anaerobic Condition

Pig Dung	Bacteria (Cfu/g)	Fungi (Sfu/g)
FUTA	$2.20 \times 10^4 \pm 4.04^c$	$9.33 \times 10^3 \pm 1.33^a$
South Gate	$4.00 \times 10^3 \pm 0.00^a$	$6.33 \times 10^3 \pm 0.88^a$
Apatapiti	$1.77 \times 10^4 \pm .88^b$	$1.50 \times 10^4 \pm 0.58^a$

3.5. Total Coliform Count (TCC)

The TCC of the pig dung is presented in Table 5. The outcome specified a significant ($p \leq 0.05$) difference in the fungal load of the pig dung from the three locations. The TCC result from the first isolation before the MFC experiment was between 3.96×10^4 cfu/g and 5.98×10^4 cfu/g; with all the dungs from the different locations were on the same significant ($p \leq 0.05$) difference level. TCC after the MFC experiment was between 0.00×10^3 cfu/g and 3.73×10^4 cfu/g; the highest significant ($p \leq 0.05$) load was from FUTA pig dung. The TCC was higher for the first isolation (before the experiment) across all the sites compared to the final isolation (after the experiment).

Table 5. Total Coliform Count (TCC)

Pig Dung	Initial (Cfu/g)	Final (Cfu/g)
FUTA	$5.98 \times 10^4 \pm 3.67^a$	$3.73 \times 10^4 \pm 3.33^b$
South Gate	$3.96 \times 10^4 \pm 9.67^a$	$0.00 \times 10^3 \pm 0.00^a$
Apatapiti	$5.93 \times 10^4 \pm 3.33^a$	$0.00 \times 10^3 \pm 0.00^a$

KEY: Values are calculated as mean \pm Standard error of the pig dung. And, values that fall under the same column bearing similar superscript are not apparently different at ($p \leq 0.05$) on applying Duncan's New Multiple Range Test on it.

Cfu/g- Colony-forming unit per gram. Sfu/g- Spore forming unit per gram.

3.6. Biochemical characterization of bacterial isolates

The biochemical characterization of the bacterial isolates is presented in Table 6. The result reveals nine (9) isolates, and the probable identity of the isolates are

Bacillus sp, *Escherichia coli*, *Shigella sp*, *Staphylococcus arlettae*, *Micrococcus luteus*, *Klebsiella singaporensis*, *Paenibacillus sp*, *Salmonella sp*, and *Yersinia intermedia*.

Table 6. Biochemical Characterization of the Bacterial Isolates

Isolate Code	Gram's Reaction	Cell Morphology	Catalase	Indole	Oxidase	Methyl Red	Voges Proskauer	Citrate Utilization	Urease	Motility	Spore Forming	Glucose	D-Mannitol	Lactose	Fructose	Galactose	Maltose	Sorbitol	Sucrose	H ₂ S production	Probable Identity
35(o)	+	C	+	-	-	-	-	-	-	-	-	+G	+G	+	+G	+G	+G	+G	(+)	-	<i>Staphylococcus arlettae</i>
17(o)	-	R	+	+	-	-	-	-	-	-	-	+	+	+G	+	+G	+G	+G	+G	-	<i>Yersinia intermedia</i>
26(o)	+	C	+	-	-	-	+	-	+	-	-	-	-	-	-	-	-	-	-	-	<i>Micrococcus luteus</i>
C(n)	-	R	+	-	+	-	+	+	+	-	-	+G	+G	+G	+G	+G	+G	+G	+	-	<i>Klebsiella singaporensis</i>
30(n)	+	R	+	-	+	-	-	-	+	+	+	+	+	-	+	+	+	+G	+G	-	<i>Paenibacillus amylolyticus</i>
17(n)	+	R	+	-	+	+	+	+	-	-	+	+	+	-	-	+	(+)	-	-	+	<i>Bacillus mycoides</i>
EC	-	R	+	+	-	-	-	-	-	+	-	+G	+G	+G	+G	+G	+G	+G	+	+	<i>Escherichia coli</i>
Shig	-	R	+	-	-	+	+	-	+	-	-	+	+	-	-	-	-	-	-	-	<i>Shigella sp</i>
Salm	-	R	+	-	-	-	-	-	-	+	-	+G	+G	+G	+G	+G	+G	+G	+G	+	<i>Salmonella sp</i>

KEY: R= Rod, C= Cocci, += Positive reaction, (-) = Negative reaction, (+) = weakly positive reaction, G = gas production

3.7. Microscopic characterization of fungal isolates

The identity of the fungi with the aid of microscopy view are presented in Table 7; this include: *Fusarium sp*,

Aspergillus flavus, *Aspergillus fumigatus*, *Aspergillus niger*, and *Penicillium chrysogenum*.

Table 7. Microscopic Characterization of Fungi Isolates from Pig Dung

Isolate Code	Characteristics	Probable Identity
1	Hyphae are septate and hyaline. Produces both macro- and microconidia from slender phialides. The macroconidia are several celled and the microconidia are one celled in chains, Phialides are cylindrical, conidiophores are medium length.	<i>Fusarium sp</i>
2	Conidiophore was thick walled, hyaline and coarsely roughened, often more noticeable with a vesicle at the top. Vesicles are globose with phialides and with short conidial chains.	<i>Aspergillus flavus</i>
3	Colonies are spreading, green with pale to bright yellow. Septate hyaline hyphae, conidiophores are branched with yellow exudate, two to three stage branched conidia and mutulae phialides are present.	<i>Penicillium chrysogenum</i>
5	Colonies changed from white to black conidia. Septate hyphae, long/tall conidiophores, smooth-walled, branched foot cells, hyaline and contained globose vesicle each covered completely with biseriata phialides. Conidia were globose, dark and rough-walled. Conidia heads were large with radiating heads, dark brown and biseriata.	<i>Aspergillus niger</i>
4	Conidial heads are long, globose to prolate. Conidial heads radiate to nearly globose, grayish near the apices with an irregular shape. Conidiophores hyaline slightly coloured, short green, particularly in the upper part, smooth-walled.	<i>Aspergillus fumigatus</i>

3.8. Frequency Distribution of Bacterial Isolates from Pig Dung in Percentage

The percentage frequency distribution of bacterial isolates, as represented in Table 8, reveals the frequency distribution of bacterial isolates from Apatapiti, South Gate, and FUTA pig dung. The percentage of occurrence includes *Paenibacillus amylolyticus* (24 %), *Yersinia intermedia* (17.24 %), and *Bacillus mycoides* (16.67 %). These three bacteria occurred before the MFC experiment and after, they had the highest frequency of occurrence in the first three orders, among others.

Table 8. Percentage Frequency Bacterial Isolates

Bacteria	Number	Frequency (%)
<i>Staphylococcus arlettae</i>	1	3.70
<i>Yersinia intermedia</i>	7	25.93
<i>Micrococcus luteus</i>	1	3.70
<i>Klebsiella singaporensis</i>	2	7.40
<i>Paenibacillus amylolyticus</i>	6	22.22
<i>Bacillus mycoides</i>	8	29.63
<i>Escherichia coli</i>	2	7.40
Total Number	27	100

3.9. Frequency Distribution of Fungal Isolates from Pig Dung in Percentage

The percentage frequency distribution of fungal isolates, as represented in Table 9, reveals the percentage frequency distribution of fungal isolates from Apatapiti, South Gate, and FUTA pig dung. The percentage of occurrence include *Aspergillus fumigatus* (55.56 %), *Aspergillus flavus* (52.94 %), and *Fusarium* sp (50 %). These three fungi occurred before the MFC experiment and after, they had the highest frequency of occurrence in the first three orders, among others.

Table 9. Percentage Frequency of Fungal Isolates

Fungi	Number	Frequency (%)
<i>Aspergillus fumigatus</i>	9	34.62
<i>Aspergillus flavus</i>	6	23.08
<i>Fusarium</i> sp	4	15.38
<i>Penicillium chrysogenum</i>	2	7.69
<i>Aspergillus niger</i>	2	7.69
Total	23	100

3.10. Molecular Based Identification of Bacteria Species with the highest percentage of occurrence

The three most occurred organisms across the sample sites were molecularly identified as; *Paenibacillus amylolyticus*, *Bacillus mycoides*, and *Yersinia intermedia*. Observation of the gels after electrophoresis of PCR products of the bacterial and fungal DNA isolated from pig dung are shown on Plates 1 and 2, respectively. The extracted DNA bands for each of the bacteria isolated from pig dung were shown to have a molecular weight of approximately 1500 bp with highly bright, bold, and clean DNA bands. Plate 2 shows the gel electrophoresis image detailed view of the amplified 18S and 26S rRNA from the fungal isolates. The extracted DNA bands for each of the fungi isolated from pig dung were shown to have a molecular weight of approximately 600 bp with highly bright, bold, and clean DNA bands.

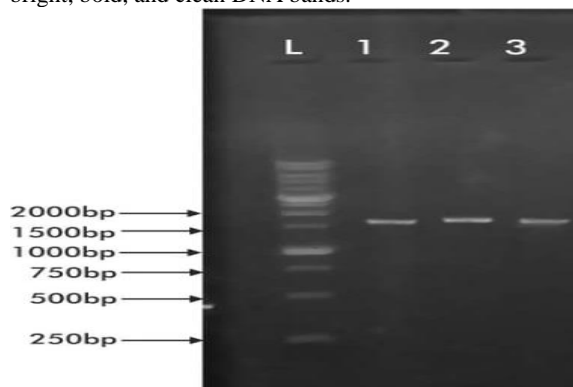


Plate 3.1: PCR amplification of genomic DNA targeted to amplify the 16S rRNA gene of the bacterial isolate on 1.5% agarose gel electrophoresis

L- Molecular marker

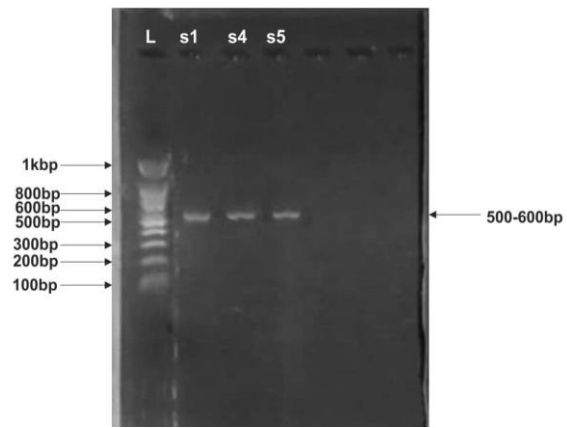


Plate 3.2. PCR amplification of genomic DNA targeted to amplify the 18S and 26S rRNA gene of the fungal isolate on 1.5% agarose gel electrophoresis.

L- Molecular marker

3.10.1. Genetic Relationship between the Bacterial Isolates

The constructed phylogenetic tree showing the relatedness of the bacterial isolates is represented in Plate 3. The phylogenetic tree of the bacterial isolates in Plate 3 showed that the isolates had two clades; from the first clade, *Yersinia enterocolitica* and *Bacillus amyloliquefaciens* (NR_028624 and NR_117946) are closely related but shared the same ancestor with *Bacillus funiculus* which is on the second clade. The evolutionary distance between the bacterial isolates is 0.04.

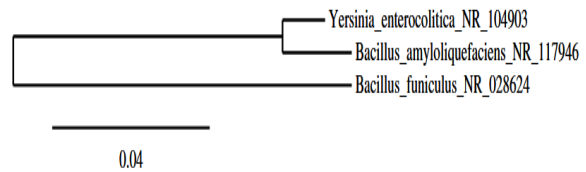


Plate 3.3. Phylogenetic tree of the bacterial isolate from pig dung.

3.10.2. Molecular Identification of isolated microorganisms from pig dung

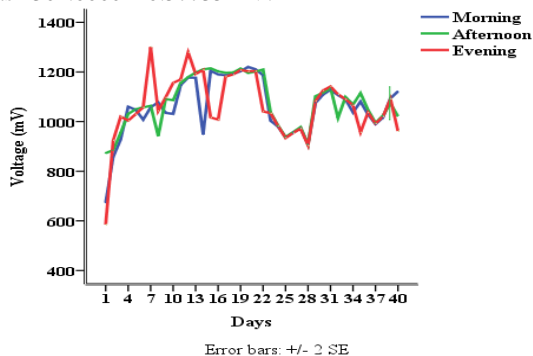
The molecular identities of the bacterial and fungal isolates are represented in Table 10. The bacterial isolates had more than 80 % similarity with those in the NCBI Gene Bank by BLASTn. The BLASTn results confirmed the bacterial isolates were similar to *Bacillus amyloliquefaciens* NR_117946, *Bacillus funiculus* NR_028624, and *Yersinia enterocolitica* subsp. palearctica NR_104903, which were culturally identified as *Paenibacillus amylolyticus*, *Bacillus mycoides* and *Yersinia intermedia*, respectively. The fungal isolates had more than 70% similarity with those in the NCBI Gene Bank by BLASTn. The BLASTn results confirmed the fungal isolates were similar to *Fusarium verticillioides* XR_001989346, *Aspergillus heteromorphus* XM_02554151 and *Aspergillus tamari* (MK_638758.1) which were culturally identified as *Fusarium* sp, *Aspergillus fumigatus*, and *Aspergillus flavus* respectively.

Table 10. Molecular Identification of isolated microorganisms from pig dung

Cultural and Biochemical Identification	Gene sequence Identification	Max Identity	Accession Number
<i>Paenibacillus amylolyticus</i>	<i>Bacillus amyloliquefaciens</i>	98.23%	NR_117946
<i>Bacillus mycoides</i>	<i>Bacillus funiculus</i>	88.92%	NR_028624
<i>Enterobacter asburiae</i>	<i>Yersinia enterocolitica</i>	93.62%	NR_104903
<i>Fusarium</i> sp	<i>Fusarium verticillioides</i>	90.1%	XR_001989346
<i>Aspergillus fumigatus</i>	<i>Aspergillus heteromorphus</i>	96.95%	XM_025541519
<i>Aspergillus flavus</i>	<i>Aspergillus tamarii</i>	73.17%	MK_638758.1

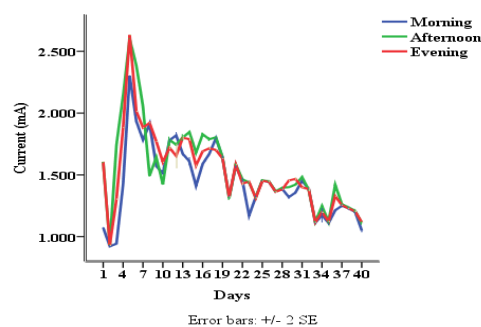
3.11. Voltage Generated from FUTA Pig Dung

The electricity generation from FUTA pig dung in terms of voltage is presented in Figure 3.1. The outcome specified a significant ($p \leq 0.05$) difference across the three sessions of the day. In the morning session; the least voltage was recorded on day 1 as 673.0000 ± 0.57735 mV while the peak voltage was recorded on day 20 as 1220.6667 ± 0.33333 mV. In the afternoon session; the least voltage ($p \leq 0.05$) were recorded on days 1 and 2 as 873.0000 ± 0.57735 mV and 885.0000 ± 0.57735 mV respectively while the peak voltage was recorded on day 15 as 1214.6667 ± 0.33333 mV. In the evening session; the least voltage was recorded on day 1 as 585.0000 ± 1.15470 mV while the peak voltage was recorded on day 7 as 1301.0000 ± 0.57735 mV.

**Figure 1.** Voltage generated from FUTA pig dung

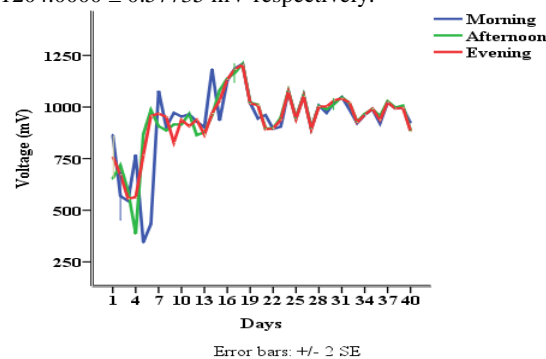
3.12. Current Generated from FUTA Pig Dung

The electricity generation from FUTA pig dung in terms of current is presented in Figure 3.2. The outcome specified a significant ($p \leq 0.05$) difference across the three sessions of the day. In the morning session; the least current was recorded on day 2 as 0.92167 ± 0.000882 mA while the peak current was recorded on day 5 as 2.30200 ± 0.000577 mA. In the afternoon session; the least current was recorded on day 2 as 0.93500 ± 0.000577 mA while the peak current was recorded on day 5 as 2.60167 ± 0.000333 mA. In the evening session; the least current was recorded on day 2 as 0.93100 ± 0.000577 mA while the peak current was recorded on day 5 as 2.63233 ± 0.000882 mA.

**Figure 2.** Current generated from FUTA pig dung

3.13. Voltage Generated from Apatapiti Pig Dung

The electricity generation from Apatapiti pig dung in terms of voltage is presented in Figure 3.3. The outcome specified a significant ($p \leq 0.05$) difference across the three sessions of the day. In the morning session; the least voltage was recorded on day 5 as 345.6667 ± 2.84800 mV while the peak voltage were recorded on days 14, 17 and 18 as 1183.3333 ± 1.20185 mV, 1187.0000 ± 0.57735 mV and 1209.0000 ± 0.57735 mV respectively. In the afternoon session; ; the least voltage was recorded on day 4 as 386.0000 ± 0.57735 mV while the peak voltage was recorded on day 18 as 1209.3333 ± 0.88192 mV. In the evening session; the least voltage were recorded on days 3 and 4 as 557.0000 ± 0.57735 mV and 563.0000 ± 0.57735 mV respectively while the peak voltage were recorded on days 17 and 18 as 1183.0000 ± 0.57735 mV and 1204.0000 ± 0.57735 mV respectively.

**Figure 3.** Voltage generated from Apatapiti pig dung

3.14. Current Generated from Apatapiti Pig Dung

The electricity generation from Apatapiti pig dung in terms of current is presented in Figure 3.4. The outcome specified a significant ($p \leq 0.05$) difference across the three sessions of the day. In the morning session; the least current was recorded on day 2 as 0.92167 ± 0.000882 mA while the peak current was recorded on day 5 as 2.30200 ± 0.000577 mA. In the afternoon session; the least current was recorded on day 2 as 0.93500 ± 0.000577 mA while the peak current on day 5 as 2.60167 ± 0.000333 mA. In the evening session; the least current was recorded on day 2 as 0.93100 ± 0.000577 mA while the peak voltage was recorded on day 5 as 2.63233 ± 0.000882 mA.

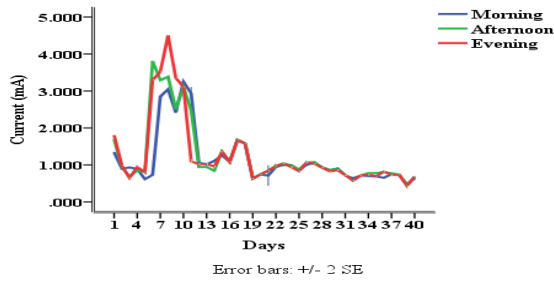


Figure 4. Current generated from Apatapiti pig dung

3.15. Voltage Generated from South Gate Pig Dung

The electricity generation from South Gate pig dung in terms of voltage is presented in Figure 3.5. The outcome specified a significant ($p \leq 0.05$) difference across the three sessions of the day. In the morning session; the least voltage was recorded on day 3 as 391.3333 ± 1.85592 mV while the peak voltage was recorded on day 17 as 1206.0000 ± 0.57735 mV. In the afternoon session; the least voltage was recorded on day 3 as 346.3333 ± 2.18581 mV while the peak voltage was recorded on day 17 as 1214.6667 ± 2.40370 mV. In the evening session; the least voltage was recorded on day 8 as 358.0000 ± 1.15470 mV while the peak voltage was recorded on day 17 as 1203.0000 ± 0.57735 mV.

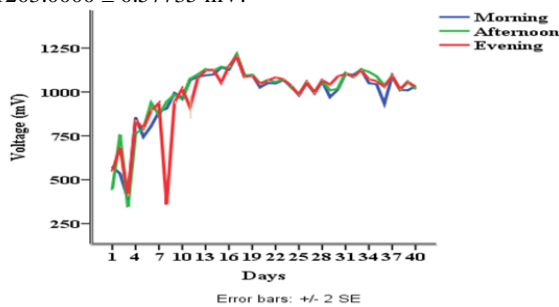


Figure 5. Voltage generated from South Gate pig dung

3.16. Current Generated from South Gate Pig Dung

The electricity generation from South Gate pig dung in terms of current is presented in Figure 3.6. The outcome specified a significant ($p \leq 0.05$) difference across the three sessions of the day. In the morning session; the least current was recorded on day 2 as 0.3050 ± 0.000577 mA while the peak current was recorded on day 18 as 1.96333 ± 0.008819 mA. In the afternoon session; the least current was recorded on day 2 as 0.31233 ± 0.004702 mA while the peak current was recorded on day 18 as 1.98000 ± 0.005774 mA. In the evening session; the peak current was recorded on day 2 as 0.33000 ± 0.006557 mA while the peak voltage was recorded on day 12 as 2.12333 ± 0.061734 mA.

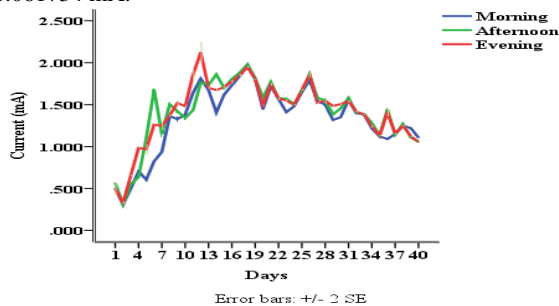


Figure 6. Current generated from South Gate pig dung.

3.17. Voltage Generated from Control MFC

The electricity generation from the control MFC in terms of voltage is presented in Figure 3.7. The outcome specified a significant ($p \leq 0.05$) difference across the three sessions of the day. The peak current was recorded on day 1 as 379.00 ± 0.00 mV. After this, there was an observable steady decrease to the minimum values till day 8.

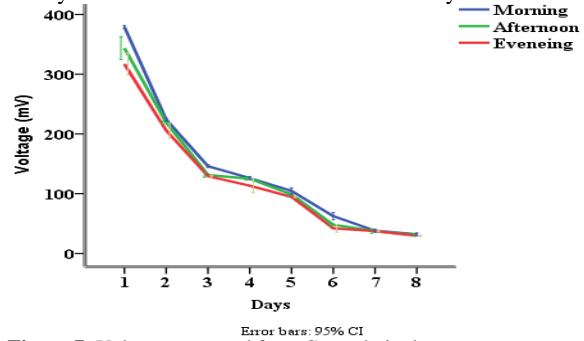


Figure 7: Voltage generated from Control pig dung

3.18. Current Generated from Control MFC

The electricity generation from the control MFC in terms of current is presented in Figure 3.8. The outcome specified a significant ($p \leq 0.05$) difference across the three sessions of the day. The peak current was recorded on day 1 as 0.030 ± 0.00 mA. After this, there was an observable steady decrease to the minimum values till day 8.

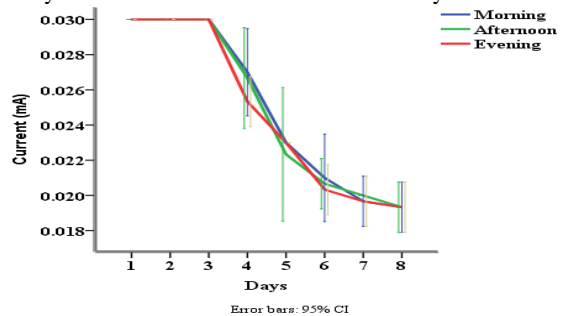


Figure 8. Current generated from Control pig dung

3.19. Testing the MFC on low appliances

The result of the combined voltage generated from the serial connection of the pig dung based MFC with a voltage generation of 3003 mV is represented in figures 9 and 10 (Light-emitting diode (LED) bulbs (red and yellow) and wall clock powered by the combined MFCs respectively). The red bulb, yellow bulb, and wall clock were powered at a voltage of 1640 mV, 1880 mV, and 1760 mV, respectively.



Figure 9: Pig dung based MFCs connected in series generated voltage of 3003 mV



Figure 10: MFC powered wall clock at a voltage of 1760 mV

4. Discussion

Pig dung was evaluated for electricity generation using KMNO_4 as an electron acceptor. Based on BLAST in the National Centre for Biotechnology Information (NCBI) database, the dominating bacterial isolates confirmed include *Bacillus amyloliquefaciens*, *Bacillus funiculus*, and *Yersinia enterocolitica*. The result revealed a slight difference in the cultural identity of these three organisms, which have been identified based on biochemical activities as *Paenibacillus amylolyticus*, *Bacillus mycoides*, and *Yersinia intermedia*, respectively. Akinyemi and Oyelakin, (2014), also reported differences between the conventional and molecular methods of bacterial identification. Conversely, results from this work demonstrated the importance of introducing 16S rDNA gene sequencing method in bacteria identification and that combining the two methods will help to improve further the identification authentication above the probable identity obtainable from the sole use of the cultural method.

Polymerase chain reaction revealed the molecular weight of the DNA of fungi in this study were between 500 bp and 600 bp. Selected fungi had more than 70 % similarity with those in the NCBI Gene Bank by BLASTn. The BLASTn results confirmed the fungal isolates were *Fusarium verticillioides*, *Aspergillus heteromorphus* and *Aspergillus tamari*. The result revealed a slight difference in the cultural identity of these three organisms, which have been identified as *Fusarium* sp, *Aspergillus funmigatus*, and *Aspergillus flavus*, respectively. This was also reported by Bechem and Afanga (2017), who reported a slight difference between the conventional and molecular methods of fungal identification.

Bacteria isolation before and after the MFC experiment revealed *Bacillus mycoides* of the phylum Firmicutes as the organism with the highest occurrence, this is in consonance with the report of Lim *et al.* (2018); they reported phylum Firmicute as the dominant phylum in all the cultured swine manure samples when the bacterial community were identified on phylum basis.

Microbial load before and after electricity generation revealed a significant population of microorganisms before and after the electric energy generation period; their presence connotes and establishes their function in facilitating the release of protons and electrons, which

brings about the overall generation of current and voltage. The control MFC generated low voltage and current; it is deduced that other factors, mainly chemical and biological owing to the difference of potential between the two chambers, contributed to the generated voltage and current. The subsequent rapid drop in the current and voltage could be hanged on the exterminated organisms (during sterilization) when compared to other MFCs in which current and voltage were continuously generated throughout the experiment as a result of the presence microbial activities in them. This agrees with the description of (Akujobi *et al.*, 2017).

The bacterial and coliform count dropped down relatively after the MFC experiment compared to its initial load in all the pig dung samples after power generation. This is a normality expected when microbial growth curve in an anaerobic environment is considered; available nutrients are competitively used up, waste accumulates, release of secondary metabolites, and the mortality rate of cells is on a rise. This is like the report of Adegunloye and Olotu, (2018); they reported that there was a decrease in the microbial population of the benthic mud used in the microbial fuel cell for electricity generation towards the later day of the experiment. The death phase is also characterized with adaptation, succession, and lysing of dying cells (their contents are spilled into the environment and thereby accessible to other bacteria). Sporulating bacteria are better survivor of the harshness in the death phase. They can go through this survival mode and resume normal growth life when the environment becomes conducive again to supports their growth (Nina *et al.*, 2017).

Results revealed that all the energy-yielding macronutrients were present with protein as the most abundant. The crude fat, crude fibre, protein, carbohydrate, and ash content showed a significant difference across the pig dung samples while the moisture content did not show significant difference across the pig dung samples. However, the feeding pattern at the various sites may be responsible for the difference in the energy yield; this statement agrees with the work of Stephen *et al.* (2013). They documented that the significant difference in crude protein, carbohydrate, and fibre between dung may be because of the difference in the feeding pattern of the animals. There was an insignificant difference in the moisture content across the samples (Wnetrzak *et al.*, 2015). The percentage of crude protein (18.26 ± 0.00 to 25.36 ± 0.00 %) obtained in the present study is higher than the 13.79 % reported by Udebuani (2012) and 14.05 % reported by Okoli *et al.* (2019), the ash value (7.07 ± 0.01 to 7.07 ± 0.01 %) was much lower than the 23.24 % obtained in Okoli *et al.* (2019), and the moisture content value (16.31 ± 0.00 to 22.35 ± 0.00 %) was higher than the 12.02 % reported by Okoli *et al.* (2019).

The energy value was high across the samples with a significant difference across the three samples; this can be attributed to the presence of energy-yielding macronutrients. The peak of the energy value obtained was from Apatapiti pig dung (703.81 Kj/Kg), this can be attributed to its highest carbohydrate and moisture content as these form the basis for energy production, this statement agrees with the findings of (Mukhtar and Capareda, 2017). They stated that nutrients in animal feed that are sources of energy include Carbohydrates which

comprises of (carbon, hydrogen, and oxygen) and other nutrients like protein, this later portions into net energy and energy losses such as in the form of faeces and urine, the inherent energy in the manure can be transformed into usable bio-energy. This statement disagrees with the work of Aneta and Grażyna, (2019), they confirmed that the calorific value of the energy of solid biofuel increases with decreasing moisture.

The present study revealed a sinusoid graphical representation in the bioelectricity generation in terms of voltage and current characterized by irregular falls and rises. This diverges from the steady and continuing increase all through the generation period documented by Meignanalakshmi *et al.* (2013) and Adegunloye and Ojo (2019); where voltage and current were generated from decayed wood. The present study revealed that pig dung generated higher current and voltage in MFC with KMnO₄ as an electron acceptor compared to H₂O as an electron acceptor in the work of Adegunloye and Faloni, (2020). This shows the effect of higher redox potential in permanganate than oxygen (Arbianti *et al.*, 2013).

Samples of pig dung from various location generated their peak voltage and current at varied times during the MFC experiment. The least voltage (345 mV) was generated from Apatapiti pig dung but was higher than the maximum voltage (195.6 mV) generated with sewage water as an electron acceptor and the maximum voltage (179.7 mV) generated with vinegar as electron acceptor as reported from the work of Kumar *et al.* (2012) where they studied cow dung for electricity generation. The highest voltage (1301 mV) was generated from FUTA pig dung in the evening of day 7; this was higher than the peak voltage (1110 mV) generated with potassium permanganate as electron acceptor reported from the work of (Pandit *et al.*, 2011), the maximum voltage (1006 mV) generated from sewage sludge with potassium ferricyanide as an electron acceptor in the work of (Parkash, 2018) and the maximum voltage (572 mV) generated from pig dung based MFCs with water as an electron acceptor in the work of (Adegunloye and Faloni, 2020). The highest value of current (4.5020 mA) was generated from Apatapiti in the evening of day 8. This was also higher than the peak current (0.319 mA) generated from pig dung based MFCs with water as an electron acceptor in the work of (Adegunloye and Faloni, 2020). The maximum voltage (1301 mV) generated by pig dung based MFC in this study has exceeded the theoretical documentation of Madigan *et al.* (2000), they stated that it was already documented that MFC voltages will never exceed a theoretical open-circuit voltage of 1140 mV.

The overall highest voltage was generated from three double chambers of pig dung based MFCs connected in series to yield a voltage output of 3003 mV. Devices including LED bulbs (red, yellow, green, and white colour) and wall clock powered with the combined voltage confirmed the functionality of the MFCs (Agho *et al.*, 2018).

5. Conclusion

It can be concluded that MFC has a high potential for use in domestic applications to reduce the odious effect of pig dung disposal into the environment and generate electrical energy to operate appliances of low power

consumption as demonstrated with LED bulbs and wall-clock, these were powered during the study. However, judging from the result of the highest voltage (3003 mV) generated from the combined MFCs when connected in series, the possibility of higher power generation for higher appliances than those powered in the study can be conceived, and this will be achievable by scaling up the MFC, thereby some of our home appliances can be made to run on renewable energy from organic sources. Results obtained from the study confirmed KMnO₄ as a good electron acceptor for electricity generation in microbial fuel cells due to its higher electrode potential, but its use will be unsustainable on a larger scale owing to cost implication. Therefore, research can be directed to source for renewable oxidizing agents to alleviate this consequence. Finally, findings from the study have revealed that pig dung has the capacity to yield a voltage output as high as 3003 mV, which is higher than the previous literature report indicating the enhancing effect of KMnO₄ on electricity generation in a microbial fuel cell.

Competing interest statement

The authors have declared that no competing interest exists in the manuscript.

Acknowledgments

We appreciate the Department of Microbiology, Federal University of Technology, Akure for their innovative ideas and support.

Funding disclosure

The authors of this research publication received no research funds/compensation from any organization. The research project and publication were sponsored by all the authors.

Contribution of individual authors

Faloni Taiwo Mercy: Conceived and designed the experiments; Performed the experiments; Analysed and interpreted the data; Contributed reagents, materials, analysis tools or data; Wrote the paper.

Adegunloye Deke Victoria: Conceived and designed the experiments; Supervised the experiment and the manuscript.

References

- Adegunloye, D. V. and Ojo, I. M. (2019). Electricity Production Potential of Decayed *Tectona grandis* Using Microbial Fuel Cell. *J Adv Microbiol.* **14**(3): 1-8
- Adegunloye, D.V. and Faloni, T.M. (2020). Evaluation of Pig Dung for Electrical Current Generation Using Microbial Fuel Cell. *J Energ Technol Policy.* **10**(1): 8-20
- Adegunloye, D. V. and Olotu, T. M. (2018). Comparative Measure of Electricity Produced from Benthic Mud of FUTA North Gate and FUTA Junction in Akure, Ondo State, Using Microbial Fuel Cell. *Innov Ener Res.* **7**: 180.
- Akinyemi, A. A. and Oyelakin, O. O. (2014). Molecular characterization of bacteria isolates from farm-raised cat fish *Clarias garipinus*. *British Microbiol Res J.* **4**(12): 1345-1352.

- Akujobi, C. O., Anuforo, H. U., Ogbulie, T. E. and Ezeji, E. U. (2017). Study on Generation of Bioelectricity Using Potassium Ferricyanide Electron Acceptor in Microbial Fuel Cell. *Chem Biomol Eng.* **2**(1): 5-13
- Aneta, S. and Grażyna Ł. (2019). The Effect of Moisture and Ash on the Calorific Value of Cow Dung Biomass. *Innovations-Sustainability-Modernity-Openness Conference (ISMO'19)*, Bialystok, Poland. Pp 22–23.
- AOAC-Association of Official Analytical Chemists. (2002). Fertilizers: water, phosphorus, nitrogen, potassium and other elements. Official method of Analysis, 16th ed. Wilson Boulevard Arlington, Virginia 22201 USA.
- AOAC- Association of Official and Analytical Chemists. (2005). **Official method of analysis of the Association of Official Analytical Chemists** (18th ed.). Washington D.C.
- AOAC- Association of Official Analytical Chemists, (2010). **Official Methods of Analysis.** 18th ed, AOAC, Washington, D.C., USA.
- Bechem, E. T. and Afanga, Y. A. (2017). Morphological and molecular identification of fungi associated with corn rot and blight symptoms on plantain (*Musa paradisiaca*) in macro-propagators. *Int J Biol Chem Sci.* **11**(6): 2793-2308
- Cao, Y., Mu, H., Liu, W., Zhang, R., Guo, J., Xian, M. and Liu, H. (2019). Electricigens in the anode of microbial fuel cells: pure cultures versus mixed communities. *Microbial Cell Fact.* **18**: 39
- Clauwert, P., Aelterman, P., Pharm, H. T., DeSchampelaire, L., Carballa, M., Rabaey, K. and Verstraete, W. (2008). Minimizing losses in bio-electrochemical systems: the road to application. *Appl Microb Biotechnol.* **79**: 901
- Energy Information Administration (EIA). (2013). International energy outlook. www.eia.gov/forecasts/ieo/more_highlights.cfm. Accessed on: 09/07/2019
- Fan, L. P. and Xue, S. (2016). Overview on Electricigens for microbial Fuel Cell. *Open Biotech J.* **10**: 398-406
- Franks, A. E. and Nevin, K. P. (2010). Microbial fuel cells, a current review. *Energies*, **3**(5): 899-919
- Ginkel, S., Oh, S. and Logan, B. (2005). Biohydrogen gas production from food processing and domestic wastewaters. *Int J Hydrogen Energy.* **30**: 1535–1542
- Iregbu, G. U., Kubkomawa, I. H., Okoli, C. G., Ogondu, E. C., Uchehgbu, M. C. and Okoli, I. C. (2014). Environmental concerns of pig waste production and its potentials as biofuel source. *J Animal Vet Sci.* **13**: 17-24
- Kumar, S., Kumar, H. D. and Babu K. G. (2012). A study on the electricity generation from the cow dung using microbial fuel cell. *J Biochem Technol.* **3**(4): 442-447
- Lim, J.S., Yang, S.H., Kim, B.S. and Lee, E.Y. (2018). Comparison of microbial communities in swine manure at various temperatures and storage times. *Asian-Australasian J Animal Sci.* **31**(8): 1373-1380
- Li, J., Fu, Q., Liao, Q., Zhu, X., Ye, D. D. and Tian, X. (2009). Persulfate: A self-activated cathodic electron acceptor for microbial fuel cells. *J Power Sour.* **194**: 269–274
- Madigan, M. T., Martinko, J. M. and Parker, J. (2000). **Brock Biology of Microorganisms**; Prentice Hall: Upper Saddle River, NJ.
- Meignanalakshmi, S., Deepika, J. and Deana, D. (2013). Bioelectricity Production From *Lysinibacillus Sphaericus* Dms-3 Isolated From Swine Waste. *Int J Adv Biotechnol Res.* **4**(3): 291-295
- Mukhtar, S. and Capareda, S. (2017). **Manure to Energy: Understanding Processes, Principles and Jargon.** *Texas Cooperative Extension*, Pp 428
- Nina, P., Mark, S., Thi Tu, A., Brian, M. F. and Philip, L. (2017). **Microbiology.** Open Stax, Rice University.
- Okoli, C. G., Edo, F. A. Ogbuewu, I. P., Nwajiobi, I. J., Enemor, V. H. A. and Okoli, I. C. (2019). Biochemical values of pig dung collected from different locations in Imo state, southeastern Nigeria. *Asian J Biol Sci.* **12**: 470-476
- Oyetayo, V. O. (2014). Molecular Identification of Trametes Species Collected from Ondo and Oyo States, Nigeria. *Jordan J Biol Sci.* **7**(3): 165-169
- Pandit, S., Sengupta, A., Kale, S. and Das, D. (2011). Performance of electron acceptors in catholyte of a two chambered microbial fuel cell using anion exchange membrane. *Biores Technol.* **102**: 2736–2744
- Parkash, A. (2018). Potential of Biomass for Electricity Generation Using Environment-Friendly MFC. *J Bioproc Biotech.* **8**(1): 314
- Potter, M.C. (1911). Electrical effects accompanying the decomposition of organic compounds. *Proc. R. Soc. Lond.*, **84**, 260–276
- Samson, R., Varga, J. (2007). *Aspergillus* systematic in the genomic era. CBS fungal Biodiversity centre Utrecht. Pg. 206
- Stephen, C., Ukpabi, C. and Esihe, T. E. (2013). Anaerobic Digester Considerations of Animal Waste. *American J Biochem.* **3**(4): 93-96
- Udebuani, A. C., Okoli, C. I., Nwigwe, H. C. and Ozoh. P. T. E. (2012). The value of animal manure in the enhancement of bioremediation processes in petroleum hydrocarbon contaminated agricultural soils. *J Agr Technol.* **8**(6): 1935-1952
- Wnetrzak, R., Hayes, D. J. M., Jensen, L. S., Leahy, J. J. and Kwapinski, W. (2015). Determination of the higher heating value of pig manure. *Waste Biomass Val.* **6**(3): 327-333

Neuroprotective Efficacy of *Dunaliella salina* Against Paraquat-Induced Neurotoxicity in *Drosophila melanogaster*

Mohamad Agus Salim^{1,*}, Muhammad Subandi² and Yeni Yuniarti³

¹Biology Department of Science and Technology Faculty of UIN Sunan Gunung Djati Bandung of Indonesia; ²Agrotechnology Department of Science and Technology Faculty of UIN Sunan Gunung Djati Bandung of Indonesia; ³Mathematic Education of Universitas Pendidikan Indonesia of Indonesia

Received: March 21, 2020; Revised: September 7, 2020; Accepted: September 11, 2020

Abstract

Microalgae of *Dunaliella salina* possesses multiple biological properties which are mainly attributed to the active compounds such as polyphenol, chlorophyll and β -carotene. However, the utilization of *D. salina* as a neuroprotective agent in the management of Parkinson's disease is still questionable. Presently, we observed the potential neuromodulatory effects of *D. salina* extract against the toxicity exposed to paraquat in fruit fly (*Drosophila melanogaster*). Male wild-type fruit flies were concomitantly induced by paraquat (3.5mM) and methanolic extract of *D. salina* (200 μ g/mL) in their diet during 4 days of observation. Paraquat-fed fruit flies exhibited a higher incidence mortality and severe influence on locomotor phenotypes (i.e. negative geotaxis) compared to the control. *D. salina* extract treatment that showed protection ability against these deleterious effects of paraquat. However, paraquat exposure caused a marked increase in malondialdehyde (MDA) levels as indicating increase lipid peroxidation process in brains of fruit flies. Meanwhile, paraquat toxicity was also related to a significant decrease on dopamine levels in head of fruit flies, which were attenuated by *D. salina* extract treatment. Results revealed that *D. salina* extract significantly reduced the toxicity of paraquat compounds exposed to fruit flies and proved the usefulness of this model as a potential therapeutic strategy for symptoms that appear in Parkinson's disease.

Keywords: locomotor, survival, malondialdehyde, dopamine.

1. Introduction

The presence of damage to dopaminergic neurons in the substantia nigra pars compacta as a hallmark of the onset of Parkinson's disease. Accordingly, the disease is predicted to double every 25 years and generally affecting the people above 65 years old with 1-2% of world's population (Siddique and Jyoti, 2017). Clinical disorders of the disease are locomotor symptoms such as resting tremor, muscle rigidity, postural imbalance and bradykinesia (Stephano *et al.*, 2018). While nonmotoric symptoms include depression, dementia and disturbed sleep (Soares *et al.*, 2017).

In recent times, researchers explained that the cause of Parkinson's disease remains unknown (idiopathic). However, it is estimated that the cause of this disease is more than 90% of environmental factors (Standaert *et al.*, 2016). One of environmental factors that cause the disease is the use of paraquat (herbicide) (Thakolwiboon *et al.*, 2017). Actually, paraquat is a free radical source which causes oxidative stress. Excessive oxidation on dopaminergic neurons reduces the production of dopamine compounds that function as neurotransmitters (Jhonsa *et al.*, 2016).

Remarkably, treatment of patients with Parkinson's disease is given by lepodova. The ability of synthetic drugs is quite helpful to replace the dopamine content that is lacking (Lazzari *et al.*, 2020). However, the use of

lepodova is very risky because it has side effects that will aggravate the symptoms of Parkinson's disease including hallucinations, foot edema, nausea and vomiting (Wells *et al.*, 2019). Considering the side effects of lepodova, researchers continue to search for natural ingredients that possess the potential to treat this neurodegenerative disorder (Mohamed *et al.*, 2018). Therefore, the expected neuroprotective agent can at least reduce the symptoms or inhibit the development of Parkinson's disease.

Microalgae are photosynthetic microorganisms that contain many bioactive substances including antioxidant compounds (Sedjati *et al.*, 2020). β -carotene pigments contained in microalgae cells of *D. salina* are expected to function as neuroameliorative dopaminergic neurons that have been damaged (Wong *et al.*, 2016). Interestingly, other antioxidant compounds such as polyphenols and chlorophyll will also act against free radicals that cause excessive oxidation in the brain.

Actually, fruit flies have been known as alternative animals model with many advantages including being easy to maintain, fast breed (female flies can produce 55 eggs during their lifetime), and a short life cycle of around 12 days (Quintero-Espinosa *et al.*, 2016). Hence, this fruit fly is very suitable for use in medical research to look for potential therapeutic solutions for diseases. This can be done because fruit flies have about 75% homologous genes that regulate disease in humans (Nelson *et al.*, 2018). Associated with Parkinson's disease, these fruit flies have dopaminergic neurons scattered in all parts of the **brain**

* Corresponding author e-mail: agus.salim@uinsgd.ac.id.

that allow a thorough study of the cellular mechanism of this disease (Jahromi *et al.*, 2015).

Considering the promising potential of *D. salina* microalgae as a source of natural antioxidant compounds, it is hypothesized that this species of microalgae may offer protection against the toxicity of paraquat. Therefore, the study aimed to investigate the protective potential of *D. salina* against paraquat-induced locomotor damage and excessive oxidation using animal models of *D. melanogaster*.

2. Methods and Materials

2.1. Culture and Harvest of Microalgae *D. salina*

Microalgae *D. salina* was obtained from stocks owned by plant physiology laboratory, Biology Department of Universitas Islam Negeri Bandung of Indonesia. Furthermore, these microalgae were cultured using Walne medium on plastic containers with a capacity of 10 L. The culture room with a temperature of 23-26 °C and lighting uses a 45 watt TL lamp with 2500 Lux intensity throughout the day for 12 hours. Microalgae were harvested using a centrifuge at 3000 rpm for 10 min and dried in an oven with a temperature of 50 °C for 10 hours. Dry biomass was crushed with mortar and stored in a refrigerator before being used for subsequent analysis.

2.2. Extraction of *D. salina*

100 mL of methanol was added to conical flask that had 10 g of dry biomass of *D. salina* microalgae. Contents were shaken for 48 hours at room temperature. This mixture was filtered with filter paper and the solvent was evaporated until a crude extract was obtained. Finally, the crude extract was packaged in an airtight container and stored in the refrigerator for further analysis.

2.3. Total Phenolics

The test was carried out to measure the total phenol levels of *D. salina* extract using the procedure of Stockum *et al.* (2019) with a slight modification. 4 µL sample was dissolved with 35 µL of 1 N Folin Ciocalteu reagent. The solution was left to stand for 3 min, then 70 ml of 15% Na₂CO₃ solution was added, followed by the addition of 284 µL of aquadest. The mixture was kept in the dark for 2 h, after which the OD was read at 760 nm. As a standard, gallic acid was used (10 - 300 µg / mL). The obtained data were represented as mg gallic acid equivalents (GAE) per 100 g of extract.

2.4. DPPH (Diphenyl-picrylhydrazyl) Scavenging Assay

This assay was carried out to obtain antioxidant activity of *D. Salina* extract using the procedure of McCann *et al.* (2019). The stable purple colour of DPPH turns light yellow when it reacts with antioxidants from *D. salina* extract. Discoloration due to a mixture of 500 µL *D. salina* extract with 250 µL DPPH solution (0.3 mM) was measured spectrophotometrically. The mixture was shaken evenly and kept in a dark room at room temperature for 30 minutes. Furthermore, the inhibition ability of *D salina* extract against DPPH free radicals were preceded by OD measurements of the mixture which were read at 520 nm and its calculation made using the following equation:

$$(\text{inhibition (\%)}) = \frac{\text{Absorbance control} - \text{Absorbance extract}}{\text{Absorbance control}} \times 100\%$$

2.5. *Drosophila Stock*

Wild type male fruit flies were obtained from the stock owned by the genetic laboratory, Department of Biology, Faculty of Science and Technology at State Islamic University (Universitas Islam Negeri) Bandung, Indonesia. Fruit flies were reared in agar medium consisting of dry yeast, sucrose, powdered milk, corn flour, and nipagin. Propionate acid was added as an anti-fungal and anti-bacterial agent. Fruit flies were reared in a 5.5 cm X 8.7 cm vial containing 10 ml of medium at constant temperature, humidity (70%) and under 12h dark/light cycle.

2.6. Survival Rates

Survival rate assay was performed to determine the number of flies still alive daily until the end of observation period (4 days). Therefore, 120 flies from each treatment group were included in survival data, and the total number of flies indicated the use of 4 replications per treatment group (30 flies/treatment replicate). In this survival rate observation, there was no change in the feed medium because it was to show its survival ability during the investigation.

2.7. Locomotor Phenotype

Negative geotaxis assay is a method used to determine the fly's locomotor phenotype. Fruit flies were anesthetized in brief ice, then carefully placed at the base of the glass column (14 cm high, 1.5 cm in diameter / 10 flies each). To start measuring, the fly's locomotor phenotype, flies gently were tapped down to the bottom of the column. Counting of climbing abilities was carried out on fruit flies that were able to pass the 5 cm in high during 6 s. The scores represent the sum of three independent replications (Sakai *et al.*, 2019).

2.8. MDA (Malondialdehyde) Assay

Measurement of lipid peroxidation level of MDA was made based on Rzezniczak *et al.* (2017). In this assay, 90 µL homogenate of fly brain was mixed with 600 µL of 1% O-phosphoric acid, 5 µL of 10 mM butyl-hydroxytoluene (BHT), 200 µL of 0.6% thiobarbic acid and 105 µL of distilled water. Then, the mixture was immediately incubated at 100°C for 10 min and spectrophotometrically the OD was read at 535 nm. The obtained data shows MDA levels as the end result of lipid peroxidation was expressed as µmol of TBARS formed / h / g tissue.

2.9. Dopamine Assay

This assay was performed to determine the dopamine content in the fly's brain using a procedure of Aryal and Lee, 2019. So, for this purpose a 40 head of flies from each group were prepared to be homogeneous in 500 µL of HCl-butanol. Next, the mixture was centrifuged at 2500 rpm for 7 min. The obtained supernatant was mixed with 250 µL of heptane and 100 µL of 0.1 M HCl and re-centrifuged at 2500 rpm for 7 min. The obtained supernatant was mixed again with 50 µL of 0.4 M HCl and 100 µL of iodine solution and incubated for 2 min. Thereafter, 100 µL of sodium sulphite and 100 µL of 10 M acetic acid were added to the mixture boiled at 100°C for 6

min. After the mixture cooled, OD was measured at 375 nm using a UV-Vis spectrophotometer.

2.10. Statistical Analysis

The obtained data was statistically analyzed using one way ANOVA followed by Duncan's multiple range test if there were significant differences at $p < 0.05$. Results were presented as mean and standard errors of mean. The statistical analysis was determined using SPSS software, version 16 for windows

3. Result

3.1. Phenolic Content and Antioxidant Activity

Phenolic content and antioxidant activity of microalgae *D. salina* extract performed by Folin-Ciocalteu protocol and DPPH assay respectively. Results of phenolic acid represented as gallic acid equivalent were 321.53 mg GAE/g extract, whereas the antioxidant strength of the *D. salina* extract can be seen from the IC_{50} value as measured by DPPH scavenging activity which is 74.49 $\mu\text{g} / \text{mL}$ with a strong category compared to IC_{50} ascorbic acid which is 4.97 $\mu\text{g} / \text{mL}$ with a very strong category.

3.2. Effectiveness of *D. salina* Extract on Survival Rate

The effect of *D. salina* extract treatment on the survival of fruit flies exposed to paraquat was observed for 4 days. As shown in Figure 1, the *D. salina* extract treatment had no effect on fruit fly survival when compared to the control group. Meanwhile, the survival rate of the fruit fly group that received paraquat treatment was seen to decrease since the first day of observation and continued to decrease until the end of the observation (day 4) with a survival rate of up to 40% (Figure 1). The administration of *D. salina* extract together with paraquat can increase the survival rate of fruit flies when compared to the fruit fly group that only received paraquat treatment (Figure 1).

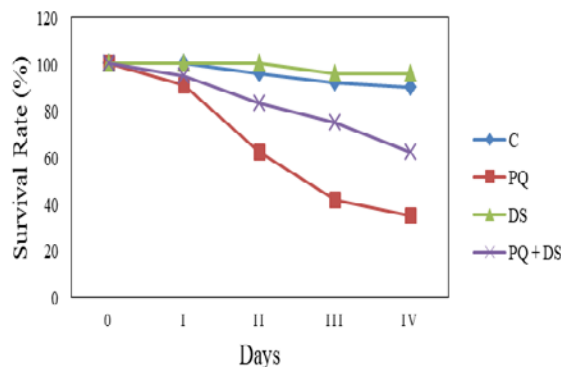


Figure 1. Effects of DS extract and PQ on survival rate (30 flies per replicate), of wild-type male fruit fly for 4 day observation. (C=control, PQ=3.5 mM paraquat, DS=200 $\mu\text{g}/\text{mL}$ extract of *D. salina*).

3.3. Effectiveness of *D. salina* Extract on Locomotor Performance.

Negative geotaxis is a common measurement to determine the locomotor ability of fruit flies. The ability of vertical climbing of fruit fly inside the tube was observed by startling them at a distance of 5 cm in 6 s. The effect of *D. salina* extract treatment not significantly change the locomotor performance of fruit flies when compared to control ($p > 0.05$). The fruit fly group exposed to paraquat

significantly impaired locomotor ability when compared to controls ($p < 0.05$) (Figure 2). More than 50% of flies treated paraquat lag below the boundary line, showing locomotor deficit caused by paraquat. The fruit fly group treated with the *D. salina* extract and paraquat showed a significant increase in locomotor ability when compared to the fruit fly group that was treated only with paraquat (Figure 2, $p < 0.05$).

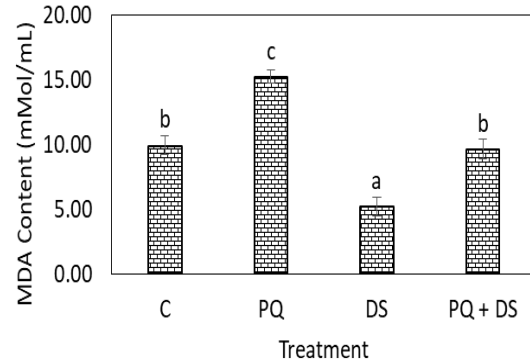


Figure 2. Effects of DS extract and PQ on negative geotaxis (10 flies per replicate), of wild-type male fruit fly at the end of observation. Error bars depict mean \pm SEM. Different alphabets respect to significant difference ($p < 0.05$). (C=control, PQ=3.5 mM paraquat, DS=200 $\mu\text{g}/\text{mL}$ extract of *D. salina*).

3.4. Effectiveness of *D. salina* extract on Lipid Peroxidation

The fruit fly group treated with *D. salina* extract significantly changed the MDA (malondialdehyde) content to be lower when compared to the control (Figure 3, $p < 0.05$). Meanwhile, the fruit fly group treated with paraquat showed a significant increase MDA content when compared to control ($p < 0.05$). However, MDA content of fruit fly group treated with *D. salina* extract and paraquat showed no significant difference when compared with the control ($p > 0.05$) (Figure 3). So, it can be seen from Figure 3 that the *D. salina* extract treatment was able to reduce the MDA content when compared to the fruit fly group that received PQ treatment (Figure 3).

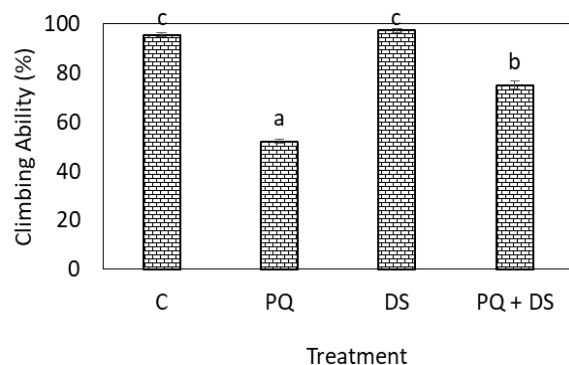


Figure 3. Effects of DS extract and PQ on MDA levels (40 flies per replicate), of wild-type male fruit fly at the end of observation. Error bars depict mean \pm SEM. Different alphabets respect to significant difference ($p < 0.05$). (C=control, PQ=3.5 mM paraquat, DS=200 $\mu\text{g}/\text{mL}$ extract of *D. salina*, MDA=malondialdehyde).

3.5. Effectiveness of *D. salina* Extract on Dopamine Levels

The fruit fly group treated with the *D. salina* extract produced almost the same dopamine levels and not

significantly different when compared to the control ($p > 0.05$). Meanwhile, the fruit fly group that received paraquat treatment produced lower dopamine levels and was significantly different when compared to the control ($p < 0.05$). For the fruit fly group treated with both the *D. salina* and paraquat extracts produced higher dopamine levels when compared to the fruit fly group that received PQ only treatment (Figure 4).

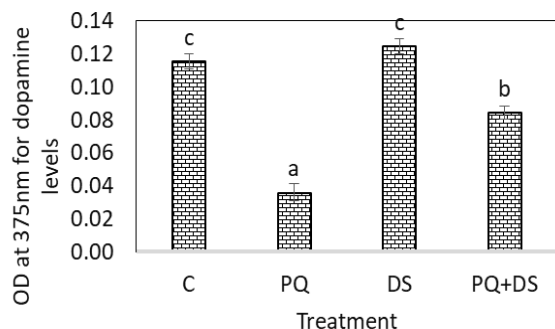


Figure 4. Effects of DS extract and PQ on dopamine levels (40 flies per replicate) of wild-type male fruit fly at the end of observation. Error bars depict mean \pm SEM. Different alphabets respect to significant difference ($p < 0.05$). (C=control, PQ=3.5 mM paraquat, DS=200 μ g/mL extract of *D. salina*, OD=optical density).

4. Discussion

At present, there is a major challenge for the medical world that there is no treatment for neurodegenerative disorders including Parkinson's disease. So, a continuous search for compounds that can prevent or inhibit damage to neurons is continually needed (Helena *et al.*, 2019). Oxidative stress is the main factor causing a variety of neurodegenerative disorders and other age-related degenerative disorders (Mohamed *et al.*, 2018). The incidence of lipid peroxidation, protein and DNA oxidation is increasing in the brain of the disease model (Xiong *et al.*, 2017). Concerning the above, various antioxidant compounds originating from natural sources have demonstrated neuroprotective abilities in models in-vitro and in-vivo which include polyphenols and β -carotene (Xiong and Yu, 2018).

According to studies of researchers in the health sector, there is a connection between Parkinson's disease and exposure to pesticides (Gupta *et al.*, 2020). The study clearly shows that paraquat neurotoxins can damage locomotor performance of fruit flies and decrease survival. This effect can be observed when using *D. salina* extract in the fruit fly culture medium. The benefits of *D. salina* extract may be at least in part from the presence of potentially antioxidant compounds which include polyphenols and β -carotene (Sedjati *et al.*, 2020). Dopaminergic neurons in the brain will be damaged or even lost due to the occurrence of oxidative stress which stimulates degeneration in the onset of the disease (Guo *et al.*, 2018). Paraquat as an herbicide is capable of damaging dopaminergic neurons which are indicated by locomotory disturbances in animal models used (Sanz *et al.*, 2017). The concurrent time between the occurrence of dopaminergic neurodegeneration and locomotor disorders is thought to have a causal relationship (Niveditha *et al.*, 2017). Although we did not specifically test for the

dopaminergic neuron degeneration, it can be seen that fruit flies treated with paraquat will show permanent locomotory disruption which is certainly related to oxidative stress causing neuronal impairment in the brain.

Although the potential of antioxidant compounds in vitro has often been demonstrated, knowledge has not been found in vivo. Therefore, in this study the use of methanol extract from *D. salina* might increase endogenous antioxidant activity which has an effect on increasing dopamine levels and reducing MDA levels in the fruit fly brain. Likewise the presence of *D. salina* extract on fruit fly culture medium will be able to increase the survival rate and also the ability of negative geotaxis as an expression of its locomotor phenotype. The ability of the *D. salina* extract against the toxicity of paraquat compounds indicates the content of antioxidant compounds such as polyphenols (321.53 mg GAE/g extract) and has strong antioxidant activity (74.49 μ g / mL).

5. Conclusion

In this study, we demonstrated that methanol extract of *D. salina* was able to protect against toxicity from paraquat as a neurotoxin agent. This capability was the contribution of potential antioxidant compounds from *D. salina* proven by its ability to increase survival rate, locomotor performance (in negative geotaxis), and ability to increase dopamine levels and reduce MDA levels as the end results of lipid peroxidation. The obtained data leads to the recognition that microalgae of *D. salina* as a neuroprotective agent have the potential to reduce symptoms found in Parkinson's disease.

Acknowledgment

This study has been supported by Biology Department of Universitas Islam Negeri Sunan Gunung Djati Bandung of Indonesia, both financially and otherwise. Hence, the authors are obliged to express their gratitude.

References

- Aryal B, Lee Y. 2019. Disease model organism for Parkinson disease: *Drosophila melanogaster*," *BMB Rep.*, **52**(4): 250-258.
- Guo JF, Lu ZL, Li K. 2018. Coding mutations in NUS1 contribute to Parkinson's disease. *Proceedings of the National Academy of Sciences. PNAS Latest Articles.*, October 2018; 1-6.
- Gupta G, Gliga A, Hedberg J, Serra A, Greco D, Wallinder IO, Fadeel B. 2020. Cobalt nanoparticles trigger ferroptosis-like cell death (oxytosis) in neuronal cells: Potential implications for neurodegenerative disease. *The FASEB Journal.*, 1-20.
- Helena XH, Peñuelas N, Miquel VM, Laguna A. 2019. Autophagic- and Lysosomal-Related Biomarkers for Parkinson's Disease: Lights and Shadows. *Cells.*, **8**(1317): 1-20.
- Jahromi JR, Haddadi M, Shivanandappa T and Ramesh SR. 2015. Attenuation of neuromotor deficits by natural antioxidants of *Decalepis hamiltoni* in transgenic *Drosophila* model of Parkinson's disease. *Neuroscience.*, **293**: 136-150.
- Jhonsa DJ, Badgular LB, Sutariya BK and Saraf MN. 2016. Neuroprotective effect of flavonoids against paraquat induced oxidative stress and neurotoxicity in *Drosophila melanogaster*. *Cur. Top. Nutra. Res.* **14**(4): 283-294.

- Lazzari FD, Sandrelli F, Whitworth AJ, Bisaglia M. 2020. Antioxidant Therapy in Parkinson's Disease: Insights from *Drosophila melanogaster*. *Antioxidants*, **9**(52): 1-17.
- McCann ME, de Graaff JC, Dorris L. 2019. Neurodevelopmental outcome at 5 years of age after general anaesthesia or awake-regional anaesthesia in infancy (GAS): an international, multicentre, randomised, controlled equivalence trial. *Lancet*, **393**: 664-77.
- Mohamed NA, Shehata MI, El-Sawaf AL, Hussein HKH, Michel PTN. 2018. The Ameliorating Effect of Erythropoietin on Diabetic Neurodegeneration by Modulating the Antioxidant-Oxidant Imbalance and Apoptosis in Diabetic Male Rats. *Jordan J. Biol. Sci.*, **11**(3): 339 - 345
- Nelson MP, Boutin M, Tse TE. 2018. The lysosomal enzyme alpha-Galactosidase A is deficient in Parkinson's disease brain in association with the pathologic accumulation of alpha-synuclein. *Neurobiol Dis.*, **110**: 68-81.
- Niveditha S, Ramesh SR and Shivanandappa T. 2017. Paraquat-induced movement disorder in relation to oxidative stress-mediated neurodegeneration in the brain of *Drosophila melanogaster*. *Neuro Res.*, **42**: 3310-3320.
- Quintero-Espinosa D, Jimenez-Del-Rio M, Velez-Pardo C. 2016. Knockdown transgenic Lrrk *Drosophila* resists paraquat-induced locomotor impairment and neurodegeneration: A therapeutic strategy for Parkinson's disease. *Brain Res.*, **1657**: 253-261.
- Rzezniczak TZ, Douglas LA, Watterson JH and Merritt TJS. 2017. Paraquat administration in *Drosophila* for use in metabolic studies of oxidative stress. *Anal Biochem.*, **419**(2): 345-347.
- Sakai R, Suzuki M, Ueyama M, Takeuchi T, Minakawa EN, Hayakawa H. 2019. E46K mutant α -synuclein is more degradation resistant and exhibits greater toxic effects than wild-type α -synuclein in *Drosophila* models of Parkinson's disease. *Plos One*, **14**(6): 1-16.
- Sanz FJ, Solana-Manrique C, Muñoz-Soriano V, Calap-Quintana P, Moltó MD, Paricio N. 2017. Identification of potential therapeutic compounds for Parkinson's disease using *Drosophila* and human cell models. *Free Rad Bio Med.*, **108**: 683-691.
- Sedjati S, Delianis P and Muhamad F. 2020. Determination of the Pigment Content and Antioxidant Activity of the Marine Microalga *Tetraselmis suecica*. *Jordan J. Biol. Sci.*, **13**(1): 55-58
- Siddique YH and Jyoti S. 2017. Alteration in biochemical parameters in the brain of transgenic *Drosophila melanogaster* model of Parkinson's disease exposed to apigenin. *Integ. Med. Res.*, **6**(3) : 245-253.
- Soares JJ, Rodrigues DT, Gonçalves MB, Lemos MC, Gallarreta MS, Bianchini MC, Gayerc MC, Puntel RL, Roehrs R and Denardi ELG. 2017. Paraquat exposure-induced Parkinson's disease-like symptoms and oxidative stress in *Drosophila melanogaster*: Neuroprotective effect of *Bougainvillea glabra* Choisy. *Biomed Pharmacotherapy*. **95**: 245-251.
- Standaert DG, Saint-Hilaire MH, Cathi A, Thomas CA, Joan and Collard R. 2016. **Parkinson's Disease Handbook**. America : Medtronic.
- Stephano F, Nolte S, Hoffmann J, El-Kholy S, von Frieling J, Bruchhaus I, Fink C and Roeder T. 2018. Impaired Wnt signaling in dopamine containing neurons is associated with pathogenesis in a rotenone triggered *Drosophila* Parkinson's disease model. *Sci. Rep.*, **8**(2372).
- Stockum SV, Sanchez-Martinez A, Corra S. 2019. Inhibition of the deubiquitinase USP8 corrects a *Drosophila* PINK1 model of mitochondria dysfunction. *life-science-alliance.*, **2**(2) : 1-16.
- Thakolwiboon S, Julayanont P and Ruthirago D. 2017. Pesticides and Parkinson's disease: A potential hazard in agricultural communities. *The Southwest Resp Crit Care Chron.* **5**(20): 60-67.
- Wells C, Brennan SE, Keon M and Saksena NK. 2019. Prionoid in the Pathogenesis of Neurodegenerative Diseases. *Front. Mol. Neurosci.*, **12** (271): 1-24.
- Wong YK, Ho YH, Ho KC, Lai YT, Tsang PM, Chow KP, Yau YH, Choi MC and Ho RSC. 2016. Effects of light intensity, illumination cycles on microgreens," *Journal of Mar. Bio. and Aquacul.*, **2**(2): 1- 6.
- Xiong Y, Dawson TM, Dawson VL. 2017. Models of LRRK2 associated Parkinson's disease," *Adv Neurobiol.*, **14**: 163-191.
- Xiong Y, Yu J. 2018. Modeling Parkinson's Disease in *Drosophila*: What Have We Learned for Dominant Traits? *Front Neurol.*, **9**(228): 1-15.

Cytokine genes expression in uteri of *Bubalus bubalis* associated with endometritis infection

Dalia A. Taha¹, Eman R. Mahfouz^{1,*}, Mona A. Bibars¹, Nagwa A. Hassan² and Othman E. Othman¹

¹Cell Biology Department, National Research Centre, Dokki, Egypt ;²Zoology Department, Faculty of Science, Ain Shams University, Egypt

Received: March 26, 2020; Revised: September 9, 2020; Accepted: September 11, 2020

Abstract

Fertility deficiency is one of the major causes which lead to a decrease in river buffalo's production that has great economic importance in Egypt. Infection of the endometrium with different types of bacteria leads to inflammations causing infertility in severe conditions. The difference in cytokines expression profiles has a role in the early detection of subclinical endometritis-infected buffalo. The present study aimed to assess some cytokine gene expressions in endometritis-infected buffaloes using RT-qPCR. The uteri samples were collected from 60 animals with inflammation signs and other 60 healthy animals. RNA was extracted from uteri samples and cDNA was synthesized from extracted RNA. Gene expressions were detected by real-time PCR using SYBR Green PCR Master-Mix and primers specific for tested genes (*IL-1 α* , *IL-1 β* , *IL-6*, *IL-10* and *TNF- α*). Cycle threshold (Ct) mean values of triplicate samples were utilized for analysis. Chi-square test was utilized to determine the significant differences ($P < 0.05$) in gene expression of tested genes using *GAPDH* as a house-keeping gene for normalization. Bacterial examination of uteri from infected buffaloes showed the presence of bacterial contamination with *Escherichia coli*, *Klebsiella pneumonia* and *Proteus vulgaris*, whereas the uteri of apparently-healthy animals did not show any of the previous pathogenic bacteria. The RT-qPCR results revealed that the gene expression of three tested cytokines; *IL-1 α* , *IL-1 β* and *IL-6* increased in endometritis-infected buffaloes with 1.3, 1.7 and 5 folds, respectively compared to their expression in healthy animals. On the contrary, the expressions of two other genes: *IL-10* and *TNF- α* showed down regulations with 0.2 and 0.4 folds, respectively in infected buffaloes when compared with those in uninfected animals. It can be concluded that the tested cytokine genes in endometritis-infected buffaloes showed different responses to the endometritis infection, where three of them: *IL-1 α* , *IL-1 β* and *IL-6* were up-regulated, whereas *IL-10* and *TNF- α* were down-regulated with different levels of significant values.

Keywords: Endometritis, Buffalo, Cytokines gene, RT-qPCR, Gene expression

1. Introduction

Buffalo is the most economically important livestock in many developing countries including Egypt where it is considered to be one of the main sources of milk and meat. Any loss in its production leads to a valuable increase in the gap between increased population and the demand for this important foodstuff. Fertility deficiency is one of the major causes leading to a decrease in buffalo's production (Mohammed, 2018).

The uteri in mammals are a sterile environment, but always - especially during coitus or parturition - they are ready to infection with different types of bacteria (Benko *et al.* 2015). This bacterial contamination leads to inflammation ranging from pelvic disease to chronic endometritis and infertility (Park *et al.* 2016). The infection of the endometrium with *E. coli* is associated with the impact on female fertility (Dahiya *et al.*, 2018).

Cytokines are natural proteins produced by immune cells and act importantly in host defense against infection and participate in specific and nonspecific immunity.

Depending on the type of simulated cells and the nature of the antigenic stimulus, the cytokine type is released from the cell. Cytokines equalize the leukocytes to respond to bacterial and microbial stimuli, and they are classified into the following six groups; L1 superfamily, TNF superfamily, IL-6 superfamily, IL-17 family, type I superfamily and type II superfamily (Muñoz Carrillo *et al.*, 2018).

Several researches reported the variations in cytokine expression in inflammatory disorders (Audet *et al.*, 2014). Sensitive detection techniques are required to observe their expression and secretion under various physiological conditions. Many techniques allow quantitation of cytokine expression at the protein level like ELISA and at the mRNA level like reverse transcriptase polymerase chain reaction (RT-PCR) (Skalnikova *et al.*, 2017).

Subclinical endometritis is difficult to detect, the animals appear healthy but they are carrier of bacteria that cause infection to other animals. Therefore, the control of subclinical endometritis is the best way to reduce the harmful effect of this disease (Molina-Coto and Lucy, 2018). Since the inflammatory responses were known to be induced by the cytokines during the infection, the

* Corresponding author e-mail: emanmahfouz27@yahoo.com.

difference in cytokines expression profiles became with valuable impact in the early detection of subclinical endometritis-infected buffalo. The present study aimed to investigate the difference in some cytokines gene expressions between healthy and endometritis-infected buffaloes reared in Egypt using RT-qPCR.

2. Materials and Methods:

2.1. Samples and bacterial identification

The uteri samples were obtained from 120 Egyptian buffaloes; 60 infected with endometritis and 60 normal ones. Buffaloes with endometritis showed abnormal secretions with signs of inflammation such as swelling, redness and hardness in the uterus.

Collected samples were streaked onto: Blood agar, Mac-Conkey agar and mannitol salt agar plates. All samples were incubated aerobically and anaerobically. Aerobic plates were incubated at 37°C for 24 h, whereas anaerobic plates were incubated in an anaerobic jar using anaerobic system (BD) at 37°C for 84-72 h. Plates were examined for colony characters, cellular morphology and the purity of the culture.

2.2. RNA extraction and cDNA synthesis

RNA was extracted from uteri samples using a total RNA purification kit (Jena Bioscience, Germany), according to the manufacturer's instructions. An aliquot of RNA was diluted in RNase free water to estimate RNA quantity. The concentration of RNA samples was determined using the NanoDrop spectrophotometer and the purity of RNA was assessed by 260/280 nm ratio.

cDNA synthesis was performed on extracted RNA, which was treated with DNase to remove any possible DNA contamination. One µl of DNase and 1 µl buffer were added to 1 µg RNA, and the volume was completed

to 10 µl by DEPC water and incubated at 37°C for 30 min. 1 µl of EDTA was added and incubated at 70°C for 10 min. The DNase-treated RNA was reverse transcribed into first-strand cDNA using the RevertAid First Strand cDNA Synthesis kit (Fermentas) according to the manufacturer's instructions.

2.3. Real-time polymerase chain reaction (Real-time PCR):

Gene expressions were detected by real-time PCR, which was performed using the Rotor-Gene Q system (Qiagen Company). A 25 µl reaction mixture consisted of 12.5 µl SYBR Green PCR Master-Mix (applied Biosciences, USA), 0.5 µl of each primer (10 PMole) [Table 1], 1 µl cDNA (50 ng) and 10.5 µl RNase free water.

The optimum amplification conditions were chosen empirically according to each tested gene. Generally, the amplification conditions include initial incubation, then 40 cycles of amplification with denaturation, annealing and extension steps. Mean cycle threshold (Ct) values of triplicate samples are used for analysis. The Ct value indicates the fractional cycle number at which the amount of amplified target reaches a fixed threshold.

2.4. Data analysis

A Chi-square test was used to evaluate the significant differences ($P < 0.05$) in gene expression of tested genes. Data from real-time PCR were analyzed using $2^{-\Delta\Delta Ct}$ method (Livak and Schmittgen, 2001). Data were represented as the fold change in target gene expression normalized to a House-Keeping gene (HKG) and relative to the control (uninfected animals). Glyceraldehyde-3-phosphate dehydrogenase (*GAPDH*) was used as a house-keeping gene to normalize input RNA amount, RNA quality and reverse transcription efficiency.

Table 1. Primer information of tested genes and the housekeeping gene

Gene	Primer sequences	Amplicon size (bp)	References
Interleukin-1 alpha (<i>IL-1α</i>)	F: AGAGGATTCTCAGCTTCCTGTG R: ATTTTCTTGGCTTTGTGGCAAT	224-bp	
Interleukin-1 beta (<i>IL-1β</i>)	F: GAG GAG CAT CCT TTC ATT CAT C R: TTC CTC TCC TTG TAC GAA GCT C	229-bp	Herath <i>et al.</i> , (2009)
Interleukin-6 (<i>IL-6</i>)	F: ATG ACT TCT GCT TTC CCT ACC C R: GCT GCT TTC ACA CTC ATC ATT C	180-bp	
Interleukin-10 (<i>IL-10</i>)	F: TACTCTGTTGCCCTGGTCTTCCT R: AGTAAGCTGTGCAATTGGTCTCT	178-bp	
Tumor necrosis factor alpha (<i>TNF-α</i>)	F: CGG TGG TGG GAC TCG TAT G R: CTG GTT GTC TTC CAG CTT CAC A	352-bp	Coussens <i>et al.</i> , (2004)
Glyceraldehyde-3-phosphate dehydrogenase (<i>GAPDH</i>)	F: CCT GGA GAA ACC TGC CAA GT R: GCC AAA TTC ATT GTC GTA CCA	214-bp	Buza <i>et al.</i> , (2003)

3. Results and Discussion

Two immunity systems are considered the key factors for controlling infectious diseases; innate and adaptive systems. Cytokines play an orchestral role in the balance between these two systems (Silva-Barrios and Protozoan, 2017). Cytokines are involved in the regulation of tissue repairing during inflammation (Grignani and Maiolo,

2000). They are secreted by immune cells and act on different target cells with major effects on the function of many immune genes including other cytokines (Carson and Kunkel, 2017). Many reports discussed the effect of uterine infection at postpartum on the ovarian function, embryo development and the decrease of the frequency of successful pregnancy. These fertility disorders lead to economic loss in livestock production, especially in buffalo (Patra *et al.*, 2013). In this respect, Osman *et al.*

(2018) suggested the existence of novel polymorphic sites in TLR4 gene in the river buffalo Egyptian breed and their accompanied with occurrence of endometritis disease. This study was considered to assess the differential expression of some cytokine genes in endometritis-infected buffalo reared in Egypt. Five cytokine genes: *IL-1 α* , *IL-1 β* , *IL-6*, *IL10* and *TNF- α* in addition to *GAPDH* (as a housekeeping gene) were included in this study.

Bacterial examination of uteri from 60 endometritis-infected buffaloes showed the presence of bacterial contamination in these samples; 33 samples with *E. coli*, 21 samples with *P. Klebsiella pneumonia* and 6 samples with *P. vulgaris*. The sixty apparently-healthy buffaloes did not show any sign of endometritis symptoms, and their uteri did not show any pathogenic bacteria.

The quantitative gene expressions of these cytokine genes were evaluated in one hundred-twenty buffaloes; sixty with endometritis infection and other sixty apparently healthy animals. Ct was calculated in triplicate for each sample and the mean was recorded for each sample.

IL-1 α is a member of the interleukin 1 family, and it is related to the inflammation production and fever promotion. So, the inhibition of this immune gene contributes in treatment of these disorders. *IL-1 α* is produced mainly by macrophages, neutrophils and epithelial cells. This cytokine has a major role in the regulation of the immune system through different physiological and hematopoietic activities including increasing of blood neutrophils and activation of fibroblasts and neutrophils proliferations (Dinarello, 2017).

The Cts for 60 infected buffaloes ranged from 19.79 to 31.77 with a mean value of 25.44, whereas their values ranged from 22.21 to 31.15 with a mean of 26.14 in normal buffaloes. The calculated $-\Delta\Delta Ct$ was 0.37; which means that the expression of this gene is up-regulated with 1.3 folds (Fig. 1). The p-value of the up-regulation of *IL-1 α* gene expression is 0.017 (<0.05) as a significant level.

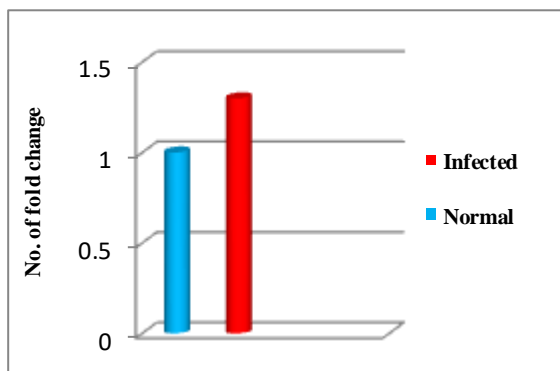


Figure 1: No. of fold changes in *IL-1 α* gene expression between normal and infected animals

Gene expression profiles of this cytokine were extensively studied in livestock infected with different diseases. Using of *Yersinia enterocolitica* as a model enteric pathogen, Dube *et al.* (2001) identified the role of *IL-1 α* for induction of pathologic inflammation during bacterial infection. Aho *et al.* (2003) recorded the enhanced expression of *IL-1 α* in Johne's disease-infected cattle compared with healthy animals using cDNA microarray and RT-qPCR. On the other hand, the pro-inflammatory mediators' expressions as *IL-1 α* was reported to be higher during the first week post partum as

well as in infertile than fertile animals (Herath *et al.*, 2009). In the same respect, mRNA of *M. avium* subsp. *paratuberculosis* infected-animals expressed elevated measures of many interleukins including *IL-1 α* comparing to the similar tissues from normal cattle (Coussens *et al.*, 2004 and DeKuiper and Coussens, 2019).

The cytokine interleukin-1 β (*IL-1 β*) has a major role in the inflammatory response, where its secretion is essential for the response and resistance of infected host to pathogens (Lopez-Castejon and Brough, 2011). The pro-inflammatory cytokine *IL-1 β* is expressed by several cells which include monocytes, macrophage, neutrophils and NK cells. The *IL-1 β* secretion and its continuity depends on the strength of stimuli and the requirement for it (Chan and Schroder, 2020).

In this study, the differential expression of this *IL-1 β* immune gene was assessed in endometritis-infected buffalo. The threshold cycles of infected animals ranged from 17.46 to 32.68 with a mean value of 23.01. The Ct values in normal animals ranged from 18.17 to 34.34 with a mean of 24.10. Relative to Ct values of *GAPDH*, the $-\Delta\Delta Ct$ was 0.76, which means; the *IL-1 β* expression was elevated in infected buffaloes with 1.7 folds (Fig. 2) compared to healthy animals. The p value of up-regulation of *IL-1 β* gene expression is 0.032 (<0.05) as a significant level.

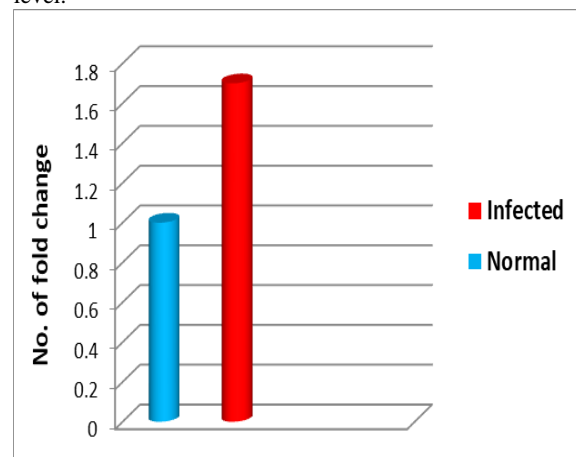


Figure 2: No. of fold changes in *IL-1 β* gene expression between infected and normal animals

The up-regulation of *IL-1 β* gene expression was recorded in some infected livestock compared with healthy ones. By comparing the expression in sheep ileal tissue for thirteen genes with three different forms of paratuberculosis, Smeed *et al.* (2007) has reported higher levels of tested cytokines including *IL-1 β* compared to normal's tissues. Confirming the hypothesis that postpartum cattle suffer from endometritis and infertility as a result of the limited inflammatory response to uterine bacterial infection, Herath *et al.* (2009) declared the elevation of *IL-1 β* expression in infected and infertile animals than that in healthy cattle. Abdel Aziz *et al.* (2014) analyzed the expression profile of three cytokine genes in response to bovines infected with *Babesia*. The results showed highly significant up-regulation of *IL-1 β* gene in *Babesia*-infected cattle compared to non-*Babesia* infected animals.

Interleukin 6 (*IL-6*) is acting as a pro-inflammatory cytokine as well as anti-inflammatory myokine, and it is an important mediator of the acute phase response and fever

(Tanaka *et al.*, 2014). In the innate immune system macrophages secrete *IL-6* responding to pathogen-associated molecular manner linked to a group of recognition receptors pattern. These receptors, which exist on the cell surface, stimulate intracellular signaling cascades that induce inflammatory cytokine production (Woo *et al.*, 2017). This interleukin can change the body's temperature setpoint through initiating Prostaglandin E2 synthesis in the hypothalamus after crossing the blood brain barrier, and it induces energy mobilization in fatty tissue and muscle that increases the body temperature (Zampronio *et al.*, 2015).

The differential expression of *IL-6* in healthy and endometritis-infected buffaloes was studied in this work. The range of threshold cycles for infected animals was detected between 18.49 and 33.11 with a mean value of 25.43, whereas it was from 16.48 to 37.3 with a mean of 28.09 in healthy buffaloes. The $-\Delta\Delta C_t$ value of this gene was 2.33, which means that the expression of *IL-6* is increased in infected animals by 5 folds (Fig. 3) compared to healthy buffaloes. The p value of up-regulation of this immune gene expression is 0.001 as a highly significant level.

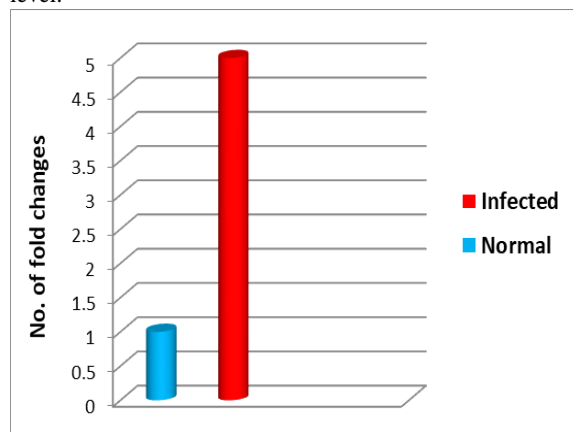


Figure 3: No. of fold changes in *IL-6* gene expression between normal and infected animals

Harris *et al.* (2000) reported the significant elevation of some cytokine molecules number including *IL-6* in gastric tissue infected with *Helicobacter pylori* comparing with the pre-infection numbers. *IL-6* mRNA expression in *M. avium* subsp. *Paratuberculosis*-infected cows was significantly greater ($P < 0.05$) than that in healthy animals, where it was more than 6.5-fold higher in infected animals (Coussens *et al.*, 2004). On the other hand, Glass and Jensen (2007) detected the gene expression of some pro-inflammatory cytokines in cattle infected with *Theileria annulata* and reported the non-significant increase of *IL-6* in infected animals compared to controls. Maranga *et al.* (2013) reported the significant ($p < 0.05$) upregulation of *IL-6* expression in experimentally *Trypanosoma brucei*-infected monkeys compared with uninfected animals. The upregulation of this cytokine expression was observed in VSV-infected swine suggesting a strong correlation between *IL-6* and the infection of pig with vesicular stomatitis virus (Velazquez-Salinas *et al.*, 2019).

Interleukin 10 (*IL-10*) is a cytokine that has strong anti-inflammatory characters and plays a major role in response to infected-host against pathogens. Therefore, the disturbance in the expression of this immune gene leads to the increased risk for infection with autoimmune diseases

(Iyer and Cheng, 2012). During the infection, *IL-10* does not only inhibit the activity of some immune cells including macrophages, which is important for pathogen clearance, but also it has a role in tissue damages. This controversial protein is produced with different types of cells, and its source may vary between different tissues and during the response to the same infection (Couper *et al.*, 2008). Upon infection, the unclear behavior of this gene was one of the main reasons for this study to shed the light on this important cytokines in order to assess its expression in endometritis-infected buffaloes.

Regarding its expression assessment, Ct values ranged from 24.01 to 32.71 with a mean of 26.74 in endometritis-infected animals, whereas the range of Ct values in healthy ones was 19-8-28.7 with a mean value of 24.86. The calculated $-\Delta\Delta C_t$ of *IL-10* in this study was -2.21, which means that the expression of *IL-10* was down-regulated in infected animals by 0.2 folds (Fig. 4). The p value for down-regulation of *IL-10* gene expression is 0.15 as non significant level.

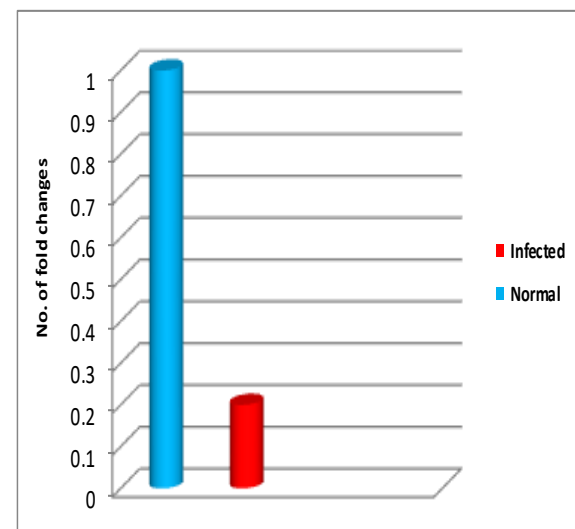


Figure 4. No. of fold changes in *IL-10* gene expression between normal and infected animals

Coussens *et al.* (2004) examined the expression of ten interleukins in addition to other three cytokines in cattle naturally-infected with Johne's disease. The differential expression of all tested genes did not require stimulation with the exception of *IL-10* which required enhancement by *M. avium* subsp. *paratuberculosis* stimulation of PBMCs from sub-clinically infected cattle. *IL-10* was not included with the cytokines whose expression was recorded to be increased during the first week postpartum (Herath *et al.*, 2009). They reported higher ratios of both interleukins 1 (α and β) mRNA expression to *IL-10* in endometritis-infected cattle. The *IL-10* expression during infection with *Fasciola hepatica* was investigated by Mendes *et al.* (2013) using Qt-PCR. They reported a synergism between *IL-10* and *IL-4* with Interferon gamma in the liver tissues of infected cattle and suggested the role of *IL-10* in modulating the immune response.

Tumor necrosis factor alpha (*TNF- α*) is a cell signaling protein which has a role in systemic inflammation process. The main source of its production is the activated macrophages in addition to other producers like neutrophils and eosinophils (Parameswaran and Patial, 2010). In addition to the role of *TNF- α* in immune system

functions like antitumor and antimicrobial activities, it has a role in physiological activities including appetite, fever and endocrine activity (Kushibiki, 2011). The disturbance of TNF regulation is implicated in some diseases including Alzheimer's disease (Swardfager *et al.*, 2010), cancer (Ma *et al.*, 2016) and bowel disease (Brynskov *et al.*, 2002).

The comparison between *TNF- α* expression in endometritis-infected and healthy buffaloes was performed in this study. The mean of Ct values in endometritis-infected animals was 25.41, where the Cts ranged from 20.08 to 31.15. The range of Ct values in healthy buffaloes was observed between 19.44 to 27.31 with a mean value of 24.38. The $-\Delta\Delta Ct$ was -1.36, meaning that the expression of *TNF- α* was down-regulated in infected buffaloes with 0.4 folds (Fig. 5) compared to healthy animals. The p value of this statistical down-regulation is 0.009 (<0.01) at a high significant level.

Using real-time RT-PCR, Smeed *et al.* (2007) reported the increased level of *TNF- α* expression in sheep's ileal tissue infected with three types of Johne's disease as indication of persistent inflammatory lesions, whereas asymptomatic animals had increased levels of *TNF α* and significantly decreased levels of *IL-18*.

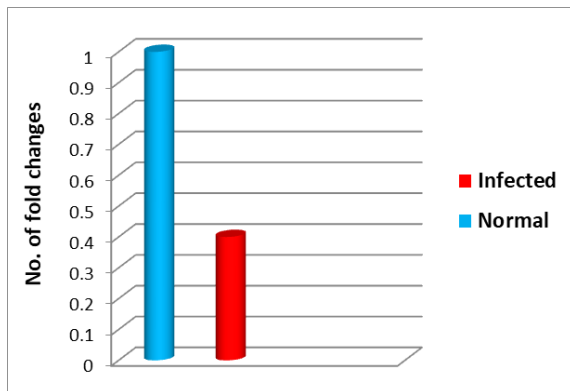


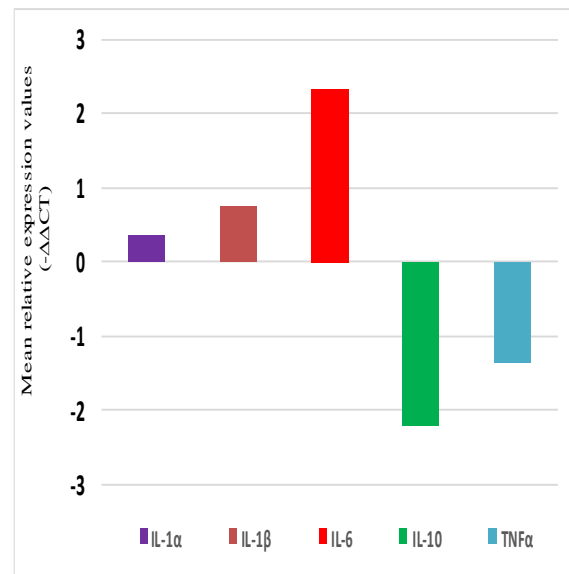
Figure 5: No. of fold changes in *TNF- α* gene expression between normal and infected animals

Aho *et al.* (2003) declared the significant high levels of gene expressions for some cytokines like *IL-1 α* in tissues from infected cattle with Johne's disease. They also reported that increased levels of TRAF1 within the lesions of Johne's-infected cattle may result in cells that are highly resistant to *TNF- α* stimulated signaling. On the contrary to the above-mentioned results, Glass and Jensen (2007) registered the absence of differences in gene expression of some immune genes including *TNF α* , *IL-1 β* and *IL-6* in infected cattle with *Theileria annulata*. Also, DeKuiper and Coussens (2019) argued that non-significant expression of cytokines like *IFN- γ* , *TNF- α* and *IL-17 α* in CD4+ T cells from cows infected with Johne's disease may be due to the exhaustion of immune T cells. In the same context, Bojaroj *et al.*, (2016) declared that there is no significant difference in the percent of PBMCs-expressing *TNF- α* in cow infected with leukemia virus even with the presence of different *TNF- α* genotypes.

Finally, it can be concluded that tested cytokines genes in endometritis-infected buffaloes differ in their response to endometritis infection, where three of them (*IL-1 α* , *IL-1 β* and *IL-6*) were up-regulated, while the other two genes: *IL-10* and *TNF- α* were down-regulated with different levels of significant values. The mean relative expression values ($-\Delta\Delta Ct$) of the five tested genes in

endometritis-infected buffaloes comparing to healthy animals were shown in Fig. 6.

Figure 6: Mean relative expression values ($-\Delta\Delta Ct$) of the tested genes in endometritis-infected buffaloes comparing to healthy animals



4. Conclusion

Innate and adaptive immune systems are considered the key factors for controlling infectious diseases. Cytokines play an orchestral role in the balance between these two systems, and they are involved in the regulation of tissue repairing during inflammation. This study was applied to determine the differential expression of some cytokine genes in endometritis-infected buffalo reared in Egypt. Five cytokine genes: *IL-1 α* , *IL-1 β* , *IL-6*, *IL-10* and *TNF- α* in addition to GAPDH (as a housekeeping gene) were included in this study. *IL-1 α* , *IL-1 β* and *IL-6* were found to be up-regulated, while the other two genes: *IL-10* and *TNF- α* were down-regulated with different levels of significant values. The identification of physiopathological pathways underlying many complex diseases may be facilitated by studying the genetic factors involved in their occurrence, which will develop our understanding for the disease in its entirety and to define the risk of developing it. This will ease and pave the way to improve the disease resistance in herds by selective breeding as well as identify and synthesize innovative drugs.

References

- Abdel Aziz KB, Khalil WKB, Mahmoud MS, Hassan NHA, Mabrouk DM and Suarez CE. 2014. Molecular characterization of babesiosis infected cattle: Improvement of diagnosis and profiling of the immune response genes expression. *Global Vet.*, **12** (2): 197-206.
- Aho AD, McNulty AM and Coussens PM. 2003. Enhanced expression of interleukin-1 α and tumor necrosis factor receptor-associated protein 1 in ileal tissues of cattle infected with *Mycobacterium avium* subsp. *Paratuberculosis*. *Infect. Immun.*, **71**(11): 6479-6486.

- Audet MC, McQuaid RJ, Merali Z and Anisman H. 2014. Cytokine variations and mood disorders: influence of social stressors and social support. *Front. Neurosci.*, **8**:416.
- Benko T, Boldizar M, Novotny F, Hura V, Valocky I, Dudrikova K, Karamanova M and Petrovic V. 2015. Incidence of bacterial pathogens in equine uterine swabs, their antibiotic resistance patterns, and selected reproductive indices in English thoroughbred mares during the foal heat cycle. *Vet. Med.*, **60**(11): 613-620.
- Bojarojc-Nosowicz B, Brym P, Kaczmarczyk E, Stachura A and Habel AK. 2016. Polymorphism and expression of the tumour necrosis factor-alpha (TNF-alpha) gene in non-infected cows and in cows naturally infected with the bovine leukaemia virus (BLV). *Vet. Med.*, **61**(1): 1-9.
- Brynskov J, Foegh P, Pedersen G, Ellervik C, Kirkegaard T, Bingham A and Saermark T. 2002. Tumour necrosis factor alpha converting enzyme (TACE) activity in the colonic mucosa of patients with inflammatory bowel disease. *Gut.*, **51**(1):37-43.
- Buza JJ, Mori Y, Bari AM, Hikono H, Hirayama S, Shu Y and Momotani E. 2003. Mycobacterium avium subsp. paratuberculosis infection causes suppression of RANTES, monocyte chemoattractant protein 1, and tumor necrosis factor alpha expression in peripheral blood of experimentally infected cattle. *Infect. Immun.*, **71**(12): 7223-7227.
- Carson WF and Kunkel SL. 2017. **Type I and II cytokine superfamilies in inflammatory responses. In: Inflammation: From Molecular and Cellular Mechanisms to the Clinic.** (Ed. by Cavailon, J.M. and Singer, M.). Weinheim, Germany: Wiley-VCH Verlag. pp. 587-618.
- Chan AH and Schroder K. 2020. Inflammasome signaling and regulation of interleukin-1 family cytokines. *J. Exp. Med.*, **217**(1): e20190314.
- Couper KN, Blount DG and Riley EM. 2008. IL-10: The master regulator of immunity to infection. *J. Immunol.*, **180**:5771-5777.
- Coussens PM, Verman N, Coussens MA, Elftman MD and McNulty AM. 2004. Cytokine gene expression in peripheral blood mononuclear cells and tissues of cattle infected with *Mycobacterium avium* subsp. *paratuberculosis*: Evidence for an inherent proinflammatory gene expression pattern. *Infect. Immun.*, **72**(3): 1409-1422.
- Dahiya S, Kumari S, Rani P, Onteru SK and Singh D. 2018. Postpartum uterine infection & ovarian dysfunction. *Indian J. Med. Res.*, **148**(Suppl 1): S64-S70.
- DeKuijper JL and Coussens PM. 2019. Inflammatory Th17 responses to infection with *Mycobacterium avium* subspecies *paratuberculosis* (MAP) in cattle and their potential role in development of Johne's disease. *Vet. Immunol. Immunopathol.*, **218**: 109954.
- Dinarello CA. 2018. Overview of the IL-1 family in innate inflammation and acquired immunity. *Immunol. Rev.*, **281**(1): 8-27.
- Dube PH, Revell PA, Chaplin DD, Lorenz RG and Miller VL. 2001. A role for IL-1a in inducing pathologic inflammation during bacterial infection. *PNAS.* **98**(19): 10881-10885.
- Glass EJ and Jensen K. 2007. Resistance and susceptibility to a protozoan parasite of cattle: Gene expression differences in macrophages from different breeds of cattle. *Vet. Immunol. Immunopathol.* **120**: 20-30.
- Grignani G and Maiolo A. 2000. Cytokines and hemostasis. *Haematologica.* **9**:967-972.
- Harris PR, Smythies LE, Smith PD and Dubois A. 2000. Inflammatory cytokine mRNA expression during early and persistent *Helicobacter pylori* infection in nonhuman primates. *J. Infect. Diseases.* **181**:783-786.
- Herath S, Lilly ST, Santos NR, Gilbert RO, Goetze L, Bryant CE, White JO, Cronin J, and Sheldon IM. 2009. Expression of genes associated with immunity in the endometrium of cattle with disparate postpartum uterine disease and fertility. *Reprod. Biol. Endocrinol.* **7**:55.
- Iyer SS and Cheng G. 2012. Role of interleukin 10 transcriptional regulation in inflammation and autoimmune disease. *Crit. Rev. Immunol.* **32**(1): 23-63.
- Kushibiki S. 2011. Tumor necrosis factor- α -induced inflammatory responses in cattle. *Anim. Sci. J.* **82**: 504-511.
- Livak KJ and Schmittgen TD. 2001. Analysis of relative gene expression data using real-time quantitative PCR and the $2^{-\Delta\Delta Ct}$ method. *Methods.* **4**: 402-408.
- Lopez-Castejon G and Brough D. 2011. Understanding the mechanism of IL-1 β secretion. *Cytokine Growth Factor Rev.* **22**(4): 189-195.
- Ma K, Zhang H and Baloch Z. 2016. Pathogenetic and therapeutic applications of tumor necrosis factor- α (TNF- α) in major depressive disorder: A systematic review. *Int J Mol Sci.* **17**: 733.
- Maranga DN, Kagira JM, Kinyanjui CK, Karanja SM, Maina NW and Ngotho M. 2013. IL-6 is upregulated in late-stage disease in Monkeys experimentally infected with *Trypanosoma brucei rhodesiense*. *Clin. Dev. Immunol.* Article ID 320509.
- Mendes EA, Mendes TA, dos Santos SL, Menezes-Souza D, Bartholomeu DC, Martins IV, Silva LM and Lima Wdos S. 2013. Expression of IL-4, IL-10 and IFN- γ in the liver tissue of cattle that are naturally infected with *Fasciola hepatica*. *Vet. Parasitol.* **195**(1-2): 177-182.
- Mohammed KME. 2018. Application of advanced reproductive biotechnologies for buffalo improvement with focusing on Egyptian buffaloes. *Asian. Pac. J. Reprod.* **7**(5): 193-205.
- Molina-Coto R and Lucy MC. 2018. Uterine inflammation affects the reproductive performance of dairy cows: A review. *Agron. Mesoam.* **29**(2):449-468.
- Muñoz-Carrillo JL, Contreras-Cordero JF, Gutiérrez-Coronado O, Villalobos-Gutiérrez PT, Ramos-Gracia LG and Hernández-Reyes VE. 2018. **Cytokine profiling plays a crucial role in activating immune system to clear infectious pathogens. In: Immune response activation and immunomodulation.** (Ed. by Tyagi RK and Bisen PS).
- Osman NM, Abou Mossallam AA, El Seedy FR and Mahfouz ER. 2018. Single Nucleotide Polymorphisms in TLR4 Gene and Endometritis Resistance in River Buffalo (*Bubalus bubalis*). *Jordan J Biol Sci.* **11** (5): 577- 583.
- Parameswaran Nand Patial S. 2010. Tumor necrosis factor- α signaling in macrophages. *Crit. Rev. Eukaryot. Gene Expr.* **20**(2): 87-103.
- Park HJ, Kim YS, Yoon TK and Lee WS. 2016. Chronic endometritis and infertility. *Clin. Exp. Reprod. Med.* **43**(4): 185-192.
- Patra MK, Kumar H and Nandi S. 2013. Neutrophil functions and cytokines expression profile in buffaloes with impending postpartum reproductive disorders. *Asian Australian. J. Anim. Sci.* **26**(10): 1406-1415.
- Silva-Barrios S and Stäger S. 2017. Protozoan parasites and type I IFNs. *Front. Immunol.* **8**:14.
- Skalnikova HK, Cizkova J, Cervenka J and Vodicka P. 2017. Advances in proteomic techniques for cytokine analysis: Focus on melanoma research. *Int. J. Mol. Sci.* **18**:2697.
- Smeed JA, Watkins CA, Rhind SM and Hopkins J. 2007. Differential cytokine gene expression profiles in the three pathological forms of sheep paratuberculosis. *BMC Vet. Res.* **3**:18.

Swardfager W, Lanctôt K, Rothenburg L, Wong A, Cappell J and Herrmann N. 2010. A meta-analysis of cytokines in Alzheimer's disease. *Biol. Psychiatry*. **68**(10): 930-941.

Tanaka T, Narazaki M and Kishimoto T. 2014. IL-6 in inflammation, immunity, and disease. *Cold Spring Harb Perspect Biol*. **6**: a016295.

Velazquez-Salinas L, Verdugo-Rodriguez A, Rodriguez LL and Borca MV. 2019. The role of interleukin 6 during viral infections. *Front. Microbiol*. **10**:1057.

Woo J, Yang Y, Ahn J, Choi YS and Choi J. 2017. Interleukin 6 secretion from alternatively activated macrophages promotes the migration of endometriotic epithelial cells. *Biol. Reprod*. **97**(5): 660-670.

Zampronio AR, Soares DM and Souza GEP. 2015. Central mediators involved in the febrile response: effects of antipyretic drugs. *Temp*. **2**(4): 506-521.

Influence of drought stress on physiological traits of crossed okra varieties

Zainab G. Ahmed¹, Magdi A. El-Sayed^{1,2,*}

¹Botany Department, Faculty of Science, Aswan University, Aswan 81528, Egypt; ²Molecular Biotechnology Program, Field of Advanced Basic Sciences, Galala University, Galala New City, Egypt

Received: June 17, 2020; Revised: Dec 2, 2020; Accepted Mar 11, 2021

Abstract

Drought and heat stresses are major constraints to agriculture worldwide, reducing crop productivity and affecting global food security. Two okra cultivars (Japanese and Egyptian) with different physiological attributes were crossbred for producing F1 hybrids. All cultivars and their hybrids were evaluated for drought stress tolerance at two water regimes (12% and 2%). At limited water condition, photosynthesis and stomatal conductance tended to decrease in Egyptian parent and Japanese × Egyptian hybrid while transpiration rate showed no significant changes in both parents and F1 hybrids. Maximum quantum yield of PSII (Fv/Fm) ratio was decreased with decreasing soil moisture content in Japanese cultivar, E×J and J×E hybrids with mean value of (0.14, 0.16 and 0.15, respectively). Chlorophyll content in both parents and their hybrids was decreased under severe drought stress. Significant high activity levels of the anti-oxidative enzymes, peroxidase (POX) and superoxide dismutase (SOD) was observed in water-stressed plants than in well-watered (12% water regime) plants. The highest activity of POX was recorded in E×J hybrid (234.9 U/g FW) and the highest activity of SOD was found in Japanese cultivar (18.69 U/g FW). Accumulation of proline content under drought severity stress in both hybrids (E×J and J×E) was recorded (16.7 and 10.4 mg/g DW, respectively). The performance of E×J hybrid was more prominent than parents because of the strong antioxidant defence system and accumulation of higher proteins, proline and chlorophyll content than other cultivars.

Keywords: *Abelmoschus esculentus*, metabolic changes, antioxidant enzymes, cross breeding

1. Introduction

Global water scarcity and change in climate are responsible for the occurrence and severity of drought, heat and salinity stresses in the environment. Combined drought and heat events are the most destructive abiotic stress to crop growth and productivity worldwide, which promote evapotranspiration and affects photosynthetic rate (Mir et al., 2012; Lamaoui et al., 2018). Drought and heat stresses are both important threat limitations impairing plants' photosynthetic rate and altering stomatal function (Silva et al., 2010). Anjum et al. (2017) concluded that exposure to environmental stresses increases reactive oxygen species (ROS) production and thus leads to harmful oxidative damage, impairing the normal cellular functions and causing damages to lipids, proteins and nucleic acids. Heat stress and water deficit also affect the electron transport rate (ETR) and damage the photosynthetic apparatus PSII (Guo et al., 2016). Chlorophyll fluorescence is a non-invasive measurement detecting the authenticity of photosystem II (PSII) (Harb and Lahham, 2013). Chl fluorescence parameters such as photosystem efficiency (Fv/Fm), minimal fluorescence (Fo) and maximal fluorescence (Fm) are useful tools for detection of drought stress severity, genetic variation and determine any damage to PSII (Rahbarian et al., 2011).

In order to cope and adapt stress conditions, plants respond by triggering molecular, physiological and biochemical processes such as altering gene expression, inducing osmolyte accumulation and activation of the antioxidant system whether enzymatic or non-enzymatic (Reddy et al., 2004; Hussien et al., 2019). Plants can regulate their rates of photosynthesis by modifying photosystem II, low electron transport rate and enhance stomatal closure (Khan et al., 2016).

Finding new strategies for maintaining crop productivity under adverse drought, salt and heat stress conditions is probably the major challenge being faced by recent agriculture (Lizana et al., 2006; Albdaiwi et al., 2019). Plant breeders exploit the genetic diversity to make significant improvement towards developing drought adapted crops.

Okra (*Abelmoschus spp.* (L) Moench) is an important cultivated vegetable crop in Egypt, and it is grown for its edible fruits. It is energy supplier to the human diet as well as carbohydrates, protein, fat, fibers, minerals and vitamins (Adejumo et al., 2018). Its usage is increasing in pharmaceutical industry due to high content of polysaccharides and bioactive compounds (Petropoulos et al., 2017). Based on Kusvuran et al. (2012) study, okra genotypes exhibited differences in physiological responses to drought stress; these differences are related to the valuable genetic variation between okra genotypes (Aaron

* Corresponding author e-mail: Magdi A. El-Sayed: magdiel_sayed@aswu.edu.eg.

et al., 2016). Genetic variation in okra is necessary for crop improvement (Sawadogo et al., 2006).

Egyptian cultivar (African variety) and Japanese cultivar (Asian variety) of okra showed differences in their morpho-physiological characteristics (Ahmed and El-Sayed, 2019) and were expected to respond differently when subjected to a drought stress. High productivity Japanese variety was crossed with local nutritional low productivity variety and the produced hybrids were tested in this study for their tolerance to water deficiency. Ultimately, this study aims to investigate the effect of drought stress on physiological traits and metabolic variability, and to assess the performance of new okra hybrids under drought stress.

2. Materials and methods

2.1. Plant material and growth conditions

The experiments were performed on cultivars of okra (*Abelmoschus esculantus*) i) Egyptian cultivar and ii) Japanese cultivar and two intraspecific F1 hybrids derived from a cross between these two parents (Ahmed and El-Sayed, 2019). These cultivars and their F1 offspring were planted in summer season in nursery under normal climatic conditions at Research Unit for Studying plants of Arid Lands (RUSPAL). They were grown in pots containing a mix of sand and clay (1:1 w/w), and three month old plants were subjected to two moisture levels including 12% (100 % pot water holding capacity as well-watered (Control) and 2% of the maximum capacity for water retention that applied for stressed plants. Healthy expanded leaf samples were collected at time of the measurement of physiological responses, metabolic content and defensive antioxidant enzymes.

2.2. Gas exchange measurements and Chlorophyll fluorescence

Gas exchange (including Photosynthesis rate (pn), transpiration rate (E), leaf intercellular CO₂ concentration, stomatal conductance (Ci)) were measured using infrared gas analyzer (IRGA, CI 340) photosynthesis system (CID Bio-Science, Inc.) on one randomly selected fully expanded healthy leaf. Timing of data recording was between 11:00 AM to 1:00 PM and between 5:00 to 7:00 PM.

The fourth last fully expanded leaf from different plant samples were used for measuring chlorophyll fluorescence including maximum fluorescence (F_m), initial fluorescence (F_o), variable fluorescence (F_v), and PSII maximum quantum efficiency of PSII (F_v/F_m) using IRGA (CI- 510 CF) chlorophyll fluorescence module.

2.3. Measurement of Enzymatic and Metabolic changes

2.3.1. Assays for PAL, SOD and POX enzymatic activities

Frozen plant tissues (200 mg) were homogenized in a medium composed of 2 ml of extraction buffer which consists of 0.2 M (pH 7.2) of phosphate buffer, 0.1 mM EDTA, 1 mM DTT, and 2 U protease inhibitor. The homogenates were centrifuged at 10,000 rpm for 5 min at 4 °C. The supernatant was collected and used for the assays of enzymatic activities.

PAL activity was determined according to (Nagarathna et al., 1993). by measuring the L-phenylalanine formation.

The supernatant was added to reaction mixture containing 100 mM Tris-HCl, 40 mM trans-cinnamic acid. The mixture was incubated at 40 °C for 1 h and an ice bath was used to stop the reaction. The absorbance was measured at 290 nm in U g⁻¹ FW using a spectrophotometer (Genesys 5, Thermo Spectronic, Rochester, NY, USA).

The method by (Giannopolitis et al., 1977) was followed to assay SOD activity. Three ml of reaction mixture contained 50 mM sodium phosphate buffer (pH 7.6), 0.1 mM EDTA, 50 mM sodium carbonate, 50 μM NBT, 10 μM riboflavin, 12 mM L-methionine and 100 μl of crude extract. To start the reaction, the tubes were placed under two 15W florescent lamps and last for 15 min. Absorbance was read through a spectrophotometer at 560 nm. The ability of SOD to inhibit NBT by 50% was considered as 1 unit for enzyme activities.

POX activity was estimated using method of Kim and Yoo, (1996). 0.2 ml of crude enzyme extract was added to reaction mixture containing 0.8 ml of 0.2 M phosphate buffer (pH 7.2), 1 ml of 15 mM guaiacol, 1 ml of 3 mM hydrogen peroxide. The absorbance was determined at 470 nm. POX activity was calculated as per extinction coefficient of its oxidation product: U/ml = [Change in absorbance min⁻¹ × Reaction mixture volume (ml) × Dilution factor] / [ε470 × Enzyme extract volume (ml)]

2.3.2. Total saponins determination

Total saponins content was assayed by spectral reading at 473 nm using spectrophotometer (Ebrahimzadeh and Niknam, 1998). Standard curve of the Diosgenin compound was used to calculate the saponin contents.

2.3.3. Total carbohydrates determination

An anthrone-sulfuric acid method was used to determine the total contents of carbohydrates following Fales (1951). The developed blue-green color was read at 620 nm spectrophotometrically.

2.3.4. Total flavonoids determination

The total contents of flavonoids of the dried leaves extract were quantified by the aluminum chloride method; the reading absorbance wavelength was at 510 nm through spectrophotometer (Chang et al., 2002). The total flavonoids concentration was calculated from a standard curve, and the result was estimated as mg quercetin equivalent per g dry weight.

2.3.5. Total proteins assay

Total proteins were assayed according to the method of (Lowry et al., 1951).

2.3.6. Determination of total phenolics

Total phenolic compounds were examined using the Folin-Ciocalteu method (Ough et al., 1988).

2.3.7. Ascorbic acid determination

Ascorbic acid content was determined according to (Omaye et al., 1979).

2.3.8. Proline determination

Proline content was examined by modification of the method of (Bates et al., 1973). Dry powdered okra leaves (250 mg) were homogenized with 10 ml of 3 % sulfo-salicylic acid and centrifuged at 3000 × g for 10 min. Two ml of the supernatant were mixed with 2.0 ml of the

prepared reagent (2.5 g ninhydrin in 40 ml of 6 m orthophosphoric acid and 60 ml glacial acetic acid), and 2.0 ml of glacial acetic acid in a test tube. The test tubes were heated at 100 °C for 1 h and 4 ml of toluene were added to each test tube after cooling. The absorbance was read at 520 nm through spectrophotometer. The concentration of proline was quantified using calibration curve of proline standard and calculated on dry weight basis.

2.3.9. Chlorophyll content assay

To quantify chlorophyll content by spectrophotometer, the method described by (Ni et al., 2009) was used.

2.4. Statistical analysis

The obtained data were analyzed by a one-way analysis of variance (ANOVA) using Minitab. Student t-test was used to compare the control with stressed plants. Statistical significance was considered at the level ($P \leq 0.05$). Values shown in the figures were reported as means \pm standard errors (SEs) of three independent replicates. The relationships among individual variables were determined using Principal Component Analysis (PCA).

3. Results

3.1. Gas exchange measurements and Chlorophyll fluorescence parameters

A significant reduction ($p < 0.05$) in net photosynthesis and stomatal conductance was detected for Egyptian

mothers and J×E hybrid (0.07 and 0.0 $\mu\text{mol s}^{-1}\text{m}^{-2}$, respectively) and (8.09 and 0.0 $\text{mmol s}^{-1}\text{m}^{-2}$, respectively) Fig.1. Declines in the intercellular CO_2 concentrations were observed following the reduction in stomatal conductance. In contrast, Japanese cultivar and E×J hybrid exhibited higher photosynthesis rate with high stomatal conductance as soil water content decreases in comparison with their unstressed plants and stressed Egyptian mothers and J×E. Transpiration rate of J×E hybrid showed significant decrease (0.06 $\text{mmol m}^{-2}\text{s}^{-1}$) at severe drought stress. Parents and E×J plants showed no significant change in transpiration rate (0.12 $\text{mmol m}^{-2}\text{s}^{-1}$) at the same drought condition.

Fig. 1 shows that the quantum efficiency (Fv/Fm) of PSII was affected significantly by the water shortage. This led to reduction in PSII efficiency. Both hybrids and Japanese cultivar showed decreasing in Fv/Fm under stress condition ranged between 0.14 and 0.15 for stressed plants ($P < 0.05$), while Egyptian mothers showed no significant change compared to unstressed plants, the Fv/Fm remained higher than other cultivars under stress 0.38. Drought stress was also affected by the efficiency of electron transfer (F0) which is necessary for regulating the primary photochemical activity.

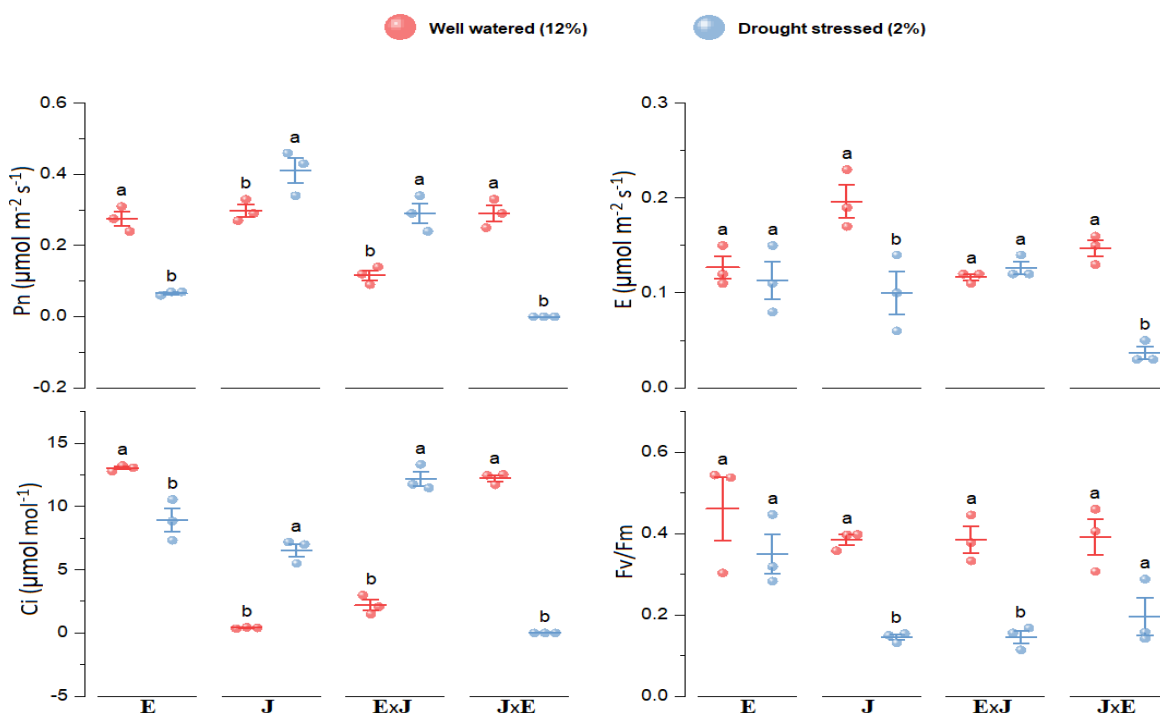


Figure 1. Diagram showing the effect of drought stress on photosynthesis rate (Pn), Transpiration rate (E), stomatal conductance (Ci) and Fv/Fm of Japanese cultivar, Egyptian cultivar, E×J and J×E at two water regimes (12% and 2%), a and b letters indicate significant changes ($P < 0.05$) between well watered and stressed plants according to Student's t-test.

3.2. Activities of Enzymatic Antioxidants under Drought Stress

Fig. 2 shows the varied significant influence of osmotic stress ($P < 0.05$) on the antioxidant enzymes (SOD),

(POD) and (PAL). The activities of SOD in Egyptian mothers, Japanese mothers, E×J and J×E were significantly increased with the severity of drought stress in comparison to the well-watered control plants. The maximum activity of SOD was observed in Japanese

cultivar at 2% water regime level (18.69 U g⁻¹ FW) followed by Egyptian mothers, J×E and E×J (17.961, 14.078 and 13.835 U g⁻¹ FW, respectively). The obtained results showed that highly significant increase in POX for E×J reaching the maximum activity value of (234 U g⁻¹ FW), followed by Japanese mothers and J×E with value of (167.5 and 101 U g⁻¹ FW, respectively). In Egyptian

mothers, there is no significant change in POX activity in well watered (62.6 U g⁻¹ FW) compared with stressed plants (60.3 U g⁻¹ FW). Activities of PAL were significantly increased in the Egyptian mothers and E×J under severe drought stress conditions while in Japanese mothers and J×E the PAL activities were decreased significantly.

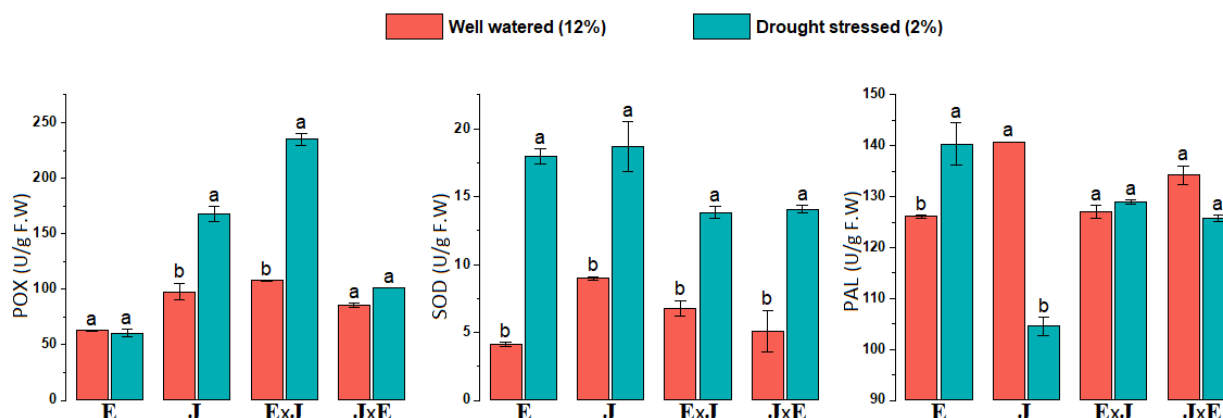


Figure 2. Antioxidant enzyme activities of peroxidase, POX; superoxide dismutase, SOD and Phenylalanine ammonia lyase, PAL representing well watered Japanese cultivar, stressed Japanese cultivar, well watered Egyptian cultivar, stressed Egyptian cultivar, well watered Japanese cultivar× Egyptian cultivar (J×E), stressed Japanese cultivar× Egyptian cultivar (J×E), well watered Egyptian cultivar × Japanese cultivar (E× J) and stressed Egyptian cultivar × Japanese cultivar (E× J). Values are means ± standard errors (SEs) of three independent replicates (n = 3), a and b letters indicate significant changes (P<0.05) between well watered and stressed plants as expressed by a Student's t-test.

3.3. Total chlorophyll content and Metabolic change

Under stress condition, the leaf chlorophyll concentration of Japanese and Egyptian parents and their J×E hybrid was decreased as compared with control from (1.84, 1.88 and 1.66 mg/g FW, respectively) to (1.66, 1.6 and 1.4 mg/g FW, respectively), while the total chl content in J×E hybrid remained constant under low water regime (1.9 mg/g FW). Changes in metabolite contents were induced by drought stress and led to different responses of the two Japanese and Egyptian mothers and their hybrids to water deficit conditions (Fig.3). Drought condition (2% water regime level) resulted in significantly higher protein content in Japanese cultivar and E×J (202.38 and 191.9 mg/g DW respectively) and in contrast, the content of protein in Egyptian and J×E decreased compared to their control plants (178.5 and 164.29 mg/g DW, respectively). Our results showed decrease in total carbohydrates content in Japanese, Egyptian and E×J while J×E hybrid showed significant increase (P < 0.05) in total carbohydrates under water deficit conditions.

In general, ascorbic acid content was unaffected by drought stress in both okra hybrids and Egyptian mothers except for Japanese mothers, where ascorbic acid contents were significantly increased (P<0.01) under 2% water

regime with mean value of (30.6 mg/g DW). Proline content was increased due to drought stress in both F1 hybrids while their parents showed decreasing in proline content. Under low water regime (2%), there is no significant change in total phenolic for all okra cultivars and their F1 hybrids. Total flavonoids and saponins contents were declined in parental cultivars and both F1 hybrids under drought stress as compared to well-watered control plants. Principle component analysis PCA indicated that physiological traits are remarkable for distinguishing parental okra cultivars and their F1 offspring at both 12% and 2% water regimes (Fig.4). The PCA analysis was used to reduce the dimension of the data among all physiological and metabolic traits. PCA 1 was the most descriptive component which explained 31.9% of the variation. PCA 1 correlates positively to parameters related to peroxidase POX, super-oxide dismutase SOD and ascorbic in which characterize the plant under low water regime (2%), while physiological parameters such as chlorophyll fluorescence, transpiration (E) and stomatal conductance (Ci) has large negative loadings on PCA components. Furthermore, smaller variation was observed on PCA 2 (21.7%), corresponding mainly to proteins and photosynthesis (pn).

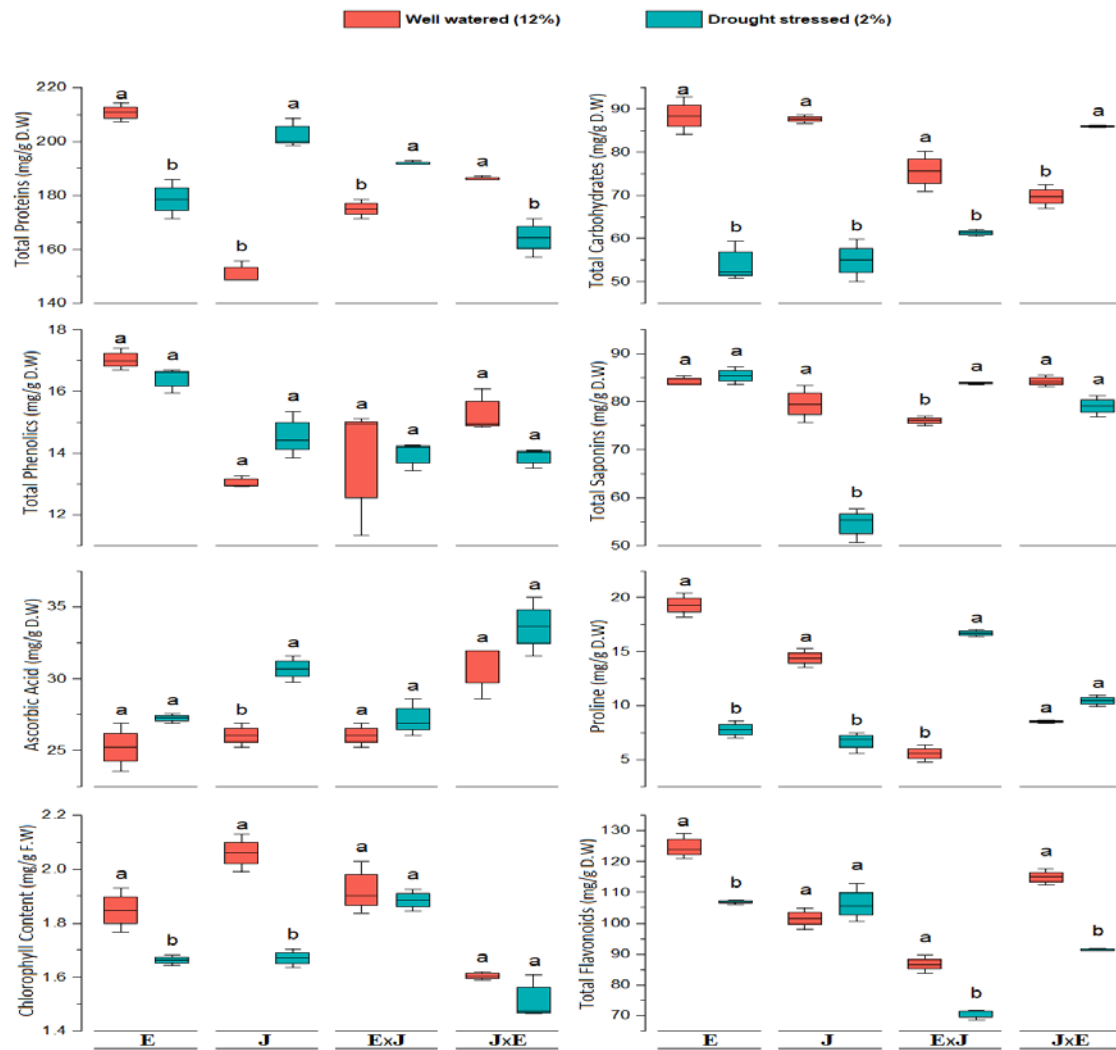


Figure 3. Differences in total protein contents, total carbohydrate contents, ascorbic acid and proline, total phenolics, flavonoids and saponins (mg/g DW) between well-watered Japanese cultivar, stressed Japanese cultivar, well watered Egyptian cultivar, stressed Egyptian cultivar, well-watered Japanese cultivar× Egyptian cultivar (J×E), stressed Japanese cultivar× Egyptian cultivar (J×E), well-watered Egyptian cultivar × Japanese cultivar (E×J) and stressed Egyptian cultivar× Japanese cultivar (E×J) Values are means ± standard errors (SEs) of three independent replicates (n = 3), a and b letters indicate significant changes (P<0.05) between well-watered and stressed plants as expressed by a Student’s t-test.

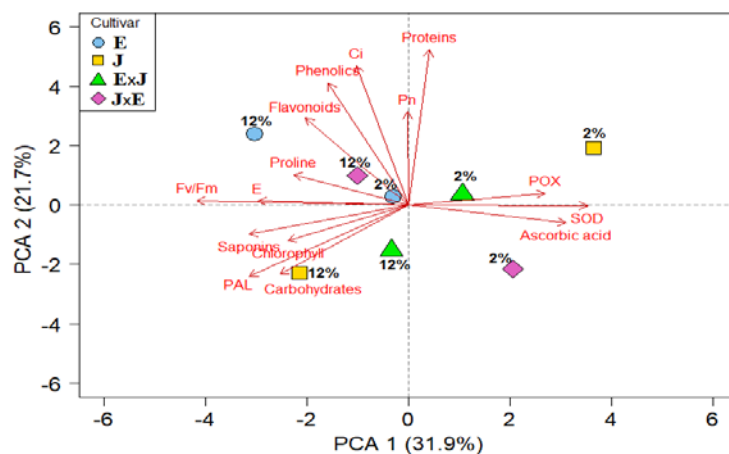


Figure 4. Principal component analysis (PCA) for identification of metabolic change and physiological attributes in two okra varieties (Egyptian and Japanese) and their hybrids (Egyptian cultivar ×Japanese cultivar and Japanese cultivar ×Egyptian cultivar) grown under two water regime 12% (well watered plants) and 2% (stressed plants). The factor loading values for variables are indicated by red arrows radiating from the center showing the direction (angle) and magnitude (length), allowing to separate well-watered and stressed plants. Arrows represent physiological traits with various length based on the impact of each trait on the separation of cultivars showing how each metabolite and physiological parameter contributes to the individual correlations represented by PCA1 (31.9%) and PCA2 (21.7%).

4. Discussion

Drought tolerance improvement and crops productivity are considered the most difficult challenges for plant breeders. Germplasm lines can be selected on the basis of their performance under conditions of water limit. Drought stress influence plant performance, by altering physiological processes such as disruptions of photosynthetic pigments, reduction of the gas exchange and regulation of stomatal function (Keyvan, 2010). Stomatal closure causes reductions in net photosynthesis rates in water stressed Egyptian okra cultivar and J×E hybrid. The stomatal closure lead to reduction in CO₂ assimilation and minimized the rate of water loss transpiration. Similar findings were addressed for medicinal plants under shortage of water (Al-Gabbiesh et al., 2015). This response enables the plant to tolerate water stress (Souza et al., 2004). Fv/Fm is considered as one of the most commonly used features to estimate plant stress. The Fv/Fm ratio decreased in all cultivars and their hybrids under drought stress. Several researchers reported that Fv/Fm decreased under severe water stress (Miyashita et al., 2005; Banks, 2018). Thus, reduction in Fv/Fm ratio indicates the protective mechanism of light absorption in response to water deficiency (Paknejad et al., 2007).

Water deficit conditions cause production of ROS, encouraging plant tissues under drought stress to produce various antioxidant enzymes to alleviate oxidative damage caused by ROS (Mattos et al., 2015). Previous researches have shown that antioxidant enzymes such as superoxide dismutase (SOD), peroxidase (POD) and phenyl ammonia lyase (PAL) act as key defendant enzymes against ROS, and the higher enzymatic activity depends on genotypes genetic potential (Park et al., 2013; Martinez et al., 2018). Peroxidase is the most important enzyme providing for plant anti-oxidant defence (Kholodova et al., 2007). In our experiments, peroxidase was highly activated in Japanese cultivar, J×E and E×J plans under stress conditions as POX is lowering the concentration of H₂O₂ and limiting the oxidative damage. SOD activity was increased in parent cultivars and their both hybrids under severe drought condition to impair the ROS production while PAL activity increased only in Egyptian mothers. The protective effect of antioxidant enzymes against water stress has been demonstrated in several plant species (Sayfzadeh and Rashidi 2011; Ahmed et al., 2002; Ahmad et al., 2015).

The photosynthetic pigment contents (chlorophylls and carotenoids) are considered influential physiological crop indicators for stress tolerance, including drought stress (Pour-Aboughadareh et al., 2020). In this study, total chlorophyll value was decreased by drought stress in all parent cultivars and their F1 hybrids (E×J and J×E). This reduction in chlorophyll pigment is believed to be a result of inhibition of chlorophyll synthesis pathway (Anjum et al., 2011). Stress proteins are expressed intensively, and their accumulation in plants is a common feature of the response to drought stress. The total proteins increased in Japanese cultivar and E×J under low water regime while, in contrast, Egyptian mothers and J×E hybrid showed decrease in total proteins content. Increasing in protein content under drought stress is in agreement with a previous study carried out by (Qaseem et al., 2019). Total carbohydrates was higher in stressed J×E in comparison to

the control while the other cultivars showed decrease in total carbohydrates, indicating that there might be a genetic variation in the accumulation of these compounds. Carbohydrates seem to play a key role in the regulation of carbon metabolism to be part of a wider mechanism for plant surviving during drought stress (Praxedes et al., 2005).

Free proline accumulation by plant tissue was dependent on the severity of osmotic stress conditions. Proline acts as osmolyte which regulates the osmotic pressure in the cytoplasm (Caballero et al., 2005). Adejumo et al. (2018) reported that accumulation of proline in okra leaves may serve as physiological tool to develop drought tolerance in okra plants. Our result revealed that proline content of well watered hybrid plants (E×J and J×E) was lower than those plants exposed to limited water condition. In contrast, the stressed parents (Japanese and Egyptian cultivars) showed lower proline content than well watered control plants. It seems that the hybrids have this drought-response character, and this result is similar to the observation by Castillo et al. (2017). PCA is the most frequently used multivariate statistical method (Liu et al., 2010). The output results of the PCA successfully identified variables which contribute most to response against drought stress amongst okra cultivars and hybrids. PCA analysis is useful tool for distinguishing between okra varieties and their hybrids based on the changes in their physiological traits and antioxidant enzymes activity (POX, PAL and SOD). Findings suggested that strong positive contributions were observed for POX and SOD on stressed hybrids, while they were in negative association with chlorophyll and carbohydrates according to PCA; also results showed that drought stress has a negative effect on photosynthesis, transpiration and proline content of parental cultivars.

Stress plants showed higher enzymatic activity and proteins content, indicating the most cultivar adapted to drought stress. Our findings in this study are in agreement with Liu et al. (2015) investigation.

5. Conclusion

In this investigation, okra cultivars and their F1 hybrids have various strategies to reduce the harmful effects of water deficit stress. It was concluded that photosynthesis and stomatal conductance tended to decrease under low water regime in parental cultivars and their hybrids. Transpiration rate was decreased in Japanese cultivar and E×J hybrid. Plants also responded against adverse conditions by up-regulation of antioxidant enzymes and accumulation of compatible solutes. The total chlorophyll, carbohydrates, proteins, proline contents were decreased across both parental cultivars under stressful conditions. In contrast, E×J hybrid was more tolerant to drought and performed better by enhancement of proline, proteins and total chlorophyll contents.

References

- Aaron TA, Elvis AB, Faustina A, Kingsley T and Edmund O. 2016. Phenotypic traits detect genetic variability in Okra (*Abelmoschus esculentus*. L. Moench). *Afr J Agr Res.*, **11**: 3169–3177.

- Adejumo SA, Ezeh OS and Mur LAJ. 2018. Okra growth and drought tolerance when exposed to water regimes at different growth stages. *Intl J Veg Sci.*, **25**: 226-258.
- Ahmad SAK, Ebadi A, Ebadi SA, Daneshian J and Ataolah SS. 2015. Changes in enzymatic and non enzymatic antioxidant defence mechanisms of canola seedlings at different drought stress and nitrogen levels. *Turk J Agr Forest.*, **39**: 601-612.
- Ahmed S, Nawata E, Hosokawa M, Domae Y and Sakuratani T. 2002. Alterations in photosynthesis and some antioxidant enzymatic activities of mungbean subjected to waterlogging. *Plant Sci.*, **163**: 117-123.
- Ahmed ZG and El-Sayed MA. 2019. Characterization and crossing two cultivars of okra (*Abelmoschus esculentus* L.) for crop improvement in Egypt. *Plant Cell Biotech Mol Biol.*, **20**:1066-1073.
- Albdaiwi RN, Khyami-Horani H and Ayad JY. 2019. Plant Growth-Promoting Rhizobacteria: An Emerging Method for the Enhancement of Wheat Tolerance against Salinity Stress- (Review). *Jordan J Biol Sci.*, **12** (5): 525-534.
- Al-Gabbiesh A, Kleinwächter M and Selmar D. 2015. Influencing the Contents of Secondary Metabolites in Spice and Medicinal Plants by Deliberately Applying Drought Stress during their Cultivation. *Jordan J Biol Sci.*, **8** (1): 1-10.
- Anjum SA, Farooq M, Wang LC, Xue LL, Wang SG, Wang L, Zhang S and Chen M. 2011. Gas exchange and chlorophyll synthesis of maize cultivars are enhanced by exogenously-applied glycinebetaine under drought conditions. *Plant Soil Environ.*, **57**: 326-331.
- Anjum SA, Ashraf U, Tanveer M, Khan I, Hussain S, Shahzad B, Zohaib A, Abbas F, Saleem MF, Ali I and Wang LC. 2017. Drought Induced Changes in Growth, Osmolyte Accumulation and Antioxidant Metabolism of Three Maize Hybrids. *Front Plant Sci.*, **6**: 69.
- Bates LS, Waldran RO and Terere ID. 1973. Rapid determination of free proline for water stress studies. *Plant Soil*, **39**: 205-208.
- Banks JM. 2018. Chlorophyll fluorescence as a tool to identify drought stress in Acer genotypes. *Environ Expr Bot.*, **155**: 118-127.
- Caballero JI, Verduzco CV, Galan J and Jimenez ESD. 2005. Proline accumulation as a symptom of drought stress in maize: a tissue differentiation requirement. *J Expr Bot.*, **39**: 889-897.
- Castillo A, Rebuffo M, Díaz P, García C, Monza J and Borsani O. 2017. Physiological and biochemical responses to water deficit in *Lotus uliginosus* × *L. corniculatus* hybrids. *Crop Pasture Sci.*, **68**: 670- 679.
- Chang C, Yang M, Wen H and Chern J. 2002. Estimation of total flavonoid content in propolis by two complementary colorimetric methods. *J Food Drug Anal.*, **10**: 178-182.
- Ebrahimzadeh H and Niknam V. 1998. A revised spectrophotometric method for determination of triterpenoid saponins. *Indian Drugs*, **35**: 379-382.
- Fales FW. 1951. The assimilation and degradation of carbohydrates by yeast cells. *J Biol Chem.*, **193**: 113-124.
- Giannopolitis CN and Reis SK. 1997. Superoxide dismutase I. Occurrence in higher plants. *Plant Physiol*, **59**: 309-314.
- Guo Y-Y, Yu HY, Kong DS, Yan F and Zhang YJ. 2016. Effects of drought stress on growth and chlorophyll fluorescence of *Lycium ruthenicum* Murr. Seedlings. *Photosynthetica*, **54**: 524-531.
- Harb AM and Lahham JN. 2013. Response of Three Accessions of Jordanian *Aegilops crassa* Boiss. and Durum Wheat to Controlled Drought. *Jordan J Biol Sci.*, **6** (2): 151-157.
- Hussain HA, Men S, Hussain S, Chen Y, Ali S, Zhang S, Zhang K, Li Y, Xu Q, Liao C and Longchang W. 2019. Interactive effects of drought and heat stresses on morpho physiological attributes, yield, nutrient uptake and oxidative status in maize hybrids. *Sci Rep.*, **9**: 3890.
- Keyvan S. 2010. The effects of drought stress on yield, relative water content, proline, soluble carbohydrates and chlorophyll of bread wheat cultivars. *J Animal Plant Sci.*, **8**:1051-1060.
- Kholodova VP, Bormotova TS, Semenov OG, Dmitrieva GA and Kuznetsov VV. 2007. Physiological mechanisms of adaptation of alloplasmic wheat hybrids to soil drought. *Rus J Plant Physiol.*, **54**: 480-486.
- Kim Y and Yoo JY. 1996. Peroxidase production from carrot hairy root cell culture. *Enzym Microb Technol.*, **18**: 531-535.
- Lamaoui M, Jemo M, Datla R and Bekkaoui F. 2018. Heat and Drought Stresses in Crops and Approaches for Their Mitigation. *Front Chem.*, **19**: 6-26.
- Lizana C, Wentworth M, Martinez JP, Villegas D, Meneses R, Murchie EH and Pinto M. 2006. Differential adaptation of two varieties of common bean to abiotic stress. *J Expr Bot.*, **57**: 685-697.
- Lowry OH, Rosebrough NJ, Farr AL and Randall RJ. 1951. 'Protein measurement with the folin phenol reagent'. *J Biol Chem.*, **193**:265-275.
- Liu Y, Zhang X, Tran H, Shan L, Kim J, Childs K and Zhao B. 2015. Assessment of drought tolerance of 49 switch grass (*Panicum virgatum*) genotypes using physiological and morphological parameters. *Biotechnol Biofuel.*, **8**: 152.
- Liu ZY, Shi JJ, Zhang LW and Huang JF. 2010. Discrimination of rice panicles by hyperspectral reflectance data based on principal component analysis and support vector classification. *J Zhejiang Univ-SCI B.*, **11**: 71-78.
- Mattos LM and Moretti CL. 2015. Oxidative stress in plants under drought conditions and the role of different enzymes. *Enzym Engineer.*, **5**: 136.
- Martinez V, Nieves-Cordones M, Lopez-Delacalle M, Rodenas R, Mestre T, Garcia-Sanchez F and Rivero R. 2018. Tolerance to Stress Combination in Tomato Plants: New Insights in the Protective Role of Melatonin. *Molecules.*, **23**: 535.
- Mir RR, Zaman-Allah M, Sreenivasulu N, Trethowan R and Varshney RK. 2012. Integrated genomics, physiology and breeding approaches for improving drought tolerance in crops. *Theor Appl Genet.*, **125**: 625-645.
- Miyashita K, Tanakamaru S, Maitani T and Kimura K. 2005. Recovery responses of photosynthesis, transpiration, and stomatal conductance in kidney bean following drought stress. *Environ Expr Bot.*, **53**: 205-214.
- Nagarathna KC, Shetty SA and Shetty HS. 1993. Phenylalanine ammonia lyase activity in pearl millet seedlings and its relation to downy mildew disease resistance. *J Expr Bot.*, **265**: 1291-1296.
- Ni Z, Kim ED and Chen ZJ. 2009. Chlorophyll and starch assay. *Protocol Exchange*. doi:10.1038/nprot.2009.12
- Omaya, S.T., Turnbull, J.D., Sauberilick, H.E., 1979. Selected methods for the determination of ascorbic acid in animal cells, tissues and fluids. *Method enzymol.*, **62**: 3-11.
- Ough CS and Amerine MA. 1988. **Methods for analysis of must and wines**. 2th Ed. New York: John Wiley & Sons.

- Paknejad F, Nasri M, Reza HMT, Zahedi H and Jami MA. 2007. Effects of Drought Stress on Chlorophyll Fluorescence Parameters, Chlorophyll Content and Grain Yield of Wheat Cultivars. *J Biol Sci.*, **7**: 841-847.
- Park S, Lee DE, Jang H, Byeon Y, Kim YS and Back K. 2013. Melatonin-rich transgenic rice plants exhibit resistance to herbicide-induced oxidative stress. *J Pineal Res.*, **54**: 258-263.
- Petropoulos S, Fernandes Â, Barros L and Ferreira ICFR. 2018. Chemical composition, nutritional value and antioxidant properties of Mediterranean okra genotypes in relation to harvest stage. *Food Chem.*, **242**: 466-474.
- Pour-Aboughadareh A, Etminan A, Abdelrahman M, Siddique K H M, and Tran, L S P. 2020. Assessment of biochemical and physiological parameters of durum wheat genotypes at the seedling stage during polyethylene glycol-induced water stress. *Plant Growth Regul.*, **92**:81-93
- Praxedes SC, DaMatta FM, Loureiro MEG, Ferrao MA and Cordeiro AT. 2005. Effects of long term soil drought on photosynthesis and carbohydrate metabolism in mature robusta coffee (*Coffea canephora* Pierre var. kouillou) leaves. *Environ Expr Bot.*, **56**: 263-273.
- Qaseem MF, Qureshi R and Shaheen H. 2019. Effects of Pre-Anthesis Drought, Heat and Their Combination on the Growth, Yield and Physiology of diverse Wheat (*Triticum aestivum* L.) Genotypes Varying in Sensitivity to Heat and drought stress. *Sci Rep.*, **9**: 6955.
- Rahbarian R, Khavari-Nejad R, Ganjeali A, Bagheri A and Najafi F. 2011. Drought Stress Effects on Photosynthesis, Chlorophyll Fluorescence and Water Relations in Tolerant and Susceptible Chickpea (*Cicer Arietinum* L.) Genotypes. *Acta Biol Cracov Ser Bot.*, **53**: 47-56.
- Reddy AR, Chaitanya KV and Vivekanandan M. 2004. Drought-induced responses of photosynthesis and antioxidant metabolism in higher plants. *J Plant Physiol.*, **161**: 1189-1202.
- Sawadogo M, Zombre G and Balma D. 2006. Behaviour of different ecotypes of okra (*Abelmoschus esculentus* L.) under water deficit during budding and flowering phases. *Biotechnol Agron Soc Environ.*, **10**: 43-54.
- Sayfzadeh S and Rashidi M. 2011. Response of antioxidant enzymes activities of sugar beet to drought stress. *J Agri Biol Sci.*, **6**: 27-33.
- Silva EN, Ferreira-Silva SL, de V, Fontenele A, Ribeiro RV, Viégas RA and Silveira JAG. 2010. Photosynthetic changes and protective mechanisms against oxidative damage subjected to isolated and combined drought and heat stresses in *Jatropha curcas* plants. *J Plant Physiol.*, **167**: 1157-1164.
- Souza RP, Machado EC, Silva JAB, Lagôa AMMA and Silveira JAG. 2004. Photosynthetic gas exchange, chlorophyll fluorescence and some associated metabolic changes in cowpea (*Vigna unguiculata*) during water stress and recovery. *Environ Expr Bot.*, **51**: 45-56.

Orange Peels Valorization For Citric Acid Production Through Single And Co-Culture Fermentation

Muddassar Zafar*, Hania Shah Bano and Zahid Anwar

Department of Biochemistry and Biotechnology, University of Gujrat, Gujrat, Pakistan.

Received: May 14, 2020; Revised: September 10, 2020; Accepted: September 11, 2020

Abstract

The present work describes fermentation of raw materials to produce citric acid through single and co-culture process using indigenous strains of *Aspergillus niger* and *Aspergillus fumigatus*. For this purpose, orange peels, peanut shells and their homogenous mixtures were used as raw material using solid state fermentation (SSF). Incubation period, pH, temperature, moisture content, inoculum size and substrate concentrations were optimized simultaneously using response surface methodology (RSM) design followed by contour plot analysis. Citric acid was separated from other by products in a non-polar C-8 column and quantified using reversed phase high performance liquid chromatography (RP-HPLC) technique. It was found that more amount of citric acid (114.68 ± 0.73 mg/mL) was produced during co-culture fermentation employing both *A. niger* and *A. fumigatus* simultaneously as compared to single culture fermentation inoculated with *A. niger* (94.92 ± 0.46 mg/mL) and *A. fumigatus* (65.13 ± 0.28 mg/mL), using 25 gms orange peels OPs as substrate, 60 % moisture content, 6 pH, 6 mL inoculum size, 6 days incubation period and 50 °C temperature as optimized fermentation conditions. The results also showed that RSM based co-culture SSF using cheap biomass can produce more amount of citric acid as compared to conventional fermentation.

Keywords: Raw materials, Citric acid, Co-culture fermentation, *A. fumigatus*, *A. niger*, HPLC, Orange peels.

1. Introduction

Citric acid is biodegradable, highly soluble and low toxic in nature (Yalcin *et al.* 2009; Artmaktadır 2010). It is considered among valuable commercial organic acids which are used in pharmaceutical, food and beverage industries (Abd El-Latif *et al.* 2020). There is a continuous need for research work to improve citric acid production systems and reduce the cost of substrates to fulfil application demands (Ema *et al.* 2020). More than two million tons of citric acid is being manufactured annually through fermentation technology (Ozidal *et al.* 2019) because production of citric acid by using chemicals is more expensive as compared to its production through biomass utilization using microbes either bacteria or fungi (Prado *et al.* 2005). This acid is used in various industrial processes, and 60 % of its production is being used in food industry with 5 % annual increase in production demand worldwide (Papagianni 2007).

By using fermentation techniques, agricultural biomass can be converted into useful products (Iqbal *et al.* 2013). Citric acid can be produced by using different raw products and agricultural wastes (Soccol *et al.* 2006) and milling products (Ema *et al.* 2020). Many organisms like bacteria, fungi and yeast are capable to produce citric acid in their culture medium through fermentation (Iqbal *et al.* 2015). As compared to bacteria, fungi especially species of *Aspergillus* have been preferred for citric acid production due to more yield (Angumeenal *et al.* 2013).

Both *Aspergillus niger* and *A. fumigatus* can grow on soil, dungs, compost piles and agriculture biomass (Cramer *et al.* 2006). The production of useful products like citric acid from biomass is influenced by fermentation parameters like incubation period, substrate, substrate concentration, inoculum size, moisture content, pH and temperature (Ali *et al.* 2002; Ajala *et al.* 2020). In this regard, Response Surface Methodology (RSM) approach during experimentation, helps to study the simultaneous interaction of various variables, optimization of different fermentation parameters as described above and their interaction with each other to provide statistically significant results (Wang *et al.* 2011).

HPLC being more reliable is an advanced technique to separate and detect the presence of citric acid in culture medium produced through biomass based fermentation as compared to conventional spectrophotometric detection. Therefore, this study has aimed to compare maximum production of citric acid through biomass valorization using single culture and co-culture fermentation techniques with different substrates and to quantify citric acid through HPLC technique.

2. Materials and Methods

2.1. Cultivation of fungal species

Fungal species *Aspergillus niger* and *Aspergillus fumigatus* were obtained from Industrial Biochemistry Laboratory, Department of Biochemistry and Biotechnology, University of Gujrat, Gujrat, Pakistan.

* Corresponding author e-mail: muddassar.zafar@uog.edu.pk.

These were cultivated on potato dextrose agar (PDA) medium (Sharma, 2010). The cultures were cultivated for 5 days in orbital shaker at 35 °C in order to obtain fresh colonies. Later, 100 µL inoculum of both *fungi* was spread into petri plates containing solidified PDA medium and placed at 35 °C for 5 days.

2.2. Screening of biomass

Biomass including Orange peels (OPs), peanut shells (PSs) and their mixture were employed as substrate for citric acid production. Three flasks containing 5g of OPs, PSs and their mixture containing 2.5 gms of each substrate along with 5mL of water were autoclaved at 121 °C temperature, 15 psi pressure for 20 min. A total of 3 mL inoculum was added to each flask then incubated at 35 °C for 5 days. The inoculum comprised of 1.5 mL overnight inoculum of each fungal strain (*A. niger* and *A. fumigatus*). After screening, the substrate producing maximum citric acid was further employed in RSM trial.

2.3. Response Surface Methodology (RSM)

In order to study and optimize the effect of incubation period, pH, temperature, substrate concentration, inoculum size and moisture content for citric acid production, solid state fermentation was performed using statistical design of Response Surface Methodology through Minitab software (version 17) (Wang *et al.* 2011). Accordingly, under RSM, fermentation experiment was carried out using different combinations of pH, temperature and incubation period and moisture content, substrate concentration and inoculum size.

2.4. Optimization of fermentation parameters through RSM

For the determination of optimum values, different concentrations and ranges of fermentation parameters were tested for maximum citric acid production. For optimum incubation period, biomass substrates were inoculated with 1.5 mL of single and co-culture consortia after addition of 5 mL distilled water to give moisture content and incubated for 1, 2, 4, 6 and 7 days. For optimum pH, inoculated substrates were treated at different values of pH (3-9) using phosphate buffer. For optimum temperature and moisture content, experiment was conducted at different range of temperature (20-55 °C) and moisture content (10-90 %). For inoculum size, inoculated biomass was treated with 1-11 mL inoculum size and for optimization of substrate, different concentrations (3-58 gms) of substrate were used to obtain maximum production of citric acid.

2.5. Fermentation

Single and co-culture fermentation was performed in separate flasks. For single culture experimentation, 5 gms of powdered OPs were moistened with 3 mL of phosphate buffer, and 1.5 mL inoculum of *A. fumigatus* and *A. niger* was added in separate flasks. For co-culture experimentation, same amount of substrate (OPs) was added to 3mL of phosphate buffer, and 1.5 mL inoculum of both *A. niger* and *A. fumigatus* was added in same flasks. The selected values of fermentation parameters including pH, temperature, incubation period, inoculum size, moisture content and substrate concentration were further employed in single and co-culture fermentation. After incubation, 50 mL of distilled water was added, and

cultures were placed in orbital shaker at 37 °C for 30 min at 180 rpm. The culture was filtered with Whatman filter paper (Number 42, pore size 2.5 µm), centrifuged at 4000 rpm for 15 min, then the supernatants were collected and used for detection of citric acid through HPLC analysis.

2.6. HPLC analysis

HPLC grade standard of citric acid was purchased from Sigma-Alrich (USA). A stock solution (1000 µg/mL) of citric acid standard was prepared and further diluted (100, 200, 300, 400 and 500 µg/mL) to draw the standard curve. The samples were analyzed on reversed phase high pressure liquid chromatograph (RP-HPLC) system (Hitachi, Japan) at room temperature using isocratic mode with distilled deionized water as mobile phase. The flow rate was set to 1.5 mL/min and absorbance of citric acid was noted at 212 nm using UV/visible detector. The stationary phase comprised of C-8 column (15cm x 4.6 mm x and 5µM). The qualitative and quantitative detection of citric acid was performed using retention time and peak area information of chromatograms, respectively.

3. Results

3.1. HPLC detection of citric acid

The amount of citric acid was quantified through HPLC analysis. The standard curve of citric acid was obtained using HPLC grade standards having different concentrations. A typical chromatogram of stock standard of citric acid has been shown in Figure 1 which shows elution of citric acid from HPLC column at 2.0 min retention time.

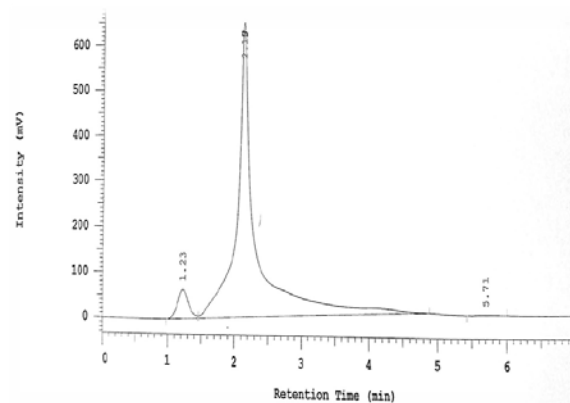


Figure 1. HPLC chromatogram of stock standard of citric acid (1 mg/ml). The analyte was eluted at retention time of 2 min and detected at 212 nm wavelength using UV/Visible detector through isocratic mode of analysis.

3.2. Biomass screening

The growth of *A. niger* and *A. fumigatus* was visible after 5 days of inoculation in separate flasks containing three different biomass (OPs, PSs and uniform mixture of OPs and PSs). The maximum production of citric acid (114.68±0.73 mg/mL) was observed in OPs substrate as analyzed through HPLC (Fig 2) as compared to PSs and their mixture by co-culturing (*A. niger* and *A. fumigatus*) technique.

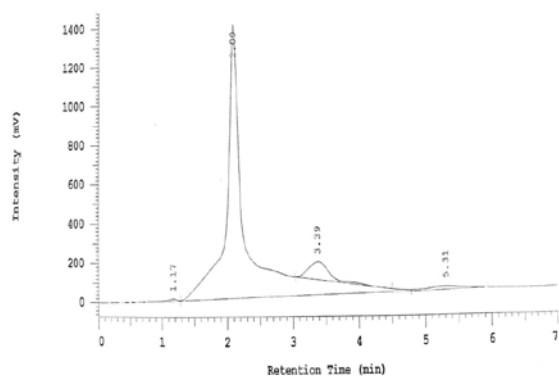


Figure 2. HPLC chromatogram of maximum amount of citric acid (114.68 ± 0.73 mg/mL) produced in orange peels (substrate) based fermentation culture using co-culturing of *A. niger* and *A. fumigatus*. The analyte was eluted at 2 min retention time and detected at 212 nm wavelength using UV/Visible detector.

3.3. Optimization of fermentation parameters through RSM

Different fermentation parameters were optimized using RSM, and effect of pH, temperature and incubation period for citric acid production through co-culture technique was observed (Table 1). The maximum production of citric acid (94.92 ± 0.46 mg/mL) as determined by HPLC analysis (Fig 3) was noted after 6 days of incubation during single culture fermentation using *A. niger* while single culture fermentation using *A. fumigatus* produced 65.13 ± 0.28 mg/mL citric acid. However, co-culturing using both *A. niger* and *A. fumigatus* yielded more amount of citric acid (114.7 ± 0.73 mg/mL) after 6 days of incubation period. For determination of optimum pH, the cultures were treated with different pH values using phosphate buffer and maximum production of citric acid was observed at pH 6. Regarding temperature, the maximum production was observed at 50 °C during co-culture among different ranges of temperature. The moisture content of 60% maximally produced citric acid during co-culture experimentation. An inoculum size of 6 mL was found optimum. In addition, upon using different concentrations of biomass substrates OPs, PSs and their mixture, maximum production of citric acid was observed at 25 gms concentration of OPs during co-culture fermentation employing both fungal strains (Table 2).

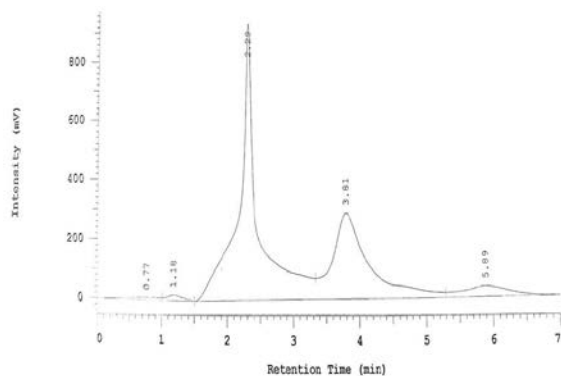


Figure 3. HPLC chromatogram of citric acid (94.92 ± 0.46 mg/mL) produced in orange peels (substrate) based fermentation culture using single culture of *A. niger*. The analyte was eluted at 2 min retention time and detected at 212 nm wavelength using UV/Visible detector.

Table 1. RSM based optimization of pH, temperature and incubation period for citric acid production through co-culture fermentation using *A. niger* and *A. fumigatus*

S #	pH	Temperature (°C)	Incubation period (Days)	Amount of citric acid (mg/mL)
1	3	55	2	50.86
2	6	35	1	29.53
3	8	50	2	42.51
4	8	20	2	11.19
5	3	20	2	10.09
6	5.5	35	4	56.18
7	6	35	4	52.09
8	5	35	4	26.89
9	9	35	4	29.07
10	3	35	4	0.572
11	3	20	6	30.50
12	3	50	4	45.28
13	8	20	6	17.43
14	6	50	6	70.76
15	5.5	35	7	16
16	6	60	4	49.28

Table 2. RSM based optimization of moisture level, substrate concentration and inoculum size for citric acid production through co-culture fermentation using *A. niger* and *A. fumigatus*

S #	Moisture level (%)	Substrate concentration (g)	Inoculum size (mL)	Amount of citric acid (mg/mL)
1	90	45	9	72.55
2	60	25	9	76.91
3	60	25	6	11.85
4	30	5	9	30.64
5	90	5	3	28.42
6	60	25	6	114.68
7	60	58	6	41.72
8	30	45	3	47.82
9	60	3	6	0.48
10	30	5	3	42.83
11	60	25	1	23.02
12	30	45	9	43.01
13	10	25	6	43.26
14	90	45	3	25.13
15	60	25	11	28.11
16	90	5	9	18

3.4. Interaction among fermentation parameters

The interaction of fermentation parameters like incubation period, pH, temperature, inoculum size, moisture content and substrate concentration were observed through RSM design and contour plots were prepared using Minitab software (version 17) to observe significant interaction among various parameters. A significant interaction shows dependency of one parameter with other while non-significant interaction shows non dependency of parameters with each other regarding production of citric acid during single and co-culture experimentation.

3.5. Interaction among parameters during single culture using *A. niger*

A significant interaction was observed between substrate concentration and moisture content during single culture inoculation with *A. niger* (Fig 4). It was observed

that maximum citric acid (94.92 ± 0.46 mg/mL) was produced with 58 gms substrate concentration and 60 % moisture content. However, the interaction between inoculum size and moisture content was non-significant (Fig 5), which shows non-dependency of both parameters for production of citric acid.

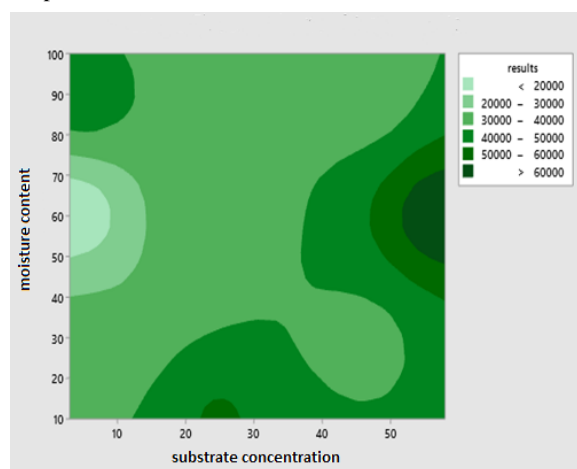


Figure 4. Contour plot showing significant interaction (p -value < 0.05) between substrate concentration and moisture content for citric acid production from orange peels (OPs) using single culture (*A. niger*). The light green colour is representing minimum and dark green colour represents more production of citric acid.

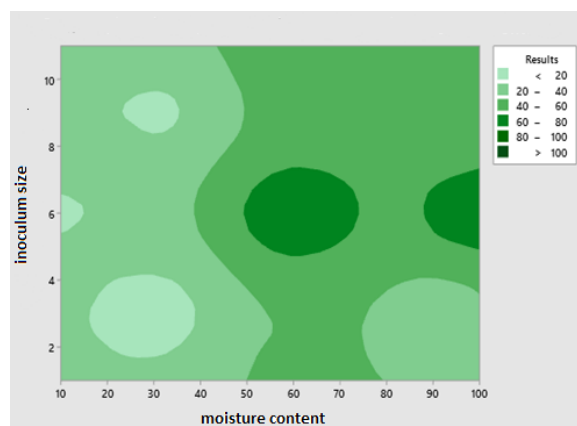


Figure 5. Contour plot showing non-significant interaction (p -value > 0.05) between moisture content and inoculum size for citric acid production from OPs using single culture (*A. niger*). The light green colour is representing minimum and dark green colour represents more production of citric acid.

3.6. Interaction among parameters during single culture using *A. fumigatus*

The maximum production of citric acid (65.13 ± 0.28 mg/mL) was observed at pH 6 and 60 °C temperature during single culture inoculation using *A. fumigatus*, showing more significant interaction between pH and temperature (Fig 6) as compared to interaction between moisture content and substrate concentration during which maximum production was observed at 60 % moisture content and 58 grams of substrate concentration however their interaction was less significant (Fig 7).

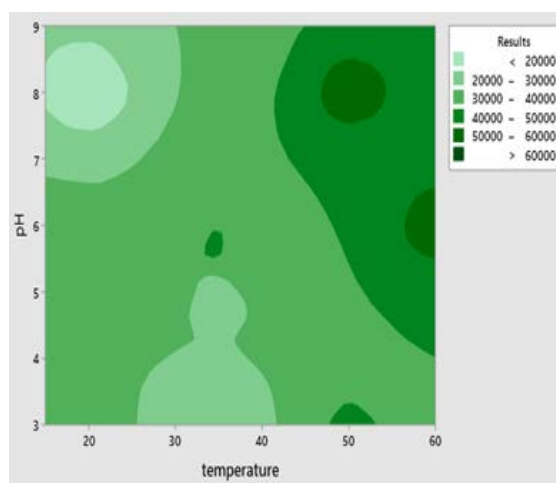


Figure 6. Contour plot showing significant interaction (p -value = 0.001) between temperature and pH for citric acid production from OPs using single culture (*A. fumigatus*). The light green colour is representing minimum and dark green colour represents more production of citric acid.

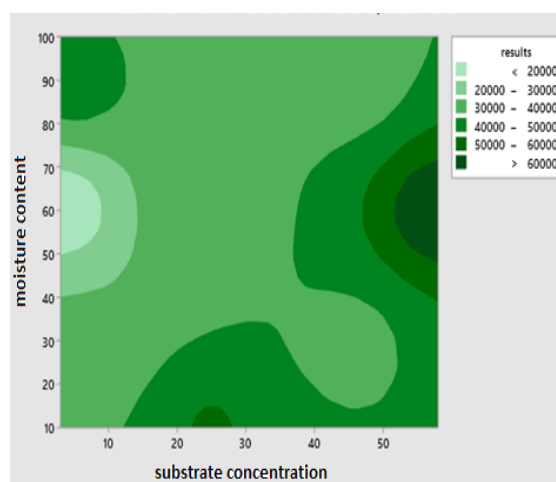


Figure 7. Contour plot showing non-significant interaction (p -value = 0.12) between substrate concentration and moisture content for citric acid production from OPs using single culture (*A. fumigatus*). The light green colour is representing minimum and dark green colour represents more production of citric acid.

3.7. Interaction among parameters during co-culture (*A. niger* and *A. fumigatus*)

It was further found that during co-culturing using both *A. niger* and *A. fumigatus*, a significant interaction appeared between temperature and pH parameters as shown in Fig 8, yielding maximum amount of citric acid at 50°C and pH 8. However, when temperature was employed as parameter with incubation period, a non-significant interaction was observed through contour plot analysis (Fig 9) producing maximum citric acid at 50°C for 6 days of incubation period.

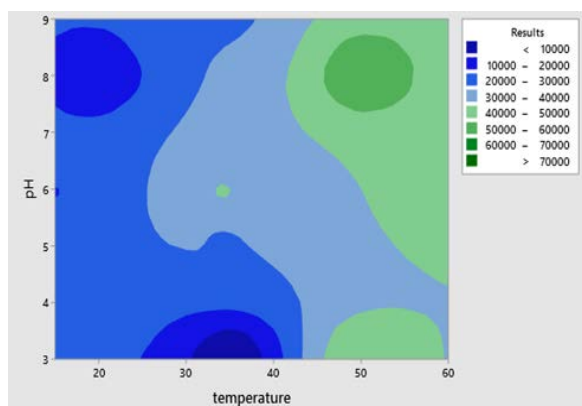


Figure 8. Contour plot showing significant interaction (p -value<0.05) between temperature and pH for citric acid production from OPs using co-culture (*A. niger* and *A. fumigatus*). The dark green colour shows more production of citric acid while light blue colour shows less production.

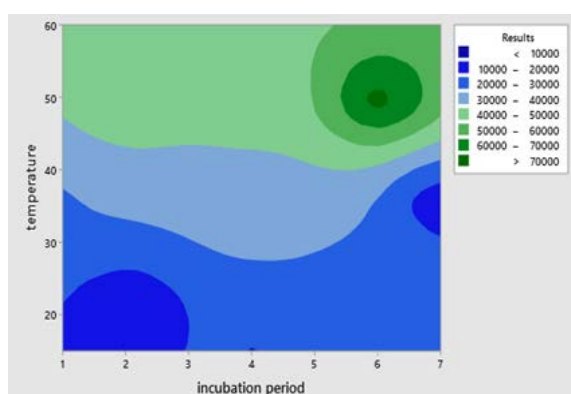


Figure 9. Contour plot showing non-significant interaction (p -value>0.05) between temperature and incubation period for citric acid production from OPs using co-culture (*A. niger* and *A. fumigatus*). The dark blue colour is representing less production while dark green colour shows more production.

4. Discussion

The results of this study showed that as compared to single culture fermentation, more amount of citric acid was produced during co-culture fermentation using indigenous strains of *A. niger* and *A. fumigatus*. It was also observed that citric acid was successfully separated from other byproducts present in the fermentation culture medium, using reversed phase (non-polar) stationary phase with polar mobile phase (distilled deionized water) in isocratic mode at 212 nm wavelength. Hence, RP-HPLC technique was found reliable to quantify organic acids produced through fermentation using different biomass.

OPs were found best biomass substrate to produce citric acid, and the possible reason for this is presence of high content of carbohydrates in its peel, which facilitates microbial growth and enhances fermentation process. Particularly, pectin is present in maximum concentration (42.5%) among components of OP as compared to other components including cellulose, hemicellulose and soluble sugars like glucose, fructose and sucrose (Rivas *et al.* 2008). Pectin mainly consists of sugar acid (galacturonic acid) units. The sugars are used as carbon source during fermentation of citric acid and concentration of these sugars is enhanced due to breakdown of pectin content of OPs through fungal pectinases. The OP substrate was more degraded due to increased production of pectinases during

co-culture as compared to single culture fermentation. Therefore, more the availability of substrate and its respective enzyme, there will be enhanced breakdown and ultimately release and consumption of monosaccharides which enhances citric acid production during fermentation.

As the maximum production of citric acid using solid state fermentation was observed with OPs as substrate, it was therefore selected to optimize other parameters of experiment. Like our strategy of SSF, Ajala *et al.* 2020 have also preferred SSF to produce citric acid and obtained more yield as compared to sub-merged fermentation. Various agro-waste bioresidues have been used by many researchers as substrates in solid state fermentation for production of useful products through microbes (Uma & Rita, 2008; Chinnasamay *et al.* 2011; Rajashri & Anand Rao, 2012). Particularly for citric acid production, biomass based substrates have been used by Kareem *et al.* 2010 using single culture solid state fermentation; however, we observed more production yield using co-culture fermentation. Regarding incubation period, better results were observed with decreased incubation period (6 days) in our study as compared to results reported by other researchers. Ambati *et al.* 2001 and Cevrimli *et al.* 2009 found 7 days as optimum incubation period for citric acid production using *A. niger*. The results of study also indicated that an acidic culture medium with $pH \leq 6$ leads to more production of organic acids using co-culture technique. Shabaan *et al.* 2020 also favored an acidic medium to enhance the production yield using potato peels and mixed grasses as raw materials. Other researchers have also favored an acidic medium for citric acid production using *Aspergillus* species (Cevrimli *et al.* 2009, El-Gamal *et al.* 2018, Ambati *et al.* 2001, Bhattacharjee *et al.* 2015).

Our findings suggest temperature of 50°C as favorable to obtain more production yield of citric acid using biomass; however, El-Gamal *et al.* 2018 found 45 °C as optimum temperature during single culture fermentation by *A. fumigatus* for citric acid production. Similarly, 60 % content was found as optimum moisture content for production of citric acid in our study while Kareem *et al.* 2010 reported 65 % content as optimum during single culture fermentation using *A. niger*. The reason for decrease in required moisture content is use of two fungi simultaneously in same fermentation medium using co-culture technique.

For substrate concentration, it is important to describe that optimum concentration of substrate depends upon composite nature of substrate and type of fermentation used during culturing. The amount of substrate (OPs) used in our method is less than that of Solomon *et al.* 2018 which used banana peel as substrate. The co-culture technique is favored due to less consumption of raw substrates (Ali *et al.* 2016). Accordingly, results of the present study indicate that co-culture fermentation should be preferred as compared to single culture fermentation because it requires less amount of substrate and yields more production of organic acids by using microbes particularly fungi.

The understanding of impact of applying multiple parameters and their combined effect on production of fermentation products in presence of different microbes is essential in order to obtain best results within least time period, and contour plot analysis is an excellent tool to

observe such effect of multiple parameters in a fermentation experiment as described above. Therefore, contour plot analysis was applied accordingly, and the results showed that a significant interaction exists between pH and temperature for production of citric acid either during single culture fermentation or co-culture fermentation and the possible reason might be interdependency of both parameters during RSM based experimentation.

5. Conclusion

The findings of present study indicate that as compared to single culture fermentation using only *A. niger*, choice of co-culturing using both *A. niger* and *A. fumigatus* is a successful strategy to degrade biomass and to obtain maximum amount of citric acid (114.68 ± 0.73 mg/mL). Among various biomass like OPs, PSs and their mixture, OPs as raw substrate can produce more amount of citric acid. In addition, described RP-HPLC technique could be more useful as compared to spectrophotometric detection of citric acid as it facilitates separation of organic acid from other products produced during fermentation, and separated analyte can be collected using fraction collector. Hence, proposed co-culture solid state fermentation method using RSM design can be employed to enhance the production of citric acid using cheap and easily available biomass resources.

Acknowledgments

This research work was funded by Department of Biochemistry and Biotechnology, University of Gujrat, Gujrat, Pakistan.

References

- Abd El-Latif H, Yasser SM and Laila EOA. 2020. Optimization of citric acid production by immobilized cells of novel yeast isolates. *Mycobiol.* **48** (2): 122-132.
- Ajala AS, Adeoye AO, Olaniyan SA and Fasonyin OT. 2020. A study on effect of fermentation conditions on citric acid production from cassava peels. *Sci Afric.* **8**: e00396.
- Ali S, Haq I, Qadeer M and Iqbal J. 2002. Production of citric acid by *Aspergillus niger* using Cane Molasses in a Stirred Fermentor. *Elect J Biotechnol.* **5**(3): 19-20.
- Ali SR, Anwar Z, Irshad M, Mukhtar S and Warraich NT. 2016. Bio-synthesis of citric acid from single and co-culture-based fermentation technology using agro-wastes. *J Radiation Res Appl Sci.* **9**(1): 57-62.
- Ambati P and Ayyanna C. 2001. Optimizing medium constituents and fermentation conditions for citric acid production from palmyra jaggery using response surface method. *World J Microbiol Biotechnol.* **17**(4): 331-335.
- Angumeenal A and Venkappayya D. 2013. An overview of citric acid production. *Food Sci Technol.* **50**(2): 367-370.
- Artmaktadir AAK. 2010. Enhanced production of citric acid by *aspergillus niger* m-101 using lower alcohols. *Turkish J Biochem.* **35**(1): 7-13.
- Bhattacharjee I and Baruah P. 2015. Isolation and screening of citric acid producing aspergillus spp. and optimisation of citric acid production by *Aspergillus niger* S-6. *J Environ Sci Toxicol Food Technol.* **9**(3): 19-23.
- Cevrimli BS, Kariptas E and Ciftci H. 2009. Effects of fermentation conditions on citric acid production from beet molasses by *Aspergillus niger*. *Asian J Chem.* **21**(4): 3211-3218.
- Chinnasamy M, Duraisamy G, Dugganaboyana GK, Ganesan R, Manokaran K and Chandrasekar U. 2011. Production, purification and characterization of protease by *Aspergillus flavus* under solid state fermentation. *Jordan J Biol Sci.* **4** (3): 137-148.
- Cramer RA, Gamcsik MP, Brooking RM, Najvar LK, Kirkpatrick WR and Patterson TF. 2006. Disruption of a nonribosomal peptide synthetase in *Aspergillus fumigatus* eliminates gliotoxin production. *Eukaryot Cell.* **5**(6): 972-980.
- El-Gamal MS, Desouky SES, Abdel-Rahman MA and Khattab ARM. 2018. Optimization of citric acid production from sugar cane molasses using a fungal isolate, *Aspergillus fumigatus* Na-1. *Elect J Biotechnol.* **15**(3): 519-532.
- Ema C, Matías N, Patricia C, María LF. 2020. Exploring the production of citric acid with *Yarrowia lipolytica* using corn wet milling products as alternative low-cost fermentation media. *Biochem Eng J.* **155**: e107463.
- Iqbal HMN, Kyazze G and Keshavarz T. 2013. Advances in the valorization of lignocellulosic materials by biotechnology: an overview. *BioRes.* **8**(2): 3157-3176.
- Iqbal J and Utara U. 2015. Isolation of *Aspergillus niger* strains from soil and their screening and optimization for enhanced citric acid production using cane molasses as carbon source. *J Appl Environ Biol Sci.* **5**(4):128-137.
- Kareem S, Akpan I and Alebiowu O. 2010. Production of citric acid by *Aspergillus niger* using pineapple waste. *Malaysian J Microbiol.* **6**(2): 161-165.
- Ozdal M, Kurbanoglu EB. 2019. Citric acid production by *Aspergillus niger* from agro-industrial by-products: Molasses and chicken feather peptone. *Waste Biomass Valoriz.* **10**(3): 631-640.
- Papagianni M. 2007. Advances in citric acid fermentation by *Aspergillus niger*: biochemical aspects, membrane transport and modeling. *Biotechnol Adv.* **25**(3):244-263.
- Prado F, Vandenberghe L, Woiciechowski A, Rodrigues-Leon J and Soccol C. 2005. Citric acid production by solid-state fermentation on a semi-pilot scale using different percentages of treated cassava bagasse. *Brazilian J Chem Engin.* **22**(4): 547-555.
- Rajashri DK and Anand Rao RJ. 2012. Optimization and scale up of cellulase-free xylanase production in solid state fermentation on wheat bran by *Cellulosimicrobium* sp. mtcc 10645. *Jordan J Biologic Sci.* **5** (4): 289-294.
- Rivas B, Torrado A, Torre P, Converti A and Domínguez JM. 2008. Submerged citric acid fermentation on orange peel autohydrolysate. *J Agric Food Chem.* **56** (7): 2380-2387.
- Shaaban ZO, Ayad HH and Ivo L. 2020. Potato peels and mixed grasses as raw materials for biofuel production. *Sci J Koya Univ.* **8** (1): 31-37.
- Sharma G. 2010. Influence of culture media on growth, colony character and sporulation of fungi isolated from decaying vegetable wastes. *J Yeast Fungal Res.* **1**(8): 157-164.
- Soccol CR, Vandenberghe LP, Rodrigues C and Pandey A. 2006. New perspectives for citric acid production and application. *Food Technol Biotechnol.* **44**(2): 457-464.
- Solomon K. 2018. Utilization of banana peel for citric acid production on solid-state fermentation using *Aspergillus niger*. *Addis Ababa Univ.*, 1- 127.
- Uma G and Ritu K. 2008. Optimization and scale up of cellulase free endo xylanase production by solid state fermentation on corn cob and by immobilized cells of a thermotolerant bacterial isolate. *Jordan J Biologic Sci.* **1** (3): 129-134.
- Wang T, Liang H and Yuan Q. 2011. Optimization of ultrasonic-stimulated solvent extraction of sinigrin from indian mustard seed (*Brassica juncea*) using response surface methodology. *Phytochem Analys.* **22**(3): 205-213.
- Yalcin SK, Bozdemir M and Ozbas Z. 2009. A comparative study on citric acid production kinetics of two *Yarrowia lipolytica* strains in two different media. *Food Technol Biotechnol.* **44**(2): 457-464.

Bioactive ingredients of different extracts of *Vitex agnus-castus* L. Fruits from Morocco and their antioxidant potential

Fatima El Kamari*, Driss Ousaid, Amal Taroq, Yassine El Atki, Iman Aouam, Badiaa Lyoussi, and Abdelfattah Abdellaoui.

Laboratory of Physiology Pharmacology and Environmental Health, Department of Biology, Faculty of Sciences Dhar Mehraz, Sidi Mohamed Ben Abdellah University, B.P. 1796, Atlas, Fez, Morocco

Received: April 4, 2020; Revised: August 22, 2020; Accepted: September 11, 2020

Abstract

The current study aimed to examine the effect of different solvents on phenols and flavonoid contents and evaluate the antioxidant activities of different extracts. At first, the Soxhlet extracts were performed with four solvents (ethanol, methanol, ethyl acetate, and water) and were examined for their polyphenolic content, flavonoid content, and antioxidant potentials using three assays (DPPH, FRAP, TAC). The dosage of phytochemical compounds (polyphenolic and flavonoid contents) revealed that the highest values were established in ethanol extract ($p < 0.05$). Additionally, the strongest antioxidant activity measured by TAC and DPPH assays was established in ethanol extract with 400 ± 00 mg AAE/g DW and 0.36 ± 0.07 mg/mL, respectively, while the methanol extract showed the best antioxidant activity as measured by FRAP with an IC_{50} value of 2.98 ± 0.2 mg/mL; the lowest value was observed in ethyl acetate extract. The *Vitex* fruits possess remarkable antioxidant potential, which may enhance their protective effects.

Keywords: *Vitex agnus-castus*, Antioxidant activity, Flavonoids, Polyphenols.

1. Introduction

The failure of antioxidant defense systems is associated with oxidative stress, which induce the overproduction of reactive oxygen species (ROS) (McCord, 2000). ROS reacts with different molecules such as membrane lipids, proteins, and DNA leading to the pathogenesis and progression of various diseases including cancer, cardiovascular diseases, diabetes, tumors, rheumatoid arthritis, and epilepsy (Halliwell and Gutteridge, 2007; Ho et al., 1992). Thus, there is a growing interest in finding natural substances with antioxidant properties. Medicinal herbs are considered as a good source of bioactive compounds. They contain a large variety of functional substances such as, polyphenols, flavonoids, vitamins, which provide protective effects (Hamli et al., 2017; Rodríguez et al., 2013).

Vitex agnus-castus L. (VAC) is a medicinal plant that grows in the Mediterranean region, Europe, and Asia; (Ahangarpour et al., 2016). It belongs to the Verbenaceae family, commonly known as the chaste tree (Yushchyshena and Tsurkan, 2014). The uses of this medicinal herb are shown to have many biological activities. The fruits of this plant have been used to treat various female conditions such as uterine cramps, menstrual disorders, lactation, and acne (Chhabra and Kulkarni, 2011). By-products of *Vitex* (essential oils and extracts) possess several biological activities including antimicrobial and antifungal activities (Ahmad et al., 2016;

Arokiyaraj et al., 2009; Asdadi et al., 2015), while the aromatic leaves of this plant are used as a spice.

V. agnus-castus L. contain different bioactive ingredients such as Iridoid glycosides, Flavonoids, Diterpenes and Essential fatty acids (Dugoua et al., 2008). *V. agnus-castus* is locally named “Angarf-lkrwaa” in the Imouzzer Ida Outanane region; the plant used as a sedative, antispasmodic, and an aphrodisiac (Abdelhai Sijelmassi, 1991).

The chemical contents and antioxidant capacities of different extracts of *Vitex agnus-castus* were determined and compared.

2. Materials and Methods

2.1. Plant material

Fruits of VAC were collected from Khenifra area (Latitude: $32^{\circ}56'05''$ Nord; Longitude: $5^{\circ}39'42''$ Ouest; altitude: 827 m), (Middle Atlas, Morocco) in June-October 2015 (flowering period). Professor A. Bari as a botanist identified our plant material (Department of Biology, FSDM, USMBA, Fez (Morocco).

2.2. Extract preparation

Before extraction, the *Vitex* fruits were washed and then dried. Next, the dried fruits were powdered. The extraction was performed with four solvents (ethanol, methanol, ethyl acetate, and water), and the solid to liquid ratio was 1/20 using Soxhlet extractor for 8 h. The rotary evaporator was used to concentrate all extracts then stored in a refrigerator at 4°C .

* Corresponding author e-mail: kamarisapiens@gmail.com.

2.3. Dosage of total polyphenolic content (TPC)

The determination of TPC of extracts was assessed by the method described by Jadouali et al., (2018) and detailed by Hamli et al., (2017) using Folin-Ciocalteu. Results of TPC were calculated as mg GAE/g DW.

2.4. Determination of Total flavonoid content (TFC)

To quantify TFC, we have chosen a modified Zhishen et al., (1999) method as detailed by Hamli et al., (2017). Results were expressed as mg RE/g DW.

2.5. Total antioxidant capacity test (TAC)

The test chosen to determine the TAC of extracts is based on the method proposed by Prieto et al., (1999). Briefly, each extract (25 μ L) was appended to 1 mL of phosphomolybdate solution. The color intensity was read at wavelength 695 nm after incubating the mixture reaction at 95 $^{\circ}$ C for 90 min used ascorbic acid as the standard calibration. Results were expressed as mg AAE/g DW.

2.6. DPPH assay

To examine the capacity to quench free radicals, we have chosen DPPH assay as described by Wu et al., (2003). 0.1 mL of the extract/standard and 1.5 mL of DPPH solution (0.1 mmol) were mixed, then the mixture was incubated 30 min in the darkness. Decline in the intensity of coloration produced was read at 517 nm. The DPPH scavenging activity was estimated by the following equation:

$$\%Inhibition = [(A_c - A_s)/A_c] \times 100$$

Where A_c is the absorbance of the control, and A_s is the absorbance of the sample. BHT served as a positive control.

2.7. FRAP assay

The FRAP of extracts was examined using the technique of Oyaizu (OYAIZU and M., 1986). Briefly, 200 μ L of the sample, 500 μ L of phosphate buffer (0.2M, pH 6.6), and 500 μ L of potassium ferricyanide [$K_3Fe(CN)_6$] 1% were mixed. Then, 500 μ L of Trichloroacetic (TCA) 10% was added and mixture was incubated during 20 min at 50 $^{\circ}$ C. The supernatant (2, 5 mL) after centrifugation, 500 μ L of deionized water, and 100 μ L of $FeCl_3$ (10%) were mixed. 700 nm was the wavelength used to read the absorbance. The outcomes were deducted as the dose of extract inhibiting 50% of FRAP.

2.8. Statistical analysis

Statistical analysis was carried out by ANOVA one-way followed by Tuckey-test, using the Graph Pad Prism 5 (Microsoft Software). Differences at $P < 0.05$ were considered significant. The outcome was also subjected to multivariate analysis (principal component analysis).

3. Results

3.1. Effects of solvent on extraction yield, polyphenol, and flavonoid contents

Table 1 resumes the results of yields. The extraction yield of water (24%) was significantly the highest followed by ethanol (7.2%), methanol (6.3%), and ethyl acetate (2.04%).

Table 1: Yield, total phenolic content and total flavonoids of different extracts

Extract	Yield (%)	Phenols (mg GAE/g DW)	Flavonoids (mg RE/g DW)
Ethanol	7.2	62.66 \pm 2.5 ^a	58.16 \pm 1.3 ^a
Methanol	6.3	46.66 \pm 2.6 ^b	31.7 \pm 0.7 ^b
Ethyl acetate	2.04	21.50 \pm 1.8 ^d	12.08 \pm 1.1 ^c
Water	24	50.46 \pm 1.2 ^{cb}	16.07 \pm 0.81 ^d

a: comparison between the ethanol extract and all extracts, b: comparison between the methanol extract and all extracts, c: comparison between the ethyl acetate extract and all extracts, d: comparison between the water extract and all extracts.

Extraction process of active ingredients was assessed by different solvents. As shown in (Table 1), the quantity of phenols of various extracts, measured by Folin-Ciocalteu method, varied significantly from 21.50 \pm 1.8 to 62.66 \pm 2.5 mg GAE/g DW.

Results of flavonoids ranged from 12.08 \pm 1.1 to 58.16 \pm 1.3 mg RE/g DW. It is clear that the ethanol extract significantly contained the highest value of flavonoids (58.16 \pm 1.3 mg RE/g DW), while ethyl acetate extract (12.08 \pm 1.1) established the lowest value of TFC.

3.2. Antioxidant activities

3.2.1. Total antioxidant capacity (TAC)

Results are documented in Figure 2; they revealed that the best value of TAC was established in ethanol extract with a value equal to 408.33 \pm 4.33(mg Eq AAE/g DW), while the ethyl acetate extract have the lowest antioxidant capacity (147.4 \pm 2.04 mg Eq AAE/g DW).

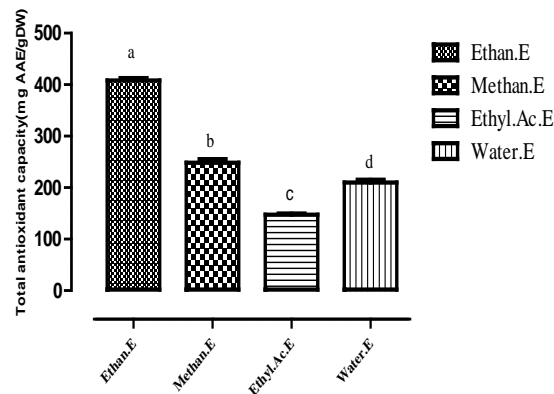


Figure 1. TAC of different extracts of V. fruits.

3.2.2. Antioxidant ability by DPPH

Results of DPPH assay are presented in Table 2. The IC_{50} values of all tested samples through the DPPH scavenging ability test ranged from 0.36 \pm 0.07 mg/mL to 2.04 \pm 0.21 mg/mL. All extracts inhibited the DPPH radical as follows: ethanol > water > methanol > ethyl acetate. The highest activity was obtained from ethanol extract (IC_{50} = 0.36 \pm 0.07 mg/mL), while the lowest activity was registered from ethyl acetate extract (IC_{50} = 2.04 \pm 0.21 mg/mL). However, the BHT exhibited the best antioxidant ability compared to all samples studied (0.10 \pm 0.03 mg/mL).

3.2.3. Ferric reducing power assay

The highest and lowest reducing power values were obtained by methanol and aqueous extracts ($2.98 \pm 0.2 - 3.54 \pm 0.22$ mg/mL), respectively. Also, the best ability tested by FRAP assay was established by BHT with value of 0.12 ± 0.01 mg/mL.

Table 1: Antioxidant activities of different extracts

Extract	DPPH	FRAP
Ethanol	0.36 ± 0.07^d	3.29 ± 0.41^c
Methanol	0.71 ± 0.33^{bd}	2.98 ± 0.2^{dc}
Ethyl Acetate	2.04 ± 0.21^a	3.14 ± 0.21^{bcd}
Water	0.52 ± 0.02^{cd}	3.54 ± 0.22^{abc}
BHT	0.10 ± 0.03^{ed}	0.12 ± 0.01^e

a: comparison between the ethanol extract and all extracts, b: comparison between the methanol extract and all extracts, c: comparison between the ethyl acetate extract and all extracts, d: comparison between the water extract and all extracts, e: comparison between the BHT and all extracts.

3.3. Correlation of Antioxidant Activities with Flavonoids and Phenols Content

To find the influence bioactive compounds (phenols and flavonoids) on the antioxidant potential of *Vitex agnus castus* extracts, we studied the relation between the antioxidant tests and the content of bioactive ingredients (polyphenols and flavonoids) using correlation test. Based on the data presented in Table 3, positive correlation was recorded between phytochemicals and their ability to scavenge free radicals ($P < 0.01$). The IC_{50} DPPH negatively correlated with TFC ($r^2 = -0.87$) and phenols ($r^2 = -0.96$).

Table 3: Pearson correlation coefficients between compounds and antioxidant activities.

Antioxidant activities	Flavonoids (TFC)	Phenols (TPC)
CAT	0.89 **	0.95 **
DPPH	-0.87 **	-0.96 **
FRAP	-0.44	-0.34

* Correlation is significant at the $P < 0.05$ level.

** Correlation is significant at the $P < 0.01$ level.

4. Discussion

The present work was designed to evaluate, for the first time, the TPC, TFC, and antioxidant capacities of *Vitex agnus castus* fruits extracts, which grow in wild habitats in Khenifra area, Morocco. Therefore, from outcomes obtained from different extracts, water gives the highest yield in comparison with other solvents. Our findings are similar to those obtained by Sağlam et al., (2007). In the literature, the nature of solvent affects the yield of extraction (Do et al., 2014). Furthermore, several factors affect the extraction process such as the extraction method, sample particle size, nature of phytochemicals (Stalikas, 2007).

Regarding phenolic quantity, the most proper solvent to extract bioactive compounds was ethanol as previously documented by Latoui et al. (2012). Furthermore, the amount of active ingredients in plants is highly related to

numerous biological parameters such as genotype, organ, ontogeny, and environmental conditions. Besides, the solvent used, polymerization, and interaction of active substances govern the solubility of phenolic compounds (Ksouri et al., 2008).

In the same context, the ethanol was the highly extractable solvent for flavonoids, while the lowest value was established in the ethyl acetate extract. The minimum yield of flavonoids extracted (7.12 ± 0.08 μ g QE / mg of extract) was also documented in the ethyl acetate extract of *Vitex agnus castus* fruits from Manisa, Turkey (Sarikurku et al., 2009). Thus, the yield of flavonoids from fruits is controlled by the nature of the solvent (Gao and Liu, 2005). Hirobe et al., (1997) reported that the bark root of plant (*Vitex*) also contained flavonoids.

In summary, according to the results obtained from all extracts, ethanol was the most proper organic solvent to extract molecules with antioxidant potential (Table 1).

An extract is qualified to have a strong antioxidant effect if the $IC_{50} < 5$ mg/mL (Abdillah et al., 2015). The methanolic extract of VAC fruits collected from Antalya possesses strong antioxidant activity (Gökbulut et al., 2010), which is in accordance of our data. The existence of some anthraquinones could be responsible for this high reducing power (Yen and Chuang, 2000). Therefore, the methanolic extract could be rich in this class of secondary metabolites.

The TPC and TFC correlate positively with antioxidant ability evaluated by TAC and negatively with DPPH, FRAP. Therefore, the activity of eliminating free radicals from extracts could be attributed to the content of phenols and flavonoids. Phenol compounds can contribute to antioxidant activity, and they have been considered as anti-inflammatory, anticancer, anticholinergic enzymes, antiviral, and antibacterial agents (Atki et al., 2019; Banji et al., n.d.; Jaiswal and Thakur, 2017; Ojo et al., 2017; Rakass, 2018; Sagbo et al., 2017; Shawarab et al., 2017).

The correlation linked the FRAP and the bioactive substances was not significant, which indicates that the FRAP assay in these extracts measures the activity of certain phytochemical classes other than phenols and flavonoids (Yen and Chuang, 2000).

5. Conclusion

Bioactive ingredients and the assessment of antioxidant quality of *Vitex agnus castus* collected from Khenifra were conducted in the present work. The outcome shows that chemical composition was affected by nature of solvent, and ethanol is evaluated as a proper solvent for extraction of molecules, which exhibits the best antioxidant ability. The outcomes revealed the possible application of evaluated *Vitex agnus castus* fruits extracts as the best source of bioactive molecules with health benefits.

References

- Sijelmassi A. 1991. Plantes médicinales du Maroc - broché - Abdelhaï Sijelmassi - Achat Livre - Achat & prix | Soldes fnac.
- Abdillah S, Tambunan RM, Farida Y, Sandhiutami NMD and Dewi RM. 2015. Phytochemical screening and antimalarial activity of some plants traditionally used in Indonesia. *Asian Pac. J. Trop. Dis.* 5: 454-457.

- Ahangarpour A, Najimi SA and Farbood Y. 2016. Effects of Vitex agnus-castus fruit on sex hormones and antioxidant indices in a d-galactose-induced aging female mouse model. *J. Chin. Med. Assoc.* **79**: 589–596.
- Ahmad B, Hafeez N, Ara G, Azam S, Bashir S and Khan I. 2016. Antibacterial activity of crude methanolic extract and various fractions of Vitex agnus castus and Myrsine africana against clinical isolates of Methicillin Resistant Staphylococcus aureus. *Pak. J. Pharm. Sci.* **29**: 1977–1983.
- Arokiyaraj S, Perinbam K, Agastian P and Kumar RM. 2009. Phytochemical analysis and antibacterial activity of Vitex agnus-castus. *Int. J. Green Pharm.* **3**.
- Asdadi A, Hamdouch A, Oukacha A, Moutaj R, Gharby S, Harhar H, El Hadek M, Chebli B and Idrissi Hassani LM. 2015. Study on chemical analysis, antioxidant and in vitro antifungal activities of essential oil from wild Vitex agnus-castus L. seeds growing in area of Argan Tree of Morocco against clinical strains of Candida responsible for nosocomial infections. *J. Mycol. Medicale.* **25**: e118-27.
- Atki YE, Aouam I, Kamari FE, Tarog A, Lyoussi B and Abdellaoui A. 2019. Antioxidant activity of two wild teucrium species from Morocco. *IJPSR.* **10**(6): 2723-2729.
- Banji A, Goodluck B, Ouluchi O and Stephen F. 2018. Antimicrobial and antioxidant activities of crude methanol extract and fractions of Andrographis paniculata leaf (Family: Acanthaceae) (Burm. f.) wall. Ex Nees. *Jordan J. Biol. Sci.* **11**(1): 23-30.
- Chhabra GS and Kulkarni KS. 2011. Vitex agnus castus - an overview. *J. Nat. Remedies.* **11**
- Do QD, Angkawijaya AE, Tran-Nguyen PL, Huynh LH, Soetaredjo FE, Ismadji S and Ju Y-H. 2014. Effect of extraction solvent on total phenol content, total flavonoid content, and antioxidant activity of Limnophila aromatica. *J. Food Drug Anal.* **22**: 296–302.
- Dugoua J-J, Seely D, Perri D, Koren G and Mills E. 2008. Safety and efficacy of chastetree (Vitex agnus-castus) during pregnancy and lactation. *Can. Pharmacol. Clin.* **15**: e74-9.
- Gao M and Liu C-Z. 2005. Comparison of techniques for the extraction of flavonoids from cultured cells of Saussurea medusa Maxim. *World J. Microbiol. Biotechno.* **21**: 1461–1463.
- Gökbulut A, Özhan O, Karacaoğlu M and Şarer E. 2010. Radical scavenging activity and vitexin content of Vitex agnus-castus leaves and fruits. *FABAD J Pharm Sci.* **35**: 85–91.
- Halliwel B and Guttridge JMC. 2007. **Free Radicals in biology and medicine.**
- Hamli S, Kadi K, Addad D and Bouzerzour H. 2017. Phytochemical screening and radical scavenging activity of whole seed of durum wheat (Triticum durum Desf.) and barley (Hordeum vulgare L.) varieties. *Jordan J. Biol. Sci.* **10**.
- Hirobe C, Qiao Z-S, Takeya K and Itokawa H. 1997. Cytotoxic flavonoids from Vitex agnus-castus. *Phytochemistry.* **46**: 521–524.
- Ho C-T, Chen Q, Shi H, Zhang K-Q and Rosen RT: 1992. Antioxidative effect of polyphenol extract prepared from various Chinese teas. *Prev. Med.* **21**: 520–525.
- Jadouali SM, Atifi H, Bouzoubaa Z, Majourhat K, Gharby S, Achemchem F, Elmoslih A, Laknifli A and Mamouni R. 2018. Chemical characterization, antioxidant and antibacterial activity of Moroccan Crocus sativus L petals and leaves. *J Mater Env. Sci.* **9**: 113–118.
- Jaiswal P and Thakur MK. 2017. The Investigation on Total Phenolic Content and in Vitro Antioxidant Potential of Different Plant Parts of Nyctanthes arbortristis (Night Jasmine). *Int. J. Pharm. Sci. Res.* **8**: 3547–51.
- Ksouri R, Megdiche W, Falleh H, Trabelsi N, Boulaaba M, Smaoui A and Abdely C. 2008. Influence of biological, environmental and technical factors on phenolic content and antioxidant activities of Tunisian halophytes. *C. R. Bio.* **331**: 865–873.
- Latoui M, Aliakbarian B, Casazza AA, Seffen M, Converti A and Perego P. 2012. Extraction of phenolic compounds from Vitex agnus-castus L. *Food Bioprod. Process.* **90**: 748–754.
- McCord JM. 2000. The evolution of free radicals and oxidative stress. *Am. J. Med.* **108**: 652–659.
- Ojo OA, Ajiboye BO, Ojo AB, Olayide II, Akinyemi AJ, Fadaka AO, Adedeji EA, Boligon AA and de Campos MMA. 2017. HPLC-DAD Fingerprinting Analysis, Antioxidant Activity of Phenolic Extracts from Blighia sapida Bark and Its Inhibition of Cholinergic Enzymes Linked to Alzheimer's Disease. *Jordan J. Biol. Sci.* **10**.
- Oyaizu M. 1986. Studies on products of browning reactions : antioxidative activities of products of browning reaction prepared from glucosamine. *Jpn J Nutr.* **44**: 307–315.
- Prieto P, Pineda M and Aguilar M. 1999. Spectrophotometric Quantitation of Antioxidant Capacity through the Formation of a Phosphomolybdenum Complex: Specific Application to the Determination of Vitamin E. *Anal. Biochem.* **269**: 337–341.
- Rakass S. 2018. Antioxidant activity of Butternut squash Skin: Effect of different extracting solvents. *Moroc. J. Chem.* **6**(3): 548-556.
- Rodríguez ML, Estrela JM and Ortega Á. 2013. Natural polyphenols and apoptosis induction in cancer therapy. *J Carcinog Mutag S.* **6**.
- Sagbo IJ, Afolayan AJ and Bradley G. 2017. Antioxidant, antibacterial and phytochemical properties of two medicinal plants against the wound infecting bacteria. *Asian Pac. J. Trop. Biomed.* **7**: 817–825.
- Sağlam H, Pabuçcuoğlu A and Kivçak B. 2007. Antioxidant activity of Vitex agnus-castus L. extracts. *Phytother. Res. Int. J. Devoted Pharmacol. Toxicol. Eval. Nat. Prod. Deriv.* **21**: 1059–1060.
- Sarikurkcü C, Arisoy K, Tepe B, Cakir A, Abali G and Mete E. 2009. Studies on the antioxidant activity of essential oil and different solvent extracts of Vitex agnus castus L. fruits from Turkey. *Food Chem. Toxicol.* **47**: 2479–2483.
- Shawarb N, Jaradat N, Abu-Qaoud H, Alkowni R and Hussein F. 2017. Investigation of antibacterial and antioxidant activity for methanolic extract from different edible plant species in Palestine. *Moroc. J. Chem.* **5**: 573–579.
- Stalikas CD. 2007. Extraction, separation, and detection methods for phenolic acids and flavonoids. *J. Sep. Sci.* **30**: 3268–3295.
- Wu H-C, Chen H-M and Shiau C-Y. 2003. Free amino acids and peptides as related to antioxidant properties in protein hydrolysates of mackerel (Scomber austriasicus). *Food Res. Int.* **36**: 949–957.
- Yen G-C and Chuang D-Y. 2000. Antioxidant properties of water extracts from Cassia tora L. in relation to the degree of roasting. *J. Agric. Food Chem.* **48**: 2760–2765.
- Yushchysheva O and Tsurkan O. 2014. Phenolic compounds content in Vitex agnus-castus L. and V. cannabifolia Sieb. growing in Ukraine. *J Med Plants Stud.* **2**: 36–40.
- Zhishen J, Mengcheng T and Jianming W. 1999. The determination of flavonoid contents in mulberry and their scavenging effects on superoxide radicals. *Food Chem.* **64**: 555–559.

Thrombin protease-activated receptor inhibitors from the peel of *Ananas comosus* (L.) Merr.: an *in silico* approach

Babatunde J. Oso¹, Ige F. Olaoye^{1,2,*}, Anne Adeyanju³ and Adepeju Aberuagba²

¹Department of Biochemistry, McPherson University, Seriki Sotayo, Ogun State, Nigeria; ²School of Pharmacy and Biomolecular Sciences, Liverpool John Moores University, Liverpool, UK; ³Department of Biochemistry, KolaDaisi University, Ibadan, Oyo State, Nigeria.

Received: April 14, 2020; Revised: August 26, 2020; Accepted: September 12, 2020

Abstract

Background: Mortality and morbidity related to coronary atherothrombotic diseases and the unpredictable adverse effect of available anticoagulant drugs prompt the need for the development of effective and safe therapeutic agents. This study assessed the metabolomic profiling and molecular docking studies of the constituents of the unripe peel fruit of *Ananas comosus* (L.) Merr. methanolic extract against thrombin protease-activated receptors (PARs). **Methods:** Metabolomics profiling of the methanolic extract of the unripe peel of *A. comosus* was carried out using gas chromatography connected with a mass spectrometer (GC/MS). Molecular docking was done to assess the affinity of the identified compounds for the active sites of PARs, and the binding behaviors were visualized with DS BIOVIA. pkCSM, a web server, screened two probable compounds which presented ideal binding with all the receptors. **Results:** The GC/MS profiling showed a total of 12 volatile compounds with benzyl alcohol being the most prominent compound. The molecular docking analysis showed 2-(4-methylphenyl)-indolizine, and 2-p-nitrobenzoyl-1,3,5-tribenzyl- α -D-ribose demonstrated optimal binding with the selected PARs. The computed pharmacokinetic and pharmacodynamics properties of the selected compounds presented 2-(4-methylphenyl)-indolizine possesses drug-like properties. **Conclusion:** The findings of this study could be explored and optimized in the development of safe and efficient plant-based anti-thrombotic agents.

Keywords: *A. comosus*, Thrombin, Molecular docking, Protease-Activated Receptors

1. Introduction

Blood is a connective tissue in humans and other vertebrates flowing through the blood vessels smoothly and efficiently to deliver to cells needed materials including oxygen and nutrients. However, this smooth flow is obstructed by thrombus resulting in coronary atherothrombotic diseases that lead to death (WHO, 2017). Other clot formation diseases include pulmonary embolism, cerebrovascular accident (CVA), myocardial, and cerebral infarction (Ashorobi and Fernandez, 2019). Atherothrombotic coronary artery disease and deep vein thrombosis are major underlying death drives worldwide (Herrington *et al.*, 2016). To substantiate this, Gryka *et al.* (2017) reported that 17 million deaths are caused yearly by cardiovascular events, and 7.3 million are caused by ischemic heart disease while 6.2 million of deaths are caused by strokes. This report was validated in WHO (2017) report whereby 31% of global death was due to these collective cardiovascular disorders and most occurs in low and middle-income countries.

Thrombosis is a fatal disease involving the blood clots formation which leads to associated coronary diseases in the circulatory system due to homeostasis imbalance (Ko *et al.*, 2004; Mahmud *et al.*, 2015). Mumaw *et al.* (2015) reported the crucial cellular component of arterial thrombin as platelet aggregation with evidence from different studies showing Protease-Activated Receptors

(PARs) as thrombin activities' mediator that enhances human platelet activation. PARs, examples of G-protein-coupled receptors (GPCR) family, expressed in different cell types cause proteolytic cleavage at the N-terminal sequence for activation (Coughlin, 2000; Hollenberg and Compton, 2002). The cleavage remainders bind intramolecularly to induce intracellular signal transduction that promotes thrombosis via receptor activation (Adams *et al.*, 2011). Human PAR1, PAR3, and PAR4 have been known for their significant role in blood coagulation via interaction with thrombin (Ma *et al.*, 2005), a known platelet agonist generated by coagulation system (Covic *et al.*, 2002). Moreover, Charlotte *et al.* (2019) reported that platelet aggregation with platelet adhesion and activation is known to be a vital pathogenic factor in the development of atherosclerosis and associated thrombosis in humans via receptor-ligand interaction. Anticoagulants have been used in the prevention and management of cardiovascular disorders that are associated with thrombosis due to their clot formation inhibiting potential (De Caterina *et al.*, 2013; da Silva and Ferreira, 2015). Several anticoagulant drugs such as heparin and warfarin are available to suppress atherothrombotic events; however, these compounds might not be healthy alternatives, besides being expensive and producing a wide spectrum of adverse effects (Gryka *et al.*, 2017; Wong *et al.*, 2017). This has prompted the search for novel cost-effective antithrombotic agents that are less toxic (Lau *et al.*, 2009). Plants from time immemorial have been known to be the

* Corresponding author e-mail: igeolarinoye@gmail.com; F.I.Olaoye@ljmu.ac.uk.

promising sources of novel drug candidates for the prevention and treatment of diseases including blood-clotting disorders. Some plant materials such as *Alium cepa*, *Panax notoginseng*, and *Orbignya phalerata* had been studied for their repositioning feasibility as anticoagulant agents for management and handling of thrombotic disorders (Azevedo et al., 2007; Shikha et al., 2014). Numerous investigations have been done on the putative effect of some phytoconstituents against platelet aggregation, towards increase fibrinolysis and coronary atherothrombotic diseases (CADs) as a whole (Yoo et al., 2014; Lee et al., 2015; Mohd Nor et al., 2016; Oso et al., 2019). Moreover, the peels and seeds of plant materials such as *Lycopersicum esculentum* Mill., *Curcuma longa* L., and *Ananas comosus* (L.) Merr. are examples of plant materials that had been reported to be prospective sources of pharmacologic agents against thrombosis (Evangelista et al., 2012).

Ananas comosus is a fruit that belongs to the family of Bromeliaceae. The inedible parts of the fruit such as the peels, crown, and core have been reported to be rich sources of beneficial biologically active phytochemicals such as polyphenols (Li et al., 2014). Also, Li et al. (2014) identified catechin, epicatechin, ferulic acid and gallic acid as the phytochemical constituents of the peel of *A. comosus* methanolic extract through HPLC-MS analysis. The classes of these phytocompounds are known to contribute immeasurably to various pharmacological properties of plant materials (Banji et al., 2018; Abdel-Mawgoud et al., 2019). Therefore, this study aimed at investigating the putative anti-thrombotic effects of the phytocompounds of the unripe peel fruit of *A. comosus* methanolic extract through *in silico* studies.

2. Material and Methods

2.1. Plant Materials

The plant materials (unripe pineapple fruit) were obtained from local suppliers in Ajebo, Ogun State, South-Western Nigeria and authenticated at the Department of Biological Sciences, McPherson University, Nigeria.

2.2. Methodology

2.2.1. Extraction of plant materials

The peel of fruit was removed, washed three times with distilled water, and dried at room temperature of $30 \pm 1^\circ\text{C}$. The dried peel was pulverized and reserved for subsequent extraction. Fifty grams of the pulverized peel were transferred into 500 ml flat-bottom and macerated with 200 ml of absolute methanol for twenty-four hours and the mixture was filtered. The filtrate was concentrated and stored at -18°C in an air-tight container (Oso et al., 2019).

2.2.2. Identification and characterization of compounds

A concentrated extract of *A. comosus* was dissolved in methanol and the solution was used for the GC/MS analysis. The analysis was performed using Agilent Technologies GC/MS (Model 7890A) equipped with Agilent 19091IS-433HP-5MS 5% Phenyl Methyl Silox column ($30\text{ m} \times 250\ \mu\text{m} \times$ film thickness $0.25\ \mu\text{m}$) coupled with mass spectrometry. Pure helium gas as carrier gas at $1.5\ \text{mL/min}$ constant rate was used. The injector temperature was 250°C . GC/MS analysis

resulting in chromatogram was compared to the complete library using a data base of the National Institute of Standard and Technology (NIST). The values were presented as the relative percentage of the chemical components expressed as a percentage by peak area. The GC/MS profiling was performed at the Department of Chemical Engineering, University of Ilorin, Ilorin, Nigeria.

2.2.3. *In silico* Molecular docking

An *in silico* molecular docking study was done to validate the binding potency of all the compounds of *A. comosus* extract to thrombin by using AutoDock 4.2 program (Trott and Olson, 2010) and visualized with DS BIOVIA using the method described by Rizvi et al. (2013). The molecular dockings were conducted by using the 3D crystal structure of the PAR1, PAR3, and PAR4, obtained from the protein data bank (www.rcsb.org) (Berman et al., 2000) with PDB IDs 3HKJ, 2PUX, and 3QDZ respectively. The selected crystal structures were obtained from the human genome except for 2PUX which was an available murine PAR3 chosen as a human homologous (Bah et al., 2007). The associated thrombin and ligand complexes were deleted using DS BIOVIA. Moreover, polar hydrogen atoms were added, and the crystal water remained. The selected ligands are thrombin (PubChem CID: 65045), benzyl alcohol (PubChem CID: 244), 2-(4-methylphenyl)-indolizine (PubChem CID: 346948), and 2-p-nitrobenzoyl-1,3,5-tribenzyl- α -D-ribose (PubChem CID: 542798). Benzyl alcohol, 2-(4-methylphenyl)-indolizine, and 2-p-nitrobenzoyl-1,3,5-tribenzyl- α -D-ribose were selected from the GC/MS chromatogram based on their respective binding affinity with a threshold determined by thrombin, a PAR agonist. The ligands were obtained from the PubChem database (Bolton et al., 2008; Kim et al., 2019). The cubic grid box was set to $-12 \times -22 \times 20$ points with a spacing of $1.0\ \text{\AA}$. The catalytic site of the grid box was centered on the following coordinates ($x=68$; $y=62$; $z=83$) to obtain the best orientations and conformations of the ligands in the binding pockets of protein. The interaction figures were generated in both 3D and 2D to visualize the specific interactions between the selected compounds and the receptors. The docking results were recorded with binding energy and bonded residues.

2.2.4. Prediction of ADMET by computational analysis

Pharmacokinetic (PK) properties of 2-(4-methylphenyl)-indolizine and 2-p-nitrobenzoyl-1,3,5-tribenzyl- α -D-ribose were investigated using the pkCSM ADMET descriptors algorithm protocol (<http://biosig.unimelb.edu.au/pkcsm/prediction>) (Douglas et al., 2015). Two important chemical descriptors relate well with PK features; the absorption of drugs relies on factors such as membrane permeability [indicated by colon cancer cell line (Caco-2)], intestinal absorption, skin permeability levels, P-glycoprotein substrate or inhibitor. The distribution of drugs relies on factors such as the blood-brain barrier (logBB), CNS permeability, and the volume of distribution (VDss). Metabolism is predicted based on the CYP models for substrate or inhibition (CYP2D6, CYP3A4, CYP1A2, CYP2C19, and CYP2C9). Excretion is predicted based on the total clearance model and renal OCT2 substrate. The safety of compounds is

foreseen based on skin sensitization, AMES toxicity, hepatotoxicity, and hERG inhibition.

3. Results

3.1. Characterization of Phytochemical Compositions

The chromatograms of the metabolomics profiling of the volatile and semi-volatile components of the extract are presented in Figures 1 and the identified compounds are presented in Table 1.

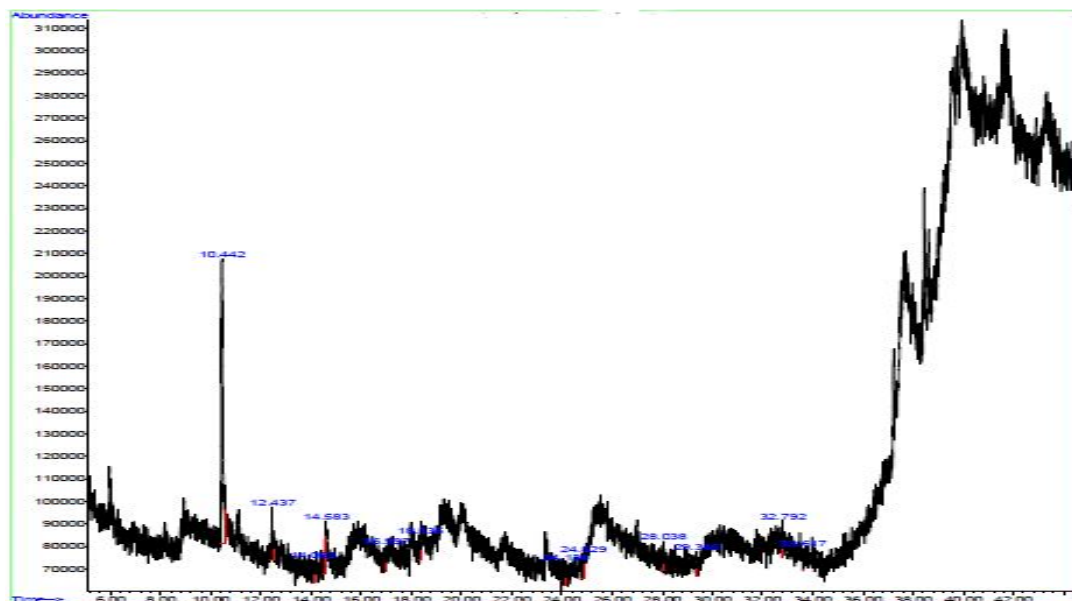


Figure 1. GC/MS chromatogram of methanol extract of the unripe peel of *A. comosus* L. with benzyl alcohol (62.52 %), 4H-1,2,4-triazol-3-amine, 4-propyl (7.12 %) and 2,5-Difluorophenylhydrazine (7.64 %) as abundant compounds

Table 1. Chemical composition of methanol extract, retention time, percentage of correlation and percentage relative composition of unripe of *A. comosus*

Compounds	RT (mins)	CM (%)	RC (%)
Benzyl alcohol	10.442	100.00	62.53
4H-1,2,4-Triazol-3-amine, 4-propyl	12.437	11.40	7.13
chloro- Acetaldehyde	14.063	3.20	2.00
2,5-Difluorophenylhydrazine	14.583	12.23	7.65
N-(3-Methylbutyl)acetamide	16.997	6.56	4.10
1,4-dinitro- Benzene	18.336	3.30	2.40
2,2-Dimethoxy-1-oxa-2-sila-1,2-dihydronaphthalene	24.134	3.66	2.29
2-p-Nitrobenzoyl-1,3,5-tribenzyl- α -D-ribose	24.829	4.29	2.68
2,3-dihydro-2,8-dimethyl- Benz[b]-1,4-oxazepine-4(5H)-thione	28.038	3.25	2.03
3-amino-3-cyano-, methyl ester Acrylic acid	29.345	5.62	3.52
5-(ethyl) (4-diethylamino-1-methyl Pyrimidine-2,4,6 (1H,3H,5H)-trione	32.792	3.29	2.05
2-(4-methylphenyl)- Indolizine	33.617	3.12	1.95

RT=Retention time; CM= Maximum Correlation; RC= Relative composition expressed in percentage of total.

3.2. Molecular docking

The inherent nature of molecular docking is the recognition process of molecules, relating to their space and energy matching. The docking results tabulated between the PARs and the ligands are shown in Figure 2a, b, and Table 2. The results showed that 2-(4-methylphenyl)-indolizine and 2-p-nitrobenzoyl-1,3,5-tribenzyl- α -D-ribose were found to possess the maximum

binding energies as -7.0 and -6.5, -8.4 and -5.1, and -8.4 and -7.2 kcal/mol respectively towards PAR1, PAR3, and PAR4 compared to thrombin except for PAR3 where 2-(4-methylphenyl)-indolizine had lower binding energy than thrombin. However, benzyl alcohol had lower binding energy towards all the PARs compared to thrombin and had its interaction towards PAR1 despite its high percentage composition in the *A. comosus* unripe peel.

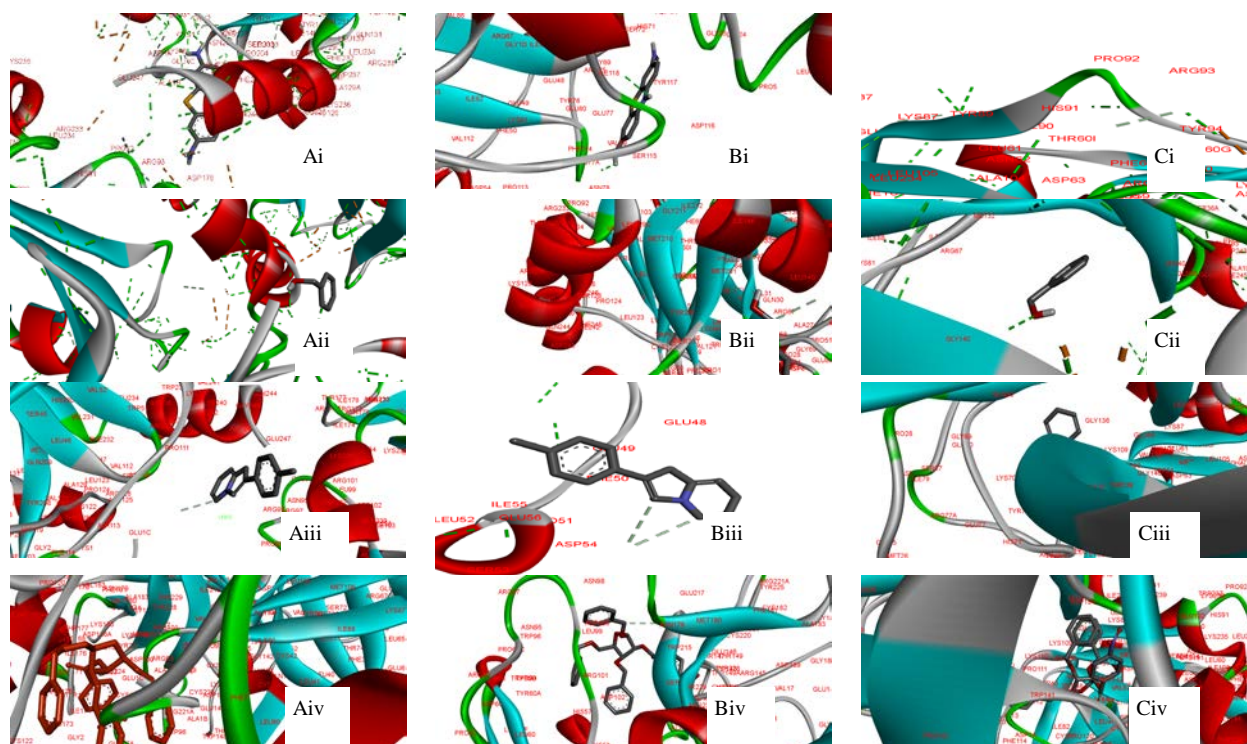


Figure 2b: 3D View of the molecular docking of PAR-1 towards and ligands: Ai thrombin, Aii benzyl alcohol, Aiii 2-(4-methylphenyl)-indolizine and Aiv 2-p-nitrobenzoyl-1,3,5-tribenzyl- α -d-ribose; PAR-3 towards and ligands: Bi thrombin, Bii benzyl alcohol, Biii 2-(4-methylphenyl)-indolizine and Biv 2-p-nitrobenzoyl-1,3,5-tribenzyl- α -d-ribose; and PAR-4 towards and ligands: Ci thrombin, Cii benzyl alcohol, Ciii 2-(4-methylphenyl)-indolizine and Civ 2-p-nitrobenzoyl-1,3,5-tribenzyl- α -d-ribose

Table 2. Docking analysis of 2-(4-methylphenyl)-indolizine and 2-p-nitrobenzoyl-1,3,5-tribenzyl- α -d-ribose from the methanolic extract of unripe of *A. comosus* L with thrombin receptors (PARs)

Ligands	PubChem ID	Molecular mass(g/mol)	Binding energy (Kcal/mol)			Amino acid residues in conventional H-bond at the binding site		
			PAR1	PAR3	PAR4	PAR1	PAR3	PAR4
Thrombin	65045	263.75	-6.1	-6.4	-6.4	Glu97	Arg 77	Asn60G, Ile88
Benzyl alcohol	244	108.14	-4.3	-5.1	-4.7	Phe232	NR	Trp96, Leu99
2-(4-methylphenyl)-indolizine	346948	209.72	-6.5	-5.1	-7.2	NR	NR	NR
2-p-nitrobenzoyl-1,3,5-tribenzyl- α -d-ribose	542798	569.61	-7.0	-8.4	-8.4	Arg 93, Asn95	NR	Leu123

NR=No residue

3.3. Prediction of ADMET by computational analysis

The ADMET properties of 2-(4-methylphenyl)-indolizine and 2-p-nitrobenzoyl-1,3,5-tribenzyl- α -d-ribose are presented in Table 3. 2-(4-methylphenyl)-indolizine had a Log P value of 3.91472 and was predicted to have Log P value of 3.92, water solubility (-3.99 log mol/L), Caco-2 permeability (1.65 log Papp in 10⁻⁶ cm/s) and 97.5 % could be absorbed through the intestine. However, 2-p-

nitrobenzoyl-1,3,5-tribenzyl- α -d-ribose showed Log P of 5.86, water solubility (-5.98 log mol/L), Caco-2 permeability (1.07 log Papp in 10⁻⁶ cm/s) and 100 % intestinal absorption. 2-p-nitrobenzoyl-1,3,5-tribenzyl- α -d-ribose was suggested as an inhibitor of P-glycoprotein and human ether-a-go-go-related gene (hERG) and a hepatotoxic agent.

Table 3. Prediction of ADMET properties of 2-(4-methylphenyl)-indolizine and 2-p-nitrobenzoyl-1,3,5-tribenzyl- α -d-ribose

Property	2-(4-methylphenyl)-indolizine	2-p-nitrobenzoyl-1,3,5-tribenzyl- α -d-ribose
Absorption		
Log P	3.92	5.86
Water solubility (log mol/L)	-3.99	-5.98
Caco2 permeability (log Papp in 10 ⁻⁶ cm/s)	1.65	1.07
Intestinal absorption (% Absorbed)	97.5	100
Skin Permeability (log Kp)	-2.11	-2.74
P-glycoprotein substrate	No	No
P-glycoprotein I inhibitor	No	Yes
P-glycoprotein II inhibitor	No	Yes
Distribution		
VDss (log L/kg)	0.20	-0.57
Fraction unbound	0.24	0.04
BBB permeability (log BB)	0.55	-1.27
CNS permeability (log PS)	-1.55	-2.93
Metabolism		
CYP2D6 substrate	No	No
CYP3A4 substrate	Yes	Yes
CYP1A2 inhibitor	Yes	No
CYP2C19 inhibitor	Yes	Yes
CYP2C9 inhibitor	No	Yes
CYP2D6 inhibitor	No	No
CYP3A4 inhibitor	No	Yes
Excretion		
Total Clearance (log ml/min/kg)	0.50	0.82
Renal OCT2 substrate	No	No
Toxicity		
AMES toxicity	No	No
MTD (log mg/kg/day)	-0.72	0.84
hERG I inhibitor	No	No
hERG II inhibitor	No	Yes
Oral Rat Acute Toxicity (LD50) (mol/kg)	2.25	2.48
Oral Rat Chronic Toxicity (log mg/kg_bw/day)	0.97	1.52
Hepatotoxicity	No	Yes
Skin Sensitisation	No	No
<i>Pyriiformis</i> toxicity (log ug/L)	0.573	0.29
Minnow toxicity (log mM)	1.7	-8.68

BBB= Blood brain barrier, CNS= Central nervous system, Cytochrome P450, Renal OCT2= organ cation transporter, MTD= Maximum tolerated dose and hERG= human Ether-à-go-go-Related Gene

4. Discussions

The metabolomic investigation on the compounds composition present in the unripe *A. comosus* methanolic extract was conducted for better clarification of the

contributions of the peel to the observed reported biological activities. Several volatile compounds seen in the extract include esters, alcohols, ketones, aldehydes, and terpenes. The results showed that 12 volatile compounds are present in the unripe *A. comosus* methanolic extract. However, only 2-(4-methylphenyl)-indolizine, and 2-p-nitrobenzoyl-1,3,5-tribenzyl- α -d-ribose depicted higher binding scores than thrombin. Benzyl alcohol with a relative composition of 62.52% was the prominent volatile compounds present in the extract followed by 4H-1,2,4-triazol-3-amine, 4-propyl. Benzyl alcohol, a relatively non-toxic and naturally occurring flavouring agent is usually an active compound in cosmetics (McCloskey *et al.*, 1986).

The binding affinities of the identified compounds: benzyl alcohol, 2-(4-methylphenyl)-indolizine, and 2-p-nitrobenzoyl-1,3,5-tribenzyl- α -d-ribose were estimated through molecular docking. The docking analysis result revealed that benzyl alcohol, the most prominent volatile compound in the extract had the least binding affinity towards PARs. This implies that the compound might not be responsible for the established antithrombotic effect of *A. comosus* peel through modulation of the PARs (Limjuco *et al.*, 2014; Go and Mariposque, 2018). Conversely, 2-p-nitrobenzoyl-1,3,5-tribenzyl- α -d-ribose had the best binding score towards the PARs including thrombin value with conventional hydrogen bond formation to basic residues (Asn and Arg) and van der Waal interaction in PAR1 binding site. Elokely and Doerksen (2013) reported that scoring systems generally rely on electrostatic interactions, Van der Waal's forces, and hydrophobic linkage. The conventional hydrogen interaction could be linked to the hirudin-like domain on PAR1, an exosite 1 that recruits thrombin to PAR1 (Vu *et al.*, 1991). Similarly, 2-p-nitrobenzoyl-1,3,5-tribenzyl- α -d-ribose had the best effective interaction with PAR3 using the same mechanism as PAR1, but no conventional hydrogen linkage was observed. The absence of a conventional hydrogen linkage may be attributed to the differences in organism genome on the receptor. In contrast to PAR1 and PAR3, 2-p-nitrobenzoyl-1,3,5-tribenzyl- α -d-ribose could be antagonist by blocking the interaction between the receptor and G protein. This could be due to its hydrophobic nature (log P value greater than 5) and prevent the internalization of signaling in the cellular part (French and Hamilton, 2016). More so, 2-(4-methylphenyl)-indolizine had a better binding score to all the PAR1 and PAR4 with no conventional hydrogen formation. This higher binding score may be attributed to the high number of alkyl and pi alkyl bond formation suggesting other mechanisms aside hirudin-like linkage (Heuberger and Schuepbach, 2019). Also, a low binding score was observed for PAR3 for 2-(4-methylphenyl)-indolizine which may be due to organism genome difference.

The distribution, metabolic, and excretion properties of 2-(4-methylphenyl)-indolizine and 2-p-nitrobenzoyl-1, 3, 5-tribenzyl- α -d-ribose were assessed through the ADMET parameters based on the pkCSM thresholds of drug ability. The computed partition coefficient (log P) which defines the respective lipophilicity of the compounds showed that 2-(4-methylphenyl)-indolizine had relative good lipophilicity as the log P is not greater than 5. This shows that it could have good absorption due to its maintain

fitting balance maintenance between the hydrophilicity and lipophilicity suggesting good system maintenance of appropriate ligand concentration. However, 2-p-nitrobenzoyl-1, 3, 5-tribenzyl- α -d-ribose could have poor oral absorption and increased risk of promiscuity and toxicity as the log P is greater than 5 (Pajouhesh and Lenz, 2005; Hughes *et al.*, 2008). Moreover, the observed lipophilicity correlates negatively to water solubility and positively to intestinal absorption. The moderate level of the lipophilicity of 2-(4-methylphenyl)-indolizine could suggest it would have no negative effect on brain exposure as indicated by the probable effect brain-blood barrier and central nervous system permeation. 2-(4-methylphenyl)-indolizine showed a comparatively better drugability score than 2-p-nitrobenzoyl-1,3,5-tribenzyl- α -d-ribose. This could also be substantiated by the inhibitory potential of 2-p-nitrobenzoyl-1,3,5-tribenzyl- α -d-ribose on P-glycoprotein and hERG. The P-glycoprotein inhibition could impair the active transport of xenobiotics in the system. Additionally, impairment in the function hERG potassium channel through inhibition may result in delayed ventricular repolarisation which could lead to a severe disturbance in the normal cardiac rhythm (Wang *et al.*, 2012). The mutagenic properties computed through AMES toxicity showed the compounds are not mutagens. However, 2-p-nitrobenzoyl-1,3,5-tribenzyl- α -d-ribose was suggested to be a hepatotoxic compound. The hepatotoxic effect of 2-p-nitrobenzoyl-1, 3, 5-tribenzyl- α -d-ribose could be related to its lipophilicity and enhanced retention within the membranes and binding to non-desired protein.

5. Conclusion

This study identified 2-(4-methylphenyl)-indolizine and 2-p-nitrobenzoyl-1,3,5-tribenzyl- α -d-ribose as potential inhibitors of PARs. They could perchance function additively in modulating the signaling event, leading to clot formation. Their therapeutic use as anti-thrombotic factors may lead to a beneficial solution against coronary atherothrombotic diseases. Further investigations on the potential toxicity of the phytocompounds through various laboratory studies are recommended.

Conflict of Interest

The authors declare that they have no conflict of interests.

Ethical Approval

This article does not contain any studies with human participants or animals performed by any of the authors.

Funding Source

This research did not receive any specific grant from funding agencies in the public, commercial, or not-for-profit sectors.

Acknowledgements

The support provided by the staff of Department Biochemistry, College of Natural and Applied Sciences,

McPherson University, Seriki Sotayo, Ogun State, Nigeria is well appreciated.

References

- Abdel-Mawgoud BM, Khedr FG and Mohammed EI. 2019. Phenolic Compounds, Antioxidant and Antibacterial Activities of *Rhus flexicaulis*. *Joradn J Biol Sci*. **12**(1):17-21
- Adams MN, Ramachandran R, Yau MK, Suen JY, Fairlie DP, Hollenberg MD and Hooper JD. 2011. Structure, function and pathophysiology of protease activated receptors. *Pharmacol Ther*. **130**: 248-282.
- Ashorobi D and Fernandez R. 2019. **Thrombosis**. Treasure Island StartPearls publishing.
- Azevedo AP, Farias JC, Costa GC, Ferreira SC, Aragão-Filho WC, Sousa PR, Pinheiro MT, Maciel MC, Silva LA, Lopes AS, Barroqueiro ES, Borges MO, Guerra RN and Nascimento FR. 2007. Anti-thrombotic effect of chronic oral treatment with *Orbignya phalerata* Mart. *J Ethnopharmacology*. **111**(1): 155-159.
- Bah A, Chen Z, Bush-Pelc LA, Mathews FS and Di Cera E. 2007. Crystal structures of murine thrombin in complex with the extracellular fragments of murine protease-activated receptors PAR3 and PAR4. *PNAS*. **104**(28): 11603-11608.
- Banji A, Goodluck B, Oluchi O and Stephen F. 2018. Antimicrobial and Antioxidant Activities of Crude Methanol Extract and Fractions of *Andrographis paniculata* leaf (Family: Acanthaceae) (Burm. f.) Wall. Ex Nees. *Jordan J Biol Sci*. **11**(1): 23-30
- Berman HM, Westbrook J, Feng Z, Gilliland G, Bhat TN, Weissig H, Shindyalov IN and Bourne PE. 2000. The Protein Data Bank. *Nucleic Acids Res*. **28**(1): 235-242.
- Bolton EE, Tiessen PA and Bryant SH. 2008. PubChem: integrated platform of small molecules and biological activities. *Annu Rep Comput Chem*. **4**: 217-241.
- Charlotte M, Julia N, Danby S, Katie RZ, Leo N, Kami P, Badr K, Sven S, Niklas B, Danny K, Thomas JS, Ludwig TW, Joachim P, Markus M, Michael J, Walter D, Tom A, Franz-Josef N, Anthony HG, Jurrien MB, Michael L and Konstantin S. 2019. Eosinophil-platelet interactions promote atherosclerosis and stabilize thrombosis with eosinophil extracellular traps. *Blood*. **134**(21): 1859-1872.
- Coughlin SR. 2000. Thrombin signalling and protease-activated receptors. *Nature*. **407**: 258-64.
- Covic L, Gresser AL, Talavera J, Swift S and Kuliopulos A 2002. Activation and inhibition of G protein-coupled receptors by cell-penetrating membrane-tethered peptides. *Proc Natl Acad Sci*. **99**: 643-648.
- da Silva L and Ferreira RM. 2015. Novel Anticoagulants in Non-Valvular Atrial Fibrillation: An Evidence- Based Analysis. *Evidence Based Medicine and Practice*. **1**(1): 101-102.
- De Caterina R, Husted S, Wallentin L, Andreotti F, Arnesen H, Bachmann F, Baigent C, Huber K, Jespersen J, Kristensen SD, Lip GY, Morais J, Rasmussen LH, Siegbahn A, Verheugt FW and Weitz JI. 2013. Vitamin K antagonists in heart disease: current status and perspectives (Section III). Position paper of the ESC Working Group on Thrombosis-Task Force on Anticoagulants in Heart Disease. *Thromb Haemost*. **110**(6): 1087-107.
- Douglas EVP, Tom LB and David BA. 2015. pkCSM: predicting small-molecule pharmacokinetic properties using graph-based signatures. *J Medicinal Chemistry*. **58**(9): 4066-4072.
- Elokely KM and Doerkse RJ. 2013. Docking challenge: protein sampling and molecular docking performance. *J Chemical Information and Modeling*. **53**(8): 1934-1945.

- Evangelista JH, De Vera MJ, Garcia RS, Joven MG, Nerosa MJA and Solidum JN. 2012. Preliminary Assessment of In vitro Anticoagulant Activity vs. Heparin 1,000IU and Cytotoxicity of Selected Philippine Medicinal Plants. *Int J Chemical and Environmental Engineering*. **3**(6): 371-376.
- French SL and Hamilton JR. 2016. Protease-activated receptor 4: From structure to function and back again. *Br. J. Pharmacol*, **173**: 2952-2965.
- Go CEO and Mariposque JRA. 2018. **Hematological effects of pineapple *Ananas comosus* L. Merr peel extracts and commercial Bromelain on male albino mice (*Mus musculus*)**. Herdin Record#: R07-USC-18082909314518
- Gryka RJ, Buckley LF and Anderson SM. 2017. Vorapaxar: The current role and future directions of a novel protease-activated receptor antagonist for risk reduction in atherosclerotic disease. *Drugs R D*. **17**: 65-72
- Herrington W, Lacey B, Sherliker P, Armitage J and Lewington S. 2016. Epidemiology of Atherosclerosis and the Potential to Reduce the Global Burden of Atherothrombotic Disease. *Circulation Res*. **118**(4): 535-546.
- Heuberger DM and Schuepbach RA. 2019. Protease-activated receptors (PARs): mechanisms of action and potential therapeutic modulators in PAR-driven inflammatory diseases. *Thrombosis J*. **17**(4): 1-24.
- Hollenberg MD and Compton SJ. 2002. International union of pharmacology. Proteinase-activated receptors. *Pharmacol Rev*. **54**: 203-217.
- Hughes JD, Blagg J, Price DA, Bailey S, Decrescenzo GA, Devraj RV, Ellsworth E, Fobian YM, Gibbs ME, Gilles RW, Greene N, Huang E, Krieger-Burke T, Loesel J, Wager T, Whiteley L and Zhang Y. 2008. Physicochemical drug properties associated with in vivo toxicological outcomes. *Bioorg Med Chem Lett*. **18**: 48725.
- Kim S, Chen J, Cheng T, Gindulyte A, He J, He S, Li Q, Shoemaker BA, Thiessen PA, Yu B, Zaslavsky L, Zhang J and Bolton EE. 2019. PubChem 2019 update: improved access to chemical data. *Nucleic acids Res*. **47**(1): 1102-1109.
- Ko HH, Hsieh HK, Liu CT, Lin CH, Teng CM and Lin CN. 2004. Structure-activity relationship studies on chalcone derivatives: The potent inhibition of platelet aggregation. *J Pharm Pharmacol*. **56**: 1333-7.
- Lau AJ, Toh DF, Chua TK, Pang YK, Woo SO and Koh HL. 2009. Antiplatelet and anticoagulant effects of *Panax notoginseng*: comparison of raw and steamed *Panax notoginseng* with *Panax ginseng* and *Panax quinquefolium*. *J Ethnopharmacology*. **125**(3): 380-386.
- Lee W, Ku SK and Bae JS. 2015. Antiplatelet, anticoagulant and profibrinolytic activities of baicalin. *Arch Pharm Res*. **38**: 893-903.
- Li T, Shen P, Liu W, Liu C, Liang R, Yan N, Chen J. 2014. Major polyphenolics in pineapple peels and their antioxidant interactions. *Int J Food Prop*. **17**, 1805-1817.
- Limjoco RP, Catalan MP and Aquino FC. 2014. Anticoagulant Activity of Pineapple (*Ananas comosus*) Extract on Human Blood Samples. *IAMURE Int J Sci Clin Lab*. **6**(1).
- Ma L, Perini R, McKnight W, Dickey M, Klein A, Hollenberg MD, Wallace JL (2005). Proteinase-activated receptors 1 and 4 counter-regulate endostatin and VEGF release from human platelets. *Proc Natl Acad Sci*. **102**: 216-220.
- Mahmud S, Samina A, Rahman MA, Aklima J, Akhter S, Merry SR, Jubair SMR, Dash R and Emran TB. 2015. Antithrombotic Effects of Five Organic Extracts of Bangladeshi Plants In Vitro and Mechanisms in In Silico Models. *Evidence-Based Compl Alt Med*. **782742**: 1-8.
- McCloskey SE, Gershanik JJ, Lertora JJ, White L and George WJ. 1986. Toxicity of benzyl alcohol in adult and neonatal mice. *J Pharm Sci*. **75**(7): 702-705.
- Mohd Nor NH, Othman F, Mohd Tohit ER and Md Noor S. 2016. Medicinal herbals with antiplatelet properties benefit in coronary atherothrombotic diseases. *Thrombosis*. 5952910.
- Mumaw MM, De La Fuente M, Arachiche A, Wahl JK and Nieman MT. 2015. Development and characterization of monoclonal antibodies against Protease Activated Receptor 4 (PAR4). *Thromb Res*. **135**: 1165-1171.
- Oso BJ, Oyewo EB and Oladiji AT. 2019. Influence of ethanolic extracts of dried fruit of *Xylopi aethiopic a* (Dunal) A. Rich on haematological and biochemical parameters in healthy Wistar rats. *Clin Phyt*. **5**: 9
- Pajouhesh H and Lenz GR. 2005. Medicinal chemical properties of successful central nervous system drugs. *Neuro RX*. **2**: 54153
- Rizvi SMD, Shakil S and Haneef M. 2013. A simple click by click protocol to perform docking: autodock 4.2 made easy for non-bioinformaticians. *EXCLI J*. **12**: 831-857.
- Shikha J, Dangi CBS, Kaur M, Singh H, Peter J and Kosta S. 2014. Plants as anticoagulant and antithrombotic agents. *World J Pharm Res*. **3**(1): 4573-4585.
- Trott O and Olson AJ. 2010. AutoDock Vina: improving the speed and accuracy of docking with a new scoring function, efficient optimization and multithreading. *J Comput Chem*. **31**(2): 455-461.
- Vu TK, Wheaton VI, Hung DT, Charo I and Coughlin SR. 1991. Domains specifying thrombin-receptor interaction. *Nature*. **353**: 674-677
- Wang S, Li Y, Wang J, Chen L, Zhang L, Yu H and Hou T. 2012. ADMET evaluation in drug discovery. 12. Development of binary classification models for prediction of hERG potassium channel blockage. *Mol Pharm*. **9**(4): 996-1010.
- WHO (2017). "Cardiovascular Diseases report". Accessed April 4, 2020.
- Wong PC, Seiffert D, Bird JE, Watson CA, Bostwick JS, Giancarli M, Allegretto N, Hua J, Harden D and Guay J. 2017. Blockade of protease-activated receptor-4 (PAR4) provides robust antithrombotic activity with low bleeding. *Sci Transl Med*. **9**: eaaf5294.
- Yoo H, Ku SK, Lee W, Kwak S, Baek YD, Min BW, Jeong G and Bae J. 2014. Antiplatelet, anticoagulant, and profibrinolytic activities of *cudraticus xanthone* A. *Arch Pharm Res*. **37**: 1069-1078.

Analysis of APXs and HSPs genes responsible to respond to heat stress in tomato plants cultivated in Central Sulawesi

Astija^{1,*}, Musdalifah Nurdin¹, Syech Zainal¹

Biology Education Study Program, Faculty of Teacher Training and Education, Tadulako University

Received: May 14, 2020; Revised: September 11, 2020; Accepted: September 12, 2020

Abstract

Central Sulawesi is one of the areas in Indonesia located on the equator which has hot temperatures. This temperature greatly affects the growth of tomato plants. However, this plant can grow well. It is not yet known what crucial genes are responsible for the heat tolerance. Therefore, a study was conducted to reveal some genes; *APX1*, *APX2*, *HSP17.4*, *HSP17.6*, *HSP70*, *HSP90*. Those genes are responsible for the heat tolerance. The study was carried out by the PCR method to determine the *APX1*, *APX2*, *HSP17.4*, *HSP17.6*, *HSP70*, *HSP90* genes. The DNA of these genes was isolated from the leaves and then cDNA was made to determine gene expression at the transcription level. Also, a qualitative analysis based on the NCBI search was used to describe the structure and function of each observed gene. The results showed that the genes; *APX1*, *APX2*, *HSP17.4*, *HSP17.6*, *HSP70*, *HSP90* were expressed in different levels in tomato plants from the Central Sulawesi region. Thus, it can be suggested that these genes have an important role in heat tolerance in the tomato plant.

Keywords: tomato, tolerant, genes, temperature, heat, temperature

1. Introduction

Tomato is one of the important food plants on earth because it functions as one of the buffering needs for humans and animals. To increase the growth and production of these plants, appropriate environmental factors are needed. Two factors including internal and external factors are very influential to limit or increase the growth and production of the tomato plants. Internal factors such as the ABA factor regulate plant growth through PGPR (Plant growth-promoting rhizobacteria) regulation (Porcel *et al.*, 2014), sugar molecules regulate metabolism and growth in wheat plants (Martínez-Barajas *et al.*, 2011). External factors also affect plant growth and development; for example, red light increases the growth and flowering of tomato plants (Cao *et al.*, 2016), fertilization using humic acid increases the productivity and quality of tomato plants (Yildirim, 2007). Meanwhile, increasing temperatures decrease biomass and metabolic activity of tomato plants (Rivero *et al.*, 2003). pH affects the absorption of nutrients in tomato plants (Wang *et al.*, 2000).

An increase in temperature results in a decrease in plant growth and development Giorno *et al.*, (2010). Furthermore, high temperatures inhibit the development of pollen, reduce pollen germination and pollen tube elongation (Astija, 2017; Firon *et al.*, 2006; Hedhly *et al.*, 2005). An important mechanism for how temperature affects the growth and development of plant cells is carried out by regulating the expression of genes (Wilson and Zang, 2009; Cordoba *et al.*, 2015). Lately, this mechanism has become an interesting concern that needs to be revealed. Disclosure of the mechanism of environmental

factors such as temperature regulating growth and development and productivity is clearly illustrated by Cabello *et al.*, (2014) through a cascade signal regulation mechanism that results in changes in stress, changes in hormones and changes in ROS signals. The result, changes in these signals will stimulate the modification of protein compounds such as enzymes from post-translational results (Huang and Xu, 2008; Baniwal *et al.*, 2004). If explored, these protein compounds or enzymes carry out activities to decipher specific compounds. The results of the enzyme activity can then affect its own activity or act as an inhibitor or even a back signal to stop the enzyme formation process (Baniwal *et al.*, 2004). Stopping enzyme productivity will inhibit the process of gene expression at the translation and transcription stages.

As for the temperature factor, many researchers have reported that temperature signals from outside will be transmitted to regulate metabolism. According to Pressman *et al.* (2012), temperature regulates growth of tomato plant through inhibition of sugar metabolism due to decreased activity of enzymes that play a role in carbohydrate metabolism. Temperature greatly influences changes in sugar metabolism and subsequently the molecules from the results of metabolism act as signals to regulate the expression of genes (Ponnu *et al.*, 2011). Later, Krasensky and Jonak (2012) revealed that temperature can reduce plant growth and productivity because it changes morphological and physiological adaptations through changes in gene expression. Also, a research conducted by Frank *et al.* (2009) had explained that temperature can increase the activity of HSPs protein (heat shock proteins). HSPs are proteins that play a role in responding to heat so that plants survive. These HSPs are

* Corresponding author e-mail: astijasurya@gmail.com.

produced from the expression of genes from the HSPs family. The results of studies have found many genes from this family such as *HSP17* (Rang *et al.*, 2011), *HSP60* (Sheoran *et al.*, 2007), *HSP70* (Ge *et al.*, 2011), *HSP90* (Astija, 2015). Genes from other families that also play a role in responding to heat stress are the peroxidase gene (APXs), for example genes belonging to the peroxidase family is widely studied being *APX1*, *APX2* (Astija, 2015).

Recently, the characteristics of the development of tomato plants in the vegetative phase have been studied (Astija and Musdalifah, 2018). Likewise, the development of reproduction in the development of pollen was investigated (Astija, 2017). Another thing that has been investigated is that many genes have been identified and proven to play a role in responding to heat stress in tomato plants, such as *HSP 17.4-CII*, *HSP 17.6-CII*, *HSP70*, *HSP90*, *APX1*, *APX2* genes (Bitra and Gerats, 2013). However, it is not known yet whether the genes are identified in tomato plant cultivated in Central Sulawesi Region. Therefore, those are identified their presences in the tomato plant. The existence of these genes was analyzed regarding the structure of nucleotides and their amino acids and the similarity between one another. All of these are to be used as candidates for important genes for crops in Central Sulawesi that have hot temperatures. Furthermore, this project can be used as a model of food crops suitable for cultivation in Central Sulawesi or to be developed into GMO crops that are resistant to heat.

2. Method

This study used a sample consisting of three leaf pieces of tomato plant each, originating from the Sidera Region. The sample was taken using "Pore Cut". Leaf sample was stored in the "Ice Box" for extract. The extraction process was conducted at the Biotechnology Laboratory of The University of Indonesia Education. The steps for extraction, gene identification by PCR and measurement of mRNA are described below.

2.1. Genomic DNA extraction and Genotypic determination of DNA using PCR

Genomic DNA was extracted from leaves. This was to verify and to determine the target genes. The procedure was done using CTAB (hexadecyltrimethylammonium bromide) as described by (Astija, 2017).

2.2. Expression assay of APXs and HSPs genes RNA extract

RNA was isolated from 5-10 mg of material/sample and work procedures were carried out following the instructions set out in the "Qiagen RNeasy Plant Mini Kit (50)". The total RNA concentration was measured by a spectrophotometer (NanoDrop 1000, Thermo scientific) on waves of 230nm, 260 nm, and 280 nm. A total of 1 µg of total RNA per sample was used for cDNA synthesis.

2.3. Synthesis of cDNA

cDNA synthesis was begun with RNA extraction. The extraction is purified by removing DNA contamination by

using DNase (Promega, Cat.M6101) by adding the following ingredients to the sample:

- 7 µL DEPC H₂O
- 1 µL RQ1 RNase-Free DNase 10X Reaction Buffer
- 1 µL RQ1 RNase-Free DNase (1 u / µL)

Then the solution was incubated at 25 °C for 15 minutes. Then 1 µL of 25 mM EDTA was added and incubated again at 65 °C for 10 minutes. A single cDNA chain was obtained from RNA synthesis by adding 1 µL oligo dT20 and 1 µL from 10 mM dNTP carried out at 65 °C for 5 minutes. Reverse transcription (Reverse transcription) is continued by adding a solution consisting of:

- 4 µL 5X First-strand Buffer
- 1 µL 0.1 M DTT
- 1 µL of SuperScript TM III RT (200 units / µl)
- 1 µL RNase OUT TM recombinant RNase inhibitor (Cat. 10777-019, 40 units / µl)

Reverse transcription is carried out at 50 °C for 45 minutes and continued at 70 °C for 15 minutes. The formed cDNA was confirmed using PCR using a reaction solution consisting of:

- 6.54 µL H₂O
- 1.05 µL 50 mM MgCl₂
- 1.5 µL 10XPCR Buffer (200 mM Tris-HCl pH 8.4, 500 mM KCl)
- 0.06 µL Taq DNA polymerase (5 u / µL)
- 0.75 µL SYBGreen (1: 20000)
- 0.6 µL 5 mM dNTP Mix
- 0.375 µL FPrimer gene
- 0.375 µL RPrimer gene
- 3.75 µL cDNA

The cycle conditions that are treated include: initial denaturation at 94 °C for 10 minutes, denaturation at 94 °C for 20 seconds, attachment at 60 °C for 20 seconds, elongation at 72 °C for 20 seconds, final elongation at 68 °C for 1 second, and hold 16. cDNA is doubled by 45 cycles. The product is separated and measured by electrophoresis on 1.5% agarose gel stained with ethidium bromide. Electrophoresis was set at 100v for 15 minutes. The gel is visualized with the GelDoc XR Imaging System (BIORAD) and Quantity One Version 4.6.3 software.

2.4. Analysis of gene expression using Real-Time PCR

Quantitative PCR is performed using the same reaction mixture used in PCR as described above with the addition of primers from certain target genes including *APX1*, *APX2*, *HSP17.4*, *HSP17.6*, *HSP70*, *HSP90*. The primers are designed using PRIMERE-BLAST software presented in table 1. The size of the resulting amplicon is then linked to the tomato sequence. Gene expression data were calculated with Corbett Rotor-Gene 6000. All amplifications were normalized to the CAC (Clathrin Adapter complex) gene.

Data from the average value of gene expression obtained from three technical replications and 3 plant biological replications were analyzed by one-way ANOVA from software XL-Stat 2018 or JMP V11.

Table 1. Primers of the *APX1*, *APX2*, *HSP17.4*, *HSP17.6*, *HSP70*, *HSP90* genes designed using PRIMER-BLAST software

Gene name	Product size (bp)	Accession number (http://www.ncbi.nlm.nih.gov/)	Primer sequence (5' – 3')	TM (°C)
<i>HSP 17.4-CII</i>	103	NM001247201	FP: ACTG TTCAGAAGCTGCCTCC	59.9
			RP: TCAAAACAGAGCAAGAAAACAGAGT	59.6
<i>HSP 17.6-CII</i>	151	NM001246984	FP: TCCTGAGCCAAAGAAACCCA	59.2
			RP: ACAGACGTGAAAACATAGCAGAA	58.6
<i>HSP70</i>	201	NM001247562	FP: AGTGTAAGCAATGGCCGGA	59.9
			RP: GGGCGACCTGATTCTTAGCA	59.8
<i>HSP90</i>	205	NM001247510	FP: TCAGCAATTCTCCGATGCTCT	60.1
			RP: TCCTTGGTTCCTGACCTTGC	59.9
<i>APX1</i>	288	NM001247853.1	FP: CACCTACTAGAACCCTTCTCTTCT	59.2
			RP: AGAGTGCCATGCAAGACGGA	61.8
<i>APX2</i>	170	NM001247859	FP: TGCTGCGGATGAAGATGCC	60.8
			RP: AACGATATCCAACAATCCAGCA	58.7

3. Result

Based on tracing through the NCBI website, we found that the *APX1* gene was located on chromosome 6 with the nucleotide position from 181740 to 185143 bp. The *APX1* gene has 1117 pairs of nucleotides that were translated into a protein with 250 amino acids. Similarly, the *APX2* gene was located in the same chromosome with the *APX1* gene, but the nucleotide was located from 170150 to 173336 bp. The *APX2* gene consists of 1197 pairs of the nucleotides and produces proteins with 250 amino acid numbers.

For the *HSP*s group, we observed that the *HSP17.4* gene was located on chromosome 8 in which the nucleotide locus from 50976534 to 50977196 bp, or the number of nucleotides was 663 nitrogen base pairs. The *HSP17.4* gene expresses a protein with a total of 155 amino acids. Meanwhile, the *HSP17.6* gene was found on chromosome 6 at locus 47701113 to 47701916 bp so that it had 822 nucleotide pairs of nitrogen bases. The *HSP17.6* gene expresses a protein composed of 154 amino acids. Another *HSP*s is the *HSP70* gene that was found on chromosome 11 from 10036518 to 10040967 nucleotides or 1980 pairs of nitrogen bases. The gene can express a protein with 692 amino acids. The last *HSP* was the *HSP90* gene that was located at the same chromosome with *HSP17.6* but the location of the nucleotide was from 25893824 to 25897169 bp. The nucleotide sequence arranges a protein with 704 amino acids.

The *APX1*, *APX2*, *HSP17.4*, *HSP17.6*, *HSP70*, *HSP90* were then tested on samples of tomato plants cultivated in Central Sulawesi. The tests using PCR, it was found that DNA from the *APX1*, *APX2*, *HSP17.4*, *HSP17.6*, *HSP70*, *HSP90* genes were obtained as shown by the DNA band in Figure 1.

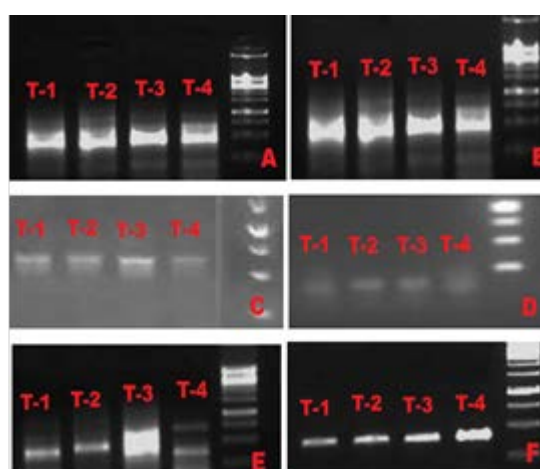


Figure 1. DNA from *APX1* (A), *APX2* (B), *HSP17.4* (C), *HSP17.6* (D), *HSP70* (E), *HSP90* (F) genes isolated from 4 tomato plants (T- 1, T-2, T-3, T-4) cultivated in Central Sulawesi.

Figure 1 shows that the four tomato plants cultivated by people in Central Sulawesi have genes that are responsible for heat tolerance including *APX1*, *APX2*, *HSP17.4*, *HSP17.6*, *HSP70*, *HSP90* genes. Furthermore, to find out whether the genes are expressed at the transcriptional stage in the form of mRNA, the gene expression testing is carried out by qPCR. In the cDNA testing phase, (unpublished data) the DNA bands were similar to the DNA bands in Figure 19.

The results of mRNA measurements via RT-qPCR of the six genes in all four plant samples are presented in Figure 2.

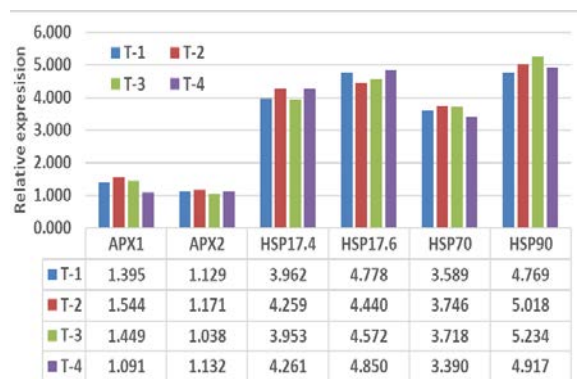


Figure 2. Expression of *APX1*, *APX2*, *HSP17.4*, *HSP17.6*, *HSP70*, *HSP90* genes from four samples of tomato plants (T-1, T-2, T-3, T-4) cultivated in Central Sulawesi. The expression of peroxidase genes (*APX1*, *APX2*) is lower than that of *HSPs* genes.

4. Discussion

Central Sulawesi, located in equatorial regions that have extreme temperatures, has an average daily temperature of 37 °C. Normally, plants that grow in areas with hot temperatures grow poorly as expressed by Krasensky and Jonak (2012) who reported that temperature can reduce plant growth and productivity because it changes morphological and physiological adaptations through changes in gene expression. However, different things happen in the Central Sulawesi, and tomato plants can grow and produce tomatoes properly. From the results of testing using the PCR method, it was found that tomato plants in the region have *APX1*, *APX2*, *HSP17.4*, *HSP17.6*, *HSP70*, *HSP90* genes. The six genes were identified based on the appearance of DNA bands through the electrophoresis process (Figure 1). DNA from all six genes was detected in all four plant samples from the region. Thus, it can be said that the DNAs are *APX1*, *APX2*, *HSP17.4*, *HSP17.6*, *HSP70*, *HSP90* genes.

DNA from the results obtained is convinced that the six genes are in tomato plants. The six genes have also previously been reported in other tomato plants (Sheoran *et al.*, 2007). Besides, from search results on the NCBI website, it was found that the six genes were also found. The interesting thing about the search results is that the two genes of the peroxidase group (*APXs*), *APX1*, and *APX2* are located in tandem in one chromosome, chromosome 6. These two genes have different nucleotide sequences and sequences (NCBI Website). The composition and sequence of the nucleotides of the two genes have a similarity rate of 93%.

Tomato plants from the Central Sulawesi can grow well because they not only have two peroxidase genes (*APXs*), *APX1* and *APX2*, but both of these genes have been transcribed into mRNA and translated into proteins. The results were based on reverse transcription that is mRNA is reversed back into DNA to obtain cDNA from both genes. Furthermore, measurement of the transcript results using RT-qPCR obtained relatively similar mRNA expressions between the *APX1* and *APX2* genes (Figure 2). The relative value of the mRNA expression obtained illustrates that both genes have the same amount of transcription results from two different DNAs but are located in one chromosome, namely chromosome 6. From the results of further searching, the expression of these two

genes does not stop until mRNA but the expression reaches a level of translation into protein. When comparing with relation to amino acids, the amino acids of the two genes have a slightly different arrangement of amino acids, which is a 96% similarity level (NCBI Website). Furthermore, the protein expressed from these two genes has reached post-transformation in the form of the enzyme ascorbic acid oxidase. The enzyme has been reported that an important substance that plays a role in oxidizing ascorbic acid to dehydroascorbic acid. Furthermore, dehydroascorbic acid is converted to 2,3-dico-1-gluconate acid. This is useful as a defense in responding to heat.

Tomato plants from the Central Sulawesi are also able to grow well because they have 4 genes responsible for responding to hot temperatures, including *HSP17.4*, *HSP17.6*, *HSP70*, and *HSP90* as shown by DNA bands from the four plants used as samples (Figure 1). These results indicate that tomato plants cultivated by people in the region have *HSPs* genes that play an important role in defending plants from heat. The role of *HSPs* in plant defense against heat has been widely reported (Wang *et al.*, 2000; Chauhan *et al.*, 2011; Al-Whaibi, 2011; Van Ooijen *et al.*, 2010; Giorno *et al.*, 2010; Baniwal *et al.*, 2004). The mechanism by which *HSPs* play an important role in responding to hot temperatures is still unclear. However, Al-Whaibi (2011) has suggested that hot temperatures cause shrinkage of protein structures. Circumstances will then cause the protein to become damaged or not functioning. This event does not occur if there is a protein from the expression of *HSPs*. *HSP* proteins will be associated to prevent structural proteins from causing damage.

The results of this research are that all four genes have been expressed in all four plants (Figure 2). The gene expression shown is an expression at the transcription stage, which is a copy of one of the DNA chains of the genes into mRNA. The mRNAs from all four genes from all four plants exhibit similar levels of expression (Figure 2). Once compared with the level of expression of peroxidase genes, *HSPs* genes have higher levels of expression. This means that all four *HSPs* genes play a greater role in the defense of heat in tomato plants in the region compared to both genes of peroxidase. No comparison has been reported between the two gene groups, *APXs* and *HSPs*. Therefore, the results of this study are important to follow up on the important role of these *HSPs* genes and other *HSPs* genes. Based on the results of this study, it is also possible that the expression of the four *HSPs* genes has been expressed at the translation stage. Unfortunately, this study did not assay the proteins from all four genes. However, the results of study based on tracing through the NCBI website obtained amino acids from proteins in the four genes (NCBI Website). The number of amino acids for *HSP17.4*, *HSP17.6*, *HSP70*, and *HSP90* can be shown in the NCBI Website. Two genes, *HSP17.6* and *HSP90*, are known to be located on the same chromosome which is chromosome 6. This also means one chromosome with the *APX1* and *APX2* genes, while the two *HSPs* genes, *HSP17.4* and *HSP70*, are located on different chromosomes, being on chromosomes 7 and 10 (NCBI Website). Thus, chromosome 6 is important in tomato plants because it contains four important genes for the defense of the plant

to heat stress. Based on alignment and phylogenetic using Clustal Omega of the four genes illustrated that *HSP17.4* and *HSP17.6* genes have a close relationship compared to the other genes. However, the two genes are located in a different chromosome in which *HSP17.6* gene is in chromosome 6 but *HSP17.4* is in chromosome 7. Thus, genes located on the same chromosome do not determine a relationship of the genes. In other words, the genes are independently expressed for certain responsibly.

5. Conclusion

The genes consisting of *APX1*, *APX2HSP17.4*, *HSP17.6*, *HSP70*, and *HSP90* are responsible genes for heat stress tolerance in tomato plants cultivated in Central Sulawesi in which those genes are expressed with different level of mRNA.

Acknowledgments

We thank FKIP Tadulako University for supporting and providing the facilities for the research.

References

- Astija. 2015. Regulation of pollen germination and pollen tube elongation and response to heat stress by cell wall invertase. PhD dissertation, The University of Newcastle, New South Well Australia.
- Astija. 2017. Pollen Germination and Pollen Tube Elongation of Tomato (*Lycopersicon esculentum* L.) Regulated by Cell Wall Invertase through Sucrose Hydrolysis. *J Agr Sci Technol.* **7**:393–400.
- Astija and Musdalifah. 2018. Effect of Watering on Tomato (*Solanum lycopersicum* L.) Plant Growth. *Int J Sci Res.* **7**(2): 194–196.
- Baniwal SK, Kapil B, Kwan YC, Markus F, Arnab G, Sachin K, Shravan K M, Lutz N, Markus P, Klaus-Dieter S, Joanna T, Christian W, Dirk Z, and Pascal VK. 2004. Heat stress response in plants: a complex game with chaperones and more than twenty heat stress transcription factors. *J Biosci.* **29**(4):471–487.
- Bitá C and Gerats T. 2013. Plant tolerance to high temperature in a changing environment: scientific fundamentals and production of heat stress-tolerant crops. *Front plant sci.* **4**: 273.
- Cabello JV, Lodeyro A F and Zurbriggen MD. 2014. Novel perspectives for the engineering of abiotic stress tolerance in plants. *Cur Opinion Biotechnol.* **26**: 62–70.
- Cao K, Cui L, Ye L, Zhou X, Bao E, Zhao H and Zou Z. 2016. Effects of Red Light Night Break Treatment on Growth and Flowering of Tomato Plants. *Front Plant Sci.* **7**: 1–8.
- Cordoba E, Denise LA-Z, Alma FH-B, Maricela R-V and Patricia L. 2015. Sugar regulation of sugar transporter protein 1 (STP1) expression in *Arabidopsis thaliana*. *J Exp Bot.* **66**(1): 147–169.
- Firon N, Shaked R, Peet MM, Pharr DM, Zamski E, Rosenfeld K, Althan L and Pressman E. 2006. Pollen grains of heat tolerant tomato cultivars retain higher carbohydrate concentration under heat stress conditions. *Scientia Hort.* **109**(3): 212–217.
- Frank G, Pressman E, Ophir L, Shaked R, Freedman M, Shen S and Firon N. 2009. Transcriptional profiling of maturing tomato (*Solanum lycopersicum* L.) microspores reveals the involvement of heat shock proteins, ROS scavengers, hormones, and sugars in the heat stress response. *J Exp Bot.* **60**(13): 3891–3908.
- Ge W, Song Y, Zhang C, Zhang Y, Alma L, Burlingame and Guo Y. 2011. Proteomic analyses of apoplastic proteins from germinating *Arabidopsis thaliana* pollen. *Biochimica et Biophysica Acta.* **1814**(12): 1964–1973.
- Giorno F, Wolter-Arts M, Grillo S, Scharf K-D, Vriezen WH and Mariani C. 2010. Developmental and heat stress-regulated expression of HsfA2 and small heat shock proteins in tomato anthers. *J Exp Bot.* **61**(2): 453–462.
- Hedhly A, Hormaza JI and Herrero M. 2005. The effect of temperature on pollen germination, pollen tube growth, and stigmatic receptivity in peach. *Plant Biol.* **7**(5): 476–483.
- Huang B and Xu C. 2008. Identification and characterization of proteins associated with plant tolerance to heat stress. *J Integ Plant Biol.* **50**(10): 1230–1237.
- Krasensky J and Jonak C. 2012. Drought, salt, and temperature stress-induced metabolic rearrangements and regulatory networks. *J Exp Bot.* **63**(4): 1593–1608.
- Martinez-Barajas E, Delatte T, Schlupepmann H, de Jong GJ, Somsen GW, Nunes CA, Primavesi LF, Coello P, Rowan AC, Mitchell and Paul MJ. 2011. Wheat grain development is characterized by remarkable trehalose 6-phosphate accumulation pregrain filling: tissue distribution and relationship to SNF1-related protein kinase1 activity. *Plant physiol.* **156**(1): 373–81.
- Ponnu J, Wahl V and Schmid M. 2011. Trehalose-6-phosphate: connecting plant metabolism and development. *Front plant sci.* **2**: 70.
- Porcel R, Zamarreño AM, García-Mina JM and Aroca R. 2014. Involvement of plant endogenous ABA in *Bacillus megaterium* PGPR activity in tomato plants. *BMC plant biol.* **14**(1): 2–12.
- Pressman E, Shaked R, Shen S, Altahan L and Firon N. 2012. Variations in carbohydrate content and sucrose-metabolizing enzymes in Tomato. *American J Plant Sci.* **03**(02): 252–260.
- Rang ZW, Jagadishb SVK, Zhoua QM, Craufurdc PQ, Heuer S. 2011. Effect of high temperature and water stress on pollen germination and spikelet fertility in rice. *Env Exp Bot.* **70**(1): 58–65.
- Rivero RM, Sánchez E, Ruiz JM and Romero L. 2003. Influence of temperature on biomass, iron metabolism and some related bioindicators in tomato and watermelon plants. *J Plant Physiol.* **160**(9): 1065–1071.
- Sheoran IS, Ross ARS, Olson DJH and Sawhney1 VK. 2007. Proteomic analysis of tomato (*Lycopersicon esculentum*) pollen. *J Exp Bot.* **58**(13): 3525–35.
- Wang HF, Takematsu N and Ambe S. 2000. Effects of soil acidity on the uptake of trace elements in soybean and tomato plants. *Appl Rad Isot.* **52**(4): 803–811.
- Wilson ZA and Zang. 2009. From arabidopsis to rice: Pathways in pollen development. *J Exp Bot.* **60**(5): 1479–1492.
- Yildirim E. 2007. Foliar and soil fertilization of humic acid affect productivity and quality of tomato. *Acta Agriculturae Scandinavica.* **57**(2): 182–186.

Effect of Garlic, Vitamin C, Vitamin E–Selenium against Bioaccumulated Organolead-Induced Cellular Injury in Liver and Spleen of Albino Rats: Pilot Study

Ziad Shraideh^{1,*}, Darwish Badran², Ahmed Alzbeede³, Duaa Alqattan⁴, Areej Alzbeede⁵, Kholoud Frieihat⁴

¹Department of Biological Sciences, School of Science, The University of Jordan, Amman, Jordan; ²Department of Anatomy and Histology, School of Medicine, The University of Jordan, Amman, Jordan; ³Department of Medical Laboratory Science, College of Science, Komar University of Science and Technology, Sulaymaniyah, Kurdistan Region, Iraq; ⁴Department of Pathology, Microbiology and Forensic Medicine, School of Medicine, The University of Jordan, Amman, Jordan; ⁵Department of Medical Laboratory Analysis, Cihan University Sulaimaniya, Sulaymaniyah, Kurdistan Region, Iraq

Received: April 4, 2020; Revised: August 13, 2020; Accepted: August 31, 2020

Abstract

Exposure to Lead (Pb²⁺) in its organic and inorganic forms is known to have deleterious effects on the health of individuals. Several studies showed that these effects are due to accumulation in vital organs and induction of oxidative stress.

This study examines the possibility of three different antioxidant substances (Aqueous garlic extract, Vitamin C and Vitamin E – Selenium) to act as chelating agents against organolead toxicity (lead acetate) by decreasing its accumulation in liver and spleen.

To achieve this purpose, forty-eight adult male albino rats were divided into eight equal groups; Group I: Control received normal water, Group II: received lead acetate (100 mg/kg/day; i.p), Group III: received garlic (100 mg/kg; orally), Group IV: received Lead (100 mg/kg/day; i.p) + Garlic (100 mg/kg; orally), Group V: received Vitamin C (100 mg/kg; orally), Group VI: received Lead (100 mg/kg/day; i.p) + Vitamin C (100 mg/kg; orally). Group VII: received Vitamin E (100 mg/kg; orally) + Selenium (0.5 mg/kg; orally) and Group VIII: received Lead (100 mg/kg/day; i.p) + Vitamin E (100 mg/kg; orally) + Selenium (0.5 mg/kg; orally). The experiments were performed over four consecutive weeks, after which blood was withdrawn from rats by heart puncture and animals were sacrificed by cervical dislocation; the liver and spleen were removed to quantify their lead content by Flame Atomic Absorption Spectroscopy (FAAS).

Analysis of the serum showed that lead acetate has significantly elevated the activity of the ALT, AST, and LDH compared to the control group, and the three selected antioxidant substances were able to minimize the activity of these enzymes significantly in comparison with lead acetate group. In addition, the results from the FAAS showed that lead concentration has significantly increased in the liver and spleen of the lead acetate group compared to the control group, and that treatment with antioxidants was not effective in reducing that effect.

It is concluded that the selected antioxidants had an ameliorative effect against the hepatotoxicity induced by lead acetate but could not be considered the suitable heavy metal chelator to overcome the bioaccumulated lead in the vital organs.

Keywords: Antioxidants, Bioaccumulation, Biochemical Markers, Lead Acetate, Metal Chelators

1. Introduction

The body of organisms is constructed with blend of different elements. Some chemical elements like carbon, hydrogen, oxygen and nitrogen are able to produce biological macromolecules which are vital for biochemical reactions and physiological functions in the organisms, and these organic biomolecules are the fundamental components of carbohydrates, protein, lipid and nucleic acid (Jonsson *et al.* 2017). Other groups of elements are minerals, or essential trace elements are important with certain daily magnitudes, any deficiency in these required elements could develop disorders that could lead to death. A group of chemical elements like gold, silver, lead,

mercury, arsenic and cadmium are not essential at all, and the presence of these toxic metals in the body induce oxidative stress status (Johnston *et al.* 2010; Maraqa *et al.* 2015; Matović *et al.* 2015).

Lead is considered a heavy metal that causes toxicity by bioaccumulation in organs and interfering with cellular signals and metabolic reactions (Brochin *et al.* 2014; Gillis *et al.* 2012; Xia *et al.* 2018). Environmental and occupational exposures are considered the significant sources of lead toxicity to humans, as the human body could absorb inorganic lead following inhalation, oral, and dermal administration (Abadin *et al.* 2007).

The prolonged exposures to lead, especially to the occupationally exposed workers resulted in decreasing the activity of delta-aminolevulinic acid dehydratase (δ -

* Corresponding author e-mail: zshraideh@ju.edu.jo.

ALAD; a key enzyme in heme biosynthesis (Shraideh *et al.* 2019) and influence the expression of calmodulin-related genes (Hussain, 2018). Also, these exposures had adverse effects on erythrocyte morphology by surface deformability and invaginations on plasma membrane (Shraideh *et al.* 2019). In addition, lead exposure induces oxidative stress by elevation of the level of superoxide dismutase (SOD), hydrogen peroxide (H₂O₂), lipid peroxidation, and decline the parameters of reduced glutathione (GSH) and total antioxidant capacity (TAOC) (Shraideh *et al.* 2018).

Antioxidants are chemical molecules mostly extracted from medicinal plants. These molecules are considered safe and effective treatment strategy to attenuate the oxidative stress status induced by hazardous environmental factors (Forni *et al.* 2019). Garlic contains chemicals with antioxidant activities; its extract contains four main classes of antioxidant compounds (alliin, allicin, allyl cysteine, and allyl disulfide), and these chemicals exhibit different patterns of free radicals scavenging capacity to protect cellular components from radical damage (Chung, 2006). In vitro studies using a cell-free system, it was reported that aged garlic extract has more inhibition capacity toward advanced glycation end products, higher total phenol content, more potent antioxidant properties compared to fresh garlic extract (Elosta *et al.* 2017).

L-Ascorbic acid; commonly known as vitamin C, is a water-soluble molecule with molecular formula C₆H₈O₆, and a molecular weight 176.12 g/mol. Vitamin C has a useful role as a potent antioxidant by scavenging oxygen and nitrogen oxide species such as superoxide radical ion, hydrogen peroxide, the hydroxyl radical, and singlet oxygen (Paciolla *et al.* 2019). Besides, it could conjugate with reactive lipid peroxide products such as malondialdehyde and 4-hydroxynonenal to neutralize the cellular stress condition. Thus, vitamin C has vital processes in the protection of cellular components from free radical-induced damage (Barja *et al.* 2014).

α-Tocopherol, commonly called vitamin E, has a chemical formula C₂₉H₅₀O₂, and a molecular weight of 430.7 g/mol. This molecule has low solubility in water due to its hydrophobic repulsion; it has been reported that vitamin E is a fat-soluble compound. Vitamin E has antioxidant activity by reducing the oxidative stress biomarkers like malondialdehyde content, protein carbonyl content, nitric oxide, xanthine oxidase, and increasing the activity of superoxide dismutase and catalase enzymes in rats with oxidative damage caused by formaldehyde (Gulec *et al.* 2006). The same study has reported that vitamin E has anti-inflammatory and anti-hepatotoxic properties (Gulec *et al.* 2006). Vitamin E has a protective effect against genotoxicity by decreasing sister chromatid exchanges and chromosomal aberration in cultured human lymphocytes with chromosomal damage induced by a platinum-based anticancer drug called oxaliplatin (Alqudah *et al.* 2018).

Selenium (Se) is a necessary trace element in the human body. Human body contains multiple families of selenium-dependent proteins such as glutathione peroxidases, thioredoxin reductases, thioredoxin-glutathione reductase, iodothyronine deiodinases, selenophosphate synthetase selenoprotein H, I, K, M, N, O, P, T, V, and W (Zoidis *et al.* 2018). These proteins are

antioxidant enzymes with anti-inflammatory, anti-viral, and chemopreventive properties (Zoidis *et al.* 2018).

The main points of this study are to evaluate the gastric administration of garlic extract, vitamin C and vitamin E-Se against the hepatotoxicity induced by organolead (lead acetate) throughout measuring of some liver enzymes, and to illustrate the ability of these selected antioxidants for chelating the bioaccumulated organolead in liver and spleen using albino rats as animal model.

2. Materials and Methods

2.1. Chemicals

Lead acetate trihydrate, vitamin C, vitamin E, and selenium, were purchased from (Sigma, USA). Nitric acid (HNO₃), hydrogen peroxide (H₂O₂), and lead standard solution were purchased from (Scharlau, Spain). All analytical grade solutions were prepared using deionized water.

2.2. Animals

This study was ethically approved by the scientific committee in the School of Science at the University of Jordan. Forty-eight adult male albino rats (6-8 weeks old, weight 140 ± 25 g) were purchased from (Animal household / The University of Jordan). These rats were randomly divided into 8 groups, each containing 6 rats. The volume of chemicals administered to rats was 0.5 ml intraperitoneal injection via insulin syringes for lead acetate, and 0.5 ml oral administration via plastic gastric tube for antioxidant solutions. Aqueous garlic extract was prepared according to (Belguith *et al.* 2010) considering the concentration of administration dose needed for this study.

Group I (Ctrl): Control receives normal water.

Group II (Pb): Lead (Pb) as lead acetate (100 mg/kg/day; i.p).

Group III (Gar): Garlic (100 mg/kg; orally).

Group IV (Pb + Gar): Lead (100 mg/kg/day; i.p) + Garlic (100 mg/kg; orally).

Group V (Vit C): Vitamin C (100 mg/kg; orally).

Group VI (Pb + Vit C): Lead (100 mg/kg/day; i.p) + Vitamin C (100 mg/kg; orally).

Group VII (Vit E-Se): Vitamin E (100 mg/kg; orally) + Selenium (0.5 mg/kg; orally).

Group VIII (Pb + Vit E-Se): Lead (100 mg/kg/day; i.p) + Vitamin E (100 mg/kg; orally) + Selenium (0.5 mg/kg; orally).

This experiment was operated and repeated daily on all animal groups for four consecutive weeks. Rats were kept in well-ventilated room at room temperature, 12/12-hours day/night period with open access to standard animal chow as feeding material with *ad libitum* for drinking water. Adult male rats were preferred to be chosen in this study because it is generally known that the adult female of mammals, including rats, could periodically enter in menstruation cycle, which could result in rhythmic fluctuations during measurement for the activity of liver enzymes.

2.3. Blood and organs collection

After four weeks, blood was withdrawn from rats by heart puncture using 3 ml disposable syringes under general ether anesthesia. Blood was left to clot in room temperature under dark condition for 1 hour and then centrifuged at 3800 rpm for 10 minutes to obtain serum for enzymatic liver tests. The liver and spleen were isolated from rats after cervical dislocation. These samples were washed with phosphate buffered saline (PBS; 0.1 M, pH 7.2) and stored in freezer at -20 °C until lead analysis.

2.4. Biochemical tests

The activity of three liver enzymes were estimated include; alanine aminotransferase (ALT), aspartate aminotransferase (AST), and lactate dehydrogenase (LDH). The chemicals kits were purchased from (BioSystem, Spain), and the process of measuring the enzymatic activity was operated according to manufacturer instructions using the serum. These colorimetric assays were performed using 1 cm light path UV-VIS single beam spectrophotometer (LI-295, Lasany, India) at wavelength (λ) of 340 nm.

2.5. Quantification of lead concentration in selected organs

All analytical grade solutions were prepared using deionized water. Glassware and tools were washed and rinsed with deionized water, dried in the oven, soaked in 10% HNO₃ for 24 hours prior to use. This method was operated according to (Massadeh³ *et al.* 2007) with some modifications. Five grams of liver or spleen were weighed and dried in the oven at 105 °C for 18 hours. A weight of 0.2 grams from each dried sample was transferred into Teflon digestion vessel and allowed for acid digestion using a mixture of 5 ml of HNO₃ with few drops of 30% v/v H₂O₂ at 80 °C for 18 hours with continuous shaking. After cooling, 5 ml of 2% HNO₃ were added to the digested extract, filtered with Whatman filter paper, and then the residue filtrate was completed to 25 ml using 2% HCO₃. This residue was directly used to determine the concentration of lead in the sample. Determination of lead in liver and spleen samples was performed using flame atomic absorption spectroscopy (SpectrAA 250 Plus, Varian, Australia). The hollow-cathode lamp of lead (Pb⁺²) was operated at $\lambda = 283.3$ nm with a spectral bandpass of 0.7 nm.

2.6. Accuracy and precision of flame atomic absorption spectroscopy

Every running of 12 samples was repeated with control blank and testing several quality control (QC) solutions. The results were within 5% of the QC values. For every sample, two replicates were taken, and each replicate was read three times and the mean reading was used for calculation purposes. In addition, concentrations of (0.1, 0.5, 1, 2, 5, 10, 15, 20 ppm) of lead standard solution prepared from stock solution were used for calibration check along with blank solution for calculating the concentration of the sample by linear calibration curve. The method was optimized and partially validated in the Department of Chemistry at The University of Jordan, Amman, Jordan.

2.7. Statistical analysis

The results from data were inserted, analyzed, and designed in figures and table using statistical software (GraphPad Prism 7.0.0, IBM, USA). The concentration differences among the groups for each individual test was tested using one-way ANOVA followed by Tukey *post hoc* considering p values <0.05, <0.01, <0.001 as significant, highly significant, extreme significant, respectively. Graph bars in figures were represent mean \pm SEM. The standard error of the mean (SEM) seems to be more accurate to be used during the interpretation of our data since each treatment group contains 6 rats only. Linear calibration curve was designed for calculating the unknown concentrations in samples and the linear regression data for each organ in this study was illustrated in the table to observe the accuracy and precision of the obtained results from flame atomic absorption spectroscopy.

3. Results

3.1. Enzymatic activity of alanine aminotransferase (ALT)

The results of this enzyme activity are illustrated in Figure (1A). The mean values of Gar, Vit C, and Vit E-Se groups for ALT did not show any significant differences against the control group at P<0.05. Pb group showed increasing in ALT activity with extremely significant result against Ctrl group at P<0.001. In addition, it had high significant result against Gar, Vit C, and Vit E-Se at P<0.001, and high significant result against Vit E-Se group at P<0.01. The groups of Pb+Gar, Pb+Vit C, and Pb+Vit E-Se did not show any significant differences against the Ctrl group at P<0.05. Also, Pb+Gar and Pb+Vit E-Se groups showed no significant differences against Pb group. Besides, Pb+Vit C group showed high significant result against Pb group at P<0.01. The inter-group comparison Gar vs. Pb+Gar; Vit C vs. Pb+Vit C; Vit E-Se vs. Pb+Vit E-Se) did not show any significant differences at P<0.05.

3.2. Enzymatic activity of alanine aminotransferase (AST)

The results of this enzyme are illustrated in Figure (1B). The mean values for Gar, Vit C, and Vit E-Se groups did not show any significant differences against the control group at P<0.05. Pb group showed about two folds increase in AST activity compared to control with extreme significant different at P<0.001. Also, Pb group showed different significant results against Vit C, Vit E-Se and Gar at P<0.05, P<0.01, and P<0.001, respectively. The result for Pb+Gar group showed no significant difference against control. Furthermore, Pb+Vit C and Pb+Vit E-Se group showed extreme significant differences against control group at P<0.001. The results of AST enzyme for Pb+Gar group showed a significant difference against Pb group at P<0.05. Besides, Pb+Vit C and Pb+Vit E-Se groups did not show any significant differences against Pb group at P<0.05. The inter-group comparison (Gar vs. Pb+Gar; Vit C vs. Pb+Vit C; Vit E-Se vs. Pb+Vit E-Se) showed no significant difference between Gar and Pb+Gar, extreme significant difference between Vit C and Pb+Vit C at P<0.001, and high significant between Vit E-Se and Pb+Vit E-Se at P<0.01.

3.3. Enzymatic activity of lactate dehydrogenase (LDH)

The results of this enzyme are illustrated in Figure 1(C). The mean values of LDH enzyme for Gar, Vit C, and Vit E-Se groups did not show any significant differences against the control group at $P < 0.05$. Pb group showed elevated level of LDH activity up to six folds compared to control group with extreme significant result at $P < 0.001$. In addition, Gar, Vit C, and Vit E-Se groups had extreme differences against Pb group at $P < 0.001$. Pb+Gar group showed about two folds increasing in the enzymatic level of LDH compared to control and Gar groups with extreme significant results at $P < 0.001$, and three folds decreasing compared to Pb group with extreme significant difference at $P < 0.001$. Also, Pb+Vit C group showed extreme significant differences against control, Pb, and Vit C groups at $P < 0.001$. The enzymatic activity of LDH in Pb+Vit E-Se group illustrated extreme significant changes against control, Pb, and Vit E-Se at $P < 0.001$.

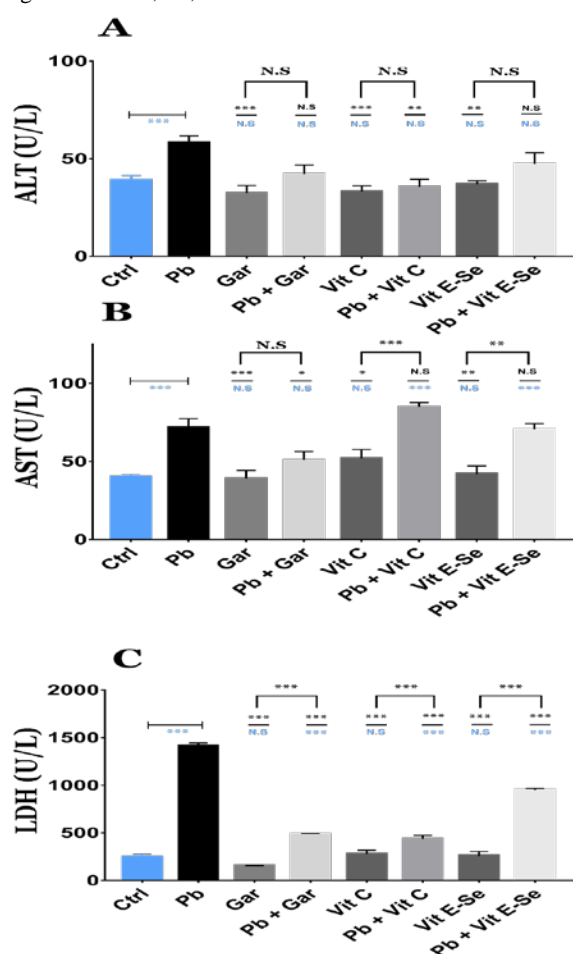


Figure 1. Graph bars represent the effect of aqueous garlic extract (Gar), Vitamin C (Vit C), and Vitamin E-Selenium (Vit E-Se) on some hepatic enzymes in parallel with the toxicity induced by the organolead (Pb). Figure (1-A) for Alanine aminotransferase (ALT); Figure (1-B) for Aspartate aminotransferase (AST); Figure (1-C) for Lactate dehydrogenase (LDH). Each bar represents the mean value of that treatment group to the biochemical test, and the error bar represents the standard error of mean value. Significant values against the control group written in blue color, whereas the significant values against the organolead group written in black color. The black-capped lines represent the significance between the inter-groups. Signs of (*, **, ***) represent $P < 0.05$, $P < 0.01$, $P < 0.001$, respectively. N.S. represents no significance when $P \geq 0.05$.

3.4. Concentrations of bioaccumulated organolead in liver

The data of linear regression for quantification of lead in liver samples is illustrated in (Table 1). Pb group showed about 17 folds increasing compared to Ctrl with statistically extreme significant difference at $P < 0.001$ (Figure 2A & C). Groups of Pb+Gar, Pb+Vit C, and Pb+Vit E-Se did not show any significant differences against Pb group but showed extreme significant differences against Ctrl group at $P < 0.001$, except Pb+Vit C at $P < 0.01$.

3.5. Concentrations of bioaccumulated organolead in spleen

The data of linear regression for quantification of lead in spleen samples is illustrated in (Table 1). Pb group showed about 16 folds increasing compared to control with statistically highly significant difference at $P < 0.01$ (Figure 2B & D). In addition, the groups of Pb+Gar, Pb+Vit C, and Pb+Vit E-Se did not show any significant differences against Pb group at $P < 0.05$. Besides, these three treatment groups showed highly significant differences against control group at $P < 0.01$.

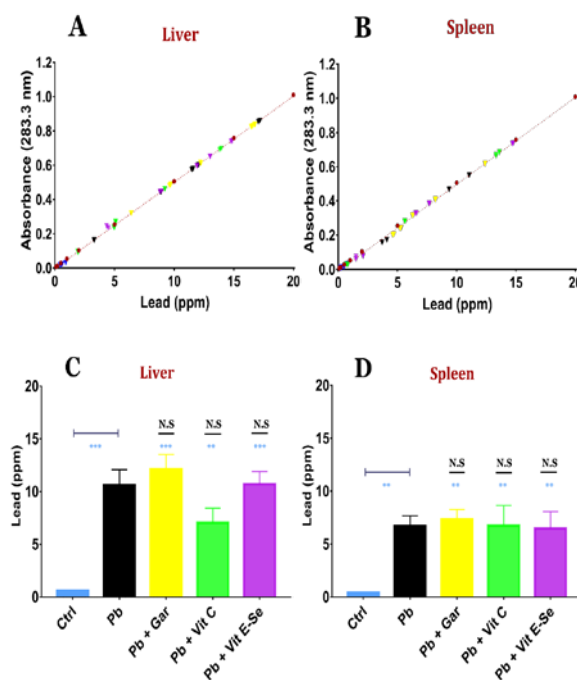


Figure 2. Results of flame atomic absorption spectroscopy (FAAS) for the concentrations of lead (Pb 2+) in the liver and spleen organs of rats after four weeks of organolead (lead acetate) exposures. Figure 2 (A-B) illustrates the absorbance generated from the liver (A) and spleen (B) of different experimental groups. Each colored inverted triangle dot represents the result of lead concentration of a single sample. The blue triangles for the control group; black for organolead; yellow for organolead + aqueous garlic extract; green for organolead + vitamin C; violet for organolead + vitamin E-Selenium. The red circular dots represent the lead standards, and the red line represents the slope of the linear calibration curve for calculating the results (absorbance versus concentration). Figure 2 (C-D) represents the bar graphs that indicates the mean \pm SEM of lead concentration per group in liver (C) and spleen (D). Significant values against the control group written in blue color, whereas the significant values against the organolead group written in black color. Signs of (*, **, ***) represent $P < 0.05$, $P < 0.01$, $P < 0.001$, respectively. N.S. represents no significance when $P \geq 0.05$.

Table 1. Linear regression data from the statistical software for the results of lead concentration in liver and spleen obtained by flame atomic absorption spectroscopy (FAAS).

Information of linear regression data		Liver	Spleen
Best-fit values ± SE	Slope	0.05029 ± 0.0001514	0.05083 ± 0.0002836
	Y-intercept	-0.001902 ± 0.001485	-0.01091 ± 0.002138
	X-intercept	0.03782	0.2147
	1/slope	19.88	19.67
95% Confidence Intervals	Slope	0.04999 to 0.05059	0.05026 to 0.0514
	Y-intercept	-0.004876 to 0.001072	-0.01519 to -0.006629
	X-intercept	-0.02141 to 0.09649	0.1315 to 0.2965
Goodness of Fit and Equation	R square	0.9995	0.9982
	Sy.x	0.006792	0.01095
	Equation	Y = 0.05029*X - 0.001902	Y = 0.05083*X - 0.01091
Is slope significantly non-zero?	F	110295	32113
	DFn, DFd	1, 57	1, 57
	P value	<0.0001	<0.0001
	Deviation from zero?	Significant	Significant

Note: This table was obtained from the statistical software after inserting the absorbance of standard concentrations and the absorbance from the samples of different experimental groups in this study by using flame atomic absorption spectroscopy. This linear regression data could deliver perception about precision and accuracy for this technique to quantify the concentrations of lead in the selected vital organs.

4. Discussion

Prolonged exposure to lead in its organic and inorganic forms induces cellular toxicity on different organisms, and this fact is consistent with the results of this study. This study showed that organolead (lead acetate) elevates liver enzymes activity of ALT, AST, and LDH. Also, quantification of lead concentration in the liver and spleen showed significant increases in the bioaccumulated metallic lead more in the liver than spleen. A previous study showed that sub-lethal exposure to lead acetate increases the enzymatic activity of ALT, AST, LDH, alkaline phosphatase, inhibition of cholinesterase activity and fluctuates the hematological and hormonal parameters in male wistar rats (Ibrahim *et al.* 2012). Also, lead acetate could induce histopathological alterations in the liver of rats which involve blood congestion with dilation of central veins and portal triads, in addition to hepatic vacuolization and degeneration (Albishtue *et al.* 2020).

This study showed that aqueous garlic extract, vitamin C and vitamin E-Se have ameliorative effect against the hepatotoxicity induced by lead acetate exposure by decreasing the activity of ALT, AST and LDH. A previous study showed that both the aqueous garlic extract and vitamin E elevate epididymal sperm count, increase the percentage of sperm motility and viability, enhance some oxidative stress biomarkers and increase the concentration of testosterone and luteinizing hormones in rats exposed to lead acetate (Asadpour *et al.* 2013). It was reported that high levels of ascorbic acid supplementation will reduce lead-induced toxic effects by slightly increasing RBCs count, hematocrit, hemoglobin, and decrease the elevation of liver enzymes in juvenile rockfish *Sebastes schlegelii* (Kim *et al.* 2017).

The second part of this study was performed to evaluate the ability of the three selected antioxidants to chelate the bioaccumulation lead in liver and spleen of the experimental animals. The results of our findings showed that these antioxidants were inactive to achieve this purpose and could not decrease the high lead accumulation in the selected organs in this study, with an exception for vitamin C that showed partial chelating ability in the liver, but not in the spleen.

Ascorbic acid showed an ameliorative effect against the toxicity of heavy metals by reducing the accumulated level of cadmium and mercury and lowering the levels of creatinine, urea, uric acid, and cystatin C protein in kidneys of heavy metals exposed rabbits (Ali *et al.* 2019). Another study stated that aqueous garlic extract could decrease the accumulated lead in different organs such as liver, kidney, heart, spleen, red blood cells in Balb/c mice exposed to 1 ppm of lead (II) nitrate $Pb(NO_3)_2$ (Massadeh *et al.* 2007), this finding is not consistent with our findings due to differences in chemical structure and dosage concentration of lead compound. A recent study illustrated that vitamin C and E significantly decreases the bioaccumulation heavy metals like lead acetate, cadmium chloride, and mercuric chloride in liver, gills, muscle, and plasma of carp fish (Sahiti *et al.* 2020).

The use of lead chelation therapies such as dimercaprol, edetate calcium disodium, and succimer is considered a controversial topic with the recommendation of their uptake in case of critical purpose, taking into consideration the concern from their potential risk of adverse drug events and lead remobilization inside human body (Gracia and Snodgrass, 2007). A recent study has suggested new therapeutic strategies against heavy metal poisoning by mixing metal chelators with antioxidants to improve excretion of heavy metal bioaccumulation and

reduce oxidative stress, which leads to restoring cell viability and inhibiting apoptosis (Kim *et al.* 2019).

5. Conclusion

The findings of this study suggest that aqueous garlic extract, vitamin C, vitamin E-Se could be considered active compounds to reduce the hepatotoxicity induced by lead acetate, but fail to chelate the bioaccumulated organolead in the liver and the spleen in albino rats.

Acknowledgement

The authors acknowledge the financial support of the Deanship of Scientific Research / The University of Jordan.

Conflict of interest

Authors declare that no conflict of interest was associated with this work.

References

- Abadin H, Ashizawa A, Stevens YW, Lladós F, Diamond G, Sage G, Citra M, Quinones A, Bosch SJ and Swartz SG. 2007. **Toxicological Profile for Lead**, first ed. Agency of Toxic Substances and Disease Registry, Atlanta.
- Albishtue A, Almhanna H, Yimer N, Zakaria M, Haron A and Almhanawi B. (2020). Effect of edible bird's nest supplement on hepato-renal histomorphology of rats exposed to lead acetate toxicity. *Jordan J Biol Sci.* **13(2)**: 213-218.
- Ali S, Hussain S, Khan R, Mumtaz S, Ashraf N, Andleeb S, ... and Ulhaq M. (2019). Renal toxicity of heavy metals (cadmium and mercury) and their amelioration with ascorbic acid in rabbits. *Environ Sci Pollut Res Int.* **26(4)**: 3909-3920.
- Alqudah MA, Al-Ashwal FY, Alzoubi KH, Alkhatatbeh M and Khabour O. (2018). Vitamin E protects human lymphocytes from genotoxicity induced by oxaliplatin. *Drug Chem Toxicol.* **41(3)**: 281-286.
- Asadpour R, Azari M, Hejazi M, Tayefi H and Zabolli N. (2013). Protective effects of garlic aqueous extract (*Allium sativum*), vitamin E, and N-acetylcysteine on reproductive quality of male rats exposed to lead. *Vet Res Forum.* **4(4)**: 251-257.
- Barja G, López-Torres M, Pérez-Campo R, Rojas C, Cadenas S, Prat J and Pamplona R. (1994). Dietary vitamin C decreases endogenous protein oxidative damage, malondialdehyde, and lipid peroxidation and maintains fatty acid unsaturation in the guinea pig liver. *Free Radic Biol Med.* **17(2)**: 105-115.
- Belguith H, Kthiri F, Chati A, Sofah AA, Hamida JB and Landoulsi A. (2010). Study of the effect of aqueous garlic extract (*Allium sativum*) on some *Salmonella* serovars isolates. *Emir J Food Agr.* **22(3)**: 189-206.
- Brochin R, Leone S, Phillips D, Shepard N, Zisa D and Angerio, A. (2014). The cellular effect of lead poisoning and its clinical picture. *GUJHS.* **5(2)**: 1-7.
- Chung LY. (2006). The antioxidant properties of garlic compounds: allyl cysteine, alliin, allicin, and allyl disulfide. *J Med Food.* **9(2)**: 205-213.
- Elosta A, Slevin M, Rahman K and Ahmed N. (2017). Aged garlic has more potent antiglycation and antioxidant properties compared to fresh garlic extract in vitro. *Sci Rep.* **7**: 39613.
- Forni C, Facchiano F, Bartoli M, Pieretti S, Facchiano A, D'Arcangelo D, ... and Tabolacci C. (2019). Beneficial role of phytochemicals on oxidative stress and age-related diseases. *Biomed Res Int.* **2019**: 8748253.
- Gillis BS, Arbieva Z and Gavin IM. (2012). Analysis of lead toxicity in human cells. *BMC Genomics.* **13**: 344.
- Gracia RC, Snodgrass WR. (2007). Lead toxicity and chelation therapy. *Am J Health Syst Pharm.* **64(1)**: 45-53.
- Gulec M, Gurel A and Armutcu F. (2006). Vitamin E protects against oxidative damage caused by formaldehyde in the liver and plasma of rats. *Mol Cell Biochem.* **290(1-2)**: 61-67.
- Hussain AH. (2018). Influence of lead exposure in the expression of calmodulin-related genes: a preliminary study on workers working in industry of batteries, in Iraq. *Baghdad Sci J.* **15(2)**: 145-149.
- Ibrahim NM, Eweis EA, El-Beltagi HS and Abdel-Mobdy YE. (2012). Effect of lead acetate toxicity on experimental male albino rat. *Asian Pac J Trop Biomed.* **2(1)**: 41-46.
- Johnston HJ, Hutchison G, Christensen FM, Peters S, Hankin S and Stone V. (2010). A review of the in vivo and in vitro toxicity of silver and gold particulates: particle attributes and biological mechanisms responsible for the observed toxicity. *Crit Rev Toxicol.* **40(4)**, 328-346.
- Jonsson AL, Roberts MA, Kiappes JL and Scott KA. (2017). Essential chemistry for biochemists. *Essays Biochem.* **61(4)**: 401-427.
- Kim JH, Oh CW and Kang JC. (2017). Antioxidant responses, neurotoxicity, and metallothionein gene expression in juvenile Korean rockfish *Sebastes schlegelii* under dietary lead exposure. *J Aquat Anim Health.* **29(2)**: 112-119.
- Kim JJ, Kim YS and Kumar V. (2019). Heavy metal toxicity: an update of chelating therapeutic strategies. *J Trace Elem Med Biol.* **54**: 226-231.
- Maraqa AD, Naik RR, Shraideh ZA and Shakya AK. (2015). Effect of mercuric chloride (HgCl₂) on cytoplasmic shuttle streaming, morphology and structure of the plasmodial slime mold: *Physarum polycephalum*. *Fresenius Environ Bull.* **24(12)**: 4567-4573.
- Massadeh^a AM, Al-Safi SA, Momani IF, Al-Mahmoud M and Alkofahi, AS. (2007). Analysis of cadmium and lead in mice organs. *Biol Trace Elem Res.* **115(2)**: 157-167.
- Massadeh^b AM, Al-Safi SA, Momani IF, Alomary AA, Jaradat QM and Alkofahi AS. (2007). Garlic (*Allium sativum* L.) as a potential antidote for cadmium and lead intoxication: cadmium and lead distribution and analysis in different mice organs. *Biol Trace Elem Res.* **120(1-3)**: 227-234.
- Matović V, Buha A, Đukić-Čosić D and Bulat Z. (2015). Insight into the oxidative stress induced by lead and/or cadmium in blood, liver and kidneys. *Food Chem Toxicol.* **78**: 130-140.
- Paciolla C, Fortunato S, Dipierro N, Paradiso A, De Leonardi S, Mastropasqua L and de Pinto, MC. (2019). Vitamin C in plants: from functions to biofortification. *Antioxidants.* **8(11)**: 519.
- Sahiti H, Bislimi K, Rexhepi A and Dalo E. (2020). Metal accumulation and effect of vitamin c and e in accumulated heavy metals in different tissues in common carp (*Cyprinus carpio*) treated with heavy metals. *Pol J Environ Stud.* **29(1)**: 799-805.
- Shraideh Z, Badran D, Hunaiti A and Battah A. (2018). Association between occupational lead exposure and plasma levels of selected oxidative stress related parameters in Jordanian automobile workers. *IJOMEH.* **31(4)**: 517-525.
- Shraideh ZA, Badran DH, Hunaiti, AA and Battah, A. (2019). Delta-Aminolevulinic acid dehydratase inhibition and RBC abnormalities in relation to blood lead among selected Jordanian workers. *Jordan J Biol Sci.* **12(2)**: 237-241.
- Xia J, Jin C, Pan Z, Sun L, Fu Z and Jin Y. (2018). Chronic exposure to low concentrations of lead induces metabolic disorder and dysbiosis of the gut microbiota in mice. *Sci Total Environ.* **631**: 439-448.
- Zoidis E, Seremelis I, Kontopoulos N and Danezis GP. (2018). Selenium-dependent antioxidant enzymes: Actions and properties of selenoproteins. *Antioxidants.* **7(5)**: 66.

The Antioxidant Activity of Kelor (*Moringa oleifera* Lam.) Leaves Based on Drying Method

Devi Dwi Siskawardani^{1,*}, Sri Winarsih¹ and Khwunta Khawwee²

¹Department of Food Technology, Faculty of Agriculture and Animal Science, University of Muhammadiyah Malang, Jl. Raya Tlogomas No 246, Malang 65144 Indonesia; ²Faculty of Natural Resources, Prince of Songkla University, Hat Yai Campus Songkhla 90110 Thailand

Received: Feb 20, 2021; Revised: March 29, 2020; Accepted April 15, 2021

Abstract

Food consumption consisting of high antioxidants could improve health conditions, and prevent cell damage caused by free radicals. *Moringa oleifera* Lam. comprised a lot of nutrition like essential vitamins, anti-inflammation, anti-aging, anti-bacteria, anti-diabetic, anti-hypertension, and antioxidants. The optimum antioxidant level depended on the thermal process such as drying. This research aimed to determine the effect of type and temperature of drying on the antioxidant of *M. oleifera* leaves. Nested with two factors, type (cabinet dryer and oven), and temperature (40 °C, 50 °C, and 60 °C) which replied three times were applied. The result indicated that antioxidant was decreased significantly with increasing drying temperature. The result showed that antioxidant, phenolic, and flavonoid content with cabinet dryer was higher than oven. The increasing temperatures tend to decrease flavonoid; it was proved with 60 °C was 0.54 mg g⁻¹ ± 0.035 mg g⁻¹. The best treatment was cabinet dryer 50 °C with the highest antioxidant 69.26 % ± 1.38 %, phenolic 1.17 mg g⁻¹ ± 0.051 mg g⁻¹, and flavonoid 1.41 mg g⁻¹ ± 0.168 mg g⁻¹.

Keywords: Flavonoid, Medicine plant, Phenolic, Radical prevention, Safe herbs.

1. Introduction

World Health Organization (WHO) admits herbal medicines as valuable and available resources for Primary Health Care. *M. oleifera* is a substantial food commodity, which has enormous attention as 'the tropics natural nutrition'. The leaves, fruit, flowers and immature pods commonly are used as a highly nutritive vegetable, and as the extracts, it is able to be effective antimicrobial (Özcan, 2020), particularly in India, Pakistan, Philippines, and several countries in Africa (Saini *et al.*, 2016; Suzauddula *et al.*, 2019).

M. oleifera is proven to have multi-system effects in the human body (Saini *et al.*, 2016); it becomes a famous herb in the community, but it is insufficient scientific evidence to explain the mechanism and validate its efficacy apparent uses. *M. oleifera* is rich in the simple sugar, rhamnose called glucosinolates and isothiocyanates (Suzauddula *et al.*, 2019). It also composed free radical inhibitor, like phenolic (phenolic acid, flavonoid, coumarin, quinone, tannin, and stilbenes), nitrogen (alkaloid, amine, B-alanine), vitamin, terpenoids (carotenoid), and another endogenous metabolites.

Previous studies proved that *M. oleifera* leaves contain β-carotene, vitamin C, protein, calcium and potassium that act as good natural antioxidants sources. Thus, it was able to increase the shelf-life of fat foods due to the presence of various types of antioxidant such as ascorbic acid, phenolic, flavonoids, and carotenoids (Suzauddula *et al.*, 2019). The high concentrations of ascorbic acid, oestrogenic and β-sitosterol, calcium, phosphorus,

vitamins A, B and C, riboflavin, α-tocopherol, folic acid, nicotinic acid, pyridoxine, β-carotene, protein, and in particular essential amino acids (methionine, cysteine, tryptophan and lysine) present in *M. oleifera* leaves made it a virtually ideal dietary supplement (Saini *et al.*, 2016; Suzauddula *et al.*, 2019).

There were several factors that affect the decreasing of antioxidant activity, such as increasing temperature and duration (Issa and Abd-Aljabar, 2013; Jiang *et al.*, 2017), extreme pH, and storage intervals (Issa and Abd-Aljabar, 2013). Therefore, optimum of drying temperature for *M. oleifera* is important to analyse. Drying refers to a process of water removed and decreasing of herbs moisture content, which aimed to prevent microbial and enzymatic activity, consequently product preservation for extend shelf life (dos Reis *et al.*, 2015; Kamaruddin *et al.*, 2020; Suwati *et al.*, 2021). The weight and volume reduction of plant will give positive consequences for distribution and storage. Nowadays, consumers are more concerned about healthy lifestyle, the demands for natural and safe herbs are tend to increase. Nevertheless, it was very little known about the *M. oleifera* leaves phytochemical components based on different drying methods and temperature. Therefore, this research aimed to determine the effect of drying process (method and temperature) on antioxidant activity, total phenolic, flavonoids content, and colour of *M. oleifera* leaves.

2. Materials and Method

M. oleifera leaves was harvested from the Temas village, Batu City, East Java, Indonesia that resulted from

* Corresponding author e-mail: devi@umm.ac.id.

directly picking of the tree, and treated on the same day. Drying equipment that was used consisted of cabinet dryer and oven. Supporting equipment used include blenders, desiccators, glassware, erlenmeyer, digital scales, wrapping plastics, cups, filter paper, and sieves (100 mesh). Nested design was applied with factor consisted of type (cabinet dryer and oven) and temperature (40 °C, 50 °C, and 60 °C) of drying.

Firstly, fresh *M. oleifera* leaves was sorted, washed, dried for controlling raw material used sun drying (T= 38 °C about 72 h), sieged, filtered used 100 mesh, then followed by parameter analysis. The parameters tested for raw materials were water content, ash content, protein, fat, fiber content, vitamin C, and antioxidants and colour followed AOAC International (Latimer, 2019).

Fresh Moringa leaves used were dark green, furthermore were washed using running water and separated from the stalks, then spread on a drying pan. The Moringa leaves were dried as treatment using a cabinet dryer and oven with a temperature of 40 °C to 60 °C for 24 h. Then powdered using a blender, sieved used 100 mesh, and followed by parameter analysis consisted antioxidants (DPPH), phenolic (Folin-Ciocalteu reagent which has been diluted with water (1:10 v/v) and 4 mL Na₂CO₃ 1M), flavonoid, and colour. The data obtained was tested using ANOVA (Analysis of Variance) and DMRT.

2.1. Determination of Total Flavonoid Content

Total flavonoid content was determined by aluminium chloride colorimetric assay adapted from Sembiring *et al.* (2018) with modification. Quercetin in concentration (30, 40, 50, 60, 70, 80, 90, 100) µg mL⁻¹ were prepared in 96 % ethanol. 50 µL of extracts (1 mg mL⁻¹) was added to 10 µL of 10 % the aluminium chloride, followed by 150 µL of 96 % ethanol. 10 µL of 1 M sodium acetate was blended to the mixture in a 96 well plate. All reagents were mixed and incubated for 40 min at room temperature protected from light. The absorbance was measured at 415 nm Spectrophotomètre.

2.2. Determination of Total Phenolic Content

The total phenolic content was based on the 96-well microplate Folin–Ciocalteu method adapted from Sembiring *et al.* (2018) with some modifications. A total of 25 µL of the diluted extract of *M. oleifera* was mixed with 100 µL of 1:4 diluted Folin–Ciocalteu reagent and shaken for 60 s in a flat-bottom 96-well microplate, then was left for 240 s and 75 µL of sodium carbonate solution (100 g L⁻¹) were added. The mixture was shaken at medium continuous speed for 1 min. After 2 h at room temperature, the absorbance was measured at 765 nm using Spectrophotomètre. Gallic acid dilutions (10 mg L⁻¹ to 200 mg L⁻¹) were used as standards for calibration.

2.3. Determination of Antioxidant Activity

Test was conducted in a 96-well plate according to Zahratunnisa *et al.* (2017) with slight modification. 20 µL extracts solution in different concentrations (100 mg L⁻¹, 500 mg L⁻¹, 1 000 mg L⁻¹, 1 500 mg L⁻¹) and 180 µL of DPPH solution 0.147 mM were added to each well. After 30 min incubation at room temperature in dark room, absorbance was read at 517 nm using Spectrophotomètre. Methanol was used as blank.

3. Result and Discussion

3.1. Raw *M. oleifera* Properties

Analysis of raw materials included water content, ash content, protein, fat, fiber, vitamin C, and antioxidants (Table 1). It showed that there were differences between the results of analysis and literature. The water content of *M. oleifera* leaf flour was 6.96 % and higher than literature (6.64 %). It due to the drying process that causes water content in material to evaporate. During drying, there is movement of water along with volatile substances. The purpose of the drying process was to reduce the moisture content, as a result material becomes more durable, reducing the volume for convenience of storage. Losses incurred during the drying process are changes in physicochemical properties and decreasing in the material quality.

Table 1. *M.oleifera* Leaf Flour Properties

Parameter	Analysis	Literature
Water Content (%)	6.96	6.64
Ash Content (%)	9.13	11.67
Protein (%)	23.17	23.37
Fat (%)	6.94	6.74
Fiber (%)	3.09	3.67
Vitamin C (mg100 g ⁻¹)	13.58	17.3
Antioxidant (%)	28.2	20

Noted: literature (Kurniawati *et al.*, 2018)

The ash content of *M. oleifera* leaf flour amounted to 9.13 %, and lower than literature 11.67 %. The increasing temperature of drying process, followed by increasing the ash content in the leaves. It is caused of water content in the leaves, which is evaporated become higher, as the result more minerals left in the material. The ash content described *M. oleifera* mineral levels, and it was potential of source essential element such as sulphur (S), magnesium (Mg), potassium (K), (Al Juhaimi *et al.*, 2017). Protein content was 23.17 % and in accordance to Al Juhaimi *et al.* (2016) that *M. oleifera* leaves have a high crude protein content up to 25 %, also contain tannins, saponins, and alkaloids (Suzauddula *et al.*, 2019). While fat content were higher about 6.94 %. This caused by differences in variety, climate, soil fertility and harvest age (Suzauddula *et al.*, 2019). Vitamin C was 13.58 mg 100 g⁻¹, it is probably due to the effect of heat on the leaves when doing bleaching with hot water. Vitamin C is easily dissolved in water. The antioxidant levels of *M. oleifera* leaf flour amounted to 43.61 %, and higher than literature. This is close related to the high temperatures that can cause some antioxidant compounds damaged (Rababah *et al.*, 2015).

3.2. Antioxidant activity of dried *M. oleifera* leaves

The drying temperature gave very significant effect ($P \leq 1$ %) on antioxidants activity, and phenolic of *M. oleifera* leaves. DPPH assay is a simple, acceptable and most widely used technique to evaluate the radical scavenging potency of plant extracts (its absorption spectrum at 515 nm to 528 nm) when it accepts a free radical species (Chithiraikumar *et al.*, 2017). The factors of decreasing antioxidant activity were increasing

temperature, extreme pH, and storage (Issa and Abd-Aljabar, 2013). The antioxidant activity was high loss in oven drying than cabinet dryer. Intense thermal process also might cause significant loss in antioxidant (Jiang *et al.*, 2017), it showed by the lowest antioxidant activity was $28.05 \pm 1.54 \%$ at oven drying 60°C (Table 2). There was found naturally in plants as well as deactivate enzymes and degrade phytochemicals (Teixeira *et al.*, 2014). The decreasing of antioxidant activities has also been correlated to Maillard- type antioxidants declined generation and accumulation.

Several literature reported there were linear correlation of antioxidant with phenolic and flavonoid content. The decreasing antioxidant levels due to the drying process also showed in the papaya leaves commodity (*Carica papaya* L.), tomatoes (*Solanum lycopersicum* L.) and ginger (*Zingiber officinale* Roscoe.) this is caused by during the drying process, loss of macromolecules such as polyphenols occurred, which was associated with the temperature and the length of time (Annegowda *et al.*, 2014 ; Gümüşay *et al.*, 2015; Yap *et al.*, 2020). Research on spearmint leaves also showed a similar downward trend based on differences in drying methods (cabinet, freeze and oven dryer) which resulted in the deactivation of degradative enzymes such as polyphenol oxidase, so as to degrade phenolic compounds (Orphanides *et al.*, 2013; Wojdylo *et al.*, 2019).

3.3. Phenolic content of dried *M. oleifera* leaves

Phenolic compounds are good electron donors that substituted with hydroxyl groups on the aromatic ring, which could directly contribute to antioxidant action (Aryal *et al.*, 2019). The phenolic compound of cabinet dryer was higher than oven treatments and tend to enhance with increasing temperature of drying (Table 2). It was shown by the highest phenolic compound was cabinet dryer with 60°C treatments about $2.75 \text{ mg g}^{-1} \pm 0.046 \text{ mg g}^{-1}$ This result was consistent with experiment in Mediterranean herbs, that drying at 40°C rapidly inactive polyphenol oxidase which caused by enzymatic processes (Nistor *et al.*, 2017; Rababah *et al.*, 2015; Udomkun *et al.*, 2015).

The drying process did not immediately deactivate degraded enzyme, it was able to degrade phenolic compounds before the sample was completely dry. The phenolic content might be responsible for the strength antioxidant activity. The increase also has been attributed to the improving phenylalanine ammonia-lyase activity (on mild heating). The key enzyme in the phenolic synthesis or to the increased extractability by solvents usage. In addition, the non-enzymatic inter-conversion between phenolic molecules and precursors of phenolic molecules availability might have contributed to increase in heating process.

3.4. Flavonoid content of dried *M. oleifera* leaves

Flavonoids are secondary metabolites with antioxidant activity, the potency of which depends on the number and position of free OH groups (Panche *et al.*, 2016). There is not significant effect of drying method and temperature on flavonoid content of *M. oleifera* leaves. Increasing drying temperature declined the flavonoid enzyme activity, which proved by the lowest was Oven with 60°C treatment with $0.54 \text{ mg g}^{-1} \pm 0.035 \text{ mg g}^{-1}$.

Drying might breakdown some phytochemicals (Wojdylo *et al.*, 2016), which affected cell wall integrity and caused some flavonoids component migration. In addition, the loss in flavonoids may be due to breakdown or leakage by chemical reactions includes oxygen, enzymes and light during drying process.

Several studies reported a linear correlation of antioxidant with phenolic and flavonoid content. The research in *Rhus flexicaulis* Baker described that high antioxidant activity might be attributed to the high phenolic and flavonoid content (Abdel-Mawgoud *et al.*, 2019).

Table 2. The effect of drying method and temperature to the *M. oleifera* leaves antioxidants, flavonoid and phenolic

Treatment	Antioxidant (%)	Phenolic (mg g ⁻¹)	Flavonoid (mg g ⁻¹)
Cabinet Dryer 40 °C	63.45 ± 1.43 c	1.92 ± 0.054 c	0.72 ± 0.071
Cabinet Dryer 50 °C	69.26 ± 1.38 c	1.17 ± 0.051 b	1.41 ± 0.168
Cabinet Dryer 60 °C	52.42 ± 2.51 b	2.75 ± 0.046 e	0.74 ± 0.056
Oven 60 °C	28.05 ± 1.54 a	2.56 ± 0.034 d	0.54 ± 0.035
Oven 50 °C	35.98 ± 1.36 a	1.03 ± 0.008 ab	1.82 ± 0.053
Oven 40 °C	46.51 ± 3.29 b	0.95 ± 0.029 a	1.31 ± 0.092

Note: The value followed by the same letter is not significantly different according to Duncan's Test $\alpha = 5 \%$

3.5. Colour

Colour is substantial choosing factor of product, mostly the acceptable of processed vegetables or fruits depend on attractive colour (dos Reis *et al.*, 2015; Sigurdson *et al.*, 2017). Based on Table 3, the decreasing level of colour in oven was higher than cabinet dryer method, while intense drying (high temperature) accelerated colour reduction. This result indicated that cabinet dryer with 40°C resulted in lighter colour. The drying affected changes in brightening, yellow, and appearance (Samoticha *et al.*, 2016). The drying method gave significant effect on lightness (L) ($P \leq 5 \%$) of leaves. Colour changes could be caused by chlorophyll pigments were reduced as the result of photo-oxidation reaction in the cells. In addition, there is a competition between peroxidase enzyme and chlorophylls (Chatatikun and Chiabchalard, 2013; Ramirez *et al.*, 2015 ; Vergara-Domínguez *et al.*, 2013), while the drying method and temperature gave very significant effect ($P \leq 1 \%$) on a colour of leaves. The trend of (a) values decreased in cabinet dryer, but increased in oven treatment with enhancing temperature. The (b) values indicated the height-browning index, the drying temperature gave significant effect ($P \leq 5 \%$) on b colour. The browning degree as well as temperature increased (Benlloch-Tinoco *et al.*, 2015; Udomkun *et al.*, 2015)

Table 3. The effect of drying type and temperature to the *M. oleifera* leaves colour

Treatment	L	a	b
Cabinet Dryer 40 °C	48.33±0.577a	6.13±0.058c	17.43±0.208c
Cabinet Dryer 50 °C	48.23±0.153a	6.33±0.058c	17±0.001bc
Cabinet Dryer 60 °C	48.20±0.173a	5.8±0.001c	16.47±0.451bc
Oven 60 °C	47.10±0.173b	1.47±0.351a	16.2±0.300b
Oven 50 °C	46.20±0.173b	2.73±0.058b	16.3±0.173bc
Oven 40 °C	46.40±0.361b	1.87±0.058a	14.43±0.404a

Noted: The value followed by the same letter is not significantly different according to Duncan's Test $\alpha=5\%$, (L = lightness; a = red/ green; b = yellow/blue)

4. Conclusion

Based on the test results, it can be concluded that *M. oleifera* leaves antioxidant of cabinet dryer was higher than oven. The treatment of cabinet dryer and temperature 50 °C showed the highest antioxidant about 69.26 % ± 1.38 %. The increasing temperature causes phenolic compounds and flavonoids decrease significantly. The best treatment is 50 °C cabinet dryer with the highest antioxidant activity 69.26 % ± 1.38 %, 1.17 mg g⁻¹ ± 0.051 mg g⁻¹ phenolic, and 1.41 mg g⁻¹ ± 0.168 mg g⁻¹ flavonoid. This treatment also in the second position of lightness 48.23 ± 0.153, and green 6.33 ± 0.058.

Acknowledgment

The authors are grateful to the Directorate of Research and Community Service (DPPM) of the University of Muhammadiyah Malang (UMM) funding number E.2.a/141/BAA-UMM/II/2019. We also thank the assistants of the Food Science and Technology Laboratory, Faculty of Agriculture and Animal Science, UMM for their support at all levels of experimentations.

References

- Abdel-Mawgoud M, Khedr FG and Mohammed EI. 2019. Phenolic compounds, antioxidant and antibacterial activities of *Rhus flexicaulis* Baker. *Jordan J Biol Sci.* **12**(1): 17–21
- AL Juhaimi F, Ghafoor K, Babiker EE, Matthaus B. and Özcan MM. 2016. The biochemical composition of the leaves and seeds meals of *moringa* species as non-conventional sources of nutrients. *J Food Biochem.* **44**(1):1-6
- AL Juhaimi F, Ghafoor K, Mohamed Ahmed IA, Babiker EE and Özcan MM. 2017. Comparative study of mineral and oxidative status of *Sonchus oleraceus*, *Moringa oleifera* and *Moringa peregrina* leaves. *Food Measure.* **11**(4): 1745–1751.
- Annegowda HV, Bhat R, Yeong KJ, Liong MT, Karim AA and Mansor S. 2014. Influence of drying treatments on polyphenolic contents and antioxidant properties of raw and ripe papaya (*Carica papaya* L.). *Int J Food Pro.*, **17**(2):283–292.
- Aryal S, Baniya MK, Danekhu K, Kunwar P, Gurung R and Koirala N. 2019. Total phenolic content, flavonoid content and antioxidant potential of wild vegetables from Western Nepal. *Plants.* **9**6:1–12.
- Benlloch-Tinoco M, Kaulmann A, Corte-Real J, Rodrigo D, Martínez-Navarrete N, and Bohn T. 2015. Chlorophylls and carotenoids of kiwifruit puree are affected similarly or less by

microwave than by conventional heat processing and storage. *Food Chem.* **187**:254–262.

Chatatikun M and Chiabchalard A. 2013. Phytochemical screening and free radical scavenging activities of orange baby carrot and carrot (*Daucus carota* Linn.) root crude extracts. *J Chem Pharm Res.* **5**(4): 97–102.

Chithiraikumar S, Gandhimathi S and Neelakantan M. 2017. Structural characterization, surface characteristics and non covalent interactions of a heterocyclic Schiff base: Evaluation of antioxidant potential by UV-visible spectroscopy and DFT. *J Mol Struct.* **1137**:569–580.

dos Reis LCR., de Oliveira VR, Hagen MEK, Jablonski A, Flores SH and de Oliveira Rios A. 2015. Carotenoids, flavonoids, chlorophylls, phenolic compounds and antioxidant activity in fresh and cooked Broccoli (*Brassica oleracea* var. Avenger) and cauliflower (*Brassica oleracea* var. Alphina F1). *LWT – Food Sci Technol.* **63**(1):177–183.

Gümüşay ÖA, Borazan AA, Ercal N and Demirkol O. 2015. Drying effects on the antioxidant properties of tomatoes and ginger. *Food Chem.* **173**: 156–162.

Kamaruddin A, Uyun AS, Soengeng R, Suherman E, Susanto H, Setyobudi RH, Burlakovs J and Vincēviča-Gaile Z. 2020. Renewable energy technologies for economic development. *E3S Web Conf.* **188**(00016): 1–8.

Latimer GW. 2019. **Official Methods of Analysis of Association of Official Analytical Chemists (AOAC International)**, 21st ed. AOAC International Rockville, Maryland, USA.

Issa N.K. and Abd-Aljabar R.S. 2013. Evaluation of antioxidant properties of *Morus nigra* L. fruit extracts [II]. *Jordan J Biol Sci.* **6**(4): 258–265.

Jiang N, Liu C, Li D, Zhang Z, Liu C, Wang D, and Zhang M. 2017. Evaluation of freeze drying combined with microwave vacuum drying for functional okra snacks: Antioxidant properties, sensory quality, and energy consumption. *LWT.*, **82**: 216–226.

Kurniawati I, Fitriyya M and Wijayanti W. 2018. Karakteristik tepung daun kelor dengan metode pengeringan sinar matahari [Characteristics of Moringa leaf flour with sunlight drying method]. *Prosiding Seminar Nasional UNIMUS.* **1**: 238–243. [in Bahasa Indonesia]

Nistor OV, Seremet L, Andronoiu DG, Rudi L and Botez E. 2017. Influence of different drying methods on the physicochemical properties of red beetroot (*Beta vulgaris* L. Var. *Cylindra*). *Food Chem.* **236**: 59–67.

Orphanides A, Goulas V and Gekas V. 2013. Effect of drying method on the phenolic content and antioxidant capacity of spearmint. *Czech J Food Sci.* **31**(5):509–513.

Özcan M.M. 2020. *Moringa spp*: Composition and bioactive properties. *S Afr J Bot.* **129**: 25–31

Panche AN, Diwan AD and Chandra SR. 2016. Flavonoids: An overview. *J Nutr Sci.* **5**(47): 1–15.

Rababah TM, Al-u'datt M, Alhamad M, Al-Mahasneh M, Erefej K, Andrade J, Altarifi B, Almajwal A and Yang W. 2015. Effects of drying process on total phenolics, antioxidant activity and flavonoid contents of common Mediterranean herbs. *Int J Agric Biol Eng.* **8**(2):145–150.

Ramirez E, Gandul-Rojas B, Romero C, Brenes M, and Gallardo-Guerrero L. 2015. Composition of pigments and colour changes in green table olives related to processing type. *Food Chem.* **166**: 115–124.

Saini RK, Sivanesan I and Keum Y. 2016. Phytochemicals of *Moringa oleifera*: A review of their nutritional therapeutic and industrial significance. *Biotech.* **6**(203): 2–14.

- Samoticha J, Wojdyło A, and Lech K. 2016. The influence of different drying methods on the chemical composition and antioxidant activity in chokeberries. *LWT*. **66**: 484–489.
- Sembiring EN, Elya B. and Sauriasari, R. 2018. Phytochemical screening, total flavonoid and total phenolic content and antioxidant activity of different parts of *Caesalpinia bonduc* (L.) Roxb. *Pharmacogn J*. **10(1)**:123–127.
- Sigurdson GT, Tang P and Giusti MM. 2017. Natural colorants: Food colorants from natural sources. *Annu Rev Food Sci Technol*. **8(1)**:261–280.
- Suwati S, Romansyah E, Syarifudin S, Jani Y, Purnomo AH, Damat D and Yandri E. 2021. Comparison between natural and cabinet drying on weight loss of seaweed *Eucheuma cottonii* Weber-van Bosse. *Sarhad J Agric*. **37(Special Issue 1)**: 01–08.
- Suzauddula Md, Miah MM, Mukta NA, Kamrul N and Hossain Md B. 2019. Kinetics study on dried *Moringa oleifera* leaves during sun drying, multi commodity solar tunnel dryer drying and oven drying. *Malays J Halal Res*. **2(1)**:10–15.
- Teixeira EMB, Carvalho MRB, Neves VA, Silva MA and Arantes-Pereira L. 2014. Chemical characteristic and fractionation of proteins from *Moringa oleifera* Lam. leaves. *Food Chem*. **147**:51–54.
- Udomkun P, Nagle M, Mahayothee B, Nohr D, Koza A, and Müller J. 2015. Influence of air drying properties on non enzymatic browning, major bio-active compounds and antioxidant capacity of osmotically pretreated papaya. *LWT*. **60 (2 :1)**: 914–922.
- Vergara-Domínguez H, Roca M and Rojas B G. 2013. Characterisation of chlorophyll oxidation mediated by peroxidative activity in olives (*Olea europaea* L.) cv. Hojiblanca. *Food Chem*. **139(1–4)**: 786–795.
- Wojdyło A, Figiel A, Legua P, Lech K, Carbonell-Barrachina ÁA, Hernández F. 2016. Chemical composition, antioxidant capacity, and sensory quality of dried jujube fruits as affected by cultivar and drying method. *Food Chem*. **207** : 170–179
- Wojdyło A, Lech K, Nowicka P, Hernandez F, Figiel A and Carbonell-Barrachina AA. 2019. Influence of different drying techniques on phenolic compounds, antioxidant capacity and colour of *Ziziphus jujube* Mill. fruits. *Molecules*. **24(13)** : 2361.
- Yap JY, Hii, CL, Ong SP, Lim KH, Abas F and Pin KY. 2020. Effects of drying on total polyphenols content and antioxidant properties of *Carica papaya* leaves. *J Sci Food Agric*. **100(7)** :2932–2937
- Zahrattunnisa N, Elya B and Noviani A. 2017. Inhibition of alpha glucosidase and antioxidant test of stem bark extracts of *Garcinia fruticosa* Lauterb. *Pharmacogn J*. **9(2)**:273–275.

Impacts of Immunostimulant Yeast (*Saccharomyces cerevisiae*) Supplemented Feed on Growth and Blood Profile of Java Barb (*Barbonymus gonionotus*)

Diana Rachmawati^{1,*}, Roy Hendroko Setyobudi², Juris Burlakovs³, Tita Elfitasari¹
and Agus Heri Purnomo⁴

¹Department of Aquaculture, Faculty of Fisheries and Marine Sciences, Diponegoro University, Jl. Prof. Soedarto SH, Tembalang, Semarang 50275, Indonesia; ²Department of Agriculture Science, Postgraduate Program, University of Muhammadiyah Malang, Jl. Raya Tlogomas No 246, Malang 65114, Indonesia; ³Department of Water Management, Estonian University of Life Sciences, Tartu, Estonia; Friedrich Reinhold Kreutzwaldi 1a, 51014 Tartu, Estonia; ⁴Ministry of Marine Affairs and Fisheries Republic of Indonesia, The Research Center for Marine and Fisheries Socio-economics, Mina Bahari 1-Building, Jl. Pasir Putih 1, Ancol, Jakarta 14430, Indonesia

Received: Feb 20, 2021; Revised: April 29, 2020; Accepted May 1, 2021

Abstract

The research aims to analyze the impacts of immunostimulant yeast (*Saccharomyces cerevisiae*) supplemented feed on growth rate and blood profile in Java Barb [*Barbonymus gonionotus* (Bleeker, 1850)] fingerlings. The Java Barb of 200 fingerlings had an average weight of 5.64 g ± 0.87 g, and an average length of 6.32 cm ± 0.58 cm. The experiments employed a Completely Randomized Design with five treatments, and each had four repetitions for a period of 49 d (days). Various dosages of *S. cerevisiae* were added to the feed. The treatments were T1 (0 g kg⁻¹ feed), T2 (1 g kg⁻¹ feed), T3 (2 g kg⁻¹ feed), T4 (3 g kg⁻¹ feed), and T5 (4 g kg⁻¹ feed). The results showed that yeast as supplemented feed could boost the growth and blood profiles of Java Barb. The blood profiles include improvement in total blood cells (TCC μL⁻¹), red blood cells (RBC), white blood cells (WBC), hematocrit (HTC) compared to control. The highest value of efficiency of feed utilization (EFU) was 72.36 % and followed by FCR (feed conversion ratio), PER (protein efficiency ratio), RGR (relative growth rate), and SR (survival rate) with the values of (1.63, 4.21, 4.18) % d⁻¹, and 92.33 % respectively. The optimal dosages of *S. cerevisiae* in the feed for EFU, FCR, PER, and RGR ranged from 2.38 g kg⁻¹ feed to 3 g kg⁻¹ feed.

Keywords: Digestibility, Enzyme, Fisheries feed, Immunity, Resistance

1. Introduction

Java Barb [*Barbonymus gonionotus* (Bleeker, 1850)] is an Indonesian native fish that is easily cultivated; hence, farmers have practiced intensively in aquaculture (Rachmawati *et al.*, 2019b). One of the problems faced by the aquaculture farmers was decreased in water quality due to unconsumed fish feeds and water waste. This condition could inhibit fish growth and rising fish diseases that could decrease fish production. Thus, it made farmers lose in profit. The studies to administrate the fish growth have been done through giving biofloc, probiotic, herb, and immunostimulant. Biofloc was implemented on fish and shrimp (Kuhn *et al.*, 2010). Moreover, de La Banda *et al.* (2010) has applied probiotic on fish and shrimp cultivation. Furthermore, Goda *et al.* (2012) also reported the *S. cerevisiae* supplemented feed could boost fish appetite; therefore, it improved growth and survival rate.

To spur growth and immunity in the fish, fish farmers could utilize immunostimulants that can be obtained from seaweed, bacteria, or yeast. Manoppo and Magdalena (2015) also discovered that the utilization of immunostimulants could raise growth and the immune system in the fish and crustaceae. According to Abu-Elala

et al. (2013), *S. cerevisiae* is one of the immune-stimulants. In addition, Tewary and Patra (2011) also suggested that *S. cerevisiae* can trigger digestibility due to digestive enzymes to boost fish growth. The *S. cerevisiae*-supplemented feed could boost the digestibility of feed and protein. It could also increase efficiency utilization of the feed and the growth (Razak *et al.*, 2017).

The immune response rate of fish could be increased by adding *S. cerevisiae* in the feed, as reported by Abu-Elala *et al.* (2013). Next, the *S. cerevisiae* could be used as an immunostimulant, because it is rich in elements such as β-1-3 glucan (50 % to 60 %). Moreover, it could generate its immunity in the fish and crustacean in which β-glucan in the yeast was able to boost the immunity and disease resistance of the fish (Manoppo and Magdalena, 2015). Moreover, Sheikhzadeh *et al.* (2012) mentioned that *S. cerevisiae* contains immunostimulants such as β-1,3 glucan, nucleate acid, manna oligosaccharide, chitin, non-starch nucleate acid, and polysaccharide. The β-1,3 glucan effectively increased the immune system in some species of fish at the dosage of 1 g kg⁻¹ feed (Dhanaraj *et al.*, 2010). Jarmolowicz *et al.* (2011) disclosed that the addition of beer yeast at the dosage of 4 % to 6 % could boost non-specific immune system in the fingerlings of pikeperch [*Sander lucioperca* Linnaeus, 1758].

* Corresponding author e-mail: dianarachmawati1964@gmail.com

Some researches on the *S. cerevisiae*-supplemented feed to boost growth and immunity were disclosed by Tewary and Patra (2011) in *Labeo rohita*, F. Hamilton, 1822; Tawwab *et al.* (2010) in *Sarotherodon galileus*, Linnaeus, 1758; Manoppo and Kolopita (2016) in *Cyprinus carpio*, Linnaeus, 1758; Jarmolowicz *et al.* (2011) in *Sander lucioperca* Linnaeus, 1758; Azevedo *et al.* (2016) in *Oreochromis niloticus*, Linnaeus 1758; Rachmawati *et al.* (2019a) in *Pangasius hypophthalmus* Sauvage, 1878; and Rachmawati *et al.* (2019b) in *Barbonymus gonionotus* Bleeker, 1850. However, previous research only observed the growth of cultivated fish, and research on the effect of blood profiles has never been carried out. Therefore, it is important to do this research which studies the impact of yeast on the blood profile of Java Barb.

Some benefits of using *S. cerevisiae* as an immunostimulant in aquaculture are that it does not leave any residues in fish and the environment, and hazard free for human beings as well. Therefore, the utilization of *S. cerevisiae* as an immunostimulant to increase growth is very important. This study aims to analyze the impacts of *S. cerevisiae* supplemented feed on growth rate and blood profile in Java Barb fingerlings.

2. Materials and Method

The study was conducted at the Laboratory for Fish Health and Environment Assessment, Muntilan, Central Java, Indonesia from April until June 2019. This experiment utilized 500 sample fingerlings of Java barb with an average weight of $5.64 \text{ g} \pm 0.87 \text{ g}$, and an average length of $6.32 \text{ cm} \pm 0.58 \text{ cm}$. (Rachmawati *et al.*, 2017). To adjust to feeding and a new environment, the sample fish was first acclimated for 1 wk (week). During acclimatization, fish were fed with commercial feed using ad satiation method. To maintain the water quality, water was being siphoned before feeding. Before the study was conducted, the sample fish fasted for 1 d (day) to clean the metabolism residues hence the initial weight was not affected by the waste weight. The yeast materials for treatments were commercial yeast (*S. cerevisiae*) brand Saf Instant produced by Saf Indonusa - Lessafre Global Group, Indonesia.

Completely Randomized Designed (CRD) was implemented in this research. There were five treatments with four replications. The treatments were a supplementation of yeast (*S. cerevisiae*) into the feed. The feeds used were commercial with brand name Comfeed fish feed, produced by JAPFA Comfeed Indonesia Tbk., composed of 30 % of raw protein, 2 % fat, 3 % raw fiber, 13 % ash, and 12 % water. Treatments were included: T1 (0 g kg^{-1} feed), T2 (1 g kg^{-1} feed), T3 (2 g kg^{-1} feed), T4 (3 g kg^{-1} feed), and T5 (4 g kg^{-1} feed). The dosages of the *S. cerevisiae* in this study were modified from Rachmawati *et al.* (2019a) study. The study recorded that 1 g kg^{-1} feed supplementation of *S. cerevisiae* was the best dosage to produce the highest feed usage efficiency in fingerling of catfish (*Pangasius hypophthalmus* Sauvage, 1878).

After the yeast was added, the protein analysis per treatment was T₀ (30 %), T₁ (30.37 %), T₂ (30.46 %), T₃ (30.39 %), and T₄ (30.53 %). The preparation of the feed was by weighing the *S. cerevisiae* based on the treatments. The weighed yeast was diluted with pure

water. The 100 mL pure water was diluted in 1 kg feed (Manurung *et al.*, 2013). The diluted yeast was evenly sprayed into the feed based on the Rachmawati *et al.*, (2019b) method. Firstly, the feed was put on the plastic tray and then sprayed by suspense yeast. When feed was being sprayed with yeast, the tray was shaken and the feed and the yeast were mixed. Then, the mixture was dried up by letting it at room temperature of 28 °C to 30 °C. After that, the mixture was put in a plastic bag. Then, the bag was labeled by treatment and stored in the refrigerator until it was ready to use. The fix feeding method was used to feed the fingerlings. The method was based on 5 % of the fish weight. The three times daily feeding implemented were in the morning (7 am), afternoon (2 pm), and evening (6 pm). The scale of the fish weight was carried out every week for 49 d. Sampling was carried out once 1 wk; therefore, a 7 wk observation is required to obtain more accurate data.

The containers used were made from fiberglass by dimension $1.5 \text{ m} \times 1.5 \text{ m} \times 1 \text{ m}$. The fish was reared in 20 containers with a stock density of 25 fish m^{-3} . Freshwater was utilized as cultivation media. Before the water was used, it has been deposited for several days in a reservoir.

The observation on blood profile has been conducted at the beginning (1st d) and the end (49th d) of the study. The observed parameters included total cells (TCC μL^{-1}), red blood cells (RBC), white blood cells (WBC), hematocrit (HCT) (referring to Mohammed *et al.*, 2013 on blood profile methodology).

The observed variables included feed efficiency (EF), the ratio of feed conversion (FCR), the protein efficiency ratio (PER), relative growth rate (RGR), and survival rate (SR) which was measured every week. Those variable observations were referring to Rachmawati *et al.* (2018) and Rachmawati *et al.* (2019b), while analysis of blood profile and water quality consisting of temperature, pH, and dissolved oxygen was measured every morning and evening, whereas ammoniac was measured in 1st d, 28th d and 49th d based on the method of APHA (1992). Water quality was maintained through the daily siphon and 30 % of water change every week after sampling. The measure variables are EFU (efficiency of feed utilization) in Equation (1) and RGR (relative growth rate) in Equation (2):

$$EFU = 100 \left(\frac{W_2 - W_1}{QF} \right) \quad (1)$$

$$RGR = 100 \left(\frac{W_2 - W_1}{T \times W_1} \right) \quad (2)$$

Note: W_1 and W_2 are the initial and final weight, respectively, QF is the feed amount consumed, and T is the days during the feeding period. FCR (feed conversion ratio), PER (protein efficiency ratio), SR (survival rate) are calculated by Equation (3), Equation (4), and Equation (5).

$$FCR = 100 \left(\frac{F_1}{WG} \right) \quad (3)$$

Note: FI is feed intake (g) and WG is weight gain (g);

$$PER = 100\left(\frac{W}{PI}\right) \quad (4)$$

Note: WG is weight gain (g) and PI is protein intake (g);

$$SR = 100\left(\frac{C_2}{C_1}\right) \quad (5)$$

Note: C_1 is an initial count of fish and C_2 final count of fish.

Analysis of variance (ANOVA) and Duncan's Multiple Range Test were used to analyze the observed variables (Rachmawati *et al.*, 2019b). The polynomial orthogonal test using SAS9 and Maple12 software was used to calculate the optimal dosage of immunostimulant yeast (*S. cerevisiae*). Water quality parameters were descriptively explained by comparing the rearing conditions to determine the viability.

3. Results and Discussions

Table 1. displayed the observed variables of EFU, FCR, PER, RGR, and SR in treatment T_0 , T_1 , T_2 , T_3 , and T_4 . The polynomial orthogonal test results of *S. cerevisiae*-supplemented feed on EFU, FCR, PER, and RGR were displayed in Figure 1, Figure 2, Figure 3, and Figure 4. Figure 1 showed that the optimal dosage of *S. cerevisiae* in the feed for EFU was 2.38 g kg^{-1} feed with the EFU value as much as 67.67 %. The best value of FCR (1.58) was obtained from *S. cerevisiae* with 2.43 g kg^{-1} feed, as shown in Figure 2.

Table 1 shows that adding yeast to feed has a significant effect on EFU, FCR, PER, and RGR, but does not show an effect on SR.

Figure 3 displayed the relationship between the dosage of yeast and the values of PER. The optimal dosage of *S. cerevisiae* for PER was 2.62 g kg^{-1} feed giving the value of 4.08. Based on Figure 4, one could calculate the optimal dosage of *S. cerevisiae* for RGR. The optimum dosage was 3 g kg^{-1} feed giving the value of 4.18 \% d^{-1} .

Table 1. The values of the variables

Experiment Data	Treatments				
	T_0	T_1	T_2	T_3	T_4
EFU (%)	48.24 ± 0.18^d	59.75 ± 0.27^c	63.35 ± 0.31^b	72.36 ± 0.19^a	55.63 ± 0.15^c
FCR	2.53 ± 0.32^c	2.18 ± 0.25^b	2.01 ± 0.25^b	1.63 ± 0.18^a	2.12 ± 0.27^b
PER	1.96 ± 0.28^d	2.85 ± 0.24^c	3.27 ± 0.23^b	4.21 ± 0.27^a	2.59 ± 0.25^c
RGR ($\% \text{ d}^{-1}$)	1.67 ± 0.14^d	2.09 ± 0.15^c	3.52 ± 0.22^b	4.18 ± 0.25^a	3.48 ± 0.22^b
SR (%)	75.33 ± 3.52^a	90.33 ± 2.67^a	90.33 ± 2.72^a	92.33 ± 2.78^a	90.33 ± 2.43^a

Note: The mean values with a different superscript in the same column showed significant difference ($P < 0.05$)

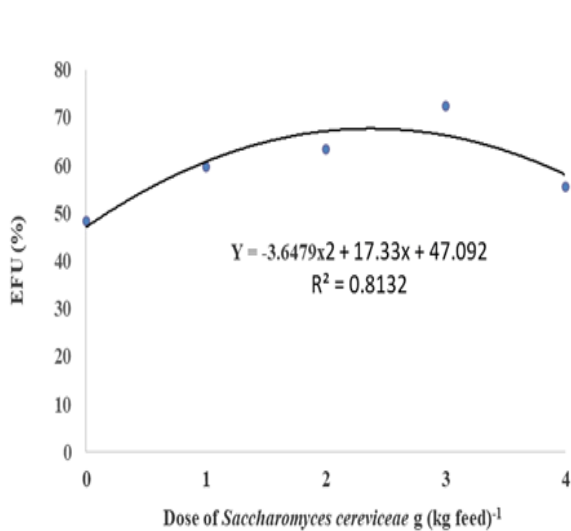


Figure 1. The relation between the immunostimulant yeast (*S. cerevisiae*) and EFU in the Java Barb fingerlings

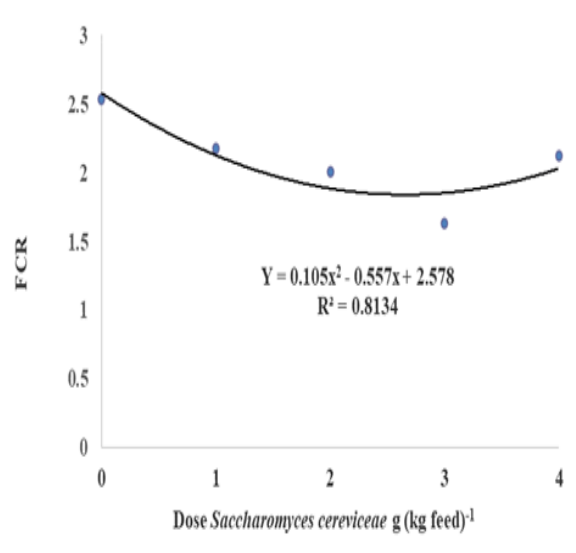


Figure 2. The relation between the immunostimulant yeast (*S. cerevisiae*) and FCR in the Java Barb fingerlings

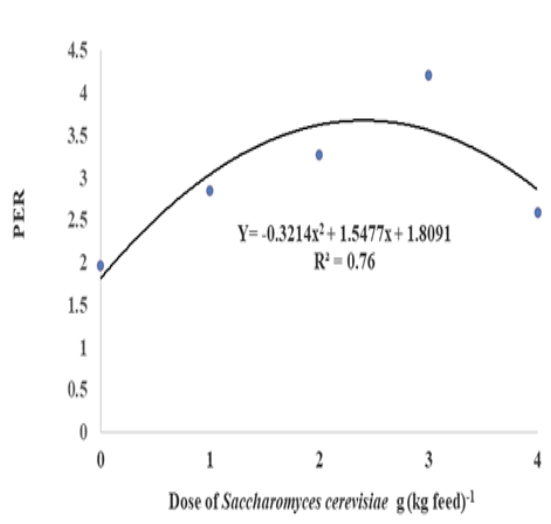


Figure 3. The relation between the immunostimulant yeast (*S. cerevisiae*) and PER in the Java Barb fingerlings

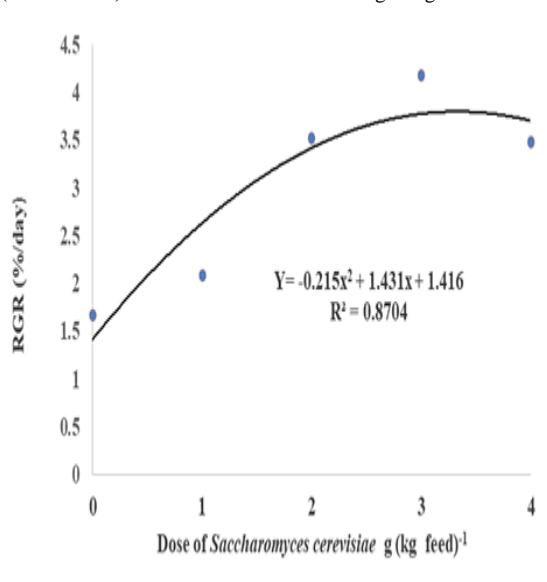


Figure 4. The Relationa between the immunostimulant yeast (*S. cerevisiae*) and RGR in the Java Barb fingerlings

The enrichment of *S. cerevisiae* with the dosages of 1 g kg⁻¹ feed to 4 g kg⁻¹ feed (T1, T2, T3, T4) in the Java barb fingerlings had higher values of EFU (55.63 % to 72.36 %) than those given the zero-supplementation yeast (48.24 %, as in the treatment T0). It was noted that the *S. cerevisiae* supplemented feed could raise the efficiency of feed utilization. Razak *et al.* (2017) discovered that the *S. cerevisiae* could boost enzymatic activities in the digestive track. Hence, it enhanced the decomposition of complex nutrients into simpler nutrients as proclaimed by Tewary and Patra (2011). The simpler nutrients were easier to absorb, and in turn this enhanced the efficiency of feed utilization. The dosage of 3 g kg⁻¹ feed (T3) produced the highest EFU (72.36 %), followed by the treatments T2, T1, T4, and T0 that had values of 63.35 %, 59.75 %, 55.63 % and 48.24 %, respectively. The optimal dosage of yeast in the feed that resulted in the highest EFU may cause the dosage appropriate to enhancing enzyme activities in the digestive track and then improve the efficiency of feed usage. Welker *et al.* (2012) discovered

that *S. cerevisiae* as an immunostimulant could enhance the production of the enzyme in the digestive tract to boost digestibility and absorption for nutrients, amino acids, vitamins, and enzymes. Similar results from other studies were reported by Tawwab *et al.* (2010) in *Sarotheredon galileus* Linnaeus 1758, Tewary and Patra (2011) in *Labeo rohita* F. Hamilton 1922, and Rachmawati *et al.* (2019a) in *Pangasius hypophthalmus* Sauvage 1978. Results of previous experiments showed that the addition of yeast to feed increases EFU.

The *S. cerevisiae* supplemented feed decreased the FCR of Java barb fingerlings. The treatment T3 with the dosage of 3 g kg⁻¹ feed generated the lowest FCR. The dosage was to make maximum feed usage efficiency, so it decreased FCR. Razak *et al.* (2017) supported this discovery. This study found that the *S. cerevisiae*-supplemented feed could raise the efficiency of feed usage and decreased the ratio of feed conversion. In addition, Jarmolowicz *et al.* (2011) discovered that the *S. cerevisiae* supplemented feed caused FCR to increase due to the increase of protein digestibility. Essa *et al.* (2010) also disclosed that the *S. cerevisiae*-supplemented feed raised the FCR and the efficiency of feed utilization.

The protein efficiency ratio (PER) is a number calling the total weight of fish produced per unit of protein in the feed (Tiamiyu *et al.*, 2014). Various dosages of *S. cerevisiae* of 1 g kg⁻¹ feed to 4 g kg⁻¹ feed given to Java barb fingerlings generated higher PER (2.59 to 4.21) compared to the PER (1.96) without the addition of yeast. Goda *et al.* (2012) mentioned that the *S. cerevisiae*-supplemented feed could surge protein digestibility; therefore, it increased the ratio of protein efficiency. Moreover, Rachmawati *et al.* (2019b) stated that the *S. cerevisiae*-supplemented feed could enhance the efficiency of feed utilization and the ratio of protein efficiency. The highest PER (4.21) was achieved in T3 (3 g kg⁻¹ feed,) while the lowest PER (1.96) was attained in T0 (0 g kg⁻¹ feed). The highest PER was because of the right dosage of the yeast to generate the ratio of protein efficiency, while the lowest PER was due to the absence of yeast.

The results on the RGR of the supplementation of *S. cerevisiae* ranged from 1 g kg⁻¹ feed to 4 g kg⁻¹ feed and between 2.09 % d⁻¹ and 4.18 % d⁻¹. These values were higher than without yeast supplementation by 1.67 % d⁻¹. The *S. cerevisiae* supplemented feed could raise RGR, which was due to the increases in protein digestibility and efficiency of feed utilization (Manoppo and Magdalena, 2015). Moreover, Rajagukguk *et al.*, (2017) disclosed that the existence of yeast (*S. cerevisiae*) in the fish digestive system could boost enzymatic activities. It can hike protein digestibility and efficiency of feed usage, and in turn, it raised RGR. The treatment T3 (3 g kg⁻¹ feed) generating the highest RGR was suggested due to the effective dosage of the yeast (*S. cerevisiae*).

The *S. cerevisiae* supplemented feed was not significant ($P > 0.05$) on the SR of Java barb fingerlings. It was suggested that the feed was not a factor for SR. The factor that affected SR was abiotic one, such as the ability to adapt to the environment, handling, density, competitors, diseases, ages, and the existence of the predators (Abu-Elala *et al.* (2013). The SR of Java barb fingerlings that were fed by supplementation of *S. cerevisiae* ranged from 90.33 % to 92.33 %, while the survival rate for those that were not fed with the

supplementation of *S. cerevisiae* was 73.33 % (Table 1). It was suggested that the yeast (*S. cerevisiae*) contained β -glucan as an agent of immunostimulant to increase the immune system; therefore, the SR was high. This phenomenon supported by Manoppo and Magdalena (2015) stated that the enrichment of β -glucan was able to be an immunostimulant to improve the immune system in the fish. The results of the blood profile were higher after the fingerlings were fed with the enrichment of *S. cerevisiae* as in Table 2.

The results of the blood profile measurement consisted of total cell count (TCC μL^{-1}), red blood cells (RBC), white blood cells (WBC), and hematocrit (HCT). Those were displayed in Table 2.

Table 2. Total cell count (TCC/ μL^{-1}), red blood cells (RBC), and white blood cells (WBC), hematocrit (HCT) in the Java Barb fingerlings

Treatments (g kg ⁻¹ feed)	TCC/ μL ($\times 10^6$)	RBC ($\times 10^6$)	WBC ($\times 10^5$)	HCT (%)
T ₁ (0)	1.39 ^b	1.92 ^b	1.38 ^b	24.49 ^b
T ₂ (1)	3.23 ^a	3.25 ^a	2.63 ^a	35.13 ^a
T ₃ (2)	3.45 ^a	3.37 ^a	2.37 ^a	36.74 ^a
T ₄ (3)	3.65 ^a	3.39 ^a	2.65 ^a	37.98 ^a
T ₅ (4)	3.56 ^a	3.29 ^a	2.83 ^a	35.83 ^a
±SD	0.127	0.132	0.263	0.221

Note: The mean values with a different superscript in the same column showed significant difference ($P < 0.05$)

Table 2 showed that the fingerlings that were fed with the *S. cerevisiae* supplemented feed had a significant increase in the total cell count (TCC/ μL^{-1}), the red blood cells (RBC), the white blood cells (WBC), and the hematocrit (HCT). It was revealed that the *S. cerevisiae*-supplemented feed increased non-specific immune response in the Java barb fingerlings. The results show that *S. Cerevisiae* is rich in β -1-3 glucan (50 % to 60 %) that increased fish immune system; therefore, fish resisted the pathogen. It was proven by the value of SR that was higher than without *S. Cerevisiae* supplementation. Manoppo and Magdalena (2015) reported that the *S. cerevisiae*-supplemented feed increased non-specific immune response. Abu-Elala *et al.* (2013) also reported that the Java barb fed with *S. cerevisiae* supplemented feed increased erythrocyte, hemoglobin, and leukocyte. Moreover, Welker *et al.* (2012) discovered that the catfish fed with *S. cerevisiae*-supplemented feed for 1 wk had higher red and white blood cells than those with no *S. cerevisiae* supplemented feed.

The observation of water quality during the experimental period was in an infeasible condition for Java Barb cultivation as indicated by the standard quality in the literature. The suitable condition of the water quality affected by the water quality was controlled according to the requirement of Java Barb need.

4. Conclusion

The supplementation of immunostimulant yeast (*S. cerevisiae*) in the feed could raise the growth and blood profiles such as total cell count, red blood cells, and white blood cells in the Java barb fingerlings. The optimal

dosages of *S. cerevisiae* in the feed for EFU, FCR, PER, and RGR ranged from 2.38 g kg⁻¹ feed to 3 g kg⁻¹ feed.

Acknowledgment

Appreciation is sincerely conveyed to the Head of Laboratory for Fish Health and Environment Assessment, Muntilan, Central Java, Indonesia who has provided the facility to carry out this research.

References

- Abu-Elala, N, Marzouk M and Moustafa M. 2013. Use of different *Saccharomyces cerevisiae* biotic forms as immunomodulator and growth promoters for *Oreochromis niloticus* challenged with some fish pathogens. *J Vet Med Sci.* **1**:21-29.
- Azevedo RV, Filho JCF, Pereira SL, Cardoso LD, Andrade DR and Júnior MVV. 2016. Dietary mannan oligosaccharide and *Bacillus subtilis* in diets for Nile tilapia (*Oreochromis niloticus*). *Acta Scientiarum.* **38**(4):347-353.
- De La Banda IG, Lobo C, Leon-Robio JM, Tapia-Paniagua S, Balebona MC, Morinigo, MA, Moreno-Venta X, Lukas LM, Linares F, Arce F and Arijji S. 2010. Influence of two closely related probiotics on juvenile Senegalese sole (*Solea senegalensis*, Kaup 1858) performance and protection against *Photobacterium damsela* ssp. Piscicida. *Aquac.* **306**:281-288.
- Dhanaraj M, Haniffaa MA, Singha SVA. Arockiarajb AJ, Ramakrishanana CM, Seetharamana S and Arthimanjua R. 2010. Effect of probiotics on growth performance of koi carp (*Cyprinus carpio*). *J App Aquac.* **22**(3): 202-209.
- Essa MA, El-Serafy SS, El-Ezabi MM, Daboor SM, Esmael NA and Lall SP. 2010. Effect of different dietary probiotics on growth, feed utilization, and digestive enzyme activities of Nile tilapia, *Oreochromis niloticus*. *J World Aquac Soc.* **5**(2): 143-162.
- Goda AMA, Mabrouk HAAH, Wafa MAE and El-Afifi TM. 2012. Effect of using baker's yeast and exogenous digestive enzymes as growth promoters on growth, feed utilization, and hematological indices of Nile tilapia, *Oreochromis niloticus* Fingerling. *J Agric Sci Technol B.* (2):15-28.
- Jarmolowicz S, Zakes Z, Siwicki A, Kowalska A, Hopko M, Glabski E, Demska Z and Partyka K. 2012. Effects of brewer's yeast extract on growth performance and health of juvenil pikeperch *Sander lucioperca* (L.). *Aquac Nutr.* **18**(4): 457-464
- Kuhn DD, Lawrence AL, Boardman GD, Patnaik S, Marsh L and Flick Jr. GJ. 2010. Evaluation of two types of bio floc derived from biological treatment of fish effluent as feed ingredients for Pacific white shrimp *Litopenaeus vannamei*. *Aquac.* **303**:28-33.
- Manoppo H and Magdalena EF. 2015. Composting bread yeast in feed increases nonspecific immune response and Tilapia growth. *Jurnal Veteriner.* **16**(2):204-211.
- Manoppo H and Kolopita MEF. 2016. Use of bread yeast (*Saccharomyces cerevisiae*) as immunostimulant to improve the resistance of carp (*Cyprinus carpio* L) against bacterial infection *Aeromonas hydrophila*. *Jurnal Budidaya Perairan.* **4**(3):37-47.
- Manurung UN, Manoppo H and Tumbol RA. 2013. The use of baker's yeast (*Saccharomyces cerevisiae*) in enhancing non specific immune response and growth of nile tilapia (*Oreochromis niloticus*). *Jurnal Budidaya Perairan.* **1**(1):8-14.
- Mohammed H, Olivares-Fuster O, Lafrentz S and Arias CR. 2013. New attenuated vaccine against columnaris disease in fish: Choosing the right parental strain is critical for vaccine efficacy. *Vaccine.* **31**:5276-5280.
- Rachmawati D, Istiyanto S and Maizirwan Mel. 2017. Effect of phytase on growth performance, feed utilization efficiency and

- nutrient digestibility in fingerlings of *Chanos chanos* (Forsskal 1775). *Philipp J Sci.* **146** (3): 237-245.
- Rachmawati D, Prihanto AA, Roy HS and Anne O. 2018. Effect of papain enzyme in feed on digestibility of feed, growth performance, and survival rate in post larvae of freshwater Lobster [*Cherax quadricarinatus* (Von Martens, 1868)]. *Proc Pakistan Acad Scies B.* **55** (3): 31-39
- Rachmawati D, Istiyanto S, Ristiawan AN and Susilowati T. 2019a. Effects of *Sacharomyces cereviceae* incorporated diet on growth performance, apparent digestibility coefficient of protein and survival rate of catfish (*Pangasius hypothalamus*). *Aquacultura Indonesiana.* **20** (1):8-14.
- Rachmawati D, Hutabarat H, Samidjan I, Herawati VE and Windarto S. 2019b. The effects of *Saccharomyces cerevisiae*-enriched diet on feed usage efficiency, growth performance and survival rate in Java barb (*Barbonymus gonionotus*) fingerlings. *Aquac Aquar Conserv Legis.* **12** (5):1841-1849.
- Rajagukguk BB, Clumenta C and Mokolensang JF. 2017. Utilization of yeast (*Saccharomyces cerevisiae*) in feed formulations in increasing the growth of tilapia (*Oreochromis niloticus*). *Jurnal Budidaya Perairan.* **5**(3):44-49.
- Razak AP, Kreckhoff RL and Watung JC. 2017. Administration of oral immunostimulant bread yeast (*Saccharomyces cerevisiae*) to increase goldfish growth (*Cyprinus carpio* L.). *Jurnal Budidaya Perairan.* **5**(2):27-36.
- Sheikhzadeh AE, Heidarich M, Pashaki AK, Nofouzi K, Farshabi MA and Akbari M. 2012. Hilyses fermented *Saccharomyces cereviceae*, enhances the growth performance and skin non-specific immune parameters in rainbow trout (*Oncorhynchus mykiss*). *Fish Shellfish Immunol.* **32** (6):1083-1087.
- Tawwab MA, Mousa MAA and Mohammed MA. 2010. Use of live baker's yeast, *Saccharomyces cerevisiae*, in practical diet, to enhance the growth performance of galilee tilapia, *Sarotherodon galilaeus* (L.), and its resistance to environmental copper toxicity. *J World Aquac Soc.* **41**(S2):214-223.
- Tewary A and Patra BC. 2011. Oral administration of baker's yeast (*Saccharomyces cerevisiae*) acts as a growth promoter and immunomodulator in *Labeo rohita* (Ham.). *J Aquac Res Dev.* **2**(1):1-7.
- Tiamiyu, LO, Victoria OA, Victor TO and Saidu U. 2014. Effect of various levels of raw *Citrullus lanatus* seed meal diets on growth performance of *Cyprinus carpio* Fingerlings. *Jordan J. Biol. Sci.* **7**(4):269-274.
- Welker T L, Lim C, Yildirim-Aksoy M and Klesius PH. 2012. Effect of short-term feeding duration of diets containing commercial whole-cell yeast or yeast subcomponents on immune function and disease resistance in channel catfish, *Ictalurus punctatus*. *J Anim Physiol Anim Nutr (Berl).* **96**:159-171.

The Moderating Effect of *Hypericum thymbrifolium* against Memory Loss and Alzheimer's Disease (Experimental Study in Mice)

Khayra Zerrouki^{1,2,*}, Nouredine Djebli¹, Leila Gadouche¹, Esra Eroglu Ozkan³ And Afife Mat³

¹Laboratory of Pharmacognosy and Api-Phytotherapy; Department of Biology FSNV- Mostaganem University, Mostaganem, Algeria; ²Department of Nutrition and Food Sciences; Nature and Life Sciences faculty -Chlef University, Chlef, Algeria; ³Department of Pharmacognosy, Faculty of Pharmacy- Istanbul University, Istanbul, Turkey

Received: Feb 15, 2020; Revised: August 26, 2020; Accepted: September, 2020

Abstract

Symptoms of neurodegenerative diseases acquired through neurologic disorder in behavior and memory are sometimes associated with severe aggression. Differences in terminology have resulted in varying estimates, but behavior disorders and memory loss appear to be characteristic of Alzheimer's disease. This work provides a brief neurologic comparison between Alzheimer's model and treated Alzheimer's with *Hypericum thymbrifolium* known as a kind of Turkish tea. The advantages of using phytotherapy against neurodegenerative diseases, including Alzheimer's, reduce the rate of cascade reactions of neurodegeneration and amyloid-beta synthetizes. *Hypericum thymbrifolium* is a species of Turkish antioxidant plant extracted and studied in Istanbul University Faculty of Pharmacy Department of Pharmacognosy. Mice were randomized into 3 groups, 6 mice each. Group 1: control; 2: Alzheimer's model (AlCl₃ orally+ IP D-Gal); 3: treated Alzheimer's with the ethanol extract of *H. thymbrifolium*. After 90 days of experimentation, neurologic tests were necessary in order to evaluate neurologic disorders; the results of these tests showed significant differences in behavior and memory between the treated Alzheimer's and Alzheimer's. A histological study was necessary to confirm the neurologic tests and check the nervous tissues state; our results confirmed the decrease of injuries of the pyramidal cells in the cerebral cortex and hippocampus of treated Alzheimer's mice.

Keywords: Alzheimer's disease (AD), antioxidant, *Hypericum thymbrifolium*, mice, phytotherapy

1. Introduction

Alzheimer's disease AD is characterized by a wide range of physical, functional, cognitive, and behavioral disorders (Moreira P.I. et al., 2008; Magali Dumont, M. Flint Beal 2011). It usually leads to a marked decrease in the cognitive, mental, and also physical skills of the affected person. In the course of time, the elderly patients with Alzheimer's disease (AD) manifest increasing difficulty in carrying out activities of daily living along with behavioral and psychological symptoms of dementia including signs of disturbed perception, thought content, mood, or behavior like hoarding, wandering, aggression, and disinhibition (Moreira P.I. et al. 2008; Magali Dumont M. and Flint Beal 2011).

Alzheimer's disease (AD) is one of the consequences of bioavailability of prooxidant, exhibited various symptoms corresponding to cerebral impairments such as loss of concentration and short term memory (Teresa M. et al., 2006).

Unfortunately, some xenobiotics are used daily in some nutrients, cosmetics, additives (dyes, anti-coagulants, firming...), in cooking utensils and in pharmacological

agents including antacids and antiperspirants, from which prooxidants enter to the human body at supraphysiological doses, thus increasing the concentration of prooxidant in the blood dramatically (ex: aluminum) (Markesberry and Carney, 1999).

Naturally, the brain is abundant in antioxidants that control and prevent the detrimental formation of reactive oxygen species (ROS) generated via Fenton chemistry involving redox-active metal-ion reduction and activation of molecular oxygen (Esra Eroglu et al., 2018).

Some species of *Hypericum* are known in Turkey as a kind of tea that can be used to improve some cases of depression. It would be of great interest to find out whether food supplements endowed with antioxidative potential could prevent/reverse or reduce neurological alterations. Experimentally, the treated Alzheimer's and Alzheimer's model is often used for pathological and pharmacological investigations (Rodger L. et al., 2017).

In this study, the effect of *H. thymbrifolium* on Alzheimer's model was investigated. The behavior and memory responses are used in order to evaluate its positive effects. The histological study is a complementary part that gives a cellular and tissular explanation of these improvements.

* Corresponding author e-mail: soumaia9@gmail.com.

2. Material & methods

2.1. Plant material

The specimens of flowering aerial parts of *H. thymbrifolium* were collected from their natural habitats on the roadsides nearby the town of Malatya located in the East Anatolia Region of Turkey. The plant materials were identified by Prof. Dr. Şükran Kültür and voucher specimens were deposited in the Herbarium of the Istanbul University Faculty of Pharmacy, Istanbul, Turkey (ISTE number is 93194).

2.1.1. Preparation of the extract

The dried flowering aerial parts of the plant (10 g) were macerated in ethanol (100 mL) for 3 days at room temperature at dark, and filtered through Whatman No-1. The residue from the filtration was extracted again twice using the same procedure. The filtrates were combined and then evaporated to dryness under reduced pressure at a temperature below 45 °C. The crude ethanol extract was lyophilized and stored at -20 °C. (Esra Eroglu et al. 2018).

2.2. Animals

Studies were performed using young adult mice (3-month-old, 22-26 g) housed in the Laboratory Animal Care of Mostaganem under a 12-hour light-dark cycle, with *ad libitum* access to food and water. Mice were obtained from PASTEUR Institute of Algiers

Mice were assigned into three groups, each containing six animals. Control Group: mice were administered freshwater orally and served as normal control. Alzheimer's model Group: mice were treated with $AlCl_3$ (100 mg/kg/day) concomitant with the IP of D-Galactose (D-Gal) in order of 200 mg respectively of the volume of (0,1mL/day). Treated Alzheimer's group: received concomitant with the Aluminum and D-Galactose dose, (0,1 mL) IP of *H. thymbrifolium* dried ethanol extract in order of 200 mg/kg/day. The experiment lasted for 3 months.

2.3. Chemical & treatment

$AlCl_3$ and D-Gal were purchased from Sigma-Aldrich Chemicals.

Both the dried ethanol extract of *H.thymbrifolium*, and the chemicals ($AlCl_3$ & D-Gal) were dissolved in distilled water, in order to be administrated for the needed dose.

2.4. Neurologic tests

2.4.1. Behavioral tests

Disturbance of behavior is enduring and creates severe difficulties for people with neurodegenerative diseases. Neurobehavioral disability (NBD) is a term that has been evolved to highlight the combination of neurological and neuropsychological origins of behavior disorders observed amongst people with this neurologic injury (Per M. Roos et al., 2006).

2.4.1.1. Stress: Forced swimming test

Forced swimming tests included two sessions, once each 24 h. On the first day, each mouse was placed individually in a glass cylinder (22 cm in diameter, 40 cm high) filled with water, kept at 25°C, at a depth of 20 cm. Animals were forced to swim, and immobility time was recorded. The mouse was considered as immobile when it stopped struggling and moved only to remain afloat,

keeping its head above the water (Persolt, R.D. et al., 1977).

2.4.1.2. Curiosity

Curiosity is one of the behavioral tests to evaluate the exploration properties of animals using a hole (deep hole test); on the other hand the anxiety would be known with the high score of this hole platform test, the visit of the hole is the score for this test.

2.4.1.3. Morris water maze

After 3 months, spatial memory was measured by the Morris water-maze (MWM) test. The water maze consisted of a circular water tank (160 cm in diameter and 35 cm in height), which was divided by four fixed points on its perimeter to four quadrants. It contained an escape platform of 10 cm in diameter of the same color as the rest of the basin (to eliminate any false-positive results due to vision), placed in a constant point of the basin throughout the trials and kept 1.5 cm below the water surface. Mice were placed at a start point in the middle of the rim of a quadrant not containing the escape area with their face to the wall. Animals had four trials per day separated by 10 minutes for 5 successive days, during which the times required to find the hidden platform were averaged.

2.4.1.4. Memory Test: Radial Arm Maze

The radial arm maze was designed for evaluating spatial learning and memory in rodents. The maze has eight arms radiating from a central platform. A small food site is at the end of one arm. The design ensures that, after checking the food site, the animal is always forced to return to the central platform before making the next choice. We used this maze to evaluate the degree of memory loss in the AD mouse model with or without drug treatment.

The maze test consisted of a 4-days training session and a 1-day testing session. Before the training session, mice were kept on a restricted diet in order to motivate the mice to seek food in the maze.

During the testing session, mice explored the maze baited at arms, and a 5-min period was provided to each mouse. Each reentry (entry to a previously visited arm) and error (entry to a non-baited arm) was recorded to evaluate working memory (short term) and reference memory (long term), respectively.

To demonstrate that mice were matched for memory ability after the treatment period, working memory and reference memory were calculated by averaging the reentries and error entries, respectively, for the 5 days of testing. To compensate for any baseline differences between Alzheimer's treated groups (the ethanol extract of *Hypericum thymbrifolium*), a regression method was used to compare the memory of Alzheimer's & Alzheimer's treated groups.

2.5. Statistical Analyses:

The data are expressed as means with S.E.M. The statistical significance of differences between groups was assessed with an analysis of variance followed by Student Newman-Keuls. A P value of 0.05 or less taken as a criterion for a statistically significant difference.

2.6. Histological study

In order to confirm the previous tests, the histological study was necessary. Mice were sacrificed, brains were quickly removed. Segments were fixed in Formol solution

and paraffin-embedded. Serial sections of 2 μ m were obtained with a Leica microtome. For histologic observation, deparaffinized sections were stained according to conventional histological and histochemical stains (H&E).

3. Results & Discussion

Obtained results have suggested that *Hypericum thymbrifolium* had an improvement on the behavioral, and memory tests clearly showed significant differences between the treated Alzheimer's and Alzheimer's model.

3.1. Behavioral tests

Conditioned avoidance response is an experimental model to study procedural type of behavior in curiosity, forced swimming test; which tested the mice performance; these tests show a remarkable difference between the treated Alzheimer's and the Alzheimer's group; the Persolt test was assessed by the immobilized time represented as a despairing time.

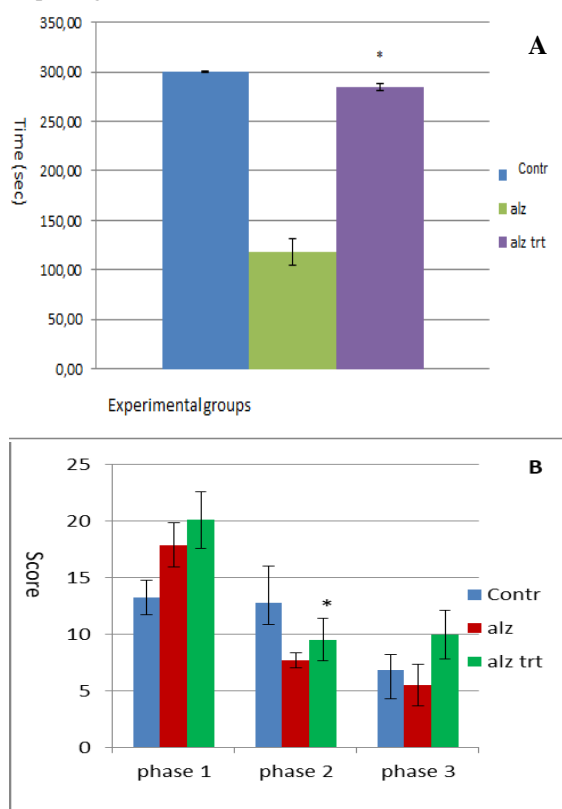


Figure 1: **A:** forced swimming test: Control mice (contr), Alzheimer's model (alz) by $AlCl_3$ (100 mg/kg) Or& D-Gal (200mg/Kg)IP and the Treated Alzheimer's with the ethanol extract of *H. thymbrifolium* (200mg/kg) orally for three months. **B:** curiosity test: Control mice (contr), Alzheimer's model (alz) by $AlCl_3$ (100 mg/kg)Or& D-Gal (200mg/Kg) IP and the Treated Alzheimer's with the extract (200mg/kg) orally for 3 months.

3.2. Memory tests

The obtained results of the Spatial Memory test preferably conditional, during the experimental tests showed that Alzheimer's mice take much longer to reach the food in the arm lit unlike control mice, treated Alzheimer's, and that put a very short time to get informed on the arm (Figure 2).

The test of long term memory, represented with Morris maze, showed a significant decrease in the retention of the learned task was observed in Alzheimer's mice, Whereas the treated mice with the ethanol extract of *H. thymbrifolium* where it had shown a significant results $P < 0.05$ noted as score per time, 5mn each day showed high activity for the Alzheimer's treated comparatively with the intoxicated group (Figure 2).

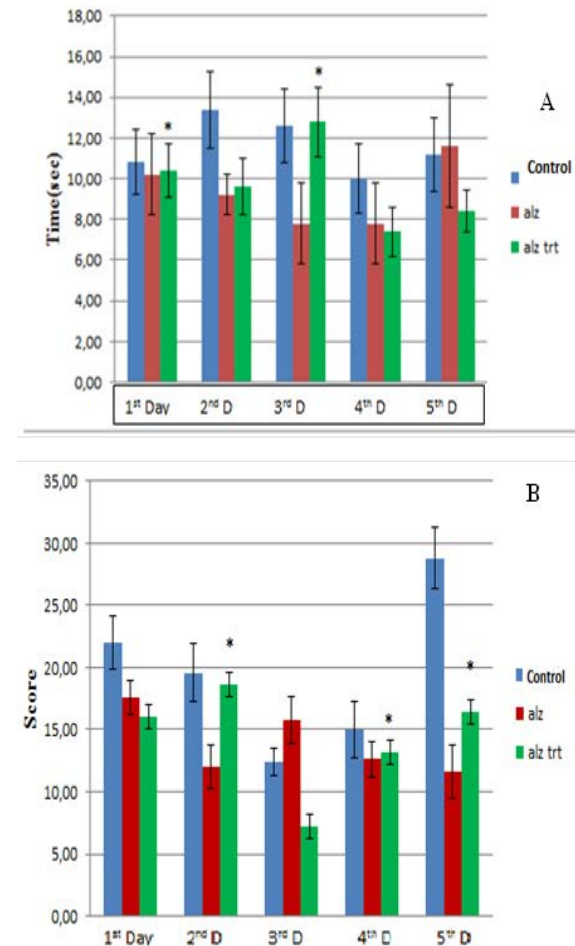


Figure 2: **A:** Work Spatial Memory; Morris aquatic test: Control mice(contr), Alzheimer's model (alz) by $AlCl_3$ (100 mg/kg)Or& D-Gal (200mg/Kg) IP and the Treated Alzheimer's with the ethanol extract of *H. thymbrifolium* (200mg/kg) orally for three months. **B:** Reference Spatial Memory; maze 8 arms test: Control mice(contr), Alzheimer's model (alz) by $AlCl_3$ (100 mg/kg)Or& D-Gal (200mg/Kg) IP and the Treated Alzheimer's with the ethanol extract of *H. thymbrifolium* (200mg/kg) orally for 3 months

3.3. Histological studies

Histological statute of nervous tissues of treated Alzheimer's in H&E staining shows that there are typical neuropathological changes in the cerebral cortex and hippocampus of Alzheimer's model, whereas the treated Alzheimer's tissues showed a shrunken decreased in all brain compartments, shows moderated neuropathological changes improved by *Hypericum thymbrifolium* administrated in parallel of $AlCl_3$.

In the control groups, the neurons were full and arranged tightly, and the nuclei were light stained. By comparison with the Alzheimer's model, the cytoplasm of neurons were shrunken, the nuclei were side moved and

dark stained, neurofibrillary degeneration and neuron loss were well identified in Alzheimer's group observed in the cerebral cortex in addition to the observed effect in the hippocampal tissues.

Hypericum thymbrifolium administration induced the neuron's protection showed in characteristic shape conservation, with reducing neurofibrillary tangles (Figure 3).

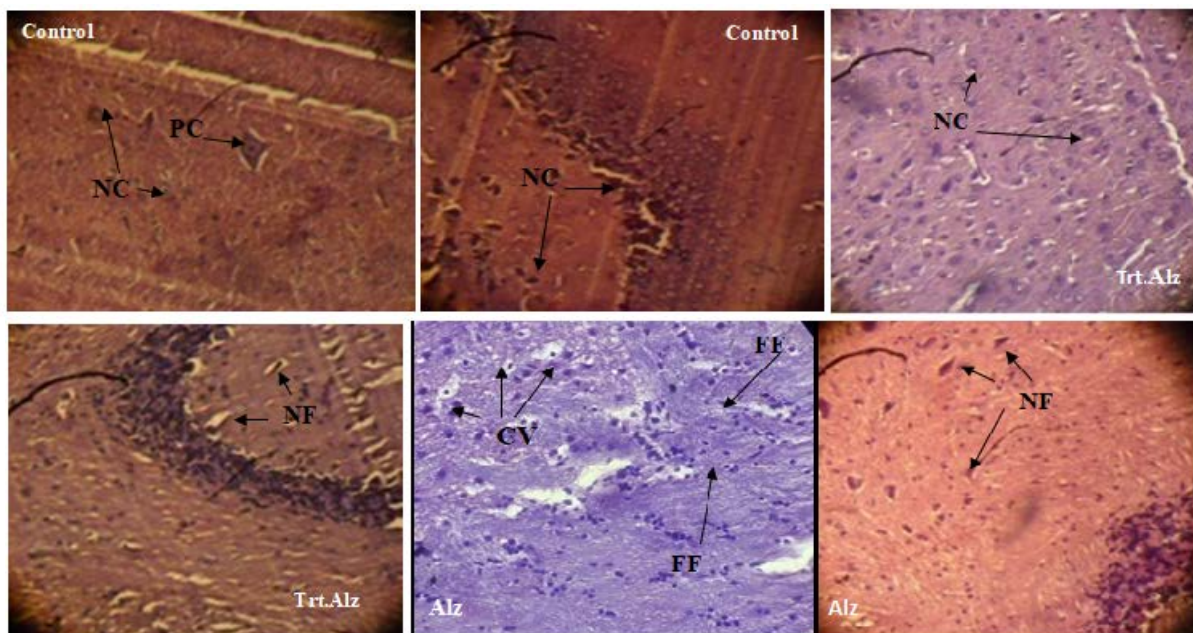


Figure 3: Microscopic study of nervous tissues of 2µm performed by H&E staining in cerebral cortex & Hippocampus of control mice (Contr); Alzheimer's mice AlCl₃ orally (100 mg/kg) and treated Alzheimer's mice (alz.trt) with the ethanol extract of *H. thymbrifolium* (200 mg/kg) for 3 months (G×400). (alz) cerebral cortex & Hippocampus characterized by a decrease in cell density and neuronal vacuolization (G×400), treated Alzheimer's (alz.trt) shows a decrease of vacuolization and a normal cells density in (G×400). NC: Normal Cell; PC: Purkinje cell; CV: Cell Vacuolisation; NF: Neurofibrillary tangles; FF: Fibrillary Form

4. Discussion

Neurodegenerative diseases are largely spread without any difference in age; they affect the young people as well as the old and are characterized by progressive pathological changes in the brain that translate into clinical signs of decline in cognitive abilities (memory), functional abilities, mood, and behavior. This pathogenesis is the result of the invasion of some contaminants, including heavy metal which we can classify Aluminum.

Alzheimer's pathological changes in the brain are characterized by deterioration and loss of neurons (nerve cells) leading to brain atrophy (Rodger L. et al., 2017).

Some solutions are actually used, but they could not resolve that neuronal loss, else the phytotherapy showed a large improvement and decrease the rate of Amyloid beta reaction cascade.

Antioxidant effects of some dietaries cooperate with the body enzymes to protect the brain from free radical damage (Piccaglia, R. et al., 1998). *Hypericum thymbrifolium* is largely used in turkey as a kind of tea, Esra et al found that this species is very rich in phenolic compounds (Trifunovic S. et al., 1998; Radulovic N. et al., 2007; Esra Eroglu et al 2018), which report a rate of this latter of 20.7 mg / g dry weight (DW). In the same previous study, the *in vitro* antioxidant activity was measured by the lipoperoxidase inhibitory power LPO test as well as the scavenging of the free radical DPPH; the results gave a relevant capacity on the LPO (4.39 ± 0.08^a) as well as DPPH scavenging (0.622 ± 0.051^a) at 50% concentration (Esra Eroglu et al 2018). That potent antioxidant activity is involved in the *in vivo* results. This

result is explicated physiologically by increasing antioxidant enzymes and the important anticholinesterase activity ($63.41 \pm 3.29a$) (Esra Eroglu et al., 2018), that conduced to a mental improvement at behavior and memory capabilities (Olton DS . et al., 1981; Sahin, G. et al., 1994), and as another benefit, this extract also have low or no side effects (Esra Eroglu et al., 2018 ; Olton DS . et al., 1981; Sahin, G. et al., 1994).

Alzheimer's was induced by Aluminum chloride (AlCl₃) orally at 100 mg/kg/day in drinking water with IP D-Gal (200mg/kg), another group Alzheimer's model was treated with the ethanolic extract of *H.thymbrifolium* orally (200 mg/kg/day) and the control group received drinking water only during 3 months.

In this investigation, the effect of *H.thymbrifolium* against Alzheimer's disease explained with behavior improvement as the memory and learning in mice tested by neurologic experiments (Olton DS. Et al.,1981) In the forced swimming test, the recorded immobility time is reduced in the Alzheimer mice compared to the other groups of mice, knowing that the immobility time in treated Alzheimer group is very close to the control group which coincides with the result of Sahin et al. (Sahin G. et al., 1994). The hole test was used to evaluate the exploration behavior exhibited by the Alzheimer's mice; for this purpose it was noted during the test that the Alzheimer's model mice are less exploratory than the treated Alzheimer's and control mice, contrary to what was found in Djebli & Rebai's work (Djebli N. and Rebai W.2008). The working spatial memory test showed that the control groups and the treated Alzheimer are more motivated than the Alzheimer's; the reference spatial memory (RSM) of control and treated Alzheimer's mice are

improved, the difference was shown by spending a short time finding the platform in the first four days unlike the Alzheimer's group (Bizon J.L. et al., 2009). In the same side of the *in vivo* study, we noted in histological study, a reducing in the fibrin form of amyloid beta in brain tissue, conduced to enhancing behavior, memory improvement and reduction of neurotoxicity in Alzheimer's disease that appeared in contrary with decreasing of cell density, deformity in tissue and fibrillary form of cell deposits (amyloid-beta). These brain moderation changes by *H. thymbrifolium* were explained by reducing oxidative damage which contributes to disease pathogenesis and AChE inhibition, were in accordance with the aim of this study which is to prove the antioxidant effect of the selected species against Alzheimer's disease, appeared in behavioral, memory and histological studies (Esra Eroglu et al 2018; Müller WE. 2006; Langosch, J. M. et al., 2002).

5. Perspectives

The mechanism of the response and the level of this moderating effect are not investigated in this study; that still needs other *in vivo* and *in vitro* studies in order to understand this treatment effect, than valorizing it to resolve health problems, which could not be resolved with the chemical treatment.

Conflict of interests

There is no conflict of interests.

References

- Bizon J.L., LaSarge C.L., Montgomery K.S., McDermott A.N., Setlow B., and Griffith W.H. 2009. Spatial reference and working memory across the lifespan of male Fischer 344 rats. *Neurobiol Aging*. **30**(4): 646–655.
- Djebli N et Rebai .,2008. "Chronic Exposure to Aluminum Chloride in Mice: Exploratory Behaviors and Spatial Learning. *Adv Biolo Res*. **2**(1-2): 26-33.
- Esra Eroglu Ozkan, Nurten Ozsoy, Tugba Yilmaz Ozden, Gul Ozhan and Afife Mat 2018. Evaluation of Chemical Composition and In-vitro Biological Activities of Three Endemic Hypericum Species from Anatolia (*H. thymbrifolium*, *H. spectabile* and *H. pseudolaevae*). *Iranian J Pharm Res*. **17**(3): 1036-1046
- Langosch, J. M., Zhou, X.-Y., Heinen, M., Kupferschmid, S., Chatterjee, S. S., Nöldner, M., & Walden, J. 2002. St John's wort (*Hypericum perforatum*) modulates evoked potentials in guineapig hippocampal slices via AMPA and GABA receptors. *European neuropsychopharmacology. J Euro College Neuropsychopharmacology*, **12**(3): 209-16.
- Magali Dumont, M. Flint Beal 2011. Neuroprotective strategies involving ROS in Alzheimer disease. *Free Rad Biol Med*. **51**(5):1014-26
- Markesberry&Carney 1999. Oxidative alterations in Alzheimer's disease. *Brain Path*. **9**(1):133-46.
- Moreira, P. I., A. Nunomura, M. Nakamura, A. Takeda, J. C. Shenk, G. Aliev, M. A. Smith and G. Perry 2008. Nucleic acid oxidation in Alzheimer disease. *Free Rad Biol Med*. **44**(8): 1493-505.
- Müller WE. 2006. St John's wort and its active principles in depression and anxiety. *Basel J Med Chem*. **49**: 5026–7.
- Olton DS, Feustle WA. 1981. Hippocampal function required for non-spatial working memory. *Exp Brain Res*. **41**: 380–389.
- Per M. Roos; Olof Vesterberg; Monica Nordberg 2006. Metals in Motor Neuron Diseases. *Exp Biol Med*. **231**(9): 1481-1487
- Persolt, R.D. Jalve, M. 1977. Poison M A new model sensitive to antidepressant treatment. *Nature*. **266**:730–732.
- Piccaglia, R., Marotti, M., Giovanelli, E., Deans, S.G., Eaglesham, E. 1993. Antibacterial and antioxidant properties of Mediterranean aromatic plants. *Ind Crops Prod*. **2**: 47–50.
- Radulovic, N., Stanko Jovanovic, V., Stojanovic, G., Smelcerovic, A., Spittler, M., Asak wa, Y. 2007. Screening of in vitro antimicrobial and antioxidant activity of nine Hypericum species from the Balkans. *Food Chem*. **103**(1): 15-21.
- Rodger L. Woodl and Andrew Worthington 2017. Neurobehavioral Abnormalities Associated with Executive Dysfunction after Traumatic Brain Injury. *Front Behavior Neurosciences*. **11**:195
- Sahin, G., Varol, I. and Temizer, A., 1994. Determination of aluminum levels in the kidney, liver and brain of mice treated with aluminum hydroxide, *Biol. Trace*.
- Teresa Montiel, Ricardo Quiroz-Baez, Lourdes Massieu, Clorinda Arias 2006. Role of oxidative stress on β -amyloid neurotoxicity elicited during impairment of energy metabolism in the hippocampus: Protection by antioxidants. *Exp Neurol*. **200**(2), 496-508
- Trifunovic S, Vajs V, Macura S, Juranic N, Djarmati Z, Jankov R, Milosavljevic S. 1998. Oxidation products of hyperforin from *Hypericum perforatum*. *Phytochem*. **49**: 1305–1310.

RAPD analysis and field screening of bread wheat and barley accessions for resistance to cereal leafminer *Syringopais temperatella*

Ihab H. Ghabeish^{1,*}, Firas A. Al-Zyoud² and Dhia S. Hassawi³

¹Department of Agricultural Sciences, As-Shoubak University College, Al-Balqa Applied University, Jordan; ²Department of Plant Protection and Integrated Pest Management, Mutah University, Karak 61710, Jordan; ³Department of Biology, Al-Anbar University, Al-Anbar, Iraq.

Received: June 23, 2020; Revised: September 3, 2020; Accepted: September 8, 2020

Abstract

(*Syringopais temperatella* Led.) is a threat to wheat and barley. Resistant varieties are preferable due to environmental and human considerations and for their sustainability. However, no attention has been focused on resistant studies against cereal leafminer worldwide. Concomitantly, this study aimed at screening wheat and barley accessions as sources of *S. temperatella* resistance under semi-arid conditions of Karak-Jordan. It was also designed to evaluate the RAPD markers potential for identifying the accessions based on their resistance. The rank accessions order resulted from least to most according to infestation percentage and presence of larvae on leaves: Acsad 1245 (wheat), Acsad 1273 (wheat), 1614 (barley) and Umkais (wheat). The rank order of the same accessions from most to least according to grain yield and straw biomass: 1614, Acsad 1245, Umkais and Acsad 1273. Data on DNA (RAPD) markers revealed higher polymorphism level among accessions. Two hundred bands were noticed; and 199 were polymorphic. Total number of amplification products/primer ranged from 16 with primer (OPI-08) to 25 with primer (OPA-10), and the PCR size products ranged between 200-3500 bp.

Keywords: Cereal leafminer, varieties identification, RAPD markers, resistant accessions, *Syringopais temperatella*

1. Introduction

Wheat and barley are important crops in semi-arid and arid regions of Jordan (Al-Bakri *et al.*, 2011). Yield gained in these regions is low and variable from year to year due to insufficient rainfall and bad distribution (FAO, 2011). Wheat and barley varieties grown in Jordan differ from one area to another, and their productivity depends on the average amount of rainfall and severity of pest attack. In Jordan, low yield or/and crop failure are common (Einfeldt, 1999), and thus Jordan is not self-sufficient in wheat and barley production, depending on imports to cover the national needs (Al-Ghazawi *et al.*, 2019; Jordan Statistical Yearbook, 2018).

Several abiotic (mainly drought, salinity and low soil fertility) and biotic factors (i.e. soil-borne diseases and insect pests) limit wheat and barley production (ICARDA, 2007). Dozens of insects' attack wheat and barley, and many of these pests cause neglected damage, others cause considerable forage and yield reductions across international borders (El-Bouhssini *et al.*, 2009; Ennahli *et al.*, 2009). As cultural practices (as control measures) have many negative effects on the biotic and abiotic factors that would suppress the pest numbers, many levels of pests have an outbreak, wreaking huge damage to crops (Harlan, 1992). Nevertheless, many pests are difficult to control with conventional control measures, and because of the low inputs on these two cereal crops in non-developing countries, enough resources are not timely available (Srivastava *et al.*, 1988).

In many West Asian countries, *Syringopais temperatella* Led. (Lepidoptera: Scythrididae) is a major pest that attacks wheat and

barley, significantly damaging the crops (Jemsi and Rajabi, 2003; Al-Zyoud, 2013b; Al-Zyoud and Ghabeish, 2015). The pest is endemic to Jordan, being reported since 1960s (Klapperich, 1968). The pest has great significance effect on wheat and barley throughout Jordan, and outbreaks of this pest have been mostly reported in Karak District since 2001 (Al-Zyoud, 2013b). Despite the intensive applications of chemical insecticides against the pest, this did not prevent further crop damage and spread of the pest in Karak, (Al-Zyoud, 2013b). Wheat infestation by *S. temperatella* in Karak District has exceeded 70% in some fields (Al-Zyoud and Ghabeish, 2015). *S. temperatella* populations increased over the years because of frequent drought, not applying the proper crop rotation and unsuitable farmer practices (Al-Zyoud, 2012).

Because of the importance of wheat and barley in Jordan; control tactics of this plague are crucial. Intensive application of chemical insecticides has been used to suppress the pest (Jemsi and Rajabi, 2003; Al-Zyoud, 2013a). Synthetic insecticide usage is neither economically feasible nor ecologically friendly; causing many side effects on humans and the environment (Gerson and Cohen 1989). In addition, the insecticides' use on wheat and barley has typically lagged as low-input crops owing to the cost constraints associated with these two crops (Debach and Rosen, 1991). As the agricultural community became increasingly aware of the negative effects of continuous reliance on chemicals, the idea that control of pests can be based on sound ecological principles reemerged. One of the most important control methods in such low-input crops is the use of resistant varieties. Finding such resistant varieties to agricultural pests are the main goal of wheat and barley breeders nowadays (Smith and Clement, 2012; Razmjou *et al.*, 2014).

* Corresponding author e-mail: ghabeish@bau.edu.jo.

Molecular biology methods are used for varieties identification and differentiation among species. Molecular markers could directly detect variations of the DNA sequences among cultivars independent of environmental effects and allow genotypes identification during earlier stages of plant development (Tar'an *et al.*, 2005). Different molecular-marker techniques have been used for accessing the genetic diversity in plants. The random amplified polymorphic DNA (RAPD) technique is used to determine the polymorphism of genomic DNA (Maric *et al.*, 2004; Sapna *et al.*, 2007), and is successfully used for wheat resistant studies (Iqbal *et al.*, 2007; Sapna *et al.*, 2007), and barley (Tinker *et al.*, 1993). The RAPD markers are dominant markers and because of its simplicity and speed, RAPD technique has been used for diversity analysis in many crops (Hernandez *et al.*, 2001; Zenglu and Randall, 2001; Mezghani-Khemakhem *et al.*, 2012).

However, no attention has been paid to studies on wheat and barley resistance to the cereal leafminer in Jordan and surrounding countries. Concomitantly, screening many wheat and barley accessions under field and laboratory conditions to investigate sources of resistance for wheat and barley to *S. temperatella* under semi-arid climatic conditions of South Jordan was our main goal. Thus, the outcomes of the current study could develop proper low cost and environmentally friendly integrated pest management (IPM) program to combat the cereal leafminer. Additionally, this research was designed to evaluate the potential of RAPD markers to determine the genetic diversity of accession included in this study.

2. Materials and Methods

2.1. *Syringopais temperatella* infestation in the field

Twenty-four accessions of bread wheat and three accessions of barley obtained from the Seed Bank of the National Agricultural Research Center (NARC, Baq'a, Jordan) were used in this study. The study was performed in a naturally *S. temperatella* infested field in Jordan, Al-Qasr, Karak area (Latitude of 31°11", Longitude of 35°42", and altitude of 845 m). The experimental site has semi-arid conditions with moderate rainfall; the long-term annual average is of 300 mm. The field soil was sandy clay loam with 1.63% organic matter.

Seeds of the different accessions were sown during the first week of December for the cropping seasons, 2011/2012 and 2012/2013 in a randomized complete block design (RCBD) with three replications. Each accession was sown in three rows (in 3 blocks), in which 30 g of seeds were sown/row of 2-m length with 25 cm spacing among rows. Seeds were directly irrigated after completion of sowing. Neither fertilizers nor insecticides were applied to the barley plants during the experiment. Routine cultural activities especially weeding have been performed every other week during seasons. Bird-net was used to prevent the plant ears from a possible attack by birds near the ripening stage of the plants. The percentage of leafminer's infestation was recorded early April for both cropping seasons. Three researchers have independently estimated the infestation percentage. In addition, the number of *S. temperatella* larvae/plant was counted. Moreover, grains and straw biomasses of all plants in each of the 3 rows (per season) for each accession were collected and weighed, then divided on the number of plants in the concerned row to find the grain and straw yields per plant.

2.2. Molecular analysis of the accessions

2.2.1. Samples collection and DNA extraction

Fresh leaf samples from each accession were collected from the wheat and barley plants and stored at -80°C for the molecular part. Then, the fresh leaves (3 g) were grounded into fine powder with liquid nitrogen. The powder was mixed with 20 ml of hot CTAB buffer (100 mM Tris-HCl, pH 8.0, 1.4 M NaCl, 20 mM EDTA, 2% CTAB, 1% PVP, 0.2% β-mercaptoethanol, 0.1% NaHSO₃). Following that, the samples were incubated in a water bath at 65°C for 1 h. After cooling at the room temperature for 10 min, equal volume of chloroform-isoamyl alcohol (24: 1) was added to each sample and gently mixed for 10 min. The samples were centrifuged at 15,000 rpm at 10°C for 15 min. The aqueous phase was transferred into a clean tube and mixed with an equal volume of cold absolute ethanol, and the tubes were kept stand at -20°C for 20 min. The samples were then gently mixed, and the precipitation was recovered with a glass rod. The precipitation was washed with 10 ml of 10 mM ammonium acetate in 76% ethanol, and then air-dried at the room temperature overnight. The samples were resuspended in 400 μl of TE buffer (10 mM Tris-HCl, pH 8, 0.1 mM EDTA). RNA that could interfere with PCR was digested with 2 μl of DNase-free RNase for each sample (Doyle and Doyle, 1987; Maguire *et al.*, 1994). The quality of DNA was estimated by calculating the ratio of the absorbance at 260 and 280 nm according to Johnson (1994).

2.2.2. Polymerase chain reaction (PCR)

A total of 10 RAPD primers (Operon Technologies, Inc) were used for PCR amplification. Amplification reactions were carried out in a total volume of 25 μl, containing 30-50 ng of genomic DNA, 1.5 mM MgCl₂, 0.25 μM 10-mer primer, 0.2 mM dNTPs, 1X PCR buffer from 10x buffer [100 mM Tris-HCl (pH 8), 500 mM KCl, 15 mM MgCl₂, 0.1% Difco Gelatin], 1 unit AmpliTaq DNA polymerase (Promega, Madison, Wis), and a drop of mineral oil to prevent evaporation. A control PCR mix containing all components, except the genomic DNA, was checked for DNA contamination. Each reaction was repeated at least twice for accuracy. The DNA amplification reactions were set up in a thermal cycler (Gene, UK) according to the following program: 1 min at 94°C for initial strand separation, followed by 40 cycles of 1 min at 94°C, then 2 min at 34°C, and 2 min at 74°C, and a final extension step of 5 min at 74°C.

2.2.3. Agarose gel electrophoresis

Amplified DNA fragments were separated on 1% agarose gel. Ethidium bromide was added to the gel to stain the DNA. The gel was viewed under ultraviolet (UV) light (BIO-RAD, USA), and then was photographed via a Video Polaroid Photograph Camera. A 100 bp-DNA ladder (Sigma Chemical Company, St. Louis) was used to estimate the molecular size of amplification products.

2.3. Statistical analysis

To validate the basic assumptions of the data to be statistically analyzed, the normal distribution and the homogeneity of variance were firstly evaluated using the Barlett method (Kohler *et al.*, 2002). After fulfilling the aforementioned two assumptions, analysis of variance was conducted using the Statistical Package Sigma Stat (SPSS) version 16.0 (Proc General Linear Model) (SPSS, 1997). For determining significant differences among means, least significant differences (LSD) test at a probability level of 0.05 was used (Abacus Concepts, 1991). Spearman's correlation analysis was performed to examine pair-wise association among the variables (number of larvae versus grain yield and straw biomass) (Zar, 1999). Data generating from

RAPD analysis were analyzed using the Nei similarity index (Nei and Li 1979). A dendrogram was constructed based on the similarity matrix data, by applying Unweighted Pair Group Method with Arithmetic Averages (UPGMA) cluster analysis using the Numerical Taxonomy System for personal computer (NTSYSpc) program (Exeter, Software, N.Y.).

3. Results

Results indicated that wheat and barley accessions varied in their susceptibility to the cereal leafminer. Averages of infestation level, number of larvae, grain yield and straw biomass showed significant differences among accessions (Tables 1&2). Results revealed that the wheat accessions, Acsad 1273 and 1245, as well as Umkais were the most resistant ones in terms of low percentage of infestation and minimal number of larval attacked plants foliage. The barley accession, 1614 (14.6% infestation) and Tadmur (15.9%) were significantly more resistant than Mutah (21.1%), and both were exhibited a low larval attack. On the contrary, the wheat accessions; 1115, 1069 and 1131 showed susceptibility based on infestation percentage and larval abundance on plant foliage. Moreover, Mutah barley accession showed susceptibility, but with a moderate number of larval attack. The harvested grain of the accessions tested, Acsad 1245 was the best one among the most wheat-resistant accessions; and located in the top 9 accessions from the standpoint of grain yield production. Furthermore, Acsad 1245 showed good straw biomass (1.86 g/plant). The most resistant barley accession, 1614 was one of the top 5 accessions from the standpoint of grain weight and one of the top 4 accessions in terms of straw biomass.

None of the resistant wheat accessions was promising in straw biomass produced. The most susceptible wheat accessions (1115 and 1131) were ranked of the worst 9 accessions in the weight of grains obtained. Results showed that the most susceptible barley accession; Mutah was the top barley accessions in grain yield production. The most susceptible accessions of wheat (Al-Raba) and barley (Mutah) showed the least straw biomass production. As expected, all the susceptible accessions were among the first-third accessions heavily attacked with the highest number of pest larvae.

Results of the Spearman correlation analysis showed significant relationship between the infestation% and the foliage larval number for wheat accessions, and showed non-significant

relationship for barley accessions. The relationship was moderately positive for wheat accessions and was weakly positive for barley accessions. Moreover, results showed significant negative relationships between foliage larval infestation and each of the grain yield and the straw biomass for wheat and barley accessions. Spearman coefficient values are higher in wheat accessions than in barley accessions (Table 2).

After an initial screening of several decamer primers available in the laboratory, amplification products of ten primers were selected for further analysis. The genomic DNA of twenty-seven wheat and barley accessions was amplified with these random 10 base arbitrary primers (Table 3). The primers that generated polymorphic amplification fragments were conspicuous and highly reproducible (Figures 1 and 2). The gel of each primer was separately analyzed by scoring the presence/absence of all fragments of PCR in individual lanes, where (+) was allocated for the presence of an amplified fragment, while (-) for its absence (Table 3).

Two hundred DNA fragments were generated by 10 random primers, averaging 20 bands/ primer. Some reactions were duplicated more than once for checking the amplified products' consistency. Among the 200 amplification products recorded, 199 bands (99.5%) were polymorphic, and only one band (0.5%) was monomorphic. The primer (OPA-10) produced the highest number of bands (25), while primer (OPI-08) produced the lowest number (16). The DNA fragments size ranged from 200 bp with primers (OPB-09) to 3500 bp with primer (OPI-08). The primer OPI-08 was the only one that generated fragments above 2000 bp molecular size (2500, 3000, and 3500 bp) with some of wheat accessions. In general, the three barley accessions (1614, Tadmur and Mutah) produced smaller fragments size ranging between 250 to 1500 bp. On the other hand, primers (OPH-15, OPJ-13 and OPK-2) generated more numbers of polymorphic bands with the aforementioned three barley accessions. RAPD data were used to produce dendrogram using cluster tree analysis, NTSYSpc (Figure 3). The 24 wheat accessions were grouped into two main clusters; the first one contained 23 accessions, while the second one contained the accession, Acsad 1129 only. The clustering pattern of the accession indicated that most of the accessions are closely related. This is expected to be caused by the selection of those accessions from a single population.

Table 1. Average (\pm SD) infestation percentage, grain yield, straw biomass and larvae number of wheat and barley accessions in both the 2011/2012 and 2012/2013 seasons.

No	Crop	Accession	Infestation (%)	Grain yield (g/plant)	Straw biomass (g/plant)	No. of larvae per plant
1	Wheat	Acsad 1273	10.6 \pm 2.69 a	0.21 \pm 0.18 abc	1.56 \pm 0.98 abcd	2.57 \pm 0.85 a
2	Wheat	Acsad 1245	13.7 \pm 4.41 ab	0.45 \pm 0.29 abcdef	1.86 \pm 0.94 bcde	2.51 \pm 1.52 a
3	Barley	1614	14.6 \pm 7.76 ab	0.53 \pm 0.35 cdef	2.08 \pm 0.89 cde	2.61 \pm 1.42 a
4	Wheat	Umkais	14.9 \pm 4.61 ab	0.32 \pm 0.27 abcdef	1.67 \pm 0.73 abcde	2.86 \pm 2.39 ab
5	Wheat	Acsad 1129	15.7 \pm 10.2 abc	0.13 \pm 0.07 a	1.85 \pm 0.44 bcde	3.21 \pm 1.56 abc
6	Barley	Tadmur	15.9 \pm 6.36 abc	0.49 \pm 0.21 bcdef	1.39 \pm 0.15 abc	2.36 \pm 1.24 a
7	Wheat	Acsad 1275	16.0 \pm 5.07 abc	0.16 \pm 0.10 ab	1.56 \pm 0.37 abcd	2.65 \pm 1.18 a
8	Wheat	Horani	17.1 \pm 6.19 abc	0.21 \pm 0.20 abc	1.96 \pm 0.29 bcde	2.34 \pm 1.31 a
9	Wheat	Horani Nawawi	17.3 \pm 9.16 abc	0.45 \pm 0.35 abcdef	2.09 \pm 0.40 cde	3.25 \pm 3.11 abc
10	Wheat	885	17.9 \pm 7.65 abc	0.63 \pm 0.30 ef	1.84 \pm 0.70 bcde	4.15 \pm 2.89 abc
11	Wheat	Al-Raba	18.5 \pm 5.53 abcd	0.39 \pm 0.16 abcdef	0.97 \pm 0.55 a	2.22 \pm 0.79 a
12	Wheat	Safra Maan	19.1 \pm 14.3 abcde	0.20 \pm 0.18 abc	2.35 \pm 0.90 de	2.51 \pm 1.82 a
13	Wheat	Sham 4	20.2 \pm 8.72 bcde	0.32 \pm 0.23 abcdef	1.65 \pm 0.86 abcde	2.85 \pm 1.04 ab
14	Wheat	Sham 1	20.3 \pm 9.22 bcde	0.37 \pm 0.26 abcdef	1.68 \pm 0.81 abcde	2.89 \pm 1.65 ab
15	Wheat	Amra	20.5 \pm 13.8 bcde	0.23 \pm 0.21 abcd	1.93 \pm 0.22 bcde	5.45 \pm 3.43 bc
16	Barley	Muta'h	21.1 \pm 9.82 bcdef	0.55 \pm 0.50 def	1.36 \pm 0.39 abc	3.89 \pm 2.05 abc
17	Wheat	Acsad 65	21.5 \pm 13.4 bcdef	0.32 \pm 0.22 abcdef	1.38 \pm 0.36 abc	3.11 \pm 2.53 abc
18	Wheat	Tari 885	22.1 \pm 5.52 bcdef	0.62 \pm 0.30 ef	1.83 \pm 0.30 bcde	2.84 \pm 1.31 ab
19	Wheat	1315	24.4 \pm 3.66 cdefg	0.32 \pm 0.31 abcdef	2.06 \pm 0.95 cde	3.57 \pm 2.63 abc
20	Wheat	Petra	26.4 \pm 7.75 cdefgh	0.26 \pm 0.22 abcd	1.97 \pm 0.99 bcde	5.67 \pm 5.04 c
21	Wheat	899	27.2 \pm 6.73 defgh	0.38 \pm 0.37 abcdef	1.40 \pm 0.80 abcd	4.33 \pm 2.94 abc
22	Wheat	981	27.5 \pm 10.7 defgh	0.65 \pm 0.31 f	1.57 \pm 0.21 abcd	3.07 \pm 1.65 abc
23	Wheat	Acsad 1187	27.8 \pm 8.41 efgh	0.41 \pm 0.15 abcdef	2.13 \pm 0.67 de	3.03 \pm 1.77 abc
24	Wheat	969	29.8 \pm 4.50 fgh	0.46 \pm 0.09 abcdef	1.97 \pm 0.73 bcde	3.88 \pm 1.36 abc
25	Wheat	1131	32.3 \pm 4.36 gh	0.30 \pm 0.26 abcde	2.05 \pm 0.47 cde	4.49 \pm 4.39 abc
26	Wheat	1069	33.0 \pm 6.94 gh	0.44 \pm 0.35 abcdef	2.03 \pm 0.75 cde	4.12 \pm 1.98 abc
27	Wheat	1115	33.6 \pm 6.21 h	0.24 \pm 0.11 abcd	1.24 \pm 0.23 ab	3.58 \pm 2.48 abc
LSD value			9.10	0.34	0.75	2.80

*Means with different letters in the same column are significantly different at 0.05

Table 2: Correlation analysis of larval population size of the leafminer *Syringopais temperatella* versus grain yield and straw biomass of the infested barley and wheat accessions during the 2011/2012 and 2012/2013 seasons.

Correlated variables	Spearman coefficient (r)	Significances
Barley:		
Infestation% vs. larval number	0.254	NS
Larvae vs. straw biomass	-0.781**	000
Larvae vs. grain yield	-0.721**	000
Wheat:		
Infestation% vs. larval number	0.440 **	000
Larvae vs. straw biomass	-0.589**	000
Larvae vs. grain yield	-0.593**	000

**Correlation is significant at the 0.01 level. NS: Not significant.

Table 3: Number of different size and monomorphic markers, and percentage of monomorphic and polymorphic markers generated by each of the ten primers with the 27 wheat and barley accessions.

Primer number	Primer sequence (5'-3')	No. of different size markers	No. of monomorphic markers	Monomorphic markers (%)*	Polymorphic markers (%)**
OPA-10	GTGATCGCAG	25	0	0%	100%
OPB-09	TGGGGGACTC	17	1	6%	94%
OPC-10	TGTCTGGGTG	18	0	0%	100%
OPD-12	CACCGTATCC	20	0	0%	100%
OPG-02	GGCACTGAGG	18	0	0%	100%
OPH-15	AATGGCGCAG	22	0	0%	100%
OPI-08	TTTGCCCGGT	16	0	0%	100%
OPJ-13	CCACACTACC	22	0	0%	100%
OPK-02	GTCTCCGCAA	20	0	0%	100%
OPO-02	ACGTAGCGTC	21	0	0%	100%
Total	-	199	1	0.5%	99.5%

*Calculated by dividing the number of common markers among accessions on the total number of markers produced by each primer.

**Calculated by subtraction the % of monomorphic markers from 100%.

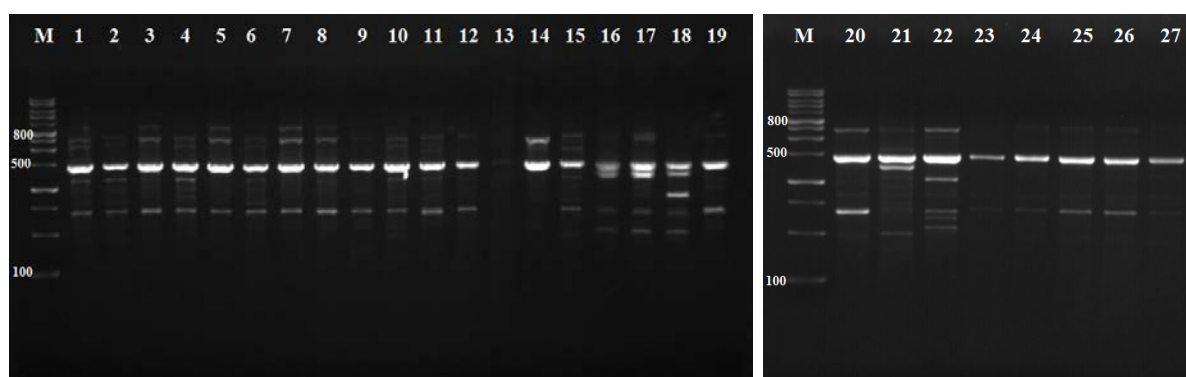


Figure 1: RAPD PCR products profile of wheat and barley accessions with primer OPI-08. M = Marker, 1 = wheat 981, 2 = wheat 1131, 3 = wheat Horani Nawawi, 4 = wheat Al-Raba, 5 = wheat Safra Maan, 6 = wheat 1069, 7 = wheat Sham 4, 8 = Acsad 1187, 9 = wheat Umkais, 10 = wheat 885, 11 = wheat Tari 885, 12 = wheat Horani, 13 = wheat Petra, 14 = wheat Amra, 15 = wheat 1115, 16 = barley Mutah, 17 = wheat Acsad 1129, 18 = barley Tadmur, 19 = wheat Sham 1, 20 = Acsad 1275, 21 = barley 1614, 22 = wheat 1315, 23 = wheat 969, 24 = wheat Acsad 65, 25 = wheat Acsad 1273, 26 = wheat Acsad 1245, 27 = wheat 899.

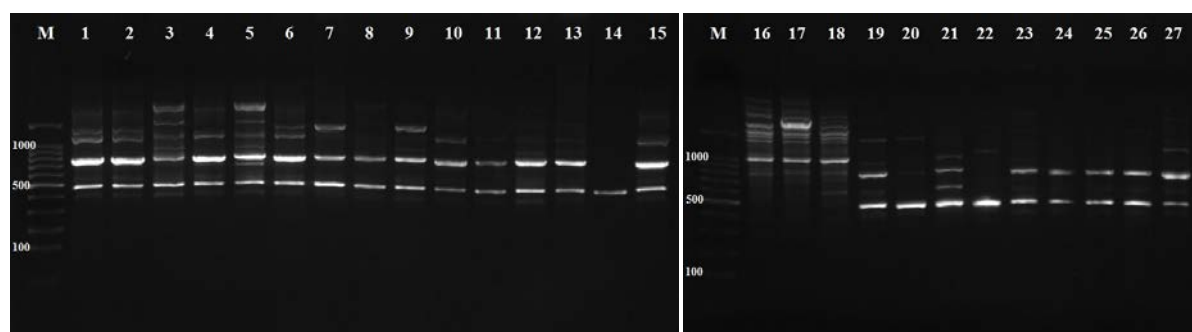


Figure 2: RAPD PCR products profile of wheat and barley accessions with primer OPJ-02. M = Marker, 1 = wheat 981, 2 = wheat 1131, 3 = wheat Horani Nawawi, 4 = wheat Al-Raba, 5 = wheat Safra Maan, 6 = wheat 1069, 7 = wheat Sham 4, 8 = Acsad 1187, 9 = wheat Umkais, 10 = wheat 885, 11 = wheat Tari 885, 12 = wheat Horani, 13 = wheat Petra, 14 = wheat Amra, 15 = wheat 1115, 16 = barley Mutah, 17 = wheat Acsad 1129, 18 = barley Tadmur, 19 = wheat Sham 1, 20 = Acsad 1275, 21 = barley 1614, 22 = wheat 1315, 23 = wheat 969, 24 = wheat Acsad 65, 25 = wheat Acsad 1273, 26 = wheat Acsad 1245, 27 = wheat 899.

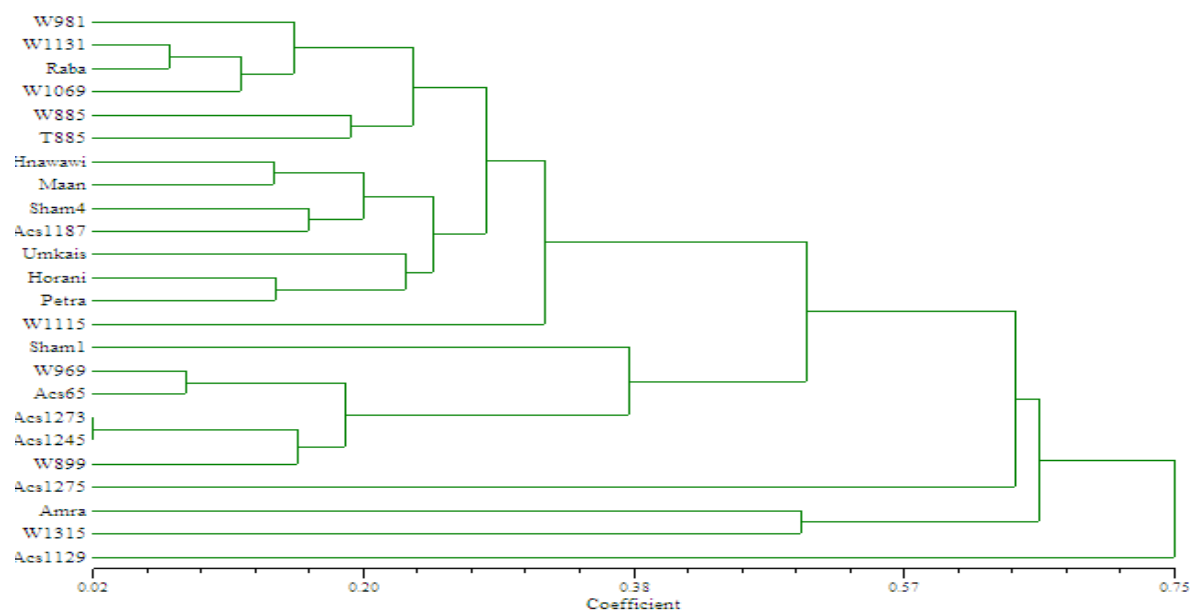


Figure 3: Dendrogram illustrating genetic relationships among 24 wheat accessions generated from RAPD data.

4. Discussion

Breeding of wheat and barley resistant varieties is of vital importance for cereal growers, since cereal crops characterizing by relatively low financial returns, and thus, costly control measures is considered undesirable. Resistant varieties usage against agricultural pests of such crops does not entail extra cost, and the only cost is the price of the seeds, and thus the use of these varieties is a desirable practice for their effectiveness, safe to environment (Singh and Weigand, 2006), and durable as well. Smith and Clement (2012) mentioned that arthropod-resistant for rice and sorghum cultivars and, to a lesser extent, wheat and raspberry cultivars are major elements of IPM programs throughout the world. Hence, this study aspires to constitute the first step for the development of resistant varieties to *S. temperatella*.

The current results indicated that some accessions, especially Acsad1273 (as it has higher resistance than 1245) (wheat) and 1614 (barley) are promising, based on the field resistance score, and could be useful as genetic source materials for further studies in breeding programs for producing *S. temperatella*-resistant cultivars. The aforementioned accessions indicated low infestation level, high grain yield and straw biomass as well as few numbers of larval populations attacking their foliage, and this is confirmed by the results of the correlation analysis; Spearman coefficients are relatively high for barley (0.78 for straw and 0.72 for grain yield vs. larvae number), and of moderate values for wheat (0.58 for straw and 0.59 for grain yield). Furthermore, results of the correlation analysis explained the low grain yield and straw biomass in the susceptible accessions which is due to the larger larval population size of the leafminer attacked their foliage and vice versa for the resistant accessions. Nevertheless, accession resistance to *S. temperatella* might be due to plant physical barriers, or variations in plant chemical composition (Al-Zyouod et al., 2009; 2015). Moreover, the accession's genetic make-up might also stand behind *S. temperatella* resistance. Although, no accession tested was completely immune to *S. temperatella*, some accessions indicated a type of resistance that is promising to the cereal leafminer and could be used in a future breeding program. Al-Zyouod et al. (2009), however, found susceptibility variations

in 12 cultivars of wheat and barley to the pest, in which Acsad 65 (wheat) and Athroh (barley) had pest resistance more than the rest of the tested cultivars. In addition, in Iraq, it was reported that Sham 6 (wheat) is more resistant to the pest, whereas Tell-After 3, Karunya and Om Rabee showed less resistance to *S. temperatella* (ICARDA, 2007).

Ten RAPD primers were selected and used in this study. The number of reproducible polymorphic fragments for wheat accessions with primers ranged between one band such as in the wheat accessions, Petra and Amra with primer OPI-08 and OPJ-13, respectively to twelve bands for the wheat accessions, Acsad 65 with primer OPA-10 and Al-Raba with primer OPO-02. For barley accessions, the number of bands ranged from three for 1614 and Tadmur with primers OPG-02 and OPO-02, respectively to twelve bands for Mutah with primer OPH-15 and Tadmur with primer OPJ-13. The fragment size ranged between 200 bp for primer OPB-09 with the accessions; wheat Tari 885, wheat Amra and barley 1614 to 3500 bp for primer OPI-08 with the wheat accessions; Horani Nawawi, Safra Maan, Sham 4, and Acsad 1187.

The PCR amplification products allowed us to investigate the genetic relationship of the accessions. The total number of bands scored for the ten primers was 200. The relatively large number of polymorphic bands (199) obtained with these primers is consistent with the earlier findings of Maric et al. (2004) and Sapna et al. (2007), who reported that both wheat and barley are highly polymorphic plant species. The results of this study revealed that the diversity of wheat and barley, which is displayed by the 27 accessions could be attributable to evolutionary forces like selection, mutation, migration and genetic drift that act continuously and result in continuous changes in allelic frequency in a population as well as genetic diversity.

All amplification patterns obtained with the ten primers were clear, but the intensity was not the same after being illustrated under UV. It is suggested that intensity of the band might reflect differences in the copy number of the amplified sequence among the different accessions (Yang and Quiros, 1993).

Genetic diversity is referred to the diversity present within different genotypes of same species. RAPD analysis indicated that wheat Acsad 1273 and Acsad 1245 are closely related to each other, as they showed similar pattern with the different RAPD

primers, and they are far related to wheat Acsad 1129; this also proved in the different RAPD patterns of this accession compared to the other two mentioned above. These three accessions showed lowest infestation%. However, RAPD patterns in this study revealed the genetic diversity of the whole genome of the accessions and not similarity or diversity of single gene polymorphisms for resistance to leafminer. RAPD primers are random and not specific; to acquire a molecular marker closely linked to leafminer resistant gene, a saturated genetic linkage map is required using other molecular markers techniques such as Amplified Fragment Length Polymorphism (AFLP), Single Nucleotide Polymorphisms (SNPs), Simple Sequence Repeats (SSRs), and Restriction fragment length polymorphism (RFLP), ...etc., which is beyond the scope of this study.

The existence of genetic diversity among wheat and barley accessions used in this study may serve as the source of desirable alleles and may assist plant breeders in breeding for leafminer resistant and new insect-pests. Additionally, the presence of genetic diversity among these accessions may permit breeders to select superior genotypes to be used as parents in hybridization programs.

5. Conclusions

None of the accessions checked in the current study have been immune to *S. temperatella*; however, some accessions were found having a promising degree of resistance to the pest infestation, which could be exploited in future breeding programs. Depending on pest infestation level and number of larvae on plants, the rank order of accessions from least to most was as follows: Acsad 1245 (wheat), Acsad 1273 (wheat), 1614 (barley) and Umkais (wheat). The rank order of the same accessions from most to least from the standpoint of grain yield and straw biomass produced was 1614, Acsad 1245, Umkais and Acsad 1273. The plant materials used in this study are well adapted to our region; thus, they could be directly used as genetic resources without any further adapting.

Genetic diversity revealed by RAPD analysis and dendrogram results for wheat accessions in relation to field resistance to leafminer indicated that accession Acsad 1129 is far related to two other accessions, Acsad 1273 and Acsad 1245; also, the three accessions showed least Infestation%. For future leafminer breeding programs and for fast and efficient release of leafminer resistant variety, accession Acsad 1129 can be crossed with Acsad 1273 as first choice and Acsad 1129 with Acsad 1245 as second choice for this purpose. RAPD analysis can help plant breeders in deciding on selecting parents in breeding programs, which otherwise is not possible to perform based solely on field resistance.

Acknowledgments

The authors express genuine thanks to the Scientific Research Support Fund (SRSF), Amman, Jordan for financially supporting this study.

References

Abacus Concepts. 1991. **SuperAnova User's Manual**, Version 1.11, Abacus Concepts, Berkeley, CA.

Al-Bakri J, Suleiman A, Abdulla F and Ayad J. 2011. Potential impact of climate change on rainfed agriculture of a semi-arid basin in Jordan. *Phys Chem Earth Parts A/B/C*. **36(5)**: 125-134.

Al-Ghzawi A, Al-Ajlouni Z, Al Sane K, Bsoul Y, Musallam I, Bani Khalaf Y, Al-Hajaj N, Al Tawaha A, Aldwairi Y and Al-

Saqqar H. 2019. Yield stability and adaptation of four spring barley (*Hordeum vulgare* L.) cultivars under rainfed conditions. *Res Crops*. **20(1)**: 10-18.

Al-Zyoud F. 2012. Effect of field history on the cereal leafminer *Syringopais temperatella* Led. (Lep., Scythrididae) and its preference to different wheat and barley cultivars. *Pak J Biol Sci*. **15**: 177-185.

Al-Zyoud F. 2013a. Efficacy of insecticides' applications against the cereal leafminer *Syringopais temperatella* Led. (Lep., Scythrididae) on barley under field conditions in Karak-Jordan. *Dirasat Agric Sci*. **39**: 65-74.

Al-Zyoud F. 2013b. Towards integrated pest management of the cereal leafminer *Syringopais temperatella* Led. (Lep., Scythrididae): Status, current and future control options. *Am-Eur J Agric Environ Sci*. **13**: 1582-1594.

Al-Zyoud F and Ghabeish I. 2015. Significance of the larval population size of the cereal leafminer *Syringopais temperatella* Led. (Lep., Scythrididae) and the diapausing depth in the soil on the yield variables of wheat and barley. *Jordan J Agric Sci*. **11**: 725-734.

Al-Zyoud F, Hassawi D and Ghabeish I. 2015. Oxalic acid as an alienate factor for wheat and barley resistance to cereal leafminer *Syringopais temperatella* (Lederer, 1855) (Lepidoptera: Scythrididae). *SHILAP Revta lipid*. **43**: 113-123.

Al-Zyoud F, Salameh N, Ghabeish I and Saleh A. 2009. Susceptibility of different varieties of wheat and barley to cereal leafminer *Syringopais temperatella* Led. (Lep., Scythrididae) under laboratory conditions. *J Food Agri Environ*. **7**: 235-238.

Debach P and Rosen D. 1991. **Biological control by natural enemies**. Cambridge University Press, Cambridge, UK.

Doyle JJ and Doyle JL. 1987. A rapid isolation procedure for small quantities of fresh leaf tissue. *Phytochem. Bul*. **19**: 11-15.

Einfeldt CHP. 1999. Effects of heterozygosity and heterogeneity on yield and yield stability of barley in the dry areas of north Syria. Ph.D. Dissertation, University of Hohenheim, Stuttgart, Germany.

El-Bouhssini M, Street K, Joubi A, Ibrahim Z and Rihawi F. 2009. Sources of wheat resistance to Sunn pest *Eurygaster integriceps* Put in Syria. *Evol*. **56**: 1065-1067.

Ennahli S, El-Bouhssini M, Grandi S, Anathakrishnan R, Niide T, Starkus L, Starkey S and Smith CM. 2009. Comparison of categories of resistance in wheat and barley genotypes against biotype 2 of the Russian wheat aphid *Diuraphis noxia* Kurdjumov. *Arthrop Pl Interact*. **3**: 45-53.

FAO. 2011. **Production Yearbooks**.

Gerson U and Cohen E. 1989. Resurgence of spider mites (Acari: Tetranychidae) induced by synthetic pyrethroids. *Exp Appl Acarol*. **6**: 29-46.

Harlan JR. 1992. **Crops and man**. Second ed., American Society of Agronomy, Madison, Wisconsin, USA.

Hernandez P, Rosa R, Rallo L and Dorado G. 2001. Development of SCAR markers in olive (*Olea europaea*) by direct sequencing of RAPD products: Application in olive germplasm evaluation and mapping. *Theor App Genet*. **103**: 788-791.

ICARDA. 2007. Iraq-ICARDA-Australia Project: Better crop germplasm and management for improved production of wheat, barley and pulse and forage legumes in Iraq. 2nd Technical Report, ICARDA, Aleppo, Syria.

Iqbal A, Khan AS, Khan FS, Ahmad A and Khan AA. 2007. Study of genetic divergence among wheat genotypes through random amplified polymorphic DNA. *Genet Mol Res*. **6**: 476-481.

- Jemsi G and Radjabi G. 2003. Study on harvesting agronomic measures and effect of chemical application in controlling the cereal leafminer *Syringopais temperatella* Led. (Lep., Elachistidae) in Khuzestan province. *App Entomol Phytopath.* **70**: 45-61.
- Johnson JL. 1994. Similarity analysis of DNAs. In: *Methods for general and molecular bacteriology*, (Gerhardt P, Murray RGE, Wood WA and Krieg NR., Eds). American Society for Microbiology, Washington, D. C., USA.
- Jordan Statistical Yearbook. 2018. Department of Statistics/**Annual Agriculture Surveys**. http://www.dos.gov.jo/dos_home_a/main/cd_yb2011/pdf/agri.pdf
- Klapperich J. 1968. Entomologisch und wirtschaftlich bedeutsame Schadinsekten in der jordanischen Landwirtschaft. *J Pest Sci.* **41**: 164-168.
- Kohler W, Schachtel W and Voleske P. 2002. **Biostatistik**. Springer-Verlag, Berlin.
- Maguire TL, Collins G, and Sedgley M. 1994. A modified CTAB DNA extraction procedure for plants belonging to family *Proteaceae*. *Plant Molecular Biology Reporter.* **12**: 106-109.
- Maric S, Bolaric S, Martincic J, Pejic I and Kozumplik V. 2004. Genetic diversity of hexaploid wheat cultivars estimated by RAPD markers, morphological traits and coefficients of parentage. *Pl Breed.* **123**: 366-369.
- Mezghani-Khemakhem M, Bouktila D, Kharrat I, Makni M and Makni H. 2012. Genetic variability of green citrus aphid populations from Tunisia assessed by RAPD markers and mitochondrial DNA sequences. *Entomol Sci.* **15**: 171-179.
- Nei M. and Li WH. 1979. Mathematical model for studying genetic variation in terms of restriction endonucleases. *Proc Natl Acad Soc.* **76**: 5269-5273.
- Razmjou J, Hemati SA and Naseri B. 2014. Comparative performance of the cotton bollworm *Helicoverpa armigera* Hubner (Lep., Noctuidae) on various host plants. *J Pest Sci.* **87**: 29-37.
- Sapna G, Pushpa K, Rekha M, Jain S and Jain RK. 2007. Assessment of genetic diversity among some Indian wheat cultivars using random amplified polymorphic DNA (RAPD) markers. *Ind J Biotech.* **6**: 18-23.
- Singh KB and Weigand S. 2006. Registration of three leafminer-resistant chickpea germplasm lines: ILC 3800, ILC 5901 and ILC 7738. *Crop Sci.* **36**: 472-472.
- Smith CM and Clement SL. 2012. Molecular bases of plant resistance to arthropods. *Ann Rev Entomol.* **57**: 309-328.
- SPSS. 1997. **Sigmastat Statistical Software Users Manual**. Statistical Product and Service Solutions Inc., Chicago, United States.
- Srivastava JP, Miller RH and van Leur. JAG. 1988. **Biotic stress in dry land cereal production: The ICARDA perspective**. In: Unger PW, Jordan WR and Sneed TV.
- Tar'an B, Zhang C, Warkentin T, Tullu A and Vandenberg A. 2005. A genetic diversity among varieties and wild species accessions of pea (*Pisum sativum* L.) based on molecular markers, and morphological and physiological characters. *Genome.* **48**: 257-272.
- Tinker NA, Fortin MG and Mather DE. 1993. Random amplified polymorphic DNA and pedigree relationship in spring barley. *Theor Appl Genet.* **85**: 976-984.
- Zenglu L and Randall LN. 2001. Genetic diversity among soybean accessions from three countries measured by RAPDs. *Crop Sci.*, **41**: 1337-1347.
- Yang X and Quiros C. 1993. Identification and classification of celery cultivars with RAPD markers. *Theor Appl Genet.* **86**: 205-212.
- Zar J. 1999. **Bio-Statistical Analysis**. Prentice Hall, Upper Saddle River, NJ, pp 663.

Cadmium and Lead Concentrations in Water, Sediment, Fish and Prawn as Indicators of Ecological and Human Health Risk in Santubong Estuary, Malaysia

Adriana Christopher Lee¹, Farah Akmal Idrus^{1,*}, Fazimah Aziz¹

¹Faculty of Resource Science and Technology, Universiti Malaysia Sarawak, 94300 Kota Samarahan, Sarawak, Malaysia;

Received: July 3, 2020; Revised: August 17, 2020; Accepted: September 16, 2020

Abstract

Cadmium (Cd) and lead (Pb) are toxic heavy metals with a growing appeal for study due to their ability to bioaccumulate in fish which may pose threat to human health through fish consumption. This study reported the concentration of Cd and Pb in water, sediment, fish, and prawn in Santubong Estuary, Malaysia. Water, sediment, fish (*Arius maculatus*) and prawn (*Fenneropenaeus merguensis*) samples were collected from three rivers namely Buntal, Penambir and Demak. These samples were digested and analyzed using Flame Atomic Absorption Spectrophotometer (FAAS) for the heavy metal contents. The potential ecological and human health risks were assessed by using the bioaccumulation factor (BAF), Geo-accumulation Index (Igeo), Enrichment Factor (EF), Provisional Tolerable Weekly Intake (PTWI), Health Risk Index (HRI) and Health Index (HI). Cd and Pb concentrations in water were within the permissible limits but were above the acceptable limits in sediment as recommended by WHO. The concentration of Cd in *A. maculatus* was (0.10 - 0.13 mg/kg) while the concentration of Cd in *F. merguensis* was (0.11 - 0.15 mg/kg), and these values were below the safety limits set by FAO/WHO and MFA. The concentration of Pb in *A. maculatus* (0.19-1.46 mg/kg) was also below the safety limits; however, the concentration of Pb in *F. merguensis* (1.35-2.97 mg/kg) surpassed these safety limits. The Igeo values were less than one, and EF values ranged between 5 and 20, suggesting that this area is polluted with heavy metals. The BAF values for Cd (0.001 - 0.002 mg/kg) and Pb (0.003 - 0.040 mg/kg) showed that there might be an appreciable chance of bioaccumulation of heavy metals in the fish and prawn. The PTWI of prawn was slightly above the acceptable PTWI of Pb recommended by FAO/WHO (2004). Comparison with the safety limits showed that the continuous consumption of these fish and prawn for a long period would impose bad impacts on health. HRI and HI in both organisms were greater than one, indicating that there were possible adverse effects. Therefore, close monitoring of this area is recommended to minimize the risks of aquatic organism consumption.

Keywords: cadmium, lead, fish, prawn, water, sediment

1. Introduction

Santubong Estuary is located at the Bako-Buntal Bay, bordered by Gunung Santubong and Bako National Park, Malaysia. It is an estuary with mangrove ecosystem. Mangroves are the most productive ecosystems due to their role as a nursery and breeding grounds for many fish species (Abu Hena *et al.*, 2017). Siddik *et al.* (2016) stated that turbid water of this ecosystem provides abundant food for juvenile fish. Surrounding areas of Santubong Estuary have been rapidly growing as an industrial area (i.e. Demak Laut Industrial Park) and the industrial activities in this area may have produced heavy metal wastes. Heavy metal pollution has been a serious global threat to the aquatic ecosystem due to its potential to cause an adverse effect on the different trophic levels through its persistence, the ability of bioaccumulation and biomagnification (Kumari *et al.*, 2018). Heavy metals are difficult to be degraded and eliminated (Lenart-Boron and Boron, 2014). Non-essential heavy metals like cadmium (Cd) and lead (Pb) have no role in biological processes,

and are very harmful even in a low concentration (Mirnategh *et al.*, 2018). Heavy metals occur in the environment by natural processes such as formation of ores, weathering of rocks and leaching of rocks, airborne dust, forest fires and vegetation (Adebayo, 2017; Olawusi-Peters *et al.*, 2017) and human activities such as disposal of untreated industrial effluent and domestic sewage, atmospheric deposition of particulate matters, runoff from agricultural land and recreational activities (Adebayo, 2017; Olawusi-Peters *et al.*, 2017; Kumari *et al.*, 2018).

Heavy metals tend not only to be accumulated in water but also may be released under certain physicochemical conditions, moving up through the food chain (Tabari *et al.*, 2010). Moreover, mangroves serve as a natural sink for heavy metals accumulations from the freshwater river before entering the sea (Mitra, 2019). Hence, heavy metals have a high tendency to accumulate in the body of aquatic organisms such as fish and prawn. Fish may absorb heavy metals through several pathways like from food ingestion and surrounding water and sediment (Adebayo, 2017). Fish have the ability to accumulate heavy metals in their tissues (Rajeshkumar and Li, 2018) and this may transfer

* Corresponding author e-mail: aifarah@unimas.my.

into higher trophic level in the food chain (Kumari *et al.*, 2018) and accumulate in the human body, which will threaten human life if exceeding the recommended limit (Sihombing *et al.*, 2019).

Various standard measures were used to assess the human health risks associated with the measured levels of heavy metal contamination. The human health risk assessment of potentially toxic heavy metals such as Health Risk Index (HRI) and Hazard Index (HI) provides an estimation of the potential health risks associated with long term exposure to chemical pollutants (Ezemonye *et al.*, 2019). Monitoring contaminants in sediments were largely recognized, and it has been extensively used as environmental indicator to assess the metal contamination. Several indices were developed to assess the heavy metal risk to environment such as Geo-accumulation Index (Igeo) and Enrichment Factor (EF) used to examine the degree of contamination of the sediments and anthropogenic influence on the sediment quality (Enuneku *et al.*, 2018). Health risks to humans arising from the toxicity of heavy metals mainly include kidney and skeletal damages, neurological disorders, endocrine disruption, cardiovascular dysfunction, and carcinogenic effects (Maurya *et al.*, 2019).

A study conducted at the Estero Salado mangrove located in Ecuador has reported that the area has been contaminated by heavy metals such as copper (Cu), chromium (Cr), Cd and Pb from the industrial wastewater (Fernandez *et al.*, 2014). Tabari *et al.* (2010) stated that fish from estuaries associated with industrial and sewage discharges have been found to be contaminated with heavy metals. Unfortunately, studies on heavy metals pollution in Santubong Estuary have not been done; hence, the status of highly toxic heavy metal such as Cd and Pb in water, sediment, fish (*Arius maculatus*) and prawn (*Fenneropenaeus merguensis*) in this estuary was still unknown. *A. maculatus* is known as the spotted catfish that comes from the family of Ariidae, and it is also called as Ikan Lundu by the locals (Froese and Pauly, 2020). *F. merguensis* comes from the family of Penaeidae and is known as banana prawn (Palomares and Pauly, 2019). Both of *A. maculatus* and *F. merguensis* are commercially important species. The polluting industries in this area are production of timber, food, furniture, electrical, paints, and the major industrial activities is steel production. Steel production generated a significant amount of air pollutants, solid by-products and residues, and waste-water sludge which contained various types of pollutants such as Cd and Pb (Musah *et al.*, 2021). This causes a major concern because large inputs of sewage from the nearby industrial area and villages may increase the concentrations of Cd and Pb, which may lead to both direct and indirect degradation of the aquatic ecosystem. Therefore, a clear

understanding of their distribution pathways, fate and effect on aquatic ecosystem must be made in order to effectively control and manage heavy metal pollution (Ayotunde *et al.*, 2012). Thus, the aim of the present study was to investigate the concentration of Cd and Pb in water, sediment, fish (*A. maculatus*) and prawn (*F. merguensis*) in Santubong Estuary. The information of this study would provide better understanding of Cd and Pb concentration in aquatic organisms in relation to the contamination level in water and sediment for better environmental monitoring, ecological risk assessment and water quality management.

2. Materials and Methods

2.1. Description of study area

This study was carried out at Santubong Estuary which is situated at the North East of Kuching, the capital city of Sarawak, Malaysia. It opens into the South China Sea through the Buntal Esplanade which is one of the openings for the entire basin. Three rivers were selected in this study namely: Buntal, Penambir and Demak. These rivers serve as important means of transportation, food source and aquaculture site for the locals and the primary occupation of the villagers in this area is fishing industry. Other than that, this area was nearby to Demak Industrial Park that is one of the biggest industrial areas in Kuching. The coordinates for the rivers were 01°41'49.38" N, 110°22'20.04" E (Buntal River), 01°39'44.28" N, 110°22'58.62" E (Penambir River) and 01°35'51.30" N, 110°23'34.08" E (Demak River) (Figure 1).

2.2. Sampling procedures

The sampling was conducted three times at three rivers (Buntal, Penambir and Demak) from April 2017 to July 2017 during the wet season. The coordinates of the river were recorded using Global Positioning Station (GPS) (Garmin, GPS 72H). Fish and prawn samples were caught by using three-layered gillnets (3.81-12.70 cm mesh sizes) that were set in the morning and then the caught samples were collected in the afternoon after approximately 6 hours. Sediment sample were collected using an Ekman grab sampler and stored in the resealable plastic bags. Water samples were collected using Van Dorn water sampler and were stored in the sample bottles. All the samples were transported back to the laboratory in cooler boxes with ice, and when they reached the laboratory they were kept in the freezer at -20°C before further analysis. Selected water quality parameters such salinity, temperature, pH and dissolved oxygen were taken using YSI (Professional Plus, Pro 10102030) handheld multi-parameter while turbidity was taken using a turbidity meter (Extech, TB400).



Figure 1. The map on the left shows the location of Santubong Estuary (located in between Santubong Peninsula and Bako) in Kuching, Malaysia while the map on the right shows the Santubong Estuary with the rivers (Buntal, Penambir and Demak).

2.3. Metals Analysis in Water and Sediment

Approximately 1 litre water samples from each river were filtered through a 0.45 μm filter paper and acidified using concentrated 65% HNO_3 for preservation at the time of collection (USEPA, 1992). Then, the water samples were analysed using FAAS (Thermo Scientific iCE 3000). The sediment samples were dried in an oven at 60°C until constant weight obtained. One gram of dried weight sample was weighed and put into 250 ml conical flask. The digestion process for sediment was done according to the standard method of USEPA (1996). After the digestion process, sample solutions were allowed to cool to room temperature, filtered through Whatman No. 41 filter paper, and the filtrate was collected in a 100 ml volumetric flask. Fifty ml of deionized water was added through filtration, and the sample was analysed using FAAS.

2.4. Metals Analysis in Fish and Prawn

The number of *A. maculatus* was collected; 22 samples at Buntal, 11 samples at Penambir and 27 samples at Demak while the number of *F. merguensis* were collected; 42 at Buntal, 80 samples at Penambir and 31 samples at Demak. Then, the muscle samples of the *A. maculatus* and *F. merguensis* were removed using ceramic knife. Muscle part was chosen because it is an edible part of the organisms. Then, they were dried in an oven at 60°C until constant weight was obtained. Dried sample was weighed for about 0.5 g. The acid digestion process for fish and prawn samples was done following the standard method by Alina *et al.*, (2012) and Mohammed *et al.* (2017). The concentrations of Cd and Pb then were determined by using FAAS.

2.5. Quality Control and Method Validation

The accuracy of the analytical methods for the analysis of heavy metal in water, sediment, fish and prawn samples were confirmed by using Certified Reference Material (CRM) MESS-4 and internal standard method. Every CRM and internal standard were analyzed three times and were compared to the certified values of metals concentration from National Research Council Canada (NRCC) and internal standard values. The recovery percentages attained for the CRM and internal standard of water, sediment, fish and prawn were between 80-120%

meeting the acceptable recovery recommended by the Environment Agency (2013).

2.6. Bioaccumulation Factor (BAF)

The BAF are the ratio of heavy metals concentration in organism to that in sediment. BAF was determined using the formula (Equation 1) suggested by Olawusi-Peters *et al.* (2017).

$$\text{BAF} = \frac{C_m}{C_s} \quad (\text{Equation 1})$$

Where: C_m = concentration of metal in organism (mg/kg). C_s = concentration of metal in sediment (mg/kg)

2.7. Assessment of Contamination Status in Sediment

The contamination status of sediment was evaluated using the Geo-accumulation Index (Igeo) and Enrichment Factor (EF). Igeo was used to determine and define metal contamination in sediments by comparing current concentration with pre-industrial levels, and the sediment is classified as unpolluted if value is less than zero (Nowrouzi and Pourkhabbaz, 2014). This index is expressed in Equation 2. Meanwhile, EF is used to estimate the anthropogenic impact on sediments by calculating differentiate between the metals originating from human activities and metals from natural source or the mixed source of the metals. The EF method normalizes the measured heavy metal content with respect to a sample reference metal such as aluminium (Al) (Zhu *et al.*, 2011). The sediment is in depletion to mineral if value is less than 2 and the EF values were calculated using Equation 3.

$$I_{\text{geo}} = \log_2 \left(\frac{C_n}{1.5B_n} \right) \quad (\text{Equation 2})$$

Where: C_n = The concentration of the examined metal in sediment. B_n = The background value for the metal n: Al (8000 ppm), Cd (0.3 ppm) and Pb (20 ppm) (Turekian and Wedepohl, 1961).

$$\text{EF} = \frac{(C_M/C_X)_{\text{Sample}}}{(C_M/C_X)_{\text{Background}}} \quad (\text{Equation 3})$$

Where: C_M = Concentration of examined metal in the sample of interest/ selected reference sample. C_X = Concentration of immobile metal in the sample of interest/ selected reference sample (Al was used in this study).

2.8. Human Health Risk Assessment Daily Intake Metal (DIM)

A survey to estimate the fish intake of villagers who lived at nearby the study region was conducted using a standard questionnaire. A total of 100 coastal villagers (male and female) with the age ranged from 17 to 87 years old were interviewed. The assessment of dietary intakes of Cd and Pb was conducted following the method of Ruaeny *et al.* (2015). The mean fish and prawn intake per week was 120 g per person and the average body weight of the villagers in this area was 60 kg. Then, the risks of dietary intakes of Cd and Pb were evaluated by comparing the weekly intake value with the provisional tolerable weekly intake (PTWI) according to FAO/WHO (2016): Cd (0.007 mg/kg) and Pb (0.025 mg/kg).

$$DIM = \frac{(Cm \times Mf)}{Mbw} \quad (\text{Equation 4})$$

Where: DIM= Daily intake of metal (mg/kg/day).

Cm= Concentration of metal in fish (mg/kg)

Mf= Mean of fish intake (g/person/day)

Mbw = Average body weight (kg)

2.9. Health Risk Index (HRI)

The HRI referred to the ratio of the daily intake of metals in the food to the oral reference dose (RfD). The oral RfD is a numerical estimate of the daily oral exposure to humans that is not likely to cause harmful effects during the lifetime (USEPA IRIS, 2006). The USEPA (2001) has established the RfD for Cd in food at 0.00003 mg/kg day. The RfD for Pb was set at 0.0035 mg/kg day by the Joint FAO/WHO Expert Committee on Food Additives (JECFA, 1993). If HRI greater than one for any metal in food indicates that the consumer population faces a health risk (Yaradua *et al.*, 2018). The value of HRI depends on the DIM value of the food stuff and the RfD. The HRI for heavy metal exposure for fish and prawn consumption was calculated using the Equation 5 of Cui *et al.* (2004):

$$HRI = \frac{DIM}{RfD} \quad (\text{Equation 5})$$

Where: RfD = Cd (0.00003 mg/kg day) and Pb (0.0035 mg/kg day)

2.10. Hazard Index (HI)

The HI is used to evaluate potential risk to human health upon exposure to more than one heavy metal (USEPA, 1989). It is assumed that the adverse effects will be proportional to the magnitude of the sum of multiple metal exposures, implying that higher metal exposure will cause a higher health risk. The HI is the sum of the HRI values as shown in Equation 6:

$$HI = \sum HRI = HRI_{Cd} + HRI_{Pb} \quad (\text{Equation 6})$$

Where: HRI_{Cd} and HRI_{Pb} = HRI values for Cd and Pb

2.11. Statistical Analysis

The metal concentrations were reported as mean \pm standard deviation (S.D). Analysis of Variance (ANOVA) with multiple comparisons using Tukey's test was performed to deduce the significant difference between the means at a significant level of 0.05. The relationship between the different variables was assessed using Pearson's correlation analysis. The statistical analysis was performed using Statistical Package for Social Sciences (SPSS) and Microsoft Excel (MS Excel).

3. Results

3.1. Physicochemical water parameters

The physicochemical parameters of water at these three rivers were shown in Table 1. The temperature of water ranged from 28.72 ± 1.28 °C at Buntal to 28.89 ± 0.46 °C at Demak. The highest turbidity was 92.37 ± 104.05 NTU in Penambir and the lowest turbidity was 59.76 ± 39.89 NTU at Buntal. The water was neutral with a pH range from 7.31 ± 0.72 to 7.64 ± 0.58 . Dissolved Oxygen (DO) ranged from 3.48 ± 0.81 mg/L to 4.19 ± 0.91 mg/L. The value of salinity was found to be significantly among the three rivers ($p < 0.05$) and the salinity ranged from 11.49 ± 3.64 ppt to 22.16 ± 0.99 ppt.

Table 1. The physicochemical water parameters in Buntal, Penambir and Demak.

Parameters	Buntal	Penambir	Demak
Temperature (°C)	28.72 ± 1.28	28.78 ± 0.58	28.89 ± 0.46
Turbidity (NTU)	59.76 ± 39.89	92.37 ± 104.05	65.83 ± 46.65
pH	7.31 ± 0.72	7.59 ± 0.85	7.64 ± 0.58
DO(mg/L)	4.19 ± 0.91	3.56 ± 0.83	3.48 ± 0.81
Salinity (ppt)	22.16 ± 0.99	19.06 ± 5.47	11.49 ± 3.64

3.2. Analysis of metals in water

The concentrations of heavy metal in water were presented in Figure 2. Cd ranged from 0.02 ± 0.001 mg/L in Penambir to 0.03 ± 0.001 mg/L in Demak while the concentration of Pb ranged from 0.01 ± 0.002 mg/L in Buntal to 0.01 ± 0.005 mg/L in Penambir. WHO (2011) stated that the recommended standard of Cd in water is 0.003 mg/L and the Pb is 0.01 mg/L; hence, the concentration of Cd and Pb in water of these rivers was within the recommended standards.

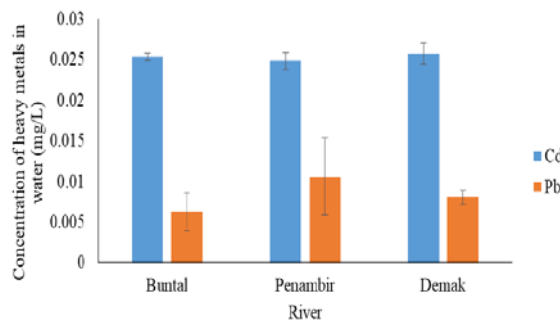


Figure 2. The mean concentration of Cd and Pb in water at Buntal, Penambir and Demak.

3.3. Analysis of heavy metals in sediment

The concentrations of heavy metal in the sediment samples were presented in Figure 3. The mean concentrations of Cd in Buntal were 0.33 ± 0.03 mg/kg, Penambir was 0.40 ± 0.02 mg/kg and Demak was 0.42 ± 0.03 mg/kg. Meanwhile, the mean concentration of Pb in Buntal was 22.86 ± 2.31 mg/kg, Penambir was 31.25 ± 2.41 mg/kg and Demak was 49.43 ± 8.31 mg/kg. WHO (2011) stated that the acceptable limits of Cd and Pb in sediments were 0.20 mg/kg and 0.30 mg/kg respectively; however, the concentrations of Cd and Pb in sediment in this study were generally higher than those limits.

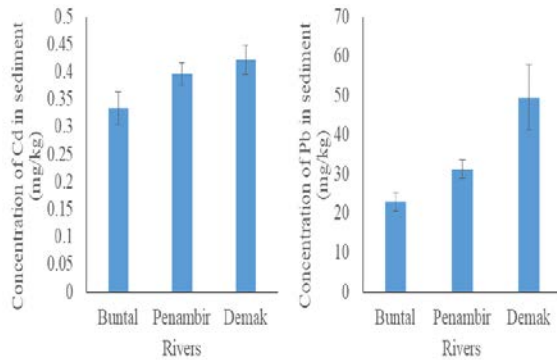


Figure 3. The mean concentration of Cd and Pb in sediment at Buntal, Penambir and Demak

3.4. Analysis of metals in fish and prawn

The heavy metal concentration in the muscle of *A. maculatus*, also called as spotted catfish, and *F. merguensis* known as banana shrimp were presented in Figure 4. In *A. maculatus*, the concentrations of Cd were in the range of 0.1 ± 0.01 mg/kg in Buntal to 0.13 ± 0.04 mg/kg in Demak while the concentration of Pb were in the range of 0.19 ± 0.11 mg/kg in Buntal to 1.46 ± 0.47 mg/kg in Demak. In *F. merguensis*, the range of Cd were in the range of 0.11 ± 0.04 mg/kg in Buntal to 0.15 ± 0.01 mg/kg in Penambir while the concentration of Pb were in the range of 1.35 ± 0.51 mg/kg in Penambir to 2.97 ± 1.13 mg/kg in Buntal.

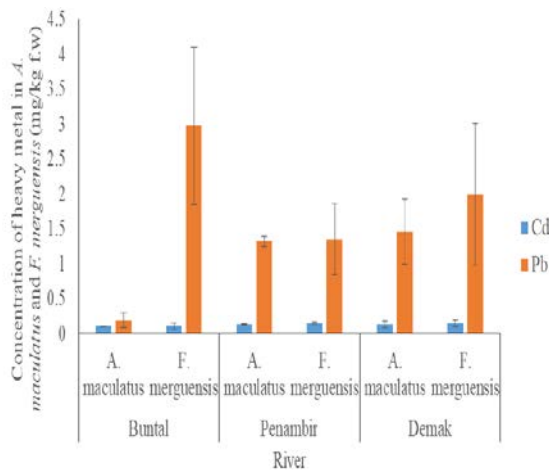


Figure 4. The mean concentration of Cd and Pb in *Arius maculatus* and *Fenneropenaeus merguensis* caught from Buntal, Penambir and Demak.

3.5. Bioaccumulation Factor (BAF)

In this study, *F. mergeunsis* showed a higher BAF values than *A. maculatus* in all the three rivers and Cd was accumulated at higher level compared to Pb (Table 2).

Table 2. The BAF of Cd and Pb in *Arius maculatus* and *Fenneropenaeus merguensis* in Buntal, Penambir and Demak.

River	Species	BAF (mg/kg)	
		Cd	Pb
Buntal	<i>Arius maculatus</i>	0.26	0.01
	<i>Fenneropenaeus merguensis</i>	0.28	0.09
Penambir	<i>Arius maculatus</i>	0.34	0.04
	<i>Fenneropenaeus merguensis</i>	0.38	0.04
Demak	<i>Arius maculatus</i>	0.34	0.04
	<i>Fenneropenaeus merguensis</i>	0.37	0.06

3.6. Assessment of Contamination Geo-accumulation index (Igeo) and Enrichment Factor (EF)

The Igeo and EF values were shown in Table 3. The Igeo values for Cd and Pb were found to be greater than one, suggesting that the area is moderately polluted. Meanwhile, the EF values for Cd and Pb were in the range of 5 to less than 20, which indicated that the area is significant contaminated. Thus, both of these indices confirmed that the sediment in this area was contaminated.

Table 3. The Igeo and EF values in Buntal, Penambir and Demak.

River	Igeo		EF	
	Cd	Pb	Cd	Pb
Buntal	0.003	0.003	6.39	6.57
Penambir	0.004	0.004	7.59	8.98
Demak	0.004	0.007	8.08	14.20

3.7. Human Health Risk Assessment Weekly Intake of Metal (WIM), Health Risk Index (HRI) and Hazard Index (HI)

The WIM of Cd in *A. maculatus* in all rivers were found to be below the PTWI of Cd recommended by the FAO/WHO (2016). However, the WIM of *F. merguensis* at Buntal and Demak were slightly above the PTWI for Pb (Table 4).

Additional comparisons with the permitted limits of heavy metal in fish and prawn set by the FAO/WHO (2011) and MFA (1983) were also shown in Table 4. In *A. maculatus*, the concentrations of Cd were below the permitted limit set by both FAO/WHO (2011) and MFA (1983) while the concentration of Pb were above the FAO/WHO (2011) but still under the MFA (1983) permitted limit. In *F. merguensis*, the concentrations of Cd were also below the permitted limit set by both FAO/WHO (2011) and MFA (1983), but the concentrations of Pb were above the permitted limit set by the FAO/WHO (2011). The concentration of Pb in *F. merguensis* was also above the permitted limit set by the MFA (1983) except at Penambir and Demak.

The HRI values of Cd in both organisms were greater than one. Meanwhile for Pb, only the HRI values of *F. merguensis* at Buntal and Demak was greater than one. The HI values in both organisms were also greater than one in every river (Table 4).

Table 4. Comparison of WIM, HRI and HI values in *Arius maculatus* and *Fenneropenaeus merguensis* with PTWI and safety limits.

River	Species	WIM		HRI		HI
		Cd	Pb	Cd	Pb	
Buntal	<i>Arius maculatus</i>	0.001	0.003	6.64	0.11	6.75
	<i>Fenneropenaeus merguensis</i>	0.002	0.04	7.19	1.69	8.88
Penambir	<i>Arius maculatus</i>	0.002	0.02	8.63	0.75	9.38
	<i>Fenneropenaeus merguensis</i>	0.002	0.02	9.79	0.77	10.56
Demak	<i>Arius maculatus</i>	0.002	0.02	8.63	0.83	9.46
	<i>Fenneropenaeus merguensis</i>	0.002	0.03	9.51	1.13	10.64
PTWI	FAO/WHO (2016)	0.007	0.025			
Safety limits	FAO/WHO (2011)	0.2	0.3			
	MFA (1983)	1	2			

Table 5. Pearson correlations analysis between physicochemical water parameters and heavy metals in the water.

	Cd	Pb	Salinity	Turbidity	pH	DO	Temperature
Cd	1						
Pb	0.076	1					
Salinity	0.193	0.216	1				
Turbidity	-0.547*	0.131	-0.309	1			
pH	0.491*	-0.001	0.135	-0.584*	1		
DO	0.497*	-0.307	0.465	-0.527*	0.622*	1	
Temperature	0.535*	0.356	0.13	-0.308	0.021	-0.228	1

* Correlation is significant at the 0.05 level.

3.8. Correlation between heavy metals in water and sediment

The result shows no correlation between Cds-Cdw with the value of $r = 0.076$, while Pbs-Pbw also showed no correlation with the value of $r = 0.107$ (Table 6). However, the Cdw-Pbs and Cds-Pbs shows positive correlations with the values of $r = 0.485$ and $r = 0.703$, respectively.

Table 6. The Pearson correlation analysis between heavy metals in water and sediments.

	Cdw	Pbw	Cds	Pbs
Cdw	1			
Pbw	0.076	1		
Cds	-0.061	0.37	1	
Pbs	0.485*	0.107	0.703*	1

* Cds is Cd in sediment, Pbs is Pb in sediment, Cdw is Cd in water and Pbw is Pb in water.

* Correlation is significant at the 0.05 level.

4. Discussion

Aquatic ecosystems are experiencing great pressure from the increasing industrial activities due to the accidental spill of waste and dumping of waste. Hence, the monitoring of the levels of pollutants is becoming increasingly urgent as a critical measure to ensure good quality of food and water. The results obtained in the current study reveal the physicochemical water parameters of water measured in the three rivers of the Santubong Estuary. The temperature falls within the acceptable value (28- 30 °C) for a survival of aquatic organism (Olawusi-Peters *et al.*, 2017; Lawson, 2011). There were no variations in water temperatures across the rivers; and this may be due to the constant flow of water, so the

temperature was not changing. The increase of temperature may affect metals uptake by organism since influx and efflux rates of metals changes (Pourang *et al.*, 2004). Turbidity is an index of water clarity, and it was higher in all the rivers. The turbidity increases constantly from the river mouth to the mangrove. The recorded salinity indicates a brackish environment with a range from 0.5 to 30 ppt (Karleskint *et al.*, 2009; Olawusi-Peters *et al.*, 2017). The salinity decreases from Buntal to Demak. The decreasing salinity values from the river mouth to the middle were similar to those of Kazemi *et al.* (2013). Arshad *et al.* (2011) also reported that salinity range increases where the river water meets the ocean. The water samples were neutral, and the pH values in this study matched with other researchers' proven view, mangrove which is near to the sea has pH of sea water of approximately 6.5-8.5 (WHO, 2011). The acidification of the aquatic environment will lower pH and reduce bioavailability of physiologically important free metals (Henry *et al.*, 2012). DO is an important aquatic parameter, whose presence is vital to aquatic fauna. It plays crucial role in the growth, distribution and behaviour of aquatic organisms. The DO level in this study was within the favourable condition (4-6 mg/L) for aquatic life to survive (Olawusi-Peters *et al.*, 2017). Thus, low DO content is potentially to cause by the presence of pollutants such as heavy metals in that area, while higher DO level indicates an adequate supply and availability of oxygen to support marine species growth and activity.

The concentration of Cd and Pb in water in this study was higher than the level in the study of Sany *et al.* (2012), but they were still within the recommended standard range set by WHO (2011). The concentrations of both heavy metals in water were not significantly different among the

three rivers ($p > 0.05$). For sediment, the concentrations of Cd and Pb were generally high and were above the acceptable limits described by WHO (2011) and the concentration of Cd and Pb in the sediments showed significant difference ($p < 0.05$) between rivers. Demak River located at the Demak Industrial Park showed the highest concentration of both metals, and this indicated that the industrial activities in this area were polluting the aquatic ecosystem. The concentrations of Cd and Pb in sediment in this study were lower compared to the study done by Sany *et al.* (2013) in Selangor, Malaysia; however, the concentration of Pb in sediment in this study was found to be higher than Langat Estuary that received high metals pollution from the industrial and shipping activity (Mokhtar *et al.*, 2015). Sediment recorded the highest metal concentrations, and this may be due to the fact that when metal pollutants are released into aquatic environment, they do not remain in aqueous phase but are adsorbed on to the sediments. Thus, the sediment acts as a sink for pollutants, hence the reason for its higher concentrations of these metals. Meanwhile, the Igeo values for Cd and Pb were found to be less than one, suggesting the area to be moderately polluted. The EF values for Cd and Pb in all rivers were between 5 and 20, which indicated that the area is significantly contaminated. The high level of metals in sediments influences the level of metals in water, which would contribute widely to the bioaccumulation in aquatic organisms.

The heavy metal concentration in the muscle of *A. maculatus* and *F. merguensis* were presented in Figure 4. The concentrations of Cd in both organisms were below the safety limits by FAO/WHO (2011) and MFA (1983); however, the concentration of Pb in *F. merguensis* surpassed these safety limits. The result observed in this study is similar to the findings in the reports of Ahmed *et al.* (2019). This showed that consuming these fish and prawn in large quantities and on a regular basis for a long period of time might also impose a bad effect on human health. Other than that, the constant and consistent exposure of fish and prawn to these metals would thereby decrease their fitness in the ecosystem. Ahmed *et al.* (2019) stated that that metal concentrations in fish muscles varied widely depending on the location and species. In this study, the *F. merguensis* had comparatively higher concentration of metals than *A. maculatus* as they live close to the bottom of sediment. The metal accumulation in fishes could be highly influenced by sampling locations and habitats. However, only the concentration of Pb in *A. maculatus* was significantly different among the three rivers ($p < 0.05$), and the concentration of Cd and Pb in *F. merguensis* was not significantly different among the three rivers ($p > 0.05$). Generally, strong correlations between specific heavy metals in the environment may reflect similar levels of contamination or release from the same sources of pollution. In this study, strong positive correlations were found between Cd in sediment and Pb in sediment (Table 5), indicating that they had the same source either natural or anthropogenic. Cd and Pb are non-essential elements; Cd and Pb originated from nearby industrial activities might end up in the aquatic ecosystem which will greatly affect the aquatic organisms that live in this area.

The level of concentration in the waters, sediments, and organisms at Santubong Estuary amongst the three rivers

follows the order $Pb > Cd$, while the sequence of the concentration of heavy metal in the rivers was Demak $>$ Penambir $>$ Buntal. This showed that the industrial activities and human settlement directly influence the metals concentration in water, sediment and aquatic organism in this estuary. This is alarming for authorities and dangerous to the local people who feed on the organisms since Cd and Pb are very toxic and harmful to human body. The correlation analysis shows that concentration of Cd in water was positively correlated with pH, DO and temperature. There were also no correlations between the heavy metal concentrations in the water with the heavy metals in sediment.

The BAF was generally high, indicating that the bioaccumulation of heavy metals occurred in these organisms. The accumulation of the metal in aquatic organism depends upon the classification of species, entry pathways, metabolic characters of the sampled tissues and the surrounding environmental condition in which the species live (Ahmed *et al.*, 2019). *F. merguensis* has the highest BAF compared to *A. maculatus* due to the fact that it is a benthic organism; thus metals in sediments may greatly contribute to high metals accumulation in *F. merguensis*. The occurrence of appreciable high BAF values in Santubong Estuary was an indication of the high human activities going on in the area. Generally, the calculated level of PTWI for Cd lies in the normal ranges, and the fishes were assumed as safe to be consumed; however, the continuous exposure of Pb to the fish and prawn may cause toxicity in future. The calculated PTWI of Cd and Pb at Kuala Terengganu by Chuan *et al.* (2018) were found to be higher than the present study, indicating the continuous consumption of the species would impose some health problem. The acceptable guideline value for HRI and HI is 1. However, the HRI and HI values in this study were exceeding 1. These high values of HRI and HI indicated that the aquatic organisms may pose serious human health risk after consumption.

5. Conclusion

The physicochemical water parameters and heavy metals concentration in water of Santubong Estuary revealed a brackish environment with low chemical pollutants burden. However, the concentration of Cd and Pb in sediment were generally higher when compared with recommended values and based on the pollution indices (Igeo and EF), the sediment was polluted. The accumulation of heavy metals is predominant in sediments compared to water and organisms because sediments act as an important sink for all contaminants. The concentration of Cd in *A. maculatus* and *F. merguensis* was within the recommended limits; however, the concentration of Pb in these organisms was considerably high and thus causing worry. The prolonged consumption of both organisms in this area will pose some serious health problem to the consumer based on the human health risk assessments since heavy metals accumulate. Thus, great attention should be given to this estuary to control the anthropogenic inputs and proper regular monitoring of heavy metal concentrations in this estuary should be conducted. The industrial activities that operate nearby this estuary also should adopt more sustainable and eco-

innovative management options to reduce potential ecological and human health risk of heavy metal pollution.

Acknowledgements

Authors extend their gratitude to University Malaysia Sarawak (UNIMAS) for research financial support through RAGS grant E14099 F07 69 1320/2015(14). Authors also wish to thank all laboratory staffs from UNIMAS and local guides during the sampling and data analysis.

References

- Abu Hena MK, Idris MH, Rajae A and Siddique, MAM. 2017. Length–weight relationships of three fish species from a tropical mangrove estuary of Sarawak, Malaysia. *J Appl Ichthyol.*, **33(4)**: 858-860.
- Adebayo, I. 2017. Determination of Heavy Metals in Water, Fish and Sediment from Ureje Water Reservoir. *J Environ Anal Toxicol.*, **7(4)**: 1-4.
- Ahmed ASS, Sultana S, Habib A, Ullah H, Musa N, Hossain MB, Rahman MM and Sarker MSI. 2019. Bioaccumulation of heavy metals in some commercially important fishes from a tropical river estuary suggests higher potential health risk in children than adults. *PLOS ONE*, **14(10)**: 1-21.
- Alina M, Azrina A, Mohd Yunus AS, Mohd Zakiuddin S, Mohd Izuan Effendi H and Muhammad Rizal R. 2012. Heavy metals (mercury, arsenic, cadmium, plumbum) in selected marine fish and shellfish along the Straits of Malacca. *Int Food Res J.*, **19(1)**: 135-140.
- Arshad AB, Ara R, Amin SMN and Effendi M. 2011. Influence of environmental parameters on shrimp post- larvae in the Sungai Pulaui seagrass beds of Johor Strait, Peninsular Malaysia. *Sci Res Essays*, **6(26)**: 5501-5506.
- Ayotunde E, Offem B and Ada F. 2012. Heavy Metal Profile of Water, Sediment and Freshwater Cat Fish, *Chrysichthys nigrodigitatus* (Siluriformes: Bagridae), of Cross River, Nigeria. *Rev Biol Trop*, **60**: 1289-1301.
- Chuan O, Aziz NM, Shazili NA and Yunus K. 2018. Selected heavy metals content in commercial fishes at different season landed at Fisheries Development Authority of Malaysia Complex (LKIM) Complex, Kuala Terengganu, Malaysia. *J Sustain Sci Manag.*, **13**: 29-38.
- Cui YJ, Zhu YG, Zhai RH, Chen DY, Huang YZ, Qui Y, Liang JZ. 2004. Transfer of metals from soil to vegetables in an area near a smelter in Nanning, China. *Environ Int.*, **30**: 785-791.
- Environment Agency. 2013. "Method implementation document for EN14385." <http://www.sa.org/Files%20Public%20Area/Documents/MID%2014385%20V3.1%20draft.pdf> (June 26, 2020).
- Enuneku A, Omoruyi O, Tongo I, Ogbomida E, Ogebeide O and Lawrence Ikechukwu E. 2018. Evaluating the potential health risks of heavy metal pollution in sediment and selected benthic fauna of Benin River, Southern Nigeria. *Appl Water Sci.*, **8 (224)**: 1-13.
- Ezemonye LI, Adebayo PO, Enuneku AA, Tongo I and Ogbomida E. 2019. Potential health risk consequences of heavy metal concentrations in surface water, shrimp (*Macrobrachium macrobrachion*) and fish (*Brycinus longipinnis*) from Benin River, Nigeria. *Toxicol. Rep.*, **6**, 1-9.
- FAO/WHO. 2016. "Joint FAO/WHO standards programme CODEX committee on contaminants in foods." http://www.fao.org/fao-who-codexalimentarius/sh-proxy/en/%3Flnk%3D1%26url%3Dhttps%25253A%25252F%25252Fworkspace.fao.org%25252Fsites%25252Fcodex%25252FMeetings%25252FCX-735-10%25252FWD%25252Fcf10_INF1e.pdf (June 26, 2020).
- FAO/WHO. 2011. "Joint FAO/WHO food standards programme codex committee on contaminants in foods fifth session." http://www.fao.org/input/download/report/758/REP11_CFe.pdf (June 26, 2020).
- Fashchuk DY. 2011. **Geographic and ecological information model of marine basin, In: Marine Ecological Geography. Environmental Science and Engineering.** Berlin, Heidelberg: Springer.
- Fernandez J, Andrade S, Silva-Coello CL and De la Iglesia R. 2014. Heavy metal concentration in mangrove surface sediments from the north-west coast of South America. *Mar Pollut Bull.*, **82 (1-2)**: 221-226.
- Froese R and Pauly D. 2020. "Species of *Arius maculatus* in FishBase." <https://www.fishbase.se/summary/Arius-maculatus> (August 28, 2020).
- Henry R, Lucu C, Onken H and Weihrauch D. 2012. Multiple Functions of the Crustacean Gill: Osmotic/ionic Regulation, Acid-Base Balance, Ammonia Excretion, and Bioaccumulation of Toxic Metals. *Front Physiol.*, **3 (431)**: 1-33.
- JECFA. 1993. "Joint FAO/WHO Expert Committee on Food Additives. Evaluation of Certain Food Additives and Contaminants: Forty-first Report of the Joint FAO/WHO Expert Committee on Food Additives. WHO Technical Report Series, No.837. Geneva." <https://apps.who.int/iris/handle/10665/36981> (August 25, 2020).
- Karleskint G, Turner RK and Small J. 2009. **Intertidal communities. Introduction to Marine Biology (3rd edition).** Belmont, CA: Cengage Learning.
- Kazemi Z, Hashim NB and Ismail, M. 2013. Estimating the Mean Salinity, Dissolved Oxygen and Temperature of the West of Johor Strait, Malaysia. Proceedings of the Land and Water Conference. Universiti Teknologi Malaysia, Skudai, Malaysia.
- Kumari P, Chowdhury A and Maiti S. 2018. Assessment of heavy metal in the water, sediment, and two edible fish species of Janshedpur Urban Agglomeration, India with special emphasis on human health risk. *Hum Ecol Risk Assess.*, **24 (6)**: 1477-1500.
- Lawson EO. 2011. Physico-Chemical Parameters and Heavy Metal Contents of Water from the Mangrove Swamps of Lagos Lagoon, Lagos, Nigeria. *Adv Biol Res.*, **5(1)**: 08-21.
- Lenart-Boron A and Boron P. 2014. The Effect of Industrial Heavy Metal Pollution on Microbial Abundance and Diversity in Soils - A Review. In: Hernandez-Soriano MC (Ed.), **Environmental Risk Assessment of Soil Contamination.** IntechOpen, United Kingdom, pp. 10.5772/57406.
- MFA. 1983. **Malaysian Food Act:Malaysian food and drug.** Kuala Lumpur: MDC Publishers Printer Sdn. Bhd.
- Maurya P, Malik DS, Yadav KK, Kumar A, Kumar S and Kamyab H. 2019. Bioaccumulation and potential sources of heavy metal contamination in fish species in River Ganga basin: Possible human health risks evaluation. *Toxicol Rep.*, **6**: 472-481.
- Mimategh SB, Shabanipour N and Sattari M. 2018. Seawater, Sediment and Fish Tissue Heavy Metal Assessment in Southern Coast of Caspian Sea. *Int J Pharmac Res Allied Sci.*, **7(3)**:116-125.
- Mitra, A. 2019. **Mangrove Forests in India.** Springer, Cham.
- Mohammed E, Mohammed T and Mohammed A. 2017. Optimization of an acid digestion procedure for the determination of Hg, As, Sb, Pb and Cd in fish muscle tissue. *MethodsX*, **4**: 513–523.

- Mokhtar F, Aris AZ and Praveena S. 2015. Preliminary Study of Heavy Metal (Zn, Pb, Cr, Ni) Contaminations in Langat River Estuary, Selangor. *Procedia Environ Sci.*, **30**: 285-290.
- Musah BI, Peng L and Xu Y. 2021. Evaluation of chromium application in the steel industry in China: Implications on environmental quality. Proceedings of the International Conference on Environmental Science and Technology. Beijing, China.
- Nowrouzi M and Pourkhabbaz A. 2014. Application of geoaccumulation index and enrichment factor for assessing metal contamination in the sediments of Hara Biosphere Reserve, Iran. *Chem Speciat Bioavailab.*, **26(2)**: 99-105.
- Olawusi-Peters O, Akinola JO and Jelili AO. 2017. Assessment of Heavy Metal Pollution in Water, Shrimps and Sediments of Some Selected Water Bodies in Ondo State. *Int J Res Agric Sci.*, **5 (2)**: 55-66.
- Palomares MLD and Pauly D. 2019. On the creeping increase of vessels' fishing power. *Ecol Soc.*, **24 (3)**: 31-37.
- Pourang N, Dennis J and Ghourchian H. 2004. Tissue Distribution and Redistribution of Trace Elements in Shrimp Species with the Emphasis on the Roles of Metallothionein. *Ecotoxicol.*, **13**: 519-533.
- Rajeshkumar S and Li X. 2018. Bioaccumulation of heavy metals in fish species from the Meiliang Bay, Taihu Lake, China. *Toxicol Rep.*, **5**: 288-295.
- Ruaeny TA, Hariyanto S and Soegianto A. 2015. Contamination of copper, zinc, cadmium and lead in fish species captured from Bali Strait, Indonesia, and potential risks to human health. *Cah Biol Mar*, **56**: 89-95.
- Sany SBT, Salleh A, Sulaiman AH, Sasekumar A, Rezayi M and Tehrani GM. 2012. Heavy metal contamination in water and sediment of the Port Klang coastal area, Selangor, Malaysia. *Environ Earth Sci*, **69**: 2013-2025.
- Siddik MAB, Chaklader MR, Hanif MA, Islam MA and Fotedar R. 2016. Length-weight relationships of four fish species from a coastal artisanal fishery, southern Bangladesh. *J Appl Ichthyol.*, **32**: 1300-1302.
- Sihombing V, Gunawan H and Sawitri R. 2019. Heavy metal residues in water and fishes at Karangsong Mangrove Conservation Area, Indramayu. Proceedings of the International Conference on Biology and Applied Science. UIN Maulana Malik Ibrahim Malang, Indonesia.
- Tabari S, Saeedi Saravi SS, Bandany G, Dehghan A and Shokrzade M. 2010. Heavy metals (Zn, Pb, Cd and Cr) in fish, water and sediments sampled from Southern Caspian Sea, Iran. *Toxicol Ind Health.*, **26**: 649-656.
- Turekian KK and Wedepohl KH. 1961. Distribution of the Elements in some major units of the Earth's crust. *Geol Soc Am Bull.*, **72**: 175-192.
- USEPA. 1992. "SW-846 test method 3005A: Acid digestion of waters for total recoverable or dissolved metals for analysis by Flame Atomic Absorption (FLAA) or Inductively Coupled Plasma (ICP) spectroscopy." <https://www.epa.gov/hw-sw846/sw-846-test-method-3005a-acid-digestion-waters-total-recoverable-or-dissolved-metals> (June 26, 2020).
- USEPA. 1996. "Method 3050B: Acid digestion of sediments, sludges, and soils." <https://www.epa.gov/homeland-security-research/epa-method-3050b-acid-digestion-sediments-sludges-and-soils> (June 26, 2020).
- USEPA. 2001. "Integrated Risk Information System Methylmercury (MeHg) (CASRN 22967-92-6)." https://cfpub.epa.gov/ncea/iris/iris_documents/documents/subst/073.htm (June 26, 2020).
- USEPA IRIS. 2006. "United States Environmental Protection Agency. Integrated Risk Information System." Washington, DC USA, <http://www.epa.gov/iris/substS> (June 26, 2020).
- USEPA. 1989. "Risk Assessment Guidance for Superfund volume 1: Human Health Evaluation Manual (Part A): Interim Final." Washington, DC, USA, https://www.epa.gov/sites/production/files/2015-09/documents/rags_a.pdf (June 26, 2020).
- WHO. 2011. "Guidelines for drinking water quality 4th ed. Geneva." https://apps.who.int/iris/bitstream/handle/10665/44584/9789241548151_eng.pdf;jsessionid=CD184970088EC72CCAC9B13667259C73?sequence=1 (June 26, 2020).
- Yaradua I, Alhassan A, Kurfi A, Nasir A, Idi A, Ibrahim M and Kanadi A. 2018. Heavy Metals Health Risk Index (HRI) in Human Consumption of Whole Fish and Water from Some Selected Dams in Katsina State Nigeria. *Asian J Fish Aquat Res.*, **1(1)**:1-11.
- Zhu L, Xu J, Wang F and Lee B. 2011. An assessment of selected heavy metal contamination in the surface sediments from the South China Sea before 1998. *J Geochem Explor.*, **108(1)**: 1-14.

Durum wheat (*Triticum turgidum ssp durum*) improvement during the past 67-year in Algeria: Performance assessment of a set of local varieties under rainfed conditions of the eastern high plateaus

Leïla Haddad^{1, 2,*}, Adel Bachir³, Nassima Ykhelef⁴, Amar Benmahammed^{5,2},
Hammena Bouzerzour^{5,2}

¹Department of Agronomic Sciences, Faculty of Life and Natural Sciences, Chadli Bendjedid University, El Tarf, 36000, Algeria;

²Laboratory for the development of biological and natural resources of the University of Sétif-1, 19000, Algeria; ³Field Crop Institute, Agricultural Experimental Station, Setif, 19000, Algeria; ⁴Department of Agronomic Sciences, Faculty of Life and Natural Sciences, Ferhat Abbas University, Setif 1, Setif, 19000, Algeria; ⁵Ecology and Plant Biology Depart, Faculty of Life and Natural Sciences, University Ferhat Abbas, Setif-1, Setif, 19000, Algeria.

Received: July 8, 2020; Revised: September 11, 2020; Accepted: September 18, 2020

Abstract

A field experiment was conducted during the 2017/18 cropping season at the Field Crop Agricultural Experimental Station Institute of Setif, Algeria. The study aimed to investigate the performance and variability of agro-morphological traits present in a set of local durum wheat varieties, registered during the 1950–2017 period and to estimate grain increase and to identify concurrent trait changes accompanying yield increase. The results indicated ample variation for the measured traits. Multivariate analysis grouped the assessed varieties into: high vs low grain yield, tall, late vs early and dwarf and high fertility, low kernel weight vs low fertility, high kernel weight varieties. Post-green revolution varieties performed significantly more than traditional varieties in terms of grain yield, yield components and harvest index. Local varieties were taller, late to head and had high straw yield. Grain yield genetic progress over time was estimated to be equal to 11.56kg/ha/year. Differences between local and recently released varieties are ascribed to Rht genes. To make the best use of desirable characteristics from local and modern varieties, it is suggested to further investigate the variation of dwarfing genes in the tested plant material. This allows to design a breeding program promoting the development of new germplasm more adapted to rain-fed south Mediterranean environments, through selection for dwarfing genes, like Rht24 and Rht8, which express minor effects on the desirable traits in low yield environment.

Keywords: *Triticum durum*, local varieties, variability, genetic progress, PCA, clustering, regression.

1. Introduction

With nearly 1.5 million hectares planted annually, durum wheat [*Triticum turgidum* (L.) Thell. ssp. *turgidum* conv. *durum* (Desf.) MacKey] remains a major field crop in Algeria (CEIC, 2017). Durum semolina is largely consumed in rural areas as couscous, leavened flat bread, frik, home-made pasta and various types of cakes (Kezih *et al.*, 2014), and straw is baled, stacked and fed to livestock during the winter months. Rainfed grown, in regions known for their high frequency of frost, drought and heat events, durum wheat production varies largely, between and within cropping seasons, from one location to another (Mekhlouf *et al.*, 2006; Chourghal *et al.*, 2015). From 1970/1971 to 2016/2017 period, the production of this crop varied from 0.42 (1974/1975) to 3.2 million tons (2016/2017), (CEIC, 2017). To reduce cereals grain imports, induced by a large domestic demand, yield improvement, under rainfed conditions, appeared as a sound alternative, although it may be possible to increase the irrigated area under cultivation, notably in the sahara (Laaboudi and Mouhouche, 2012; Haddad *et al.*, 2016;

Belagrouz *et al.*, 2018). In spite of the fact that traditional varieties are still cultivated, here and there, on large scale, this strategy resulted, in recent years, in an increased number of newly released varieties proposed to replace old ones (Benbelkacem, 2014; Rabti *et al.*, University of Algeria, personal communication). Several studies, conducted mainly under favorable environments, reported that replacement of traditional cultivars was accompanied by positive changes in grain yield, yield components, harvest index, earliness and plant height reduction (Battenfield *et al.*, 2013; Fischer *et al.*, 2014; Sanchez-Garcia *et al.*, 2013; Gizzi and Gambin, 2016; Laidig *et al.*, 2017; Wang *et al.*, 2017; Rabti *et al.*, University Algeria, personal communication). In this context, Joudi *et al.* (2014) reported a rate of grain yield increase varying from 20 and 30 kg/ha/year, under respectively rainfed and irrigation conditions. Battenfield *et al.* (2013) reported a rate of 14.6 kg/ha/year. Cargnin *et al.* (2009), quantifying the genetic progress of rainfed wheat varieties released between 1976 and 2005, reported an estimated yield increase of 37 kg/ha/year. Sun *et al.* (2014) noted that plant height decreased by almost 44 %, from 140.7 to 79.5 cm, from ancient to newly released cultivars.

* Corresponding author e-mail: tarffac@yahoo.fr.

Investigating yield stability, Flintham *et al.* (1997) mentioned that mean grain yields of dwarf and tall wheat isolines were similar in low yielding environment; however, dwarf varieties yielded significantly more under favorable environments. In contrast, tall varieties produced significantly more straw than their shorter counterparts, suggesting that cultivation of tall wheat varieties is beneficial in semi-arid environments where yield is below 2.5 t/ha, and where straw has a value (Flintham *et al.*, 1997). Rabti *et al.* University of Algeria, personal communication, found that modern varieties outperformed the old ones in terms of grain yield, spike number, spike weight, number of kernels per square meter, harvest index, spike fertility and stay green. Old varieties outperformed the modern ones in terms of straw yield, lateness, tallness and flag leaf area. Modern varieties were more responsive to improved growth conditions, showing agronomic stability, while old varieties were stress tolerant and less responsive to improved environmental conditions, exhibiting biological stability (Rabti *et al.*, University of Algeria, personal communication). Modern varieties were selected on grain yield basis from plant materials carrying reduced height genes (Rht-B1b). Because of pleiotropic effects exerted by dwarfing genes on several plant traits, this selection resulted in high-yielding semi-dwarf wheat varieties that respond to increased inputs without lodging (Brancourt-Hulmel *et al.*, 2003; Rebetzke *et al.*, 2012; Bai *et al.*, 2013). Consequently, plant height reduction was targeted in many breeding programs, because this trait was associated with lodging, under application of high levels of N-fertilizer and added irrigation water (Griffiths *et al.*, 2012). However, under water limited environments, lodging is a rare event and the presence of reduced height genes negatively impacted root elongation, early seedling vigor, coleoptiles length and plant height that are useful traits for cultivation in dry prone environments. In fact, seedling vigor and longer coleoptiles enhance deep sowing, allowing access to soil moisture during germination and crop establishment periods (Rebetzke *et al.*, 2012; Bai *et al.*, 2013). Furthermore, tall varieties possess the ability to store more assimilates in the stem which are transferred to the grain to minimize yield

reduction under severe terminal heat and drought stresses (Rebetzke *et al.*, 2012; Bai *et al.*, 2013; Belkharouch *et al.*, 2015). Tall varieties produce more straw, which is valuable under conservation agriculture, where wheat stubbles serve as soil cover to limit water and wind erosion (Chennafi *et al.*, 2011). Straw is also a valuable fodder source in small farms practicing livestock rearing to complement cereal production (Benider *et al.*, 2017). The present study aimed to investigate varietal differences and genetic gain achieved by a set of local durum wheat varieties registered at different periods during the past 67-year under rainfed conditions of the eastern high plateaus of Algeria. The genetic gain of the durum wheat species could provide a visionary perspective to identify within the framework of breeding and improvement programs, the varieties as well as the genetic characters suitable for environments reduced in water. Special attention will be paid to local varieties which present, as much as modern varieties, a very interesting genetic source to study to try to discern the characteristics favorable to dry environments. It is a way by which these varieties will be maintained and conserved sustainably.

2. Materials and methods

2.1. Site, plant materials and experimental design.

Plant materials under study consisted of 16 genotypes of durum wheat (Table 1). These genotypes, registered at different time periods (mainly before 1970 and after 1970) were evaluated in a randomized complete block design with three replications, under rainfed conditions, at the Field Crop Institute, Agricultural Experimental Station of Setif (AES-ITGC, Setif, Algeria, 36°15'N, 5°37'E, 1081 m altitude), during the 2017-2018 cropping season. Plot dimensions were 6 rows, 5 m long, and 20 cm apart. The experiment, sown on December 8th 2017, was fertilized with 100 kg/ha of triple superphosphate (46% P₂O₅), and 80 kg/ha of urea (35% N) were broadcasted at jointing growth stage. Weed control was performed chemically by application of Zoom herbicide.

Table 1. Names, Pedigree, Origin and registration date of the set of the assessed varieties:

Order	Name	Pedigree	Origin	Registration date	abbreviation
1	Oued Zenati368	Pure line Selection from Guelma landrace	INRAA	1950	OZ
2	Hedba3	Pure line Selection from El Khroub landrace	INRAA	1950	H3
3	Gloire de Montgolfier	Pure line Selection from Tiaret landrace	INRAA	1950	GLR
4	Mohamed Ben Bachir	Pure line Selection from Setif landrace	INRAA	1950	MBB
5	Bidi 17	Pure line Selection from Guelma landrace	INRAA	1950	B17
6	Guemgoum Rkhem	Pure line Selection from Tiaret landrace	INRAA	1950	GGR
7	Polonicum	Triticum polonicum/Zenati bouteille	INRAA	1950	POL
8	Waha	Plc/Ruffi//Gta's/3/Rolette CM 17904	Cimmyt Icarda	1985	WAH
9	Vitron	Turkey77/3/Jori/Anhinga/Flamingo	Cimmyt Icarda	1985	VIT
10	Ziban	Zb/Fg's//Lk/3/Ko120/4/Ward	Cimmyt Icarda	1985	ZBA
11	Gaviota durum	Crane/4/PolonicumPI ₁₈₅₃₀₉ //T.glutin en/2* Tc60/3/Gil	Cimmyt Icarda	1990	GTA
12	Ofanto	Appulo/Adamello	Italy	1990	OFA
13	Bousselam	Heider/Martes//Huevos de Oro.	Cimmyt Icarda	1995	BOU
14	Setifis	Bousselam/Ofanto	ITGC-Setif	2009	SET
15	Boutaleb	Hedba3/Ofanto	ITGC-Setif	2013	BTL
16	Montpellier	Old variety INRAFrance	INRAFrance	--	MPL

INRAA = Institut Nationale de la Recherche Agronomique d'Algérie (National Institute of Agronomic Research of Algeria), ITGC = Institut Technique des Gandes Cultures (Technical Institute of Field Crops).

2.2. Notations and Measurements

The following agro morphological traits were measured. Number of days to heading (DHE, days) was counted as number of days from sowing to the date when 50% of the spikes were halfway out from the flag leaf sheath. Plant height (PHT, cm) was measured at maturity from the soil surface up to the tip of the spike, excluding awns. Aboveground biomass (BIO, g/m²), spike number (SN, #/m²), spike weight (SW, g/m²), straw yield (STW, g/m), and grain yield (GY, g/m²) were recorded from a vegetative sample harvested from one row, 1.0 m long per plot. Harvest index (HI, %) was derived as the ratio of grain yield to aboveground biomass. Economical yield (Yeco, g/m²) was derived as grain yield plus 0.3 times straw yield, according to Annicchiarico *et al.* (2005).

2.3. Data Analysis

Collected data were subjected to an analysis of variance (Anova) according to a complete block design with three replicates, as per Steel and Torrie (1982), using balanced Anova subroutine implemented in Cropstat version 7.2 (2007) software. Mean comparisons were made using the F-protected least significant difference test (F-protected LSD). The LSD was calculated according to Steel and Torrie, (1982) as follows: $LSD_{5\%} = t_{5\%} (\sqrt{2\sigma^2_e})/r$, where $t_{5\%}$ is the tabulated t value at 5% probability level, σ^2_e = mean square error and r = number of replications. Variables showing statistical significance were further explored through correlation, principal components, and cluster analyses to determine pertinent traits association useful for genotypes classification. Correlation, principal components and cluster analyses were performed using past software version 3 (Hammer *et al.*, 2001). Statistical significance of correlation coefficients was checked versus r table values at the 5% and 1% probability levels (Steel and Torrie, 1982). Principal components and cluster analyses were run using Euclidean distances of normalized variables and Ward's method as linkage criterion. Principal components showing Eigen value greater than unity were deemed significant and discussed. Genotypic differences between old and recently release varieties were tested for significance via a single degree of freedom contrast. Rate of grain yield increase was derived as the linear regression coefficient of the grain yield means of the local varieties versus time. Variance components and broad sense heritability were derived from the genotypic and error mean squares according to Acquah, (2012).

3. Results

3.1. Traits variability and heritability

Results of the analysis of variance of the measured traits are reported in table 2. Significant genotypic effect

was observed for all the analyzed traits (Table 2). This effect emerged from genetic and environmental differences among the assessed varieties. Genetic variance (σ^2_g) was, however, somewhat higher than the residual variance (σ^2_e), as this is indicated by the CVg/CVe ratio which varies from 1.2 for Yeco to 23.9 for DHE (Table 2). Mean PHT varied from 66.9 cm to 91.4 cm with an overall average of 78.9 cm. SN varied from 142.7 to 270.7 spikes/m². Ample variation was also observed for GY which varied from 201.2 to 363.2 g/m², DHE from 117.0 to 133.3 days, NGM from 3.3 to 6.9 thousand kernels /m², STW from 248.8 to 582.0 g/m² and HI from 29.1 to 51.4 %. BIO varied from 467.2 to 826.4 g /m², NKS from 21.6 to 32.9 kernels per spike, TKW from 42.1 to 62.0 g and Yeco from 282.5 to 486.0 g/m² (Table 2). Mean values of the measured traits were within the range of the values usually observed under the conditions of the experimental site where this study was carried out. From the same environment, Haddad *et al.* (2016) reported that grain yield means, measured in 2013, 2014, and 2015 cropping seasons, averaged over varieties, were 511.0, 93.7 and 227.5 g/m², respectively. Grain yield differences between seasons and varieties could arise from management factors, biotic and abiotic stresses which prevail under water-limited environments (Mekhlouf *et al.*, 2006; Adjabi *et al.*, 2007; Royo *et al.*, 2010; Angus *et al.*, 2015). Broad sense heritability values were low (< 70%) for PHT, BIO, SW, NGM, GY and Yeco; intermediate (>70% < 80%) for SN and NKS; and high (> 80%) for TKW, STW, HI and DHE (Table 2). These results partially corroborated Salmi *et al.* (2019) findings who reported that this parameter took high values for days to heading and plant height, intermediate values for spike number and number of kernels per spike, and low values for grain yield; and findings of Mohsin *et al.* (2009) who found high broad-sense heritability for harvest index; but these results contradict findings of Graziani *et al.* (2014), who reported high grain yield broad sense heritability. Generally, broad sense heritability values, based on one environment (site x year) data, are biased upward, because genotype x environment variance is confounded with genetic component, and selection based on these values is usually misleading. In this context, from a multi-season trial, Laala *et al.* (2017) reported that only days to heading and plant height showed an intermediate heritability leading to effective selection response, while the other traits exhibited low heritability and selection inefficiency, because of the high magnitude of the GxE interaction variance component.

Table 2. Analysis of variance mean squares, variance components, broad sense heritability, traits mean characteristic of the set of the varieties assessed and relative deviation between old and recently released varieties.

Source (DF)	PHT	BIO	SW	SN	NKS	NGM	
Replication (2)	183.3	1446.3	132.0	2.3	0.4	0.0	
Genotype (15)		189.2**	42035.8**	11322.9**	3676.4**	31.3**	2.8**
Old vs Modern (1)	507.7**	15222.8ns	8369.4**	9459.7**	9.1ns	4.8**	
Error (30)	27.3	5705.3	1765.5	391.0	3.2	0.4	
σ^2_e	27.3	5705.3	1765.5	391.0	3.2	0.4	
σ^2_g	54.0	12110.2	3185.8	1095.1	9.4	0.8	
σ^2_p	81.3	17815.5	4951.3	1486.1	12.6	1.2	
CVe	6.6	11.4	11.6	10.1	6.6	11.6	
CVg	9.3	16.6	15.5	17.0	11.3	17.1	
CVp	11.4	20.1	19.4	19.8	13.1	20.7	
CVg/CVe	1.4	1.5	1.3	1.7	1.7	1.5	
H ² bs	66.4	68.0	64.3	73.7	74.5	68.7	
\bar{Y} overall	78.9	664.6	363.4	194.8	27.0	5.2	
\bar{Y} Max	91.4	826.4	474.2	270.7	32.9	6.9	
\bar{Y} Min	66.9	467.2	259.5	142.7	21.6	3.3	
\bar{Y} Old	85.2	699.5	337.5	167.2	27.9	4.6	
\bar{Y} Modern	73.9	637.5	383.7	216.3	26.3	5.7	
Deviation	-11.3**	-62.0ns	46.2**	49.1**	-1.5ns	1.1**	
%Deviation	-13.3	-8.9	13.7	29.3	-5.4	23.9	
LSD5%	8.7	125.9	70.1	33.0	3.0	1.0	
Source (DF)	TKW	GY	STW	Yeco	HI	DHE	
Replication (2)	3.0	111.6	840.7	335.5	3.1	3.6	
Genotype (15)	73.9**	6959.8**	36909.7**	9731.6**	189.9**	118.3**	
Old vs Modern (1)	0.8ns	12932.8**	56218.0**	1814.0ns	521.8**	540.4**	
Error (30)	2.0	905.5	2465.3	1827.7	9.2	1.6	
σ^2_e	2.0	905.5	2465.3	1827.7	9.2	1.6	
σ^2_g	23.9	2018.1	11481.5	2634.6	60.2	38.9	
σ^2_p	26.0	2923.6	13946.8	4462.4	69.5	40.5	
CVe	2.8	11.4	12.4	11.1	22.7	1.3	
CVg	9.6	17.1	26.7	13.4	148.4	31.1	
CVp	10.0	20.5	29.4	17.4	171.1	32.4	
CVg/CVe	3.4	1.5	2.2	1.2	6.5	23.9	
H ² bs	92.2	69.0	82.3	59.0	86.7	96.0	
\bar{Y} overall	50.7	263.4	401.2	383.8	40.6	124.9	
\bar{Y} Max	62.0	363.2	582.0	486.0	51.4	133.3	
\bar{Y} Min	42.1	201.2	248.8	282.5	29.1	117.0	
\bar{Y} Old	51.0	231.1	468.4	371.7	34.2	129.9	
\bar{Y} Modern	50.5	288.5	349.0	393.2	46.9	119.8	
Deviation	-0.4ns	57.4**	-119.4*	21.5ns	12.7**	-10.1**	
%Deviation	-0.8	24.8	-25.5	5.8	37.1	-7.8	
LSD5%	2.4	50.2	82.8	71.3	5.1	2.1	

PHT= plant height (cm), BIO=biomass (g/m²), SW= spikes weight (g/m²), SN= spikes number, NKS = number of kernels per spike, NGM= number of grains/m², TKW= 1000-kernel weight (g), GY= grain yield (g/m²),STW= straw yield (g/m²), Yeco = economical yield (g/m²), HI= harvest index (%), DHE = days to heading.

3.2. Relationships between measured variables

PHT showed significant and positive correlations with DHE (0.631**) and with STW (0.555*). Tall varieties were late to head, showing high straw yield. DHE was negatively and significantly correlated with SN (-0.611*) and with GY (-0.619*). Late genotypes, among those tested, were low grain yielding, showing low spike number. BIO was positively correlated with SW (0.506*), STW (0.891**) and with Yeco (0.844**). Within the set of the assessed varieties, straw yield, economical yield and spike weight appear as the main contributors to biomass expression. SW, besides its correlation with BIO, exhibited

significant correlations with SN (0.652**), NGM (0.671**) and with GY (0.876**). SN showed significant correlations with NGM (0.806**), GY (0.781**) and Yeco (0.610*). Spike number and spike weight contributed substantially to grain yield and biomass formation. NKS and TKW were significantly and negatively correlated to each other (-0.553*), suggesting that high spike fertility is made possible at the detriment of thousand kernel weight because of compensation effect among these two yield components. GY, besides its significant correlations with DHE, SW, SN, NGM, showed a positive and significant correlation with Yeco (0.674**). These correlations suggested that high grain yielding varieties headed early,

exhibiting high spike weight, spike number, number of kernels /m² and high economical yield. Similarly, varieties, having high economical yield, exhibited high biomass, spike number, number of kernels/ m² and high grain yield (Table 3). These results were in line with those reported by Graziani *et al.* (2014), who found that, among the yield components, the number of grains/m² showed the strongest correlation with grain yield. Mohsin *et al.* (2009) found that grain yield correlated positively with biomass, number of spikes and harvest index. Fellahi *et al.* (2015) reported positive and significant correlations yield with biomass,

spike weight, and spike number. They reported also that biomass had the highest effect, explaining more than 83.0% of grain yield variation, suggesting that any increase in biological yield, particularly the spike weight fraction, affected positively grain yield. Straw yield was positively related to spike number while thousand kernel weight and plant height exhibited significant and negative correlations with spike fertility. Fellahi *et al.* (2015) and Keser *et al.* (2017) reported a significant positive correlation between plant height and yield under severe drought stress conditions.

Table 3. Spearman's rank coefficients of correlations between the measured traits (Above diagonal probability, under diagonal coefficients of correlations:

	PHT	DHE	BIO	SW	SN	NKS	NGM	TKW	GY	STW	Yeco
PHT		0.009	0.210	0.395	0.124	0.471	0.316	0.803	0.109	0.026	0.791
DHE	0.631**		0.667	0.225	0.012	0.480	0.058	0.655	0.010	0.134	0.636
BIO	0.331	0.117		0.046	0.380	0.097	0.200	0.451	0.368	0.000	0.000
SW	-0.228	-0.322	0.506*		0.006	0.506	0.004	0.542	0.000	0.506	0.000
SN	-0.401	-0.611*	0.236	0.652**		0.450	0.000	0.974	0.000	0.749	0.012
NKS	0.194	0.190	0.429	0.179	-0.203		0.200	0.026	0.704	0.092	0.188
NGM	-0.268	-0.484	0.338	0.671**	0.806**	0.338		0.172	0.000	0.888	0.004
TKW	-0.068	-0.121	-0.203	0.165	0.009	-0.553*	-0.359		0.485	0.188	0.854
GY	-0.416	-0.619*	0.241	0.876**	0.781**	0.103	0.785**	0.188		0.594	0.004
STW	0.555*	0.391	0.891**	0.179	-0.087	0.435	0.038	-0.347	-0.144		0.019
Yeco	0.072	-0.128	0.844**	0.850	0.610*	0.347	0.676**	-0.050	0.674**	0.579**	

PHT= plant height (cm), BIO=biomass (g/m²), SW= spikes weight (g/m²), SN= spikes number, NKS = number of kernels per spike, NGM= number of grains/m², TKW= 1000-kernel weight (g), GY= grain yield (g/m²),STW= straw yield (g/m²), Yeco = economical yield (g/m²), HI= harvest index (%), DHE = days to heading.

Furthermore, according to Royo *et al.* (2007), grain yield increases have been mostly associated to increases in harvest index and number of grains/m² arising from enhanced number of spikes and grains set. Mansouri *et al.* (2018) reported highly significant rank correlations between biomass, spike number and grain yield, while moderate and significant correlations were found between plant height and 1000-kernel weight, and between kernels/spike and harvest index.

3.3. Classification of the assessed varieties

Principal component analysis (PCA) is used to identify traits which were decisive in varietal differentiation. Most of the variability existing within the data analyzed is absorbed by the first three principal components which showed latent roots greater than unity. In fact, these three PC's explained 88.08% of the total variance (Table 4). This percentage is appreciably high to discriminate between the assessed varieties on the basis of the measured traits. Spike weight (SW, 0.404), spike number (SN, 0.376), grain yield (GY, 0.418), number of kernels/ m² (NGM, 0.427) and economical yield (Yeco, 0.407) were the major contributors to PC1. All 5 traits were positively related to this axis which explained 45.69% of the total variation, suggesting that PC1 is indicator of genotypic grain yielding ability (Table 4, Figure 1). PC2 accounted for 29.35% of variation with PHT (0.382), DHE (0.387), BIO (0.432) and STW (0.511) as the major loaded factors. PC2 is indicator of biomass production, earliness and plant height. PC3 accounted for another 13.04% of the total variation, with NKS and TKW as the major loaded factors. This axis represents the opposition of spike fertility to kernel weight (Table 4).

Table 4. Eigenvalues, % variance, % cumulative variances and eigenvectors of the first three principal components for the measured variables of the tested varieties.

Parameters	PC1	PC2	PC3
Eigenvalue	5.03	3.23	1.43
% variance	45.69	29.35	13.04
% cumulative variances	45.69	75.04	88.08
Traits	Loading		
SW	0.404	0.009	0.277
SN	0.376	-0.212	0.038
NGM	0.427	-0.015	-0.187
GY	0.418	-0.115	0.148
Yeco	0.407	0.201	0.150
PHT	-0.162	0.382	0.354
DHE	-0.241	0.387	0.190
BIO	0.255	0.432	0.100
STW	0.090	0.511	0.042
NKS	0.094	0.339	-0.401
TKW	-0.081	-0.207	0.713

PHT= plant height (cm), BIO=biomass (g/m²), SW= spikes weight (g/m²), SN= spikes number, NKS = number of kernels per spike, NGM= number of grains/m², TKW= 1000-kernel weight (g), GY= grain yield (g/m²),STW= straw yield (g/m²), Yeco = economical yield (g/m²), HI= harvest index (%), DHE = days to heading.

Varieties GTA (4.053), VIT (4.021), BTL (2.587), ZBA (1.604), B17 (-1.533), H3 (-2.543) and GGR (-4.438) exhibited high scores on PC1. Based on the sign of their scores, GTA, VIT, BTL and ZBA were categorized as high grain yielding cultivars. This capacity resulted from their high genetic ability to produce numerous and heavy spikes besides numerous kernels /m². By contrast B17, H3 and GGR were somewhat lacking this genetic ability and

consequently were classified as low grain yielding varieties (Figure 1). GLR (3.02), MBB (2.212), POL (1.526), BOU (-2.522) and OFA (-2.583) had high scores on PC2. Based on the sign of their scores, GLR, MBB and POL were classified as late and tall, exhibiting high biomass and straw yields. BOU and OFA had the opposite features, being early, short and showing low biomass and straw yields. OZ (1.952), MPL (-0.788), WAH (-1.488) and Setifis (-1.991) diverged for NKS and TKW. OZ had

high TKW (54.4 g) associated with low NKS (21.1 grains/spike); while MPL, WAH and SET had, on average, low kernel weight and high spike fertility (Figure 1). Cluster analysis classified the tested genotypes, based on their resemblance/dissimilarity degree, into three major groups. BTL, ZBA, GTA and VIT were grouped in cluster C1. Cluster C2 contained OZ, GLR, MBB, POL, H3 and B17; while GGR, WAH, MPL, SET, BOU and OFA were classified in cluster C3 (Figure 1).

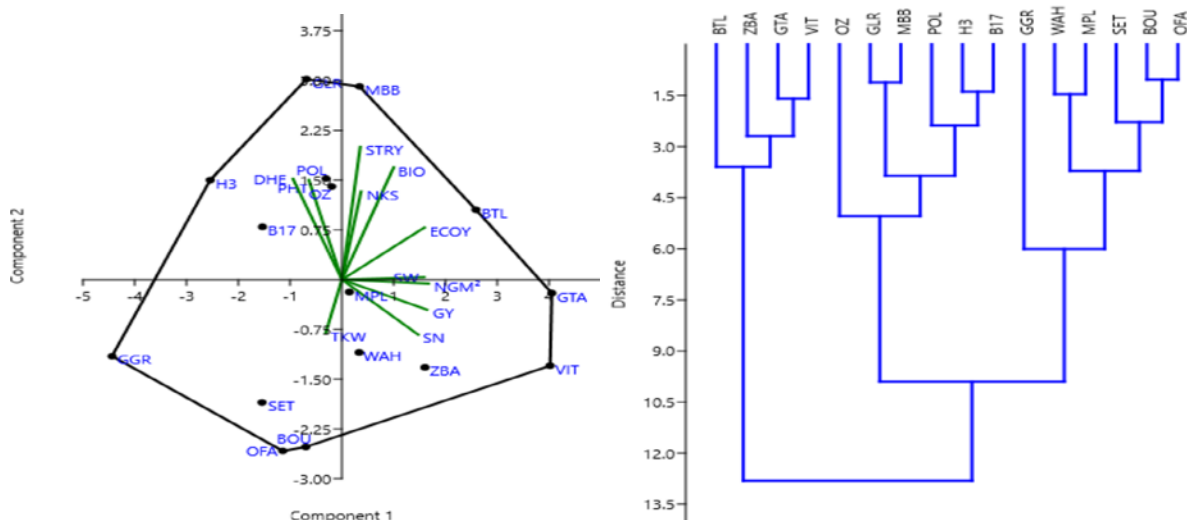


Figure 1. PC1-PC2 biplot and cluster(dendrogram) of the assessed varieties based on 10 measured variables (PHT= plant height (cm), BIO=biomass (g/m²), SW= spikes weight (g/m²), SN= spikes number, NKS = number of kernels per spike, NGM= number of grains/m², TKW= 1000-kernel weight (g), GY= grain yield (g/m²),STW= straw yield (g/m²), Yeco = economical yield (g/m²), HI= harvest index (%), DHE = days to heading. BOU= Boussselam, BTL= Boutaleb, B17= Bidi 17,GTA= Gaviota durum, MBB= Mohamed Ben Bachir, GLR= GM= Gloire de montgolfier, GGR= Guemgoum Rkhem, WAH= Waha, OFA= Ofanto, VIT= Vitron, SET= Setifis, H3= Hedba3, POL= Polonicum, MPL= Montpellier, ZBA= ZB/Fg/Lds/3/ Ward's).

Average values for the measured traits of the three clusters are reported in table 5. These figures indicated that C1 varieties concurrently carry several desirable characteristics among which are high grain and economical yields, spike number, spike weight, number of kernels/ m², 1000-kernel weight and harvest index. These varieties were, on average, 11 days earlier and 7.9 cm shorter than C2 varieties, from which they did not differ significantly for biomass and spike fertility. The lastly registered variety, BTL, was classed among these varieties. Majority of traditional varieties, which were tall, late,

exhibiting high straw yielding capacity, low spike number and low harvest index, belonged to C2. Varieties included in cluster C3 show globally intermediate features between those characterizing C1 and C2 varieties (Table 5). WAH and BOU, largely grown along the traditional cultivar MBB in the experimental site area, were classed among the varieties grouped in C3 cluster. Using multivariate analysis, Abu-Zaitoun *et al.* (2018) categorized the studied varieties into three main clusters: High yielding, tall and late and high grain weight varieties.

Table 5. Cluster average values E for the measured traits of the tested varieties.

Cluster	PHT	DHE	BIO	SW	SN	NKS	NGM	TKW	GY	STW	Yeco	HI
C1	76.3	120.4	729.7	453.7	239.0	27.0	6.4	52.1	335.5	394.1	453.8	46.1
C2	84.2	131.2	738.2	343.8	170.7	28.8	4.8	49.1	235.8	502.4	386.5	32.1
C3	75.2	121.4	547.6	323.0	189.6	25.2	4.8	51.4	243.0	304.7	334.4	45.3

PHT= plant height (cm), BIO=biomass (g/m²), SW= spikes weight (g/m²), SN= spikes number, NKS = number of kernels per spike, NGM= number of grains/m², TKW= 1000-kernel weight (g), GY= grain yield (g/m²),STW= straw yield (g/m²), Yeco = economical yield (g/m²), HI= harvest index (%), DHE = days to heading. C1 = cluster I, C2= Cluster II, C3= Cluster III.

3.4. Traits mean change between traditional and recently released varieties.

Performances comparison of traditional (registered before 1970) and recently released varieties (registered after 1970) indicated significant differences for PHT, SW, SN,NGM, GY, STW and non-significant differences for BIO, NKS, TKW and Yeco, as suggested by the single

degree of freedom contrast (Table 2). Relative deviations ($[(100 * (\bar{Y}_{recent} - \bar{Y}_{old}) / \bar{Y}_{old})]$) of modern varieties from old ones, for the measured traits, are indicated in Figure 2. Post-green revolution varieties exhibited significant increase in SW (13.7%), SN (29.3%), NGM (23.9%), GY (24.8%), and HI (37.1%) and significant decrease in PHT (-13.3%), STW (-25.5%) and DHE (-7.8%). No significant

change was observed for BIO, NKS, TKW and Yeco (Table 2, Figure 2).

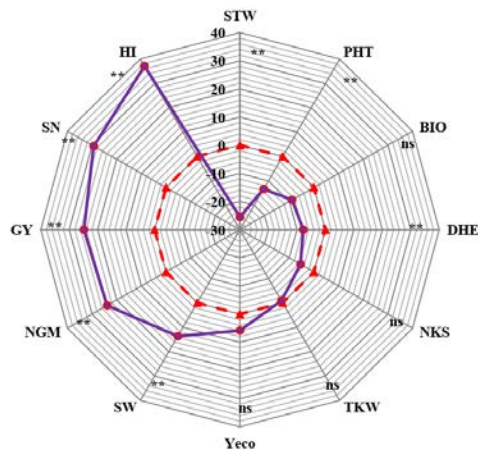


Figure 2. Relative deviation [$100 \times (\bar{Y}_{\text{recent}} - \bar{Y}_{\text{old}}) / \bar{Y}_{\text{old}}$] between traits mean of recent vs traditional varieties (PHT= plant height (cm), BIO=biomass (g/m²), SW= spikes weight (g/m²), SN= spikes number, NKS = number of kernels per spike, NGM= number of grains/m², TKW= 1000-kernel weight (g), GY= grain yield (g/m²), STW= straw yield (g/m²), Yeco = economical yield (g/m²), HI= harvest index (%), DHE = days to heading).

These results corroborated findings of Alvaro et al. (2008) who mentioned that, compared with ancient

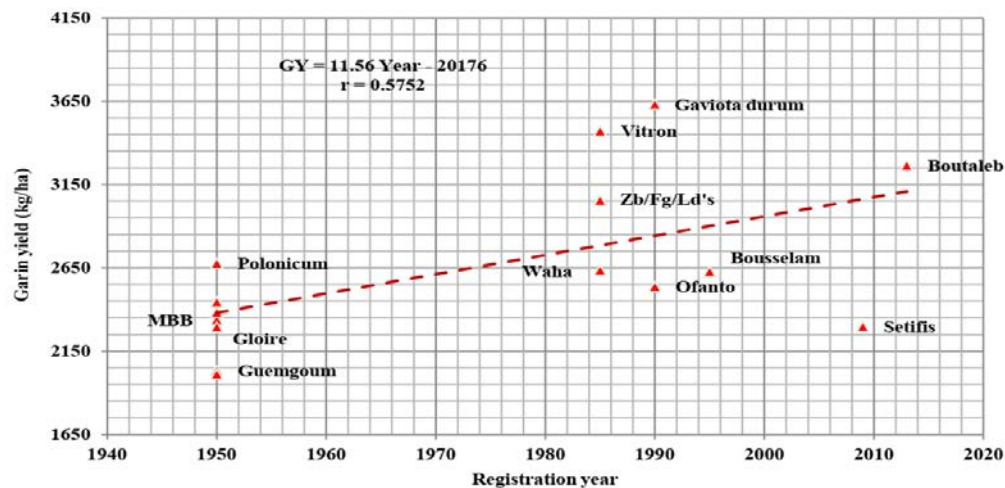


Figure 3. Durum wheat grain yield linear increase over the past 50-year period (1970 to 2020) estimated under rainfed conditions of the eastern high plateaus of Algeria.

4. Discussion

Durum wheat is a major field crop in Algeria. Rainfed grown, its production varies largely and remains below the domestic demand justifying the need to increase grain yield. Durum wheat breeding begins at the end of World War II, selecting the best types from the diversity available within the landraces (Benbelkacem, 2014). At the beginning of the seventies, massive introductions from post-green revolution high yielding plant materials were made to be used as such, on large scale, and for selection and crossing purposes. Several new varieties were developed and some of which are nowadays large scale cultivated along with pure line varieties derived from landraces. Comparison of both sources of germplasm indicates trait changes accompanying grain yield increase. Such information helps identify traits to select for and which source of germplasm to use, to design future grain

varieties, modern ones were early, had improved harvest index, more spikes/ m² and grains/ spike, with no significant difference for grain weight between the two sources of germplasm. Rate of grain yield increase is generally approached using linear or bi-linear regression models, fitting the relationship between yield and year (Keser et al., 2017). In the present study, yield trend was investigated using yield performances of the old varieties dating back to 1950 and the post-green revolution varieties, released after 1970. Linear regression analysis indicated that grain yield increased by an amount of 11.56 kg/ha/year (Figure 3). These figures were well below what has been found by Zhou et al. (2007) who reported that grain yield increase rates varied from 32.0 to 72.1 kg/ha/year for wheat cultivars released after 1970. But they were close to the minimal value reported by Royo et al. (2008) who mentioned that grain yield genetic gains varied from 17.0 kg/ha/year to a maximum of 24.0 kg/ha/year. Keser et al. (2017) reported, for low-yielding sites, a grain yield increase of 6.1 kg/ha/year and 18.0 kg/ha/year for high yielding sites. Differences in grain yield increase are usually explained by variation in site potentialities, genotypic potentialities, genotype x environment interactions and management factors (Laidig et al., 2017).

yield improvement in water-limited environments. Results of the present study indicated the presence of appreciable variability, as suggested by the CVg/CVe which took values greater than unity, for most of the traits measured. Trait mean values were within the range of the values usually observed under the conditions of the experimental site where the experience was carried out. This environment is known for its large year-to-year variation and significant genotype x environment interaction (Mekhlouf et al., 2006; Adjabi et al., 2007; Haddad et al., 2016). Broad sense heritability values were, on average higher because based on one year data, and as such are biased upward, but still agreed with results from Salmi et al. (2019) and Mohsin et al. (2009), and contradicted findings of Graziani et al. (2014) for grain yield broad sense heritability. Careful examination of trait relationships suggested that within the assessed plant materials, tall varieties tended to be late to head, having high straw yield. Late genotypes were low grain yielding,

bearing low spike number. Spike number and spike weight make sizable contribution to grain yield and biomass. Compensation effect is operating between spike fertility and kernel weight. Altogether, the correlations suggested that high grain yielding varieties were early, producing heavy and numerous spikes resulting in numerous kernels /m² and exhibiting high economical yield. These results were in line with those reported by Mohsin *et al.* (2009), Graziani *et al.* (2014), Fellahi *et al.* (2015) and Mansouri *et al.* (2018). Used to identify traits which were decisive in varietal differentiation, principal components analysis indicated that the first principal component discriminates between high (4 varieties) and low (3 varieties) grain yielding varieties, based on their differential genetic ability to produce numerous and heavy spikes besides numerous kernels /m². The second principal component discriminates the assessed varieties based on lateness/earliness, tallness/shortness, and differential yielding ability for biomass and straw (3 vs 2 varieties). The third principal component discriminates between varieties having high kernel weight and low spike fertility (1 variety) and those exhibiting high spike fertility and low kernel weight (3 varieties). Cluster analysis confirmed somewhat principal components analysis and categorized the tested genotypes into three major clusters. Varieties belonging to cluster I were high yielding, 7.9 cm shorter and 11 days earlier, on average. Varieties of cluster C2 were tall, late, exhibiting high straw yield, low grain yield and low harvest index. Varieties included in cluster C3 had globally intermediate features between those characterizing C1 and C2 varieties. These results were in line with findings of Abu-Zaitoun *et al.* (2018) who reported three main clusters: High yielding varieties, tall and late varieties and varieties showing high grain weight. Performances comparison of traditional and recently released varieties indicated that post-green revolution varieties exhibited significant increase in grain yield and grain yield components and harvest index and significant decrease in plant height, straw yield and lateness; with no significant changes in biomass, spike fertility and kernel weight, on average. These results corroborated findings of several researches (Alvaro *et al.*, 2008; Battenfield *et al.*, 2013; Fischer *et al.*, 2014; Sanchez-Garcia *et al.*, 2013; Gizzi and Gambin, 2016; Laidig *et al.*, 2017; Wang *et al.*, 2017; Rabi *et al.*, University of Algeria, personal communication). Rate of grain yield increase was estimated to be equal to 11.56 kg/ha/year, which is well below figures reported from favorable environments (Zhou *et al.*, 2007 ; Cargnin *et al.*, 2009; Joudi *et al.*, (2014), but closer to those reported from similar water -limited environments (Royo *et al.*, 2008; Battenfield *et al.*, 2013; Keser *et al.*, 2017). The overall findings suggested that in order to improve grain yield under low yielding environment, it is important to look for dwarfing genes which affect less the expression of the desirable traits such as early vigor, rooting depth, coleoptiles length and plant height in the targeted environment. Chosen genes need to be suited to achieve the desired reduction in plant height and minor effects on other useful agronomic traits (Lopes *et al.*, 2012; Joudi *et al.*, 2014; Zhang *et al.*, 2016). Tian *et al.* (2017) suggested the use of Rht24 and Rht8, which had less adverse effects on yield and plant height under a broad range of climatic conditions compared to Rht-B1b locus. The resulting plant height increase positively impacts biomass and grain yield.

This conservative approach may achieve reasonable genetic gains under water limited environment. In fact, Morgounov *et al.* (2010) reported a substantial yield increase from a breeding program based uniquely on semi-tall and tall varieties targeted for drought conditions. The identified clusters reported in this study could be easily integrated into breeding program to accumulate desirable traits which enhance yielding ability and stress tolerance. Knowing that favorable genes for grain yield and earliness exist in post green revolution varieties while genes controlling expression of tall plant height and high straw yield exist in the traditional varieties, it is necessary to investigate variation of dwarfing genes in the tested plant material. This allows to design a breeding program promoting the development of new germplasm more adapted to rain-fed south Mediterranean environments, through selection for dwarfing genes, like Rht24 and Rht8, with minor effects on desirable traits in low yield environment.

5. Conclusion

The results of this study suggested that traditional and modern varieties complement each other as far as yield performance and adaptation to low yielding environment are concerned. To best use desirable traits coming from both source of germplasm, it is essential to investigate variation of reduced height genes present in the assessed varieties, looking for Rht genes which impact less the desirable traits in low yielding environment. Varieties carrying such Rht genes could be used in breeding program targeting high grain yield and adaptation among tall or semi tall genotypes.

Acknowledgment

Special thanks are addressed to the experimental and research institute ITGC (Technical Institute of field crops) of Setif in Algeria and its entire staff for the supply of seeds and assistance in the management of trials. Gratitude is due to its director Mr. LOUAHDI Nasr Eddin for opening the doors of the institute for conducting this research. Special thanks are also due for our partner and collaborator Mr. BACHIR Adel for all the help he gave, in particular field help from seed preparation to harvest.

References

- Abu-Zaitoun SY, Chandrasekhar K, Assili S, Shtaya MJ, Jamous RM, Mallah OB, Nashef K, Sela H, Distelfeld A, Alhajaj N, Ali-Shtayeh MS, Peleg Z and Roi Ben-David. 2018. Unlocking the genetic diversity within a Middle-East panel of Durum Wheat landraces for adaptation to semi-arid climate. *Agron.* 8: 1-12.
- Acquaah G. 2012. **Principles of plant genetics and breeding**, 2nd ed. Wiley Blackwell, Oxford, UK.
- Adjabi A, Bouzerzour H, Lelarge C, Benmahammed A, Mekhlouf A and Hanachi A. 2007. Relationships between grain yield performance, Temporal Stability and Carbon Isotope discrimination in Durum wheat (*Triticum durum* Desf.) under Mediterranean conditions. *J Agron.* 6: 294-301.
- Álvaro F, Isidro J, Villegas D, García del Moral L.F and Royo C. 2008. Old and modern durum wheat varieties from Italy and Spain differ in main spike components. *Field Crops Res.* 106: 86-93.

- Angus JF, Kirkegaard JA, Hunt JR, Ryan MH, Ohlander L and Peoples MB. 2015. Break crops and rotations for wheat. *Crop Pasture Sci.* **66**: 523-552.
- Annicchiarico P, Abdellaoui Z, Kelkouli M, and Zerargui H. 2005. Grain yield, straw yield and economic value of tall and semi-dwarf durum wheat cultivars in Algeria. *J Agr Sci.* **143**(1): 57-64.
- Bai C, Liang Y and Hawkesford MJ. 2013. Identification of QTLs associated with seedling root traits and their correlation with plant height in wheat. *J. Exp. Bot.* **64**: 1745-1753.
- Battenfield SD, Klatt AR and Raun WR. 2013. Genetic yield potential improvement of semi-dwarf winter wheat in the Great Plains. *Crop Sci.* **53**: 946-955.
- Belagrouz A, Chennafi H, Bouzerzour H, Hakimi M, Razim R and Hadj Sahraoui A. 2018. Relationships among water use efficiency and the physio-agronomic traits in durum wheat (*Triticum durum* Desf.) cultivars assessed under rainfed conditions of the eastern high plateaus of Algeria. *Agr Forestry.* **64**: 159-172.
- Belkharouch H, Benbelkacem A, Bouzerzour H and Benmahammed A. 2015. Flag Leaf and Awns Ablation and Spike Shading Effects on Spike Yield and Kernel Weight of Durum Wheat (*Triticum Turgidum* L. Var. *Durum*) Under Rainfed Conditions. *Adv Env Biol.* **9**: 184-191.
- Benbelkacem A. 2014. The history of wheat breeding in Algeria. In Porceddu E. (ed.), Damania A.B. (ed.), Qualset C.O. (ed.). Proceedings of the International Symposium on Genetics and breeding of durum wheat Bari: *CIHEAM Options Méditerranéennes: Série A. Séminaires Méditerranéens.* **110**: 363-370.
- Benider C, Madani T, Bouzerzour H and Guendouz A. 2017. Reflectance estimation in cereal/pea intercropping system based on numerical images analysis method. *Indian J. Agric. Res.* **51**: 615-618.
- Brancourt-Hulmel M, Doussinault G, Lecomte C, Berard P, Le Buanec B and Trottet M. 2003. Genetic improvement of agronomic traits of winter wheat cultivars released in France from 1946 to 1992. *Crop Sci.* **43**(1): 37-45.
- Cargnin A, Souza MA, Fronza V and Fogaça CM. 2009. Genetic and environmental contributions to increased wheat yield in Minas Gerais, Brazil. *Sci. Agric.* **66**: 317-322.
- CEIC. 2017. <https://www.ceicdata.com/en/algeria/agricultural-production/agriculture-production-vegetable-cereals-durum-wheat>.
- Chennafi H, Hannachi A, Touahria O, Fellahi ZEA, Makhlof M and Bouzerzour H. 2011. Tillage and residue management effect on durum wheat [*Triticum turgidum* (L.) Thell. ssp. *turgidum* conv. *Durum* (Desf.) MacKey] growth and yield under semi- arid climate. *Adv Env Biol.* **5**: 3231-3240.
- Chourghal N, Lhomme JP, Huard F and Aidaoui A. 2015. Climate change in Algeria and its impact on durum wheat. *Reg Env Change.* 1-13.
- Cropstat version 7.2. (2007). Software package for windows. Manila, International Rice Research Institute (IRRI).
- Fellahi ZEA, Hannachi A, Bouzerzour H, and Benbelkacem A. 2015. Inheritance pattern of metric characters affecting grain yield in two bread wheat (*Triticum aestivum* L.) crosses under rainfed conditions. *Jordan J Biol Sci.* **8**: 175-181.
- Fischer T, Byerlee D and Edmeades G. 2014. Crop yields and global food security. Will yield increase continue to feed the world? ACIAR Monograph No. 158. Canberra: Aust. Centre for Intern. Agricultural Research.
- Flintham JE, Borner J, Worland A and Gale M. 1997. Optimizing wheat grain yield: Effects of Rht (gibberellin-insensitive) dwarfing genes. *J Agr Sci.* **128**: 11-25.
- Gizzi G and Gambin BL. 2016. Eco-physiological changes in sorghum hybrids released in Argentina over the last 30 years. *Field. Crop. Res.* 188: 41-49.
- Graziani M, Maccaferri M, Royo C, Salvatorelli F, and Tuberosa R. 2014. QTL dissection of yield components and morpho-physiological traits in a durum wheat elite population tested in contrasting thermo-pluviometric conditions. *Crop Pas Sci.* **65**: 80-95.
- Griffiths S, Simmonds J, Leverington M, Wang Y, Fish L, Sayers L, Alibert L, Orford S, Wingen L and Snape J. 2012. Meta-QTL analysis of the genetic control of crop height in elite European winter wheat germplasm. *Mol. Breeding.* **29**: 159-171.
- Haddad L, Bouzerzour H, Benmahammed A, Zerargui H, Hannachi A, Bachir A, Salmi M, Fellahi ZEA, Nouar H, Laala Z. 2016. Analysis of genotype × environment interaction for grain yield in early and late sowing date on Durum Wheat (*Triticum durum* Desf.) genotypes. *Jordan J Biol Sci.* **9**: 139-146.
- Hammer O, Harper DAT, Ryan PD. PAST 2001. Paleontological statistics software package for education and data analysis. *Palaeontologia Electronica.* **4**: 1-9.
- Joudi M, Ahmadi A, Mohammadi V, Abbasi A, Mohammadi H. 2014. Genetic changes in agronomic and phonologic traits of Iranian wheat cultivars grown in different environmental conditions. *Euphytica.* **196**: 237-249.
- Keser M, Gummadov N, Akin B, Belen S, Mert Z, Taner S, Topal A, Yazar S, Morgounov A, Sharma RC and Ozdemir F. 2017. Genetic gains in wheat in Turkey: Winter wheat for dryland conditions. *crop j.* **5**: 533-540.
- Kezih R, Bekhouche F and Merazka A. 2014. Some traditional Algerian products from durum wheat. *African J Food Sci.* **8**: 30-34.
- Laaboudi A and Mouhouche B. 2012. Water Requirement Modelling for Wheat under Arid Climatic Conditions. *Hydrolog Curr Res.* **3**: 130-139.
- Laala Z, Benmahammed A, Fellahi ZEA and Bouzerzour H. 2017. Response to F3 Selection for Grain Yield in Durum Wheat [*Triticum turgidum* (L.) Thell. ssp. *Turgidum* conv. *durum* (Desf.) Mac Key] under South Mediterranean Conditions. *Annual Res Rev Biol.* **21**: 1-11.
- Laidig F, Piepho HP, Rentel D, Drobek T, Meyer U and Huesken A. 2017. Breeding progress, environmental variation and correlation of winter wheat yield and quality traits in German official variety trials and on-farm during 1983–2014. *Theor. Appl. Genet.* **130**: 223-245.
- Lopes MP, Reynolds MP, Jalal-Kamali MR, Moussa M, Feltaous Y, Tahir ISA, Barma N, Vargas M, Mannes Y and Baum M. 2012. The yield correlations of selectable physiological traits in a population of advanced spring wheat lines grown in warm and drought environments. *Field Crops Res.* **128**: 129-136.
- Mansouri A, Oudjehih B, Benbelkacem A, Fellahi ZEA and Bouzerzour H. 2018. Variation and relationships among agronomic traits in durum wheat [*Triticum turgidum* (L.) Thell. Ssp. *Turgidum* conv. *Durum* (Desf.) Mackey] under south Mediterranean growth conditions: Stepwise and path analyses. *Int J Agron.* **2018**: 1–11.
- Mekhlof A, Bouzerzour H, Benmahammed A, Hadj Sahraoui A and Harkati N. 2006. Adaptation des variétés de blé dur (*Triticum durum* Desf.) au climat semi-aride. *Sécheresse.* **17**: 507-513.
- Mohsin T, Khan N and Naqvi FN. 2009. Heritability, phenotypic correlation and path coefficient studies for some agronomic characters in synthetic elite lines of wheat. *J Food Agr Env.* **7**: 278-282.

- Morgounov A, Zykin V, Belan I, Roseeva L, Zelenskiy Y, Gomez-Becerra HF, Budak H and Bekes F. 2010. Genetic gains for grain yield in high latitude spring wheat grown in Western Siberia in 1900–2008. *Field Crop Res.* **117**: 101-112.
- Rebetzke GJ, Ellis MH, Bonnett DG, Mickelson B, Condon AG and Richards RA. 2012. Height reduction and agronomic performance for selected gibberellin-responsive dwarfing genes in bread wheat (*Triticum aestivum* L.). *Field Crops Res.* **126**: 87–96.
- Royo C, Álvaro F, Martos V, Ramdani A, Isidro J, Villegas D and García del Moral LF. 2007. Genetic changes in durum wheat yield components and associated traits in Italian and Spanish varieties during the 20th century. *Euphytica.* **155**: 259-270.
- Royo C, Maccaferri M, Álvaro F, Moragues M, Sanguineti MC, Tuberosa R, Maalouf F, García del Moral LF, Demontis A, Rhouma S, Nachit M, Nserallah N and Villegas D. 2010. Understanding the relationships between genetic and phenotypic structures of a collection of elite durum wheat accessions. *Field Crops Res.* **119**: 91-105.
- Royo C, Martos V, Ramdani A, Villegas D, Rharrabti Y and García del Moral LF. 2008. Changes in yield and carbon isotope discrimination of Italian and Spanish durum wheat during the 20th century. *Agron. J.* **100**: 352-360.
- Salmi M, Benmahammed A, Benderradji L, Fellahi ZEA, Bouzerzour H, Oulmi A and Bendelkacem A. 2019. Generation means analysis of physiological and agronomical targeted traits in durum wheat (*Triticum durum* Desf.) cross. Generation means analysis of physiological and agronomical targeted traits in durum wheat (*Triticum durum* Desf.) cross. *Rev. Fac. Nac. Agron. Medellín.* **72**: 8971-8981.
- Sanchez-Garcia M, Royo C, Aparicio N, Martín-Sánchez JA and Álvaro F. 2013. Genetic improvement of bread wheat yield and associated traits in Spain during the 20th century. *J Agr Sci.* **151**(1): 105-118.
- Steel RGD and Torrie JH. 1982. **Principles and procedures of statistics**, McGraw-Hill Books, NY, USA.
- Sun YY, Wang XL, Wang N, Chen YL and Zhang SQ. 2014. Changes in the yield and associated photosynthetic traits of dry-land winter wheat (*Triticum aestivum* L.) from the 1940s to the 2010s in Shaanxi Province of China. *Field Crops Res.* **167**: 1-10.
- Wang Z, Sadras VO, Yang X, Han X, Huang F and Zhang S. 2017. Synergy between breeding for yield in winter wheat and high-input agriculture in North-West China. *Field Crops Res.* **209**: 136-143.
- Tian X, Wen W, Xie L, Fu L, Xu D, Fu C, Wang D, Chen X, Xia X, Chen Q, He Z and Cao S. 2017. Molecular Mapping of Reduced Plant Height Gene Rht24 in Bread Wheat. *Front. Plant Sci.* **8**: 1379.
- Zhang DQ, Song XP, Feng J, Ma XP, Wu BJ, Zhang CL. 2016. Detection of dwarf genes Rht-B1b, Rht-D1b and Rht8 in huang-huai valley winter wheat areas and the influence on agronomic characteristics. *J. Triticeae Crops.* **36**: 975-981.
- Zhou LL, Bai GH, Carver B, Zhang DD. 2007. Identification of new sources of aluminum resistance in wheat. *Plant Soil.* **297**: 105-118.

Influence of Fasting and Feed Constituents Size Variation on Broiler Performance and Intestinal Demonstrations

Asad Ali Khaskheli^{1,*} and Li Chou²

¹Centre for Nutrition and Food Sciences, Queensland Alliance for Agriculture and Food Innovation, The University of Queensland,

Brisbane Qld 4072 Australia; ²Kasetsart University, Thailand

Received: July 17, 2020; Revised: September 3, 2020; Accepted: September 8, 2020

Abstract

Investigation was performed to elucidate the effects of fasting and feed constituents' size variation on broilers performance and GIT demonstrations. Experiment was performed on 90 newly hatched chicks by dividing them into 3 treatment groups including T1, T2 and T3. Chicks in group T1 were fasted for 48 hours, T2 were fed a coarsely ground diet and T3 were finely ground mash diet. Results showed significant difference for residual egg yolk weight (2.54 ± 0.29^a) and final body weight (50.1 ± 0.3^b) in group T1; however, concerning weight of proventriculus + gizzard significant difference occurred in the group T2 (8.20 ± 0.08^a). Chicks in group T1 possessed significantly higher weight of pancreas (0.32 ± 0.00^b), jejunum (2.28 ± 0.05^b) and ileum (1.98 ± 0.14^b), while length of duodenum appeared higher in group T2 (25.92 ± 0.51^a) followed by T3 (20.32 ± 0.77^b) and T1 (18.24 ± 0.29^c). Length of jejunum (41.44 ± 0.82^a) and ileum (40.22 ± 0.93^a) was significantly different in group T2. Duodenum villi height, cell area and muscularis externa thickness were significantly different in the group T1; however, body weight gain, diet intake and feed conversion efficiency showed significant difference in the group T2. Study concludes that post hatch fasting negatively affects the growth performance, gross and histological structures of digestive organs in broilers.

Keywords: Broilers, Intestinal morphology, Villi, Post hatching

1. Introduction

In broiler industry, baby chicks are not given instantaneous water and feed. Hatched birds are only transferred from the incubators, when majority of chicks have been hatched, and it takes 12 - 24 hours (Wang and Peng, 2008). Furthermore, hatchery operation procedures like vaccination, sexing, packaging and transportation are also key factors responsible for fasting of chicks (Batal and Parsons, 2002). Although, chicks start their growth and search for feed immediately after hatching, but due to late feed supply, chicks suffer starvation of 1 or 1.5 day and that results sufficient loss of body weight, dehydration, energy depletion and slow immune and GIT system development (Boersma *et al.*, 2003). In such cases, inherited nutrients from yolk sac are only liveliness source before appropriate diet utilization. The GIT develops quickly compared to other organs following hatching and act as an important part for chicks' growth during early stage (Henderson *et al.*, 2003). The GIT serves as vital part for nutrients digestion and assimilation in the body. Intestinal development can only be assessed through the measurement of crypts, site of new intestinal cells formation, villus height and surface area (Franco *et al.*, 2006). Recent past studies have reported that GIT development depends on fed, alterations in villus shape and the type of species. It may be severely impaired by delayed feeding, because fasting depresses the expression

of transcription factors *cdxA* and *cdxB*, which plays major role in the intestinal development and maintenance (Geyra *et al.*, 2001).

Although growth rate of broiler chicks is much faster, but it is influenced by intestinal development which undergoes dramatic changes during first few days of chicks' life to accommodate the rapid conversion and utilization of external nutrients (Krás *et al.*, 2013). These dramatic changes include rapid increase in mass, villi number, villi length, enterocytes number, proliferating cells and depth of crypts (Friedman *et al.*, 2003). Compared to carcass, weight of small intestines increases more quickly, and it peaks on 6 to 10th day. The length and weight of intestine have direct correlation with nutrients digestion and absorption which in turn influence the weight gain of chicks (Mateos *et al.*, 2012). Further, the type of strain and species of birds are also key variables to affect the weight and length of the small intestines (Hassouna, 2001). Gross and histological researches have reported that the duodenum, jejunum and ileum are three main parts which comprises the small intestine, while tunica serosa, tunica muscularis and tunica mucosa are 3 sheets which compose their wall (Rougière *et al.*, 2009). Inner mucosal layer is again divided into three sub-layers like laminae submucosa, muscularis mucosae and propria. Likewise, muscularis tunica is divided into two sub-layers like lamina longitudinalis and lamina subserosa. Tunica mucosa contains villi. These villi are actually hair like structures towards the lumen (Silva *et al.*, 2007).

* Corresponding author e-mail: khaskheli@gmail.com, a.ali1@uqconnect.edu.au

Numerous microvilli are also found on surface that comprise the brush. Transportation as well as absorption of monosaccharides, fatty acids and amino acids is carried by enterocytes (Pourreza *et al.*, 2012). Furthermore, mucus producing cells and intraepithelial lymphocytes are also present besides the enterocytes. Mucus secreting cells are dispersed on epithelial lining, while lumen is roofed by microvilli. They produce mucin and glycoproteins for protection (Khambualai *et al.*, 2009). Depth of mucosa and villi height are key indicators, though are commonly used for evaluating the intestinal status of chickens and differential growth of epithelium (Incharoen and Maneechote, 2013). However, Jia *et al.* (2010) stated that the growth of villi depends on the feeding.

It is assumed that the use of whole grains or coarsely ground feed has significant influence on the gastrointestinal functions and health of chicks (Huang *et al.*, 2006). The presence of gizzard is a unique feature of the poultry birds which enables chicks to take up and digest coarse feed particles, thus it is less advantageous to grind the feed for achieving better digestion. Poultry birds prefer larger feed particles instead of smaller ones (Peron *et al.*, 2005), but the precondition is complete development of digestive system otherwise their performance will decrease. By reviewing past literature, it has been found that the influence of feed particle size variation on performance parameters has rarely been investigated in the broilers (Svihus *et al.*, 2010). Current study was thus planned in order to observe the influence of fasting and feed particle size variation on the growth performance and intestinal demonstrations in broiler chicks, especially during the starter period.

2. Materials and methods

Current research was performed at the Poultry Research Station, department of Animal Science, Kasetsart University, Thailand. All the experiments and procedures were carried by trained researcher under the guidelines verified by Animal Care and Use Committee (KU - AQ570503) of Kasetsart University. Experimental trial included a total of One Hundred newly hatched Ross 308 broiler chicks. From Hundred, total of 90 birds were allocated into 3 groups *viz.*, T1, T2 and T3 containing 30 chicks in each. Chicks in group T1 were fasted for 48 hours, T2 were fed a coarsely ground diet, while in group T3 were fed a finely ground mash diet. Chicks were individually examined and weighed. Though having uniform weights, they were tibia tagged and reared into 15 battery cages. After 48 hours, chicks were reweighed again and a total of 5 were slaughtered from every group for observing visceral organs. The GIT and concerned organs were collected for further study in the laboratory like gross and histological examinations. For gross examination, length, position, shape, size, width and weight of all visceral organs like residual yolk, liver, proventriculus, gizzard, pancreas, ceca, duodenum, jejunum and ileum were focused. However, for histological observation, small portions of all visceral organs were collected and fixed into the fixative solution. Specimen size ranged from 2 to 3 cm. Specimens were washed with Phosphate Buffered Saline (PBS) having molarity 0.1. Fixed samples were implanted in paraffin then cut into sections of 5 μ m size. Glass slides were cleaned, and transverse segments were

mounted on different glass slides. Staining was carried using hematoxylin as well as eosin. Last, slides were examined by microscope. Height and area of villi, area of cell, thickness of mucosa, muscularis externa of the intestinal parts were key variables to measure for intestinal morphology.

Moreover, chicks of each group were reared for further period of 14 days. Treatment groups remained same *viz.* T1, T2 and T3. Diet was given on ad libitum to the birds, while photoperiod was continuous lighting of 24hours. Temperature was adjusted to 32°C on day numbered first and then gradually reduced according to usual brooding practice. Data regarding different parameters like body weight, weight gain, feed intake and feed conversion efficiency was recorded.

2.1. Diet composition for chicks

For meeting the nutrients requirement of chicks, maize and soya meal-based diet was formulated (Table 1). Composed diet for different treatment groups contained same kinds of nutrients excepting particle size which was varying with treatment group. The coarse and finely ground mash diets were prepared by grinding the corn and soybean meal in the hammer mill to pass through 6 mm or 3 mm screen and their mixture were combined with other feed components.

Table 1. Diet composition of experimental birds

Ingredients	Dry matter basis (%)
Corn meal	40.00
Rice bran	15.00
Soybean meal	40.00
Palm oil	1.00
DL-Methionine	0.20
Dicalcium phosphate	2.00
Calcium carbonate	0.90
Sodium chloride	0.40
Premix	0.50
Chemical composition	
Crude protein	22.00
Ether extract	4.00
Crude fiber	4.00
Crude ash	6.00
Calcium	0.80
Available phosphorus	0.45
ME (kcal / kg)	3,000

2.2. Statistical Analysis

Results regarding all study parameters were analyzed by using software, Statistix version 8.1. The data was expressed in terms of means \pm SE. Means were compared by applying Duncan's multiple range test. Difference was considered significant at $P < 0.05$.

3. Results and Discussion

3.1. Intestinal demonstrations

Results regarding the different parameters like initial body weight (grams), final body weight (grams), weight of visceral organs (grams), weight of intestine (grams) and length of intestine (centimeters) in different treatment groups are shown in the Table 2. Results indicate that initial body weight was higher in the group T2 (40.9 ± 0.3)

followed by T3 (40.7 ± 0.5) and T1 (39.7 ± 0.4) liver weight was higher in group T1 (3.54 ± 0.06) followed by T3 (3.50 ± 0.12) and T2 (3.32 ± 0.13), ceca weight was higher in group T3 (1.60 ± 0.19) followed by T1 (1.40 ± 0.09) and T2 (1.38 ± 0.08), while duodenum weight was found higher in group T2 (1.88 ± 0.17) followed by T3 (1.87 ± 0.05) and T1 (1.86 ± 0.06). Although means varied from one another, but statistically no significant ($P > 0.05$) difference was found among all groups for initial body weight, ceca weight, liver weight and duodenum weight.

Results further indicate no significant ($P > 0.05$) variation in the group T3 (62.8 ± 0.7^a) and T2 (63.8 ± 0.5^a), but the group T1 (50.1 ± 0.3^b) statistically differed from group T2 and T3 against final body weight. Regarding residual yolk weight, significant difference ($P < 0.05$) was found in the group T1 (2.54 ± 0.29^a), while between group T3 (1.48 ± 0.29^b) and T2 (1.28 ± 0.09^b) no significant ($P > 0.05$) change was noticed. Regarding weight of proventriculus + gizzard significant ($P < 0.05$) difference occurred in the group T2 (8.20 ± 0.08^a) but among group T1 (7.10 ± 0.24^b) and T3 (7.10 ± 0.16^b) no significant ($P > 0.05$) difference was observed.

Table 2. Growth rate, visceral organs weight, intestinal weight and intestinal length of chicks under the influence of fasting and feed particle size variation

Study parameters	Treatment groups		
	T1	T2	T3
Growth rate (g / bird)			
Initial body weight	39.7 ± 0.4	40.9 ± 0.3	40.7 ± 0.5
Final body weight	50.1 ± 0.3^b	63.8 ± 0.5^a	62.8 ± 0.7^a
Visceral organ weight (g / 100 BW)			
Residual Yolk	2.54 ± 0.29^a	1.28 ± 0.09^b	1.48 ± 0.29^b
Liver	3.54 ± 0.06	3.32 ± 0.13	3.50 ± 0.12
Proventriculus + gizzard	7.10 ± 0.24^b	8.20 ± 0.08^a	7.10 ± 0.16^b
Pancreas	0.32 ± 0.00^b	0.44 ± 0.02^a	0.44 ± 0.02^a
Ceca	1.40 ± 0.09	1.38 ± 0.08	1.60 ± 0.19
Intestinal weight (g / 100 BW)			
Duodenum	1.86 ± 0.06	1.88 ± 0.17	1.87 ± 0.05
Jejunum	2.28 ± 0.05^b	3.30 ± 0.15^a	3.22 ± 0.25^a
Ileum	1.98 ± 0.14^b	2.64 ± 0.09^a	2.90 ± 0.21^a
Intestinal length (cm / 100 BW)			
Duodenum	18.24 ± 0.29^c	25.92 ± 0.51^a	20.32 ± 0.77^b
Jejunum	34.00 ± 1.41^b	41.44 ± 0.82^a	36.30 ± 0.95^b
Ileum	31.44 ± 1.02^b	40.22 ± 0.93^a	33.24 ± 0.17^b

^{a-c}Means within each row differ with letter designations ($P < 0.05$)

Table 3. Growth performance of broiler chicks under the influence of fasting and feed particle size (Mean \pm SE)

Study parameters	Treatment groups		
	T1	T2	T3
Body weight (g / bird)	399.7 ± 4.8^b	432.2 ± 3.0^a	403.3 ± 6.7^b
Weight gain (g / bird)	360.2 ± 5.1^b	391.5 ± 2.9^a	363.7 ± 7.1^b
Feed intake (g / bird)	566.7 ± 11.4^a	594.8 ± 7.5^a	511.7 ± 18.3^b
Feed efficiency	0.67 ± 0.02	0.69 ± 0.02	0.73 ± 0.03

^{a-b}Means within each row differ with letter designations ($P < 0.05$)

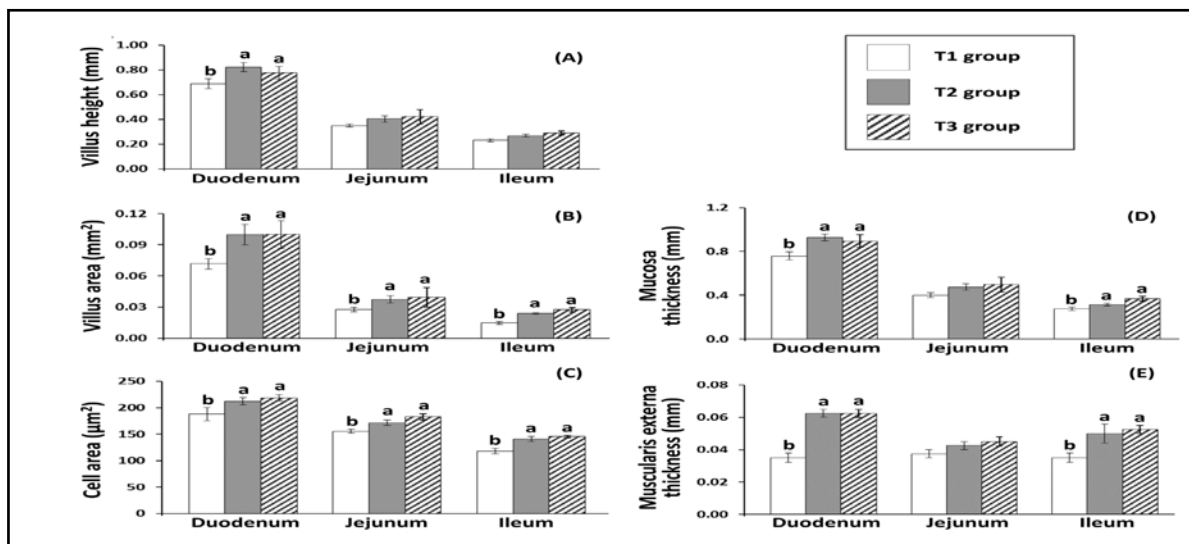
Regarding weight of pancreas, no significant ($P > 0.05$) difference appeared in the group T2 (0.44 ± 0.02^a) and T3 (0.44 ± 0.02^a), whereas group T1 (0.32 ± 0.00^b) showed significant ($P < 0.05$) difference compared to group T2 and T3. These results are in concomitant with (Bhanja *et al.*, 2009) who indicated that the feed intake significantly influences the GIT and visceral organs' development. Several other scientists also reported similar kinds of findings and recommended that baby chicks following hatching need instant feed for assurance of appropriate growth of GIT and its affiliated organs (Incharoen *et al.*, 2010). In connection to our study, it has also been reported that the post hatch withdrawal of water and feed impairs weight of all digestive organs (Maiorka *et al.*, 2003). Table 2 further depicts no significant ($P > 0.05$) difference in the group T3 (3.20 ± 0.25^a) and T2 (3.30 ± 0.15^a), whereas group T1 (2.28 ± 0.05^b) found statistically different ($P < 0.05$) from group T2 and T3 for weight of jejunum. Concerning weight of ileum, no significant ($P > 0.05$) difference was found in the group T3 (2.90 ± 0.21^a) and T2 (2.64 ± 0.09^a), while group T1 (1.98 ± 0.14^b) showed prominent ($P < 0.05$) variation compared to birds in group T2 and T3. Regarding the duodenum length, significant ($P < 0.05$) difference appeared in the group T2 (25.92 ± 0.51^a) followed by T3 (20.32 ± 0.77^b) and T1 (18.24 ± 0.29^c). Group T2 (41.44 ± 0.82^a) also showed significant ($P < 0.05$) difference against length of jejunum, but the group T3 (36.30 ± 0.95^b) and T1 (34.00 ± 1.41^b) showed no significant ($P > 0.05$) difference. Further, significant ($P < 0.05$) difference appeared in the group T2 (40.22 ± 0.93^a), and no significant ($P > 0.05$) difference in group T3 (33.24 ± 0.17^b) and T1 (31.44 ± 1.02^b) for the length of ileum. These results with (Jimenez-Moreno *et al.*, 2010), where authors reported that the variation in the diet causes structural change in duodenum and its concerning parts.

Results regarding the villus height (mm), villus area (mm^2), cell area (mm^2), mucosa thickness (mm) and muscularis externa thickness (mm) are presented in the Figure 1. Results indicate significant ($P < 0.05$) difference in the group T1 against villus height of duodenum, while group T2 and T3 showed no significant ($P > 0.05$) difference compared to group T1. Regarding the villus height of jejunum and ileum no significant ($P > 0.05$) difference appeared in group T1; however, change was significant ($P < 0.05$) for area of villus, ileum jejunum and duodenum. Regarding cell area, group T2 and T3 showed no significant ($P > 0.05$) difference, however T1 varied considerably ($P < 0.05$). Figure 1 further shows no prominent ($P > 0.05$) change in the group T2 and T3 against mucosa thickness of duodenum and ileum, whereas variation was significant ($P < 0.05$) in the group T1. Concerning mucosa thickness of jejunum, although all the

means showed slight variation, statistically they were not different ($P > 0.05$) from each other. Comparatively, significant difference ($P < 0.05$) was seen in the group T1 and no significant difference among groups T2 and T3 against muscularis externa thickness of duodenum and ileum. Against muscularis externa thickness of jejunum, statistically no difference ($P > 0.05$) was found among all the groups.

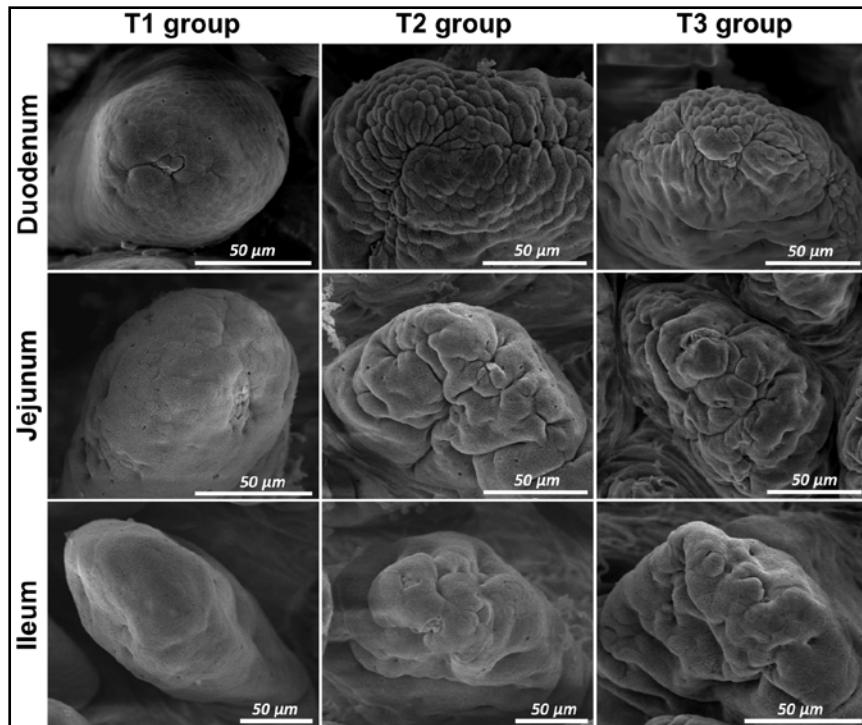
Our findings possess similarity with results of (Tabedian *et al.*, 2010) who stated that the height of villi in

jejunum and duodenum diminishes considerably ($P < 0.05$) with the increase of feed withdrawal period. It is also supportive that feed deprivation of 5 - 6 days prominently ($P < 0.05$) reduces the number of enterocytes and villi height (Yamauchi *et al.*, 2010). Further, morphological alterations in the villi of broilers are reliant on digested nutrients in the intestinal lumen (Panda *et al.*, 210). Cellular alterations in the apical surface of villi were observed under the electron microscope and observations are displayed in the Figure 2.



^{a-b}Means with different letter designations are significantly different ($P < 0.05$)

Figure 1. Villus height (A), villus area (B), cell area (C), mucosa thickness (D) and muscularis externa thickness (E) in the duodenum, jejunum and ileum of chicks subjected to fasting and feed particle size variation.



Scale bar = 50 μm, magnification: ×1000

Figure 2. Scanning electron microscopic observations of apical surface of duodenum, jejunum and ileum in broiler chicks subjected to fasting and feed particle size variation.

Duodenal cellular morphology of chicks among different groups showed great variability in the appearance. Surface of villi was made up of only layer of epithelial cells in the group T1, while villi in group T2 followed by T3 possessed copious cell groups accumulated by several protruded epithelial layers surrounding sulcus centrale. Regarding cellular morphology of jejunum and ileum, copious bunches of cells were grouped and many epithelia surrounding the central sulcus were seen in the group T3. However, in group T1, villus apical surface was composed of many single epithelial cells only (Figure 2).

3.2. Growth performance

Results regarding different growth parameters are shown in the Table 3. Table indicates significant ($P < 0.05$) difference in the group T2 (432.2 ± 3.0^a), while among groups T3 (403.3 ± 6.7^b) and T1 (399.7 ± 4.8^b) no significant ($P > 0.05$) variation was observed for initial body weight. Weight gain significantly ($P < 0.05$) differed in the group T2 (391.5 ± 2.9^a), but among groups T3 (363.7 ± 7.1^b) and T1 (360.2 ± 5.1^b) change was non-significant ($P > 0.05$). Reported results of (Noy and Sklan, 1998) and (Hetland *et al.*, 2002) are also much similar to our study, when studying the newly hatched chicks in contrast to feeding practices. They showed 10.5 percent higher weight compared to chicks though they were fed following fasting of 2 days. It may be presumed that the late feeding of chicks may cause few stimulations in their GIT. Panda *et al.* (2010) have also reported supportive findings. According to their results, chicks (though accessed feed after fasting of two days) attained considerably lesser weight compared to that of those were early fed. Adverse effects of fasting of two days on chicks' development have also been stated by Juul-madsen *et al.* (2004). It was reported that fasting one day is adequate for appropriate performance of birds.

Table 3 further shows that no significant ($P > 0.05$) difference was found in the group T2 (594.8 ± 7.5^a) and T1 (566.7 ± 11.4^a), while group T3 (511.7 ± 18.3^b) was statistically ($P < 0.05$) different from the group T1 and T2 against feed intake. As for feed efficiency, group T3 (0.73 ± 0.03) showed higher mean value followed by T2 (0.69 ± 0.02) and T1 (0.67 ± 0.02) but statistically no significant ($P > 0.05$) difference was found among all groups. Similar kinds of results have also been reported by other scientists like Mohiti-Asli *et al.* (2012) and Sklan *et al.* (2003), who revealed that fasting of short duration (0.5 day) positively influences the performance of broilers. In another study, it was found that the GIT performance of broilers is stimulated by proper concentration of dietary fiber fed from day 1st to 28th (Gonzalez-Alvarado *et al.*, 2008). It has also been reported that hulls derived from oat increase the retention of nutrients in the GIT because of higher level of insoluble fiber. Further, gizzard activity and overall digestibility are also enhanced during starter period that results in increased growth performance (Hetland and Svihus, 2001).

4. Conclusion

Current study concludes that post hatch fasting significantly affects the utilization of yolk sac, feed intake, gross and histological structures of digestive organs. Fasting for first few hours of hatching does not negatively

influence the birds, but fasting of 48 hours adversely impairs the performance, gross and histological structures of intestine and its affiliated organs as reported in the findings of current study. Thus, fasting of chicks for longer periods should be avoided.

References

- Batal AB and Parsons C M. 2002. Effect of fasting versus feeding oasis after hatching on nutrient utilization in chicks. *Poult Sci.* **81**: 853-859.
- Bhanja S K, Devi C A, Panda A K and Sunder G S. 2009. Effect of post hatch feed deprivation on yolk-sac utilization and performance of young broiler chickens. *Asian-Aust J Anim Sci.* **22**: 1174-1179.
- Boersma S I, Robinson F E, Renema R A and Fassenko G M. 2003. Administering oasis hatching supplement prior to chick placement increases initial growth with no effect on body weight uniformity of female broiler breeders after three weeks of age. *J Appl Poult Res.* **12** (4): 428-34.
- Franco J R G, Murakami AE, Natali M R M, Garcia E R M and Furlan A C. 2006. Influence of delayed placement and dietary lysine levels on small intestine morphometrics and performance of broilers. *Braz J Poult Sci.* **8**: 233-241.
- Friedman A, Bar S E and Sklan D. 2003. Ontogeny of gut associated immune competence in the chick. *World's Poult Sci J.* **59**: 209-219.
- Geyra A, Uni Z and Sklan D. 2001. Enterocyte dynamics and mucosal development in the Post hatch chick. *Poult Sci.* **80**: 776-82.
- Gonzalez-Alvarado J M, Jimenez-Moreno E, Valencia D G, Lazaro R and Mateos G G. 2008. Effects of fiber source and heat processing of the cereal on the development and pH of the gastrointestinal tract of broilers fed diets based on corn or rice. *Poult Sci.* **87**: 1779-1795.
- Hassouna E M A. 2001. Some anatomical and morphometrical studies on the intestinal tract of chicken, duck, goose, turkey, pigeon, dove, quail, sparrow, heron, jackdaw, hoopoe, kestrel and owl. *Ass Vet Med J.* **44**: 47-78.
- Henderson S N, Vicente J L, Pixely C M, Hargis B M and Tellez G. 2008. Effect of an early nutritional supplement on broiler performance. *Int J Poult Sci.* **7**: 211-214.
- Hetland H and Svihus B. 2001. Effect of oat hulls on performance, gut capacity and feed passage time in broiler chickens. *Brit Poult Sci.* **42**: 354-361.
- [11] Hetland H, Svihus B and Olaisen V. 2002. Effect of feeding whole cereals on performance, starch digestibility and duodenal particle size distribution in broiler chickens. *Brit Poult Sci.* **43** (3): 416-423.
- Huang D S, Li D F, Xing J J, Ma Y X and Li Z J. 2006. Effects of feed particle size and feed form on survival of Salmonella Typhimurium in the alimentary tract and Salmonella Typhimurium reduction in growing broilers. *Poult Sci.* **85**: 831-836.
- Incharoen T and Maneechote P. 2013. The effects of dietary whole rice hull as insoluble fiber on the flock uniformity of pullets and on the egg performance and intestinal mucosa of laying hens. *Am J Agri Bio Sci.* **8**: 323-329.
- Incharoen T, Yamauchi K and Thongwittaya N. 2010. Intestinal villus histological alterations in broilers fed dietary dried fermented ginger. *J Anim Phys & Anim Nutr.* **94**: 130-137.
- Jia W and Slominski B A. 2010. Means to improve the nutritive value of flaxseed for broiler chickens: The effect of particle size, enzyme addition, and pelleting. *Poult Sci.* **89**: 261-269.

- Jimenez-Moreno E, Chamorro S, Frikha M, Safaa H M and Lazaro R. 2011. Effects of increasing levels of pea hulls in the diet on productive performance, development of the gastrointestinal tract and nutrient retention of broilers from one to eighteen days of age. *Anim F Sci Tech*. **168**: 100-112.
- Juul-Madsen H R, Su G and Sørensen P. 2004. Influence of early or late start of first feeding on growth and immune phenotype of broilers. *Br Poult Sci*. **45**: 210-222.
- Khambualai O, Ruttanavut J, Kitabatake M, Goto H and Erikawa T. 2009. Effects of dietary natural zeolite including plant extract on growth performance and intestinal histology in Aigamo ducks. *Brit Poult Sci*. **50**: 123-130.
- Krás R V, Kessler A M, Ribeiro A M L, Henn J D and Bockor L. 2013. Effect of dietary fibre, genetic strain and age on the digestive metabolism of broiler chickens. *Braz J Poult Sci*. **15**: 83-90.
- Maiorka A, Santin E, Dahlke F, Boleli I and Furlan R. 2003. Post hatching water and feed deprivation affect the gastrointestinal tract and intestinal mucosa development of broiler chicks. *J Appl Poult Res*. **12**: 483-492.
- Mateos G G, Jimenez-Moreno E, Serrano M P and Lazaro R P. 2012. Poultry response to high levels of dietary fiber sources varying in physical and chemical characteristics. *J Appl Poult Res.*, **21**: 156-174.
- Mohiti-Asli M, Shivazad M, Zaghari M, Rezaian M and Aminzadeh S. 2012. Effects of feeding regimen, fiber inclusion and crude protein content of the diet on performance and egg quality and hatchability of eggs of broiler breeder hens. *Poult Sci*. **91**: 3097-3106.
- Noy Y and Sklan D. 1998. Yolk utilization in the newly hatched poult. *Br Poult Sci*. **39**: 446-451.
- Panda A K, Raju M V L N, Rama R S V, Shyam S G, Reddy M R. 2010. Effect of post-hatch feed deprivation on growth, immune organ development and immune competence in broiler chickens. *Anim Nutr F Tech*. **10**: 9-17.
- Peron A, Bastianelli D, Oury F X, Gomez J and Carre B. 2005. Effects of food deprivation and particle size of ground wheat on digestibility of food components in broilers fed on a pelleted diet. *Br Poult Sci*. **46**: 223-230.
- Pourreza J, Zamani F, Tabeidian A A and Toghyani M. 2012. Effect of early feeding or feed deprivation on growth performance of broiler chicks. *Res Op Anim & Vet Sci*. **2**: 136-140.
- Rougière N, Gomez J, Mignon-Grasteau S and Carré B. 2009. Effects of diet particle size on digestive parameters in D+ and D-genetic chicken lines selected for divergent digestion efficiency. *Poult Sci*. **88**: 1206-1215.
- Silva A V, Majorka A, Borges S A, Santin E and Boleli I C. 2007. Surface area of the tip of the enterocytes in small intestine mucosa of broilers submitted to early feed restriction and supplemented with glutamine. *Int J Poult Sci*. **6**: 31-35.
- Sklan D, Smirnov A and Plavnik I. 2003. The effect of dietary fibre on the small intestines and apparent digestion in the turkey. *Br Poult Sci*. **44**: 735-740.
- Svihus B, Sacranie A, Denstadli V and Choct M. 2010. Nutrient utilization and functionality of the anterior digestive tract caused by intermittent feeding and inclusion of whole wheat in diets for broiler chickens. *Poult Sci*. **89**: 2617-2625.
- Tabedian S A, Samie A, Pourreza J and Sadeghi G H. 2010. Effect of fasting or post-hatch diet's type on chick development. *J Anim & Vet Adv*. **9 (2)**: 406-413.
- Wang J X and Peng K M. 2008. Developmental morphology of the small intestine of African ostrich chicks. *Poult Sci*. **87**: 2629-2635.
- Yamauchi K, Incharoen T and Yamauchi K. 2010. The Relationship between intestinal histology and function as shown by compensatory enlargement of remnant villi after midgut resection in chickens. *The Anat Rec Adv Integ Anat & Ev Bio*. **293 (12)**: 2071-2079.

Diversity of *Phaseolus lunatus* L. in East Java, Indonesia based on PCR-RAPD technique

Elly Purwanti¹, Mohamad Amin², Siti Zubaidah², Maftuchah Maftuchah³,
Siti Nur Hidayati⁴, and Ahmad Fauzi^{1,*}

¹Department of Biology Education, Faculty of Teacher Training and Education, University of Muhammadiyah Malang, Jl. Raya Tlogmoas No. 246, Malang 65144, Indonesia; ²Department of Biology, Faculty of Mathematics and Natural Science, Universitas Negeri Malang, Semarang No. 5, Malang 65145, Indonesia; ³Department of Agrotechnology, Faculty of Agriculture and Animal Science, University of Muhammadiyah Malang, Indonesia; ⁴Department of Biology, Middle Tennessee State University, Murfreesboro, TN 37132, USA

Received: April 1, 2021; Revised: May 9, 2021; Accepted May 10, 2021

Abstract

Phaseolus lunatus L. is one of the legume plants found in some parts of Indonesia and has potential as alternative food rich in protein. This current research aimed at analysing genetic accessions of *P. lunatus* distributed in some areas in East Java, Indonesia, based on the RAPD (Random Amplified Polymorphic Deoxyribonucleic acid) marker. 15 accessions originated from four locations were analysed. Ten primers were used and produced 68 bands out of 67 were polymorphic. The percent polymorphism was 96% to 100%. Ten unique bands were detected in eight accessions (Prb1, Prb2, Prb5, Mdr12, Mdr16, Mdr19, Mdr4, and Mdr6). Using the Neighbor-Joining method, a phylogenetic tree was yielded by a similarity coefficient of 64% to 100%. On the genetic similarity coefficient (GSC) of 0.6, there were two clusters: the first and second major clusters (Cluster A and B). The former contained the accessions 7, 8, 13, and 14, while the latter comprised 2, 4, 16, 18, Prb1, Prb2, Prb3, Prb4, and Prb5. In conclusion, based on phylogenetic trees formed, *P. lunatus* from the same region cluster in the same cluster.

Keywords: Genetic diversity; Lima bean, Phylogeny, Polymerase Chain Reaction, Random Amplified Polymorphic Deoxyribonucleic acid

1. Introduction

Phaseolus lunatus L. is categorized as a legume plant with great potential to become nutritious food. In Indonesia, *P. lunatus* can be found in some islands, such as Java and Madura (Purwanti and Fauzi, 2019). The distribution of *P. lunatus* in this country implies the probability of various accessions existing in Indonesia. The diversity of *P. lunatus* accessions and relative ease offered to cultivate the plant bring about probability for Indonesian societies as well as government to make use of it as an alternatively functional food source (Diniyah *et al.*, 2013; Diniyah *et al.*, 2015; Herry *et al.*, 2013; Nafi *et al.*, 2015). Nowadays, Indonesia is dealing with the severe issue of protein shortage in some areas (Diana *et al.*, 2017; Ickowitz *et al.*, 2016; Madanijah *et al.*, 2016), so maximizing consumer consumption *P. lunatus* will be an effective solution.

With respect to elevating *P. lunatus* as one of food sources, identification on genetic diversity typifying the accessions with high protein content needs actualization. The obtainability of information regarding genetic diversity of intra- and inter-species is the most essential foundation to run all the programs of food source enhancement (Bhanu, 2017). Also, information that pinpoints natural variability and difference that lies on the plant itself is used as the primary capital to design a

betterment scheme for the species since the beginning of systematic plant breeding (Bhanu, 2017). Furthermore, such information can be used to reach a phase of sustainable crop production (Fu, 2015). Moreover, the research underpinning genetic diversity in a particular plant also leads to conservation (Carvalho *et al.*, 2019). For that reason, to support the attempt, a series of assessments on genetic diversity have been routinely administered using numerous techniques such as morphological identification, biochemical characterization, and analysis of molecular markers (Govindaraj *et al.*, 2015). Related to those techniques, the selection of molecular markers is considered more appropriate and effective to avoid any bias due to environmental influence and provide eclectic information about genetic diversity in a more acceptable way (Fu, 2015). Some molecular markers are included and considered particularly promising in helping analyse genetic diversity, such as RAPD, RFLP, and SCAR.

Among those markers, RAPD (Random Amplified Polymorphic Deoxyribonucleic acid) is the most popular marker in many research projects (AIRawashdeh and AIRawashdeh, 2015; Ben-Ari and Lavi, 2012). RAPD constitutes a PCR-based (Polymerase Chain Reaction) technique that involves a primary set with a relatively short size and can be a PCR-based technique that involves a relatively short size and can randomly amplify many DNA segments (Kumari and Thakur, 2014). This

* Corresponding author e-mail: ahmad_fauzi@umm.ac.id.

technique is equipped with outstanding excellence compared to others, which occupies a universal primary set without undergoing the DNA sequencing phase in its actual implementation. In addition, the RAPD marker is effective to demonstrate reasonable speed and is deemed more efficient (Kumar and Gurusubramanian, 2011), as it can be used for limited DNA samples, is not costly (Kumari and Thakur, 2014), and is applicable for various laboratory situations (Kumar and Gurusubramanian, 2011). Therefore, RAPD has often been used as a genetic marker in much research on the genetic variation of various legumes.

However, analyses of the genetic diversity of *P. lunatus* in Indonesia are still rare. In fact, in some parts of the world, such kinds of analyses are intensively published, such as in North America (Serrano-serrano *et al.*, 2010), Central America (Camacho-Pérez *et al.*, 2018), and South America (Silva *et al.*, 2019). On the one hand, in Indonesia, research about *P. lunatus* was still limited on its potency as an alternative food source (Diniyah *et al.*, 2013; Herry *et al.*, 2014) alongside its essential substances (Diniyah *et al.*, 2015; Praseptianga *et al.*, 2018; Sukatiningsih *et al.*, 2013; Tejasari, 2016). In addition, researches that study the diversity of *P. lunatus* are still restricted to its morphological characteristics (Purwanti and Fauzi, 2019). Therefore, this research is focused on the genetic diversity of *P. lunatus* based on the RAPD marker.

2. Material and Methods

2.1. Collection of Samples

P. lunatus used in this present study was originated from seeds collected from some areas in East Java, Indonesia, such as Madura, Tulungagung, Malang, and Probolinggo. Based on the result of identification in previous research (Purwanti and Fauzi, 2019), the collection of *P. lunatus* consisted of 15 accessions. All those fifteen are listed in the following Table 1. Further, each of the accessions was planted in a polybag in which one polybag was distanced one meter long from the next one. In addition, the plantation was done without any extraneous additions of neither fertilizer nor other kinds of growth agents.

Table 1. List of accessions to analyze

Accession Codes	Origins
2	Madura
4	Madura
7	Madura
8	Madura
12	Madura
13	Madura
14	Madura, Tulungagung
16	Madura
18	Madura
19	Madura
Prb1	Probolinggo
Prb2	Probolinggo
Prb3	Probolinggo
Prb4	Probolinggo, Malang
Prb5	Probolinggo, Madura

2.2. DNA Isolation

DNA isolation was administered based on the CTAB method of Doyle and Doyle (1984), which was modified by Maftuchah and Zainuddin (2010). The used tissue stemmed from the leaf organ of 3 mo (month-old) plants. First, leaves were cut out and were crushed using liquid nitrogen. Then, Natrium bisulfited was weighed for each of 12 samples and dissolved into the buffer. The results of isolated DNA were stored under a temperature of -20 °C.

Table 2. List of primers

Primers	Sequence 5'-3'	GC Content (%)
OPA6	GGTCCCTGAC	70
OPA8	GTGACGTAGG	60
OPA10	GTGATCGCAG	60
OPA20	GTTGCGATCC	60
OPC19	GTTGCCAGCC	70
OPD8	GTGTGCCCCA	70
OPD12	CACCGTATCC	60
OPE8	TCACCACGGT	60
OPE15	ACGCACAACC	60
OPE16	GGTGACTGTG	60

2.3. PCR-RAPD

Ten primers having 60 to 70 GC content were used in this present study (Table 2). The total volume of PCR reaction used signified 22.5 µL, containing the mixture of liquid DNA of *taq* polymerase and 10-fold buffer of *taq* polymerase (100 mM Tris-Cl, pH 8.3; 500 mM KCl; 15 mM MgCl₂; 0.01% gelatin); *dNTP'S mix* (dGTP, dATP, dTTP and dCTP) (Roche); dH₂O; and 30 ng DNA template. The condition for PCR reaction was designed under the pre-denaturation temperature of 94 °C (in 5 min), denaturation temperature of 94 °C (in 1 min), primary attachment temperature of 36 °C (in 1 min), extension temperature of 72 °C (in 2 min), the post-extension temperature of 72 °C (in 5 min), and post PCR reaction temperature of 4 °C (in 2 min). For multiplication, the cycle of the PCR reaction was repeated 36 times.

2.4. Agarose Gel Electrophoresis

There were three stages of procedure to confirm the result of isolation process and PCR reaction after implementation. The first stage was creating agarose gel with a concentration of 0.8% (for isolation result) and 1% (for PCR result) as a medium of running DNA. Next, the stage was labelled electrophoresis with the electrophoresis buffer of TBE (1×), loading dye (6×) under the condition of 60 V, 400 mA within 45 min. At last, the stage was the coloration using 10%-concentrated ethidium-bromide and the documentation of the DNA using UV-Trans illuminator.

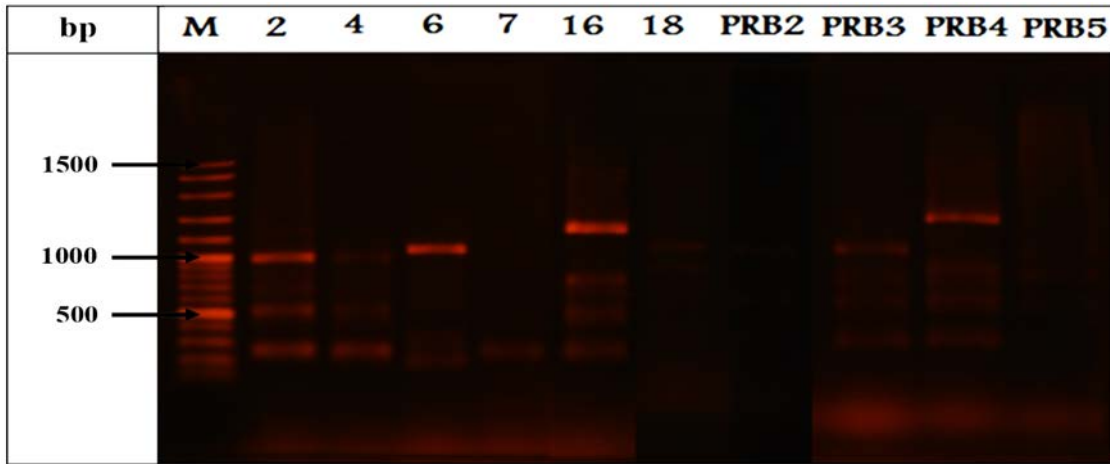
2.5. Analysis on the DNA Bands Yielded from RAPD

Data analysis was performed by observing the pattern of visible bands from the electrophoresis process in each primary locus. In addition, DNA bands were converted into binary data (0 and 1), indicating the existence and inexistence of bands typifying specific sizes. Afterward, the existing bands were observed to identify the percentage of polymorphic and monomorphic bands and create a phylogenetic tree by creating a phylogenetic tree with Popgen software version 3.1 (Yeh and Boyle, 1997).

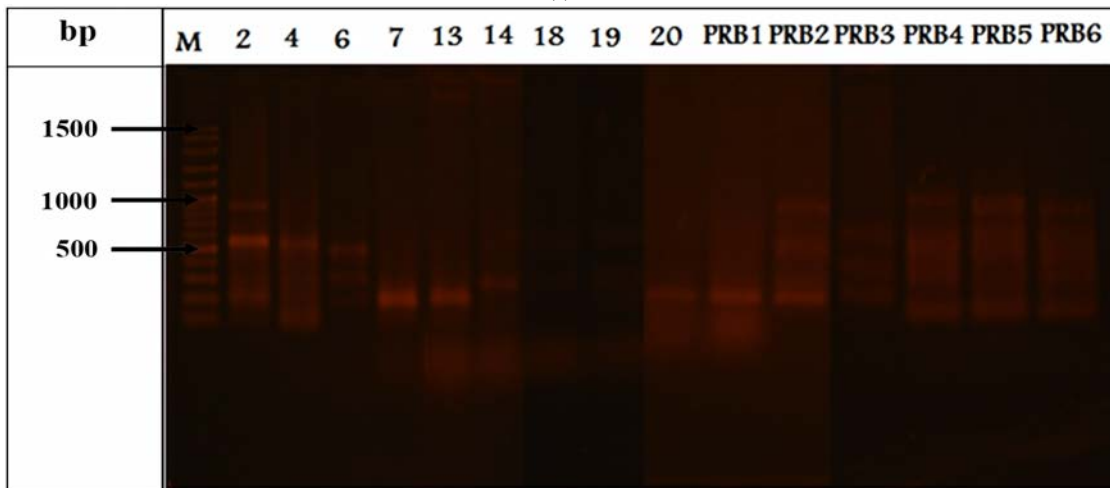
3. Results and Discussion

In this current research, ten primers were occupied for DNA amplification at 15 genotypes of *P. lunatus* L. Further, as a result of PCR-RAPD amplification at those

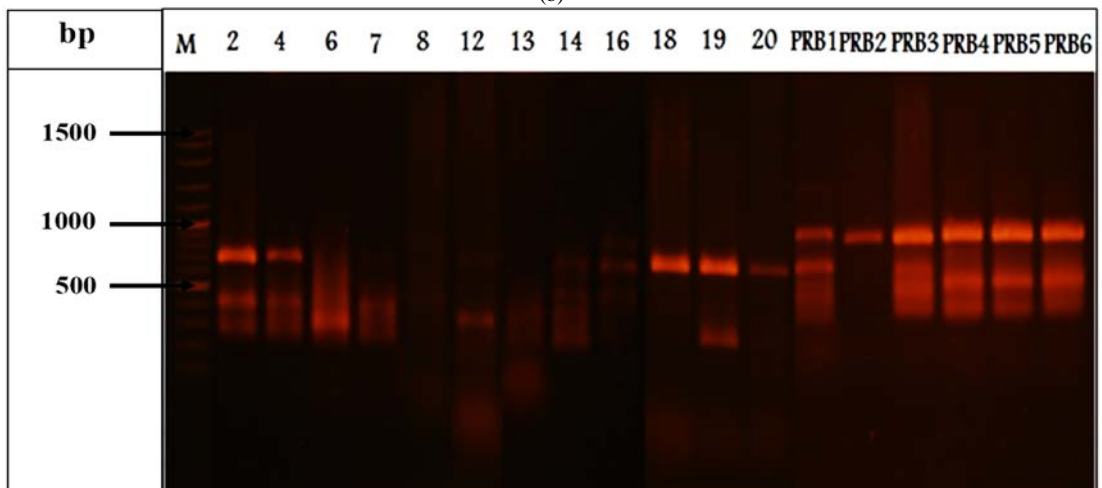
genotypes (Figure 1), the bands were assessed based on the binary data, with the description of 1 for the amplified band and 0 for unamplified. The following Table 3 showed the record of the number of loci found.



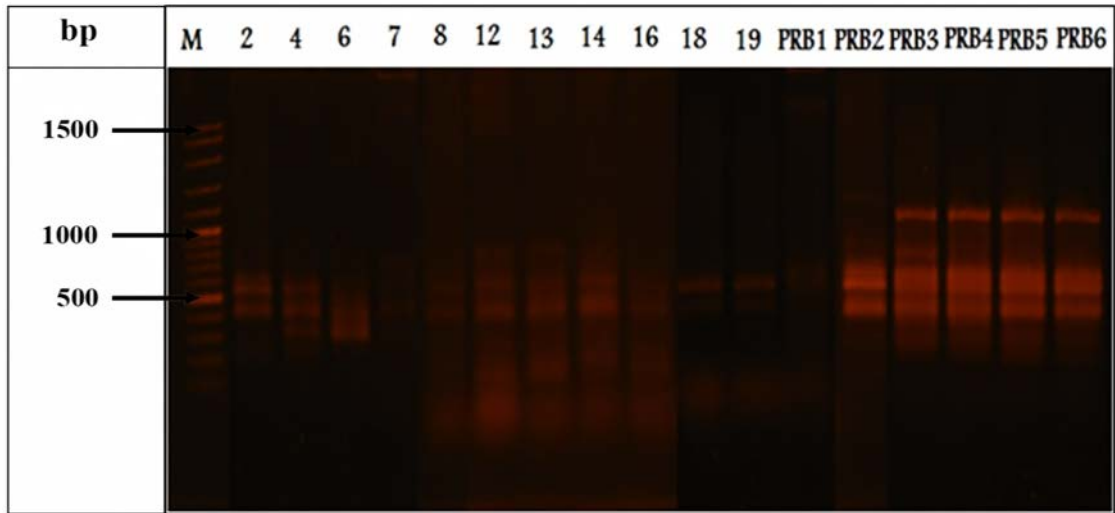
(a)



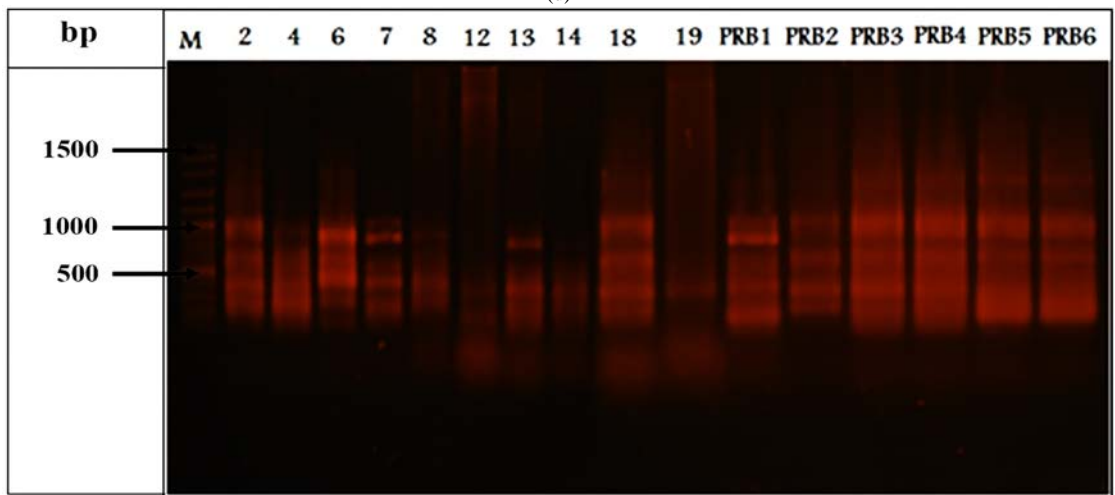
(b)



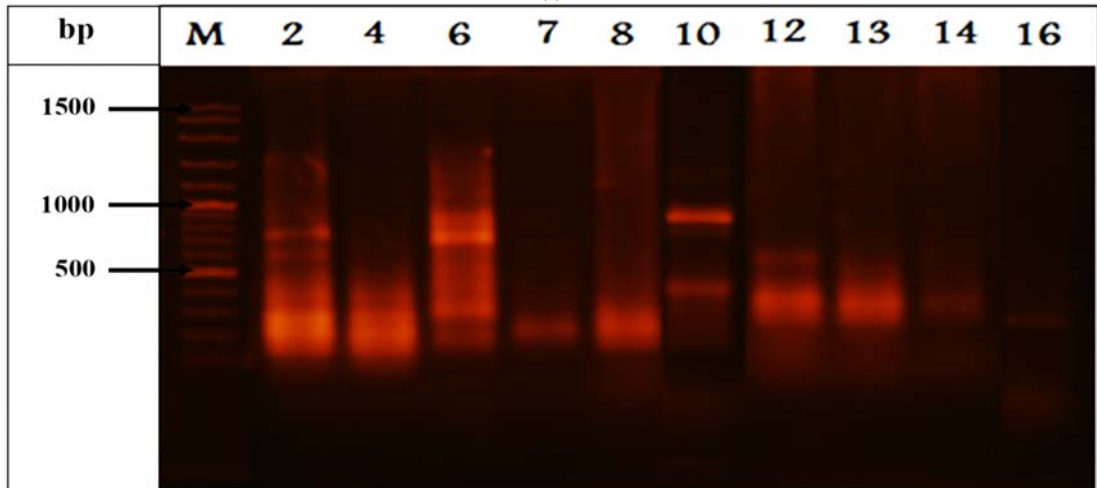
(c)



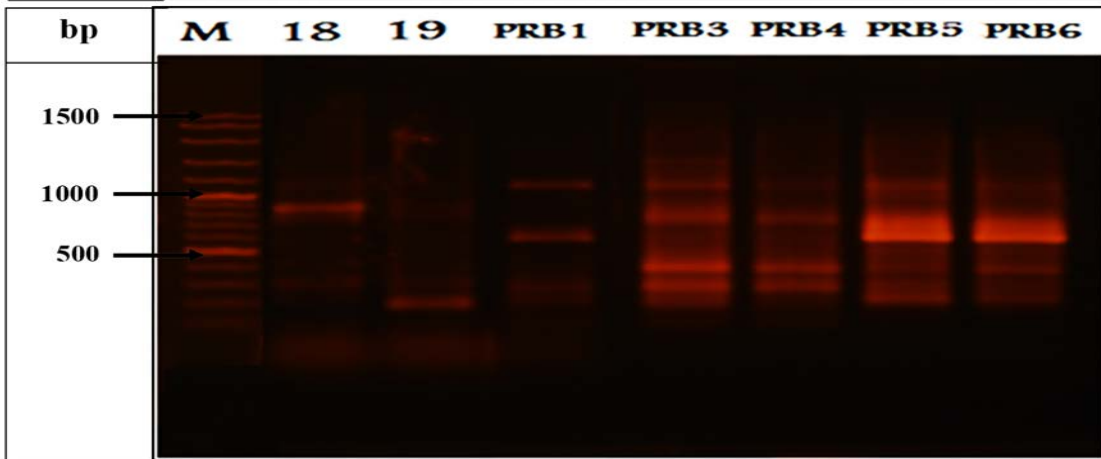
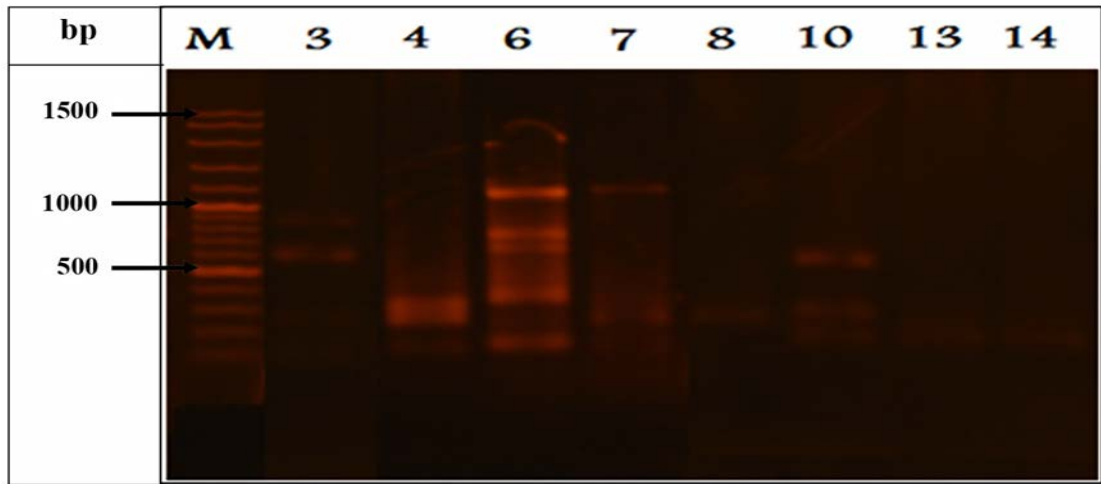
(d)



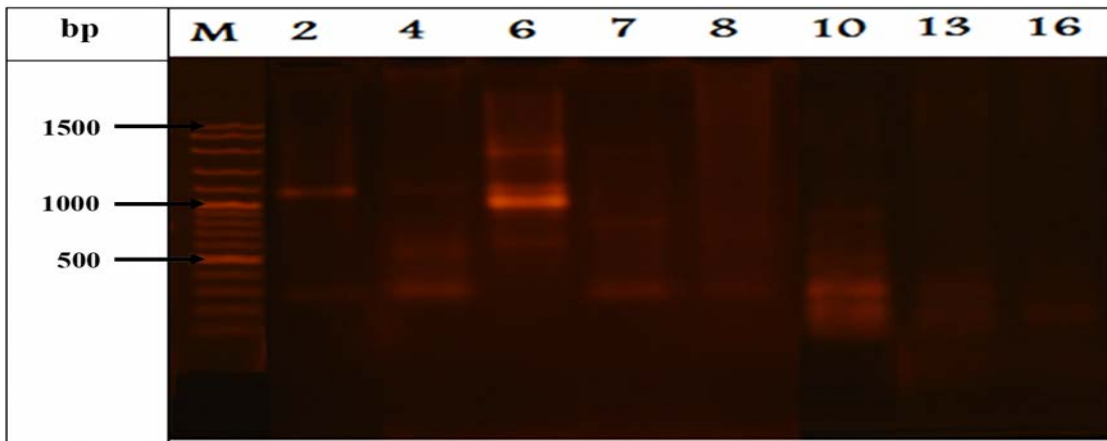
(e)



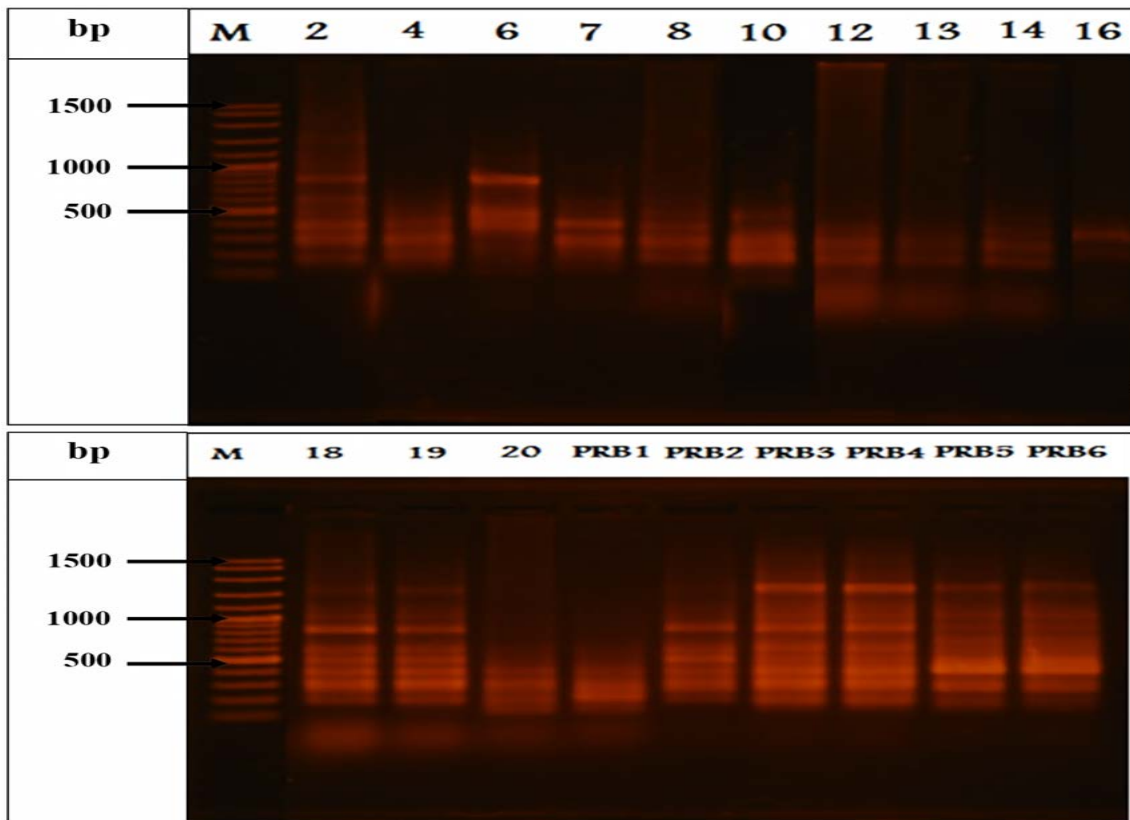
(f)



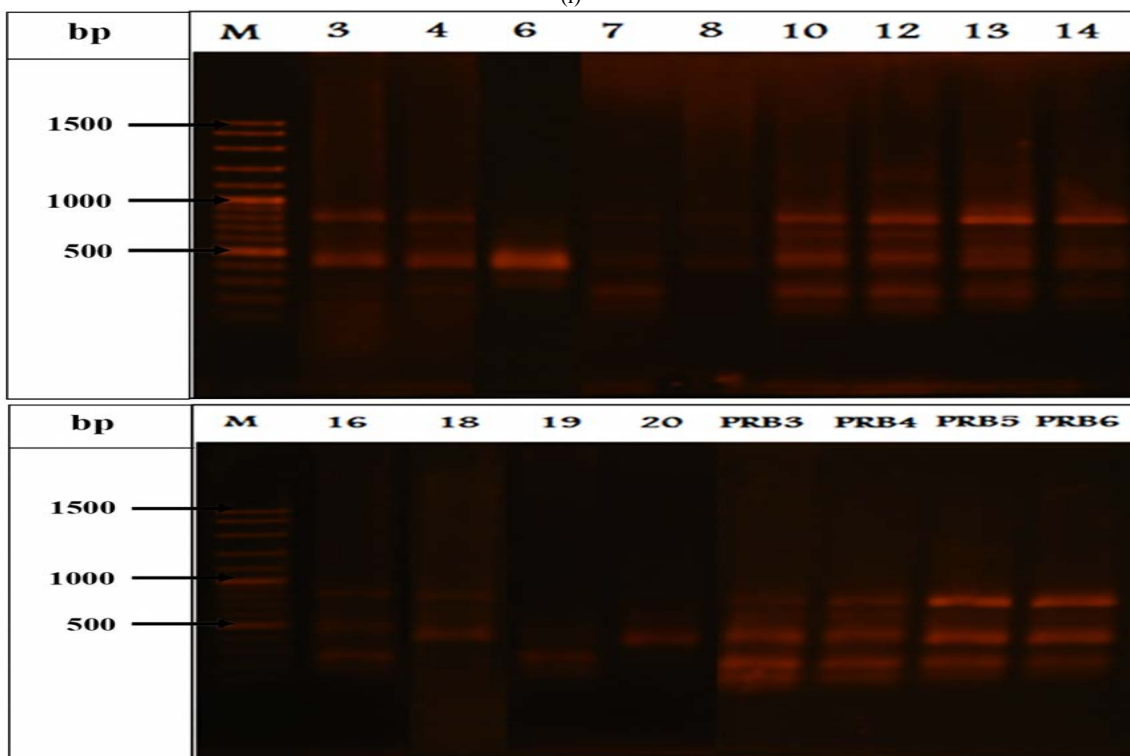
(g)



(h)



(i)



(j)

Figure 1. Gel electrophoresis profiles for PCR-RAPD results using (a) OPA6, (b) OPA8, (c) OPA10, (d) OPA20, (e) OPA19, (f) OPD8, (g) OPD12, (h) OPE8, (i) OPE15, (j) OPE16. M is the DNA size ladder

Table 3. The record of the number of locus found at 15 genotypes of *P. lumatus* using 10 random primary

Codes	Locus (bp)												
	100	200	300	400	500	600	700	800	900	1000	1100	1200	1300
2	0	1	1	1	1	1	1	1	1	1	1	0	0
4	1	1	1	1	1	1	1	1	0	1	1	0	0
7	1	1	1	1	0	0	1	1	0	1	1	0	0
8	0	1	1	1	1	0	0	1	0	1	0	0	0
12	1	1	1	1	1	1	1	1	0	0	0	0	0
13	1	1	1	1	1	0	0	1	0	1	0	0	0
14	1	1	1	1	1	0	1	1	0	0	0	0	0
16	0	1	1	1	1	1	1	1	1	1	1	0	0
18	1	1	1	1	1	1	1	1	1	0	1	1	0
19	0	1	1	1	1	1	1	1	0	0	1	1	0
Prb1	1	1	1	1	1	1	1	0	1	1	1	0	0
Prb2	0	1	1	1	1	1	1	1	1	1	1	0	0
Prb3	1	1	1	1	1	1	1	1	1	1	1	1	0
Prb4	1	1	1	1	1	1	1	1	1	1	1	1	0
Prb5	1	1	1	1	1	1	1	1	1	0	1	1	1

Description: (1): DNA band was existent, (0): DNA band was non-existent.

After PCR was conducted, DNA fragments of diverse sizes (polymorphic) were produced (Table 4). A total of 68 amplified bands were obtained, out of 67 were polymorphic. The percent polymorphism was 96% to 100%. The total number of amplified bands varied

between 5 (OPA10 and OPA20) to 9 (OPA12), with an average of 6.8 bands per primer. Ten unique bands were detected in several accessions. The size of the unique band ranged from 200 (Mdr6) to 1 300 bp (Prb5).

Table 4. RAPD primers used for diversity analysis of *P. lumatus*.

No.	Markers (100 bp–2000 bp)	Σ Band	Polymorphic	% Polymorphic	Unique band		
					Total	Locus	Accession
1	OPA 6	8	8	100%	2	700 200	Mdr16 Mdr6
2	OPA 8	7	7	100%	0	-	-
3	OPA 10	5	5	100%	0	-	-
4	OPA 20	5	5	100%	1	300	Mdr4
5	OPC 19	6	5	96%	0	-	-
6	OPD 8	8	8	100%	1	500	Prb1
7	OPD 12	9	9	100%	2	1 200 900	Prb3 Mdr19
8	OPE 8	7	7	100%	2	1 300 500	Prb5 Mdr4
9	OPE 15	7	7	100%	0	-	-
10	OPE 16	6	6	100%	2	700 500	Mdr12 Mdr16
Total		68	67		10		

The cluster analysis upon the 68 RAPD bands was administered. The phylogenetic tree using Neighbor-Joining method was produced, equipped with similarity coefficient that ranged from 64% to 100%, or there was genetic variation with the range of 0% to 36% (Figure 2). In GSC of 0.6, *P. lumatus* accessions were formed into two main clusters, i.e. Cluster A (comprising 7, 8, 13, 14 genotypes) and Cluster B (comprising 2, 4, 16, 18, Prb1, Prb2, Prb3, Prb4, Prb5 genotypes). Cluster A contained several sub-clusters, which were A1 with GSC of 0.932

(including 8, 12, 13, 14 genotypes), A2 with GSC of 0.73 (including genotype 7). Meanwhile, Cluster B comprised several sub-clusters, too, with B1 (including 19, Prb5, Prb4, Prb3, 18 genotypes) and B2 (including Prb1, 4, Prb2, 16, 2 genotypes). At GSC of 1.0, there were 2, 4, 16, Prb2, Prb3, Prb4 genotypes. The coefficient was considered higher if it approached the point of 1, indicating that the genetic similarity amongst the genotypes was significantly close.

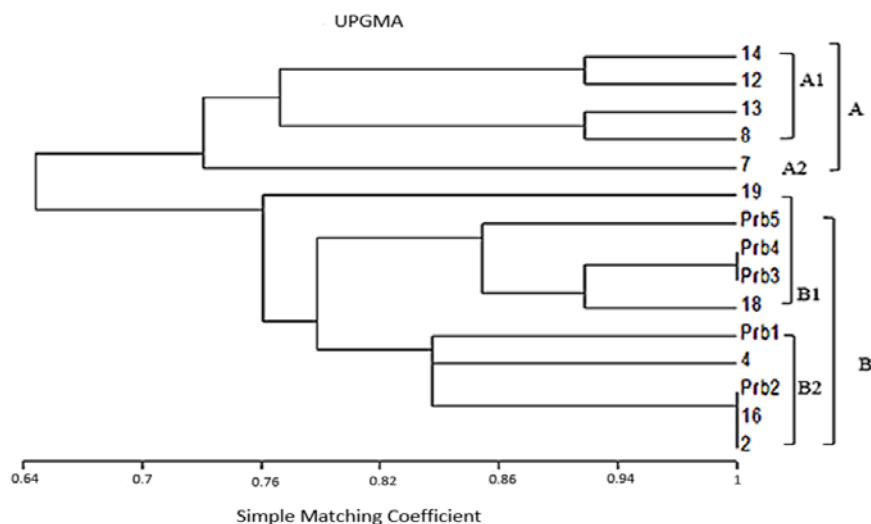


Figure 2. The dendrogram showing the connection amongst 15 accessions of *P. lunatus* referring to RAPD marker

P. lunatus under analysis through this current research was planted using conventional method in some parts of Indonesia of which environmental conditions were of diversity. The result of analysis indicated that the polymorphic level of *P. lunatus* was relatively high (ranging from 96% to 100%). This kind of finding was in line with previous studies that discussed genetic diversity of *P. lunatus* in some areas of Mesoamerica (Camacho-Pérez *et al.*, 2018; Chacón-Sánchez and Martínez-Castillo, 2017). The existing high polymorphism had indicated the vast range of genetic diversity from the accessions under analysis.

In nature, polymorphism constitutes a series of parameters to define genetic diversity on particular species (Singh and Kulathinal, 2013). The level of polymorphism in intra-species depended on the level of divergence between the genotypes. Regarding the information, *P. lunatus* used in this research was originated from different types of the gene pool. According to the previous study, the 15 accessions of *P. lunatus* included in the current research were originated from five different gene pools, name Sieva-Big, Potato-Sieva, Big lima, Sieva, and Potato-Sieva (Purwanti and Fauzi, 2019). Genetic diversity, moreover, was also a result of ecological situations that differed (Huang *et al.*, 2016). The ecological condition was closely interconnected with the agro-climatic zone in which it was grown. The origins where the samples were taken had different agro-climatic zone (Syuaib, 2016).

The genetic diversity considered high had brought about an urgent implication in terms of crop improvement attempt, including the breeding procedure for quality improvement (Bhanu, 2017; Fu, 2015). As previously reported, *P. lunatus* contained anti-nutritional components that became a confounding factor why its seeds were not effective as the main food resource (Doria *et al.*, 2012). Consequently, the process of maturation in *P. lunatus* seeds needed proper and acceptable process; thus it could reduce the anti-nutritional substances (Sukatiningsih *et al.*, 2013). Further, it was quite probable that the generation of *P. lunatus* would remain low anti-nutritional or without anti-nutritional factors. In addition, the breeding procedure could be designed that way to yield the generation of

P. lunatus with highly pest-resistant performance and a shorter period of maturation phase.

Next, concerning the phylogenetic tree formed, the population tended to be clustered based on the geographical origins of those accessions. In fact, Madura accessions were more dominant within Cluster A, while in Cluster B, Probolinggo clusters were superior. Furthermore, there was also shown a trend of connection between similarity of morphological characteristics amongst accessions grouped in the same cluster. Previous studies have reported that most of Probolinggo accessions possessed better characteristics of seed weight, seed length, leaf length, leaf width, and pod width compared to other accessions. Accession 4 constituted the one of which morphological character was close in characteristics to Probolinggo accessions (Purwanti and Fauzi, 2019).

Despite this fact, cluster analysis also indicated the existence of accessions of which pod lengths were quite different but still grouped in the same cluster. In contrast, when the pod length was not significantly different, cluster analysis classified those accessions in different clusters. This was probably due to DNA related to the RAPD marker used in this current research being unrelated to the character set. For that reason, a further study that highlights types of gen is needed to encode those characters.

In accordance with this research, the use of RAPD was not only affordable but also not complex. Also, it could be used to cluster a collection of accessions that could be connected to their agronomic characteristics. Further, reproducibility and sustainability of RAPD marker in the study of genetic variation were still contested in some previous researches. However, there were some studies of genetic variation on germplasm of beans that were successful by utilizing RAPD, such as some researches about *P. vulgaris* in India (Bukhari *et al.*, 2015), South Africa (Adesoye and Ojobo, 2012), Turkey (Ince and Karaca, 2011), and in Vicia Faba, Palestine (Basheer-Salimia *et al.*, 2013). In fact, the result of RAPD shown in this current research shared information which was in line with other generic variation researches by the use of other types of marker, such as ISSR (Camacho-Pérez *et al.*, 2018) and SNP (Chacón-Sánchez and Martínez-Castillo,

2017). In short, this current research has advocated the credibility of RAPD in the study of genetic variation in beans, such as in *P. lunatus*.

4. Conclusion

In this research, the genetic variations of 15 accessions of *P. lunatus* originated from Malang, Probolinggo, Tulungagung, and Madura were analysed. The result of RAPD using ten primers resulted in 68 bands in which nine primers possessed 100% level of polymorphism, and one primary was equipped with 96% level of polymorphism. In addition, ten unique bands were detected in eight accessions, i.e. Prb1, Prb2, Prb5, Mdr12, Mdr16, Mdr19, Mdr4, and Mdr6. Based on cluster analysis, there were two major clusters, Cluster A and B. The former contained the accessions of 7, 8, 13, and 14, while the latter comprised the 2, 4, 16, 18, Prb1, Prb2, Prb3, Prb4, and Prb5.

References

- Adesoye OA and Ojubo OA. 2012. Genetic diversity assessment of *Phaseolus vulgaris* L. landraces in Nigeria's mid-altitude agroecological zone. *Int. J. Biodivers. Conserv.* **4** (13): 453–460.
- AlRawashdeh IM and AlRawashdeh NQ. 2015. Evaluating the genetic relatedness within *Lupinus pilosus* L. species based on RAPD analysis. *Jordan J. Biol. Sci.* **8** (1): 61–64.
- Basheer-Salimia R, Shtaya M, Awad M, Abdallah J and Hamdam Y. 2013. Genetic diversity of Palestine landraces of Faba bean (*Vicia faba*) based on RAPD markers. *Genet. Mol. Res.* **12** (3): 3314–3323.
- Ben-Ari G and Lavi U. 2012. Marker-assisted selection in plant breeding. In: Chapter 11, **Plant Biotechnology and Agriculture**. Academic Press. Elsevier. USA. pp 163–184
- Bhanu AN. 2017. Assessment of genetic diversity in crop plants - An overview. *Adv. Plants Agric. Res.* **7** (3): 279–286.
- Bukhari A, Bhat MA, Ahmad M and Saleem N. 2015. Examination of genetic diversity in common bean (*Phaseolus vulgaris* L.) using random amplified polymorphic DNA (RAPD) markers. *Afr. J. Biotechnol.* **14** (6):451–458.
- Carvalho YGS, Vitorino LC, de Souza UJB and Bessa LA. 2019. Recent trends in research on the genetic diversity of plants: Implications for conservation. *Diversity.* **11** (4): 1–21.
- Diana A, Mallard SR, Hazzard JJ, Purnamasari DM, Nurulazmi I, Herliani PD, Nugraha GI, Gibson RS and Houghton L. 2017. Consumption of fortified infant foods reduces dietary diversity but has a positive effect on subsequent growth in infants from Sumedang district, Indonesia. *PLoS One.* **12** (4): 1–17.
- Diniyah N, Windarti WS and Maryanto. 2013. Pengembangan teknologi pangan berbasis koro-koroan sebagai bahan pangan alternatif substitusi kedelai [Development of food technology based on koro-koroan as an alternative food material to substitute soybeans] Seminar Nasional Pengembangan Sumber Daya Lokal untuk Mendorong Ketahanan Pangan dan Ekonomi. UPN Veteran, Surabaya, Indonesia.
- Diniyah N, Windarti WS and Riady S. 2015. Sifat fungsional tepung koro kratok hitam, merah dan putih (*Phaseolus lunatus* L.) dengan perlakuan lama perendaman [The functional properties of black, red and white koro kratok flour (*Phaseolus lunatus* L.) with long soaking treatment. *Jurnal Hasil Penelitian Industri.* **28** (2):70–77.
- Doria E, Campion B, Sparvoli F, Tava A and Nielsen E. 2012. Anti-nutrient components and metabolites with health implications in seeds of 10 common bean (*Phaseolus vulgaris* L. and *Phaseolus lunatus* L.) landraces cultivated in southern Italy. *J Food Compos Anal.* **26** (1–2): 72–80.
- Doyle J J. and Doyle JL. 1984. A rapid DNA isolation procedure for small quantities of fresh leaf tissue. *Phytochem. Bull.* **19**: 11–15.
- Fu YB. 2015. Understanding crop genetic diversity under modern plant breeding. *Theor. Appl. Genet.* **128** (11): 2131–2142.
- Govindaraj M, Vetriventhan M. and Srinivasan M. 2015. Importance of genetic diversity assessment in crop plants and its recent advances: An overview of its analytical perspectives. *Genet. Res. Int.* **ID 431487**: 1–14
- Herry B, Windarti WS and Nuru. 2014. Potensi koro-koroan sebagai sumber bahan lokal untuk pembuatan aneka produk olahan berprotein [The potential of koro-koroan as a source of local ingredients for the manufacture of various processed protein products] Prosiding Seminar Nasional. Universitas Muhammadiyah Jember, Jember, Indonesia.
- Huang W, Zhao X, Zhao X, Li Y and Lian J. 2016. Effects of environmental factors on genetic diversity of *Caragana microphylla* in Horqin Sandy Land, northeast China. *Ecol. Evol.* **6** (22): 8256–8266.
- Ickowitz A, Rowland D, Powell B and Salim MA. 2016. Forests, trees, and micronutrient-rich food consumption in Indonesia. *PLoS One* **11** (5): 1–15.
- Ince AG and Karaca M. 2011. Genetic variation in common bean landraces efficiently revealed by Td-DAMD-PCR markers. *Plant Omics.* **4** (4): 220–227.
- Kalaminasih D. 2013. Pengaruh proporsi kacang koro sayur (*Phaseolus lunatus*) dan kacang koro pedang (*Canavalia ensiformis* L.) terhadap mutu organoleptik tempe koro [Effect of the proportion of *Phaseolus lunatus* and *Canavalia ensiformis* L.) on the organoleptic quality of tempe koro]. *E-Journal Boga.* **2** (3): 104–113.
- Kumar NS and Gurusubramanian G. 2011. Random amplified polymorphic DNA (RAPD) markers and its applications. *Sci. Vis.* **11** (3): 116–124.
- Kumari N and Thakur SK. 2014. Randomly amplified polymorphic DNA-A brief review. *Am J Anim Vet Sci.* **9**(1): 6–13.
- Lim TK. 2012. *Lablab purpureus*. In: **Edible Medicinal And Non-Medicinal Plants, Vol. 2, Fruits**. Springer Netherlands. pp. 730–741.
- Madanijah S, Briawan D, Rimbawan R, Zulaikhah Z, Andarwulan N, Nuraida L, Sundjaya T, Murti L, Shah Priyali, Bindels J. 2016. Nutritional status of pre-pregnant and pregnant women residing in Bogor district, Indonesia: A cross-sectional dietary and nutrient intake study. *Br J Nutr.* **116**: 1–10.
- Maftuchah and Zainuddin. 2006. Pengembangan metode isolasi DNA genom pada tanaman jarak pagar (*Jathropa curcas* L.) [Development of genomic DNA isolation methods in *Jathropa curcas* L.]. *Humanity.* **2** (1): 63–69.
- Nafi A, Diniyah N. and Hastuti, FT. 2015. Karakteristik fisikokimia dan fungsional teknis tepung koro kratok (*Phaseolus lunatus* L.) termodifikasi yang diproduksi secara fermentasi spontan [Physicochemical and technical functional characteristics of modified *Phaseolus lunatus* L. flour produced by spontaneous fermentation]. *Agrointek.* **9** (1): 24–32.
- Praseptiangga D, Tryas A A, Affandi DR, Atmaka W, Ariyantoro AR and Minardi S. 2018. Physical and chemical characterization of composite flour from Canna flour (*Canna edulis*) and Lima bean flour (*Phaseolus lunatus*). *AIP Conf Proc.* **1927** (030020): 1–6.

- Purwanti E and Fauzi A. 2019. The morphological characteristics of *Phaseolus lunatus* L. in different areas of East Java, Indonesia. *IOP Conf. Ser. Earth Environ. Sci.* **276** (012017):1–10
- Serrano-serrano ML, Hernández-torres J, Castillo-villamizar G, Debouck DG and Chacón, MI. 2010. Molecular phylogenetics and evolution gene pools in wild Lima bean (*Phaseolus lunatus* L.) from the Americas: Evidences for an Andean origin and past migrations. *Mol. Phylogenet. Evol.* **54** (1): 76–87.
- Silva RNO, Lopes ACA, Gomes RLF, Pádua JG and Burle ML. 2019. High diversity of cultivated Lima beans (*Phaseolus lunatus*) in Brazil consisting of one Andean and two Mesoamerican groups with strong introgression between the gene pools. *Genet. Mol. Res.* **18** (4): 1–15.
- Singh RS and Kulathinal RJ. 2013. Polymorphism. In: Maloy S and Hughes K (Eds.). **Brenner's Encyclopedia of Genetics 2nd Edition**. Academic Press - Elsevier. Cambridge, Massachusetts, USA, pp. 398–399.
- Sukatiningsih, Yustian AM and Windarti SW. 2013. Penambahan isolat protein kedelai dan sukrosa racun pada kecambah koro kratok [*Phaseolus lunatus* (L) sweet] [Addition of soy protein isolate and toxic sucrose to the sprouts of *Phaseolus lunatus* (L) sweet. *Agritrop Jurnal Ilmu-Ilmu Pertanian.* **11** (1): 1–7.
- Syuaib MF. 2016. Sustainable agriculture in Indonesia: Facts and challenges to keep growing in harmony with environment. *Agri Eng Int: CIGR J.* **18** (2):170–184.
- Yeh, F.C., and T.J.B. Boyle. 1997. Population genetic analysis of codominant and dominant markers and quantitative traits. *Belgian J. Bot.* **129**:157–163.

Increasing Liquidity of SSDM-Based Red Chili Farmers through Agricultural Insurance

Sri Ayu Andayani^{1,*}, Yayan Sumekar², Reny Sukmawani³, Agus Yadi Ismail⁴, Dadan Ramdani Nugraha⁵ and Sri Umyati⁶

^{1,5,6}Faculty of Agriculture, Universitas Majalengka;²Faculty of Agriculture, Universitas Padjadjaran;³Faculty of Agriculture, Universitas Muhammadiyah Sukabumi;⁴Faculty of Forestry, Universitas Kuningan, Indonesia

Received: February 27, 2020; Revised: May 2, 2020; Accepted: May 18, 2021

Abstract

Red chilies have good demand prospects but still have problems. Apart from the fact that production is seasonal, so it often faces crop failure, it also experiences fluctuating prices, there is no certainty of selling, weak market access and risks are interrelated. In this regard, research has been carried out in Garut Regency, West Java, which is one of the development of red chili clusters. This paper has the aim of looking at the linkages of risks that occur and proposing policy scenarios in mitigating possible risks. This research was designed qualitatively and quantitatively with a case study method through a soft system dynamic methodology (SSDM) approach. The results showed that the risks that occur in the red chili agribusiness cluster can be indicated in the production risk, market risk, and institutional risk which are interrelated and have an impact on financial risk. The simulation results of the implementation of policy scenarios through agricultural insurance on red chili commodities increased farmer liquidity of about 20 percent starting from the 292nd day. This has a tendency for red chili farmers to mitigate risks. Meanwhile, the application of insurance is currently limited to rice commodities.

Keywords: Red Chili Agribusiness, Production Risk, Market Risk, Agricultural Insurance

1. Introduction

It is important to develop the agricultural sector, even though during the last decades the growth of this sector is parallel with several other dynamics and has complex and diverse phenomena (Santeramo F.G, 2021). The same applies to horticulture, which often experiences price fluctuation and occurs every year, especially at the beginning of the rainy season, including in this case the red chili commodity (Hariyani, et al, 2017).

Red chili is one of the horticultural commodities that has a tendency to increase production, but has high price fluctuations (Andayani, et al, 2016). The total production of red chilies is still lower than potential productivity due to weather constraints (Haryiani, N et al, 2017). The agricultural sector in Indonesia is prone to risks due to climate change (Boer & Suharnoto, 2014), including red chilies. Even though red chilies have good demand prospects, this commodity still faces many obstacles in its cultivation, such as often facing the risk of crop failure, lack of certainty of selling, fluctuating prices, weak market access, unable to meet the Bank's technical requirements. This indicates that in red chili farming there are risks that are interrelated (Andayani, et al, 2020), so that the agricultural sector needs treatment in plant growth through effective applications (A Walaa, et al, 2020)

The agricultural sector is always considered to be a business activity that has a tendency towards various risks (Ghalavand, 2012). Farmers are required to have the

ability to control risks and uncertainties caused by climate change through capital, mastery of technology and skills which are still constrained until now. Agricultural characteristics have uncertainty about agricultural products (Du Yilong, 2018). Climate change has a negative impact on the agricultural sector (Mashiza, 2019). Different cultivars and ensuring that are not affected by environmental conditions is one strategy that is needed even though it is long, expensive, and complex (Sidiq Y, et al, 2020). Fruit farmers in the United States also experience various risks due to climate change (Tsyrr et al, 2018). Price and production risks are also high for horticulture (Hasan F, et al, 2016).

The agricultural sector plays an important role in the rural economy (Wardhana D, et al, 2017). Bank Indonesia took the initiative in developing red chili peppers in West Java, especially in Garut district, which is one of the centers for red chili production in West Java. The cluster aims to reduce costs, create innovation, and increase productivity so that it can manage various risks due to limited resources (Teekasap, 2009). Clusters are also an important factor in understanding the effect of intermediaries in increasing small producers in the development of agricultural economic clusters (Ramirez M, et al 2018).

Seeing this condition, farmers are required to have the ability to control risks and uncertainties caused by climate change through capital, mastery of technology and skills, which are still constrained until now. The choice of risk management strategy must be appropriate because it can

* Corresponding author e-mail: sriayuandayani@unma.ac.id.

affect the cost of agricultural production and resource allocation (Vigani, M et al, 2019). Likewise, marketing choices for red chilies are influenced by transaction costs as well as price risks (Pham et al, 2020). Agricultural insurance is a form of risk management to protect losses in agriculture and can be used as a tool to spur rural development and modernization in the agricultural sector (Nnadi et al, 2013). With agricultural insurance, cocoa farmers in Nigeria can be saved from losses due to crop damage (Falola, et al, 2013). The government implemented insurance starting from 2015 to reduce the impact of agricultural risks even though it was limited to rice crops, but the level of farmer participation was still low despite the imposition of subsidies (Dadang, M, 2019).

The results of the preliminary study explain that the collaboration that has occurred since 2011 in the Garut cluster has not provided satisfaction to all parties involved, and the low supply of red chili from farmers through cooperatives in the industry indicates that there are various risks, one of which is the risk of production.

Based on the phenomena and description above, the cluster has the potential to develop red chili commodity, but in reality there are still many problems due to indications of various risks. For this reason, researchers have conducted research with the following problem formulations: (1) how is the risk relationship that occurs in the Garut red chili agribusiness cluster, (2) the proposed scenario through agricultural insurance can increase farmer liquidity so that it can mitigate the risks that occur. The emphasis of this research is to understand the risks and mitigations of the red chili commodity from the integration of stakeholders at the network level in order to improve cluster performance which is practically a scientific learning tool while methodologically using the soft system dynamic methodology (SSDM) approach in assessing agricultural problems, while ever The SSDM approach is carried out in the field of manufacturing and the social security problems of citizens and poverty (Teekasap, 2009), (Rodriguez, 2011).

2. Methodology

This research was designed in a descriptive qualitative and quantitative manner with a case study method and was carried out in Garut Regency, West Java. The determination of informants was done purposively. In analyzing the risk linkages that occur in the Garut red chilli agribusiness cluster and proposing risk mitigation scenarios that occur, it is used with systems thinking, namely soft system dynamic methodology (SSDM). SSDM can be said to be a combination of two methodologies, namely system dynamics (SD) and soft

system methodology (SSM), which can study complex social problem situations in systemic intervention (Rodriguez and Caceres, 2009). This model will be used as part of an intervention in improving existing systems or designing new systems (Pidd, 2004).

In the SSDM approach, the steps are: (1) stage to understanding unstructured problems through a rich picture in understanding the phenomena that occur and this is part of the SSM process, (2) stage to problem transformation and express it through CATWOE analysis, (3) stage to build a system dynamics model from existing phenomena and describe it in each sub-model with its various possible behaviors, (4) stage to compare stage number (4) and stage (7) by emphasizing in the observation and validation of each root cause and solution, (5) stage to determining the feasible or desirable change to improve the problematic behavior, (6) stage to building a dynamic model for solving problem situations which are in stage (4) to change real-world behavior through a simulation model which can be done by changing its parameters or structure, (7) stage to looking at the root of the mass solving orientation to change properly what is desired by CATWOE analysis through the transformation process, (8) stage to the implementation of the desired changes or changes that are feasible to be implemented, (9) and (10) stage to learning points prepared for study and reflection of time to time and future interventions (Rodriguez-Ulloa, 2004).

3. Results And Discussion

3.1. Understanding Unstructured Problems through The Rich Picture

The description of all red chili agribusiness cluster activities can be seen clearly in the following rich picture which includes actors, stakeholders, namely farmers, farmers groups, Heinz ABC industry, BRI Bank, USAID, Cagarit cooperatives. The activity process starts from the meeting of the actors, planning the planting schedule, providing input, cultivating red chili, harvesting and post-harvest activities including sorting to selling red chili for traditional markets and structured markets, which are indicated by arrows as a series of activity processes on picture. In the process of activities, many obstacle were found including the large number of crops that were rejecting, crop failure, resulting in fluctuations in production. Various obstacles are symbolized in the image with an oval shape, and subsequently various risks occur. The results of the mapping in this image were carried out through external validation by conducting focus group discussions.

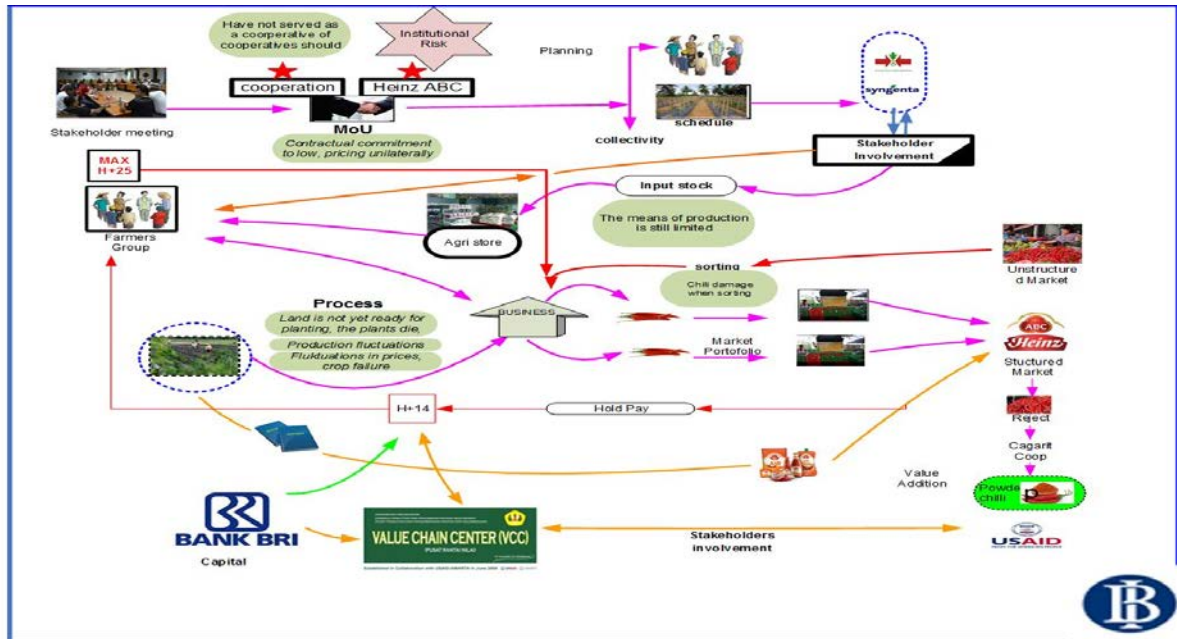


Figure 1. Rich Picture of Red Chili Agribusiness Cluster

3.2. Transformation of Problems through CATWOE Analysis

Based on the problems in the cluster, a CATWOE analysis was made in transforming events through observation and dialogue with stakeholders, looking at the relationship between the roles of actors, values and norms (Checkland and Scholes, 1990).

Formulation of Transformation (T)

T: increasing liquidity of red chili farmers through risk mitigation.

CATWOE analysis is as follows: Customer; C (beneficiaries): farmers in the red chili cluster, Actors; A (actors who carry out the transformation): farmer group association, cluster member red chili farmers, cooperative, Transformation; T (change): increase the liquidity of red chili farmers through risk mitigation, weltanschauung; W (meaningful perspective): multistakeholder collaboration

in supporting risk mitigation, Owners; O (party that might stop the transformation process / user): farmer group association, cluster member red chili farmers, cooperative, Environmental; E (environmental constraints): farmer skills, climate anomalies, access to information and technology.

3.3. Building a System Dynamics Model in the Elaboration of each Sub Model Production Risk Sub Model

In Figure 2, can be seen from the growth stage to the production activities that indicate a risk. The structure of death due to the effects of climate anomalies occurs during the growing period, and there is also death due to fusarium wilt and anthracnose attack about 50% during the production period and damaged chili peppers or physical defects occur around 10%. This red chili plant is very susceptible to weather, pests, and diseases.

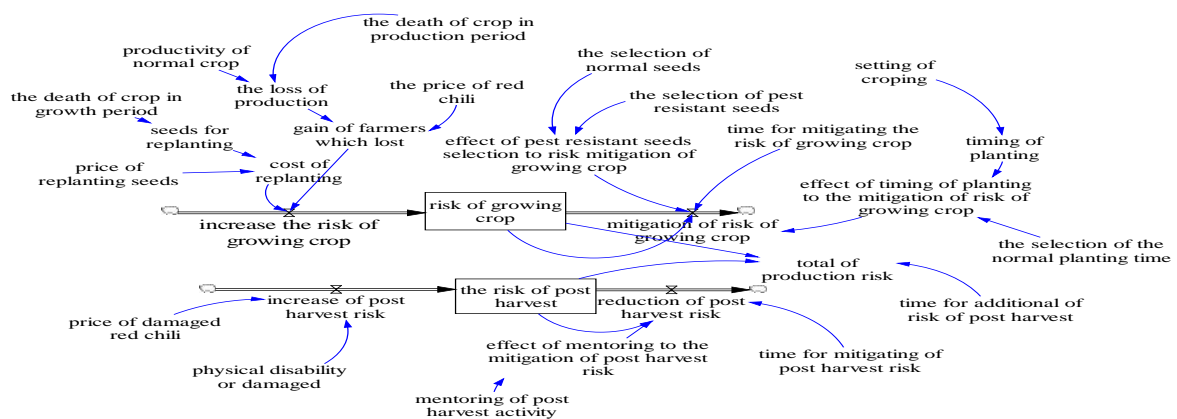


Figure 2. Production Risk Sub Model Diagram

3.4. Market Risk Sub Model

In Figure 3, it can be seen that there is a market risk that is influenced by the price of chili because its availability in the market is determined by production, which has fluctuated frequently due to pest attacks, climate

anomalies, and low technology application (Andayani, 2015). The partnership that has existed since 2011 until this research was carried out, has not optimally provided satisfaction for all parties involved. Many commitments to cooperation are still being violated, and this partnership is still far from the expectations of farmers.



Figure 3. Market Risk Sub Model Diagram

3.5. Behavior Model Behavior Model by Looking at the Behavior of Production and Skilled Farmers of Red Chili

Modeling and simulation results obtained information that the production of red chili tends to increase by showing its dynamic behavior. It can be seen in Figure 4, the simulation results for the 876th day, that the number of skilled farmers continues to increase, driven by the trend of high market demand. However, on day 1095 production decreased due to the influence of climate anomalies which indicate risks, although skilled farmers were not affected by this. In real conditions, this red chili cluster cannot meet the continuity of supply to the industry according to the contractual commitment due to these problems.

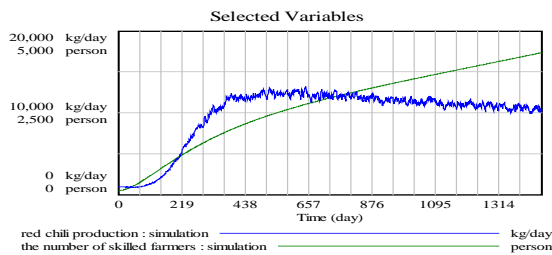


Figure 4. Farmers' Red Chilli Production by Skilled Farmers

3.6. Develop model to change behavior through simulation scenarios proposed Policy Proposed Scenario Policy Agricultural Insurance As One Risk Mitigation Alternatives At Red Chili Farmers

Figure 5 illustrates a sub-model with the addition of the agricultural insurance structure. With the compensation or compensation received by farmers, it can be used as capital for the next planting season. The trial implementation of agricultural insurance still needs to be done by expanding the area to provide a complete picture of insurance in Indonesia, and it is also hoped that the application of horticultural commodities should be implemented so that this policy proposal needs to be implemented in red chilies because so far agricultural insurance is still limited to rice commodities.

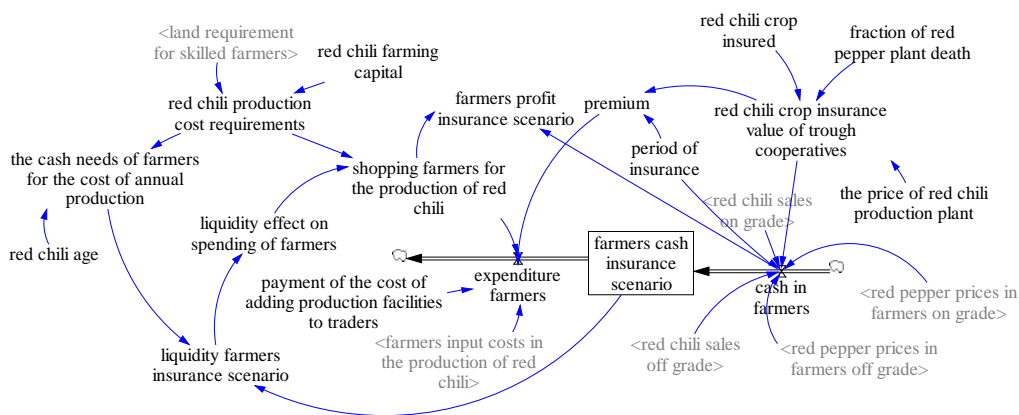


Figure 5. Sub Farmer Scheme of Insurance Scenario

3.7. Impact of the Application of Agricultural Insurance Policy Scenarios

In Figure 6, it can be seen that paying additional insurance premiums does not become a burden for farmers because there is still a guarantee if production failure and will not cause continuous losses for the farmers

themselves. It is also seen in Figure 6 on the 292th day that there is an increase in the liquidity of farmers for those who have applied insurance. Farmers will be more effective in reducing losses due to production failure by providing coverage for dead chili plants. Thus, it can be said that farmers who have applied insurance will continue to be able to carry out chili farming in a sustainable manner.

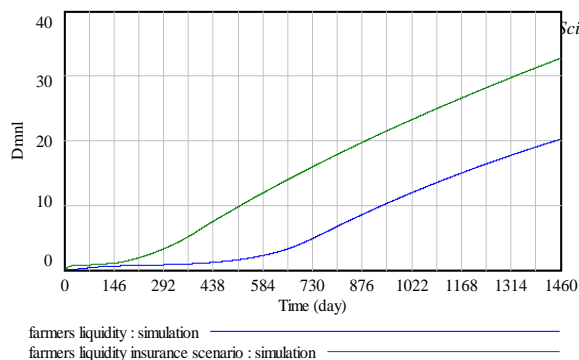


Figure 6. Red Chili Farmers Liquidity of Insurance Scenarios

4. Conclusion

The risks occurring in red chili agribusiness cluster can be indicated in the risks of production, market risk, and institutional risk. These risks are interrelated where production risks and market risks occur due to institutional risks, and the accumulation of these risks has an impact on financial risks.

One of the proposed policy scenarios as an effort to manage risk is agricultural insurance which has an impact on increasing farmers' liquidity of around 20 percent starting from day 292. Farmers will get guarantees if they experience crop failure so that they will be able to continue farming. In addition, the synergy between related parties supported by a better collaboration can provide satisfaction to the various parties involved.

It is necessary to accelerate the implementation of Law No. 19 of 2013 through the allocation of APBN/APBD funds in the form of insurance premium subsidies as a social assistance program in the agricultural sector. It would be much better if the government could also make a pilot application of loss insurance in red chili commodity.

Acknowledgement

This article is part of a study entitled *The Partnership Model For Red Chili Agribusiness Cluster To Manage Risk*. We thank the Director General of Higher Education for funding this research. Thanks are also due to Majalengka University, for giving us the opportunity to conduct this research, and to Padjadjaran University, especially the Faculty of Agriculture.

References

- A Walaa, Ramdan, and Gazeia M.Soliman. 2020. Effect of Different Applications of Bio-agent *Achromobacter Xylooxidans* Against *Meloidogyne Incognita* and Gene Expression in Infected Eggplant. *Jordan J Biol Sci.* **13**(3) : 363-370.
- Andayani Sri Ayu, Silvianita, and K Somantri. 2020. Risk Detection of Curly Red Chili (*Capsicum annum L*) Production with House of Risk. *J Agr Sci Sri Lanka.* **15** (2) : 273-279.
- Andayani, S.A, Sulistyowati Lies and Perdana Tomy. 2016. The Development of Red Chili Agribusiness Cluster with Soft System Methodology Approach in Garut. *J Mimbar.* **32** (2) : 302-310.
- Andayani, S.A. 2015. Model kemitraan Klaster Agribisnis Cabai Merah untuk Mengelola Risiko, Dr dissertation, Pasca Sarjana Universitas Padjadjaran, Bandung, Indonesia.
- Boer, Rizaldi, and Yuli Suharnoto. 2014. Climate Change Impact on Indonesia Food Crop. Paper presented at The Sixth Executive Forum on Natural Resource Management: Water & Food in a

Changing Environment at SEARCA Headquarters, Los Baños, The Philippines.

Checkland, P and Scholas,J, 1990. **Soft System Methodology in Action**, John Wiley and Sons, Chichester

Dadan Wardhana, Rico Ihle and Wim Heijman. 2017. Agro Cluster and Rural Poverty: A Spatial Perspective for West Java. *J Bul Indonesian Eco Stu.* **53** (2) : 161-186.

Fabio G Santeramo. 2021. Exploring The Link among Food Loss, Waste and Food Security; What The Research Should Focus on? *Santeramo Agric Food Secur.* **10**:26.

Mutaqin Dadang, Jainal and Koichi Usami. 2019. Smallholder farmers Willingness to Pay for Agricultural Production Cost Insurance In Rural West Java Indonesia: A Contingent Valuation Methode (CVM) Approach. Graduate School of International Development (GSID), Nagoya University. Nagoya 464-8601. Japan.

Du Yilong. 2018. Article of The Risk Pricing Mechanism of Order Agriculture Supply Chain. *Manag Eng Brighton East.* **31**: 61-67.

Falola A, Ayinde, and Agboola. 2013. Willingness to Take Agricultural Insurance by Cocoa Farmers in Nigeria. *Int J Food and Agr Eco.* **1**(1) : 97-107.

Fuad Hasan, Dwidjono Hadi Darwanto, Masyhuri Masyhuri, and Witono Adiyoga. 2016. Risk Management Strategy on Shallot Farming in Bantul and Nganjuk Regency. *Agr Sci.* **1**(2).

Ghalavand K, Karim, and Hashemi. 2012. Agriculture Insurance as a Risk Management Strategy in Climate Change Scenario: A Study in Islamic republic of Iran. *Int J Agr Crop Sci.* **4**(13) : 831-838.

Maura Vigani, and Jonas Kathage. 2019. To Risk or Not to Risk and Risk Management and Farm Productivity. *American J Agr Eco.* **101**(5) :1432-1454.

Matiaz Ramirez, Lan Clarke, and Laurens Klerk. 2018. Analysing Intermediary Organisations and Their Influence on Upgrading in Emerging Agricultural Clusters. *SAGE J Env Planning A : Eco Space.* **50**(6) : 1314-1335.

Mashiza Tinashe M. 2019. Adapting to Climate Change: Reflections of Peasant Farmers In Mashonaland West Province Of Zimbabwe. *JAMBA J Disaster Risk Stu.* **11**(1).

Nining Hariyani, Djoko Koestiono and A. Wahib Muhaimin. 2017. The Risk Level of Production and Price of Red Chili Farming in Kediri Regency, East Java Province. Indonesia. *AGRISE.* **17** (2).

Nnadi F. N, Chikaire J, Echetama, J. A, Ihenacho, R.A, Umunnakwe P.C, and Utazi, C.O. 2013. Agricultural Insurance: A Strategic tool for Climate Change Adaptation in The Agricultural Sector. *Int J Agr Sc.* **1**(1) : 1-9.

Porter, M.E, 2000: **Cluster and The New Economics of Competition**, Harvard Business Review

Pham Quoe Hung, Huynh Viet Khai. 2020. Transaction Cost marketing Chanel Decision of Small-Scale Chili Farmers in Tra Vinh Province Vietnam. *Asian J Agr Rural Dev Karachi.* **10**(1): 68-80.

Pidd, Michael. 2004. **System Modelling: Theory and Practice**. West Sussex: Wiley & Sons Ltd.

Ricardo Rodriguez-Ulloa, Alberto Montbrun, and Silvio Martinez Vicante. 2011. Soft System Dynamics Methodology in Actio: A study of the problem of citizen Insecurity in an Argentinean Province.

Caceres P, and Rodriguez. 2006. **An Application of SSDM. Manchester Metropolitan University Business School.** Manchester UK and Andean Institute of System (IAS) Lima, Peru.

Rodriguez, Caceres P. 2009. **Soft System Dynamics Methodology (SSDM):** Combination of Soft System Methodology (SSM) and System Dynamics (SD), IAS, Peru.

Sidiq Yasir, Aprilia Sufi Subiastuti, Wiko Arif Wibowo, and Budi Setiadi Daryono. 2020. Development of SCAR Marker Linked to Begomovirus Resistance in Melon (*Cucumis melo* L). *Jordan J Biol Sci.* **13** (2) : 145-151.

Teekasap P. 2009. Cluster Formation and Government Policy System Dynamics Approach. Proceedings of the 27th International Conference of The System Dynamics Society, Albuquerque, New Mexico, USA

Tsyr-Shuay, Jennifer E Ifft, Bradley J, Rickard and Calum G Turvey. 2018. Alternative Strategies to Manage Weather Risk in Perennial Fruit Crop Production. *Agr Resurce Eco J Rev.* **17** (3).

1-Pentacosanol Isolated from Stem Ethanolic Extract of *Cayratia trifolia* (L.) is A Potential Target for Prostate Cancer-*In SILICO* Approach

Sundaram Sowmya¹, Palanisamy Chella Perumal², Subban Ravi³, Palanirajan Anusooriya¹, Piramanayagam Shanmughavel⁴, Eswaran Muruges⁴, Karri Krishna Chaithanya⁵ and Velliyur Kanniappan Gopalakrishnan^{5,*}

¹Department of Biochemistry, Karpagam Academy of Higher Education, Coimbatore, Tamil Nadu, India 641 021; ²School of Food Science and Engineering, Qilu University of Technology, Shandong Academy of Science, Jinan, China; ³Department of Chemistry, Karpagam Academy of Higher Education, Coimbatore, Tamil Nadu, India 641 021; ⁴Department of Bioinformatics, Bharathiar University, Coimbatore, Tamil Nadu, India 641 046; ⁵Department of Chemistry, College of Natural and Computational Sciences, Aksum University, Axum, Ethiopia.

Received: June 13, 2020; Revised: September 24, 2020; Accepted: October 2, 2020

Abstract

Cayratia trifolia (L.) are the traditional medicinal plants used in the Indian Ayurvedic system of medicine. The main objective of the study was to isolate and characterize the structure and function of bioactive compound from ethanolic extract of stem parts of *Cayratia trifolia* (L.) against prostate cancer targets such as PTEN, AKT, SMO and E2F3 by *in silico* approach. Column, Thin layer chromatography, UV-visible spectrophotometer (UV), Fourier Transform Infrared (FTIR), ¹H and ¹³C Nuclear Magnetic Resonance (NMR) spectroscopy suggested that the isolated natural bioactive compound probably like 1-pentacosanol. The molecular docking results revealed that AKT, E2F3, PTEN and SMO complex with 1-pentacosanol have good glide score of -3.428, -3.573, -3.964 and -3.987 Kcal/mol and the glide energy is -36.846, -31.761, -39.270 and -34.919 Kcal/mol respectively when compared with standard drug, i.e. Finasteride (complex with AKT, E2F3, PTEN and SMO (no interaction) has low glide score and glide energy -3.1/22.168, -3.8/-41.588 and -3.1/-40.050 Kcal/mol, respectively. The ADME property of the isolated natural compound of 1-pentacosanol was under acceptable range. Based on the results, it can be concluded that the isolated 1-pentacosanol compound may act as novel inhibitors against prostate cancer targets.

Keywords: *Cayratia trifolia*, Chromatography techniques, NMR studies, 1-pentacosanol, Molecular docking, ADME properties.

1. Introduction

Cancer is associated with multiple genetic and regulatory aberrations in the cell. It is a highly heterogeneous disease, both morphologically and genetically (Yan *et al.*, 2007). Prostate cancer is the second most common malignancy (after lung cancer) in men worldwide, counting 1,276,106 new cases and instigating 358,989 deaths (3.8% of all deaths caused by cancer in men) in 2018 (Bray *et al.*, 2018). Prostate cancer is an assorted disease visible in varying pathological and clinical forms. It is complicated to diagnose and treat as prostate cancer tumors may be detected only during autopsy. Significant advancement has been achieved in prostate cancer diagnosis with the introduction of prostate-specific antigen (PSA) screening (Wang *et al.*, 1979). Structural biology and balanced drug design, proteomics and cell imaging contain major role in understanding receptor and drug interactions in prostate cancer (Reynolds, 2008).

Analysis of cancer pathways shows a number of interrelated markers responsible for oncogenesis. The recent studies suggest that, Phosphatase and tensin homolog (PTEN), Protein kinase B (AKT), Smoothened (SMO) and E2F3 overexpression and amplification have central roles in the initiation, progression and metastasis of prostate cancer (Pradip and William, 2005; Feng *et al.*, 2007; Mehrian *et al.*, 2007; Sinosh *et al.*, 2010). A large proportion of the world population depends on the traditional medicine because of the shortage and high expenses of orthodox medicine (Perumal *et al.*, 2014), compared with synthetic compounds, natural products provide inherent larger-scale diversity and have been the major resource of bioactive agents for new drug discovery. From the point of view of research, natural products are rapidly being utilized as source for drug discovery and development (Poornima *et al.*, 2014). From 2003-2012, 22 and 14 natural bioactive compounds having potent antitumor activity, which were isolated from marine fungi and marine red algae respectively (Pejin *et al.*, 2013; Pejin *et al.*, 2015).

* Corresponding author e-mail: vkgopalakrishnan@gmail.com.

Cayratia trifolia (L.) is the medicinal plant which belongs to the family of Vitaceae, and it has been reported to contain huge number of bioactive compounds such as yellow waxy oil, steroids, terpenoids, flavonoids and tannins (Gupta and Sharma, 2007; Gupta *et al.*, 2012). Whole plant is used in the treatment of tumors, neuralgia, hepatic problems (Guru kumar *et al.*, 2011). This plant extract has also been reported to have antibacterial, antioxidants, antiviral, antiprotozoal, hypoglycaemic activity etc (Kumar *et al.*, 2012; Sowmya *et al.*, 2014, Perumal *et al.*, 2015.). Therefore, the aim of the present study is to isolate, structurally characterize and analyze the anti-prostate cancer potential of isolated compound from stem ethanolic extract of *Cayratia trifolia*.

2. Materials and Methods

2.1. Plant collection

The stem parts of *Cayratia trifolia* (L.) were collected from and around the area of Kumbakonam, Tamil Nadu, India and authenticated by Dr. P. Sathyanarayanan, Botanical survey of India, Tamil Nadu Agricultural University Campus, Coimbatore. The voucher number is BSI/SRC/5/23/2010-2011/Tech.1527 (Perumal *et al.*, 2012). The fresh stem plant material was washed under the running tap water, dipped on saline overnight, air dried and finely powdered for further use.

2.2. Extract preparation

200 g of powdered plant material was weighed and extracted with 1000 ml of ethanol for 72 hours using occasional shaker. The supernatant was collected and concentrated at 40°C in reduced pressure using a rotary evaporator. The dried extract was stored at 4°C for further study.

2.3. Isolation and Identification of bioactive compound

2.3.1. Column chromatography

Chromatographic techniques are based on separation of substances between a stationary and a mobile phase. The mobile phase moves relative to the stationary one. Components of a mixture to be separated move together, with the mobile phase due to their different interactions with the phases. The column chromatography (4 × 100 cm) was performed using 60-120 mesh silica gel to elute out individual compounds from the stem parts of ethanolic extract. After loading with the plant extract (5 g) mixed with 10-20 g of activated silica gel and the column was run with varying solvent polarities with different ratios like Petroleum ether (100%), Petroleum ether: Chloroform (9:1, 8:2, 7:3, 6:4, 5:5, 4:6, 3:7, 2:8, 1:9), Chloroform (100%), Chloroform: Ethyl acetate (9:1, 8:2, 7:3, 6:4, 5:5, 4:6, 3:7, 2:8, 1:9), Ethyl acetate (100%), Ethyl acetate: Methanol (9:1, 8:2, 7:3, 6:4, 5:5, 4:6, 3:7, 2:8, 1:9) and Methanol (100%). The fractions were collected and tested by Thin Layer Chromatography (TLC) for single spot.

2.3.2. Thin layer chromatography

Thin layer chromatography is an easy and highly useful technique in research laboratories to separate and identify unknown compounds. It is used for the separation of a mixture into individual components using a stationary and mobile phase (Sadasivam and Manikam, 2004).

The optimized conditions were used for the identification of active constituents present in the plant extract. The fractions collected from chromatographic columns were monitored by TLC in different solvent systems. These plates were placed in the solvent chamber containing mobile phase. The solvent was allowed to rise to the maximum height of the TLC plate, then they were removed from solvent chamber, dried and the spots were detected by placing the TLC plates in a chamber containing iodine vapour. Fractions identified single spots in iodine chamber, R_f value was calculated and pooled together and proceeded for further analysis.

2.4. Functional group analysis and structure characterization

2.4.1. UV-Visible Spectroscopy

The UV-Visible spectroscopy offers a simple, cheap and easy-to-use technique to identify and quantify the main phytochemicals in relation to the polarity of the extraction solvent (Zavoi *et al.*, 2011). Each isolated fraction was determined using the UV region (200-400nm) and visible region (400-800nm) using the UV-Vis-2450, Shimadzu instrument.

2.4.2. Fourier Transform Infrared (FTIR) spectroscopy

FTIR has proven to be a valuable tool for the characterization and identification of compounds or functional groups (chemical bonds) present in an unknown mixture of plants extract (Eberhardt *et al.*, 2007). In addition, FTIR spectra of pure compounds are usually unique, acting as a “molecular fingerprint” (Hazra *et al.*, 2007).

The Shimadzu FTIR Spectrum instrument consists of global and mercury vapour lamp as sources, an interferometer chamber comprising of KBr and Mylar beam splitters followed by a sample chamber and detector. Entire region of 450-4000 cm^{-1} is covered by this instrument. The spectrometer works under purged conditions. Solid samples are dispersed in KBr or polyethylene pellets depending on the region of interest. This instrument has a typical resolution of 1.0 cm^{-1} . Signal averaging, signal enhancement, base line correction and other spectral manipulations are possible.

2.4.3. Nuclear Magnetic Resonance (NMR) spectroscopy

NMR spectroscopy is used to determine the molecular structure based on the chemical environment of the magnetic nuclei like ^1H , ^{13}C , 2D NMR etc., even at low concentrations. This is one of the most powerful non-destructive techniques in elucidating the molecular structure of biological and chemical compounds and used in organic chemistry, biology, medicine, pharmaceuticals, etc., for characterization of compounds. This technique is used in JEOL GSX 400 NB FT-NMR spectrometer. The spectra of samples containing low abundant nuclei like ^1H , ^{13}C , etc. are thus easily obtained. Also, dynamic studies are possible by relaxation measurements. Homo and hetero ^1H decoupling are also possible.

2.5. In silico analysis

The 3D structure of AKT (PDB ID: 4GV1), E2F3, PTEN (PDB ID: 1D5R) and SMO (PDB ID: 4QIM) was retrieved from the Protein Data Bank (www.rcsb.org), and proteins were prepared by protein preparation wizards (standard methods) that are available in grid-based ligand

docking with energetic (Protein Preparation Wizard, 2012). The active site (binding pocket) and functional residues of AKT, E2F3, PTEN and SMO were identified and characterized by site-map module from Schrodinger package. The isolated bioactive compound was used in molecular docking studies. These ligands were prepared using the LigPrep 2.4. The structure of each ligands was optimized. All docking analysis were performed by using the standard precision (SP) which is Standard mode of Glide (Grid based Ligand Docking with Energetic) module from Schrodinger 2012. The isolated bioactive compound was docked in to

the binding site AKT, E2F3, PTEN and SMO using GLIDE. ADME properties predictions were carried out using QikProp 2.3 module. QikProp helps in analysing the pharmacokinetics and pharmacodynamics of the ligand by accessing the drug like properties. Significant ADME properties such as molecular weight (MW), H-bond donor, H-bond acceptor and log P (O/W) were predicted.

3. Results

Column chromatography was performed in the stem ethanolic extract of *Cayratia trifolia* (L.) by varying solvent polarities with different ratios like Petroleum ether (100%), Petroleum ether : Chloroform (9:1, 8:2, 7:3, 6:4, 5:5, 4:6, 3:7, 2:8, 1:9), Chloroform (100%), Chloroform : Ethyl acetate (9:1, 8:2, 7:3, 6:4, 5:5, 4:6, 3:7, 2:8, 1:9), Ethyl acetate (100%), Ethyl acetate : Methanol (9:1, 8:2, 7:3, 6:4, 5:5, 4:6, 3:7, 2:8, 1:9) and Methanol (100%). Totally 223 fractions were collected and analysed by TLC which is shown in table 1.

Table 1. Isolated fractions of stem ethanolic extract of *Cayratia trifolia* Separation of fractions by column chromatography

Solvents	Ratio	Fractions collected
Petroleum ether	(100%)	1-20
Petroleum ether:	9:1, 8:2, 7:3,	21-30, 31-37, 38-45, 56-58,
Chloroform	6:4, 5:5, 4:6,	49-55, 56-60, 61-69, 76-80
	3:7, 2:8, 1:9	
Chloroform	100%	81-109
Chloroform: Ethyl	9:1, 8:2, 7:3,	110-116, 117-120, 121-125,
acetate	6:4, 5:5, 4:6,	126-129, 130-132, 133-137,
	3:7, 2:8, 1:9	138-147, 148-150, 151-153
Ethyl acetate	100%	154-160
Ethyl acetate:	9:1, 8:2, 7:3,	161-163, 164-169, 170-178,
Methanol	6:4, 5:5, 4:6,	179-182, 183-188, 189-195,
	3:7, 2:8, 1:9	196-198, 199-201, 202-205
Methanol	100%	206-223

TLC is a simple, rapid, and inexpensive procedure that gives a quick answer as to how many components are in a mixture. From the TLC analysis 202-205 showed clear single spot with same R_f value 0.6cm and 50 mg was yielded from ethyl acetate: methanol (1:9) ratio fraction of *Cayratia trifolia* stem parts, shown in figure 1.



Figure 1. Thin Layer Chromatography of isolated compound of *Cayratia trifolia*

In UV-Visible spectroscopy analysis, the 202-205 fractions show the maximum absorbance at 271nm, so it confirmed that the compound doesn't have double bond and that bond was not weak (Figure 2).

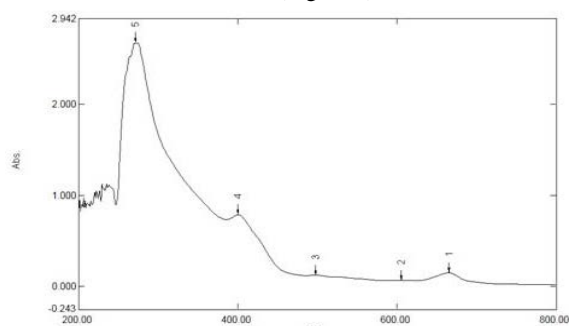


Figure 2. UV Visible Spectroscopy of isolated compound of *Cayratia trifolia*

FTIR confirmed to be a valuable tool for the characterization and identification of compounds or functional groups (chemical bonds) present in an unknown mixture of plants extract. The FTIR analysis showed the presence of O-H at 3442 cm^{-1} , C-H at 2927 cm^{-1} and C-O at 1061 cm^{-1} , groups (Figure 3 and Table 2).

Table 2. FTIR spectrum peak values and functional groups of 202-205th fractions

Functional Groups	Type of Vibration	Characteristic Absorptions (cm^{-1})
O-H Alcohol	Stretch	3442
C-H Alkane	Stretch	2927
C-O Alcohol	Stretch	1061

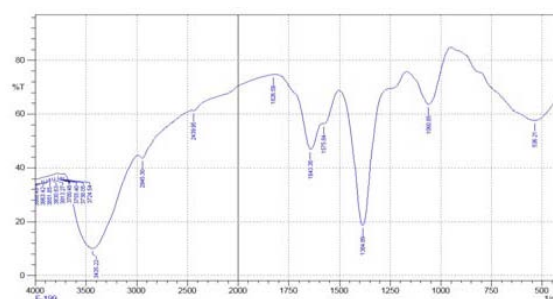


Figure 3: FTIR Spectroscopy of isolated compound of *Cayratia trifolia*

The ^1H NMR spectrum showed the presence of a triplet at δ 0.86 for a terminal methyl group, a broad singlet at δ 1.25 showing the presence of a long chain of methylene groups, at δ 2.34 for a methylene α - to the oxy methylene

group, at δ 2.17 for a β - methylene to a oxy methylene group and a pair of multiplet signals at δ 3.6 to a oxy methylene group (OCH_2) (Figure 4).

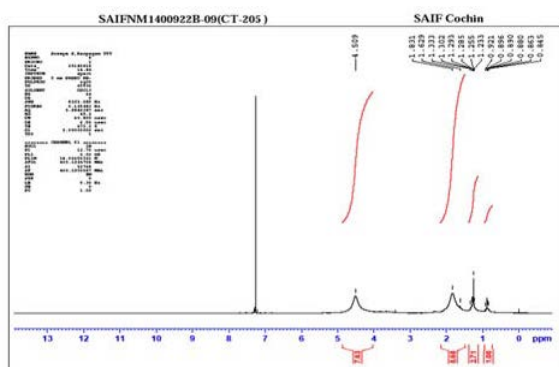


Figure 4. ^1H NMR Spectroscopy of isolated compound of *Cayratia trifolia*

^{13}C NMR spectrum indicates the presence of long chain methylene groups (Figure 5). Based on the chromatographic and spectrum techniques indicated that the isolated compound is a 1-pentacosanol (Figure 6 and Table 3).

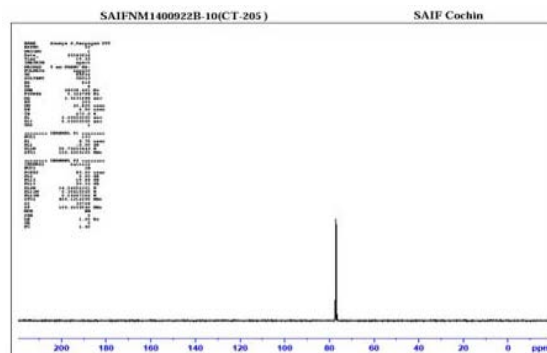


Figure 5. ^{13}C NMR Spectroscopy of isolated compound of *Cayratia trifolia*



Figure 6. Structure of the isolated compound

Table 3. Isolated compound from stem ethanolic extract of *Cayratia trifolia*

Compound Name	1-pentacosanol
Molecular Formula	$\text{C}_{25}\text{H}_{52}\text{O}$
Molecular Weight	368.68 g/mol
IUPAC Name	Pentacosan-1-ol

IUPAC=International Union of Pure and Applied Chemistry

3.1. Molecular Docking analysis

The isolated natural compound was docked with targeted proteins such as AKT and E2F3, PTEN and SMO using Glide module from Schrodinger suite. Based on glide score and glide energy, the docking results were analysed. The docking result of the isolated 1-pentacosanol compound was complex, and the interaction of amino acids with AKT, E2F3, PTEN and SMO protein is shown in table 4.

Table 4. Docking Results of isolated natural compound and standard drug complexed with AKT, E2F3, PTEN and SMO proteins

Target protein	Amino Acids interaction		Ligand atom		Glide Gscore/ Glide energy	
	Finasteride	Pentacosanol	Finasteride	Pentacosanol	Finasteride	Pentacosanol
AKT	ALA 230 (H)	LYS 276(H)	O	O	-3.1/-22.168	-3.42/-34.919
		LYS 179(H)	O	O		
		ASP 292(C)	H	H		
E2F3	SER 147 (O)	GLN 303(O)	O	H	-3.8/-41.588	-3.57/-36.846
		ARG 121(O)	H	H		
PTEN	LYS 330 (H)	ASP 153(O)	O	H	-3.1/-40.050	-3.96/-39.27
		ARG 172(H)	H	O		
SMO	No Interaction	ILE 413 (O)	No Interaction	H	No Interaction	-3.98/-31.761

The molecular docking results revealed that AKT (Fig. 7), E2F3 (Fig. 8), PTEN (Fig. 9) and SMO (Fig. 10) complex with 1-pentacosanol has good glide score of -3.428, -3.573, -3.964 and -3.987 Kcal/mol and the glide energy is -36.846, -31.761, -39.270 and -34.919 Kcal/mol respectively. When compared with standard drug, i.e., Finasteride (complex with AKT, E2F3, PTEN and SMO (no interaction) has low glide score and glide energy -3.1/22.168, -3.8/-41.588 and -3.1/-40.050 Kcal/mol respectively. An ADME property of the isolated natural compound of 1-pentacosanol is shown in Table 5 and was under acceptable range. Perumal *et al.*, (2016) reported that the bioactive compound, epifriedelanol isolated from the ethanolic extract of *Cayratia trifolia* having binding affinities against few proteins (HER2, EGFR and CXCR4) might act as good inhibitor against ovarian cancer.

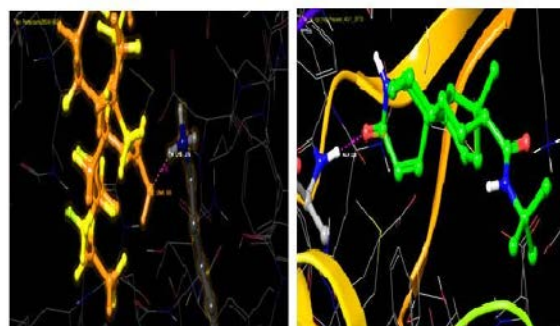


Figure 7: The 3D structure of 1-pentacosanol and finasteride complexed with AKT protein7: (a) 1-pentacosanol 7: (b) Finasteride

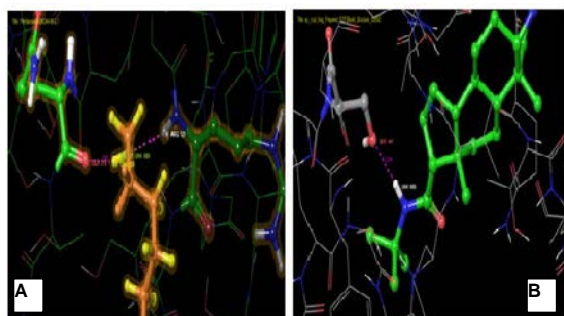


Figure 8. The 3D structure of 1-pentacosanol and finasteride complexed with E2F3 protein 8: (a) 1-pentacosanol 8: (b) Finasteride

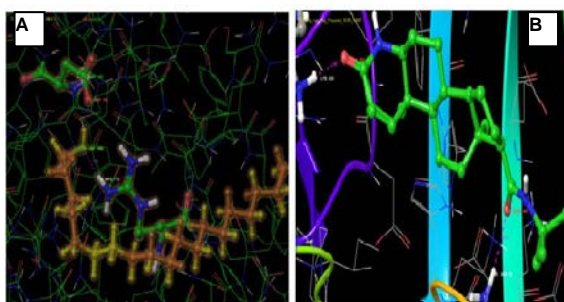


Figure 9. 3D structure of 1-pentacosanol and finasteride complexed with PTEN protein 9: (a) 1-pentacosanol 9: (b) Finasteride

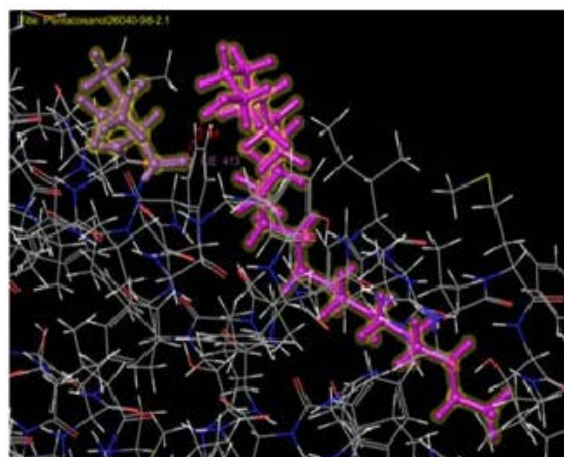


Figure 10. 3D structure of 1-pentacosanol complexed with SMO

Table 5. ADME properties of 1-pentacosanol

Ligand	Molecular weight (g/mol)	H-Bond donar	H-Bond acceptor	Log P (O/W)
1-pentacosanol	368.68 g/mol	1	1	12.2

ADME=Absorption, Distribution, Metabolism and Excretion

4. Discussion

Nature has been a source of medicinal agent for thousands of years and an impressive number of modern drugs have been isolated from natural sources (Nair *et al.*, 2005). Natural products discovered from medicinal plants have played an important role in combating cancer irrespective of their multifactorial origin (Rajkumar *et al.*, 2012). Isolation of pharmacologically active compounds from medicinal plants persist today. Investigation of the chemical composition and secondary metabolites from medicinal plants is an active research field and is the base for drug discovery, due to the demand for identifying and

analysing the target proteins with their active sites and potential drug molecules that can bind to these sites specifically.

Cayratia trifolia (Vitaceae), known as fox grape in English, a perennial climber having trifoliolate leaves (2–3 cm), is native to India, Asia and Australia. The methanolic extract is more effective than aqueous extract of *Cayratia trifolia* were found to be defending against esophageal cancer in rodents (Rejitha and Das 2009). *Cayratia trifolia* (L.) leaves contain stilbenes such as piceid, reveratrol, viniferin and ampelopsin. Stem, leaves and roots are reported to possess hydrocyanic acid and delphinidin. The leaves were used to cure swelling, injury and infection for bullock (Kumar *et al.*, 2011). Sowmya *et al.* (2016), also reported that more phytochemical and bioactive compounds were present in the stem ethanolic extract of *Cayratia trifolia* (L.) confirmed by FTIR, HPTLC and GC-MS analysis. The ethanolic root extract of *Cayratia trifolia* having antidiabetic activity was reported by Mohammed *et al.* (2017).

Many databases are available today to describe the medicinal plants and compound (Nonita *et al.*, 2012). The current study provides useful insights to research in isolation and identification of potential anticancer chemo preventive metabolites from stem parts of ethanolic extract of *Cayratia trifolia*. The identification of natural compounds using chromatography and spectroscopic techniques may provide efficient information concerning qualitative and quantitative composition of herbal medicines (Barbosa *et al.*, 2013). Docking is a method which predicts the preferred direction of one molecule to a second when bound to each other to form a stable complex (Tripathi *et al.*, 2012).

The target of ligand-protein docking is to predict the predominant binding model of a ligand with a protein of known three-dimensional structure (Srivastava *et al.*, 2010). The highest negative value of glide score and glide energy indicated that these complexes may have good affinity (Srinivasan *et al.*, 2014). In the present study, the isolated natural compound 1-pentacosanol has comparable good affinity with selected prostate cancer targets of PTEN, AKT, SMO and E2F3 when compared with FDA approved drug of Finasteride.

5. Conclusion

Based on the results, it can be concluded that the isolated bioactive compound of 1-pentacosanol may act as a good inhibitor to the selected targets and a novel anti-prostate cancer agent in future. However, the molecular docking studies alone cannot completely support to control the prostate cancer. The combined *in silico* approach has been translated into *in vitro* and *in vivo* molecular studies which have provided encouraging *in silico* results against the prostate cancer.

Funding

This research did not receive any specific grant from funding agencies in the public, commercial, or not-for-profit sectors.

Conflict of Interest

The authors declare that there is no conflict of interest regarding the publication of this paper.

Acknowledgement

The authors are thankful to our Chancellor, Chief Executive Officer, Vice-Chancellor and Registrar of Karpagam Academy of Higher Education, Coimbatore, India for providing facilities and encouragement. Our thanks are also due to Sophisticated Analytical Instrument Facility (SAIF), Cochin University of Science and Technology, Cochin, India for successful NMR analysis.

References

- Barbosa pereira L, Pocheville A, Angulo I, Paseiro losada P and Cruz JM. 2013. Fractionation and purification of bioactive compounds obtained from a brewery waste stream. *Biomed Res Int.* **2013**: 408-491.
- Bray F, Ferlay J, Soerjomataram I, Siegel RL, Torre LA and Jemal A. 2018. Global cancer statistics 2018: GLOBOCAN estimates of incidence and mortality worldwide for 36 cancers in 185 countries. *CA Cancer J Clin.* **68**: 394-424.
- Eberhardt TL, Li X, Shupe TF and Hse CY. 2007. Chinese Tallow Tree (*Sapium sebiferum*) utilization: Characterization of extractives and cell-wall chemistry. *Wood Fiber Sci.* **39**: 319-324.
- Feng YZ, Shiozawa T, Miyamoto T, Kashima H, Kurai M, Suzuki A, Song JY and Konishi I. 2017. Overexpression of hedgehog signalling molecules and its involvement in the proliferation of endometrial carcinoma cells. *Clin Cancer Res.* **13**: 1389-1398.
- Glide. 2012. Schrödinger version 5.6, LLC, New York.
- Gupta K and Sharma M. 2007. Review on Indian Medical Plant. Delhi, India: ICMR. **5**: 879-82.
- Gupta J, Kumar D and Gupta A. 2012. Evaluation of gastric anti-ulcer activity of methanolic extract of *Cayratia trifolia* in experimental animals. *Asian Pac J Trop Dis.* **2**: 99-102.
- Guru kumar D, Sonumol VM, Rathi MA, Thirumoorthi L, Meenakshi P and Gopalakrishnan VK. 2011. Hepatoprotective Activity of *Cayratia trifolia* (L.) Domin Against Nitrobenzene Induced Hepatotoxicity. *Lat Am J Pharm.* **30**: 546-9.
- Hazra KM, Roy RN, Sen SK and Laska S. 2007. Isolation of antibacterial pentahydroxy flavones from the seeds of *Mimusops elengi* Linn. *Afr. J. Biotechnol.* **6**: 1446-1449.
- Kumar D, Kumar S, Gupta J, Arya R and Gupta A. 2011. A review on chemical and biological properties of *Cayratia trifolia* Linn. (Vitaceae). *Phcog Rev* **5**: 184-188.
- Kumar D, Gupta J, Kumar S, Arya R, Kumar T and Gupta A. 2012. Pharmacognostic evaluation of *Cayratia trifolia* (Linn.) leaf. *Asian Pacif J Trop Biomed.* **2**: 6-10.
- LigPrep. 2012. Schrödinger version 2.4, LLC, New York.
- Mehrian-Shai R, Chen CD, Shi T, Horvath S, Nelson SF, Reichardt JKV and Sawyers CL. 2007. Insulin growth factor-binding protein 2 is a candidate biomarker for PTEN status and PI3K/Akt pathway activation in glioblastoma and prostate cancer. *PNAS.* **104**: 5563-5568.
- Mohammed SI, Salunkhe NS, Vishwakarma KS and Maheshwari VL. 2017. Experimental Validation of Antidiabetic Potential of *Cayratia trifolia* (L.) Domin: An Indigenous Medicinal Plant. *Ind J Clin Biochem.* **32**: 153-162
- Nair T, Kalariya T and Chanda S. 2005. Antibacterial activity of some selected Indian medicinal flora, *Turk J Biol.* **29**: 47-53.
- Nonita P. Peteros and Mylene M. 2010. Antioxidant and cytotoxic activities and phytochemical screening of four Philippine medicinal plants. *J Med Plants Res.* **4**: 407-414.
- Pejin B, Jovanovic KK, Mojovic M and Savic AG. 2013. New and Highly Potent Antitumor Natural Products from Marine-Derived Fungi: Covering the Period from 2003 to 2012. *Cur Topics Med Chem.* **13**: 2745 – 2766.
- Pejin B, Jovanovic KK and Savic AG. 2015. New antitumor natural products from marine red algae: covering the period from 2003 to 2012. *Mini Rev Med Chem.* **15**: 720-730.
- Perumal PC, Sophia D, Arulraj C, Ragavendran P, Starlin T and Gopalakrishnan VK. 2012. *In vitro* antioxidant activities and HPTLC analysis of ethanolic extract of *Cayratia trifolia* (L.). *Asian Pacif J Trop Dis.* **S952-S956**.
- Perumal PC, Sowmya S, Pratibha P, Vidya B, Anusooriya P, Starlin T, Vasanth R, Sharmila DJS and Gopalakrishnan VK. 2014. Identification of novel PPAR γ agonist from GC-MS analysis of ethanolic extract of *Cayratia trifolia* (L.): a computational molecular simulation studies. *J App Pharm Sci.* **4**: 006-011.
- Perumal PC, Sowmya S, Pratibha P, Vidya B, Anusooriya P, Starlin T, Ravi S and Gopalakrishnan VK. 2015. Isolation, structural characterization and *in silico* drug-like properties prediction of bioactive compound from ethanolic extract of *Cayratia trifolia* (L.). *Pharmacog Res.* **7**: 121-125.
- Perumal PC, Sowmya S, Velmurugan D, Sivaraman T and Gopalakrishnan VK. 2016. Assessment of dual inhibitory activity of epifriedelanol isolated from *Cayratia trifolia* against ovarian cancer. *Bangladesh J Pharmacol.* **11**: 545 -551.
- Poornima K, Perumal PC and Gopalakrishnan VK. 2014. Protective effect of ethanolic extract of *Tabernaemontana divaricata* (L.) R. Br. against DEN and Fe NTA induced liver necrosis in Wistar Albino rats. *Biomed Res Int.* **2014**: 1-9.
- Pradip KM and William RS. 2005. AKT-regulated pathways in prostate cancer. *Oncogene.* **24**: 7465-7474.
- Protein Preparation Wizard Maestro. 2012. Schrödinger LLC, New York.
- QikProp. 2012. Version 3.2. Schrodinger, LLC, New York.
- Rajkumar V, Gunjan G and Ashok Kumar R. 2012. Isolation and bioactivity evaluation of two metabolites from the methanolic extract of *Oroxylum indicum* stem bark. *Asian Pac J Trop Biomed.* **S7-S11**.
- Rejitha G and Das A. 2009. Cytotoxic effect of *Cayratia carnosia* leaves on Human Breast Cancer Cell Lines. *Int J Cancer Res.* **5**: 115-22.
- Reynolds MA. 2008. Molecular alterations in prostate cancer. *Cancer Lett.* **271**: 13-24.
- Schrodinger. 2012. LLC, New York.
- Sadashivam. S and Manickam A. 2004. **Biochemical Methods.** 2nd Edition New Age International (P) Limited, New Delhi, India.
- Sinosh S, Rao Shruthi K and Usha BB. 2010. *In Silico* Investigation and Docking Studies of E2F3 Tumor Marker: Discovery and Evaluation of Potential Inhibitors for Prostate and Breast Cancer. *Int J Pharm Sci Drug Res.* **2**: 254-260.
- Sowmya S, Perumal PC, Anusooriya P, Vidya B, Pratibha P, Malarvizhi D and Gopalakrishnan VK. 2014. Comparative Preliminary Phytochemical Analysis Various Different Parts (Stem, Leaf and Fruit) of *Cayratia trifolia* (L.). *Indo-Am J Pharm Res.* **4**: 218-223.
- Sowmya S, Perumal PC and Gopalakrishnan VK. 2016. chromatographic and spectrophotometric analysis of bioactive compounds from *Cayratia trifolia* (L.) stem. *Int J Pharm Pharm Sci.* **8**: 56-64

Srinivasan P, Perumal PC and Sudha A.2014. Discovery of Novel Inhibitors for Nek6 Protein through Homology Model Assisted Structure Based Virtual Screening and Molecular Docking Approaches. *Scientific World J.* **2014**: 1-9.

Srivastava V, Gupta SP, Siddiqi MI and Mishra BN 2010.Molecular docking studies on quinazoline antifolate derivatives as human thymidylate synthase inhibitors. *Bioinform.* **4**: 357-365.

Tripathi SK, Singh SK, Singh P, Chellaperumal P, Reddy KK and Selvaraj C. 2012. Exploring the selectivity of a ligand complex with CDK2/CDK1: a molecular dynamics simulation approach. *J Mol Recognit.* **25**: 504-512.

Wang MC, Valenzuela LA, Murphy GP and Chu TM. 1979.Purification of a human prostate specific antigen. *Invest Urol.* **17**: 159-163.

Yan L, Yijun Y, Pengyuan L, Weidong W, Michael J, Daolong W and Ming Y.2007. Common Human Cancer Genes Discovered by Integrated Gene-Expression Analysis. *PLoS ONE.* **2**: 1149.

Zavoi S, Florinela F, Floricuta R, Raluca M, Anca B and Carmen S 2011. Comparative Fingerprint and Extraction Yield of Medicinal Herb Phenolics with Hepatoprotective Potential, as Determined by UV-Vis and FT-MIR Spectroscopy. *Not. Bot. Horti Agrobi.* **39**: 82-89.

Cloning, expression and purification of *Leishmania major* PSA-sfGFP fusion protein

Aisha Al-jaghasi¹, Abdul-Qader Abbady^{2,4}, Sahar Al-Khatib¹ and Chadi Soukkarieh^{1,3,*}

¹Dept. of Animal Biology, Faculty of Sciences, Damascus University, Damascus, Syria; ²Dept. of Molecular Biology and Biotechnology, Atomic Energy Commission of Syria (AECS), ³Damascus, Syria; ⁴Faculty of Pharmacy, Syrian Private University, Damascus, Syria
⁵Faculty of Pharmacy, International University for Science and Technology, Damascus, Syria

Received: June 16, 2020; Revised: September 24, 2020; Accepted: October 21, 2020

Abstract

PSA (Promastigote Surface Antigen) is one of the immunogenic antigens in *L. major*. Protection depends on the source of PSA antigen, whereas native protein and plasmid DNA encoding PSA, but not recombinant PSA purified from *E. coli* provided significant protection. The green fluorescent protein (GFP) is commonly used as an excellent expression tag for fusion proteins, which can improve their expression while retaining their function and native-like structure. Trying to develop anti cutaneous leishmaniasis vaccine based on PSA (as recombinant protein or DNA vaccine), this study evaluated the cloning, expression, of the secreted PSA protein from *L. major* as a fusion partner to the superfolder form of green fluorescent protein (sfGFP) in both *E. coli* and HEK-293T cells. This included constructing protein expression plasmids pRSET-sfGFP-PSA and pcDNA-sfGFP-PSA, then producing the recombinant of 6× His tagged sfGFP-PSA protein (65 kDa) that was confirmed by SDS-PAGE and western blotting. Although sfGFP-PSA fusion protein was expressed with full length in both types of cells, a partial separation of sfGFP protein was observed when the fusion protein was expressed in *E. coli*.

Here we presented an efficient method to produce the full length of PSA as a fusion protein with sfGFP, which could greatly facilitate its uses as a vaccine against cutaneous leishmaniasis.

Keywords: PSA, sfGFP, Gene cloning, Protein expression

1. Introduction

Cutaneous leishmaniasis is endemic in more than 70 countries worldwide, and 90% of cases happen in Afghanistan, Algeria, Brazil, Pakistan, Peru, Saudi Arabia, and Syria (Reithinger *et al.*, 2007; Von Stebut, 2015). Leishmaniasis remains one of the promising parasitic diseases for vaccine development since defective cellular immune responses are restored after effective chemotherapy and hosts who recover from leishmaniasis are typically insusceptible to further infection (Handman, 2001).

Leishmania secreted factors and surface proteins are key players in the pathogenesis of the disease; they mainly facilitate the parasite's initial contact with the host cells, and interfere with immune cells' functions such as antigen presentation, cytokine production and cell activation (Soto *et al.*, 2009). The interest in *Leishmania* excreted molecules was confirmed by past studies showing interesting properties in terms of protection, which is likely to be special targets for the immune system (Holzmüller *et al.*, 2005; Lemesre *et al.*, 2005; Tonui *et al.*, 2004). Promastigote Surface Antigen (PSA) is an abundant glycolipid-anchored protein on the surface of the promastigote form of most *Leishmania* species (Devault and Bañuls, 2008; Jiménez-Ruiz *et al.*, 1998). It belongs to

a unique family of membrane-bound and secreted proteins, and has a specific Leucine Rich Repeats signature, which is involved in protein-protein interactions and pathogen recognition (Devault and Bañuls, 2008; Kędzierski *et al.*, 2004). PSA protein is involved in *Leishmania* attachment and invasion of host macrophages via interactions with the complement receptor 3 (CR3), and in resistance to complement lysis (Kędzierski *et al.*, 2004; Lincoln *et al.*, 2004). It has been proven that this protein is a major immunogenic component of secreted antigens (Brag-Gonçalves *et al.*, 2014). The development of vaccines based on the PSA protein was evaluated in several experimental models. PSA isolated from *L. amazonensis* promastigotes, as well as recombinant vaccine viruses expressing this protein, have been demonstrated to induce a protective immune response against infection with *L. amazonensis* in BALB/c mice (Champsy and McMahon-Pratt, 1988; McMahon-Pratt *et al.*, 1993). With the recently available whole genome sequences of some *Leishmania* species, thirty-two PSA genes were described in *L. major* genome (Devault and Bañuls, 2008). Moreover, the presence of Th1-type memory to PSA in humans and the ability of the antigen to protect injected mice against *L. major* infection make PSA an attractive candidate to be used as vaccine against human cutaneous leishmaniasis (Kemp *et al.*, 1998). Protection depends on the source of PSA antigen, whereas protection was

* Corresponding author e-mail: soukkarieh@gmail.com..

observed with the protein purified from *L. major* membrane (native PSA) or expressed as a recombinant protein in *L. mexicana*, vaccination with the PSA expressed in bacteria did not give protection (Handman *et al.*, 1995; Sjölander *et al.*, 1998a). However, the immunization with PSA DNA vaccine induced an exclusive Th1 response and mice were protected against an *L. major* challenge (Sjölander *et al.*, 1998b).

Several protocols are currently available to improve protein expression including fusion of the protein with a more soluble partner like GFP, where it dramatically aids in protein folding and increases its stability; furthermore, it rarely adversely affects biological activity (Waldo *et al.*, 1999). A superfolder form of GFP was engineered by Waldo and colleagues (*sfGFP*), that is more resistant to denaturation and aggregation during refolding, and improved folding kinetics (Andrews *et al.*, 2007; Pedelacq *et al.*, 2006). The development of an efficient and low-cost technique to produce PSA protein could greatly facilitate its uses as a vaccine against leishmaniasis. In this study, we report the steps of producing *L. major* PSA protein as fusion with *sfGFP* (as recombinant protein and DNA vaccine); *sfGFP*-PSA fusion protein production was confirmed in *E. coli* and HEK-293T cells by SDS-PAGE and Western blotting.

2. Methods

2.1. Bacterial strains and plasmids:

E. coli strains TOP10 (Invitrogen) and BL21 (DE3) Gold (Novagen) were used in cloning and protein expression. *E. coli* strain transformants were grown at 37°C in Luria Broth (LB) (Bio Basic INC) that contained ampicillin (100 µg/ml) for selection of clones containing recombinant plasmid constructs. Plasmids used in this study were the plasmid pRSET (Invitrogen), pRSET-*sfGFP* (Al-Homsi *et al.*, 2012), and the plasmid pcDNA-*sfGFP* which was kindly provided by Dr. Abbady, Atomic Energy Commission of Syria (AECS). Schematic diagrams of plasmid constructs were generated using Geneious pro 4.8.4.

2.2. Cloning of PSA

L. major (Dermatology and Venereology Hospital in Damascus, Syria) was used as the parental strain for amplifying the PSA gene. *LMJF_31_1450* gene, which expresses the secreted PSA form, was amplified by polymerase chain reaction (PCR) technique. The full sequence of PSA gene was obtained from GenBank *Leishmania major* freidlin strains; Gene ID: 5654076, while the forward and reverse primers were designed based on it: the forward primer: (5'ATATATGTCGACGCAGGATCCATGCCCATGCTGCTGCTCCG3') containing a *Bam*HI restriction site, and the reverse primer: (5'ATATATGGTACCGAATTCTTACTAGCACGCGTTGGCTGTCGAGC3') containing an *Eco*RI restriction site. The Pfu DNA polymerase kit (Thermo) was used according to the manufacturers' instructions. PCR was performed by thermal cycler (Peqlap, Germany) under standard protocol of a 94 C for 2 min, 30 cycles of 94 C for 30 s, 58 C for 30 s, 72 C for 1 min and 72 C for 7 min as a final extension step. The obtained PCR product and the plasmid pRSET (Invitrogen) were digested with the

restriction enzymes *Bam*HI and *Eco*RI (Fermentas). Digestion products were extracted from the agarose gels using the QIAquick Gel Extraction Kit (Qiagen) and then ligated using T4 DNA ligase (Fermentas). The new plasmid construct pRSET-PSA was transformed into *E. coli* strain TOP10 (Invitrogen) by the heat shock method. Positive clones were confirmed by Colony PCR screening using PSA cloning primers, and then plasmid constructs were isolated from some positive clones by Plasmid Miniprep Kit (Qiagen). DNA sequencing and digestion with restriction enzymes were performed to confirm successful cloning.

2.3. DNA sequencing

DNA sequencing for pRSET-PSA construct was performed on a Genetic 114 Analyzer system ABI-310 by the dideoxynucleotide chain-termination method, and the homology searches were performed using the BLAST program with NCBI Reference Sequence: XM_001685079.1.

2.4. Subcloning of PSA

The PSA gene was subcloned into pRSET-*sfGFP* and pcDNA-*sfGFP* (prokaryotic and eukaryotic expression plasmids respectively) as a fusion partner at the C-terminus of *sfGFP* gene. The new recombinant constructed plasmids pRSET-*sfGFP*-PSA and pcDNA-*sfGFP*-PSA were verified by restriction enzyme digestion. pRSET-*sfGFP*-PSA was digested by *Eco*RI and (*Bam*HI or *Xba*I) enzymes while pcDNA-*sfGFP*-PSA was digested by *Hind*III and *Eco*RI compared with the pcDNA-*sfGFP* plasmid.

2.5. Expression of PSA and *sfGFP*-PSA fusion protein in *E. coli*

pRSET-PSA and pRSET-*sfGFP*-PSA constructions were transformed into *E. coli* strain BL21 (DE3) Gold (Novagen) competent cells by thermal shock. One positive clone of each construct was grown, and the expression of the recombinant proteins was induced in *E. coli* Gold cells by the addition IPTG (Isopropyl β-D-1-thiogalactopyranoside) to 0.5 mM final concentration, for 16 h. The induction of protein expression was done at 20 C for PSA, and 16 C for *sfGFP*-PSA fusion protein. Bacterial cells were harvested by centrifugation at 10000 rpm for 10 min at 4 C. The harvested cells were prepared for protein purification, so cell pellets were suspended in PBS 1X, then the lysates were loaded to the frenchpress (Constant systems), and pressure applied (Total processing time, 10 min; 1 Kbr), after that the disrupted extracts were centrifuged at 10000 rpm for 10 min at 4 C. Purification of PSA and *sfGFP*-PSA proteins from cytoplasmic extract was done on immobilized-metal affinity chromatography, using the Ni-NTA agarose beads; finally, eluted proteins were analyzed by 12% SDS-PAGE and western blotting.

2.6. Expression of *sfGFP*-PSA fusion protein in eukaryotic cells

HEK-293T cells were transfected with pcDNA-*sfGFP*-PSA using polyethylenimine (PEI) Transfection Reagent (Roche, Germany). After two passages, the cells were seeded in four-well plate (100×10³ cells/well), and grown in RPMI 1640 medium supplemented with 10% fetal calf serum, 1% glutamine, 100 U/ml of penicillin, and

100 mg/ml streptomycin (all from Sigma Chemical) for 48 h. Transfection solution for each well contained 50 μ l of serum-free RPMI medium, PEI (1:3 ratio) and 1.5 μ g of plasmid either pcDNA-*sfGFP*-PSA or pcDNA-*sfGFP* (control). The previous mixture was incubated for 30 min at room temperature and then it was added dropwise to the 60-70% confluent cells with gentle shaking. The plate was incubated for 48 h and the production of *sfGFP*-PSA fusion protein was evaluated by fluorescence microscopy at 12, 24, and 48 hours after transfection; finally, it was confirmed in the supernatants medium by western blotting.

2.7. SDS-PAGE and Western Blotting

Three protein samples (PSA and *sfGFP*-PSA) expressed in bacteria and HEK cells were separated on 12% SDS-PAGE followed by western blotting. The proteins were diluted in reducing SDS sample buffer and heated at 95 C for 5 min, and the electrophoresis (Bio-Rad) was performed at 140V. After electrophoresis, the gels were stained in coomassie blue buffer. Other SDS-PAGEs were performed, and the polypeptides from the gels were transferred to 0.45 μ m nitrocellulose membranes using a wet blotting system (Bio-Rad). The membranes were blocked with PBS 1X containing 5% skim milk and 0.05% Tween 20 for overnight at 4 C. Then the blot of PSA protein was incubated for 1 h with (1:2000) dilution of mouse anti-6 \times His antibodies (R&D Systems), while the blots of the fusion *sfGFP*-PSA proteins were incubated with (1:3000) dilution of a polyclonal rabbit anti-GFP (Al-Homsi *et al.*, 2012). After washing, the membranes were incubated for 1 h with secondary antibody conjugated to Alkaline Phosphatase (AP), either Rabbit anti-mouse (1:2000; Sigma, Germany), or goat anti-rabbit (1:2000; Bio-Rad). The proteins were detected with NBT 1%, BCIP 0.5% (Bio-Rad, Germany) staining.

3. Results

3.1. Cloning of PSA

Using the gene-specific primers with *L. major* genomic DNA as the template, a 909 bp long PSA gene was successfully amplified. Amplified PSA gene, as well as the pRSET plasmid, was digested with the restriction enzymes *Bam*HI and *Eco*RI, then they were purified from the gel and used in a ligation reaction in an appropriate molar ratio of 1:3 (plasmid: insert).

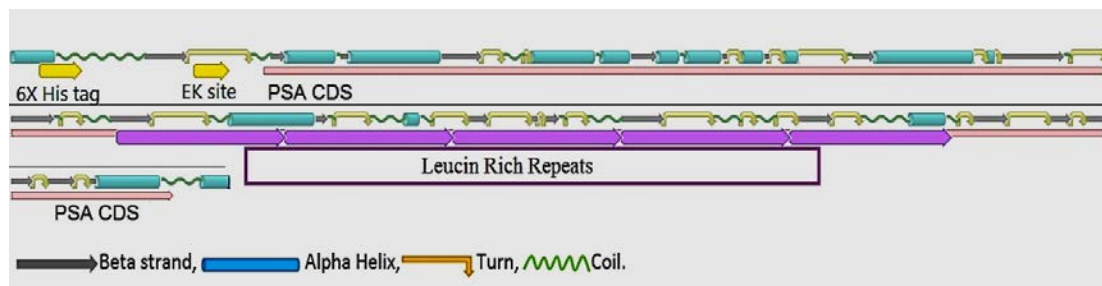


Figure 2. Diagrammatic representation of the Secondary structure of PSA protein, where LRR domains have been matched with NCBI Reference Sequence: XP_001685131.1. The model for PSA protein was generated using Geneious pro 4.8.4.

3.3. Subcloning of PSA

PSA gene was subcloned into pRSET-*sfGFP* and pcDNA-*sfGFP* plasmids as a fusion partner to the *sfGFP*. PSA gene was introduced directly at the C-terminus of the

sfGFP gene, and the two genes were in-frame cloning construct. The recombinant constructed plasmids pRSET-*sfGFP*-PSA and pcDNA-*sfGFP*-PSA were prepared from positive PCR colonies by plasmid miniprep Kit and the enzyme digestion was used to verify them (Figs. 3, 4).

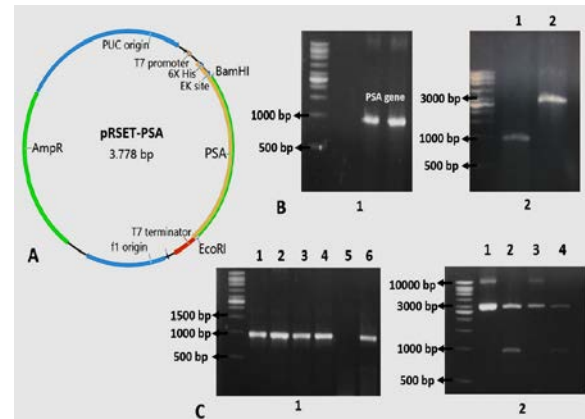


Figure 1. Cloning of PSA into pRSET plasmid.

A: Schematic diagram of pRSET-PSA construct. **B: B-1** Agarose gel electrophoresis of PCR products. The full-length of *L. major* PSA gene (909 bp) was separated on a 1% agarose gel. **B-2** DNA bands of pRSET plasmid and PSA PCR amplified gene after being digested with *Bam*HI and *Eco*RI restriction enzymes. Lane 1: PSA gene; Lane 2: pRSET plasmid. **C: C-1** Results of colony PCR screening performed on 6 randomly selected clones. Lanes 1, 2, 3, 4 and 6: positive clones, which contain full-length PSA gene (909bp); Lane 5: a negative colony that doesn't contain the PSA gene. **C-2** Identification of recombinant pRSET-PSA plasmid by restriction enzyme digestion. Lanes 1, 3: circular pRSET-PSA Plasmid; Lanes 2, 4: pRSET-PSA double-digested with *Bam*HI and *Eco*RI. DNA ladder (1 kb).

3.2. Sequence analysis of the PSA gene

Sequencing analysis revealed that no changes were presented during the cloning process and the pRSET-PSA construct was exact. Open reading frame, which includes the full length of PSA gene and protein binding 6His tag followed by EK protease site, was composed of 1,032 nucleotides and the predicted molecular weight of the recombinant PSA protein was 38 kDa (Fig. 2).

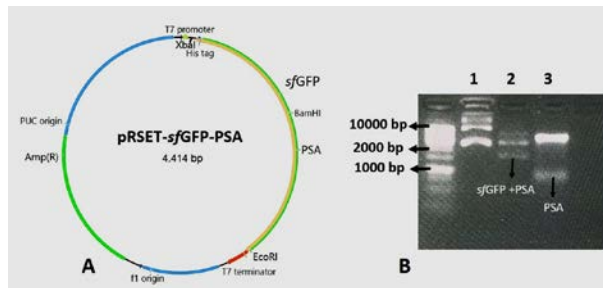


Figure 3. Cloning of PSA into pRSET-*sfGFP* plasmid.

A: Schematic diagram of pRSET-*sfGFP*-PSA construct. **B:** Identification of recombinant pRSET-*sfGFP*-PSA plasmid by restriction enzyme digestion. Lane 1: pRSET-*sfGFP*-PSA circular Plasmid; Lane 2: pRSET-*sfGFP*-PSA double-digested with *Xba*I and *Eco*RI (expected digested fragment: PSA and *sfGFP* genes); Lane 3: pRSET-*sfGFP*-PSA double-digested with *Bam*HI and *Eco*RI (expected digested fragment: PSA gene). DNA ladder (1 kb).

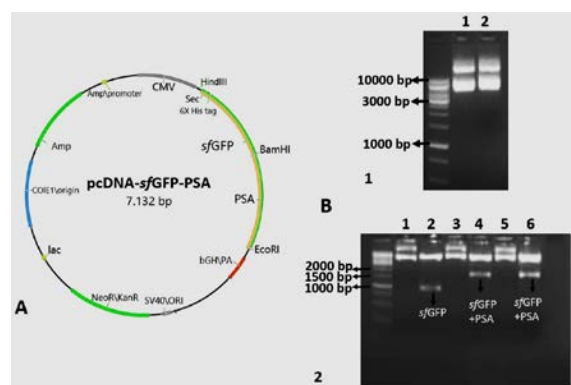


Figure 4. Cloning of PSA into pcDNA-*sfGFP* plasmid.

A: Schematic diagram of pcDNA-*sfGFP*-PSA construct. **B:** **B-1** Recombinant pcDNA-*sfGFP*-PSA plasmid was extracted from two of the positive colonies by miniprep. Lanes 1, 2: pcDNA-*sfGFP*-PSA Plasmid. **B-2** Identification of recombinant pcDNA-*sfGFP*-PSA plasmid by restriction enzyme digestion. Lane 1: pcDNA-*sfGFP* plasmid (control) without digestion; Lane 2: pcDNA-*sfGFP* double-digested with *Hind*III and *Eco*RI (expected digested fragment: *sfGFP* gene); Lanes 3, 5: pcDNA-*sfGFP*-PSA plasmid without digestion; Lanes 4, 6: pcDNA-*sfGFP*-PSA double-digested with *Hind*III and *Eco*RI (expected digested fragment: PSA and *sfGFP* genes). DNA ladder (1 kb).

3.4. Expression of protein

3.4.1. Expression of PSA and *sfGFP*-PSA fusion protein in *E. coli*:

The production of PSA and PSA-*sfGFP* proteins were obtained after the transformation of *E. coli* BL21 (DE3) Gold cells with the confirmed pRSET-PSA and pRSET-*sfGFP*-PSA constructs. Following positive bacterial cells growth, protein expression was induced overnight by IPTG and Low temperature. PSA protein was shown a significant expression with a molecular weight of around 38 kDa as observed in SDS-PAGE (acrylamide 12%). His-tagged PSA was not successfully purified as a single band through Ni-NTA affinity chromatography, and this recombinant protein

appeared as lightly band at a smaller size on the western blotting (Fig. 5A).

The expected size of the *sfGFP*-PSA fusion protein is 65 kDa, but we observed two bands, one of them at the correct size and the other around 30 kDa (indicating separation product). We confirmed it was *sfGFP* through western blotting using polyclonal anti-GFP. To improve fusion product, we used protease inhibitors before its purification; however, that did not give any significant effect (Fig. 5B).

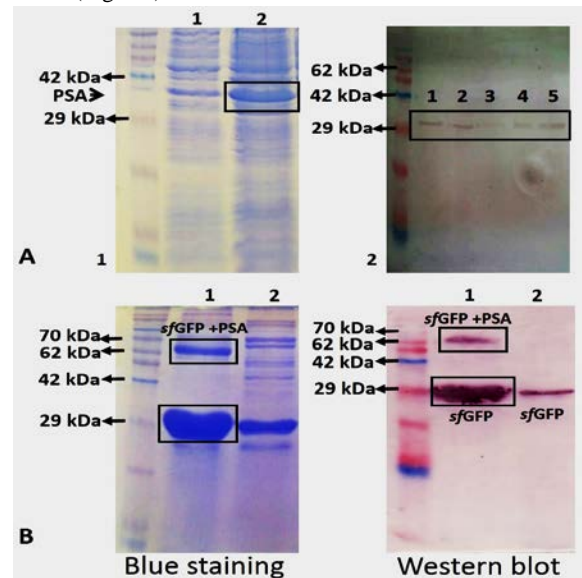


Figure 5. Expression of PSA and *sfGFP*-PSA fusion protein in *E. coli*.

A: **A-1** Detection of PSA expression with a molecular weight of 38 kDa in total cell cytoplasmic extract by SDS-PAGE separation (acrylamide 12 %) and coomassie blue staining. Lane 1: T0 expression; Lane 2: overnight expression. **A-2** Detection of the purified PSA protein, protein samples obtained after different steps purification were analyzed by western blotting, visualized using anti-6 × His tag antibodies. Lane 1: T0 expression; Lane 2: overnight expression; Lane 3: flowthrough sample; Lane 4: wash sample; Lane 5: Pure PSA protein.

B: Detection of the purified *sfGFP*-PSA (65 kDa) was done after SDS-PAGE separation (acrylamide 12 %), either by blue staining or by western blotting using anti-GFP antibodies. Lanes 1: Pure *sfGFP*-PSA fusion protein; Lanes 2: Pure *sfGFP* protein (control). Molecular mass standard (in kDa).

3.4.2. Expression and detection of *sfGFP*-PSA fusion protein in eukaryotic cells:

HEK-293T cells were transfected with pcDNA-*sfGFP*-PSA construct. Evaluation of fusion protein PSA-*sfGFP* expression by fluorescence microscopy at 12, 24, and 48 h after transfection showed that the construct was efficiently expressed in HEK cells. The expression of the *sfGFP*-PSA fusion protein with a molecular weight of 65 kDa was verified in the supernatants medium by western blotting using polyclonal anti-GFP, so that the correct length of the fusion protein has been demonstrated and there was no separation for *sfGFP*-PSA fusion product (Fig. 6).

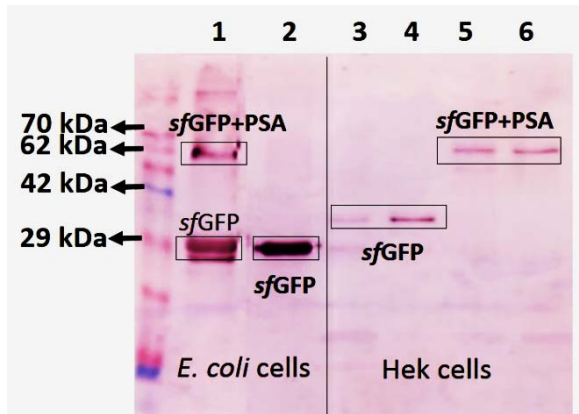


Figure 6. Expression of *sfGFP-PSA* fusion protein in HEK-293T cells.

Detection of *sfGFP-PSA* fusion protein (65 kDa) produced in HEK-293T cells. The Supernatants medium of transfected HEK-293T cells was analyzed by western blotting after 48 h of incubation, *sfGFP-PSA* fusion protein was detected by polyclonal rabbit anti-GFP antibodies. Lane 1: *sfGFP-PSA* fusion protein expressed in bacteria; Lane 2: *sfGFP* protein expressed in bacteria (control); Lanes 3, 4: *sfGFP* protein expressed in HEK-293T cells (control); Lanes 5, 6: *sfGFP-PSA* fusion protein expressed in HEK-293T cells. Molecular mass standard (in kDa).

4. Discussion

It is well-established that *L. major*-secreted molecules are highly immunogenic and can confer protective effects when introduced into experimental subjects (Tonui *et al.*, 2004). Therefore, current efforts are directed towards assessing Leishmanial secreted proteins as future candidates for vaccines and targets for medications. Currently, the success of subunit vaccines based on recombinant proteins or peptides has been variable to poor, and more efforts are needed to reach optimal results (Kumar and Engwerda, 2014). Our data showed that prokaryotic-based systems succeeded in producing the full-length PSA when it was fused with *sfGFP*, which may be significant in the development of PSA-based vaccines.

In the context of developing vaccines based on proteins and peptides, several factors should be considered such as the properties of the proteins of interest, which are largely determined by its amino acid sequence, and the specific post-translational modifications taking place during or after synthesis of the polypeptide chain (Walsh *et al.*, 2005). Some polypeptides such as PSA need to be in their native conformation to maintain its immunogenicity and *Escherichia coli* derived recombinant proteins may not achieve this requirement (Handman *et al.*, 1995; Sjölander *et al.*, 1998a). This problem could be solved by exploitation of the parasites themselves by overexpression of parasitic antigens in transfected nonpathogenic *Leishmania* strains and by the development of a DNA based vaccine (Chamakh-Ayari *et al.*, 2014; Petitdidier *et al.*, 2016; Sjölander *et al.*, 1998b). DNA vaccine is attractive because they ensure appropriate folding of the polypeptide, and it is simple production technology (Alarcon *et al.*, 1999; Handman, 2001; Hasan *et al.*, 1999). Although many alternative organisms and expression systems are also used to produce PSA protein, *E. coli* rests

the least expensive, easiest and quickest (Demain and Vaishnav, 2009). The GFP is commonly used as an excellent expression tag for many fusion protein, and it has been expressed in a variety of organisms, including bacteria, and mammals (Gerdes and Kaether, 1996; Waldo *et al.*, 1999). An increased solubility was observed for several proteins when fused to *sfGFP*, proving the importance of this tag as a mean to improved protein expression, detection, and purification (Andrews *et al.*, 2007). Here, due to the difficulty expressing and purifying PSA protein in *E. coli*, *sfGFP* was fused to PSA. We constructed a recombinant plasmids pRSET-*sfGFP-PSA* and pcDNA-*sfGFP-PSA* that can produce *sfGFP-PSA* fusion protein in *E. coli*, and eukaryotic cells respectively. In *E. coli*, the *sfGFP* separation may have resulted from overexpression of the fusion protein, and we probably need to change the whole expression system or one of its factors (promoter, cell strain, induction period) to decrease the overexpression rate and, therefore, separation. *sfGFP* protein as a fusion partner allowed us to monitor the existence of *sfGFP-PSA* fusion protein through expression and purification steps, as well as verify fusion protein production with the correct molecular weight by western blotting using anti-GFP.

5. Conclusion

In this study, we described an approach to expression of full-length PSA as a fusion protein with *sfGFP*. Our data showed that prokaryotic-based systems succeeded in producing the full-length PSA when it was fused with *sfGFP*; also, the plasmid DNA encoding *sfGFP-PSA* protein was expressed in eukaryotic cells indicating that the designing and cloning of the recombinant construct is correct and applicable. The potential protection by these vaccine candidates against experimental *L. major* infection will be evaluated in animal models.

Acknowledgments

The authors would like to thank Damascus University and the Director General of the Atomic Energy Commission of Syria for their continuous support throughout this work.

References

- Al-Homsi L, Assaad JM and Kweider M. (2012). Construction of pRSET-*sfGFP* Plasmid for Fusion-Protein Expression, Purification and Detection. *Jordan J Biol Sci.* **147**:1-9.
- Alarcon JB, Waive GW and McManus DP. (1999). DNA vaccines: technology and application as anti-parasite and anti-microbial agents. *Adv parasitol.* **42**: 343-410.
- Andrews BT, Schoenfish AR, Roy M, Waldo G and Jennings PA. (2007). The rough energy landscape of superfolder GFP is linked to the chromophore. *J mol biol.* **373**:476-490.
- Bras-Gonçalves R, Petitdidier E, Pagniez J, Veyrier R, Cibrelus P, Cavaleyra M, Maquaire S, Moreaux J and Lemesre J-L. (2014). Identification and characterization of new *Leishmania* promastigote surface antigens, LaPSA-38S and LiPSA-50S, as major immunodominant excreted/secreted components of *L. amazonensis* and *L. infantum*. *Infect Gen Evol.* **24**:1-14.
- Chamakh-Ayari R, Bras-Gonçalves R, Bahi-Jaber N, Petitdidier E, Markikou-Ouni W, Aoun K, Moreno J, Carrillo E, Salotra P

- and Kaushal H. (2014). In vitro evaluation of a soluble Leishmania promastigote surface antigen as a potential vaccine candidate against human leishmaniasis. *PLoS One*. **9**:e92708.
- Champsi J and McMahon-Pratt D. (1988). Membrane glycoprotein M-2 protects against *Leishmania amazonensis* infection. *Infect Imm*. **56**:3272-3279.
- Demain AL and Vaishnav P. (2009). Production of recombinant proteins by microbes and higher organisms. *Biotechnol Adv*. **27**:297-306.
- Devault A and Bañuls A-L. (2008). The promastigote surface antigen gene family of the Leishmania parasite: differential evolution by positive selection and recombination. *BMC Evol Biol*. **8**:292.
- Gerdes H-H and Kaether C. (1996). Green fluorescent protein: applications in cell biology. *FEBS Lett*. **389**:44-47.
- Handman E. (2001). Leishmaniasis: current status of vaccine development. *Clinical microbiology reviews*, **14**:229-243.
- Handman E, Symons FM, Baldwin TM, Curtis JM and Scheerlinck J. (1995). Protective vaccination with promastigote surface antigen 2 from *Leishmania major* is mediated by a Th1 type of immune response. *Infect Imm*. **63**:4261-4267.
- Hasan U, Abai A, Harper D, Wren B and Morrow W. (1999). Nucleic acid immunization: concepts and techniques associated with third generation vaccines. *J Imm methods*. **229**:1-22.
- Holzmueller P, Cavaleyra M, Moreaux J, Kovacic R, Vincendeau P, Papierok G and Lemesre J-L. (2005). Lymphocytes of dogs immunised with purified excreted-secreted antigens of *Leishmania infantum* co-incubated with Leishmania infected macrophages produce IFN gamma resulting in nitric oxide-mediated amastigote apoptosis. *Vet Imm Immunopath*. **106**:247-257.
- Jiménez-Ruiz A, Boceta C, Bonay P, Requena JM and Alonso C. (1998). Cloning, sequencing, and expression of the PSA genes from *Leishmania infantum*. *Euro J Biochem*. **251**:389-397.
- Kedzierski L, Montgomery J, Bullen D, Curtis J, Gardiner E, Jimenez-Ruiz A and Handman E. (2004). A leucine-rich repeat motif of Leishmania parasite surface antigen 2 binds to macrophages through the complement receptor 3. *J Imm*. **172**:4902-4906.
- Kędzierski Ł, Montgomery J, Curtis J and Handman E. (2004). Leucine-rich repeats in host-pathogen interactions. *Arch Immunol Ther Exp*. **52**:104-112.
- Kemp M, Handman E, Kemp K, Ismail A, Mustafa MD, Kordofani AY, Bendtzen K, Kharazmi A and Theander TG. (1998). The Leishmania promastigote surface antigen-2 (PSA-2) is specifically recognised by Th1 cells in humans with naturally acquired immunity to *L. major*. *FEMS Imm Med Microbiol*. **20**:209-218.
- Kumar R and Engwerda C. (2014). Vaccines to prevent leishmaniasis. *Clin trans Imm*. **3**:e13.
- Lemesre J-L, Holzmueller P, Cavaleyra M, Gonçalves RB, Hottin G and Papierok G. (2005). Protection against experimental visceral leishmaniasis infection in dogs immunized with purified excreted secreted antigens of *Leishmania infantum* promastigotes. *Vaccine*. **23**:2825-2840.
- Lincoln LM, Ozaki M, Donelson JE and Beetham JK. (2004). Genetic complementation of Leishmania deficient in PSA (GP46) restores their resistance to lysis by complement. *Molecular & Biochem Parasitol*. **1**:185-189.
- McMahon-Pratt D, Rodriguez D, Rodriguez J, Zhang Y, Manson K, Bergman C, Rivas L, Rodriguez J, Lohman K and Ruddle N. (1993). Recombinant vaccinia viruses expressing GP46/M-2 protect against Leishmania infection. *Infect Imm*. **61**:3351-3359.
- Pedelacq JD, Cabantous S, Tran T, Terwilliger TC and Waldo GS. (2006). Engineering and characterization of a superfolder green fluorescent protein. *Nat Biotechnol*. **24**:79-88.
- Petitdidier E, Pagniez J, Papierok G, Vincendeau P, Lemesre J-L and Bras-Gonçalves R. (2016). Recombinant forms of *Leishmania amazonensis* excreted/secreted promastigote surface antigen (PSA) induce protective immune responses in dogs. *PLoS Neg Trop Diseases*. **10**:e0004614.
- Reithinger R, Dujardin J-C, Louzir H, Pirmez C, Alexander B and Brooker S. (2007). Cutaneous leishmaniasis. *The Lancet infectious diseases*, **7**:581-596.
- Sjölander A, Baldwin TM, Curtis JM, Bengtsson KL and Handman E. (1998a). Vaccination with recombinant Parasite Surface Antigen 2 from *Leishmania major* induces a Th1 type of immune response but does not protect against infection. *Vaccine*. **16**:2077-2084.
- Sjölander A, Baldwin TM, Curtis JM and Handman E. (1998b). Induction of a Th1 immune response and simultaneous lack of activation of a Th2 response are required for generation of immunity to leishmaniasis. *J Imm*. **160**:3949-3957.
- Soto M, Ramírez L, Pineda MA, González VM, Entringer PF, de Oliveira CI, Nascimento IP, Souza AP, Corvo L and Alonso C. (2009). Searching genes encoding Leishmania antigens for diagnosis and protection. *Schol Res Exchange*. **2009**.
- Tonui WK, Mejia JS, Hochberg L, Mbow ML, Ryan JR, Chan AS, Martin SK and Titus RG. (2004). Immunization with *Leishmania major* exogenous antigens protects susceptible BALB/c mice against challenge infection with *L. major*. *Infect Imm*. **72**:5654-5661.
- Von Stebut E. (2015). Leishmaniasis. *JDDG: Journal der Deutschen Dermatologischen Gesellschaft*. **13**:191-201.
- Waldo GS, Standish BM, Berendzen J and Terwilliger TC. (1999). Rapid protein-folding assay using green fluorescent protein. *Nat Biotechnol*. **17**:691.
- Walsh CT, Garneau-Tsodikova S and Gatto Jr GJ. (2005). Protein posttranslational modifications: the chemistry of proteome diversifications. *Angewandte Chemie International Edition*. **44**:7342-7372.

Relevance of Nanoparticles on Micropropagation, Antioxidant Activity and Molecular Characterization of *Sequoia sempervirens* L. Plant.

Iman M. El-Sayed¹, Walaa H. Salama^{2*}, Rasha G. Salim³, Lobna S. Taha¹

¹Department of Ornamental Plants and Woody Trees, Agricultural and Biological Research Division, National Research Centre (NRC), Egypt; ²Department of Molecular Biology, Genetic Engineering and Biotechnology Research Division, National Research Centre (NRC), Egypt; ³Department of Microbial Genetic, Genetic Engineering and Biotechnology Research Division, National Research Centre (NRC), Egypt.

Received: June 21, 2020; Revised: November 2, 2020; Accepted: November 28, 2020

Abstract

Micropropagation is essential in plant biology for the propagation of economic trees, plant improvement, genetic manipulation and bioactive compounds production. In recent years, the nanoparticles application has had successes in the improvement of plant characters, root induction, enhancing secondary metabolites. So, this study aims to examine the effect of three concentrations of Fe, Al, Zn and Ti nano oxides (2.5, 5 and 10 mg/L) on the improvement of growth behavior, pigment content, total phenolic and flavonoid contents, and specific activities of redox enzymes. In addition, to detect the genetic polymorphism between untreated and the best treated *Sequoia sempervirens* L. plant. Murashig and Skoog (MS) media at 75% of the original concentration containing 0.2 mg/L BA were individually fortified with nano Fe, Al, Zn, and Ti oxides, under standard control conditions *in vitro*. Selected morphological characters, total chlorophyll and total phenolic and flavonoid contents of treated explants were determined and compared with the untreated plant (control). The specific activities of peroxidase, catalase and polyphenol oxidase of plant groups were calculated using guaiacol, hydrogen peroxide and catechol as substrates under enzyme assay conditions, respectively. The results showed that the highest shoot number and length were 18.09 and 75.71 mm as well as the greatest root percentage and root number were 55.55% and 3.088 of shootlets treated with 10 mg/L Ti NPs. Whereas, the highest total chlorophyll, total phenolic and flavonoid contents were 220.35 mg/100g F.W, 3.41±0.28 mg GAE/g D.W and 1.67±0.12 mg CE/g D.W, respectively, with 5 mg/L Ti NPs treated shootlets. In addition, the treatment of shootlets with 10 mg/L Fe NPs has significantly increased the activities of the selected enzyme, whereas the maximum specific activity of polyphenol oxidase was 18.60 U/mg with shootlets fortified with 10 mg/L Ti NPs. Moreover, RAPD-PCR indicated that the superlative treatment with Ti NPs (10 mg/L) showed a low similarity comparable with control (74%). Briefly, Ti NPs shows a great enhancement in the morphological behavior of plant and, therefore, a high production *in vivo* in a short time.

Keywords: *Sequoia sempervirens* L., Nanoparticles, antioxidant enzyme, shooting, rooting, polymorphism, RAPD-PCR.

1. Introduction

Sequoia sempervirens L. known as redwood belongs to *Cupressaceae* Family (*Taxodiaceae*) and sets on the California Coast. Yet in addition, it is cultured in the whole world as ornamental plants in many gardens and parks. Many studies are interested in studying *S. sempervirens* L. because of its economic impact importance and on the other hand, for its beauty (Tosta *et al.*, 2012). This species is being considered as an evergreen tree; also, it is the highest tree in the world and its diameter is very large (Farjon *et al.*, 2006).

In vitro culture medium is an effective tool for faster growth and secondary metabolites induction (Khan, 2015 b). The methyl jasmonate (Me-J) and phenyl acetic acid (PAA) were used as elicitors for biosynthesis of many secondary metabolites *in vitro*. (Saeed *et al.*, 2017; Kazmi *et al.*, 2019). Many compounds with medical importance

were extracted from *Sequoia sempervirens* L. Arafat (2018) demonstrated the antitumor effect of the methanol extracts of various parts of Sequoia against colon, breast and lung tumors. Unfortunately, there are few *in vitro* studies on micropropagation of this coniferous tree by application varies sources of the explants (Sul *et al.*, 1998). This may be according to previous studies mentioning that Sequoia is very difficult for formation roots, and its rooting percentage is very weak (Tosta *et al.*, 2012; Sul and Korban, 2005).

Recently, various nanomaterials have been successfully used as new stimulators to improve the growth and characters of commercially important crops and plants as well as to enhance the accumulation and synthesis of the secondary metabolites. Therefore, the elucidation of the mechanism of interaction between plant and nanoparticles has been interesting to identify the activities of plants under control conditions in physiological, biochemical and

* Corresponding author e-mail: walaahsalama82@gmail.com.

molecular levels. (Khan *et al.*, 2019; 2020 and Kumar *et al.*, 2020).

In addition, application of modern agricultural biotechnology such as tissue culture technique can play an important role in improving the propagation of economic and commercial trees such as *S. sempervirens* L. Also, using the micropropagation tool for plants gave the highest production in a short time (Chadipiralla *et al.*, 2020; Shatnawi *et al.*, 2004; Chebet *et al.*, 2003).

Furthermore, to meet the requirements of genetic variation in the horticulture industry, modern molecular techniques have been developed ranging from morphological characterization to different DNA-based markers include randomly amplified polymorphic DNA (RAPD), restriction fragment length polymorphism (RFLP), amplified fragment length polymorphism (AFLP) and simple sequence repeats (SSR) (Ferdousi *et al.*, 2013). For the conservation and utilization of plant genetic resources, the identification and characterization of germplasm is very crucial (Suvakanta *et al.*, 2006). So, molecular marker is a perfect tool to characterize and preserve genetic assets of the plant. Besides, the Molecular characterization helps to determine the breeding behavior of species, individual reproductive success and consequently, the existence of gene flow, the movement of alleles within and between populations of the same or similar species, and its implications (Papa and Gepts, 2003).

In numerous plant species for population studies, genetic linkage mapping, and varieties analysis, RAPD procedure has been broadly used (Rout *et al.*, 2003). The optimization of the RAPD analysis built upon the primers was selected. Though, this technique based on screening of several random sequences of primer to select primers gave positive amplification products. So, this work is implemented to detect the polymorphism between the control and three variable treatments of *Sequoia sempervirens* L. by using RAPD. Thus, this research will contribute basic knowledge in the aspect of their phylogenetic relationships and intra specific diversity.

In previous studies, different materials and methods were used as attempts to improve the induction of rooting formation in *Sequoia sempervirens* L. *in vitro* such as exposure of different laser radiation (red, blue, and green) (Taha *et al.*, 2014), and various growth regulators as (NAA, BAP and Kinetin in the culture medium) (Menegnzi *et al.*, 2019). However, the results showed an improvement in shooting characters of *Sequoia sempervirens* L., but negative results in enhancing root formation (Taha *et al.*, 2014; Menegnzi *et al.*, 2019). Therefore, the application of nanoparticles in MS culture media to understand the interaction between nanoparticles and *Sequoia sempervirens* L. plant gives attention not only to improve the morphological characters and stimulate the secondary metabolites of *Sequoia sempervirens* L. *in vitro* but also to enhance the root formation. So, this is the first attempt for studying the effect of the selected nano oxides (Fe, Al, Ti, Zn) on enhancing the root formation of the valuable *Sequoia sempervirens* L. tree *in vitro*.

This study aims to assess the effectiveness of different concentrations of the selected nano oxides (Fe, Zn, Al and Ti) on shooting and rooting ability, chemical composition, enzymes activities, and detection of the genetic variation of micropropagated *Sequoia sempervirens* L. Plantlets

using *in vitro* culture technique for improving the formation of the roots of healthy quantitatively and qualitatively plants.

2. Materials and Methods

The experimental study was carried out during years 2018 and 2019 on *Sequoia sempervirens* L. at Central laboratories, Tissue Culture Technique Lab, Department of Ornamental Plants and Woody Trees, National Research Centre (NRC), Egypt.

2.1. Plant materials

The explants (stem node) of *Sequoia sempervirens* L. were taken from the adult tree at Orman Garden, Giza, Egypt, washed with liquid soap for 30 min, and then rinsed with running tap water for 1 h. The washed explants were immersed in 70% ethyl alcohol for 30 sec, then exposed to 15% sodium hypochlorite NaOH (Clorox +0.01% Tween 20) for 7 min, and then rinsed with sterile water three times. The explants were then sterilized in 0.1% HgCl₂ solution for 5 min, rinsed three times in sterile water under aseptic conditions.

2.2. Culture medium

The explants were cultured on MS culture medium at 3/4 strength of basal salts. The culture medium added with 0.2 mg/L of 6- benzyladenine (BA) and supplemented with sucrose 25g/L and solidified with 0.7% agar, adjusted to pH 5.7 with HCl and NaOH, then autoclaved at 121°C and 1.2Kg/ cm².

2.3. Culture condition parameters

The *in vitro* cultures were incubated in a growth chamber at 24 ± 1°C under fluorescent lamps with the light intensity of 3k lux at 16 h photoperiods.

2.4. Experiments treatments

The selected nanoparticles (NPs) used in this study were purchased from Sigma Co., USA, and the characterization of the selected NPs was done in Electron Microscope unit, NRC. The NPs were suspended in distilled water and dispersed uniformly according to Zafar *et al.* (2016) method. The MS culture media were grouped and treated separately by four nanoparticles Nano- Ferric Oxide (Fe NPs), Nano-γ-Alumina (Al NPs), Nano-Zinc Oxide (Zn NPs) and Nano-Titanium Oxide (Ti NPs) with varying concentrations (2.5, 5, and 10mg/L) as follow:

S1: Control (3/4 strength of MS +0.2mg/L BA)

S2: Control + Fe NPs 2.5mg/L

S3: Control+ Fe NPs 5 mg/ L

S4: Control+ Fe NPs 10 mg/ L

S5: Control+ Al NPs 2.5 mg/ L

S6: Control+ Al NPs 5 mg/ L

S7: Control+ Al NPs 10 mg/ L

S8: Control+ Zn NPs 2.5 mg/ L

S9: Control+ Zn NPs 5 mg/ L

S10: Control+ Zn NPs 10 mg/ L

S11: Control+ Ti NPs 2.5 mg/ L

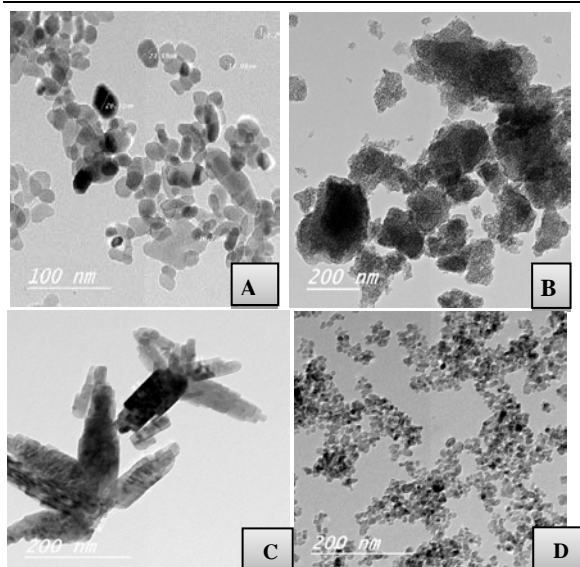
S12: Control+ Ti NPs 5mg/ L

S13: Control+ Ti NPs 10mg/ L

The specification of used nanoparticles is indicated in Table (1) and Figure (1; A, B, C and D).

Table 1. Specification of used nanoparticles.

Specification Test method		
Nano- Iron Oxide		
Phase	Hematite	XRD
Particle size	<50 nm	TEM
Surface area	>50m ² /g	BET (P/Po: up to 0.35)
Nano- γ - Alumina		
Phase	Gamma	XRD
Particle size	<100 nm	TEM
Surface area	>300m ² /g	BET (P/Po: up to 0.35)
Nano- Zinc Oxide		
Phase	ZnO	XRD
Particle size	<30 nm	TEM
Surface area	~20m ² /g	BET (P/Po: up to 0.35)
Nano- Titanium Oxide		
Phase	Anatase	XRD
Particle size	<50 nm	TEM
Surface area	>100m ² /g	BET (P/Po: up to 0.35)

**Figure 1.** Scanning electron microscopy image of nanoparticles; A: Fe oxide NPs; B: Nano- γ -Alumina, C: Zn oxide NPs and D: Ti oxide NPs.

2.4.1. Shooting behavior

After incubation period of the experiment (three months), a number of formed shootlets per explant and Shootlet length (mm) were calculated for each group.

2.4.2. Rooting behavior

Percentage of roots formation (%), Number of roots /shootlet and Root length (mm) were determined for each group.

2.4.3. Hardening off

The number of roots produced, root length, and shoot height were registered after three months. Some of rooted plantlets were removed, washed, and then transferred from the rooting media to plastic pots containing a 1:1:1 ratio of peat, perlite, and clay. Newly potted plantlets were covered with polythene bags for three weeks before being moved to the green house.

2.5. Extraction and analysis

2.5.1. Photosynthetic pigments

The plants were grounded to powder using a mortar and extracting with 85% methanol. After that, the extracts were centrifuged for 10 min at 8000 rpm. The Photosynthetic pigments were assayed for the obtained supernatant according to Saric (1967) protocol using a UV-Visible spectrophotometer (UV-1280, Shimadzu, Japan). The equations and specific absorption in the wavelength are 660, 640, 440 nm to determine chlorophylls a, b and carotenoids, respectively.

2.5.2. Assessment of total phenolic and flavonoid content:

Total phenolic concentration was carried out according to Velioglu *et al.* (1998) using Folin-Ciocalteu reagent and gallic acid as a standard. Total phenols were monitored at 750 nm and the results are expressed as mg gallic acid equivalent (GAE)/ g dry weight tissue. Whereas, the total flavonoid content was calculated using a modified colorimetric method using AlCl₃ according to Zhishen *et al.* (1999) and used catechin as a standard. The absorbance was monitored at 510 nm and the results expressed as mg catechin equivalent (CE)/ g dry weight tissue.

2.5.3. Enzymatic assays

2.5.3.1. Peroxidase enzyme:

Peroxidase activities of the prepared plant extracts were carried out according to Miranda *et al.* (1995). The reaction mixture of 8 mM H₂O₂, 40 mM guaiacol and 0.1 ml crude extract to a final volume of 1 ml of 20 mM sodium acetate buffer, pH 5.5. The adjustment in absorbance at 470 nm was recorded for 1 min. One unit of peroxidase activity was defined as the enzyme concentration which increases the absorbance 1.0 per min under standard assay conditions and the specific activity is considered as units/mg protein.

2.5.3.2. Catalase enzyme:

The specific activity of catalase was determined according to Aebi (1974) using H₂O₂ as a substrate. The decrease in absorbance at 240 nm was recorded for 1 min and one unit of enzyme activity was defined as the enzyme concentration that hydrolyzes 1 μ m of H₂O₂ per min under standard assay conditions. The specific activity is considered as units/mg protein.

2.5.3.3. Polyphenol oxidase enzyme:

The activity of polyphenol oxidase was assayed using catechol as a substrate according to Concellon *et al.* (2004). The increase in absorbance at 410 nm is recorded for 3 min. One unit of enzyme activity is defined as the enzyme concentration that causes a change of 0.1 in absorbance per min under standard assay conditions. The specific activity is considered as units/mg protein.

2.6. Extraction of genomic DNA.

Extraction of genomic DNA using DN easy plant mini kit (Qiagen Sciences, Maryland, USA) was carried out according to the manufacturer's instruction manual.

2.7. DNA fingerprinting

DNA fingerprinting was performed using ten RAPD-PCR primers to detect the polymorphism of three samples of *Sequoia sempervirens* L., these primers were synthesized by Metabion Corp., Germany. The sequences

of primers are showed in table (2). Reactions were performed in 25 µl assay mixture composed of 1x reaction buffer, 0.2 mM of dNTPs, 1.5 mM MgCl₂, 0.2 µM of primer, 0.5 unit of *Taq* polymerase (Qiagen Ltd., Germany) and 50 ng of template DNA in sterile dist. water.

2.7.1. Amplification of RAPD-PCR

PCR amplification of the DNA was carried out using Perkin Elmer thermal cycler 9700. The temperature profile in the different cycles describes as follow: an initial strand separation cycle at 94°C for 5 min followed by 40 cycles comprised of a denaturation step at 94°C for 1min, an annealing step at 36°C for 1 min and an extension step at 72°C for 1.5 min, finally, the termination cycle for 10 min at 72°C. The PCR products were mixed with 5 µl of loading dye and resolved in 1.5 % agarose gel containing 0.5 mg/ml ethidium bromide in 1x TBE buffer at 100 volts using vertical gel electrophoresis apparatus. The resolved bands were visualized under TMXR+ Gel Documentation System (Bio-Rad).

2.7.2. Data analysis

For determination of genetic relationships between control and three selected treatment groups, the RAPD-PCR bands patterns were analyzed and compared with control group. The distinct and clear PCR products were scored as 1 for presence and 0 for the absence of bands. Bands of the same mobility have an identical score. The genetic similarity coefficient between control and the treatment groups were calculated according to Dice coefficient PAST program.

Table 2. RAPD primers name and sequence.

Primer name	Sequence (5'-3')
OPA-09	GGGTAACGCC
OPA-11	CAATCGCCGT
OPA-13	CAGCACCCAC
OPA-18	AGGTGACCGT
OPB-10	CTGCTGGGAC
OPB-11	GTAGACCCGT
OPB-12	CCTTGACGCA
OPB-15	GGAGGGTGTT
OPB-18	CCACAGCAGT
OPC-01	TTCGAGCCAG

2.8. Statistical analysis

The data were analyzed using a randomized complete design with three replicates per each treatment and were conducted using COSTATV-63 (Duncan, 1955); one way ANOVA (analysis of variance) was used to calculate the significance by new multiple range tests at $p < 0.05$.

3. Results and Discussion

3.1. In vitro growth behavior

Micropropagation is one of the main advantages of use nanoparticles in agricultural biotechnology. Shooting and rooting characters that represent the *in vitro* growth behavior as a result of the application of four nanoparticles (Fe, Al, Zn and Ti oxides) at different concentrations (2.5, 5 and 10 mg/L) on *Sequoia sempervirens* L. were detected as shown in Table (3) and Figure 2. Shoot and root parameters include number and length of shootlets, rooting percentage, number and length of roots per shoot of untreated and treated groups were observed, calculated and compared with the control group (untreated explants in MS culture medium). Overall, number and length of shoots and roots of treated groups with different nanoparticles treatments were increased as compared to untreated group. Significantly, the highest values of shoot number and length were observed on shootlets that MS culture medium supplemented with Ti oxide NPs at concentration of 10 mg/L (18.09 and 75.71mm respectively) as compared to other treatments and control groups, whereas the minimum value of shoot number and length was observed in MS culture medium added with Zn oxide NPs at 5 mg/L (11.33 and 45.00 mm respectively). The same trend was observed for rooting behavior. Similarly, the highest rooting percentage and root number were recorded in the shootlets treated with Ti oxide NPs at 10 mg/L by (55.55% and 3.08) comparing with control and treated groups, while the longest root length was recorded on the shootlets treated with Al oxide NPs at 10 mg/L by 123.75 mm. In contrast, non-rooting was noticed in both untreated shootlets and medium treated with 2.5 and 5 mg/L of Zn oxide NPs.

These findings were confirmed by Zheng *et al.* (2005) who reported that Ti NPs increased germination and growth of spinach plant. Similarly, Albersheim *et al.* (2011) demonstrated that Ti NPs enhanced root and shoot length in the wheat seedling. These might be attributed to the small size of Ti NPs which help in increasing the ability to penetrate the seed and stimulate fast germination and growth of the plant. Furthermore, TiO₂ NPs was shown affectivity in the stimulation of gene expression of photosynthetic content, plant hormones metabolism and nitrogen metabolism (Yang *et al.*, 2006; Albrecht *et al.*, 2006) and these biosynthesis pathways might promote cell division, growth of plant and differentiation of plant cells (Song *et al.*, 2013; Frazier *et al.*, 2014). In other studies, Owje *et al.* (2019) improved the formation of roots of Fenugreek *in vitro* using Al NPs in the culture medium. Also, Zia *et al.* (2020) enhanced rooting reaction, number of roots/plant and root length in carnation cultivars by Ag NPs *in vitro*. Additionally, the application of Fe oxide NPs improved shoot and root growth parameters of *Moringa oleifera*, *Antigonon leptopus* and *stivia rebaudiana* plants (El-Sayed *et al.*, 2019; El-Ziat *et al.*, 2020; Khan *et al.*, 2020). On the other hand, Desai *et al.* (2015) demonstrated that using Zn NPs reduced the morphological parameters of *Stevioside rebaudiana* plant *in vitro*.

Table 3. Effect of varied concentrations of four nanoparticles on *in vitro* shooting and rooting ability of *Sequoia sempervirens* L. plant.

Treatments	Shoot number	Shoot length mm	Root %	Root number	Root length mm
S1:Control ((3/4 strength of MS +0.2mg/L BA)	10.01 e	43.77 h	---	---	---
S2:Control+ Fe NPs 2.5 mg/L	12.00de	48.00 g	16.60 d	0.50 d	50.00 e
S3:Control+ Fe NPs 5 mg/L	12.90 cd	68.00 cd	33.33 c	1.50 c	122.00 a
S4::Control+ Fe NPs 10 mg/L	11.60 de	66.25 d	33.33 c	2.00 bc	70.50 d
S5:Control + Al NPs 2.5 mg/L	15.30 b	68.70 c	49.95 b	3.00 a	120.00 a
S6:Control + Al NPs 5 mg/L	10.19 e	60.36 f	16.65 d	0.60 d	50.00 e
S7:Control+ Al NPs 10 mg/L	13.50 b-d	63.66 e	49.95 b	2.06 bc	123.75 a
S8:Control+ Zn NPs 2.5 mg/L	12.00 de	47.33 g	---	---	---
S9:Control+ Zn NPs 5 mg/L	11.33 de	45.00 h	---	---	---
S10:Control + Zn NPs 10 mg/L	11.50 de	68.66 e	16.65 d	0.70 d	70.50 d
S11:Control+ Ti NPs 2.5 mg/L	11.88 de	61.66 ef	33.33 c	2.00 bc	80.33 c
S12:Control+ Ti NPs 5 mg/L	14.55 bc	71.25 b	33.33 c	1.50 c	118.33 a
S13:Control + Ti NPs 10 mg/L	18.09 a	75.71 a	55.55 a	3.08 a	110.66 b

Averages (means) having the same letter(s) within the same column are not significantly different according Duncan's multiple range tests at 5% level of probability.

3.2. Hardening off

Rooted plantlets of *Sequoia sempervirens* L. obtained from *in vitro* culture media supplemented with different

concentration of Fe, Al, and Ti NPs were acclimatized and transferred to the greenhouse in the peat: perlite: clay (1:1:1 v/v/v) as shown in Figure 2.

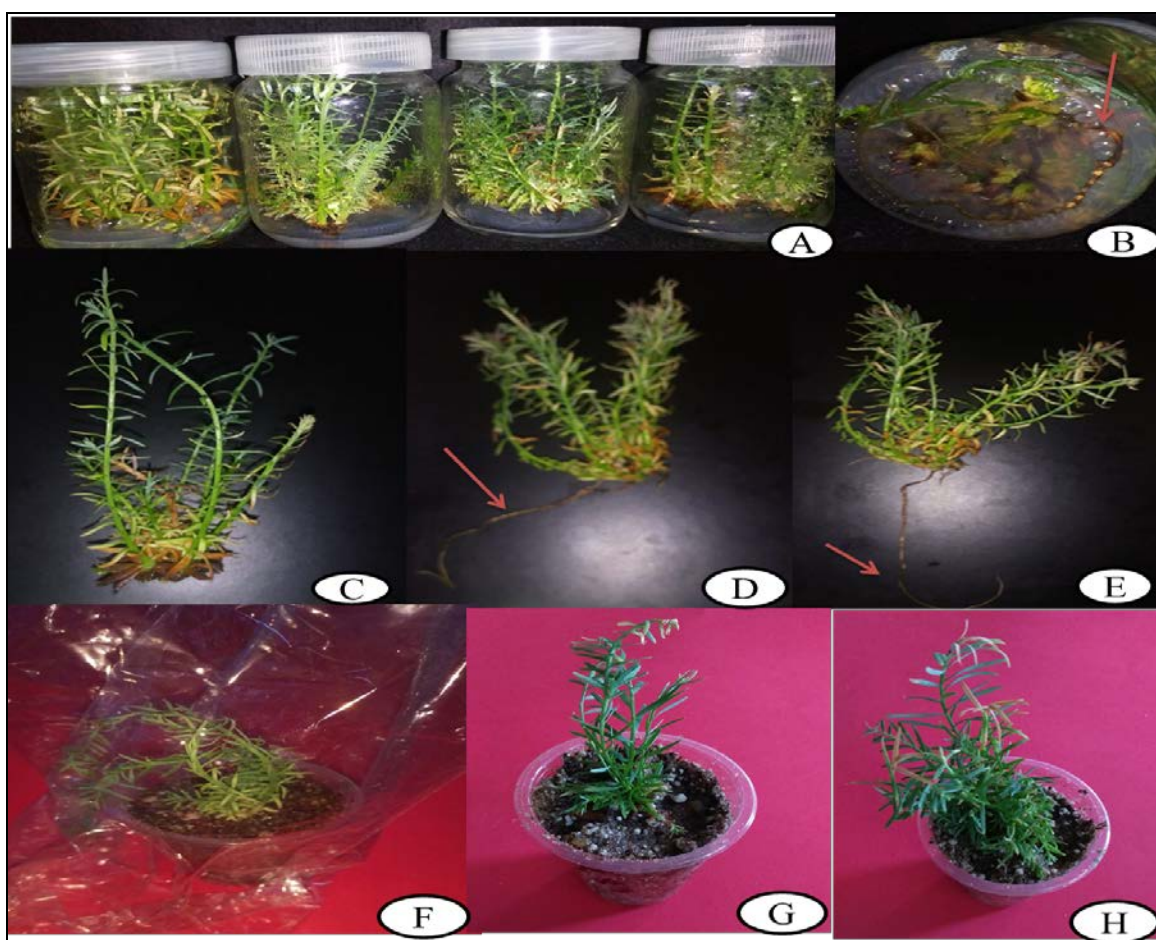


Figure 2. In vitro growth behavior; A: Shoot proliferation and rooting induction *in vitro* with application of 10mg/L Ti NPs, B: non-rooting plantlets (control), C: rooting on plantlets treated with Al NPs 10 mg/L and Ti NPs 10 mg/L, D,E: Prepared plantlets to hardening off stage and F to H: Acclimatization plants to greenhouse.

3.3. Photosynthetic pigments

The influence of different concentrations of nanoparticles (2.5, 5 and 10 ppm) on both chlorophylls and carotenoids contents of treated shootlets were determined and compared with untreated (control). The results in

Table (4) showed an increase in chlorophyll a, b, total chlorophylls and carotenoids contents in shootlets that were cultured on MS media supplemented with the various nanoparticles treatments. The highest contents of chlorophylls a, b, total chlorophyll and carotenoids were noticed with 5 mg/L Ti NPs (150.88, 69.37, 220.35 and

98.69mg/100g F.W., respectively). Whereas, the lowest contents of chlorophyll a, b, total chlorophyll and carotenoids were recorded with the addition of 2.5 mg/L Zn NPs (43.55, 19.38, 61.93 and 44.44 mg/100g F.W., respectively). It could be concluded that supplementation of Ti NPs in the culture medium was stimulated the accumulation of chlorophyll content in *Sequoia sempervirens* L. comparing with untreated (control) and other treatments.

These results are in agreement with Duhan *et al.* (2017) who reported that Fe and Zn NPs increased the leaf photosynthetic pigments and photosynthesis characters. In addition, El-Mahdy and Elazab (2020) demonstrated that using 1 and 2.5mg/L of Zn-NPs in culture medium increased chlorophyll a and b contents. This might be due to the presence of zinc and iron in both catalytic sites of many enzymes and structure of proteins and pigments that induced photosynthesis activity (Rout and Sahoo, 2015; Mohammadi *et al.*, 2018).

Table 4. Effect of different concentrations of nanoparticles on photosynthetic pigments of *Sequoia sempervirens* L.

Pigment (mg/100g F.W.)	Chlorophyll a mg /100 g F.W.	Chlorophyll b mg/100 g F.W.	Total chlorophyll mg/100 g F.W.	Carotenoids mg/100 g F.W.
Treatments				
S1:Control l(3/4 strength of MS+0.2 mg/L)	40.78 e	19.22 h	59.0 k	42.33 l
S2:Control + Fe NPs 2.5 mg/L	45.99 de	20.63 gh	66.62 j	45.63 jk
S3:Control + Fe NPs 5 mg/ L	49.29 de	22.17 fg	71.46 i	49.55 i
S4:Control + Fe NPs 10 mg/ L	72.37 c	29.89 e	100.88 f	62.2 f
S5:Control + Al NPs 2.5 mg/ L	57.22 d	24.17 f	81.39 h	52.98 g
S6:Control + Al NPs 5 mg/ L	46.56 de	21.22 gh	67.78 ij	47.06 j
S7:Control + Al NPs 10 mg / L	88.57 b	38.79 d	127.03 d	66.1 d
S8:Control + Zn NPs 2.5 mg/ L	43.55 de	19.38 h	61.93 k	44.44 k
S9:Control + Zn NPs 5 mg / L	70.37 c	27.71 e	94.08 g	55.98 g
S10:Control + Zn NPs 10 mg / L	137.05 a	62.93 c	192.98 c	86.92 c
S11:Control + Ti NPs 2.5 mg/ L	83.44 bc	37.93 d	120.37 e	64.33 e
S12:Control + Ti NPs 5 mg / L	150.88 a	69.37 a	220.35 a	98.69 a
S13:Control + Ti NPs 10 mg / L	139.09 a	66.45 b	203.54 b	91.92 b

Average (means) having the same letter(s) within the same column are not significantly different according Duncan's multiple range tests at 5% level of probability.

3.4. Total Phenolic and flavonoid content

Data in Table (5) indicated the influence of individual supplementation of the selected nano oxides at different concentrations in culture media on the contents of total phenolics and flavonoid compounds of shootlets. The highest contents of phenolic and flavonoid compounds were 3.41 mg GAC/g tissue and 1.67 mg CE/g tissue of shootlets treated with Ti oxide NPs at 5 mg/ L, respectively. On the other hand, the minimal phenolic and flavonoid contents of shootlet were 1.05 mg GAC/g and 0.52 mg CE/g tissue estimated in shootlets treated with 2.5 mg/ L of Fe NPs treated group compared to other treatments and control groups, respectively. In addition, the increasing of concentrations of Zn NPs showed a gradual increase in the contents of total phenolic and flavonoid of treated shootlets compared with untreated explant. Whereas, the total phenolic and flavonoid contents were increased to 2.14 mg GAC/ g tissue and 0.95 mg CE/ g tissue with the treatment of Al NPs at 10 mg/ L compared with the other concentrations of Al NPs treatments and control. The total phenolic and flavonoid contents were significantly increased with zinc oxides nanoparticles treatments. This may be due to the ability of zinc to induce and accumulate secondary metabolites production (Javed *et al.*, 2017)

These findings agreed with Raei *et al.* (2014) who reported that the maximum production of aloin was found when *Aloe vera* plant was treated with titanium oxide nanoparticles. Similarity, Al-oubaidi and Kasid (2015) showed that *Cicer arietinum* contents of gallic,

chlorogenic, o-coumaric, tannic and cinnamic acids were increased when MS medium was augmented with TiO₂ NPs (4.5-6.0 mg/ L). Another study by Poborilova *et al.* (2013) reported that using Al₂O₃ NPs (0-100 gm/ L) in MS culture medium was increased the phenolic contents of tobacco plant. Similarly, Owje *et al.* (2019) indicated that supplementation of Al NPs in the culture medium increased lignin content of fenugreek plant. Also, addition of Ag NPs and Au NPs in culture medium resulted in high accumulation of phenolics and flavonoid contents of *prunella vulgars* L. plant (Fazal *et al.* 2016). Recently, Khan *et al.* (2020) noticed that fortification of high and low levels of Fe NPs increased total phenolics and flavonoids contents as well as increased accumulation of stevioside and rebaudioside of *Stavia rebaudiana* plant. Interestingly, we noticed a good correlation between these findings with shooting and rooting proliferation results and biochemical assays that were determined in this study. Thus, secondary metabolites accumulation and production are necessary to stimulate photosynthesis activity and increase the level of flavonoids, phenolics and tannins and to enhance the carrying of carbohydrate to different parts inside the plants (Ghasemzadeh *et al.*, 2011; Khan *et al.*, 2020).

Table 5. Effect of different concentrations of selected nanoparticles on the contents of total phenolics (mg GAE/g tissue) and total flavonoids (mg CE /g tissue) of *Sequoia sempervirens* L.

Treatments	Contents	Total phenolics (mg GAE/ g tissue)	Total flavonoids (mg CE/ g tissue)
S1:Control ((3/4 strength of MS +0.2mg/ L BA)		1.43±0.12 g	0.79±0.05 f
S2:Control + Fe NPs 2.5 mg/ L		1.05±0.09 h	0.52±0.04 j
S3:Control + Fe NPs 5 mg/ L		1.41±0.12 g	0.68±0.05 hi
S4:Control + Fe NPs 10 mg/ L		1.78±0.15 e	0.85±0.07 e
S5:Control + Al NPs 2.5 mg/ L		1.65±0.14 f	0.79±0.06 f
S6:Control + Al NPs 5 mg/ L		1.05±0.095 h	0.65±0.04 i
S7:Control + Al NPs 10 mg/ L		2.14±0.18 b	0.95±0.08 c
S8:Control + Zn NPs 2.5 mg/ L		1.41±0.11g	0.72±0.06 gh
S9:Control + Zn NPs 5 mg/ L		1.63±0.13 f	0.74±0.05 fg
S10:Control + Zn NPs 10 mg/ L		2.03±0.16 c	0.91±0.08 cd
S11:Control + Ti NPs 2.5 mg/ L		1.88±0.16 d	0.89±0.07 de
S12:Control + Ti NPs 5 mg/ L		3.41±0.28 a	1.67±0.12 a
S13:Control + Ti NPs 10 mg/ L		2.19±0.18 b	1.01±0.09 b

Data are mean of three replicate ± SD at $P \geq 0.01$. Means having the same letter(s) within the same column are not significantly different according Duncan's multiple range tests 5% level of probability.

3.5. Enzyme activity

The impact of different nanoparticles at 2.5, 5 and 10 mg/ L separately in MS culture media on the enzymatic activities of oxidoreductase enzymes such as peroxidase, catalase and polyphenol oxidase of *Sequoia sempervirens* L. shootlets was determined and described in Table (6). The application of different NPs was enhanced activities of tested enzymes compared with untreated explants. In addition, increasing the concentrations of these NPs was shown a dose-dependent increase in the activities of these enzymes. The treatment of explants with 10 mg L⁻¹ of Fe NPs has significantly increased the activities of peroxidase, catalase and polyphenol oxidase to 51.60, 54.60 and 17.50 U/mg compared with other treatments and untreated explant. Whereas, the highest specific peroxidase activity was 70.50 U/mg for shootlets treated with 10 mg/L of Zn NPs comparable with other NPs and control explants. Similarly, the maximum activity of polyphenol oxidase was 18.60 U/mg for the group treated with 10 mg/L Ti NP comparable with control and other treated explants groups.

In agreement with our results, Lu *et al.* (2002) noticed the enhancement of antioxidant activity and nitrate reductase activity in soybean plant supplemented with TiO₂ NP during germination and growth. Similarly, Mathpal *et al.* (2015) observed the increase of activity of enzyme by using Zn NP, and attributed that to the role of Zn in the stimulation of enzymes incorporated in carbohydrate and protein metabolism of plant. Many researchers suggested that Zn and Fe NPs are playing the fundamental key of induction of different oxido-reductase enzymes which are responsible for phytohormone building, absorption of nutrients and metabolic biosynthesis (Dhir *et al.*, 2011). Additionally, Owje *et al.* (2019) showed that using Al NPs increase the CAT activity of Fenugreek plant., and Khan *et al.* (2020)

reported that applied Fe NPs at (90 µg/ L) increase the enzymatic activities of antioxidant enzymes (SOD, POD, and CAT) on *Stavia rebaudiana* plant.

Table 6. Effect of different concentration s of nanoparticles on activities of enzymes of *Sequoia sempervirens* L.

Treatments	Determinations (U/mg)	Peroxidase (U/mg)	Catalase (U/mg)	Polyphenol oxidase (U/mg)
S1:Control ((3/4 strength of MS +0.2mg/ L BA)		12.70	14.00	5.030
S2:Control + Fe NPs 2.5 mg/ L		13.10	17.30	5.30
S3:Control + Fe NPs 5 mg/ L		18.30	33.40	9.20
S4:Control + Fe NPs 10 mg/ L		51.60	54.60	17.50
S5:Control +Al NPs 2.5 mg/ L		13.00	17.30	6.40
S6:Control +Al NPs 5 mg/ L		13.70	24.40	7.50
S7:Control + Al NPs 10 mg/ L		16.30	32.60	10.90
S8:Control + Zn NPs 2.5 mg/ L		14.30	24.00	5.50
S9:Control + Zn NPs 5 mg/ L		22.40	18.30	7.30
S10:Control + Zn NPs 10 mg/ L		70.50	16.80	16.00
S11:Control + Ti NPs 2.5 mg/ L		22.10	19.60	6.70
S12:Control + Ti NPs 5 mg/ L		39.50	21.80	17.60
S13:Control + Ti NPs 10 mg/ L		29.70	41.70	18.60

3.6. DNA fingerprinting using RAPD-PCR

To study the genetic difference between the treatments lines (Fe NPs 10mg/L, Al NPs 10mg/ L, and Ti NPs 10mg/ L and control), ten selected RAPD primers were used. RAPD-PCR analysis offers the advantages of simplicity and rapidly conferred by the PCR product procedure to confirm the treatment lines 6 out of ten primers produced reproducible PCR products with a clear pattern for each line and showing easily scrabble RAPD profiles and informative as shown in Figure 3. The total bands were detected among the treatment lines and control (Table7). Only 23 of 52 total bands were polymorphic markers, and these primers produced multiple band profiles with a number of amplified DNA fragments varying from 4 to 13. The highest number of bands (13 bands) was generated by using the primer OPB-12, while the lowest was 4 bands and generated with primer OPC-01. Control and treatment lines gave distinct DNA fingerprint patterns. A dendrogram was constructed based on the RAPD-PCR data analysis as shown in Table (8) and Figure 4. The data also showed that the closest relationship between control and treatment Al NPs 10mg/ L was 89% and the low similarity with Ti NPs at 10mg/ L was 74%. This technique permits the characterization and detection of the diversity and identity between treated plantlets evaluated in this study. This application seems to be useful for organization and differentiation between the different treatments of Sequoia that may provide useful information on the level of polymorphism and diversity in Sequoia plantlets. These results would be useful for better management and differentiation of new clones. Toral *et al.* (2009) also used RAPD-PCR to analyze the genotype identification and gene diversity for *Sequoia sempervirens* L. (D. Don) Endl. in Chile and concluded that the variation of RAPD marker is powerful in identifying genetic relationships between Sequoia clones, so in the future, the presence of more clones in the RAPD analysis and molecular data complementation with other techniques will improve the resolution of genetic relationships and the

potential use in *Sequoia* plantations in Chile. Correspondingly, Parsad (2014) established that RAPD technique is reliable and promising for the characterization of the *Hibiscus germplasm*. Thus, these RAPD markers show a capability for characterization and identification genetic diversity within the varieties in a species. This may

also help in *Hibiscus* breeding system and conservation biology of these plants. In addition, Rafi *et al.* (2012) used RAPD-PCR to detect the association and the genetic variation between the geographical origin of 48 accessions of physic nut, *Jatropha curcas* L.

Table 7. The statistical analysis of RAPD-PCR primers used in this study

Similarity matrix between control and three treatment of <i>Sequoia sempervirens</i> L.				
Name	Control	Fe NPs 10 mg/l	Al NPs 10 mg/l	Ti NPs 10 mg/l
Control	100			
Fe NPs 10 mg/l	80	100		
Al NPs 10 mg/l	89	81	100	
Ti NPs 10 mg/l	74	75	70	100

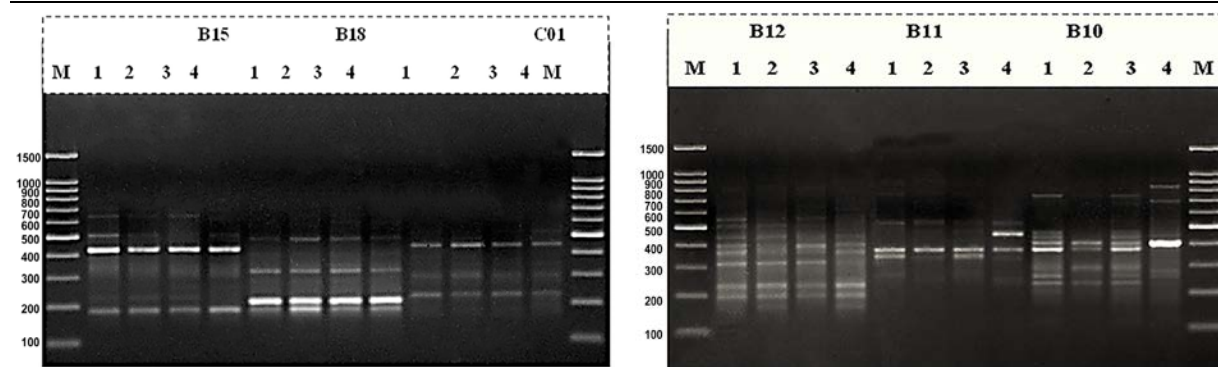


Figure 3. The PCR amplification profile of RAPD-PCR primers for the control and three treatment (Lane 1-4); **1:** Control, **2:** Fe NPs 10mg L⁻¹, **3:** Al NPs10 mg L⁻¹, **4:** Ti NPs 10 mg L⁻¹ and **M:** 100 bp DNA ladder.

Table 8. The Similarity matrix based on analysis of RAPD-PCR of control and three treatments of *Sequoia sempervirens* L.

No	Name of primer	Monomorphic bands	Polymorphic bands	Number of Unique bands	Total bands	Polymorphism (%)	MW range (bp)	Mean of frequency
1	OPB-10	5	7	0	12	58	148-810	0.7
2	OPB-11	4	5	1	10	60	206-901	0.7
3	OPB-12	1	8	4	13	92	117-862	0.6
4	OPB-15	4	2	0	6	33	188-642	0.9
5	OPB-18	5	1	1	7	29	188-556	0.8
6	OPC-01	3	0	1	4	25	227-488	0.8
Total		22	23	7	52			4.5
Average		3.66	3.83	1.16	8.6	49.5		0.75

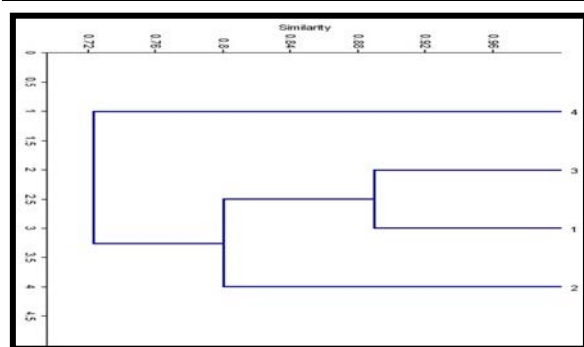


Figure 4. Dendrogram demonstrating the relationships between the control and treatments based on RAPD-PCR analysis. The numbers from 1 to 4 represent the following groups; **1:** Control, **2:** Fe NPs 10mg/l, **3:** Al NPs 10 mg/l, **4:** Ti NPs 10 mg/l.

4. Conclusion

Briefly, these findings demonstrated the benefits of using nanoparticles as an external elicitor to *Sequoia sempervirens* L. plant, and showed the high capability of Ti NPs compared with Fe, Zn and AL NPs for stimulation the shooting and rooting behavior includes shoot number, shoot length, root percentage, and root number, in addition, enhancement the content of photosynthetic pigments and secondary metabolites with increasing the activities of peroxidase, catalase and polyphenol oxidase enzymes. Additionally, RAPD-PCR is a good tool to study the genetic diversity between the control and the significant treatment Ti NPs 10 mg/L for shooting and rooting behavior. This will help in increasing the propagation of this economic tree and wide production of this valuable plant (growth), which will lead to an increase in the economic income.

Acknowledgements

The authors sincerely acknowledge the National Research Centre, Egypt, for financial support. (Grant number; 1103052).

Declaration of interest: None

References

- Aebi H. 1974. **Catalase: Methods of enzymatic analysis.** In: Bergmeyer, H.U. New York, San Francisco, London: Verlag Chemie Weinheim/Academic Press, pp. 673–684.
- Albersheim P. 2011. **Plant Cell Walls: From Chemistry to Biology**, New York, USA, Garland Science.
- Albrecht MA, Evans CW and Raston CL. 2006. Green chemistry and the health implications of nanoparticles. *Green Chem.* **8**: 417–432.
- Al-oubaidi HKM and Kasid NM. 2015. Increasing phenolic and flavonoids compounds of *Cicer arietinum* L. from embryo explant using titanium dioxide nanoparticle in vitro. *World J Pharm Res.* **4**: 1791–1799.
- Arafat MA M. 2018. Comparative pharmacognostical study and tissue culture of *Sequoia sempervirens* (D. Don Endl) and *Taxodium distichum* (L. Rich) cultivated in Egypt. MSc dissertation, Cairo University, Cairo, Egypt.
- Chadipiralla K, Gayathri P, Rajani V and Reddy PVB. 2020. **Plant tissue culture and crop improvement, Sustainable Agriculture in the Era of Climate Change**, Springer, Cham, pp. 391-412.
- Chebet DK, Okeno JA and Mathenge P. 2003. Biotechnological approaches to improve horticultural crop production. *Acta Hort.* **625**: 473-7.
- Concellon A, Anon MC and Chaves AR. 2004. Characterization and changes in polyphenol oxidase from eggplant fruit (*Solanum elaeagnifolium* L.) during storage at low temperature. *Food Chem.* **88**: 17-24.
- Desai CV, Desai HB, Suthar KP, Singh D, Patel RM and Taslim A. 2015. Phytotoxicity of zinc nanoparticles and its influence on steviol glycoside production in *Stevia rebaudiana* Bertoni. *Appl. Biol. Res.* **17**: 1-7.
- Dhir B, Sharmila P, Pardha SP, Sharma S, Kumar R and Mehta D. 2011. Heavy metal induced physiological alterations in *Salvinia natans*. *Ecotoxicol Environ Saf.* **74**(6):1678–1684.
- Duhan JS, Kumar R, Kumar N, Kaur P, Nehra K and Duhan S. 2017. Nanotechnology: the new perspective in precision agriculture. *Biotechnol Rep.* **15**(2):11-23.
- Duncan DB, 1955. Multiple range and multiple F-tests. *Biometrics.* **11**(1):1-42.
- El-Mahdy MT. and Elazab DS. 2020. Impact of zinc oxide nanoparticles on pomegranate growth under *in vitro* conditions. *Russ J Plant Physiol.* **67**(1): 162-167.
- El-Sayed IM, Taha LS, Mazhar AM and Kandil MM. 2019. Iron oxide nanoparticles role in micropropagation of *Moringa oleifera* L. under salinity stress. *Middle East J.* **8**(4): 1123-1132.
- El-Zaiat RA, El-sayed IM, Taha LS, Ibrahim EA. 2020. Enzyme activity of micropropagated *Antigonon leptopus* plant under effect of salinity stress. *Plant Arch.* **20**: 3599-3605.
- Farjon, A. and members of the Conifer Specialist Group. 2006. *Sequoia sempervirens*. In: IUCN 2006. 2006 IUCN Red List of Threatened Species. www.iucnredlist.org
- Fazal H, Abbasi BH, Ahmad N and Ali M. 2016. Elicitation of medicinally important antioxidant secondary metabolites with silver and gold nanoparticles in callus cultures of *Prunella vulgaris* L. *App biochem biotechnol.* **180**(6): 1076-1092.
- Ferdousi B, Aminul Islam AKM, GolamRasul M, KhalequeMian MA and Hossain M. 2013. Morphological diversity of eggplant (*Solanum melongena*) in Bangladesh. *Emir. J. Food Agric.* **25**(1): 45-51.
- Frazier TP, Burklew CE and Zhang B. 2014. Titanium dioxide nanoparticles affect the growth and microRNA expression of tobacco *Nicotiana tabacum*. *Funct integr. Genomics.* **14**:75-83.
- Ghasemzadeh A and Jaafar HZE. 2011. Effect of CO2 enrichment on synthesis of some primary and secondary metabolites in ginger (*Zingiber officinale* Roscoe). *Int J Mol Sci.* **12**(2): 1101–1114.
- Javed R, Usman M, Yücesan B, Zia M and Gürel E. 2017. Effect of zinc oxide (ZnO) nanoparticles on physiology and steviol glycosides production in micropropagated shoots of *Stevia rebaudiana* Bertoni. *Plant Physiol Biochem.* **110**:94–99.
- Kazmi A, AliKhan M, Mohammad S, Ali A, Kamil A and Ali H. 2019. Elicitation directed growth and production of steviol glycosides in the adventitious roots of *Stevia rebaudiana* Bertoni. *Ind. Crops Prod.* **139**(1):111530.
- Khan MA, Ali A, Mohammad S, Ali H, Khan T, Jan A, and Ahmad P. 2020. Iron nano modulated growth and biosynthesis of steviol glycosides in *Stevia rebaudiana*. *Plant Cell, Tissue Organ Cult. (PCTOC).* **143**(1): 121-130.
- Khan MA, Khan T Mashwani Z and Riaz MS. 2019. Plant cell nanomaterials interaction: growth, physiology and secondary metabolism. *Compr Anal Chem.* **84**: 23-54.
- Khan MA, Abbasi B H, Shah N A, Yu'cesan B, Ali H. 2015. Analysis of metabolic variations throughout growth and development of adventitious roots in *Silybum marianum* L. (Milk thistle), a medicinal plant. *Plant Cell, Tissue Organ Cult. (PCTOC).* **123**: 501–510.
- Kumar G, Srivastava A and Singh R. 2020. Impact of nanoparticles on genetic integrity of Buckwheat (*Fagopyrum esculentum* Moench). *Jordan J of Biol Sci.* **13**(1): 17-20.
- Lu CM, Zhang CY, Wen JQ, Wu GR and Tao MX. 2002. Research of the effect of nanometer on germination and growth enhancement of Glycine max and its mechanism. *Soybean Science.* **21**(3):168-172.
- Mathpal B, Srivastava PC, Shankhdhar D and Shankhdhar SC. 2015. Improving key enzyme activities and quality of rice under various methods of zinc application. *Physiol. Mol. Biol. Plants,* **21**(4): 567–572.
- Meneguzzi A, Konzen ER, Navroski MC, Camargo SS, Pereira M, Rufato L and Lovatel QC. 2019. Shoot multiplication of two *Sequoia sempervirens* genotypes with addition of small concentrations of kinetin. *Brazil. J. Forest Res.* **39**: 1-8.
- Miranda MV, Lahore HF and Cascone O. 1995. Horseradish peroxidase extraction and purification by aqueous two-phase partition. *Appl. Biochem. Biotechnol.* **53**: 147-154.
- Mohammadi M, Hoseini NM, Chaichi MR, Alipour H, Dashtaki M and Safikhani S. 2018. Influence of Nano-iron oxide and zinc sulfate on physiological characteristics of peppermint. *Commun Soil Sci Plant Anal.* **49**(18): 2315–2326.
- Owji H, Hemmati S, Heidari R. and Hakimzadeh M. 2019. Effect of alumina (Al₂O₃) nanoparticles and macroparticles on *Trigonella foenum-graceum* L. *in vitro* cultures: assessment of growth parameters and oxidative stress-related responses. *3 Biotech.* **9**(11):419.

- Papa R and Gepts P. 2003. Asymmetry of gene flow and differential geographical structure of molecular diversity in wild and domesticated common bean (*Phaseolus vulgaris* L.) from Mesoamerica. *Theor Appl Genet.* **106**: 239-250.
- Parsad M.P. 2014. Molecular characterization and genetic diversity determination of *Hibiscus* species using RAPD molecular marker. *Asian J plant sci res.* **4(3)**: 50-56.
- Poborilova Z, Opatrilova Rand Babula P. 2013. Toxicity of aluminum oxide nanoparticles demonstrated using a BY-2 plant cell suspension culture model. *Environ. Exp. Bot.* **91**: 1-11.
- Raei M, Abdolhamid AS, Omidi M and Khodayari M. 2014. Effect of abiotic elicitors on tissue culture of *Aloe vera*. *Int. J. Biosci.* **5**: 74-81.
- Rafii MY, Shabanimofrad M, Edaroyati MW and Latif MA. 2012. Analysis of the genetic diversity of physic nut, *Jatropha curcas* L. accessions using RAPD markers. *Mol Biol Rep.* **39**: 6505-651.
- Rout GR, Bhattacharya D, Nanda RM, Das PND. 2003. Evaluation of genetic relationships in *Dalbergia* species using RAPD markers. *Biod Conserv.* **12**: 197-206.
- Rout GR and Sahoo S. 2015. Role of iron in plant growth and metabolism. *Rev Agr Sci.* **3**: 1-24.
- Saeed S, Ali H, Khan T, Kayani W and Khan A M. 2017. Impacts of methyl jasmonate and phenyl acetic acid on biomass accumulation and antioxidant potential in adventitious roots of *Ajuga bracteosa* Wall ex Benth., a high valued endangered medicinal plant. *Physiol. Mol. Biol. Plants* . **23(1)**: 229-237.
- Saric, MR, Kastrori-Cupina, T. and Gergis, I. 1967. Chlorophyll determination Univ. UnovenSadu-Praktikum is KiziologizeBilika-Beograd, HaucuaAnjiga. 215.
- Shatnawi M, Johnson K and Torpy F. 2004. In Vitro Propagation and Cryostorage Of *Syzygium Francisii* (Myrtaceae) By Encapsulation-Dehydration Method. *In vitro Cell Dev Biol. Plant.* **40(4)**: 403-7.
- Song U, Shin M, Lee G, Roh J, Kim Yand Lee E J. 2013. Functional analysis of TiO₂ nanoparticle toxicity in three plant species. *Biol trace elem res.* **155(1)**: 93-103.
- Sul IW and Korban SS. 2005. Direct shoot organogenesis from needles of three genotypes of *Sequoia sempervirens*. *Plant Cell, Tissue Organ Cult.* **80**:353-358.
- Sul IW and Korban SS. 1998. Effect of media, carbon source and cytokinins on shoot organogenesis in the Christmas tree, Scot pine (*Pinus sulvestris*). *J. Hort Sci Biotech.* **73**: 822-827.
- Suvakanta B, Senapati S K, Subhashree A, Anuradha-Mohapatra Rout G (2006), "Identification and genetic variation among Hibiscus species (Malvaceae) using RAPD markers", *Biosciences*, Vol. **61**, No. 1, pp. 123-128.
- Taha LS, Taie HA, Metwally SA. and Fathy HM .2014. Effect of laser radiation treatments on *in vitro* growth behavior, antioxidant activity and chemical constituents of *Sequoia sempervirens*. *Res J Pharm Biol Chem Sci.* **5(4)**: 1024-1034.
- Toral M, Ceru M, Herrera M, Gonzalez L, Martin L, Miranda J and Navarro-Cerrillo R. 2009. Clones identification of *Sequoia sempervirens* (D. Don) Endl. in Chile by using PCR-RAPDs technique. *J Zhejiang Univ Sci. B.* **10(2)**:112-119.
- Tosta MS, Oliveira CVF, Freitas RMO, Porto VCN, Nogueira NW and Tosta PAF. 2012. Ácido indolbutírico na propagação vegetativa de cajaraneira (*Spondias sp.*). *Semina: Ciências Agrárias.* **33**: 2727-2740.
- Velioglu YS, Mazza G, Gao L and Oomah BD. 1998. Antioxidant activity and total phenolics in selected fruits, vegetables, and grain products. *J Agric Food Chem.* **46**: 4113-4117.
- Yang F, Hong F, You W, Liu C, Gao F, Wu C and Yang P .2006. Influences of nano-anatase TiO₂ on the nitrogen metabolism of growing spinach. *Biol Trace Elem Res.* **110**: 179-190.
- Zafar H, Ali A, Ali JS, Haq IU and Zia M. (2016). Effect of ZnO nanoparticles on *Brassica nigra* seedlings and stem explants: growth dynamics and antioxidative response. *Front Plant Sci.* **7**: 535.
- Zheng L, Hong F, Lu S and Liu C. 2005. Effects of Nano-TiO₂ on strength of naturally aged seeds and growth of spinach. *Biol Trace Elem Res.*, **104**: 83-92. <https://doi.org/10.1385/BTER:104:1:083>
- Zhishen J, Mengcheng T. and Jianming W. 1999. The determination of flavonoid contents in mulberry and their scavenging effects on superoxide radicals. *Food Chem.* **64**: 555-559.
- Zia M, Yaqoob K, Mannan A, Nisa S, Raza G. and ur Rehman R. 2020. Regeneration response of carnation cultivars in response of silver nanoparticles under *in vitro* conditions. *Vegetos.* **33(1)**: 11-20.

Jordan Journal of Biological Sciences

An International Peer – Reviewed Research Journal

Published by the Deanship of Scientific Research, The Hashemite University, Zarqa, Jordan



Name: الاسم:
 Specialty: التخصص:
 Address: العنوان:
 P.O. Box: صندوق البريد:
 City & Postal Code: المدينة: الرمز البريدي:
 Country: الدولة:
 Phone: رقم الهاتف:
 Fax No.: رقم الفاكس:
 E-mail: البريد الإلكتروني:
 Method of payment: طريقة الدفع:
 Amount Enclosed: المبلغ المرفق:
 Signature: التوقيع:
 Cheque should be paid to Deanship of Research and Graduate Studies – The Hashemite University.

I would like to subscribe to the Journal

For

- One year
 Two years
 Three years

One Year Subscription Rates

	Inside Jordan	Outside Jordan
Individuals	JD10	\$70
Students	JD5	\$35
Institutions	JD 20	\$90

Correspondence

Subscriptions and sales:

The Hashemite University
 P.O. Box 330127-Zarqa 13115 – Jordan
 Telephone: 00 962 5 3903333
 Fax no. : 0096253903349
 E. mail: jjbs@hu.edu.jo

المجلة الأردنية للعلوم الحياتية Jordan Journal of Biological Sciences (JJBS)

<http://jjbs.hu.edu.jo>

المجلة الأردنية للعلوم الحياتية: مجلة علمية عالمية محكمة ومفهرسة ومصنفة، تصدر عن الجامعة الهاشمية وبدعم من صندوق دعم البحث العلمي والإبتكار – وزارة التعليم العالي والبحث العلمي.

هيئة التحرير

رئيس التحرير

الأستاذ الدكتورة منار فايز عتوم
الجامعة الهاشمية، الزرقاء، الأردن

مساعد رئيس التحرير

الدكتور مهند عليان مساعدة
الجامعة الهاشمية، الزرقاء، الأردن

الأعضاء:

الأستاذ الدكتور جميل نمر اللحام
جامعة اليرموك

الاستاذ الدكتور زهير سامي عمرو
جامعة العلوم و التكنولوجيا الأردنية

الأستاذ الدكتورة حنان عيسى ملكاوي
جامعة اليرموك

الأستاذ الدكتور عبدالرحيم أحمد الحنيطي
الجامعة الأردنية

الاستاذ الدكتور خالد محمد خليفات
جامعة مؤتة

فريق الدعم:

المحرر اللغوي

الدكتور شادي نعامنة

تنفيذ وإخراج

م. مهند عقده

ترسل البحوث الى العنوان التالي:

رئيس تحرير المجلة الأردنية للعلوم الحياتية
الجامعة الهاشمية

ص.ب , 330127 , الزرقاء, 13115 , الأردن

هاتف: 0096253903333

E-mail: jjbs@hu.edu.jo, Website: www.jjbs.hu.edu.jo



المملكة الأردنية الهاشمية



المجلة الأردنية



للعلوم الحياتية

مجلة علمية عالمية محكمة

تصدر بدعم من صندوق دعم البحث العلمي و الابتكار



<http://jjbs.hu.edu.jo/>